## Title

From One-Coordination to Multiple Bonding: Enforcing Unusual Molecular Geometries at Aluminum and Lead Using m Terphenyl Ligands and the Competition of Steric and Dispersion Force Effects



## Author

Queen, Joshua

## Publication Date

2022

Peer reviewed|Thesis/dissertation

# From One-Coordination to Multiple Bonding: Enforcing Unusual Molecular Geometries at Aluminum and Lead Using *m*-Terphenyl Ligands and the Competition of Steric and Dispersion Force Effects

By

JOSHUA D. QUEEN
DISSERTATION

Submitted in partial satisfaction of the requirements for the degree of

DOCTOR OF PHILOSOPHY

in

Chemistry

in the

OFFICE OF GRADUATE STUDIES

of the

UNIVERSITY OF CALIFORNIA

DAVIS

Approved:

Philip P. Power, Chair

Alan L. Balch

Louise A. Berben

Committee in Charge

2022

## ABSTRACT

The use of sterically demanding *m*-terphenyl ligands to kinetically stabilize unusual low coordinate molecular geometries in organometallic complexes of aluminum and lead are described. The influence of attractive intramolecular interligand London dispersion forces on their structures was also studied. In Chapter 2, rare examples of diplumbynes, dilead analogues of alkynes, of the formula RPbPbR with lead-lead multiple bonding were prepared and structurally characterized. Using the *m*-terphenyl ligands $C_6H_3$-2,6-($C_6H_2$-2,4,6-$^tBu_3)_2$ ($Ar^{tBu6}$) and $C_6H$-2,6-($C_6H_2$-2,4,6-$^iPr_3)_2$-3,5-$^iPr_2$ ($Ar^{iPr8}$) gave multiply bonded structures in the solid state. Calculations in collaboration with Prof. Stefan Grimme, Markus Bursch, Jakob Seibert, and Leonard Maurer showed that dispersion energies also contributed significantly to the stability of these molecules. Chapter 3 describes stable *m*-terphenyl lead(II) hydrides that were isolated in the preparation of the diplumbynes.

Chapter 4 describes the metathesis reactions of heavy group 14 element alkyne analogues of Ge, Sn, and Pb with Mo-Mo single and triple bonds. These compounds reversibly dissociate in solution to monomeric radicals. By their direct reaction with $(CO)_3(\eta^5\text{-}C_5H_5)Mo–Mo(\eta^5\text{-}C_5H_5)(CO)_3$ and $(CO)_2(\eta^5\text{-}C_5H_5)Mo{\equiv}Mo(\eta^5\text{-}C_5H_5)(CO)_2$, the energetically favored group 14 element-Mo bonds are formed.

Chapter 5 describes the synthesis of the first isolated species with a one-coordinate aluminum atom. The sterically demanding $Ar^{iPr8}$ ligand stabilizes this geometry. Nonetheless, calculations showed that a dimer, the dialuminene $Ar^{iPr8}AlAlAr^{iPr8}$, is slightly favored. This is supported by the facile reactivity of $:AlAr^{iPr8}$ with $H_2$. In Chapter 6 the reaction of $:AlAr^{iPr8}$ with several organoazides is described. When the m-terphenyl azide $Ar^{Me6}N_3$ ($Ar^{Me6}$ = $C_6H_3$-2,6-($C_6H_2$-2,4,6-

$Me_3)_2$ is used, the first compound with an Al-N triple bond $Ar^{iPr8}AlNAr^{Me6}$ was isolated. The attractive dispersion forces between the two terphenyl substituents on the Al and N atoms contribute a stabilization energy that is on the same order of magnitude as the Al-N π-type bonds in the molecule.

Chapter 7 describes a new route to dialuminenes of the formula RAl=AlR. These species are highly reactive towards arene solvents in which they are soluble. By using a terphenyl ligand substituted by the $-SiMe_3$ group, $C_6H_2$-2,6-($C_6H_3$-2,6-$^iPr_2)_2$-4-$SiMe_3$ ($Ar^{iPr4}$-4-$SiMe_3$) we anticipated increasing the solubility of the dialuminene in solvents with which it would not react. Direct reduction of the iodide precursors to 4-$SiMe_3Ar^{iPr4}Al$=$AlAr^{iPr4}$-4-$SiMe_3$ failed, so a new route through the comproportionation of $Al(Et_2O)I_2Ar^{iPr4}$-4-$SiMe_3$ or $(AlIAr^{iPr4}$-4-$SiMe_3)_2$ with the dialuminyne salt $Na_2(AlAr^{iPr4}$-4-$SiMe_3)_2$ was used. In hexanes or ether, this reaction mixture turns deep purple before rapidly decomposing. However, in benzene the dialuminene-benzene [4+2] cycloaddition complex is stoichiometrically obtained from the comproportionation reaction.

## ACKNOWLEDGEMENTS

I thank my lab mates and friends at UC Davis for their friendship and help during the course of my degree. I especially thank Sam Cao and Dr. Kristian Mears who have provided much support near the end of my degree. I also thank Dr. Cary Stennett, who has always been reliable, and Dr. David Liptrot who have provided great help and conversation over the years. Special thanks to Dr. Carla Saunders and Heineken 😈 for being great housemates.

Next, I would like to acknowledge lab members that laid the foundations for several of these projects. Dr. Bobby Ellis was the first to prepare two of the new diplumbynes, $Ar^{iPr4}PbPbAr^{iPr4}$ and $4\text{-}SiMe_3Ar^{iPr4}PbPbAr^{iPr4}\text{-}4\text{-}SiMe_3$, that are described in Chapter 2. Dr. Christine Caputo discovered the reaction between the distannynes and Mo-Mo bonded compounds that is described in Chapter 4 – I also thank Alice Phung for help preparing these tin complexes.

I am also grateful to our collaborators who have carried out the calculations to quantify the dispersion force attractions in our molecules. Prof. Stefan Grimme and his students Markus Bursch, Jakob Seibert, and Leonard Maurer provided calculations for the diplumbynes described in Chapter 2. Heikki Tuononen and his students Annika Lehmann and Sini Irvankoski performed calculations on the aluminum compounds described in Chapters 5 and 6. Dr. Jim Fettinger has provided much help with preparing X-ray diffraction data for publication, and his practical instruction on solving crystal structures has been incredibly helpful.

TABLE OF CONTENTS

## Chapter 1. General Introduction

In the early 20th century, attempts to make compounds containing multiple bonds between heavier main group elements (third period and below) were unsuccessful, instead resulting in other singly bonded compounds or oligomers.[1–4] A partial explanation for this was the weak overlap of the larger 3p orbitals compared to the 2p orbitals due to their greater physical separation as well as core-core repulsion derived from the higher number of core electrons in the heavier elements.[5] This led to the assumption that there existed a "double bond rule" which stated that the main group elements of principal quantum number greater than 2 do not form multiple bonds.[6] Work in the 1970s and 80s however showed this principle to be false. Organic compounds with aromatic π systems were synthesized incorporating heavy heteroatoms including P, As, Sb, and Bi.[7] Lappert found that the stannylene $:Sn\{CH(SiMe_3)_2\}_2$, while monomeric in solution, formed a weakly bonded Sn-Sn dimer in the crystal phase.[8] In 1981, West and coworkers reported the structure of the disilene $(2,4,6\text{-}Me_3C_6H_2)_2Si{=}Si(C_6H_2\text{-}2,4,6\text{-}Me_3)$ containing an Si=Si double bond,[9] and Yoshifuji and coworkers reported the P=P doubly bonded diphosphene $(2,4,6\text{-}{}^tBu_3C_6H_2)P{=}P(C_6H_2\text{-}2,4,6\text{-}{}^tBu_3C_6H_2)$ [10] which were shown to possess "normal" double bonds. The use of large ligands at the heavy main group elements in these compounds was key to their stabilization and isolation. Pauli repulsion between alkyl groups of the ligands (i.e. steric effects) provides kinetic stabilization by protecting the multiple bonds and preventing oligomerization. The following decades saw the synthesis of series of alkene and alkyne analogues of the heavier group 13, 14, and 15 elements[11,12] employing the same strategy of

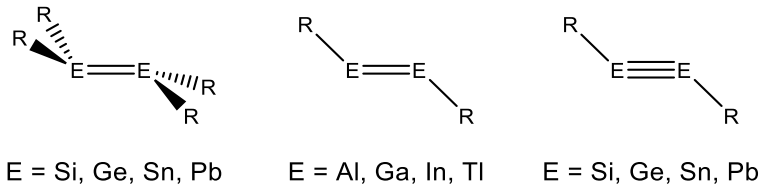


**Figure 1.1** General structures of group 13 and group 14 alkene and alkyne analogues showing pyramidalized or trans-bent geometries.

using sterically hindering ligands to protect the multiple bonds. Nonetheless, X-ray diffraction studies on the resultant group 14 $R_2EER_2$ (E = Si–Pb) compounds revealed they had unusual pyramidalized geometries around the group 14 element (Figure 1.1). Likewise, the group 13 and group 14 REER compounds (E = Al–Tl; Si–Pb) showed trans-bent cores in their solid-state structures. This differs markedly from the lighter element congeners in which molecular geometries can be well described and predicted by VSEPR and valence bond theories utilizing sp, $sp^2$, and $sp^3$ hybrid orbitals. However, these distorted structures (i.e. pyramidalized or bent) are significant as they indicate fundamental changes in the nature of the multiple bonding between the heavier elements.

Application of classical valence bond or molecular orbital theory bonding models to the heavier element compounds has led to much debate.[13,14] Alternative descriptions of the bonding in these compounds have been developed to explain their nonclassical structures. A simple treatment of the bond in the group 14 $R_2E{=}ER_2$ species is the double donor-acceptor model by Lappet[8] (Figure 1.2, bottom left). Carter, Goddard, Malrieu, and Trinquier further elaborated this model on the basis of the ground states of the heavy carbene or carbyne analogue moieties.[15,16] Methylene $R_2C$: and methyne RC:· fragments have triplet and

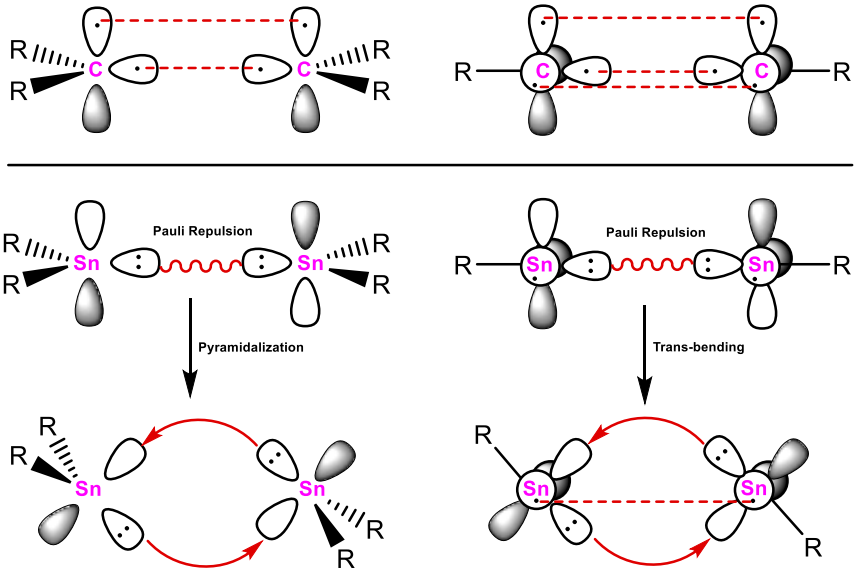


**Figure 1.2** Double donor-acceptor model for the dimerization of $R_2C$: and RC:· fragments (top) compared with the tin analogues (bottom).

quartet ground states respectively, with two or three unpaired electrons. Dimerization of these fragments to form the trigonal planar or linear geometries in alkenes and alkynes is facile (Figure 1.2, top). For the heavier elements, pairing of the electrons is more stable and the $R_2E$: and RE:· moieties have singlet and doublet ground states, respectively. The now filled orbitals do not overlap due to Pauli repulsion and the molecule distorts so these can engage in donor-acceptor interactions with the empty p orbital on the opposite main group element fragment (Figure 1.2, bottom).

Another interpretation invokes a second-order Jahn-Teller distortion starting from classical trigonal planar $R_2EER_2$ or linear REER structures.[17] Upon bending from the linear $D_{\infty h}$ geometry, symmetry allowed mixing of frontier molecular orbitals in the new $C_{2h}$ point group results in a

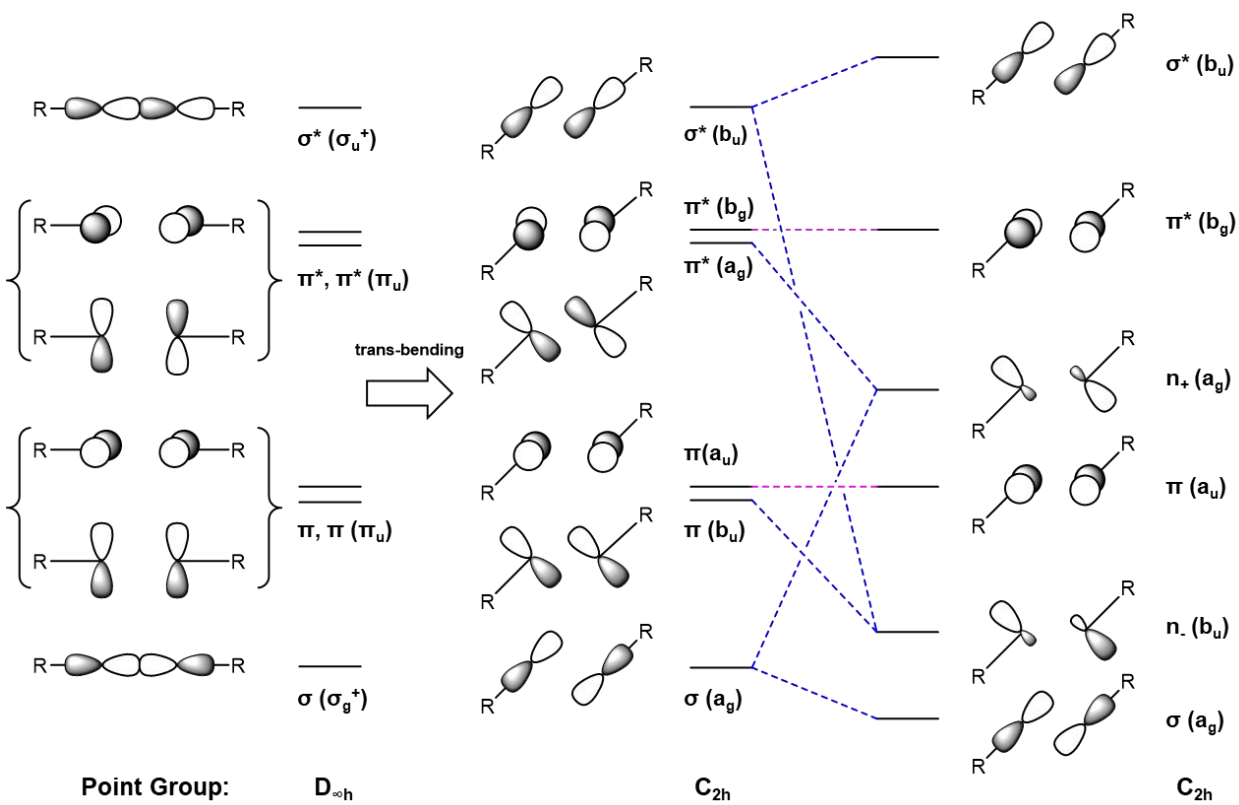


**Figure 1.3.** Second order Jahn-Teller distortion diagram for the frontier molecular orbitals of REER species (E = Al–Tl, Si–Pb). The classical linear $D_{\infty h}$ structure (left) undergoes trans-bending to a structure with $C_{2h}$ symmetry (middle). Symmetry allowed mixing of the frontier orbitals (right) stabilizes the now "slipped" π ($n_-$) and π* ($n_+$) orbitals.

significant lowering in energy (i.e. stabilization) of one of the π and π* orbitals (Figure 1.3). This is facilitated by the smaller energy gaps between the frontier orbitals in the heavier element compounds due to the decreasing E-E bond strength. Ultimately, the second period elements appear to be the exception rather than the rule, and the linear or trigonal planar geometries they adopt are not energetically favorable in their heavier counterparts. This has been attributed to the efficient 2s/2p mixing (i.e. 'hybridization') of the second row elements due to their unique 1s orbital core structure. This causes the next shell, i.e., the 2s and 2p orbitals, to have almost equal radii thereby facilitating hybridization.[18,19] As the difference between the radial extension of the ns and np orbitals increases upon descending the groups, their mixing becomes less efficient. Thus, the R-E and E-E bonding orbitals of the heavier elements have more p character which results in narrowing of the R-E-E angle.

Beyond their structural novelty, these compounds are of wide interest for their reactivity. The weak multiple bonds tend to be reactive towards small molecules and unsaturated organic compounds.[20] Indeed, the first activation of dihydrogen[21] and ethylene[22] by main group element compounds under ambient conditions involved multiply bonded complexes. The frontier orbitals of these compounds (which include the heavy element multiple bonds) interact with those of small molecules, e.g. $H_2$ or $C_2H_4$, in a manner resembling their interaction with d-orbitals on transition metals.[23] Recent years have seen growing interest in developing main group element based reagents for catalytic processes.[24,25]

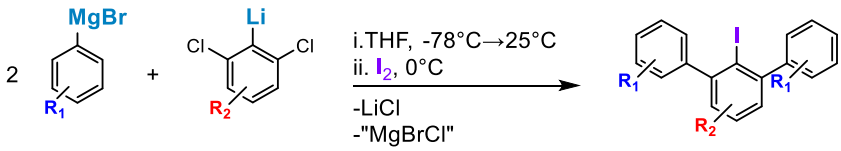


**Scheme 1.1.** General route to *m*-terphenyl ligands. $R_1$ and $R_2$ signify substitution patterns on the flanking and central aryl rings e.g., for $Ar^{iPr4}$-4-$SiMe_3$ $R_1$ = 2,6-$^iPr_2$ and $R_2$ = 4-$SiMe_3$.

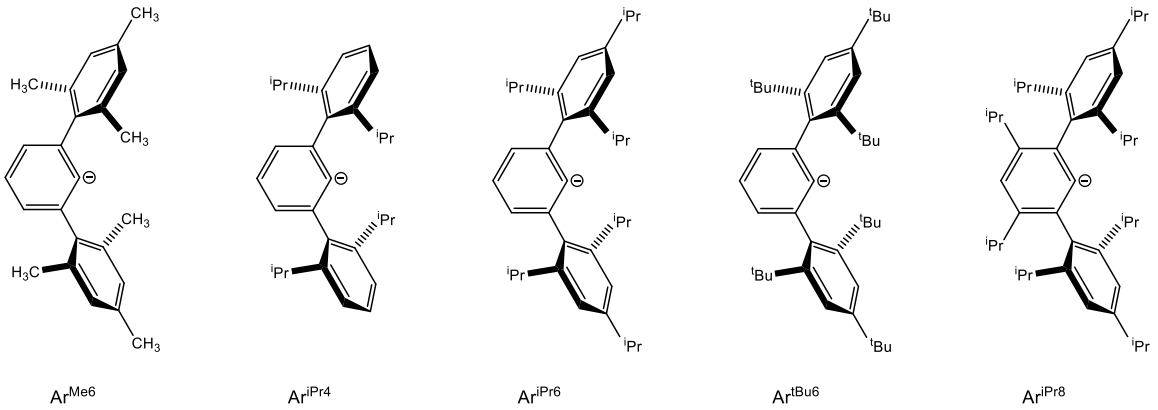


**Figure 1.4.** Commonly used *m*-terphenyl ligands and their abbreviations. The steric demand of the ligand roughly increases left to right.

Our group has synthesized several multiply bonded compounds of the heavy group 13 and 14 elements of the general formula REER (E = Al-Tl, Ge-Pb) and some of their reduced counterparts $[REER]^{-}$ and $[REER]^{2-}$ using *m*-terphenyl ligands to confer steric protection. These ligands are readily prepared at large scale and good yield in a "one-pot" procedure[26,27] (Scheme 1.1). The steric demand of the terphenyl ligand can be adjusted by varying the alkyl groups and their substitution pattern on the flanking aryl rings. Additionally, substitution at the *meta* positions of the central ring restricts the rotation of the flanking rings and pushes them slightly forward, increasing the steric protection of the element bound to the *ispo* position.[28] This allows some 'tuning' of the steric effects to control oligomerization–thus trimeric, dimeric, and even monomeric metal complexes can be accessed for an element by adjusting the ligand. Common *m*-terphenyl ligands used by our group are listed in Figure 1.4 in roughly increasing size along with their abbreviations.

Recently the influence of dispersion forces on the formation and structures of organometallic complexes has been recognized.[29,30] The attraction between alkyl groups on adjacent organic ligands, including terphenyls, can lead to structures that are counterintuitive to what may be predicted based on steric effects alone. In order to explore and exploit the balance of steric

repulsions and dispersion force attractions, the work in this dissertation is mainly focused on the use of the very sterically demanding ligand $Ar^{iPr8}$ to enforce unusual geometries at Pb and Al – two elements for which low coordinate low, oxidation state compounds are exceedingly rare. This general introduction will survey the known multiply bonded REER compounds of the group 13 and 14 elements and their monomeric counterparts with which they are in equilibrium in solution, as well as introduce the use of dispersion force attraction for the stabilization of unusual molecules.

**Group 13 compounds**

*Boron compounds*: Reduction of the terphenyl boron halides $BX_2Ar$ (X = Cl, Br; Ar = $Ar^{Me6}$, $Ar^{iPr6}$) with alkali metals did not give B-B multiple bonded species but instead resulted in formation of the transient borylenes :BAr.[31] These species activated the C-C bond between the flanking aryl ring and its *ortho* substituent to give 9-borafluorene derivatives.[31] Braunschweig and coworkers have isolated transition metal complexes of these $:BAr^{Me6}$ and $:BAr^{iPr6}$ fragments which can release the free borylene under photolytic or thermal conditions, allowing controlled studies of their reactivity.[32–35] It has only been through coordination of N-heterocyclic carbene (NHC) ligands that the diborenes (NHC)RB=BR(NHC) (R = H, alkyl) have been stabilized and isolated.[36,37]

*Aluminum compounds*: The dialuminenes RAlAlR have yet to be isolated and structurally characterized. The Al=Al bonds in these compounds appear to be inherently stable (see Chapter 7) and are highly reactive with arenes, resulting in activation of the benzene or toluene solvents in which they dissolve. Reduction of $AlI_2Ar^{iPr4}$ with $KC_8$ in $Et_2O$ afforded the dialuminene $Ar^{iPr4}AlAlAr^{iPr4}$ which was isolated only as its [2+4] cycloaddition product with toluene[38] and later its [2+2] cycloaddition product with $Me_3SiCCSiMe_3$.[39] Tokitoh and coworkers prepared bis(aryl)dialuminenes by reduction of Ar(Br)Al-Al(Br)Ar (Ar = $C_6H_3$-2,6-$\{CH(SiMe_3)_2\}_2$ or

$C_6H_2$-2,6-{$CH(SiMe_3)_2$}$_2$-4-$^t$Bu) with $KC_8$ in benzene, affording their dialuminene/benzene cycloaddition complexes.[40,41] The benzene moiety in these compounds was shown to reversibly dissociate to afford the reactive dialuminene in solution.[40] This allowed the study of the addition of the dialuminenes to naphthalene, anthracene, dihydrogen,[42] and substituted acetylenes.[40,41] Furthermore, at high temperature the benzene solution of the dialuminene appeared to liberate the monomer :AlAr which underwent [1+2] cycloaddition with PhCCPh.[41] The only Al-Al double bonded species isolated and characterized to date utilize Lewis base complexation by NHC ligands,[43,44] or chelating amido-phosphine ligands[45] to stabilize the reactive Al=Al moiety.

Reduction of $AlI_2Ar^{Me6}$ and $AlI_2Ar^{iPr4}$ with excess Na metal afforded the trimeric $Na_2(AlAr^{Me6})_3$, which features a metalloaromatic 2 π-electron $Al_3$ core, and the dimeric dialuminyne $Na_2(AlAr^{iPr4})_2$.[46] The Na cations in these compounds are complexed by the flanking aryl rings of adjacent terphenyl ligands which is probably crucial to their stability.

*Gallium compounds*: The anionic compounds $Na_2(GaAr^{iPr6})_2$,[13] $Na_2(GaAr^{Me6})_3$,[47] and $K_2(GaAr^{Me6})_3$[48] were first prepared by Robinson and coworkers by reduction of $GaCl_2Ar$ (Ar = $Ar^{iPr6}$, $Ar^{Me6}$) with Na or K metal. However reduction of $GaCl_2Ar^{iPr6}$ with K afforded the cluster $K_2\{Ga_4(Ar^{iPr6})_2\}$.[49] The neutral digallenes $Ar^{iPr4}GaGaAr^{iPr4}$ and $Ar^{iPr6}GaGaAr^{iPr6}$ were synthesized by treatment of GaI with the terphenyl lithium salts.[50,51] These could be reduced with Na to $Na_2(GaAr^{iPr4})_2$ and $Na_2(GaAr^{iPr6})_2$. Substitution of the *para* position of the central ring of the terphenyl afforded the digallenes 4-tBu$Ar^{iPr6}GaGaAr^{iPr6}$-4-tBu and 4-$CF_3Ar^{iPr6}GaGaAr^{iPr6}$-4-$CF_3$.[52] When the *meta* positions on the central ring were substituted with isopropyl groups, instead the one-coordinate Ga species :$GaAr^{iPr8}$ and :Ga($C_6H$-2,6-($C_6H_3$-2,6-$^iPr_2$)$_2$-3,5-$^iPr_2$) are isolated as crystalline solids.[52] Reactivity studies and computational analysis on the isolable dimer and

monomer compounds revealed that the dimer rather than the monomer is the reactive species towards olefins and dihydrogen.[53]

*Indium compounds*: The monomeric :$InAr^{iPr6}$ was prepared by addition of $LiAr^{iPr6}$ to InCl and showed no In⋯In contacts in the solid state (the shortest In-In distance was 6.890(2)Å).[54] The one-coordinate In atom acted as a Lewis base by addition to $MnCp(CO)_2(THF)$ to afford $Ar^{iPr6}$In-$MnCp(CO)_2$. By decreasing the size of the ligand, the diindene $Ar^{iPr4}InInAr^{iPr4}$ was isolated[55] and remains the only structurally characterized diindene to date. Upon treatment with $B(C_6F_5)_3$, the complex $Ar^{iPr4}$In-$B(C_6F_5)_3$ was isolated, indicating the lability of the In-In bond to yield :$InAr^{iPr4}$ fragments in solution. Further decreasing the size of the terphenyl ligand, the addition of $LiAr^{Me6}$ to InCl yielded the cluster $In_8(Ar^{Me6})_4$ with a distorted cubic $In_8$ core.[56]

*Thallium compounds*. Similar to indium, the addition of $Li(Et_2O)Ar^{iPr6}$ to TlCl afforded the monomeric complex :$TlAr^{iPr6}$ with no close Tl⋯Tl contacts.[57] The dithallene $Ar^{iPr4}TlTlAr^{iPr4}$ was isolated from the reaction of $LiAr^{iPr4}$ and TlCl.[58] Again dissociation to :$TlAr^{iPr4}$ was evidenced by the formation of $Ar^{iPr4}$Tl-$B(C_6F_5)_3$. The dark red compound "$TlAr^{Me6}$" was found to be unstable[57] and no structural characterization has been obtained for it. However, the addition of $LiC_6H_3$-2,6-$(C_6H_3$-2,6-$Me_2)_2$ to TlCl afforded the isolable trimer $\{TlC_6H_3$-2,6-$(C_6H_3$-2,6-$Me_2)_2\}_3$ featuring a $Tl_3$ triangular core.[58]

Selected structural parameters for the E-E bonds, R-E-E bending angles, and R-E-E-R torsion angles in these group 13 compounds are presented in Table 1.1.

**Table 1.1** Selected bond length and angle data for heavier group 13 multiple bonded REER and $[REER]^{2-}$ compounds and some related trimeric species. The E-E bonded atoms are in bold red font.

| | **Al—Al (Å)** | **R–Al–Al (°)** | **R–Al–Al–R (°)** | *Ref* |
|---|---|---|---|---|
| $^{t}Bu_2MeSi(NHC)$**AlAl**$(NHC)SiMe^{t}Bu_2$ [a] | 2.3943(16) | — | — | 43 |
| (Trip)(NHC)**AlAl**(NHC)(Trip) [a,b] | 2.4039(8) | — | — | 44 |
| $Na_2[Ar^{iPr4}$**AlAl**$Ar^{iPr4}]_2$ | 2.428(1) | 131.71(7) | 180 | 46 |
| $Na_2[$**Al**$Ar^{Me6}]_3$ | 2.520(2) | — | — | 46 |
| | | | | |
| | **Ga—Ga (Å)** | **R–Ga–Ga (°)** | **R–Ga–Ga–R (°)** | |
| $Ar^{iPr4}$**GaGa**$Ar^{iPr4}$ | 2.6268(7) | 123.16(7) | 180 | 50 |
| 4-$^{t}BuAr^{iPr6}$**GaGa**$Ar^{iPr6}$-4-$^{t}Bu$ | 2.596(4)<br>2.512(7)<br>2.552(4) | 2.012(5), 2.021(2)<br>2.039(7), 2.019(3)<br>2.006(3), 2.053(3) | 158.6(2)<br>-179.7(3)<br>163.4(2) | 51 |
| 4-$CF_3Ar^{iPr6}$**GaGa**$Ar^{iPr6}$-4-$CF_3$ | 2.6031(8) | 121.68(5), 128.53(5) | 176.26(8) | 51 |
| $Na_2[Ar^{iPr4}$**GaGa**$Ar^{iPr4}]$ | 2.347(1) | 130.7(1) | 180 | 50 |
| $Na_2[Ar^{iPr6}$**GaGa**$Ar^{iPr6}]$ | 2.319(3) | 128.5(4), 133.5(4) | -173.2(8) | 13 |
| $Na_2[$**Ga**$Ar^{Me6}]_3$ | 2.441(1) | — | — | 47 |
| $K_2[$**Ga**$Ar^{Me6}]_3$ | 2.4260(5),<br>2.4317(5),<br>2.4187(5) | — | — | 48 |
| | | | | |
| | **In—In (Å)** | **R–In–In (°)** | **R–In–In–R (°)** | |
| $Ar^{iPr4}$**InIn**$Ar^{iPr4}$ | 2.9786(5) | 121.23(6) | 180 | 55 |
| | | | | |
| | **Tl—Tl (Å)** | **R–Tl–T l(°)** | **R–Tl–Tl–R (°)** | |
| $Ar^{iPr4}$**TlTl**$Ar^{iPr4}$ | 3.0936(8) | 119.74(14) | 180 | 58 |
| $\{$**Tl**$C_6H_3$-2,6-$(C_6H_3$-2,6-$Me_2)_2\}_3$ | 3.2144(3)<br>3.3782(3) | — | — | 58 |

[a]NHC = 1,3-diisopropyl-4,5-dimethyl-imidazolin-2-ylidene. [b]Trip = 2,4,6-$^{i}Pr_3C_6H_2$.

## Group 14 compounds

*Silicon compounds*: The first stable disilyne **Si′**Si≡Si**Si′**) (**Si′ =** Si{CH(SiMe$_3$)$_2$}$_2$$^i$Pr) was isolated by Sekiguchi and coworkers using Si- substituted ligands and is stable as a green solid.[59] One electron reduction with K afforded the radical anion complex [K(CH$_3$OC$_2$H$_4$OCH$_3$)$_4$] [**Si′**Si≡Si**Si′**].[60] An asymmetric disilyne **Si′**Si≡Si(Si{CH(SiMe$_3$)$_2$}$_2$CH$_2$C(CH$_3$)$_3$) was prepared and was found to undergo rearrangement and cyclization to the cyclotrisilene.[61] A diaryldisilyne Ar′Si≡SiAr′ (Ar′ = C$_6$H$_2$-2,6-{CH(SiMe$_3$)$_2$}$_2$-4-C(SiMe$_3$)$_3$) was synthesized by treatment of the dibromodisilene Ar′(Br)Si=Si(Br)Ar′ with Li$^t$Bu at -100°C. Elimination of LiBr and $^t$BuBr afforded the disilyne which slowly decomposed in solution.[62] A dialkyl derivative has been prepared using the ligand -C(SiMe$_3$)$_2$CH$_2$$^t$Bu.[63]

*Germanium compounds*: Reduction of Ar$^{iPr4}$(Cl)Ge=Ge(Cl)Ar$^{iPr4}$ with K afforded the first digermyne Ar$^{iPr4}$GeGeAr$^{iPr4}$.[64] The derivatives 4-SiMe$_3$Ar$^{iPr4}$GeGeAr$^{iPr4}$-4-SiMe$_3$, 4-ClAr$^{iPr4}$GeGeAr$^{iPr4}$-4-Cl as well as Ar$^{iPr8}$GeGeAr$^{iPr8}$ and Ar$^{iPr6}$GeGeAr$^{iPr6}$ were prepared similarly.[65,66] Ar′Ge≡GeiAr′ has also been reported.[67] These diaryldigermynes feature wide C-Ge-Ge-C bending angles in the solid state. Using bulky amide ligands can force the trans bending angle to decrease and the Ge-Ge bond to lengthen.[68–70] The terphenyl substituted digermynes can be singly or doubly reduced with alkali metals, affording the monoanionic radicals, or the dianions.[66,71]

*Tin Compounds*: The distannynes ArSnSnAr have been isolated with the terphenyl ligands Ar$^{iPr4}$, Ar$^{iPr6}$, Ar$^{tBu6}$, and Ar$^{iPr8}$ as well as the *para* substituted ligands Ar$^{iPr4}$-4-SiMe$_3$, Ar$^{iPr4}$-4-GeMe$_3$, Ar$^{iPr4}$-4-tBu, Ar$^{iPr4}$-4-Cl, Ar$^{iPr4}$-4-OCH$_3$ generally by the reduction of Sn(Cl)Ar by alkali metals.[65,72,73] Two isomeric forms were found in the solid state structures of the distannynes differing in their trans-bending angles and consequently their Sn-Sn distances.[65] The energy

difference between these isomers was calculated to be very small (≤ 5 kcal $mol^{-1}$) and therefore likely influenced by crystal packing effects.[65,74] Characterized examples of bulky amide and borylamide substituted derivatives appear to favor the highly trans-bent geometry in the solid state.[70,75] The terphenyl substituted distannynes have been found to be in equilibrium with monomeric SnAr (Ar = *m*-terphenyl ligand) radicals in solution, evidenced by $^{1}H$ NMR and EPR experiments[76] as well as evidenced by their C-H activation of benzylic groups.[77] Both the single and double reduction of distannynes to anionic species have been reported.[66,71,78]

*Lead compounds*: Prior to the work in this dissertation, only one diplumbyne $Ar^{iPr6}PbPbAr^{iPr6}$ had been reported.[79] In that compound the Pb-Pb distance (3.1881(1) Å) was longer than the single bond in $Ph_3PbPbPh_3$ (Pb−Pb = 2.844(4) Å)[80] and the C-Pb-Pb bending angles approached 90°. This suggested the Pb-Pb bond was formed by overlap of the essentially unhybridized 6p orbitals of the Pb atoms. Rather than being synthesized via the reduction of $\{Pb(\mu\text{-}Br)Ar^{iPr6}\}_2$ with alkali metals, treatment of the bromide derivative with $Al(^{i}Bu)_2H$ formed the lead hydride intermediate $\{Pb(\mu\text{-}H)Ar^{iPr6}\}_2$ which afforded the diplumbyne with release of $H_2$. The existence of this proposed hydride was confirmed when it was independently isolated by Wesemann and coworkers who found it to be unstable above -40°C in solution.[81]

Selected structural parameters for the E-E bonds, R-E-E bending angles, and R-E-E-R torsion angles in these group 14 compounds are presented in Table 1.2.

**Table 1.2.** Selected bond length and angle data for heavier group 14 multiple bonded REER, $[REER]^{\cdot-}$ and $[REER]^{2-}$ compounds. The E-E bonded atoms are in bold red font.

| | **Si—Si (Å)** | **R–Si–Si (°)** | **R–Si–Si–R (°)** | *Ref* |
|---|---|---|---|---|
| **Si′SiSiSi′**[a] | 2.0623(9) | 137.44(3) | 179.42(3) | 59 |
| $[K(CH_3OC_2H_4OCH_3)_4]$[**Si′SiSiSi′**][a] | 2.173(1) | 112.84(5), 113.97(5) | -177.68(5) | 60 |
| **Si′SiSi**$(Si\{CH(SiMe_3)_2\}_2CH_2C(CH_3)_3)$[a] | 2.057(1) | 137.90(6), 138.78(6) | 178.36(6) | 61 |
| $\{$**Si**$C_6H_2$-2,6-$CH(SiMe_3)_2$-4-$SiMe_3\}_2$ | 2.108(4) | 133.0(3) | -164.2(5) | 62 |
| $^tBuH_2(SiMe_3)_2C$**SiSi**$C(SiMe_3)_2CH_2{}^tBu$ | 2.0863(13) | 132.05(7) | 180 | 63 |
| | | | | |
| | **Ge—Ge (Å)** | **R–Ge–Ge (°)** | **R–Ge–Ge–R (°)** | *Ref* |
| $Ar^{iPr4}$**GeGe**$Ar^{iPr4}$ | 2.2850(8) | 128.67(8) | 180 | 64 |
| 4-$SiMe_3$-$Ar^{iPr4}$**GeGe**$Ar^{iPr4}$-4-$SiMe_3$ | 2.2438(8) | 128.44(16) | 180 | 65 |
| 4-Cl-$Ar^{iPr4}$**GeGe**$Ar^{iPr4}$-4-Cl | 2.3071(3) | 128.44(16) | 180 | 65 |
| $Ar^{iPr8}$**GeGe**$Ar^{iPr8}$ | 2.2125(13) | 136.13(17) | 165.8(2) | 65 |
| $Na[Ar^{iPr6}$**GeGe**$Ar^{iPr6}]$ | 2.3089(8) | 114.2(1) | 176.9(2) | 66 |
| $K[Ar^{iPr4}$**GeGe**$Ar^{iPr4}]$ | 2.3331(4) | 115.55(5) | -173.82(9) | 66 |
| $Li_2[Ar^{iPr4}$**GeGe**$Ar^{iPr4}]$ | 2.455(9) | 102.97(9) | 180 | 66 |
| $Na_2[Ar^{iPr6}$**GeGe**$Ar^{iPr6}]$ | 2.394(1) | 102.37(8) | 180 | 71 |
| $K_2[Ar^{iPr6}$**GeGe**$Ar^{iPr6}]$ | 2.3912(6) | 112.14(7) | 180 | 66 |
| $\{$**Ge**$C_6H_2$-2,6-$CH(SiMe_3)_2$-4-$SiMe_3\}_2$ | 2.2060(7)<br>2.2260(7) | 136.18(14), 126.19(13)<br>138.66(14), 123.60(13) | 160.2(3)<br>168.9(3) | 67 |
| $[$**Ge**$N(SiMe_3)\{C_6H_2$-2,6-$(CHPh_2)_2$-4-$CH_3\}]_2$ | 2.7093(7) | 100.09(6) | 180 | 68 |
| $[$**Ge**$N(Si^iPr_3)\{C_6H_2$-2,6-$(CHPh_2)_2$-4-$^iPr\}]_2$ | 2.3568(3) | 120.39(4), 121.03(4) | -161.68(8) | 69 |
| $[$**Ge**$N(SiMe_3)\{B(NC_6H_3$-2,6-$^iPr_2)_2(CH)_2\}]_2$ | 2.6003(6) | 103.09(9), 102.43(9) | 135.6(4) | 70 |
| $[$**Ge**$N(SiPh_3)\{B(NC_6H_3$-2,6-$^iPr_2)_2(CH)_2\}]_2$ | 2.6022(10) | 107.62(8), 108.11(8) | 175.5(1) | 70 |
| | | | | |
| | **Sn—Sn (Å)** | **R–Sn–Sn (°)** | **R–Sn–Sn–R (°)** | *Ref* |
| $Ar^{iPr4}$**SnSn**$Ar^{iPr4}$ | 2.6675(4) | 125.24(7) | 180 | 72 |
| 4-$SiMe_3$-$Ar^{iPr4}$**SnSn**$Ar^{iPr4}$-4-$SiMe_3$ | 3.0577(2) | 99.07(3) | 180 | 65 |
| 4-$GeMe_3$-$Ar^{iPr4}$**SnSn**$Ar^{iPr4}$-4-$GeMe_3$ | 3.077(12) | 97.79(17) | 180 | 65 |
| 4-Cl-$Ar^{iPr4}$**SnSn**$Ar^{iPr4}$-4-Cl | 2.672(2) | 121.8(4) | 180 | 65 |
| 4-MeO-$Ar^{iPr4}$**SnSn**$Ar^{iPr4}$-4-OMe | 2.6480(12) | 124.2(2) | 180 | 65 |
| 4-$^tBu$-$Ar^{iPr4}$**SnSn**$Ar^{iPr4}$-4-$^tBu$ | 2.6461(3) | 123.98(5) | 180 | 65 |
| $Ar^{tBu6}$**SnSn**$Ar^{tBu6}$ | 2.8547(7) | 105.07(10), 117.25(11) | 160.0(2) | 73 |
| $Ar^{iPr8}$**SnSn**$Ar^{iPr8}$ | 2.7205(12)- 2.7360(14)[b] | 125.1(2)-127.6(2)[b] | 152.1(3)-166.3(4)[b] | 65 |
| $[K(THF)_6][Ar^{iPr4}$**SnSn**$Ar^{iPr4}]$ | 2.8081(9) | 97.91(16) | 180 | 66 |
| $[K(THF)_6][Ar^{iPr6}$**SnSn**$Ar^{iPr6}]$ | 2.8123(9) | 95.20(13) | 180 | 78 |
| $[K(18\text{-crown-}6)(THF)_2][Ar^{iPr6}$**SnSn**$Ar^{iPr6}]$ | 2.782(1) | 95.0(4), 93.6(4) | 180 | 66 |
| $[(THF)_3Na\{Ar^{iPr6}$**SnSn**$Ar^{iPr6}\}]$ | 2.8107(13) | 97.9(3), 98.0(4) | -179.9(5) | 66 |
| $Na_2[Ar^{iPr6}$**SnSn**$Ar^{iPr6}]$ | 2.789(1) | 104.8(2) | -179.3(4) | 66 |
| $K_2[Ar^{iPr4}$**SnSn**$Ar^{iPr4}]$ | 2.7754(3) | 106.02(5) | 180 | 66 |
| $K_2[Ar^{iPr6}$**SnSn**$Ar^{iPr6}]$ | 2.7763(9) | 107.5(1) | 178.8(3) | 71 |
| $[$**Sn**$N(Si^iPr_3)\{C_6H_2$-2,6-$(CHPh_2)_2$-4-$^iPr\}]_2$ | 3.1434(5) | 104.53(10), 103.48(11) | 148.5(2) | 75 |
| $[$**Ge**$N(SiPh_3)\{B(NC_6H_3$-2,6-$^iPr_2)_2(CH)_2\}]_2$ | 3.0638(7) | 103.01(6), 97.83(6) | -177.73(9) | 70 |
| | | | | |
| | **Pb—Pb (Å)** | **R–Pb–Pb (°)** | **R–Pb–Pb–R (°)** | *Ref* |
| $Ar^{iPr6}$**PbPb**$Ar^{iPr6}$ | 3.1881(1) | 94.26(4) | 180 | 79 |

[a]**Si′** = $Si\{CH(SiMe_3)_2\}_2{}^iPr$. [b]A ranges of values given for disordered Sn atoms sites in the crystal structure.

## Terphenyl ligands as dispersion energy donors

London dispersion (LD) interactions arise from attraction between instantaneous dipoles in the electron clouds of molecules.[82] They are generally weak and their intensity rapidly decreases with a distance (r) dependence of $r^{-6}$. When many of these interactions are present, they can sum to significant amounts in or between molecules (10s of kcal·mol$^{-1}$).[83] The role of LD interactions in stabilizing molecular structures has come to the attention of chemists in recent years and they have been manifested in several ways. For example, the fact that $Ph_3C\cdot$ (Gomberg's radical) does not dimerize to hexaphenylethane, $Ph_3C\text{-}CPh_3$ but instead forms a quinoid structure (Figure 1.5) was puzzling.[84] Curiously, the substituted derivative $(3,5\text{-}^tBu_2C_6H_3)_3C\text{-}C(C_6H_3\text{-}3,5\text{-}^tBu_2)_3$ was isolable and had a long C-C bond length of 1.67(3) Å.[85] Calculations revealed that the attractive dispersion interactions between $^t$Bu groups (up to 40 kcal mol$^{-1}$) across the molecule are responsible for its stability.[86] Other hexaphenylethane derivatives have been examined by using substituents such as cyclohexyl and 1- adamantyl[87,88] and the dispersion attraction energy is found to increase with the size of the substituent.

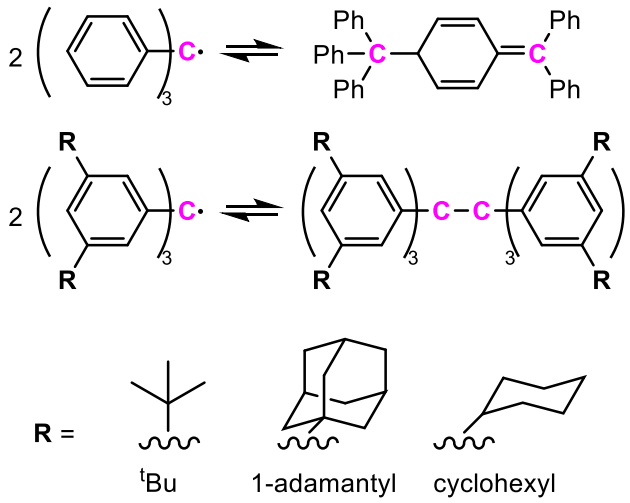


**Figure 1.5.** Dimerization of Gomberg's radical does not form hexaphenylethane. The radicals with all *meta* substitution with $^t$Bu, 1-adamantyl, or cyclohexyl groups do dimerize to ethane derivatives.[85,88]

Ligands that confer these stabilizing effects have been termed dispersion energy donors (DEDs).[86,89] Recently, Dr. C. R. Stennett applied DED ligands to the synthesis of the second reported example of a solution stable distannene[90] and the first time the stabilizing role of LD interactions in these compounds was recognized. Using a cyclohexyl substituted aryl ring, the

compound $\{2,4,6\text{-}(C_6H_{11})_3C_6H_2\}_2Sn{=}Sn\{C_6H_2\text{-}2,4,6\text{-}(C_6H_{11})_3\}_2$ was isolated with a dispersion contribution of -38 kcal mol$^{-1}$. Solution $^{119}Sn\{^1H\}$ NMR spectroscopy indicated that the Sn-Sn double bond remains intact up to at least 100°C. In contrast, the less sterically hindered species $:Sn(C_6H_2\text{-}2,4,6\text{-}Ph_3)_2$ remains a monomer in the solid state and rapidly decomposes in solution at ambient temperature.

Another unusual case involved the stability of high oxidation state transition metal alkyls $M(1\text{-norbornyl})_4$ (M = Ti–Co)[91] and $FeR_4$ (R = cyclohexyl, 2-adamantyl).[92] Attractive dispersion interactions between C-H moieties were found to play an important role in their stability[93,94] with dispersion contributions of ca. -40 kcal mol$^{-1}$. These alkyls of the later compounds were formed from the metal(II) or metal(III) halide starting materials. Disproportionation, apparently driven partly by dispersive attractions, gives the $MR_4$ species. Similarly, Dr. C. L. Wagner found that addition of $LiN(SiMe_3)(2,6\text{-}^iPr_2C_6H_3)$ to CuI in hexanes afforded the first two-coordinate $Cu^{II}$ amide $Cu\{N(SiMe_3)(2,6\text{-}^iPr_2C_6H_3)\}_2$ with concomitant precipitation of Cu metal.[95] Again the disproportionation appears to be driven by attractive dispersion interactions (-20.8 kcal mol$^{-1}$) between the ligands. These were previously quantified in the compounds $M\{N(SiMe_3)(2,6\text{-}^iPr_2C_6H_3)\}_2$ (M = Fe, Co, Ni), prepared by Dr. C.-Y. Lin, to be worth ca. -20 to -30 kcal mol$^{-1}$.[96]

The potential for *m*-terphenyl ligands to act as DED ligands was first noticed by our group during the structural characterization of group 14 dithiolates $:E(SAr)_2$ (E = Si–Pb; Ar = $Ar^{Me6}$, $Ar^{iPr4}$, $Ar^{iPr6}$, $Ar^{iPr8}$) by Dr. B. D. Rekken (Figure 1.6, a).[97] As the bulk of the terphenyl substituent was increased, the S-E-S bending angle was found to narrow, counter to what is expected from steric repulsion. A similar pattern was subsequently noted in the C-E-C (E = Ge, Sn, Pb) angle of the group 14 diaryls $:EAr_2$ (Ar = $Ar^{Me6}$, $Ar^{iPr4}$, $Ar^{iPr6}$).[98] Ziegler computed the dispersion energies arising from attraction between isopropyl groups across the molecules in the series $Ar^{iPr4}EEAr^{iPr4}$

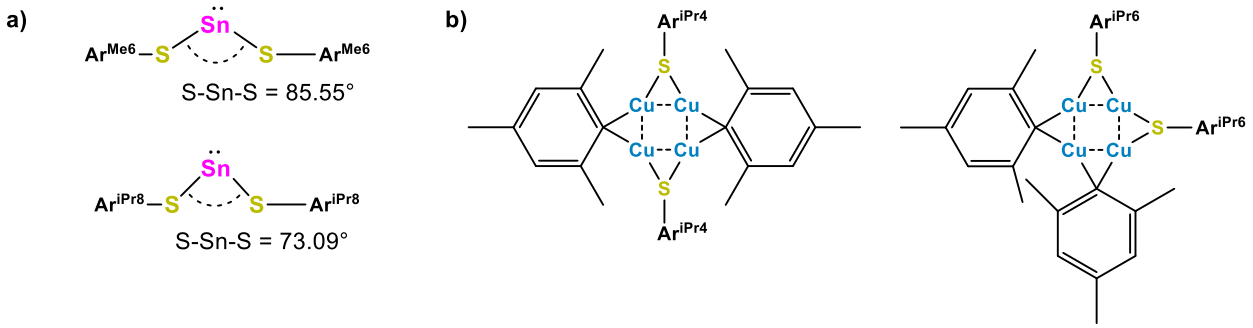


**Figure 1.6** Examples of *m*-terphenyl substituted sterically counterintuitive structures that have been attributed to LDF effects. a) The S-Sn-S angle of a stannylene decreases when the size of the terphenyl groups increases.[97] b) Increasing the size of the terphenyl ligand in mixed terphenylthiol/aryl Cu(I) tetramers causes the structure to adopt a *cis* rather than *trans* arrangement of ligands.[100]

(E = Si–Sn) and $Ar^{iPr6}PbPbAr^{iPr6}$. Stabilizations of -27.5 kcal/mol (Si), -29.1 kcal/mol (Ge), and -26.2 kcal/mol (Sn) were found while in the case of the Pb compound, which had four additional $^{i}$Pr groups, it was -44.0 kcal mol$^{-1}$.[99] W. Zou of our group prepared a series of mixed aryl/thiol copper tetramers.[100] While $\{(CuMes)_2(CuSAr^{Me6})_2\}$ and $\{(CuMes)_2(CuSAr^{iPr4})_2\}$ feature alternating ligands as expected due to steric repulsion, in $\{(CuMes)_2(CuSAr^{iPr6})_2\}$ the terphenyl thiol ligands are on adjacent Cu atoms (Figure 1.6, b). Comparing the calculated and experimental "*cis*-" and "*trans*-" isomers showed that with the larger $SAr^{iPr6}$ ligand the *cis*-structure is favored by ca. 15.8 kJ mol$^{-1}$ (ca. 3.8 kcal mol$^{-1}$) whereas the *cis*-structure $SAr^{iPr4}$ is only favored by 0.2 kJ mol$^{-1}$ (ca. 0.05 kcal mol$^{-1}$). Eventually the $SAr^{iPr8}$ ligand is too large and $\{(CuMes)_3CuSAr^{iPr8}\}$ is obtained with only one thiol group incorporated.

## Discussion

From the survey of multiply bonded REER compounds of group 13 and 14, it can be seen that those of Al and Pb remain exceedingly rare. In order to expand the library of these compounds, we exploited the repulsive effects of sterically encumbering terphenyl ligands while trying to incorporate groups prone to dispersion force attractions to hold together the weak or reactive E-E cores. In Chapter 2, a series of diplumbynes was synthesized and examined computationally using

the ligands $Ar^{iPr4}$, $Ar^{iPr4}$-4-$SiMe_3$, $Ar^{iPr6}$, $Ar^{tBu6}$, and $Ar^{iPr8}$. The largest terphenyl ligands $Ar^{tBu6}$ and $Ar^{iPr8}$ result in a widening of the C-Pb-Pb angles with a simultaneous shortening of the Pb-Pb bond in the solid state. This change in geometry gives the Pb-Pb bond multiple bonding character. Dispersion energy stabilization in these compounds was found to account for a significant portion of the interaction energy. En route to the diplumbynes, some of the intermediate lead(II) hydrides were found to be insoluble in the diethyl ether solvent in which they were prepared. These compounds precipitated as solids that could be isolated in good yield and handled near ambient temperature as described in Chapter 3.

The heavier *m*-terphenyl substituted group 13 and group 14 REER compounds are known to be in equilibrium with monomeric EAr (Ar = *m*-terphenyl ligand) fragments in solution. In Chapter 4 this is exploited to form new E–Mo and E≡Mo (E = Ge, Sn, Pb) bonds by direct reaction of the dimetallynes (as their monomer fragments) with $(CO)_3CpMo–MoCp(CO)_3$ or $(CO)_2CpMo≡MoCp(CO)_2$. The decreasing strength of the E-E bond down the group can be seen by the facile reaction of the MoMo bonded species with the diplumbyne, while the distannyne reaction proceeds slowly at room temperature and is accelerated with heat. The reaction with the digermyne requires high temperature to proceed and no reaction is observed at ambient temperature.

In Chapter 5, a monomeric alanediyl (i.e. alumylene, :Al-R) is prepared using the extremely encumbering ligand $Ar^{iPr8}$ to enforce one-coordination at the Al atom. Calculations suggested a weak association energy (ca. 5 kcal $mol^{-1}$) in solution to the dimer $Ar^{iPr8}AlAlAr^{iPr8}$, which was further evidenced by the rapid reaction of $:AlAr^{iPr8}$ with $H_2$ (cf. the monomer $:GaAr^{iPr8}$ is unreactive towards $H_2$, while the dimer $Ar^{iPr4}GaGaAr^{iPr4}$ is highly reactive). Chapter 6 describes the reaction of $:AlAr^{iPr8}$ with some organic azides $RN_3$ (R = $SiMe_3$, 1-adamantyl, $Ar^{Me6}$). The

monomeric aluminum imide $Ar^{iPr8}AlNAr^{Me6}$ was isolated and structural characterization revealed an Al-N triple bond. The dispersion energy contribution between the two terphenyl ligands on the Al and N atoms was found to be on the same magnitude as the Al-N π-bonds (ca. -21 kcal $mol^{-1}$).

Further attempts to isolate a dialuminene RAl=AlR are described in Chapter 7. The comproportionation reactions between a dialuminyne salt and aluminum iodides are reported. The resulting dialuminene is unstable when prepared in hexane or diethyl ether solvents. However, when it is prepared in benzene, the dialuminene-benzene [2+4] cycloaddition product is obtained stoichiometrically and cleanly.

**References**


(1) Dasent, W. E. *Nonexistent Compounds: Comounds of Low Stability*; Marcel Dekker, 1965.

(2) Taylor, M. J. *Metal-to-Metal Bonded States of the Main Group Elements*; Academic Press, 1975.

(3) Cowley, A. H. Stable Compounds with Double Bonding between the Heavier Main-Group Elements. *Acc. Chem. Res.* **1984**, *17*, 386–392.

(4) West, R. Multiple Bonds to Silicon: 20 Years Later. *Polyhedron* **2002**, *21*, 467–472.

(5) Pitzer, K. S. Repulsive Forces in Relation to Bond Energies, Distances and Other Properties. *J. Am. Chem. Soc.* **1948**, *70*, 2140–2145.

(6) Several main group compounds containing multiple bonds with elements beyond the second period were already known prior to this time, for example S=C=S and the oxyacids. The existence of some of the latter, such as $HClO_4$ was rationalized on the basis π-backbonding from the O 2p orbital into the empty n+1 d orbitals on the main group element: see Cruickshank, D. W. J. *J. Chem. Soc.* **1961**, 5486–5504. The participation of d orbitals in main group element bonding is now widely disregarded: see Reed, A. E.; Schleyer, P. v. R. *J. Am. Chem. Soc.* **1990**, *112*, 1434–1445.

(7) Jutzi, P. New Element-Carbon (p-p)π Bonds. *Angew. Chem. Int. Ed.* **1975**, *14*, 232–245.

(8) Goldberg, D. E.; Harris, D. H.; Lappert, M. F.; Thomas, K. M. A New Synthesis of Divalent Group 4B Alkyls $M[CH(SiMe_3)_2]_2$ (M = Ge or Sn), and the Crystal and Molecular and Molecular Strcuture of the Tin Compound. *J. Chem. Soc., Chem. Commun.* **1976**, No. 7, 261–262.

(9) West, R.; Fink, M. J.; Michl, J. Tetramesityldisilene, a Stable Compound Containing a Silicon-Silicon Double Bond. *Science* **1981**, *214*, 1343–1344.

(10) Yoshifuji, M.; Shima, I.; Inamoto, N.; Hirotsu, K.; Higuchi, T. Synthesis and Structure of Bis(2,4,6-Tri-Tert-Butylphenyl)Diphosphene: Isolation of a True Phosphobenzene. *J. Am. Chem. Soc.* **1981**, *103*, 4587–4589.

(11) Power, P. P. π-Bonding and the Lone Pair Effect in Multiple Bonds between Heavier Main Group Elements. *Chem. Rev.* **1999**, *99*, 3463–3504.

(12) Fischer, R. C.; Power, P. P. π-Bonding and the Lone Pair Effect in Multiple Bonds Involving Heavier Main Group Elements: Developments in the New Millennium. *Chem. Rev.* **2010**, *110*, 3877–3923..

(13) Su, J.; Li, X.-W.; Crittendon, R. C.; Robinson, G. H. How Short Is a -Ga⁝Ga- Triple Bond? Synthesis and Molecular Structure of $Na_2[Mes^*_2C_6H_3\text{-}Ga⁝Ga\text{-}C_6H_3Mes^*_2]$ (Mes* = 2,4,6-i-$Pr_3C_6H_2$): The First Gallyne. *J. Am. Chem. Soc.* **1997**, *119*, 5471–5472.

(14) GALLIUM "TRIPLE BONDS" UNDER FIRE. *Chem. Eng. News Arch.* **1998**, *76*, 31–35.

(15) Carter, E. A.; Goddard, W. A. III. Relation between Singlet-Triplet Gaps and Bond Energies. *J. Phys. Chem.* **1986**, *90*, 998–1001.

(16) Trinquier, G.; Malrieu, J. P. Nonclassical Distortions at Multiple Bonds. *J. Am. Chem. Soc.* **1987**, *109*, 5303–5315.

(17) Wedler, H. B.; Wendelboe, P.; Power, P. P. Second-Order Jahn–Teller (SOJT) Structural Distortions in Multiply Bonded Higher Main Group Compounds. *Organometallics* **2018**, *37*, 2929–2936.

(18) Kutzelnigg, W. Chemical Bonding in Higher Main Group Elements. *Angew. Chem., Int. Ed.* **1984**, *23*, 272–295.

(19) Lein, M.; Krapp, A.; Frenking, G. Why Do the Heavy-Atom Analogues of Acetylene $E_2H_2$ (E = Si−Pb) Exhibit Unusual Structures? *J. Am. Chem. Soc.* **2005**, *127*, 6290–6299.

(20) Power, P. P. Reactions of Heavier Main-Group Compounds with Hydrogen, Ammonia, Ethylene and Related Small Molecules. *Chem. Rec.* **2012**, *12*, 238–255.

(21) Spikes, G. H.; Fettinger, J. C.; Power, P. P. Facile Activation of Dihydrogen by an Unsaturated Heavier Main Group Compound. *J. Am. Chem. Soc.* **2005**, *127*, 12232–12233.

(22) Peng, Y.; Ellis, B. D.; Wang, X.; Fettinger, J. C.; Power, P. P. Reversible Reactions of Ethylene with Distannynes Under Ambient Conditions. *Science* **2009**, *325*, 1668–1670.

(23) Power, P. P. Main-Group Elements as Transition Metals. *Nature* **2010**, *463*, 171–177.

(24) Weetman, C.; Inoue, S. The Road Travelled: After Main-Group Elements as Transition Metals. *Chem.Cat. Chem.* **2018**, *10*, 4213–4228.

(25) Hanusch, F.; Groll, L.; Inoue, S. Recent Advances of Group 14 Dimetallenes and Dimetallynes in Bond Activation and Catalysis. *Chem. Sci.* **2021**, *12*, 2001–2015.

(26) Du, C. J. F.; Hart, H.; Ng, K. K. D. A One-Pot Synthesis of m-Terphenyls, via a Two-Aryne Sequence. *J. Org. Chem.* **1986**, *51*, 3162–3165.

(27) Terphenyl Ligands and Complexes in Inorganic Syntheses, vol 37. Ed. Power, P. P. Wiley, 2018.

(28) Stanciu, C.; Richards, A. F.; Fettinger, J. C.; Brynda, M.; Power, P. P. Synthesis and Characterization of New, Modified Terphenyl Ligands: Increasing the Rotational Barrier for Flanking Rings. *J. Organomet. Chem.* **2006**, *691*, 2540–2545.

(29) Liptrot, D. J.; Power, P. P. London Dispersion Forces in Sterically Crowded Inorganic and Organometallic Molecules. *Nat. Rev. Chem.* **2017**, *1*, 1–12.

(30) Mears, K. L.; Power, P. P. Beyond Steric Crowding: Dispersion Energy Donor Effects in Large Hydrocarbon Ligands. *Acc. Chem. Res.* **2022**, *55*, 1337–1348.

(31) Grigsby, W. J.; Power, P. P. Isolation and Reduction of Sterically Encumbered Arylboron Dihalides: Novel Boranediyl Insertion into C−C σ-Bonds. *J. Am. Chem. Soc.* **1996**, *118*, 7981–7988.

(32) Braunschweig, H.; Dewhurst, R. D.; Hörl, C.; Radacki, K.; Tate, C. W.; Vargas, A.; Ye, Q. Reductive Borylene–CO Coupling with a Bulky Arylborylene Complex. *Angew. Chem. Int. Ed.* **2013**, *52*, 10120–10123.

(33) Nutz, M.; Borthakur, B.; Dewhurst, R. D.; Deißenberger, A.; Dellermann, T.; Schäfer, M.; Krummenacher, I.; Phukan, A. K.; Braunschweig, H. Synthesis and Trapping of Iminoboranes by M=B/C=N Bond Metathesis. *Angew. Chem., Int. Ed.* **2017**, *56*, 7975–7979.

(34) Nutz, M.; Borthakur, B.; Pranckevicius, C.; Dewhurst, R. D.; Schäfer, M.; Dellermann, T.; Glaab, F.; Thaler, M.; Phukan, A. K.; Braunschweig, H. Release of Isonitrile- and NHC-Stabilized Borylenes from Group VI Terminal Borylene Complexes. *Chem. Eur. J.* **2018**, *24*, 6843–6847.

(35) Braunschweig, H.; Dewhurst, R. D.; Hupp, F.; Nutz, M.; Radacki, K.; Tate, C. W.; Vargas, A.; Ye, Q. Multiple Complexation of CO and Related Ligands to a Main-Group Element. *Nature* **2015**, *522*, 327–330.

(36) Wang, Y.; Quillian, B.; Wei, P.; Wannere, C. S.; Xie, Y.; King, R. B.; Schaefer, H. F.; Schleyer, P. v. R.; Robinson, G. H. A Stable Neutral Diborene Containing a BB Double Bond. *J. Am. Chem. Soc.* **2007**, *129*, 12412–12413.

(37) Bissinger, P.; Braunschweig, H.; Damme, A.; Hörl, C.; Krummenacher, I.; Kupfer, T. Boron as a Powerful Reductant: Synthesis of a Stable Boron-Centered Radical-Anion Radical-Cation Pair. *Angew. Chem., Int. Ed.* **2015**, *54*, 359–362.

(38) Wright, R. J.; Phillips, A. D.; Power, P. P. The [2 + 4] Diels−Alder Cycloadditon Product of a Probable Dialuminene, Ar‘AlAlAr‘ (Ar‘ = $C_6H_3$- 2,6-$Dipp_2$; Dipp = $C_6H_3$-2,6-$Pr^i_2$), with Toluene. *J. Am. Chem. Soc.* **2003**, *125*, 10784–10785.

(39) Cui, C.; Li, X.; Wang, C.; Zhang, J.; Cheng, J.; Zhu, X. Isolation of a 1,2-Dialuminacyclobutene. *Angew. Chem. Int. Ed.* **2006**, *45*, 2245–2247.

(40) Agou, T.; Nagata, K.; Tokitoh, N. Synthesis of a Dialumene-Benzene Adduct and Its Reactivity as a Synthetic Equivalent of a Dialumene. *Angew. Chem. Int. Ed.* **2013**, *52*, 10818–10821.

(41) Agou, T.; Nagata, K.; Sasamori, T.; Tokitoh, N. Reaction of a Dialumene-Benzene Adduct with Diphenylacetylene: Formation of 3,4-Dialuminacyclobutene and 5,6-Dialuminabicyclo[2.1.1]Hex-2-Ene Derivatives. *Chem. Asian J.* **2014**, *9*, 3099–3101.

(42) Nagata, K.; Murosaki, T.; Agou, T.; Sasamori, T.; Matsuo, T.; Tokitoh, N. Activation of Dihydrogen by Masked Doubly Bonded Aluminum Species. *Angew. Chem. Int. Ed.* **2016**, *55*, 12877–12880.

(43) Bag, P.; Porzelt, A.; Altmann, P. J.; Inoue, S. A Stable Neutral Compound with an Aluminum–Aluminum Double Bond. *J. Am. Chem. Soc.* **2017**, *139*, 14384–14387.

(44) Weetman, C.; Porzelt, A.; Bag, P.; Hanusch, F.; Inoue, S. Dialumenes – Aryl vs. Silyl Stabilization for Small Molecule Activation and Catalysis. *Chem. Sci.* **2020**, *11*, 4817–4827.

(45) Falconer, R. L.; Byrne, K. M.; Nichol, G. S.; Krämer, T.; Cowley, M. J. Reversible Dissociation of a Dialumene. *Angew. Chem. Int. Ed.* **2021**, *60*, 24702–24708.

(46) Wright, R. J.; Brynda, M.; Power, P. P. Synthesis and Structure of the "Dialuminyne" $Na_2[Ar'AlAlAr']$ and $Na_2[(Ar''Al)_3]$: Al—Al Bonding in $Al_2Na_2$ and $Al_3Na_2$ Clusters. *Angew. Chem. Int. Ed.* **2006**, *45*, 5953–5956.

(47) Li, X.-W.; Pennington, W. T.; Robinson, G. H. Metallic System with Aromatic Character. Synthesis and Molecular Structure of $Na_2[[(2,4,6\text{-}Me_3C_6H_2)_2C_6H_3]Ga]_3$ The First Cyclogallane. *J. Am. Chem. Soc.* **1995**, *117*, 7578–7579.

(48) Li, X.-W.; Xie, Y.; Schreiner, P. R.; Gripper, K. D.; Crittendon, R. C.; Campana, C. F.; Schaefer, H. F.; Robinson, G. H. Cyclogallanes and Metalloaromaticity. Synthesis and Molecular Structure of Dipotassium Tris((2,6-Dimesitylphenyl)Cyclogallene), $K_2[(Mes_2C_6H_3)Ga]_3$ (Mes = 2,4,6-$Me_3C_6H_2$): A Structural and Theoretical Examination. *Organometallics* **1996**, *15*, 3798–3803.

(49) Twamley, B.; Power, P. P. Synthesis of the Square-Planar Gallium Species $K_2[Ga_4(C_6H_3\text{-}2,6\text{-}Trip_2)_2]$ (Trip=$C_6H_2$-2,4,6-$^iPr_3$): The Role of Aryl–Alkali Metal Ion Interactions in the Structure of Gallium Clusters. *Angew. Chem. Int. Ed.* **2000**, *39*, 3500–3503.

(50) Hardman, N. J.; Wright, R. J.; Phillips, A. D.; Power, P. P. Synthesis and Characterization of the Neutral "Digallene" Ar′GaGaAr′ and Its Reduction to $Na_2$Ar′GaGaAr′ (Ar′=2,6-$Dipp_2C_6H_3$, Dipp=2,6-$^iPr_2C_6H_3$). *Angew. Chem. Int. Ed.* **2002**, *41*, 2842–2844.

(51) Hardman, N. J.; Wright, R. J.; Phillips, A. D.; Power, P. P. Structures, Bonding, and Reaction Chemistry of the Neutral Organogallium(I) Compounds $(GaAr)_n$ (n = 1 or 2) (Ar = Terphenyl or Related Ligand): An Experimental Investigation of Ga−Ga Multiple Bonding. *J. Am. Chem. Soc.* **2003**, *125*, 2667–2679.

(52) Zhu, Z.; Fischer, R. C.; Ellis, B. D.; Rivard, E.; Merrill, W. A.; Olmstead, M. M.; Power, P. P.; Guo, J. D.; Nagase, S.; Pu, L. Synthesis, Characterization and Real Molecule DFT

Calculations for Neutral Organogallium(I) Aryl Dimers and Monomers: Weakness of Gallium—Gallium Bonds in Digallenes and Digallynes. *Chem. Eur. J.* **2009**, *15*, 5263–5272.

(53) Caputo, C. A.; Koivistoinen, J.; Moilanen, J.; Boynton, J. N.; Tuononen, H. M.; Power, P. P. Counterintuitive Mechanisms of the Addition of Hydrogen and Simple Olefins to Heavy Group 13 Alkene Analogues. *J. Am. Chem. Soc.* **2013**, *135*, 1952–1960.

(54) Haubrich, S. T.; Power, P. P. Monomeric $InC_6H_3$-2,6-$Trip_2$ (Trip = -$C_6H_2$-2,4,6-i-$Pr_3$) and Its Manganese Complex ($\eta^5$-$C_5H_5$)$(CO)_2MnInC_6H_3$-2,6-$Trip_2$: One-Coordinate Indium in the Solid State. *J. Am. Chem. Soc.* **1998**, *120*, 2202–2203.

(55) Wright, R. J.; Phillips, A. D.; Hardman, N. J.; Power, P. P. The "Diindene" ArInInAr (Ar = $C_6H_3$-2,6-$Dipp_2$, Dipp = $C_6H_3$-2,6-$Pr^i_2$). Dimeric versus Monomeric In(I) Aryls: Para-Substituent Effects in Terphenyl Ligands. *J. Am. Chem. Soc.* **2002**, *124*, 8538–8539.

(56) Eichler, B. E.; Hardman, N. J.; Power, P. P. $In_8(C_6H_3$-2,6-$Mes_2)_4$ (Mes = $C_6H_2$-2,4,6-$Me_3$): A Metal-Rich Main-Group Cluster with a Distorted Cubane Structure. *Angew. Chem. Int. Ed.* **2000**, *39*, 383–385.

(57) Niemeyer, M.; Power, P. P. Synthesis and Solid-State Structure of 2,6-$Trip_2C_6H_3Tl$ (Trip=2,4,6-$^iPr_3C_6H_2$): A Monomeric Arylthallium(I) Compound with a Singly Coordinated Thallium Atom. *Angew. Chem., Int. Ed.* **1998**, *37*, 1277–1279.

(58) Wright, R. J.; Phillips, A. D.; Hino, S.; Power, P. P. Synthesis and Reactivity of Dimeric Ar'TlTlAr' and Trimeric $(Ar''Tl)_3$ (Ar', Ar'' = Bulky Terphenyl Group) Thallium(I) Derivatives: Tl(I)−Tl(I) Bonding in Species Ligated by Monodentate Ligands. *J. Am. Chem. Soc.* **2005**, *127*, 4794–4799.

(59) Sekiguchi, A.; Kinjo, R.; Ichinohe, M. A Stable Compound Containing a Silicon-Silicon Triple Bond. *Science* **2004**, *305*, 1755–1757.

(60) Kinjo, R.; Ichinohe, M.; Sekiguchi, A. An Isolable Disilyne Anion Radical and a New Route to the Disilenide Ion upon Reduction of a Disilyne. *J. Am. Chem. Soc.* **2007**, *129*, 26–27.

(61) Murata, Y.; Ichinohe, M.; Sekiguchi, A. Unsymmetrically Substituted Disilyne $Dsi_2{}^iPrSi$—Si≡Si—$SiNpDsi_2$ (Np = $CH_2{}^tBu$): Synthesis and Characterization. *J. Am. Chem. Soc.* **2010**, *132*, 16768–16770.

(62) Sasamori, T.; Hironaka, K.; Sugiyama, Y.; Takagi, N.; Nagase, S.; Hosoi, Y.; Furukawa, Y.; Tokitoh, N. Synthesis and Reactions of a Stable 1,2-Diaryl-1,2-Dibromodisilene: A Precursor for Substituted Disilenes and a 1,2-Diaryldisilyne. *J. Am. Chem. Soc.* **2008**, *130*, 13856–13857.

(63) Ishida, S.; Sugawara, R.; Misawa, Y.; Iwamoto, T. Palladium and Platinum $\eta^2$-Disilyne Complexes Bearing an Isolable Dialkyldisilyne as a Ligand. *Angew. Chem., Int. Ed.* **2013**, *52*, 12869–12873.

(64) Stender, M.; Phillips, A. D.; Wright, R. J.; Power, P. P. Synthesis and Characterization of a Digermanium Analogue of an Alkyne. *Angew. Chem. Int. Ed.* **2002**, *41*, 1785–1787.

(65) Peng, Y.; Fischer, R. C.; Merrill, W. A.; Fischer, J.; Pu, L.; Ellis, B. D.; Fettinger, J. C.; Herber, R. H.; Power, P. P. Substituent Effects in Ditetrel Alkyne Analogues: Multiple vs. Single Bonded Isomers. *Chem. Sci.* **2010**, *1*, 461–468.

(66) Pu, L.; Phillips, A. D.; Richards, A. F.; Stender, M.; Simons, R. S.; Olmstead, M. M.; Power, P. P. Germanium and Tin Analogues of Alkynes and Their Reduction Products. *J. Am. Chem. Soc.* **2003**, *125*, 11626–11636.

(67) Sugiyama, Y.; Sasamori, T.; Hosoi, Y.; Furukawa, Y.; Takagi, N.; Nagase, S.; Tokitoh, N. Synthesis and Properties of a New Kinetically Stabilized Digermyne: New Insights for a Germanium Analogue of an Alkyne. *J. Am. Chem. Soc.* **2006**, *128*, 1023–1031.

(68) Li, J.; Schenk, C.; Goedecke, C.; Frenking, G.; Jones, C. A Digermyne with a Ge–Ge Single Bond That Activates Dihydrogen in the Solid State. *J. Am. Chem. Soc.* **2011**, *133*, 18622–18625.

(69) Hadlington, T. J.; Hermann, M.; Li, J.; Frenking, G.; Jones, C. Activation of $H_2$ by a Multiply Bonded Amido-Digermyne: Evidence for the Formation of a Hydrido-Germylene. *Angew. Chem., Int. Ed.* **2013**, *52*, 10199–10203.

(70) Kelly, J. A.; Juckel, M.; Hadlington, T. J.; Fernández, I.; Frenking, G.; Jones, C. Synthesis and Reactivity Studies of Amido-Substituted Germanium(I)/Tin(I) Dimers and Clusters. *Chem. Eur. J.* **2019**, *25*, 2773–2785.

(71) Pu, L.; Senge, M. O.; Olmstead, M. M.; Power, P. P. Synthesis and Characterization of $Na_2\{Ge(C_6H_3\text{-}2,6\text{-}Trip_2)\}_2$ and $K_2\{Sn(C_6H_3\text{-}2,6\text{-}Trip_2)\}_2$ (Trip = $-C_6H_2$-2,4,6-i-$Pr_3$): A New Class of Multiply Bonded Main Group Compounds. *J. Am. Chem. Soc.* **1998**, *120*, 12682–12683.

(72) Phillips, A. D.; Wright, R. J.; Olmstead, M. M.; Power, P. P. Synthesis and Characterization of 2,6-$Dipp_2$-$H_3C_6SnSnC_6H_3$-2,6-$Dipp_2$ (Dipp = $C_6H_3$-2,6-$Pr^i_2$): A Tin Analogue of an Alkyne. *J. Am. Chem. Soc.* **2002**, *124*, 5930–5931.

(73) Perla, L. G.; Kulenkampff, J. M.; Fettinger, J. C.; Power, P. P. Steric and Electronic Properties of the Bulky Terphenyl Ligand ArtBu6 ($Ar^{tBu6}$ = $C_6H_3$-2,6-($C_6H_2$-2,4,6-$^tBu_3)_2$) and Synthesis of Its Tin Derivatives $Ar^{tBu6}SnCl$, $Ar^{tBu6}SnSn(H)_2ArtBu_6$, and $Ar^{tBu6}SnSnAr^{tBu6}$: A New Route to a Distannyne via Thermolysis of the As. *Organometallics* **2018**, *37*, 4048–4054.

(74) Takagi, N.; Nagase, S. Tin Analogues of Alkynes. Multiply Bonded Structures vs Singly Bonded Structures. *Organometallics* **2007**, *26*, 469–471.

(75) Hadlington, T. J.; Jones, C. A Singly Bonded Amido-Distannyne: $H_2$ Activation and Isocyanide Coordination. *Chem. Commun.* **2014**, *50*, 2321–2323.

(76) Lai, T. Y.; Tao, L.; Britt, R. D.; Power, P. P. Reversible Sn–Sn Triple Bond Dissociation in a Distannyne: Support for Charge-Shift Bonding Character. *J. Am. Chem. Soc.* **2019**, *141*, 12527–12530.

(77) Lai, T. Y.; Fettinger, J. C.; Power, P. P. Facile C–H Bond Metathesis Mediated by a

Stannylene. *J. Am. Chem. Soc.* **2018**, *140*, 5674–5677.

(78) Olmstead, M. M.; Simons, R. S.; Power, P. P. Synthesis and Characterization of $[Sn_2\{C_6H_3\text{-}2,6(2,4,6\text{-i-}Pr_3C_6H_2)_2\}_2]\text{-}\bullet$: A Singly Reduced Valence Isomer of a "Distannyne." *J. Am. Chem. Soc.* **1997**, *119*, 11705–11706.

(79) Pu, L.; Twamley, B.; Power, P. P. Synthesis and Characterization of 2,6-$Trip_2H_3C_6PbPbC_6H_3$-2,6-$Trip_2$ (Trip = $C_6H_2$-2,4,6-i-$Pr_3$): A Stable Heavier Group 14 Element Analogue of an Alkyne. *J. Am. Chem. Soc.* **2000**, *122*, 3524–3525.

(80) Preut, H.; Huber, F. Die Kristall- Und Molekülstruktur Des Hexaphenyldiplumbans. *Z. Anorg. Allg. Chem.* **1976**, *419*, 92–96.

(81) Schneider, J.; Sindlinger, C. P.; Eichele, K.; Schubert, H.; Wesemann, L. Low-Valent Lead Hydride and Its Extreme Low-Field 1H NMR Chemical Shift. *J. Am. Chem. Soc.* **2017**, *139*, 6542–6545.

(82) London, F. The General Theory of Molecular Forces. *Trans. Faraday Soc.* **1937**, *33*, 8b–26.

(83) Wagner, J. P.; Schreiner, P. R. London Dispersion in Molecular Chemistry—Reconsidering Steric Effects. *Angew. Chem., Int. Ed.* **2015**, *54*, 12274–12296.

(84) McBride, J. M. The Hexaphenylethane Riddle. *Tetrahedron* **1974**, *30*, 2009–2022.

(85) Stein, M.; Winter, W.; Rieker, A. Hexakis(2,6-Di-Tert-Butyl-4-Biphenylyl)Ethane—The First Unbridged Hexaarylethane. *Angew. Chem., Int. Ed. English* **1978**, *17*, 692–694.

(86) Grimme, S.; Schreiner, P. R. Steric Crowding Can Stabilize a Labile Molecule: Solving the Hexaphenylethane Riddle. *Angew. Chem., Int. Ed.* **2011**, *50*, 12639–12642.

(87) Rösel, S.; Balestrieri, C.; Schreiner, P. R. Sizing the Role of London Dispersion in the Dissociation of All-Meta Tert-Butyl Hexaphenylethane. *Chem. Sci.* **2017**, *8*, 405–410.

(88) Rösel, S.; Becker, J.; Allen, W. D.; Schreiner, P. R. Probing the Delicate Balance between Pauli Repulsion and London Dispersion with Triphenylmethyl Derivatives. *J. Am. Chem. Soc.* **2018**, *140*, 14421–14432.

(89) Solel, E.; Ruth, M.; Schreiner, P. R. London Dispersion Helps Refine Steric A-Values: Dispersion Energy Donor Scales. *J. Am. Chem. Soc.* **2021**, *143*, 20837–20848.

(90) Stennett, C. R.; Bursch, M.; Fettinger, J. C.; Grimme, S.; Power, P. P. Designing a Solution-Stable Distannene: The Decisive Role of London Dispersion Effects in the Structure and Properties of $\{Sn(C_6H_2\text{-}2,4,6\text{-}Cy_3)_2\}_2$ (Cy = Cyclohexyl). *J. Am. Chem. Soc.* **2021**, *143*, 21478–21483.

(91) Bower, B. K.; Tennent, H. G. Transition Metal Bicyclo[2.2.1]Hept-1-Yls. *J. Am. Chem. Soc.* **1972**, *94*, 2512–2514.

(92) Casitas, A.; Rees, J. A.; Goddard, R.; Bill, E.; DeBeer, S.; Fürstner, A. Two Exceptional Homoleptic Iron(IV) Tetraalkyl Complexes. *Angew. Chem. Int. Ed.* **2017**, *56*, 10108–10113.

(93) Li, H.; Hu, Y.; Wan, D.; Zhang, Z.; Fan, Q.; King, R. B.; Schaefer, H. F. Dispersion Effects in Stabilizing Organometallic Compounds: Tetra-1-Norbornyl Derivatives of the First-Row Transition Metals as Exceptional Examples. *J. Phys. Chem. A* **2019**, *123*, 9514–9519.

(94) Liptrot, D. J.; Guo, J.-D.; Nagase, S.; Power, P. P. Dispersion Forces, Disproportionation, and Stable High-Valent Late Transition Metal Alkyls. *Angew. Chem. Int. Ed.* **2016**, *55*, 14766–14769.

(95) Wagner, C. L.; Tao, L.; Thompson, E. J.; Stich, T. A.; Guo, J.; Fettinger, J. C.; Berben, L. A.; Britt, R. D.; Nagase, S.; Power, P. P. Dispersion-Force-Assisted Disproportionation: A Stable Two-Coordinate Copper(II) Complex. *Angew. Chem. Int. Ed.* **2016**, *55*, 10444–10447.

(96) Lin, C.-Y.; Guo, J.-D.; Fettinger, J. C.; Nagase, S.; Grandjean, F.; Long, G. J.; Chilton, N. F.; Power, P. P. Dispersion Force Stabilized Two-Coordinate Transition Metal–Amido Complexes of the −N($SiMe_3$)Dipp (Dipp = $C_6H_3$-2,6-$Pr^i_2$) Ligand: Structural, Spectroscopic, Magnetic, and Computational Studies. *Inorg. Chem.* **2013**, *52*, 13584–13593.

(97) Rekken, B. D.; Brown, T. M.; Fettinger, J. C.; Lips, F.; Tuononen, H. M.; Herber, R. H.; Power, P. P. Dispersion Forces and Counterintuitive Steric Effects in Main Group Molecules: Heavier Group 14 (Si–Pb) Dichalcogenolate Carbene Analogues with Sub-90° Interligand Bond Angles. *J. Am. Chem. Soc.* **2013**, *135*, 10134–10148.

(98) McCrea-Hendrick, M. L.; Bursch, M.; Gullett, K. L.; Maurer, L. R.; Fettinger, J. C.; Grimme, S.; Power, P. P. Counterintuitive Interligand Angles in the Diaryls E{$C_6H_3$-2,6-($C_6H_2$-2,4,6-$^iPr_3$)$_2$}$_2$ (E = Ge, Sn, or Pb) and Related Species: The Role of London Dispersion Forces. *Organometallics* **2018**, *37*, 2075–2085.

(99) Seidu, I.; Seth, M.; Ziegler, T. Role Played by Isopropyl Substituents in Stabilizing the Putative Triple Bond in Ar′EEAr′ [E = Si, Ge, Sn; Ar′ = $C_6H_3$-2,6-($C_6H_3$-2,6-$Pr^i_2$)$_2$] and Ar*PbPbAr* [Ar* = $C_6H_3$-2,6-($C_6H_2$-2,4,6-$Pr^i_3$)$_2$]. *Inorg. Chem.* **2013**, *52*, 8378–8388.

(100) Zou, W.; Fettinger, J. C.; Vasko, P.; Power, P. P. The Unusual Structural Behavior of Heteroleptic Aryl Copper(I) Thiolato Molecules: Cis vs Trans Structures and London Dispersion Effects. *Organometallics* **2022**, *41*, 794–801.

## Chapter 2. Isolation and Computational Studies of a Series of Terphenyl Substituted Diplumbynes with Ligand Dependent Lead−Lead Multiple-Bonding Character

Joshua D. Queen,[†] Markus Bursch,[‡] Jakob Seibert,[‡] Leonard R. Maurer,[‡] Bobby D. Ellis,[†,§] James C. Fettinger,[†] Stefan Grimme,*[,‡] and Philip P. Power*[,†]

†Department of Chemistry, University of California, Davis, One Shields Avenue, Davis, California 95616, United States

‡ Mulliken Center for Theoretical Chemistry, Institut für Physikalische und Theoretische Chemie, Rheinische Friedrich-Wilhelms-Universitat Bonn, Beringstr. 4, 53115 Bonn, Germany



**Abstract:** A series of four formally triply bonded diplumbyne analogues of alkynes of the general formula ArPbPbAr (Ar = terphenyl ligand with different steric properties) were synthesized by two routes. All diplumbyne products were synthesized by a simple reduction of the corresponding Pb(II) halide precursor ArPb(Br) by DIBAL-H with yields in the range 8-48%. For one of the diplumbynes $Ar^{iPr4}PbPbAr^{iPr4}$ ($Ar^{iPr4}$ = $C_6H_3$-2,6-($C_6H_3$-2,6-$^iPr_2)_2$) it was shown that reduction of $Ar^{iPr4}Pb(Br)$ using a magnesium(I) beta-diketiminate afforded a much improved yield in comparison (29 vs. 8%) to that obtained by reduction with DIBAL-H. The most sterically crowded diplumbyne $Ar^{iPr8}PbPbAr^{iPr8}$ ($Ar^{iPr8}$ = $C_6H$-3,5-$^iPr_2$-2,6-($C_6H_2$-2,4,6-$^iPr_3)_2$) displayed a shortened Pb–Pb bond with a length of 3.0382(5) Å and wide Pb–Pb–C angles of 114.73(7) and 116.02(6)° consistent with multiple-bond character with a bond order of up to 1.5. The others displayed longer metal-metal distances and narrower Pb–Pb–C angles that were consistent with a lower bond order that approached one. Computational studies of all diplumbynes yielded detailed insight of the

unusual bonding and explained the similar electronic spectra for all diplumbynes arising from the flexibility of the C–Pb–Pb–C core in solution. Further, the importance of London dispersion interactions for the stabilization of the diplumbynes was demonstrated.

## Introduction

The first stable, heavier group 14 analogue of an alkyne was the diplumbyne $Ar^{iPr6}PbPbAr^{iPr6}$ ($Ar^{iPr6}$ = $C_6H_3$-2,6-($C_6H_2$-2,4,6-$^iPr_3$)$_2$) (**1**), the syntheses and characterization of which was reported in 2000.[1] The following four years saw the synthesis of the remaining heavy element compounds of the series REER (E = Si, Ge, Sn; R = aryl, silyl)[2–6] and a growing number of group 14 dimetallynes of the elements Si-Sn continue to appear in the literature.[7–15] No further examples of diplumbynes have been characterized, however.

As a class the heavier group 14 element analogues have garnered interest because of their peculiar structures and bonding that differ markedly from their carbon congeners. Unlike the carbon-based alkynes, they all possess trans-bent REER cores (**B**, Figure 2.1). whose bending increases as the group is descended, until it reaches nearly 90° in the case of lead (**C**, Figure 2.1) (cf. 94.26(4)°, experimental value for the diplumbyne **1** below).[1]

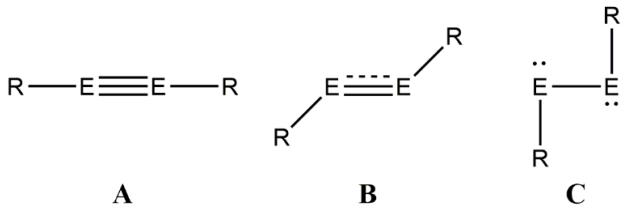


**Figure 2.1.** Bonding motifs of REER (E = C-Pb, R = alkyl, aryl, amide, silyl).

In effect, the increasing atomic number upon descending the group results in increasing non-bonding, lone pair character at the group 14 element. The original triple bond in the carbon-based alkynes is transformed into a single bond and two non-bonded pairs in the case of lead. These pairs are now mostly 6s in character and the remaining single bond is a result of head-to-head overlap

of a 6p orbital from each lead atom which affords an unusually long Pb–Pb bond (3.1881(1) Å in **1**), (cf. 2.9 Å expected from the sum of the single bond radii).[16] This result is consistent with decreasing hybridization of the elements that occurs upon descending the group.[17]

Early calculations by Frenking and coworkers suggested that the single bonded structure of the diplumbyne $Ar^{iPr6}PbPbAr^{iPr6}$ in the crystalline phase is partially stabilized by packing forces and indicated via calculations on less crowded model terphenyl ligands that structures having wider bending angles and some multiple Pb–Pb bond character were more stable.[18] Later calculations by Takagi and Nagase proposed that the diplumbyne assumes a less trans-bent multiple bonded isomeric form in solution and that the multiple and single bonded forms might be distinguishable by UV-visible spectroscopy.[19]

Previous work by our group on terphenyl substituted distannynes, which generally take multiply bonded trans-bent structures in the crystalline phase, showed that use of a para-substituent on the central ring of the terphenyl ligand can afford a single bonded distannyne in the crystalline form.[7] Presumably, this occurs as a result of changed packing forces, but this possibility has not been examined in detail, however. Nonetheless, UV-visible spectroscopy has shown that the spectra of all distannynes are similar in solution and consistent with a multiple bonded structure.[20] Furthermore, calculations have shown that the energy difference between the single and multiple bonded structures is relatively small—only ca. 5 kcal $mol^{-1}$ for 4-$Me_3Si$-$Ar^{iPr4}SnSnAr^{iPr4}$-4-$SiMe_3$—an amount that is similar in energy to packing force (i.e. intermolecular London dispersion force) effects.[20–23] Ziegler and co-workers showed that isopropyl groups on the terphenyl substituents play an important role in stabilizing the group 14 alkyne analogue structures via intramolecular dispersion force interactions (cf. -44.0 kcal·$mol^{-1}$ stabilization energy in the case of $Ar^{iPr6}PbPbAr^{iPr6}$).[24]

Given these observations, and the calculations of Takagi and Nagase which assume that in a gas phase structure without packing forces the multiple bonded structure is preferred, we sought to isolate an array of the multiple bonded diplumbyne isomers by altering the substituents on the terphenyl ligand. These investigations have afforded a series of new diaryl-diplumbynes, ArPbPbAr, (Ar = terphenyl) (Scheme 2.1) that show a considerable variation of the trans-bending and torsion angles as well as the lead-lead distance in the $C_{ipso}PbPbC_{ispo}$ core, including the highly substituted $Ar^{iPr8}PbPbAr^{iPr8}$ ($Ar^{iPr8}$ = $C_6H$-2,6-($C_6H_2$-2,4,6-$^iPr_3$)$_2$-3,5-$^iPr_2$) which contains a shortened Pb–Pb bond with a calculated bond order between 1.2 and 1.5.

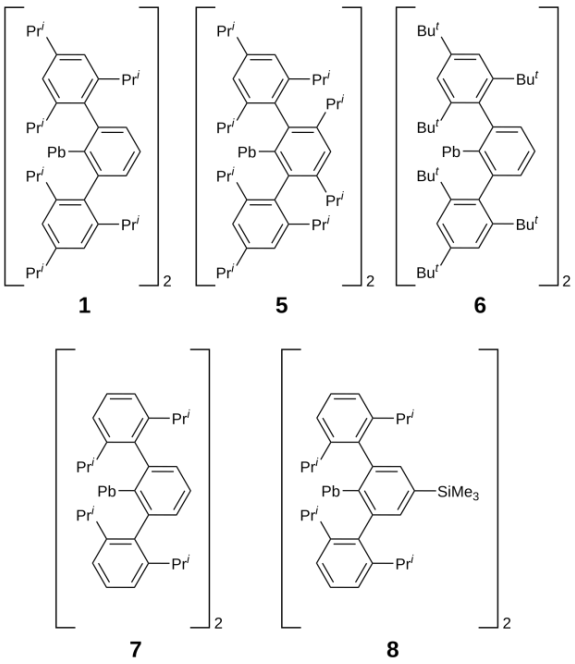


**Scheme 2.1.** Lewis representations of compounds **1**, **5-8**.

## Experimental

**General Procedures.** All manipulations were carried out using modified Schlenk techniques or in a Vacuum Atmospheres OMNI-Lab drybox under a $N_2$ or argon atmosphere. Manipulations of the lead compounds were carried out with careful exclusion of light when possible due to the tendency of low-valent lead compounds to decompose or disproportionate. Solvents were dried over columns of activated alumina using a Grubbs type purification system[25] (Glass Contour), stored over Na ($Et_2O$) or K (hexanes, pentane, toluene) mirrors, and degassed via three freeze-pump-thaw cycles prior to use. $^1H$ and $^{13}C\{^1H\}$ spectra were recorded on a Varian Inova 600 MHz spectrometer and were referenced to the residual solvent signals in $C_6D_6$.[26] UV-Visible spectra

were recorded in dilute hexane solutions in 3.5 mL quartz cuvettes using an Olis 17 Modernized Cary 14 UV-Vis/NIR spectrophotometer. Melting points were measured in glass capillary tubes sealed under argon using a Mel-Temp II apparatus and are uncorrected.

[Li($Et_2O$)$Ar^{iPr8}$] was synthesized from $Ar^{iPr8}I$[27] (see Supporting Information). [Li($Et_2O$)$_2Ar^{tBu6}$][28] ($Ar^{tBu6}$ = $C_6H_3$-2,6-($C_6H_2$-2,4,6-$^tBu_3$)$_2$), Li$Ar^{iPr4}$-4-$SiMe_3$[29] ($Ar^{iPr4}$-4-$SiMe_3$ = $C_6H_2$-4-$SiMe_3$-2,6-($C_6H_3$-2,6-$^iPr_2$)$_2$), {Pb(μ-Br)$Ar^{iPr4}$}$_2$[30] ($Ar^{iPr4}$ = $C_6H_3$-2,6-($C_6H_3$-2,6-$^iPr_2$)$_2$), and [$Mg^{Mes}$Nacnac]$_2$ ($^{Mes}$Nacnac = [HC{MeCN($C_6H_2$-2,4,6-$Me_3$)}$_2$])[31] were synthesized according to literature methods. $PbBr_2$ and DIBAL-H (neat or 1.0 M in hexanes) were purchased commercially and used without further purification.

**{Pb(μ-Br)$Ar^{iPr8}$}$_2$ (2).** A solution of [Li($Et_2O$)$Ar^{iPr8}$] (3.12 g, 4.82 mmol) in $Et_2O$ (ca. 40 mL) was added dropwise over ca. 30 min to a stirred suspension of $PbBr_2$ (1.77 g, 4.82 mmol) in $Et_2O$ (ca. 10 mL) cooled to ca. 0°C in an ice bath. The mixture was allowed to warm to ambient temperature and stirred for a further 16 h. The ether solvent was removed under reduced pressure and the orange residue was extracted with ca. 60 mL hexanes. The filtrate was concentrated to ca. 15 mL under reduced pressure and allowed to stand at ambient temperature overnight to give orange crystals of **2**. Yield: 2.15 g (52%). mp 159-162 °C (dec). $^1$H NMR (600 MHz, $C_6D_6$, 298 K): δ 7.59 (s, 2H, Ar*H*), 7.24 (s, 8H, Ar*H*), 3.01 (sept, $^3J$ = 6.9 Hz, 8H, -C*H*($CH_3$)$_2$), 2.80 (sept, $^3J$ = 6.9 Hz, 4H, - C*H*($CH_3$)$_2$), 2.71 (sept, $^3J$ = 6.8 Hz, 4H, - C*H*($CH_3$)$_2$), 1.44 (d, $^3J$ = 6.8 Hz, 24H, -CH(C*H*$_3$)$_2$), 1.27 (d, $^3J$ = 6.7 Hz, 24H, -CH(C*H*$_3$)$_2$), 1.24 (d, $^3J$ = 6.9 Hz, 24H, -CH(C*H*$_3$)$_2$), 1.15 (d, $^3J$ = 6.8 Hz, 24H, -CH(C*H*$_3$)$_2$). $^{13}$C{$^1$H} NMR (151 MHz, $C_6D_6$, 298 K): δ 156.0, 149.3, 147.6, 141.8, 134.2, 122.7, 121.4, 34.8, 30.7, 30.6, 26.1, 25.5, 25.4, 24.3. UV-Vis (hexanes): $\lambda_{max}$ 456 nm ($\varepsilon$ = 750 L mol$^{-1}$ cm$^{-1}$).

**{Pb(μ-Br)Ar$^{tBu6}$}$_2$ (3).** A solution of [Li(Et$_2$O)$_2$Ar$^{tBu6}$][28] (1.19 g, 1.65 mmol) in Et$_2$O (ca. 30 mL) was added dropwise over ca. 5 min to a stirred suspension of PbBr$_2$ (0.606 g, 1.65 mmol) in Et$_2$O (ca. 10 mL) cooled to ca. 0°C in an ice bath. The mixture was warmed to ambient temperature after ca. 30 min and stirred for 18h. The ether solvent was removed under reduced pressure and the yellow-orange solid was extracted twice with ca. 60 mL hexanes. The combined filtrates were concentrated to ca. 20 mL under reduced pressure and stored at ca. 8 °C overnight to give yellow crystals of **3**. Yield: 0.625 g (44%). mp 215-220 °C (dec). $^1$H NMR (600 MHz, C$_6$D$_6$, 298 K): δ 8.41 (d, $^3J$ = 7.6 Hz, 4H, Ar*H*), 7.61 (s, 8H, Ar*H*), 7.11 (t, $^3J$ = 7.6 Hz, 2H, Ar*H*), 1.35 (s, 72H, -C(C*H*$_3$)$_3$), 1.34 (s, 36H, -C(C*H*$_3$)$_3$). $^{13}$C{$^1$H} NMR (151 MHz, C$_6$D$_6$, 298 K): δ 149.8, 148.1, 141.6, 123.5, 39.1, 35.0, 31.5. UV-Vis (hexanes): $\lambda_{max}$ 415 nm ($\varepsilon$ = 960 L mol$^{-1}$ cm$^{-1}$).

**{Pb(μ-Br)Ar$^{iPr4}$-4-SiMe$_3$}$_2$ (4).** A solution of LiAr$^{iPr4}$-4-SiMe$_3$[29] (1.73 g, 3.36 mmol) in Et$_2$O (ca. 20 mL) was added dropwise over ca. 10 min to an Et$_2$O (ca. 10 mL) suspension of PbBr$_2$ (1.33 g, 3.62 mmol) cooled to ca. 0°C in an ice bath. The green mixture was warmed to room temperature and stirred for three days to afford an orange solution. The ether solvent was removed under reduced pressure and the orange residue was extracted twice with hexanes (ca. 80 mL). The combined extracts were concentrated to ca. 15 mL under reduced pressure and stored at ca. -18 °C to give yellow crystals of **4**. Yield: 1.35 g (51%). mp 206-210 °C (dec). $^1$H NMR (600 MHz, C$_6$D$_6$, 298K) δ 8.25 (s, 4H, Ar*H*), 7.23 (t, $^3J$ = 7.4 Hz, 4H, Ar*H*) 7.16 (d, $^3J$ = 7.4 Hz, 8H, Ar*H*), 3.13 (sept, $^3J$ = 6.8 Hz, 8H, -C*H*(CH$_3$)$_2$), 1.34 (d, $^3J$ = 6.8 Hz, 24H, -CH(C*H*$_3$)$_2$) 1.03 (d, $^3J$ = 6.8 Hz 24 H, -CH(C*H*$_3$)$_2$), 0.25 (s, 18H, -Si(C*H*$_3$)$_3$). $^{13}$C{$^1$H} NMR (151 MHz, C$_6$D$_6$ 298K) δ 147.9, 146.8, 142.6, 138.9, 137.4, 129.3, 123.7, 30.8, 26.2, 23.7, -1.3. UV-Vis (hexanes): $\lambda_{max}$ 423 nm ($\varepsilon$ = 840 L mol$^{-1}$ cm$^{-1}$).

**$Ar^{iPr8}PbPbAr^{iPr8}$·1.5 $C_7H_8$ (5·1.5 $C_7H_8$).** A solution of **2** (0.429 g, 0.250 mmol) in $Et_2O$ (ca. 30 mL) was cooled to ca. -78°C with an ethanol/dry ice bath. A freshly prepared solution of DIBAL-H (0.10 mL, 0.56 mmol) in $Et_2O$ (ca. 15 mL) was added dropwise over ca. 10 min. The mixture was slowly warmed over 2h to ambient temperature then stirred for an additional ca. 30 min. The volatile components were removed under reduced pressure and the dark red residue was extracted with hexanes (ca. 40 mL). The solvent was removed under reduced pressure and the residue was dissolved in ca. 3 mL of toluene. Storage at ca. -30 °C overnight gave **5** as red crystals. Yield: 0.196 g (48%). mp 141-146 °C (dec). $^1$H NMR (600 MHz, $C_6D_6$, 298 K): δ 6.96 (s, 8H, Ar*H*), 5.77 (s, br, 2H, Ar*H*), 3.10 (sept, br, $^3J$ = 8H), 3.01 (sept, $^3J$ = 7.0Hz, 4H), 2.37 (sept, $^3J$ = 6.7 Hz, 4H), 1.43 (d, $^3J$ = 6.9 Hz, 24H), 1.36 (d, $^3J$ = 6.6 Hz, 24 H), 1.30 (d, $^3J$ = 6.5 Hz, 24H), 1.16 (d, $^3J$ = 6.7 Hz, 24H). $^{13}$C{$^1$H} NMR (151 MHz, $C_6D_6$, 298 K): δ 149.7, 147.4, 137.9, 133.4 129.3, 128.6, 125.7, 125.1, 34.6, 31.9, 30.89, 26.4, 24.8, 24.2, 21.5. UV-Vis (hexanes): $\lambda_{max}$ 429 nm ($\varepsilon$ = 9300 L mol$^{-1}$ cm$^{-1}$), 757 ($\varepsilon$ = 2700 L mol$^{-1}$ cm$^{-1}$).

**$Ar^{tBu6}PbPbAr^{tBu6}$ (6).** A solution of **3** (0.200 g, 0.117 mmol) in $Et_2O$ (ca. 15 mL) was cooled to ca. -78 °C with an ethanol/dry ice bath. A freshly prepared solution of DIBAL-H (0.45 mL, 0.25 mmol) in $Et_2O$ (ca. 5 mL) was added dropwise over ca. 2 min. The mixture was warmed to ambient temperature over 1 h and stirred for an additional ca. 30 min. The solvent was removed under reduced pressure and the dark green residue was extracted with pentane (ca. 30 mL). The solution was concentrated to ca. 10 mL and stored at ca. -30 °C overnight to give **6** as green blocks. Yield: 0.045 g (23%). mp 132-140 °C (dec). $^1$H NMR (600 MHz, $C_6D_6$, 298 K): δ 7.91 (d, $^3J$ = 7.5 Hz, 2H, Ar*H*), 7.62 (s, 4H, Ar*H*), 6.63 (t, $^3J$ = 7.6 Hz, 1H, Ar*H*), 1.43 (s, 18 H, p-C(C*H*)$_3$), 1.26 (s, 36H, o-C(C*H*)$_3$). $^{13}$C{$^1$H} NMR (151 MHz, $C_6D_6$, 298 K): δ 157.2, 150.6, 148.3, 143.1, 136.4,

123.6, 39.3, 37.5, 34.9, 34.3, 32.5, 31.6, 31.5. UV-Vis (hexanes): $\lambda_{max}$ 388 ($\varepsilon$ = 7000 L mol$^{-1}$ cm$^{-1}$), 668 ($\varepsilon$ = 900 L mol$^{-1}$ cm$^{-1}$).

**Ar$^{iPr4}$PbPbAr$^{iPr4}$ (7).** Method A: A solution of {Pb(μ-Br)Ar$^{iPr4}$}$_2$[30] (0.525 g, 0.383 mmol) in $Et_2O$ (50 mL) was cooled to ca. -78 °C with an ethanol/dry-ice bath and 1.0 DIBAL-H in hexanes (0.78 mL, 0.78 mmol) was added via syringe. The mixture was warmed to room temperature over 30 min and stirred an additional 2 h. The reaction mixture was filtered and the solution was stored at ca. -18°C for 2 weeks to give amber blocks of **7**. Yield: 0.035 g (8%).

Method B: A solution of {Pb(μ-Br)Ar$^{iPr4}$}$_2$ (0.400 g, 0.292 mmol) in ether (ca.15 mL) was cooled to ca. 0°C in an ice/water bath. A solution of [Mg$^{Mes}$Nacnac]$_2$[29] (0.210 g, 0.292 mmol) in ether (ca. 10 mL) was added dropwise over ca. 3 min, resulting in an immediate darkening of the solution. The reaction mixture was removed from the cooling bath and stirred a further 15 min. The ether was decanted and the dark powder washed with hexanes (ca. 15 mL). The olive-green powder was identified as **7** by its $^1$H NMR spectrum and sharp melting point (dec). Yield: 0.104 g (29%). mp = 168-171°C (dec). $^1$H NMR (600 MHz, $C_6D_6$, 298 K): δ 7.66 (d, $^3J$ = 7.5 Hz, 4H, Ar*H*) 7.24 (t, $^3J$ = 7.7 Hz, 4H, Ar*H*) , 6.99 (d $^3J$ = 7.8 Hz, 8H, Ar*H*) 6.69 (t, $^3J$ = 7.5 Hz, 2H, Ar*H*) 3.29 (sept, $^3J$ = 6.9 Hz, 8H, -C*H*(CH$_3$)$_2$), 1.09 (d, $^3J$ = 6.8 Hz, 24H, -CH(C*H*$_3$)$_2$), 0.93(d, $^3J$ = 7.0 Hz, 24H, -CH(C*H*$_3$)$_2$). $^{13}$C{$^1$H} NMR (151 MHz, $C_6D_6$, 298 K): δ 148.2, 136.5, 133.0, 128.7, 128.4, 124.7, 31.7, 28.8, 26.7. UV-Vis (hexanes): $\lambda_{max}$ 682 ($\varepsilon$ = 1200 L mol$^{-1}$ cm$^{-1}$), 400 ($\varepsilon$ = 11000 L mol$^{-1}$ cm$^{-1}$).

**4-Me$_3$Si-Ar$^{iPr4}$PbPbAr$^{iPr4}$-4-SiMe$_3$·Et$_2$O (8·Et$_2$O).** A solution of **4** (0.600 g, 0.396 mmol) in diethyl ether (ca. 30 mL) was cooled to ca. -78 °C in an ethanol/dry ice bath and 1.0 M DIBAL-H in hexanes (0.79 mL, 0.79 mmol) was added via syringe. The mixture was warmed to ambient temperature over ca. 30 min and stirred an additional 2 h. The solvent was removed under reduced

pressure and the residue extracted with pentane (ca. 20 mL). The filtrate was concentrated to ca. 10 mL and stored at ca. -30°C overnight to give amber-green dichroic blocks of **8**·$Et_2O$. Yield: 0.173 g (32%). mp = 151-156 °C (dec). $^1$H NMR (600 MHz, $C_6D_6$, 298 K): δ 7.49(s, 4H, Ar*H*), 7.34 (t, $^3J$ = 7.7 Hz, 4H, Ar*H*), 7.22 (d, $^3J$ = 7.7 Hz, 8H, Ar*H*), 2.95 (sept, $^3J$ = 6.8 Hz, 8H, -C*H*$(CH_3)_2$), 1.16 (mult, $^3J$ = 6.9 Hz, 48H, -CH(C*H*$_3)_2$), 0.21 (s, 18H, -Si(C*H*$_3)_3$). $^{13}$C{$^1$H} NMR (151 MHz, $C_6D_6$, 298 K): δ 147.0, 140.4, 140.2, 140.1, 133.1, 133.0, 128.5, 31.0, 30.8, 24.50, 24.46, 24.39, 24.35, -1.2. UV-Vis (hexanes): $\lambda_{max}$ 410 ($\varepsilon$ = 18000 L mol$^{-1}$ cm$^{-1}$), 655 ($\varepsilon$ = 860 L mol$^{-1}$ cm$^{-1}$).

**X-ray Crystallography.** Crystals of **2-8** were removed from a Schlenk flask under a stream of nitrogen and immediately covered with hydrocarbon oil. A suitable crystal was selected, attached to a glass fiber on a copper pin and placed in the cold $N_2$ stream on the diffractometer. Data were collected at 90 K on a Bruker APEX II diffractometer with Mo Kα radiation (λ = 0.71073 Å). Absorption corrections were applied using SADABS[32] (**2**,**3**,**5**,**6**,**8**) or TWINABS[33] (**4**, **7**) The crystal structures were solved by intrinsic phasing methods using SHELXT[34] and refined by full matrix least-squares procedures using SHELXL.[35] All non-H atoms were refined anisotropically. Disordered solvent in **3** was treated using the SQUEEZE algorithm.[36]

**Computational Methods.** Quantum mechanical calculations were performed with the TURBOMOLE 7.0.2[37,38], ORCA 4.1.0[39,40], xtb 6.1.0[41] and NBO6.0[42] program packages. Geometries were pre-optimized in the gas-phase from the experimental structures applying the GFN2-xTB[43] extended tight-binding method. All structures were further optimized at TPSS[44]-D3(BJ)[45,46]-ATM[47,48]/def2-TZVP[49] level of theory. Gibbs free energies were calculated at PBE0[50] and B3-LYP[51]+COSMO-RS[52,53](toluene)/def2-TZVPP level in combination with the D3 and D4[54,55] dispersion correction schemes. All bond order and orbital analyses were conducted at

TPSS-D3(BJ)-ATM/def2-TZVP level of theory. UV/Vis spectra were calculated at sTDA-xTB[56](GBSA(toluene))/TPSS-D3(BJ)-ATM/def2-TZVP and sTD[57]-BHLYP[58]/def2-TZVP level. Molecular dynamics simulations were performed at GFN2-xTB(GBSA(toluene)) level For further computational details see the Supporting Information.

## Results and Discussion

**Synthesis and spectroscopy.** The terphenyl lead(II) bromide precursors **2-4** were synthesized following established procedures[30,59,60] by addition of a diethyl ether solution of the terphenyl lithium salt to a diethyl ether suspension of $PbBr_2$. During the preparation of **4**, the reaction mixture assumed a dark green color, likely due to some formation of the diarylplumbylene $Pb(Ar^{iPr4}\text{-}4\text{-}SiMe_3)_2$. Continued stirring of the reaction mixture for an extended time (ca. 3 days) leads to redistribution with the remaining unreacted $PbBr_2$ to afford **4**. The aryl lead bromides form yellow to orange crystals which are thermally stable up to their melting points, but are prone to decomposition by light over extended periods of time, noted by a darkening of color or deposition of lead metal.

The diplumbyne **1** was originally synthesized in ca. 10% yield by addition of $LiAlH_4$ to $\{Pb(\mu\text{-}Br)Ar^{iPr6}\}_2$ in diethyl ether solution at ca. -78°C.[1] The diplumbynes **5-8** were synthesized by addition of a DIBAL-H solution in diethyl ether or hexanes to the respective aryl lead bromide cooled to ca. -78°C with an ethanol/dry ice bath as shown in Scheme 2. It was proposed originally[1] that an aryl lead hydride "Pb(H)Ar" is formed as an intermediate, which upon warming releases dihydrogen to form the diplumbyne. More recent work by

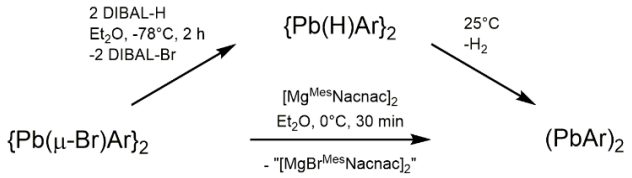


**Scheme 2.2** Synthetic routes for diplumbynes. Reduction of the aryl lead(II)bromides with DIBAL-H forms the lead(II) hydride *in situ*. Which releases $H_2$ upon warming to give compounds **1**, **5-8**. Alternatively, reduction with $[Mg^{Mes}Nacnac]_2$ was used to give **1** and **7**.

Wesemann and his group have shown that this hypothesis is essentially correct and the hydride can be isolated and structurally characterized as the hydrogen-bridged dimeric species {Pb(μ-H)$Ar^{iPr6}$}$_2$ which, however, decomposes to the diplumbyne and dihydrogen above ca. -40 °C.[61] The resulting diplumbyne **1** and compounds **5**-**8** also have limited thermal stability and are sensitive to light, which limits the yields of the reactions and necessitates quick workup and isolation of the products. They are stable for extended periods of time in the solid state but tend to decompose in solution at ambient temperature, resulting in a deposition of lead metal and protonated ligand, likely due to H atom abstraction from solvent molecules. The diplumbyne **5** is stable in solution for at least several weeks at ambient temperature in the absence of light, while **7** and **8** are stable in solution only at low temperature, ca. -20 °C, and slowly decompose at ambient temperature. Diplumbyne **6** decomposes in solution at temperatures as low as -30 °C and rapidly decomposes at ambient temperature.

Compound **7** exhibited poor solubility in common hydrocarbon and ethereal solvents, and as a result only low yields (< 10%) could be isolated from the treatment of {Pb(μ-Br)$Ar^{iPr4}$}$_2$ with DIBAL-H. Additionally, the low stability of **7** in solution and the comparatively high solubility of the protonated terphenyl ligand formed by decomposition prevented an accurate determination of the purity of **7** by $^1$H NMR spectroscopy (only ca. 1:1 ratios of **7** and $Ar^{iPr4}$H were observed in $C_6D_6$ at 298 K). However, the crystals of **7** showed a sharp melting/decomposition point in the range 168-171°C, during which the amber colored crystals turned black. We found that higher yields (ca. 30%) of **7** (as well as of **1**–see Supporting Information) could be isolated by reduction of {Pb(μ-Br)$Ar^{iPr4}$}$_2$ with the magnesium(I) reagent [$Mg^{Mes}$Nacnac]$_2$[31] reported by Jones and coworkers. Addition of one equivalent of [$Mg^{Mes}$Nacnac]$_2$ to {Pb(μ-Br)$Ar^{iPr4}$}$_2$ in diethyl ether at 0°C resulted in an immediate color change from yellow-orange to dark brown. After removing the

volatile components under reduced pressure and washing the solid with hexanes, **7** was obtained as an olive-green powder which had a decomposition point matching that of crystalline **7** and identical $^{1}H$ and $^{13}C\{^{1}H\}$ NMR spectra.

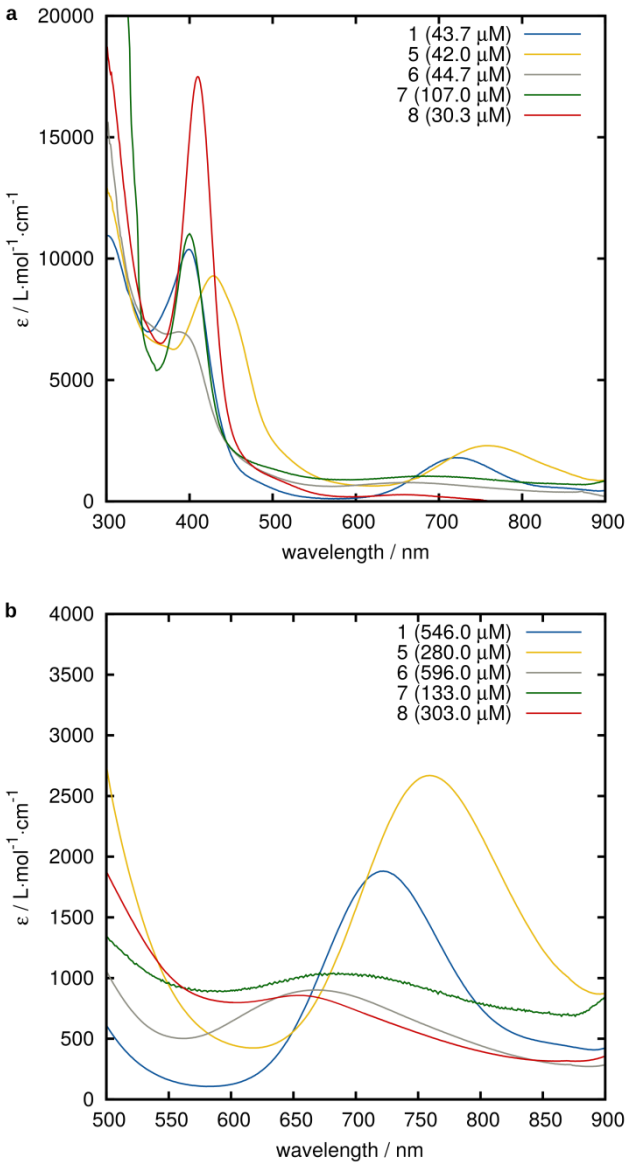


**Figure 2.2.** UV-Vis spectra **5-8** in the range 300-900 nm (a) and 500-900 nm (b).

The UV-visible spectra of **5-8** in hexanes show two absorptions: one between 388-429 nm and another in the range of 655-759 nm. (Figure 2.2 and Table 2.1) The observation of two absorptions in the solution spectra are consistent with predicted spectra for structures containing multiple bond character in solution (a single absorption, $n_{+} \rightarrow \pi$, would be expected for a single-bonded, strongly trans-bent structure), and have previously been calculated to belong to the $n_{-} \rightarrow n_{+}$ and $\pi \rightarrow \pi^{*}$ transitions.[19,20] The absorbances appear at lower energy in comparison to those of the analogous digermynes (320-380 nm, 430-510 nm) and distannynes (402-403 nm, 582-612 nm),[7] consistent with the decreasing strength of the E–E bond as the group is descended.

**Table 2.1.** Summary of key structural and spectroscopic data for **1**, **5-8.** [a]Ref 1, [b]This work.

| | $(PbAr^{iPr6})_2$[a] (**1**) | $(PbAr^{iPr8})_2$[b] (**5**) | $(PbAr^{tBu6})_2$[b] (**6**) | $(PbAr^{iPr4})_2$[b] (**7**) | $(PbAr^{iPr4}\text{-4-}SiMe_3)_2$[b] (**8**) |
|---|---|---|---|---|---|
| Pb–Pb / Å | 3.1881(1) | 3.0382(6) | 3.0394(9) | 3.1751(4) | 3.2439(9)<br>2.945(5) (6%) |
| C–Pb / Å | 2.303(2) | 2.311(3)-<br>2.314(2) | 3.357(6)-<br>3.366(6) | 2.301(2) | 2.3076(17)<br>2.282(3) |
| C–Pb–Pb / ° | 94.30(9) | 114.73(7)-<br>116.02(6) | 101.77(14)-<br>103.93(15) | 98.60(5) | 95.22(5)<br>100.82(15) |
| C–Pb–Pb–C / ° | 180 | -133.64(9) | 136.8(2) | 180 | 180 |
| $\lambda_{max}$ / nm ($\varepsilon$ / L mol$^{-1}$ cm$^{-1}$) n_ → n+ | 397 (10000)[b] | 429 (9300) | 388 (7000) | 400 (11000) | 410 (18000) |
| $\lambda_{max}$ / nm ($\varepsilon$ / L mol$^{-1}$ cm$^{-1}$) $\pi \rightarrow \pi^*$ | 719 (1800)[b] | 759 (2700) | 668(900) | 682 (1200) | 655 (860) |

**X-ray structures**. The structures of the diplumbynes are shown in Figure 2.3. The most important structural parameters of the diplumbynes **5-8** are the Pb–Pb bond lengths and the $C_{ipso}$–Pb–Pb bending and torsion angles. These and other selected structural data are summarized in Table 2.1. Diplumbynes **5** and **6** have the shortest aggregate Pb–Pb distances of 3.0382(6) Å and 3.0394(9) Å respectively. Both structures are non-centrosymmetric, the $C_{ispo}$–Pb–Pb angles in **5** being 114.73(7)° and 116.02(6)° (cf. 94.30(9)° in the original diplumbyne **1**) with a $C_{ipso}$–Pb–Pb–$C_{ipso}$ torsion angle of -133.64(9)°, while **6** has $C_{ipso}$–Pb–Pb angles of 101.77(17)° and 103.93(15)°, and a $C_{ipso}$–Pb–Pb–$C_{ipso}$ torsion angle of 136.8(2)°. In **7** the Pb–Pb distances is 3.1751(4) Å and the structure is centrosymmetric with $C_{ipso}$–Pb–Pb angles of 98.60(5)°. The two lead atoms in the core of **8** are disordered over two sites in 94% and 6% occupancies. Both components are centrosymmetric, with the major component having a Pb–Pb distance of 3.2439(9) Å and a $C_{ispo}$–Pb–Pb angle of 95.22(5)°, while the minor component has a Pb–Pb bond length of 2.945(5) Å and the $C_{ispo}$–Pb–Pb angle is 100.82(15)°. These parameters may be compared to the Pb–Pb distance (3.1881(1) Å), $C_{ipso}$–Pb–Pb angle (94.30(9)°) and 180° torsion angle in the original diplumbyne **1**.

Unlike in the structure of **6**, the $C_{ipso}$–Pb–Pb bond angles in **5** are substantially widened compared to that in the original **1**. This is likely due to the steric demand of the highly substituted $Ar^{Pri8}$ ligand and corresponds to a shortening of the Pb–Pb bond by about 0.15 Å in comparison to **1** (3.1881(1) Å). The wide angle, approaching 120°, suggests a multiple bonded isomer of the diplumbyne analogous to the structures seen for its Si, Ge, and Sn analogues. The bond parameters of **5** are very close to the Pb–Pb distance (3.071 Å), C–Pb–Pb trans-bending angle (117.7°), and

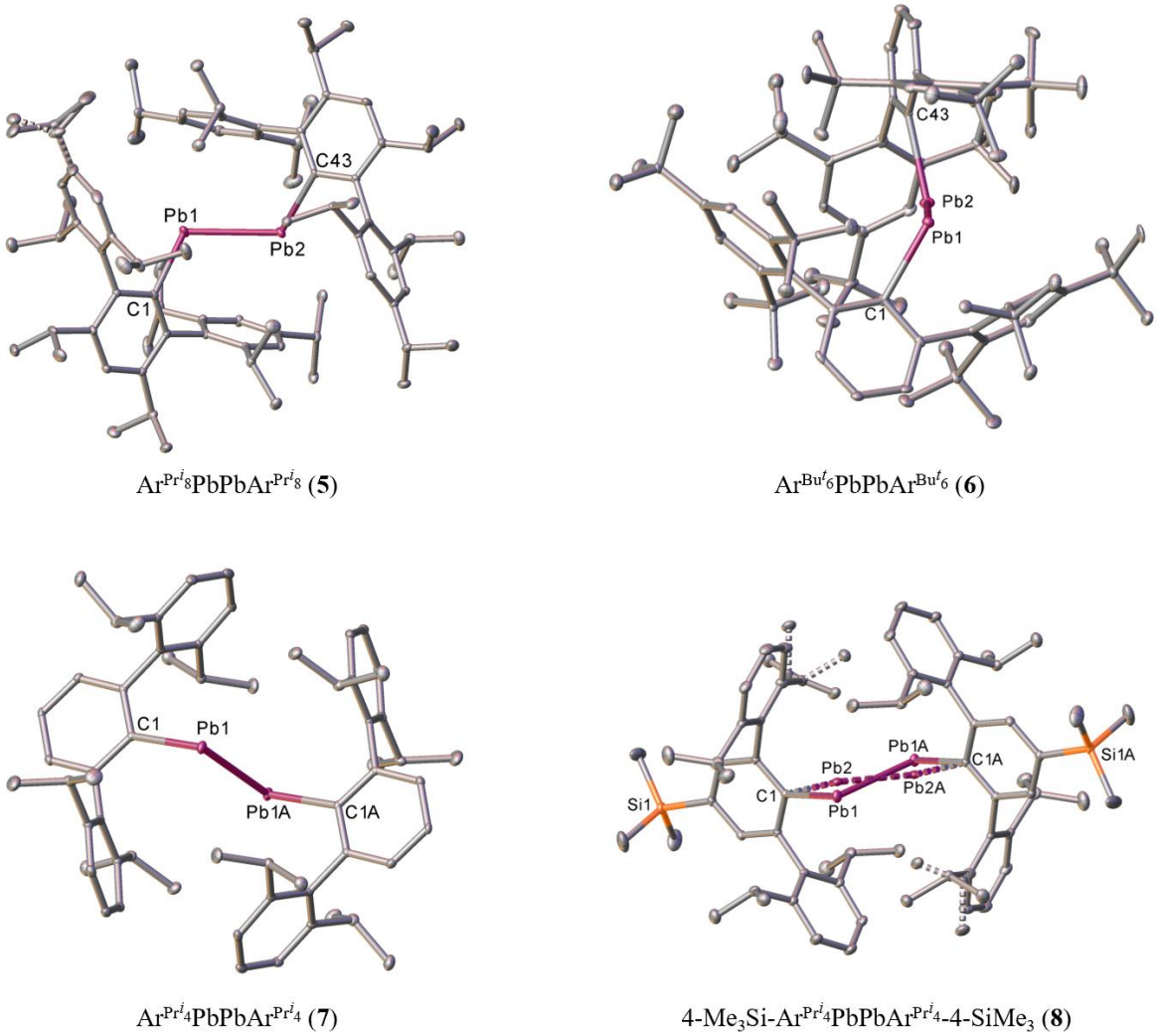


$Ar^{Pri8}PbPbAr^{Pri8}$ (**5**)

$Ar^{Bu^t6}PbPbAr^{Bu^t6}$ (**6**)

$Ar^{Pri4}PbPbAr^{Pri4}$ (**7**)

4-$Me_3Si$-$Ar^{Pri4}PbPbAr^{Pri4}$-4-$SiMe_3$ (**8**)

**Figure 2.3.** Thermal ellipsoid plots (30%) of the new diplumbynes **5**-**8**. Hydrogen atoms are not shown for clarity. Dashed bonds designate the minor components of disordered groups.

the C–Pb–Pb–C torsion angle (119.8°—although fixing the torsion angle at 140° only raised the energy by 0.7 kcal $mol^{-1}$) predicted by Nagase and Takagi for the multiply bonded isomer of **1**.[19]

The bond parameters of **7** and the major component of **8** are close to the Pb–Pb bond (3.1881(1) Å) and the $C_{ipso}$-Pb–Pb angles (94.30(9)°) originally reported in **1** and are consistent with a Pb–Pb single bonded structure. The structures of **6** and the minor component of **8** have short Pb–Pb bonds comparable to **5** but relatively narrow angles near 100° similar to **1** and **7**. This is in contrast with the singly bonded distannynes 4-$Me_3Si$-$Ar^{iPr4}SnSnAr^{iPr4}$-4-$SiMe_3$ and 4-$Me_3Ge$-$Ar^{iPr4}SnSnAr^{iPr4}$-4-$GeMe_3$ which show lengthened Sn–Sn bonds at angles of 97.79(17)- 99.07(3)°.[7] The short bonds in **5**, **6**, and **8** (Pb2–Pb2A) are still longer than typical Pb–Pb singles bonds in diplumbanes (cf. 2.84 Å in $Ph_3PbPbPh_3$),[62] but are similar to the Pb–Pb distances in reported diplumbenes said to contain Pb–Pb double bonds: 3.0515(3) Å in $Trip_2Pb{=}PbTrip_2$[63] (Trip = 2,4,6-$^iPr_3C_6H_2$), 2.9899(5) Å in Trip(Hyp)Pb=Pb(Hyp)Trip[64] (Hyp = $Si(SiMe_3)_3$) and 2.9033(9) Å in Mes(Hyp)Pb=Pb(Hyp)Mes.[65]

**Computational studies.** To investigate the structure-bonding relationship and the influence of intramolecular London dispersion interactions in compounds **1** and **5-8**, their molecular structures cut out of the crystal structures were optimized in the gas-phase with and without the D3 dispersion correction. In addition, the opposing structural motif (strongly trans-bent with longer Pb–Pb bond (Figure 2.1, structure **C**) vs. less trans-bent with short Pb–Pb bond (Figure 2.1, structure **B**)) was generated from the basic structure of the corresponding crystal structure cutout.

The generated structures are denoted by an asterisk (e.g. **1***). In all structures, the underlying structure motif **B** or **C** is retained after geometry optimization. This reflects the existence of two dominant structural minima. The structures with a shorter Pb–Pb bond and a less pronounced trans-bent angle (**5**, **6**, **1***, **7***, **8***) are unusual. For the experimental structures, the dispersion corrected

optimized gas-phase structures show fair agreement of the key structural parameters: the Pb–Pb bond length (d(Pb-Pb)), the trans-bent angle (φ(C-Pb-Pb)) and the torsion angle of the C–Pb–Pb–C unit (θ(C-Pb-Pb-C)) (Table 2.2). Upon neglecting the dispersion correction (Table 2.2, values in parentheses), both a stretching of the Pb–Pb bond and a pronounced increase of the trans-bending angle are observed. This indicates a large influence of intramolecular dispersion interactions on the molecular structure by partial compensation of steric repulsion between the large terphenyl ligands. The intramolecular dispersion interaction energy ($\Delta E_{Disp.}$) varies unsystematically between the structures in a range of 20-33 kcal·mol$^{-1}$ (PBE0) or 30-51 kcal·mol$^{-1}$ (B3LYP), respectively (Table 2.3).

**Table 2.2.** Selected calculated gas-phase bond parameters for **1**, **5-8 and 1***, **5*-8*** at TPSS-D3(BJ)-ATM/def2-TZVP level of theory. Non-dispersion corrected values are given in parentheses.

| | **1** | **5** | **6** | **7** | **8** | **1*** | **5*** | **6*** | **7*** | **8*** |
|---|---|---|---|---|---|---|---|---|---|---|
| d(Pb-Pb) / Å | 3.216 (3.314) | 2.972 (2.965) | 3.079 (3.192) | 3.207 (3.268) | 3.207 (3.270) | 3.022 (3.072) | 3.294 (3.468) | 3.281 (3.379) | 3.001 (3.073) | 3.003 (3.077) |
| d(C-Pb1) / Å | 2.329 (2.349) | 2.319 (2.328) | 2.389 (2.387) | 2.321 (2.341) | 2.318 (2.338) | 2.337 (2.335) | 2.358 (2.368) | 2.355 (2.375) | 2.324 (2.333) | 2.323 (2.331) |
| d(C-Pb2) / Å | 2.329 (2.349) | 2.318 (2.332) | 2.390 (2.384) | 2.321 (2.341) | 2.317 (2.338) | 2.336 (2.333) | 2.366 (2.367) | 2.354 (2.375) | 2.325 (2.334) | 2.323 (2.332) |
| φ(C-Pb1-Pb2) / ° | 93.5 (100.5) | 118.2 (131.6) | 98.9 (114.2) | 94.8 (102.4) | 94.3 (102.4) | 110.4 (120.7) | 102.0 (109.8) | 99.7 (104.8) | 111.6 (118.8) | 110.9 (118.6) |
| φ(C-Pb2-Pb1) / ° | 93.5 (100.5) | 118.5 (128.9) | 100.3 (105.5) | 94.8 (102.4) | 94.2 (102.0) | 109.6 (119.9) | 99.3 (109.7) | 99.7 (104.8) | 111.2 (119.3) | 110.9 (119.0) |
| θ(C-Pb1-Pb2-C) / ° | 180.0 (180.0) | −145.3 (144.2) | 133.9 (131.9) | 180.0 (180.0) | −178.9 (−179.8) | −109.2 (−113.7) | −174.4 (−177.0) | 180.0 (180.0) | −119.8 (−120.0) | −117.8 (−119.5) |

**Table 2.3.** Gibbs free energies and dispersion interaction energy contributions for **1**, **5-8** and **1***, **5*-8*** at PBE0/def2-TZVPP//TPSS-D3(BJ)-ATM/def2-TZVP and B3-LYP/def2-TZVPP/TPSS-D3(BJ)-ATM/def2-TZVP (in parentheses) level of theory. All values given in kcal·mol$^{-1}$.

| | **1** | **5** | **6** | **7** | **8** | **1*** | **5*** | **6*** | **7*** | **8*** |
|---|---|---|---|---|---|---|---|---|---|---|
| $\Delta G_{diss.}$ | −11.9 (−23.7) | −19.1 (-31.3) | −16.0 (−28.1) | −4.6 (−14.5) | −6.3 (−16.8) | −13.1 (−26.7) | −28.8 (−42.5) | −23.8 (−34.0) | −10.3 (−23.3) | −13.4 (−27.0) |
| $\Delta G_{diss.}$(D3) | 16.4 (19.7) | 9.4 (12.1) | 16.2 (20.8) | 18.6 (22.0) | 17.9 (21.1) | 13.0 (14.6) | 0.1 (1.7) | 3.9 (8.1) | 12.2 (13.3) | 9.1 (10.2) |
| $\Delta G_{diss.}$(D4) | 14.8 (15.2) | 7.5 (7.2) | 14.1 (15.4) | 17.3 (18.0) | 16.5 (17.1) | 11.5 (10.2) | −1.6 (−3.1) | 1.5 (2.3) | 11.0 (9.4) | 8.0 (6.3) |
| $\Delta E_{Disp.}$(D3) | −30.9 (−48.2) | −28.8 (−44.1) | −33.1 (−51.0) | −24.9 (−40.0) | −25.0 (−40.0) | −26.8 (−42.0) | −29.1 (−44.8) | −28.7 (−43.8) | −21.2 (−33.9) | −21.3 (−34.1) |
| $\Delta E_{Disp.}$(D4) | −29.9 (−44.4) | −27.5 (−40.1) | −31.7 (−46.4) | −24.2 (−36.7) | −24.3 (−36.9) | −25.3 (−38.4) | −27.8 (−40.5) | −27.3 (−39.7) | −20.2 (−30.5) | −20.4 (−30.8) |
| $\Delta G_{G\text{-}G^*}$(D3) | 3.5 (5.1) | 9.3 (10.4) | 12.2 (12.8) | 6.5 (8.6) | 8.8 (10.9) | | | | | |
| $\Delta G_{G\text{-}G^*}$(D4) | 3.3 (5.0) | 9.0 (10.3) | 12.6 (13.1) | 6.2 (8.6) | 8.5 (10.8) | | | | | |

Previous studies showed that the D3 and especially the D4 dispersion corrections for the repulsive B3LYP hybrid functional correlate well with the dispersion energy contribution to the interaction energy obtained from DLPNO-CCSD(T) local energy decomposition calculations.[66] It is noteworthy that the calculated dispersion interaction energies far exceed the dissociation free energies ($\Delta G_{diss.}$) for all systems and are a dominant factor in the stabilization of diplumbynes against dissociation into two doublet fragments. For all compared structure pairs, the experimental structure motifs are favored over the generated model systems in terms of free energy, with the difference in-creasing with increasing congestion of the terphenyl ligands. This is supported by a qualitative conformer search at GFN2-xTB(GBSA(toluene)) level applying the iMTD-GC algorithm within the CREST67 program, which confirms the experimental structure motifs being favored in solution for all studied compounds.

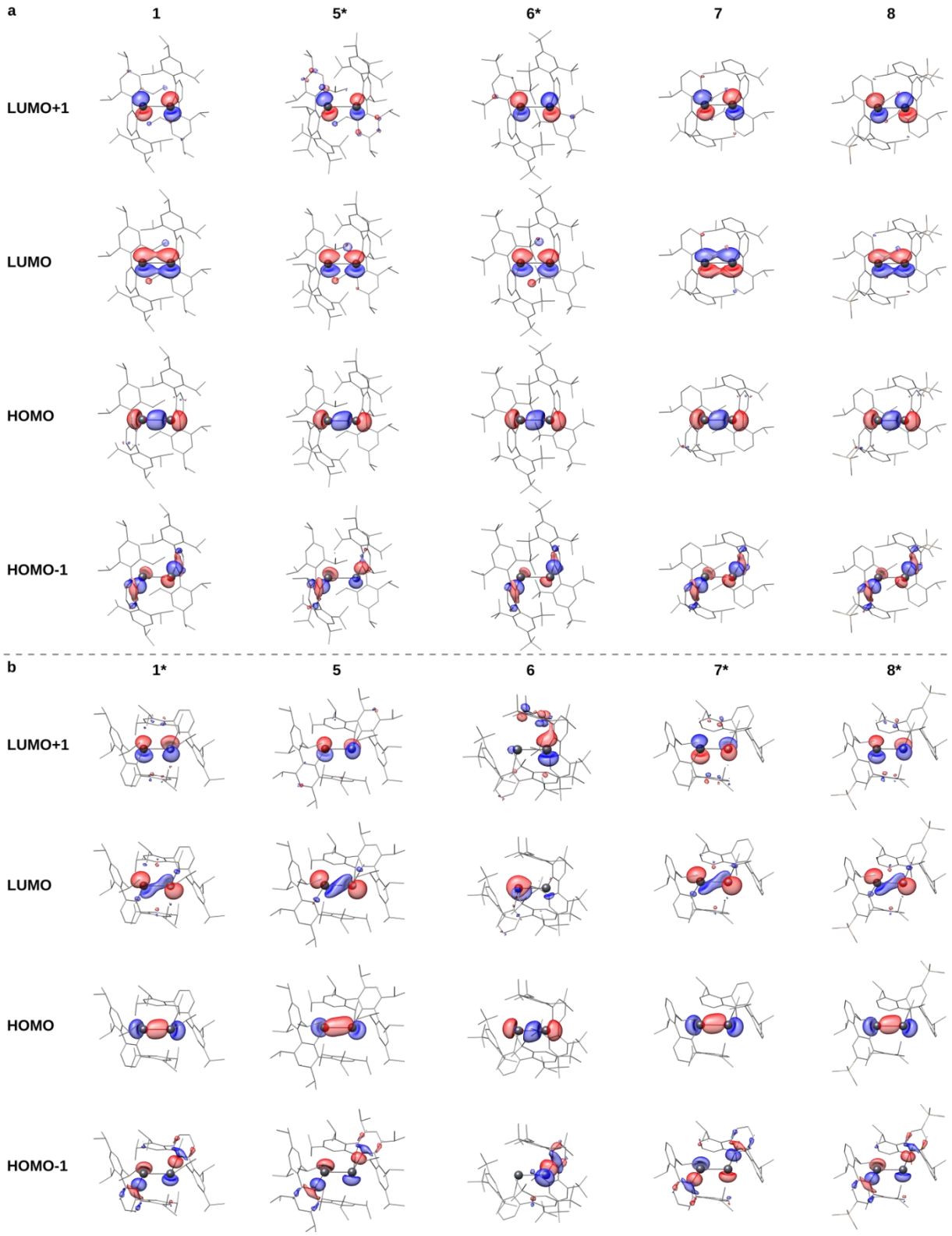


**Figure 2.4.** Selected frontier Kohn-Sham orbitals for bonding motifs **C** (a) and **B** (b) of **1**, **5**-**8** (experimental structures) and **1***, **5***-**8*** (generated structures) at TPSS-D3(BJ)-ATM/def2-TZVP level of theory. Isosurface value = 0.05 $e^{-1/2}\cdot bohr^{-3/2}$.

**Bonding in diplumbynes**. Electronic structure calculations, analysis of the Kohn-Sham frontier orbitals (Figure 2.4) and NBO analyses (Figure 2.5) yield insight in the correlation of the Pb–Pb bonding in the structural motifs B and C and their key structural features. All structures with motif C show a HOMO which reflects a σ bond consisting of symmetrical overlap of two Pb centered 6p orbitals. With a widening of the trans-bent angle and stronger torsion of the C–Pb–Pb–C unit in motif B, the HOMO is twisted and now resembles an out-of-plane p-p single bond.

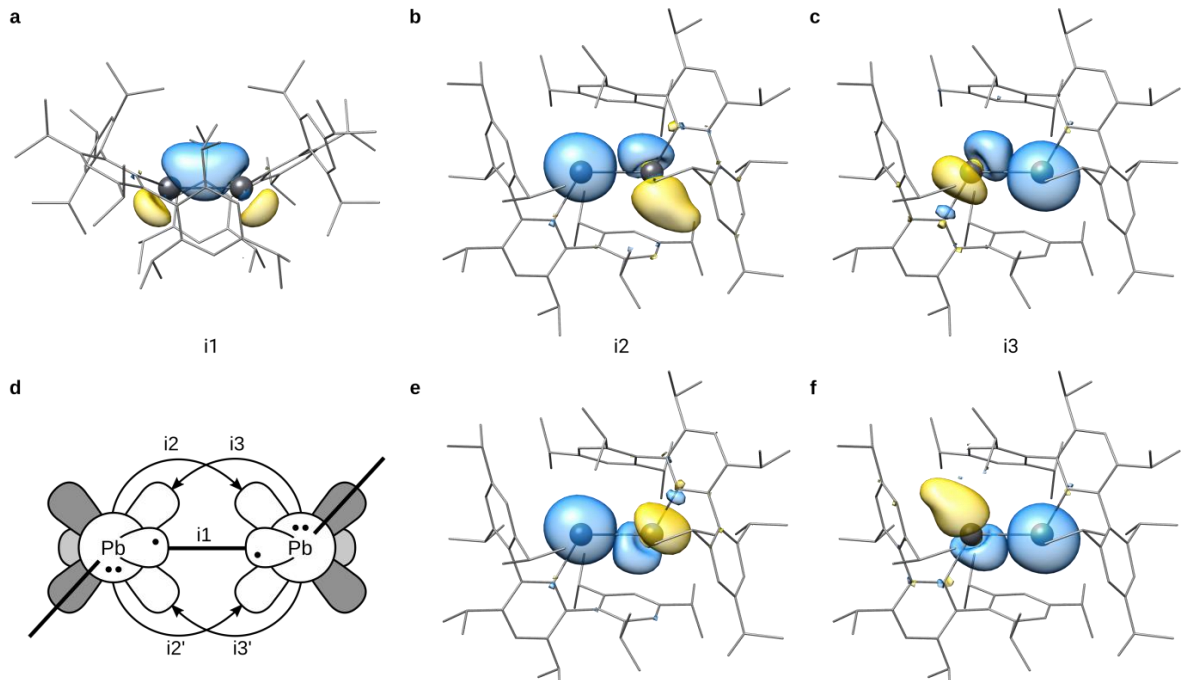


**Figure 2.5.** Schematic illustration of the bonding in **5**. NBO of the Pb-Pb single bond in **5** (i1) and NBO combinations reflecting the Pb(s)→Pb(p) donor-acceptor interactions (i2, i3, i2', i3'). Isosurface value = 0.05 $e^{-1/2}\cdot bohr^{-3/2}$.

For both structural motifs, the analysis of the Kohn-Sham molecular orbitals does not reveal any characteristics of a π-like multiple bond. However, the NBO analysis reveals a decisive difference between the two structural motifs. While the NBO analysis (in agreement with Foster-Boys localized MOs) for motif C yields only one Pb–Pb single bond corresponding to the shape of the HOMO, all structures with motif B show distinct donor-acceptor interactions between a Pb centered 6s-lone pair and a vacant 6p orbital at the opposite Pb atom (Figure 2.5). The severity of these interactions is strongly dependent on the trans-bent and torsion angles and is reflected by the

second order perturbation estimate (ΣE(2)) from the NBO analysis. The observation of a single bond with donor-acceptor contributions in motif **B** is also consistent with Wiberg, Mayer, Löwdin, and NLMO/NPA bond orders (BO) that do not exceed a maximum of 1.5 for the terphenyl substituted systems (Table 2.4, Figure 2.6). For motif **C** no E(2) contributions between the Pb atoms are present and all bond orders are close to or are slightly below a value of one. A two-dimensional scan of φ(C–Pb–Pb) (0 to 130°) and θ(C–Pb–Pb–C) (90 to 180°) for a model system Ph–Pb–Pb–Ph yields further detailed insight into the dependence of the discussed quantities on the trans-bent angle and torsion angle (Figure 2.7).

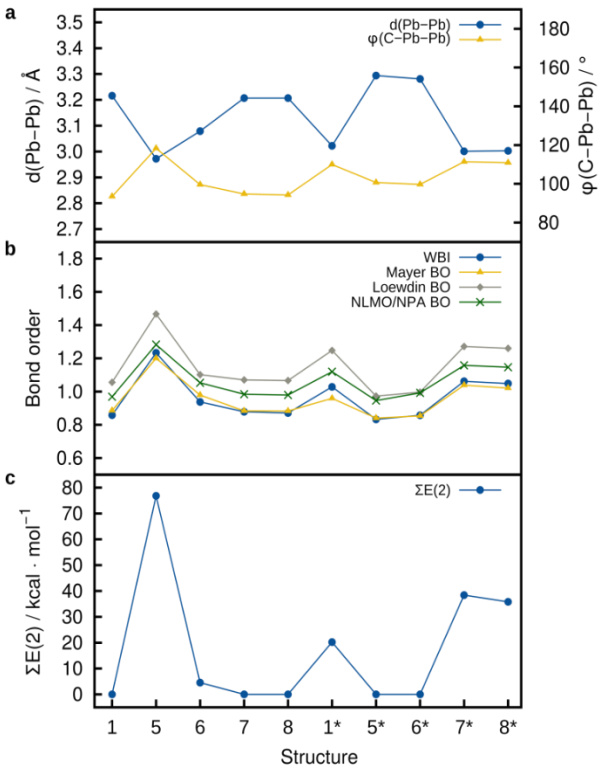


**Figure 2.6.** Summary of key structural parameters of the Pb-Pb bonding (a), bond order analyses (b), and second order perturbation estimate (ΣE(2)) of Pb(s)→Pb(p) donor-acceptor interactions in the NBO basis (c).

sTD-DFT calculations of the UV/vis excitation spectra confirm a relationship between structure and pronunciation of the excitation at longer wavelengths (Figure 2.8a,b). This only occurs in minimum structures of motif **B** and corresponds to a HOMO→ LUMO+1 excitation (Figure 2.8b). Molecular dynamics simulations at GFN2-xTB(GBSA(toluene)) level reveal, that the manifestation of the absorption band at longer wavelengths (approx. 600-800 nm) only provides a limited indication of the structural motif of the observed minimum structure. The high flexibility of the C–Pb–Pb–C unit in regard to the trans-bent angle as well as the Pb–Pb bond length leads to

approximately comparable UV/Vis spectra for the minimum structures of both structural motifs (Figure 2.8c, d).

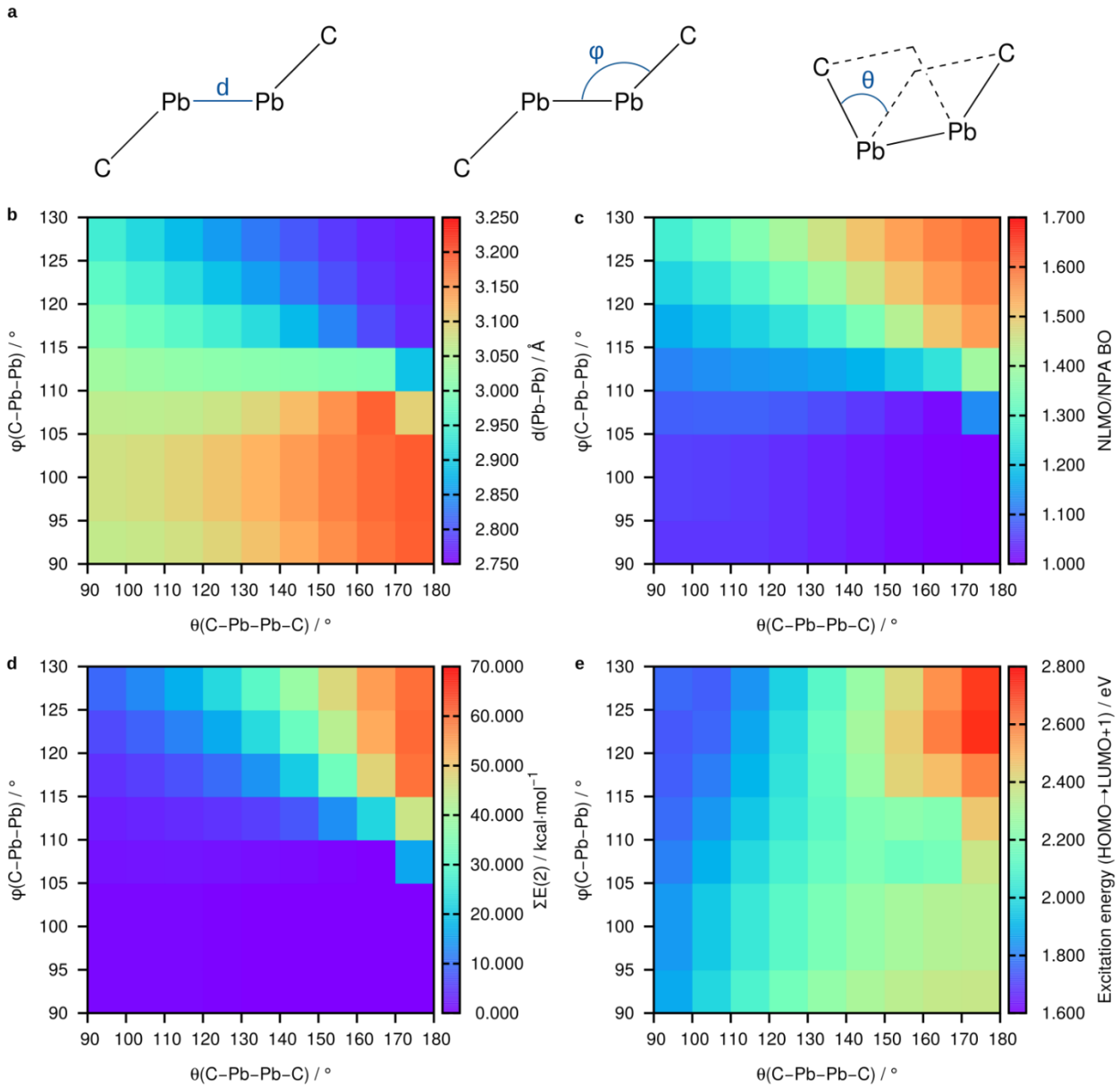


**Figure 2.7**. 2D structure scan of the trans-bent angle φ(C-Pb-Pb) (0 to 130°) and dihedral angle θ(C-Pb-Pb-C) (90 to 180°) for a model system Ph-Pb-Pb-Ph at TPSS-D3(BJ)-ATM/def2-TZVP level. a) Structure parameter definition; b) Pb-Pb bond length; c) NLMO/NPA BO; d) ΣE(2); e) Excitation energy (sTD-BHLYP/def2-TZVP) of the HOMO→LUMO+1 transition.

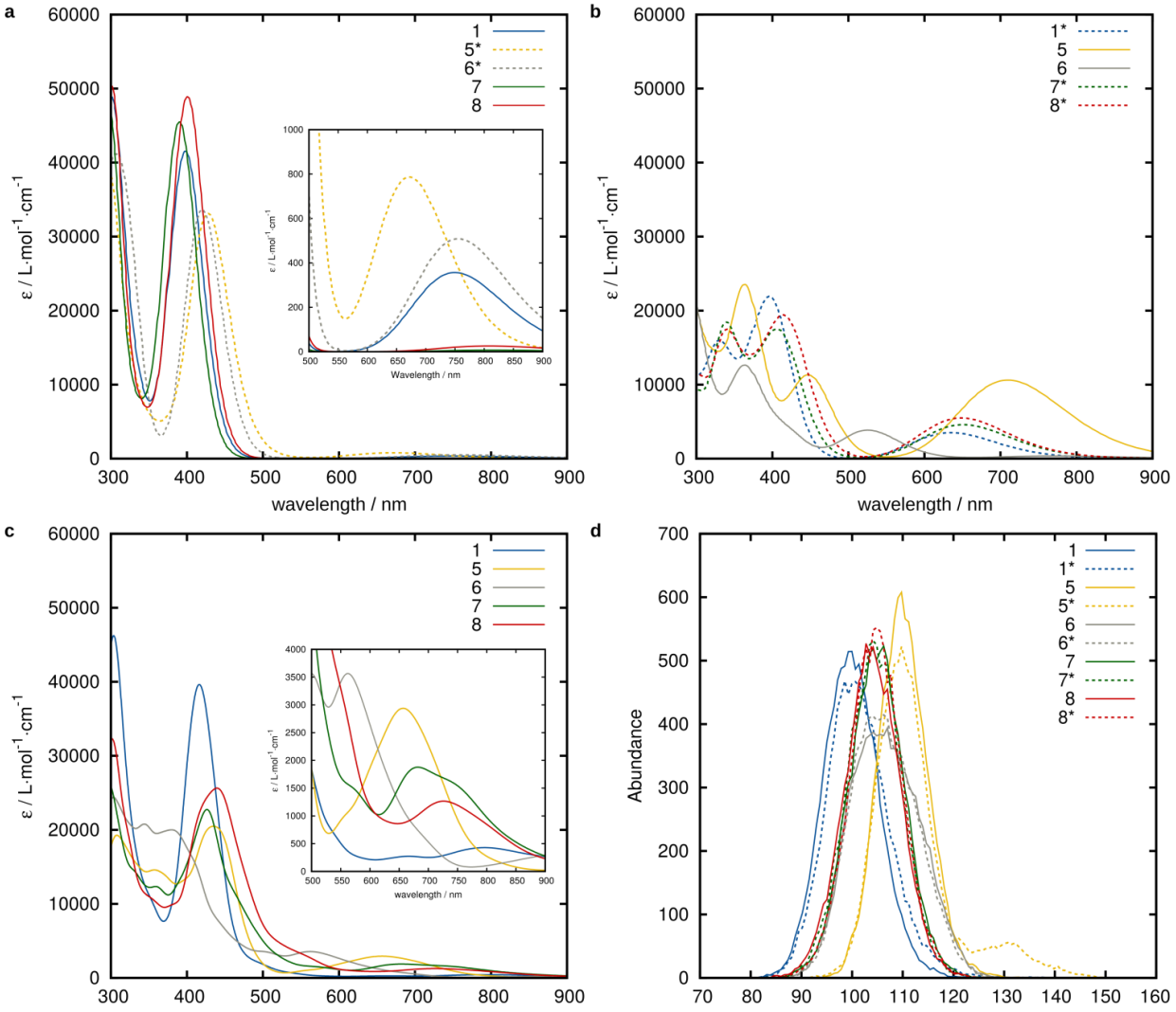


**Figure 2.8.** Calculated UV/Vis spectra for the minimum structures of motif **C** (a) and **B** (b) at sTD-BHLYP(CPCM(*n*-hexane))/def2-TZVP//TPSS-D3(BJ)-ATM/def2-TZVP level (applied shift = −0.2 eV). MD based averaged UV-Vis spectra for structures **1**, **5-8** (c) at sTD-BHLYP(CPCM(*n*-hexane))//GFN2-xTB(GBSA(toluene)) level of theory (applied shift = –0.2eV). (d) φ(C-Pb-Pb) angle distributions for the MD simulation of all investigated structures. MD simulation time of 1 ns.

**Table 2.5.** Tabulated absorption band maxima of the calculated UV-Vis spectra of **1**, **5-8** and **1***, **5*-8*** between 350 and 900 nm (applied shift = –0.2eV). $\varepsilon$ in L mol$^{-1}$ cm$^{-1}$ are given in parentheses.

| | | **1** | **5** | **6** | **7** | **8** | **1*** | **5*** | **6*** | **7*** | **8*** |
|---|---|---|---|---|---|---|---|---|---|---|---|
| single structure | λ / nm ($\varepsilon$ / L mol$^{-1}$ cm$^{-1}$) | 397 (41530), 751 (357) | 364 (23541), 448 (11314), 708 (10616) | 364 (12638), 525 (3847), 770 (364) | 390 (45496) | 410 (48898) | 331 (15994), 396 (21931), 636 (3510) | 428 (33129), 670 (787) | 420 (33605), 756 (509) | 340 (18433), 405 (17520), 653 (4585) | 341 (17488), 413 (19419), 649 (5499) |
| MD averaged | λ / nm ($\varepsilon$ / L mol$^{-1}$ cm$^{-1}$) | 416 (39630), 667 (274), 797 (429) | 357 (14590), 435 (20480), 657 (2939) | 344 (20780), 379 (20000), 562 (3565) | 359 (12340), 426 (22740), 682 (1878) | 440 (25630), 726 (1265) | 411 (32120), 550 (1412), 847 (313) | 366 (18510), 377 (18530), 425 (18190), 638 (3134) | 385 (20600), 515 (3534), 562 (3667) | 420 (22000), 658 (1245), 749 (1160) | 356 (12220), 437 (25940), 706 (1772) |

## Conclusions

A series of new diplumbynes has been synthesized by two facile routes. Their structures show a large variation in their Pb–Pb bond lengths and $C_{ispo}$–Pb–Pb angles in the solid state. The Pb–Pb distances range from 3.0382(6) Å for $Ar^{iPr8}PbPbAr^{iPr8}$ (**5**) to 3.2439(9) Å for 4-$Me_3Si$-$Ar^{iPr4}PbPbAr^{iPr4}$-4-$SiMe_3$ (**8**) (cf. 2.945(5) Å in its minor component) with respective bond angles of 114.73(7)-116.02(6)° in **5** and 95.22(5)° in **8**. Thus, the variation in Pb–Pb distance is ca. 0.3 Å, ca. 10%). The apparent 'softness' of the Pb–Pb distances and bending angles are in agreement with the calculations of Frenking and coworkers indicating that they are susceptible to alteration by changes in the packing effects (i.e. London dispersion interactions).[18] Additionally, the structure of **5** is in good agreement with structural parameters predicted by Nagase and coworkers for the isomer of $Ar^{iPr6}PbPbAr^{iPr6}$ (**1**) containing multiple bond character.[19]

DFT computational studies verify the different bonding in the observed structural motifs, highlighting a donor-acceptor interaction augmentation of the Pb–Pb bond upon widening of the trans-bent angle, resulting in shortened Pb–Pb bonds with bond orders up to 1.5. London dispersion interactions prove crucial for stabilizing all sterically congested diplumbynes investigated in this

study, strongly influencing the trans-bent angle. High steric congestion and the associated ligand fixation enable the stabilization of less trans-bent structural motifs. sTD-DFT calculations reveal a clear correlation between changes in the Pb–Pb bonding due to the trans-bent angle and the appearance of the electronic spectra of the minimum structures. Further MD simulations show that the high flexibility of the C–Pb–Pb–C unit leads to similar UV/vis spectra for both structure motifs with increased intensity of the HOMO→ LUMO+1 excitation.

**Acknowledgment**

We wish to acknowledge the US National Science Foundation (CHE-1565501) for support of this work and for purchase of a dual-source X-ray diffractometer (CHE-0840444). The German Science Foundation (DFG) is gratefully acknowledged for financial support in the framework of the Gottfried Wilhelm Leibniz prize to S.G.

**References**

(1) Pu, L.; Twamley, B.; Power, P. P. Synthesis and Characterization of 2,6-$Trip_2H_3C_6PbPbC_6H_3$-2,6-$Trip_2$ (Trip = $C_6H_2$-2,4,6-i-$Pr_3$): A Stable Heavier Group 14 Element Analogue of an Alkyne. *J. Am. Chem. Soc.* **2000**, *122*, 3524–3525.

(2) Phillips, A. D.; Wright, R. J.; Olmstead, M. M.; Power, P. P. Synthesis and Characterization of 2,6-$Dipp_2$-$H_3C_6SnSnC_6H_3$-2,6-$Dipp_2$ (Dipp = $C_6H_3$-2,6-$Pr^i_2$): A Tin Analogue of an Alkyne. *J. Am. Chem. Soc.* **2002**, *124*, 5930–5931.

(3) Stender, M.; Phillips, A. D.; Wright, R. J.; Power, P. P. Synthesis and Characterization of a Digermanium Analogue of an Alkyne. *Angew. Chem., Int. Ed.* **2002**, *41*, 1785–1787.

(4) Sekiguchi, A.; Kinjo, R.; Ichinohe, M. A Stable Compound Containing a Silicon-Silicon Triple Bond. *Science* **2004**, *305*, 1755–1757.

(5) Wiberg, N.; Niedermayer, W.; Fischer, G.; Nöth, H.; Suter, M. Synthesis, Structure and Dehalogenation of the Disilene RClSi=SiClR [R = $(t\mathrm{Bu}_3\mathrm{Si})_2$MeSi]. *Eur. J. Inorg. Chem.* **2002**, 1066–1070.

(6) Wiberg, N.; Vasisht, S. K.; Fischer, G.; Mayer, P. Disilynes. III [1]: A Relatively Stable Disilyne RSi≡SiR (R = $\mathrm{SiMe(Si}t\mathrm{Bu}_3)_2$). *Z. Anorg. Allg. Chem.* **2004**, *630*, 1823–1828.

(7) Peng, Y.; Fischer, R. C.; Merrill, W. A.; Fischer, J.; Pu, L.; Ellis, B. D.; Fettinger, J. C.; Herber, R. H.; Power, P. P. Substituent Effects in Ditetrel Alkyne Analogues: Multiple vs. Single Bonded Isomers. *Chem. Sci.* **2010**, *1*, 461–468.

(8) Pu, L.; Phillips, A. D.; Richards, A. F.; Stender, M.; Simons, R. S.; Olmstead, M. M.; Power, P. P. Germanium and Tin Analogues of Alkynes and Their Reduction Products. *J. Am. Chem. Soc.* **2003**, *125*, 11626–11636.

(9) Hadlington, T. J.; Jones, C. A Singly Bonded Amido-Distannyne: $H_2$ Activation and Isocyanide Coordination. *Chem. Commun.* **2014**, *50*, 2321–2323.

(10) Li, J.; Schenk, C.; Goedecke, C.; Frenking, G.; Jones, C. A Digermyne with a Ge–Ge Single Bond That Activates Dihydrogen in the Solid State. *J. Am. Chem. Soc.* **2011**, *133*, 18622–18625.

(11) Hadlington, T. J.; Hermann, M.; Li, J.; Frenking, G.; Jones, C. Activation of $H_2$ by a Multiply Bonded Amido-Digermyne: Evidence for the Formation of a Hydrido-Germylene. *Angew. Chem., Int. Ed.* **2013**, *52*, 10199–10203.

(12) Sugiyama, Y.; Sasamori, T.; Hosoi, Y.; Furukawa, Y.; Takagi, N.; Nagase, S.; Tokitoh, N. Synthesis and Properties of a New Kinetically Stabilized Digermyne: New Insights for a Germanium Analogue of an Alkyne. *J. Am. Chem. Soc.* **2006**, *128*, 1023–1031.

(13) Sasamori, T.; Hironaka, K.; Sugiyama, Y.; Takagi, N.; Nagase, S.; Hosoi, Y.; Furukawa, Y.; Tokitoh, N. Synthesis and Reactions of a Stable 1,2-Diaryl-1,2-Dibromodisilene: A Precursor for Substituted Disilenes and a 1,2-Diaryldisilyne. *J. Am. Chem. Soc.* **2008**, *130*, 13856–13857.

(14) Murata, Y.; Ichinohe, M.; Sekiguchi, A. Unsymmetrically Substituted Disilyne $Dsi_2{}^{i}PrSi$—Si≡Si—$SiNpDsi_2$ (Np = $CH_2{}^{t}Bu$): Synthesis and Characterization. *J. Am. Chem. Soc.* **2010**, *132*, 16768–16770.

(15) Ishida, S.; Sugawara, R.; Misawa, Y.; Iwamoto, T. Palladium and Platinum $\eta^2$ -Disilyne Complexes Bearing an Isolable Dialkyldisilyne as a Ligand. *Angew. Chem., Int. Ed.* **2013**, *52*, 12869–12873.

(16) Pyykkö, P. Additive Covalent Radii for Single-, Double-, and Triple-Bonded Molecules and Tetrahedrally Bonded Crystals: A Summary. *J. Phys. Chem. A* **2015**, *119*, 2326–2337.

(17) Kutzelnigg, W. Chemical Bonding in Higher Main Group Elements. *Angew. Chem., Int. Ed.* **1984**, *23*, 272–295.

(18) Chen, Y.; Hartmann, M.; Diedenhofen, M.; Frenking, G. Turning a Transition State into a Minimum—The Nature of the Bonding in Diplumbylene Compounds RPbPbR (R=H, Ar). *Angew. Chem., Int. Ed.* **2001**, *40*, 2051–2055.

(19) Takagi, N.; Nagase, S. Do Lead Analogues of Alkynes Take a Multiply Bonded Structure? *Organometallics* **2007**, *26*, 3627–3629.

(20) Takagi, N.; Nagase, S. Tin Analogues of Alkynes. Multiply Bonded Structures vs Singly Bonded Structures. *Organometallics* **2007**, *26*, 469–471.

(21) Yousung, J.; Marcin, B.; Power, P. P.; Head-Gordon, M. Ab Initio Quantum Chemistry Calculations on the Electronic Structure of Heavier Alkyne Congeners: Diradical Character and Reactivity. *J. Am. Chem. Soc.* **2006**, *128*, 7185–7192.

(22) Wilfling, P.; Schittelkopf, K.; Flock, M.; Herber, R. H.; Power, P. P.; Fischer, R. C. Influence of Ligand Modifications on Structural and Spectroscopic Properties in Terphenyl Based Heavier Group 14 Carbene Homologues. *Organometallics* **2015**, *34*, 2222–2232.

(23) Liptrot, D. J.; Power, P. P. London Dispersion Forces in Sterically Crowded Inorganic and Organometallic Molecules. *Nat. Rev. Chem.* **2017**, *1*, 0004.

(24) Seidu, I.; Seth, M.; Ziegler, T. Role Played by Isopropyl Substituents in Stabilizing the Putative Triple Bond in Ar′EEAr′ [E = Si, Ge, Sn; Ar′ = $C_6H_3$-2,6-($C_6H_3$-2,6-$Pr^i_2$)$_2$] and Ar*PbPbAr* [Ar* = $C_6H_3$-2,6-($C_6H_2$-2,4,6-$Pr^i_3$)$_2$]. *Inorg. Chem.* **2013**, *52*, 8378–8388.

(25) Pangborn, A. B.; Giardello, M. A.; Grubbs, R. H.; Rosen, R. K.; Timmers, F. J. Safe and Convenient Procedure for Solvent Purification. *Organometallics* **1996**, *15*, 1518–1520.

(26) Fulmer, G. R.; Miller, A. J. M.; Sherden, N. H.; Gottlieb, H. E.; Nudelman, A.; Stoltz, B. M.; Bercaw, J. E.; Goldberg, K. I. NMR Chemical Shifts of Trace Impurities: Common Laboratory Solvents, Organics, and Gases in Deuterated Solvents Relevant to the Organometallic Chemist. *Organometallics* **2010**, *29*, 2176–2179.

(27) Stanciu, C.; Richards, A. F.; Fettinger, J. C.; Brynda, M.; Power, P. P. Synthesis and Characterization of New, Modified Terphenyl Ligands: Increasing the Rotational Barrier for Flanking Rings. *J. Organomet. Chem.* **2006**, *691*, 2540–2545.

(28) Bukhryakov, K. V.; Schrock, R. R.; Hoveyda, A. H.; Müller, P.; Becker, J. Synthesis of 2,6-Hexa- Tert -Butylterphenyl Derivatives, 2,6-(2,4,6-t-$Bu_3C_6H_2$)$_2C_6H_3X$, Where X = I, Li, OH, SH, $N_3$, or $NH_2$. *Org. Lett.* **2017**, *19*, 2607–2609.

(29) Rivard, E.; Fischer, R. C.; Wolf, R.; Peng, Y.; Merrill, W. A.; Schley, N. D.; Zhu, Z.; Pu, L.; Fettinger, J. C.; Teat, S. J.; Nowik, I.; Herber, R. H.; Takagi, N.; Nagase S.; Power, P. P. Isomeric Forms of Heavier Main Group Hydrides: Experimental and Theoretical Studies of the $[Sn(Ar)H]_2$ (Ar = Terphenyl) System. *J. Am. Chem. Soc.* **2007**, *129*, 16197–16208.

(30) Hino, S.; Olmstead, M. M.; Phillips, A. D.; Wright, R. J.; Power, P. P. Terphenyl Ligand Stabilized Lead(II) Derivatives: Steric Effects and Lead-Lead Bonding in Diplumbenes. *Inorg. Chem.* **2004**, *43*, 7346–7352.

(31) Hicks, J.; Juckel, M.; Paparo, A.; Dange, D.; Jones, C. Multigram Syntheses of Magnesium(I) Compounds Using Alkali Metal Halide Supported Alkali Metals as Dispersible Reducing Agents. *Organometallics* **2018**, *37*, 4810–4813.

(32) Sheldrick, G. M. *SADABS*; University of Göttingen, Germany, 1996.

(33) Sheldrick, G. M. *TWINABS*; University of Göttingen, Germany, 2012.

(34) Sheldrick, G. M. SHELXT - Integrated Space-Group and Crystal-Structure Determination. *Acta Cryst.* **2015**, *A71*, 3–8.

(35) Sheldrick, G. M. Crystal Structure Refinement with SHELXL. *Acta Cryst.* **2015**, *C71*, 3–8.

(36) Spek, A. L. PLATON SQUEEZE: A Tool for the Calculation of the Disordered Solvent Contribution to the Calculated Structure Factors. *Acta Cryst.* **2015**, *C71*, 9-18.

(37) Furche, F.; Ahlrichs, R.; Hättig, C.; Klopper, W.; Sierka, M.; Weigend, F. Turbomole. *WIREs Comput. Mol. Sci.* **2014**, *4*, 91–100.

(38) TURBOMOLE V7.0.2 2015, a Development of University of Karlsruhe and Forschungszentrum Karlsruhe GmbH, 1989-2007, TURBOMOLE GmbH, since 2007; Available from Http://Www.Turbomole.Com.

(39) Neese, F. The ORCA Program System. *WIREs Comput. Mol. Sci.* **2012**, *2*, 73–78.

(40) Neese, F. ORCA: An Ab Initio, Density Functional and Semiempirical Program Package , V. 4.1.0; MPI Für Chemische Energiekonversion: Mülheim a. d. Ruhr, Germany, 2019.

(41) Grimme, S. XTB, V. 6.1; Mulliken Center for Theoretical Chemistry, University of Bonn. **2019**.

(42) Glendening, E. D.; Badenhoop, J. K.; Reed, A. E.; Carpenter, J. E.; Bohmann, J. A.; Morales, C. M.; Landis, C. R.; Weinhold, F. NBO 6.0. Theoretical Chemistry Institute, University of Wisconsin: Madison 2013.

(43) Bannwarth, C.; Ehlert, S.; Grimme, S. GFN2-XTB - An Accurate and Broadly Parametrized Self-Consistent Tight-Binding Quantum Chemical Method with Multipole Electrostatics and Density-Dependent Dispersion Contributions. *J. Chem. Theory Comput.* **2018**, *15*, 1652–1671.

(44) Tao, J.; Perdew, J. P.; Staroverov, V. N.; Scuseria, G. E. Climbing the Density Functional Ladder: Nonempirical Meta–Generalized Gradient Approximation Designed for Molecules and Solids. *Phys. Rev. Lett.* **2003**, *91*, 146401.

(45) Grimme, S.; Antony, J.; Ehrlich, S.; Krieg, H. A Consistent and Accurate Ab Initio Parametrization of Density Functional Dispersion Correction (DFT-D) for the 94 Elements H-Pu. *J. Chem. Phys.* **2010**, *132*, 154104.

(46) Grimme, S.; Ehrlich, S.; Goerigk, L. Effect of the Damping Function in Dispersion Corrected Density Functional Theory. *J. Comput. Chem.* **2011**, *32*, 1456–1465.

(47) Axilrod, B. M.; Teller, E. Interaction of the van Der Waals Type between Three Atoms. *J. Chem. Phys.* **1943**, *11*, 299–300.

(48) Muto, Y. Force between Nonpolar Molecules. *Proc. Phys. Math. Soc. Jpn.* **1943**, *17*, 629–631.

(49) Weigend, F.; Ahlrichs, R. Balanced Basis Sets of Split Valence, Triple Zeta Valence and Quadruple Zeta Valence Quality for H to Rn: Design and Assessment of Accuracy. *Phys. Chem. Chem. Phys.* **2005**, *7*, 3297.

(50) Adamo, C.; Barone, V. Toward Reliable Density Functional Methods without Adjustable Parameters: The PBE0 Model. *J. Chem. Phys.* **1999**, *110*, 6158–6170.

(51) Becke, A. D. Density-Functional Thermochemistry. III. The Role of Exact Exchange. *J. Chem. Phys.* **1993**, *98*, 5648–5652.

(52) Klamt, A. Conductor-like Screening Model for Real Solvents: A New Approach to the Quantitative Calculation of Solvation Phenomena. *J. Phys. Chem.* **1995**, *99*, 2224–2235.

(53) Eckert, F.; Klamt, A. Fast Solvent Screening via Quantum Chemistry: COSMO-RS Approach. *AIChE J.* **2002**, *48*, 369–385.

(54) Caldeweyher, E.; Bannwarth, C.; Grimme, S. Extension of the D3 Dispersion Coefficient Model. *J. Chem. Phys.* **2017**, *147*, 034112. https://doi.org/10.1063/1.4993215.

(55) Caldeweyher, E.; Ehlert, S.; Hansen, A.; Neugebauer, H.; Spicher, S.; Bannwarth, C.; Grimme, S. A Generally Applicable Atomic-Charge Dependent London Dispersion Correction. *J. Chem. Phys.* **2019**, *150*, 154122. https://doi.org/10.1063/1.5090222.

(56) Grimme, S.; Bannwarth, C. Ultra-Fast Computation of Electronic Spectra for Large Systems by Tight-Binding Based Simplified Tamm-Dancoff Approximation (STDA-XTB). *J. Chem. Phys.* **2016**, *145*, 54103.

(57) Grimme, S. A Simplified Tamm-Dancoff Density Functional Approach for the Electronic Excitation Spectra of Very Large Molecules. *J. Chem. Phys.* **2013**, *138*, 244104.

(58) Becke, A. D. A New Mixing of Hartree-Fock and Local Density-Functional Theories. *J. Chem. Phys.* **1993**, *98*, 1372–1377.

(59) Pu, L.; Twamley, B.; Power, P. P. Terphenyl Ligand Stabilized Lead(II) Derivatives of Simple Organic Groups: Characterization of $Pb(R)C_6H_3$-2,6-$Trip_2$ (R = Me, t-Bu, or Ph; Trip = $C_6H_2$-2,4,6-i-$Pr_3$), $\{Pb(\mu\text{-}Br)C_6H_3\text{-}2,6\text{-}Trip_2\}_2$, $Py\cdot Pb(Br)C_6H_3$-2,6-$Trip_2$ (Py = Pyridine), and the Bridged Plumbylyne Complex $[\{W(CO)_4\}_2(\mu\text{-}Br)(\mu\text{-}PbC_6H_3\text{-}2,6\text{-}Trip_2)]$. *Organometallics* **2000**, *19*, 2874–2881.

(60) Weiß, S.; Auer, M.; Eichele, K.; Schubert, H.; Wesemann, L. η 3 -Allyl Coordination at Pb(II). *Organometallics* **2019**, *38*, 417–423.

(61) Schneider, J.; Sindlinger, C. P.; Eichele, K.; Schubert, H.; Wesemann, L. Low-Valent Lead Hydride and Its Extreme Low-Field 1H NMR Chemical Shift. *J. Am. Chem. Soc.* **2017**, *139*, 6542–6545.

(62) Preut, H.; Huber, F. Die Kristall- Und Molekülstruktur Des Hexaphenyldiplumbans. *Z. Anorg. Allg. Chem.* **1976**, *419*, 92–96.

(63) Stürmann, M.; Saak, W.; Marsmann, H.; Weidenbruch, M. Tetrakis(2,4,6-Triisopropylphenyl)Diplumbene: A Molecule with a Lead-Lead Double Bond. *Angew. Chem., Int. Ed.* **1999**, *38*, 187–189.

(64) Stürmann, M.; Saak, W.; Weidenbruch, M.; Klinkhammer, K. W. A Heteroleptic Diplumbene and a Magnesium Dibromide Stabilized Plumbylene Dimer. *Eur. J. Inorg. Chem.* **1999**, 579–582.

(65) Klinkhammer, K. Dihypersilylstannylene and Dihypersilylplumbylene—Two Lewis-Amphoteric Carbene Homologues. *Polyhedron* **2002**, *21*, 587–598.

(66) Bursch, M.; Caldeweyher, E.; Hansen, A.; Neugebauer, H.; Ehlert, S.; Grimme, S. Understanding and Quantifying London Dispersion Effects in Organometallic Complexes. *Acc. Chem. Res.* **2019**, *52*, 258–266.

(67) Grimme, S. Exploration of Chemical Compound, Conformer, and Reaction Space with Meta-Dynamics Simulations Based on Tight-Binding Quantum Chemical Calculations. *J. Chem. Theory Comput.* **2019**, *15*, 2847–2862.

**Author Contributions**

**J.D. Queen:** Synthesized and spectroscopically characterized the reported lead compounds, collected X-Ray diffraction data, and prepared the manuscript.

**B. D. Ellis:** Was the first to prepare the diplumbynes **7** and **8**.

**P. P. Power**: Supervised the synthetic work and manuscript preparation.

**J. C. Fettinger:** Prepared the X-ray crystallographic data for publication.

**M Bursch, J. Seibert, L. Maurer, and S. Grimme**: Performed DFT calculations including geometry optimization for the two trans-bent forms of each of the diplumbynes **1**, **5-8**, and simulated electronic spectra. Wrote the computational results sections of the manuscript and prepared the relevant figures.

**Supporting Information**

**Preparation and characterization of [Li(Et$_2$O)Ar$^{iPr8}$].** Ar$^{iPr8}$I[S1] (12.0 g, 17.3 mmol) was dissolved in a mixture of hexanes (ca. 80 mL) and Et$_2$O (ca. 20 mL) and cooled to 0°C in an ice/water bath. 1.7 M *tert*-BuLi in pentane (20.8 mL, 35.5 mmol) was added dropwise over 10 min. The mixture was allowed to come to ambient temperature and stirred for 12 h. The volatile components were removed under reduced pressure and the solids extracted with hexane (ca. 60 mL). The pale-yellow solution was concentrated to ca. 20 mL and stored at -18ºC overnight to give colorless crystals of the lithium salt. Yield: 9.3 g (83%) mp = 143-145°C (turns yellow with gas evolution) $^1$H NMR (400 MHz, C$_6$D$_6$, 298 K): δ 7.32 (s, 1H, Ar*H*), 7.16 (s, 4H, Ar*H*), 3.39 (sept, br, 4H, -C*H*(CH$_3$)$_2$), 2.87 (m, 4H, -C*H*(CH$_3$)$_2$), 2.66 (q, br, 4H, O(C*H*$_2$CH$_3$)$_2$), 1.36 (m, 24H, -CH(C*H*$_3$)$_2$), 1.29 (d, 12H, -CH(C*H*$_3$)$_2$), 1.21 (d, 12H, -CH(C*H*$_3$)$_2$), 0.49 (t, br, 6H, O(CH$_2$C*H*$_3$)$_2$). $^{13}$C{$^1$H} NMR (101 MHz, C$_6$D$_6$, 289 K): δ 147.5, 146.2, 145.5, 144.7, 141.2, 121.0, 120.7, 117.2, 65.8, 34.7, 32.0, 31.0, 30.0, 26.2, 25.5, 24.5, 24.4, 23.1, 14.4, 14.1. $^7$Li{$^1$H} (155 MHz, C$_6$D$_6$, 289 K): δ 0.95.

**Synthesis of Ar$^{iPr6}$PbPbAr$^{iPr6}$ (1).** A solution of {Pb(μ-Br)Ar$^{iPr6}$}$_2$[S2] (1.00 g, 0.650 mmol) in Et$_2$O (ca. 20 mL) was cooled to 0°C in an ice/water bath. A solution of (Mg$^{Mes}$Nacnac)$_2$ (0.468 g 0.650 mmol) in Et$_2$O (ca. 5 mL) was added dropwise over 2 min, resulting in an immediate color change from yellow to dark brown. The solution stirred for 30 min and the volatile components were removed under reduced pressure. The dark residue was extracted with hexanes (ca. 30 mL) and stored at -30°C for 2 days to give large brown blocks of **1**·hexane (0.608 g, 0.415 mmol, 64%), identified by the $^1$H NMR spectrum in C$_6$D$_6$.

**Table 2.S1.** Selected X-ray Crystallographic data for **2** – **8**.

| **Compound** | **2** | **3+[solvent]** | **4** | **5·1.5 $C_7H_8$** | **6** | **7** | **8·$Et_2O$** |
|---|---|---|---|---|---|---|---|
| **Formula** | $C_{84}H_{122}Br_2Pb_2$ | $C_{84}H_{122}Br_2Pb_2$ | $C_{66}H_{90}Br_2Si_2Pb_2$ | $C_{189}H_{268}Pb_4$ | $C_{84}H_{122}Pb_2$ | $C_{60}H_{74}Pb_2$ | $C_{70}H_{100}Si_2Pb_2$ |
| **Formula Weight (g mol$^{-1}$)** | 1706.02 | 1706.02 | 1513.76 | 3368.83 | 1546.19 | 1209.57 | 1428.05 |
| **T (K)/λ (Å)** | 90(2)/0.71073 | 90(2)/0.71073 | 90(2)/0.71073 | 90(2)/0.71073 | 90(2)/0.71073 | 90(2)/0.71073 | 90(2)/0.71073 |
| **Crystal System** | Monoclinic | Monoclinic | Triclinic | Monoclinic | Monoclinic | Triclinic | Monoclinic |
| **Space Group** | $P2_1/n$ | C2/c | P-1 | $P2_1/n$ | C2/c | P-1 | $P2_1/c$ |
| **Z** | 4 | 4 | 1 | 2 | 8 | 1 | 2 |
| **Crystal color and habit** | Yellow block | Yellow block | Yellow plate | Red parallelepiped | Green block | Amber block | Amber/green block |
| **a (Å)** | 14.946(2) | 14.6489(14) | 11.3682(9) | 18.3288(13) | 20.3372(17) | 9.1688(8) | 11.4812(12) |
| **b (Å)** | 19.052(3) | 26.975(3) | 12.7595(10) | 23.6315(17) | 18.4518(14) | 12.7083(11) | 25.639(3) |
| **c (Å)** | 28.498(4) | 22.733(2) | 12.9493(10) | 20.2841(15) | 38.674(3) | 13.0164(12) | 12.8116(14) |
| **α (°)** | 90 | 90 | 94.5630(12) | 90 | 90 | 64.2950(10) | 90 |
| **β (°)** | 98.929(2) | 105.4841(13) | 103.1496(10) | 104.2710(10) | 90.3948(15) | 81.6790()10 | 114.5876(13) |
| **γ (°)** | 90 | 90 | 114.1017(10) | 90 | 90 | 69.5720(10) | 90 |
| **V (Å$^3$)** | 8016(2) | 8656.9(14) | 1637.9(2) | 8514.7(11) | 14512(2) | 1280.6(2) | 3429.4(6) |
| **ρ (mg mm$^{-3}$)** | 1.414 | 1.309 | 1.535 | 1.314 | 1.415 | 1.568 | 1.383 |
| **Abs. coeff (mm$^{-1}$)** | 5.231 | 4.844 | 6.425 | 3.992 | 4.677 | 6.601 | 4.976 |
| **F(000)** | 3440 | 3440 | 748 | 3460 | 6320 | 598 | 1440 |
| **Crystal size (mm)** | 0.361 x 0.331 x 0.248 | 0.194 x 0.099 x 0.092 | 0.520 x 0.312 x 0.078 | 0.252 x 0.125 x 0.068 | 0.086 x 0.068 x 0.053 | 0.160 x 0.158 x 0.141 | 0.538 x 0.438 x 0.216 |
| **$\theta$ range (°)** | 1.799 to 30.615 | 1.628 to 30.598 | 1.782 to 27.485 | 1.595 to 30.000 | 1.490 to 25.250 | 1.736 to 30.510 | 1.920 to 27.570 |
| **Reflns collected** | 93991 | 49125 | 7514 | 96170 | 44040 | 7751 | 29678 |
| **Ind. Reflns.** | 24555 | 13272 | 7514 | 24841 | 13165 | 7751 | 7912 |
| **R(int)** | 0.0290 | 0.0880 | – | 0.0419 | 0.0956 | – | 0.0201 |
| **Obs. reflns ($I$>2σ($I$))** | 21212 | 9197 | 7230 | 18353 | 9320 | 7178 | 7496 |
| **Completeness to 2$\theta$ = 25.242°** | 99.9% | 99.9% | 99.9% | 100.0% | 100.0% | 100.0% | 100.0% |
| **Goodness-of-fit on $F^2$** | 1.055 | 0.986 | 1.051 | 1.005 | 0.975 | 1.081 | 1.034 |
| **Final R ($I$>2σ($I$))** | R1 = 0.0216 | R1 = 0.0372 | R1 = 0.0402 | R1 = 0.0283 | R1 = 0.0420 | R1 = 0.0232 | R1 = 0.0162 |
| | wR2 = 0.0441 | wR2 = 0.0788 | wR2 = 0.1091 | wR2 = 0.0576 | wR2 = 0.0783 | wR2 = 0.0597 | wR2 = 0.0408 |
| **R (all data)** | R1 = 0.0287 | R1 = 0.0658 | R1 = 0.0416 | R1 = 0.0489 | R1 = 0.0734 | R1 = 0.0268 | R1 = 0.0174 |
| | wR2 = 0.0456 | wR2 = 0.0882 | wR2 = 0.1100 | wR2 = 0.0644 | wR2 = 0.0863 | wR2 = 0.0611 | wR2 = 0.0413 |

## NMR Spectra

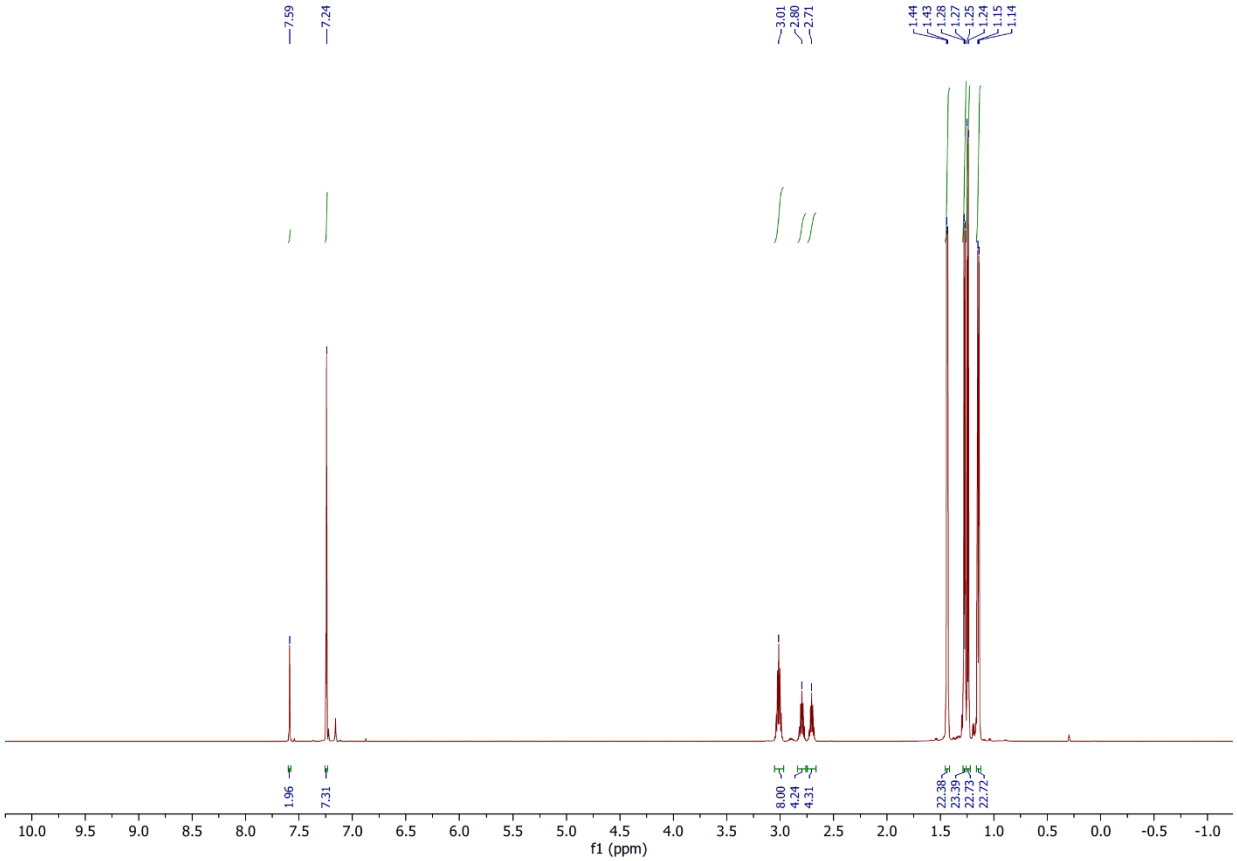


**Figure 2.S1.** $^{1}$H NMR spectrum of $\{Pb(\mu\text{-}Br)Ar^{iPr8}\}_2$ (**2**) in $C_6D_6$ at 25°C.

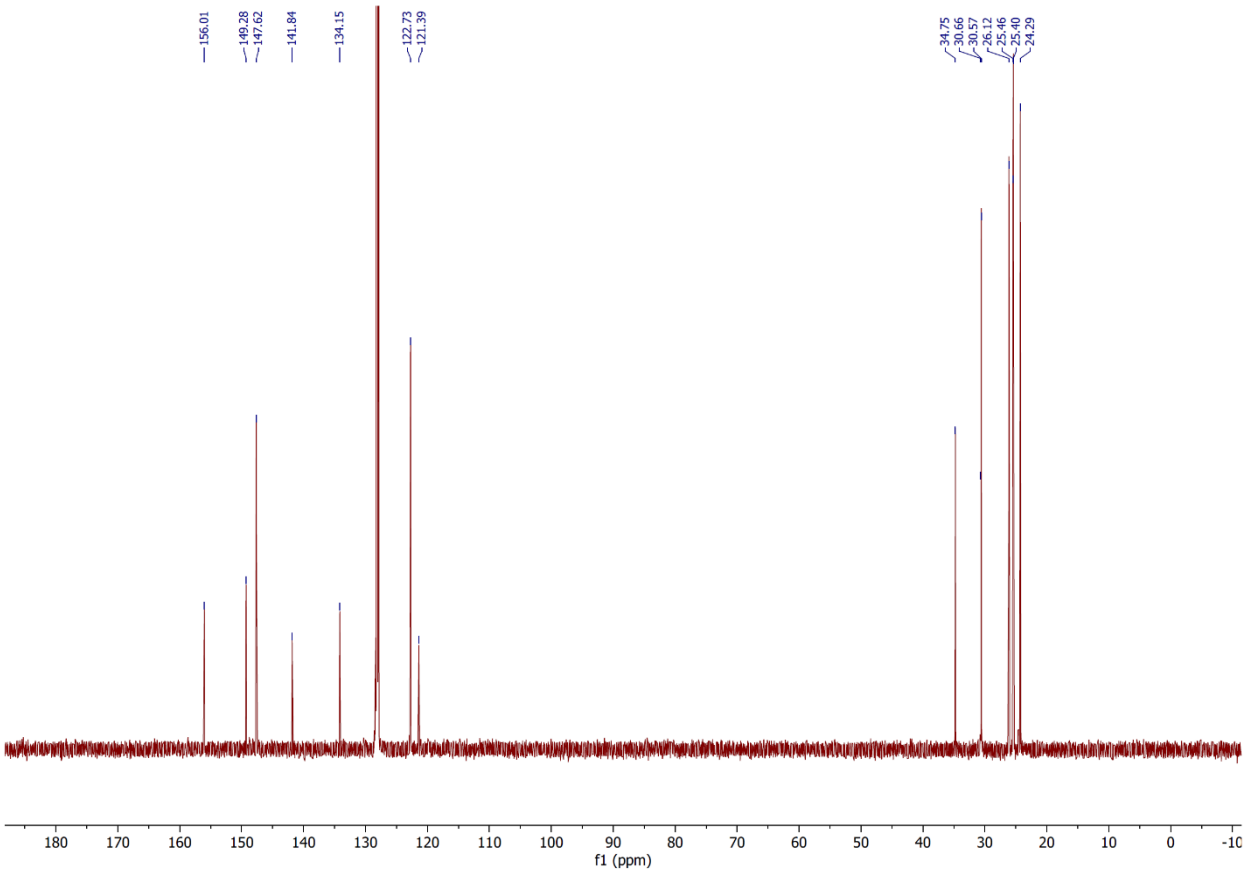


**Figure 2.S2.** $^{13}C\{^{1}H\}$ NMR spectrum of $\{Pb(\mu\text{-}Br)Ar^{iPr8}\}_2$ (**2**) in $C_6D_6$ at 25°C.

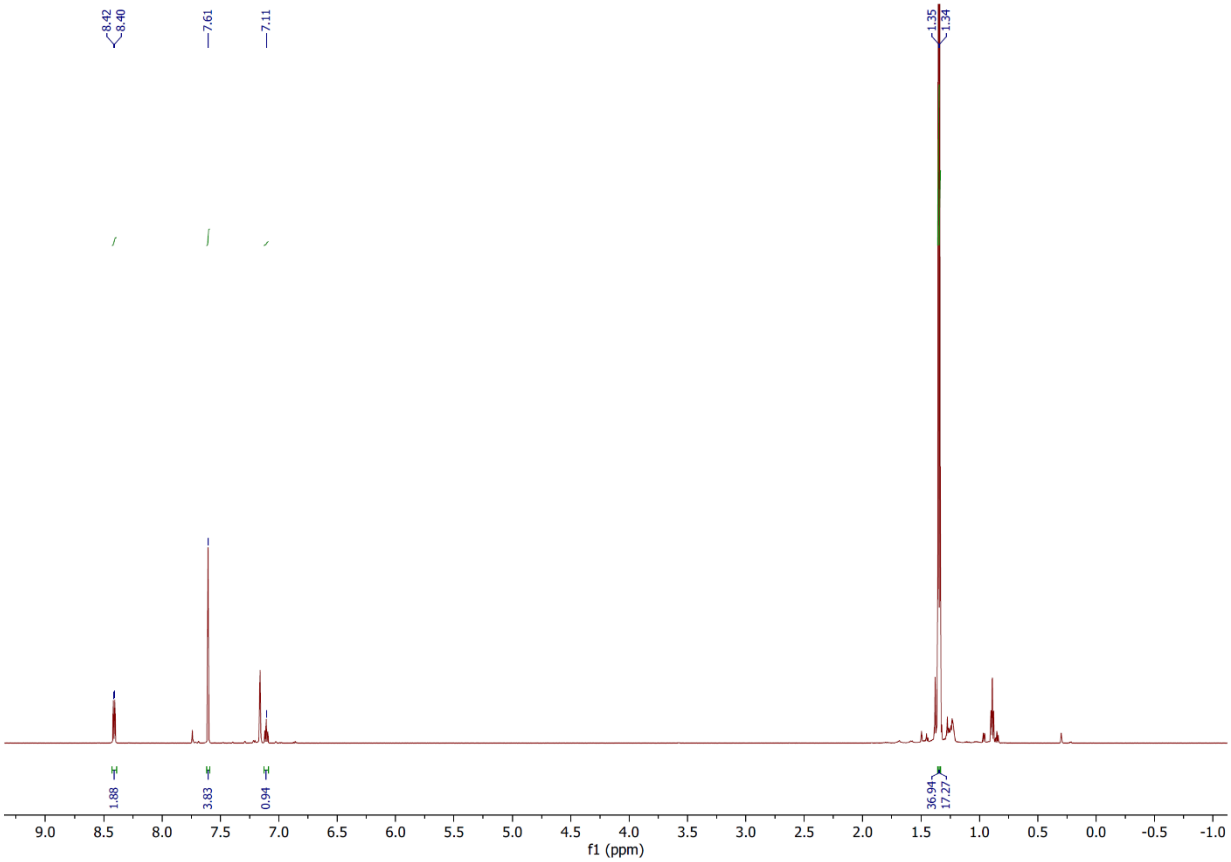


**Figure 2.S3.** $^{1}$H NMR spectrum of {Pb(μ-Br) Ar$^{tBu6}$}$_2$ (**3**) in $C_6D_6$ at 25°C.

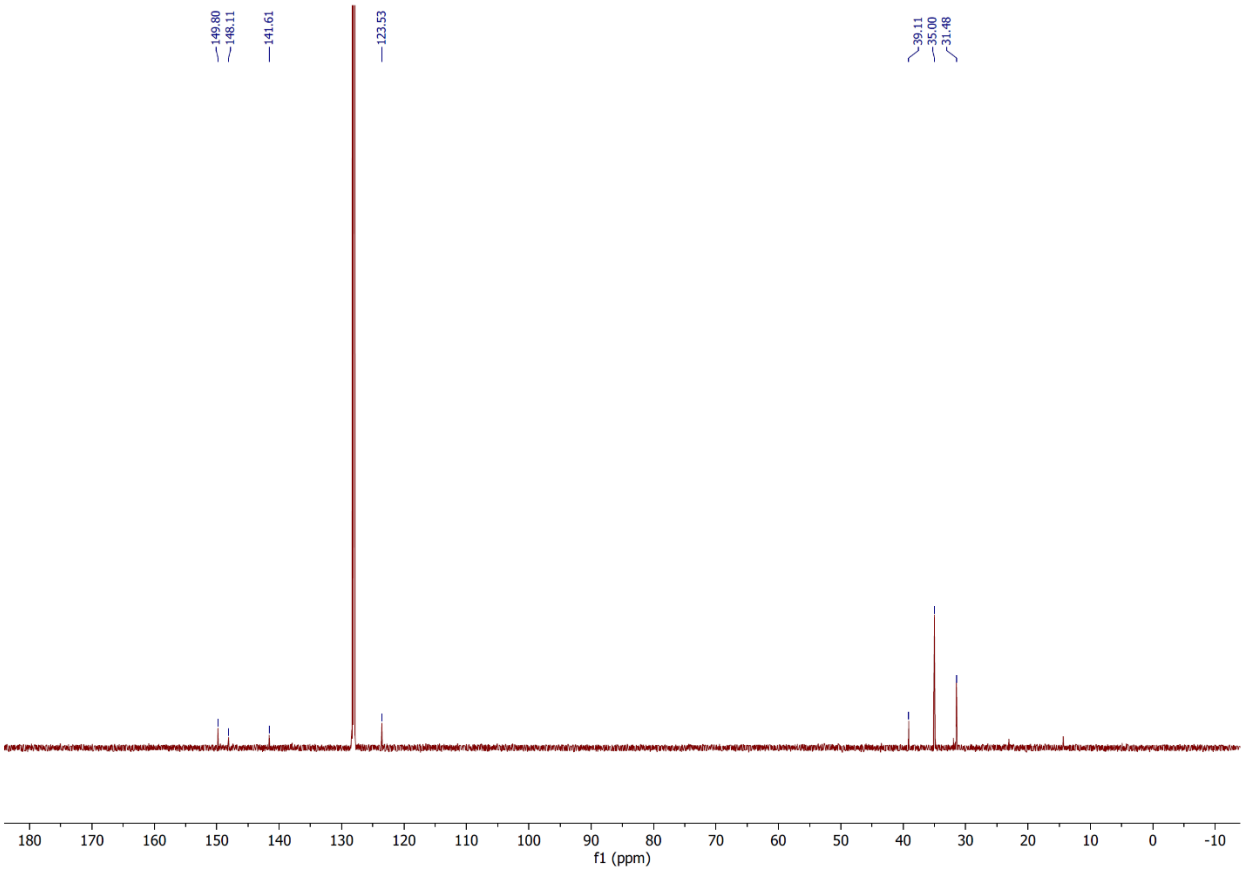


**Figure 2.S4.** $^{13}C\{^{1}H\}$ NMR spectrum of $\{Pb(\mu\text{-}Br)Ar^{tBu6}\}_2$ (**3**) in $C_6D_6$ at 25°C.

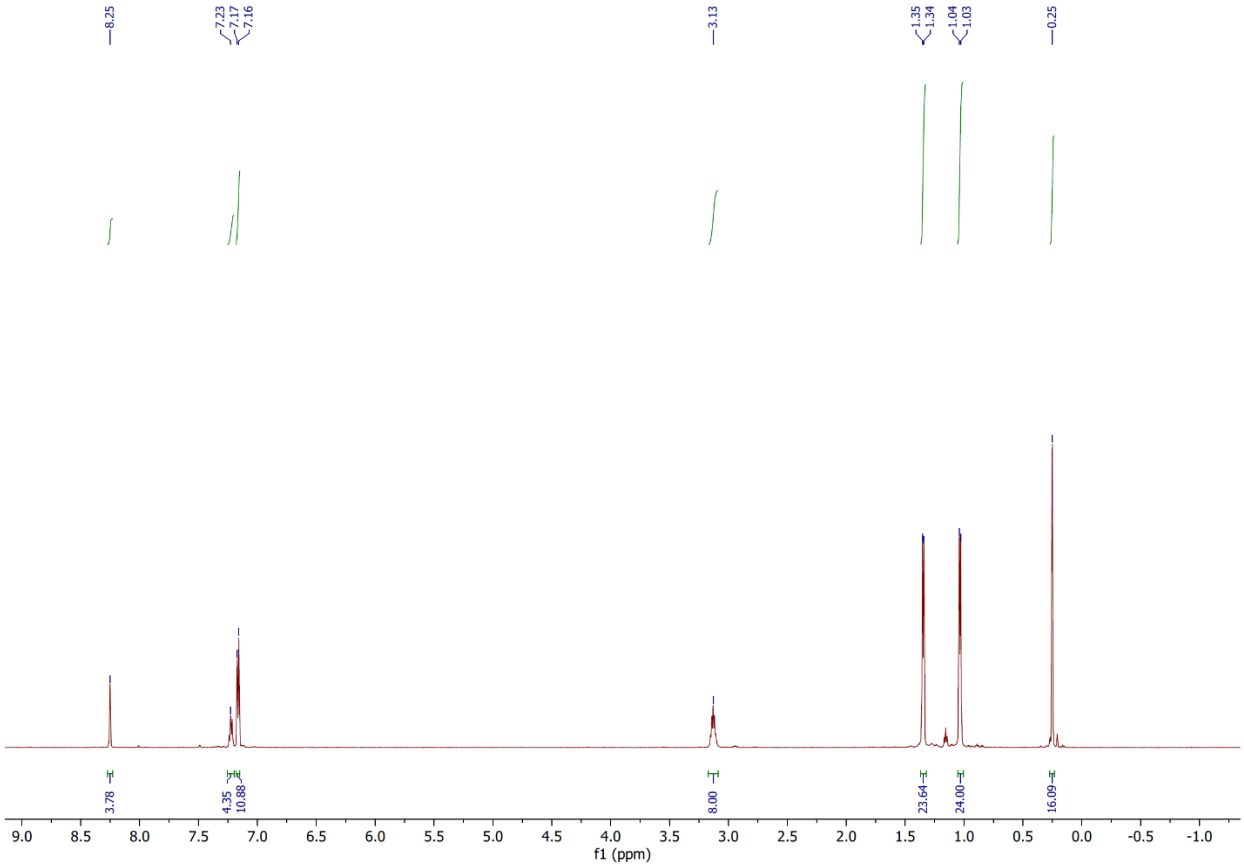


**Figure 2.S5.** $^{1}$H NMR spectrum of $\{Pb(\mu\text{-}Br)(4\text{-}SiMe_3\text{-}Ar^{iPr4})\}_2$ (**4**) in $C_6D_6$ at 25°C.

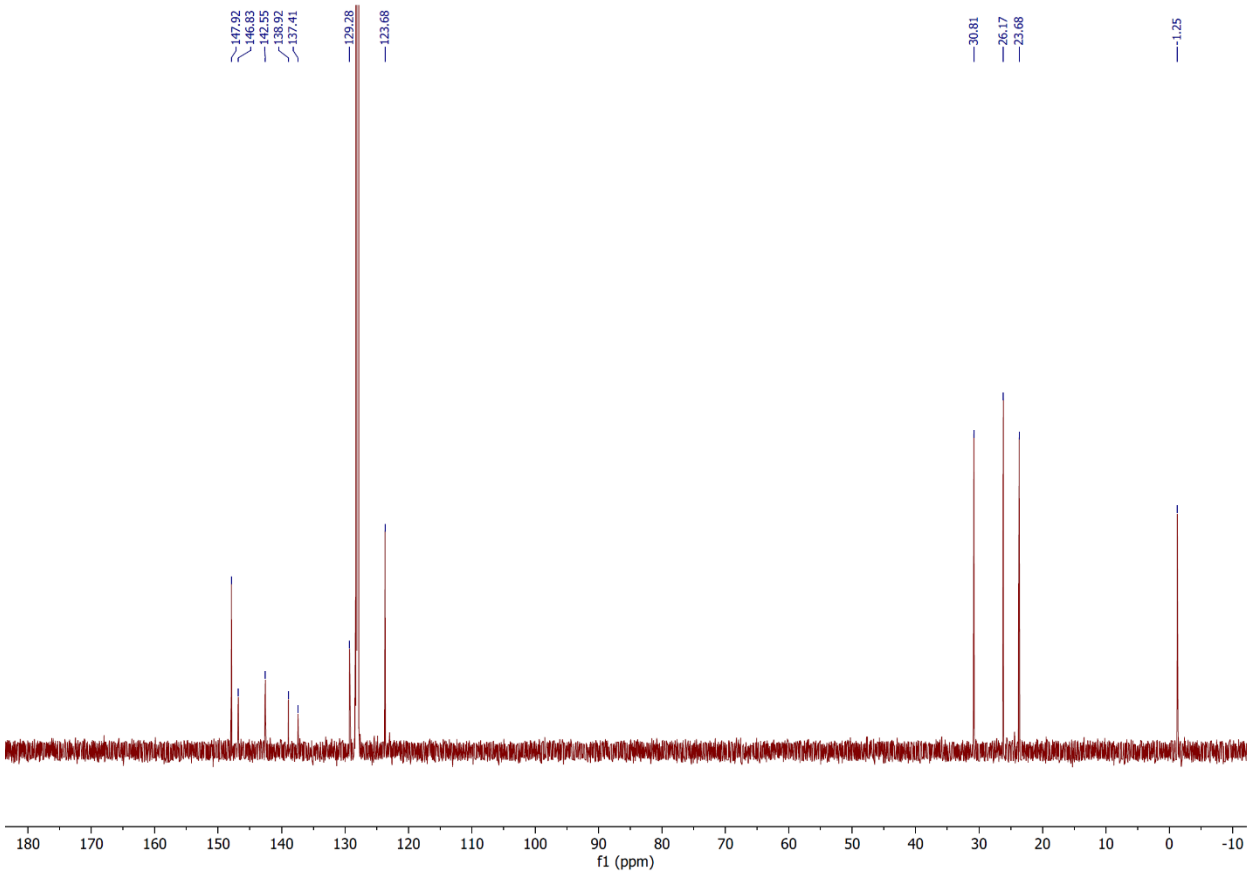


**Figure 2.S6.** $^{13}C\{^{1}H\}$ NMR spectrum of $\{Pb(\mu\text{-}Br)(4\text{-}SiMe_3\text{-}Ar^{iPr4})\}_2$ (**4**) in $C_6D_6$ at 25°C.

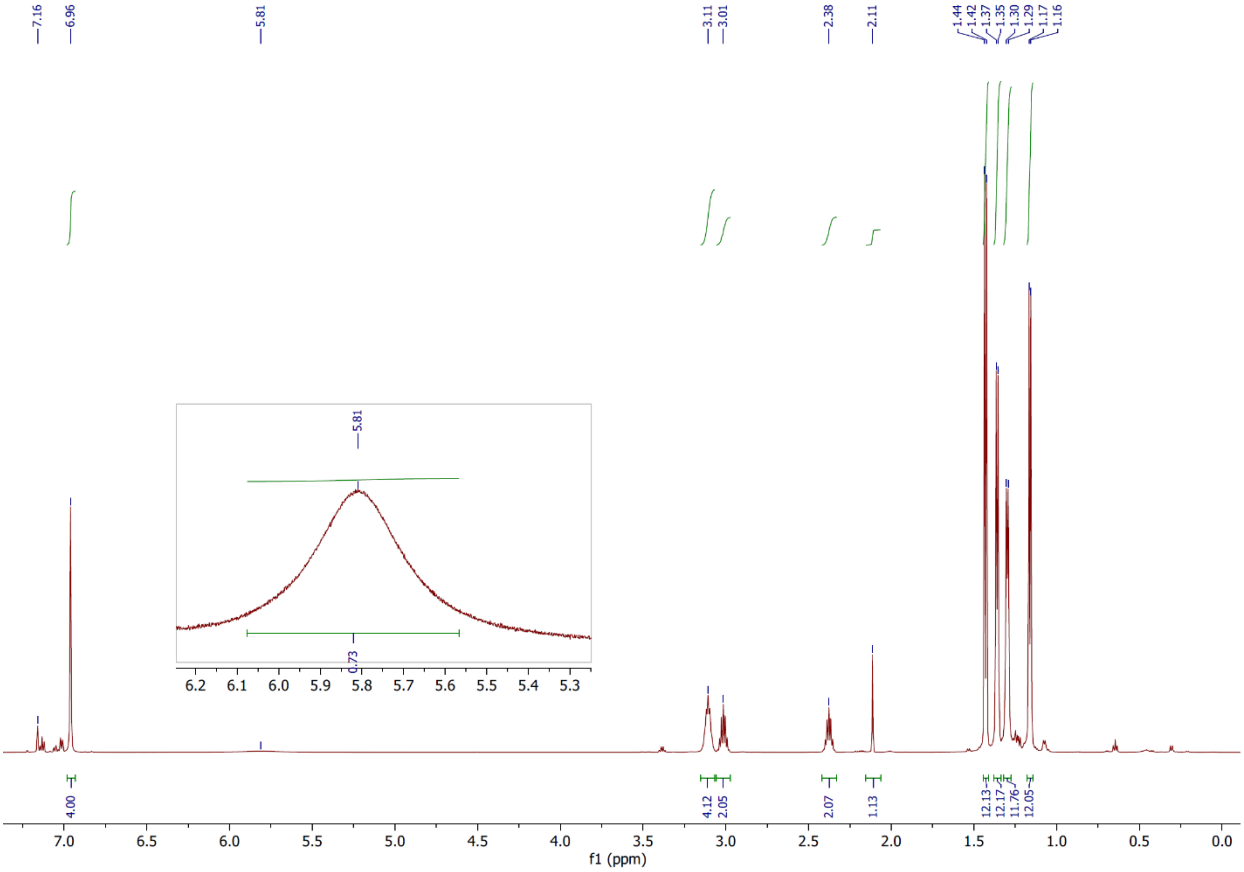


**Figure 2.S7.** $^{1}$H NMR spectrum of $(PbAr^{iPr8})_2$ (**5**) in $C_6D_6$ at 25°C. Inset shows the resonance of the para-H on the central aryl ring.

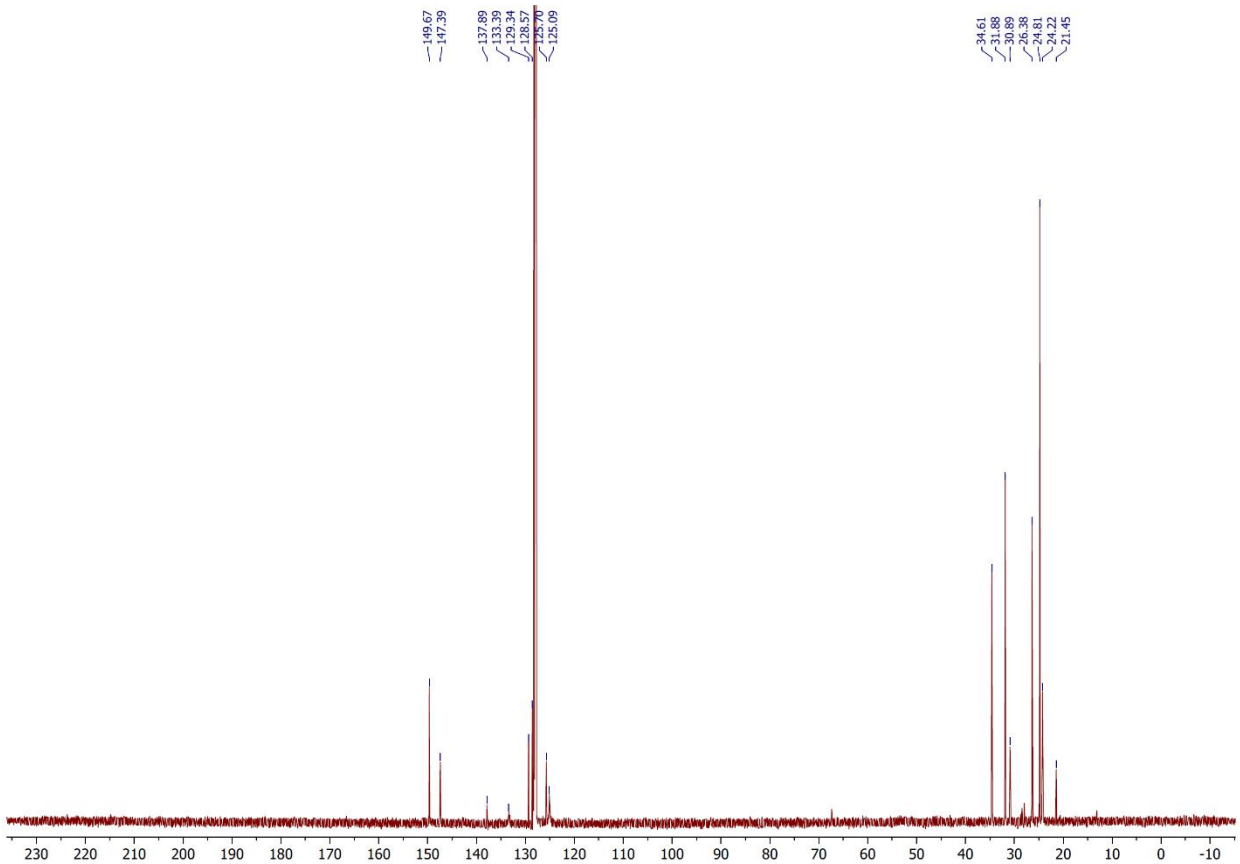


**Figure 2.S8.** $^{13}C\{^{1}H\}$ NMR spectrum of $(PbAr^{iPr8})_2$ (5) in $C_6D_6$ at 25°C.

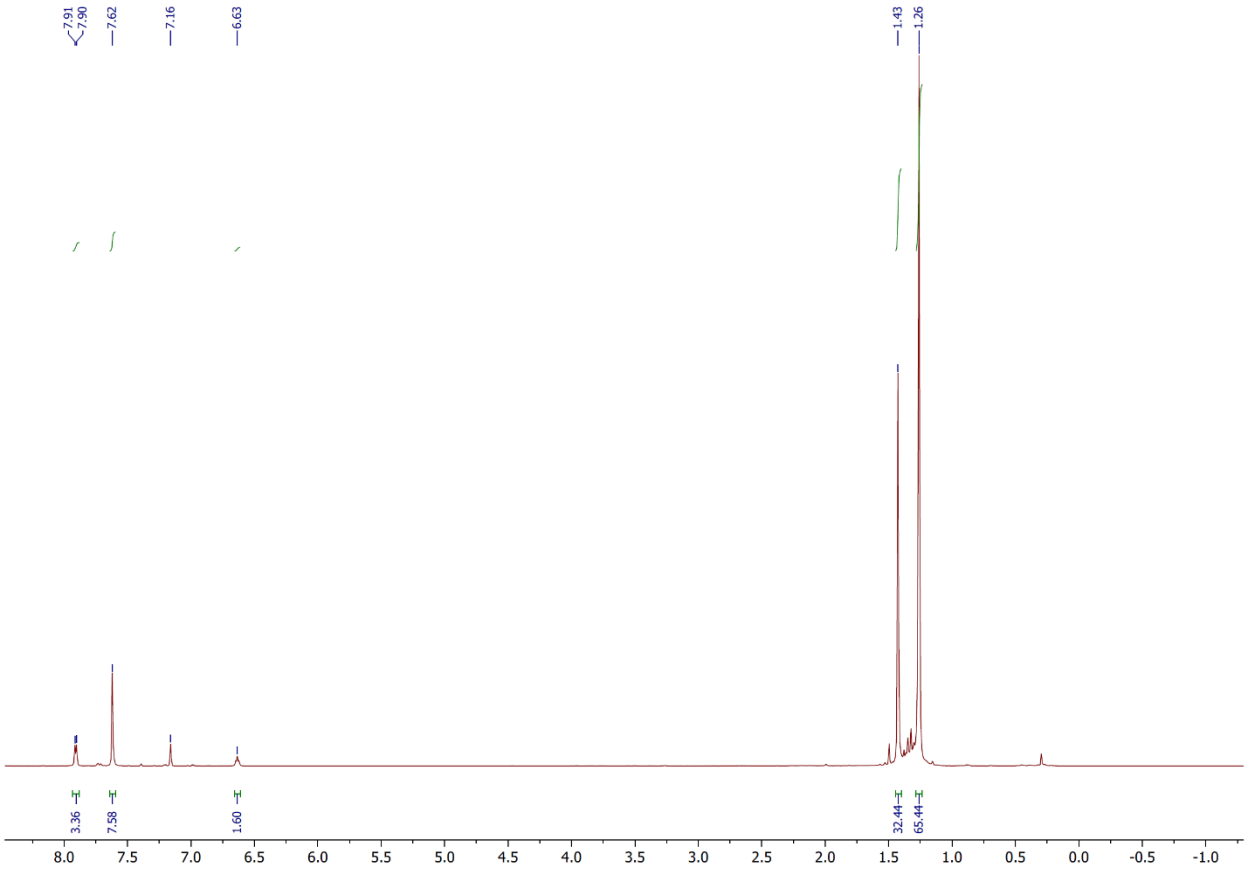


**Figure 2.S9**. $^{1}$H NMR spectrum of $(PbAr^{tBu6})_2$ (**6**) in $C_6D_6$ at 25°C.

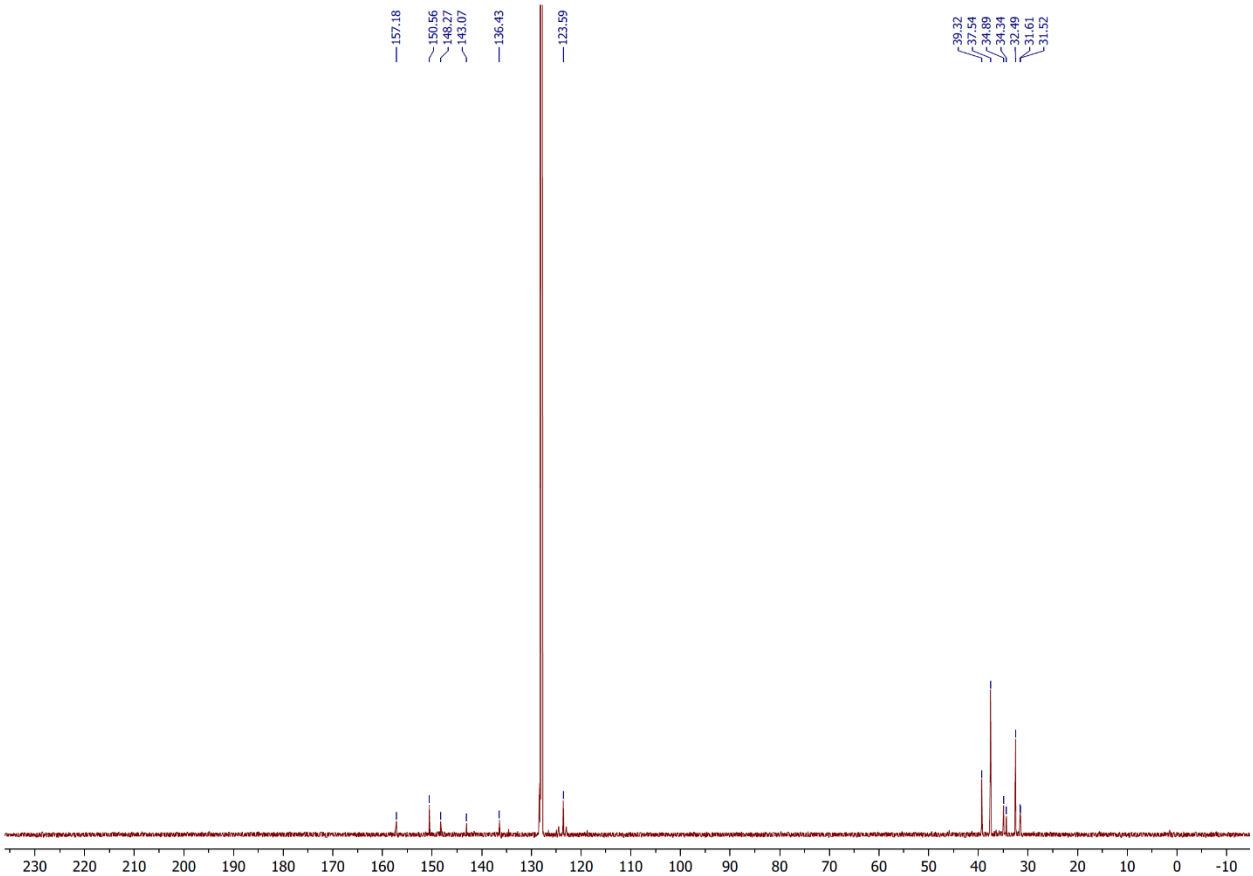


**Figure 2.S10.** $^{13}C\{^{1}H\}$ NMR spectrum of $(PbAr^{tBu6})_2$ (**6**) in $C_6D_6$ at 25°C.

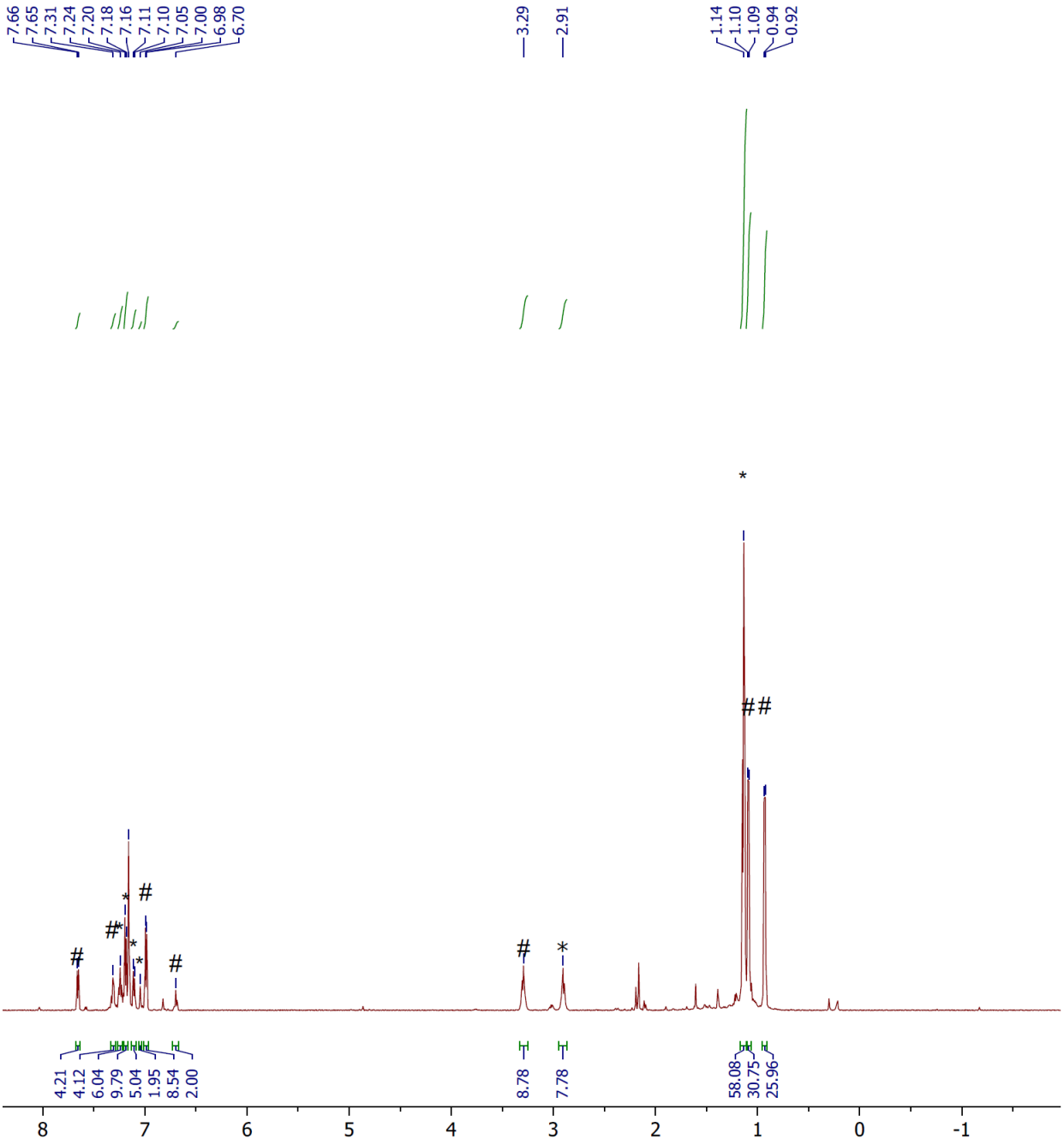


**Figure 2.S11.** $^{1}$H NMR spectrum of $(PbAr^{iPr4})_2$ (**7**, #) + $Ar^{iPr4}H$ (*) in $C_6D_6$ at 25°C.

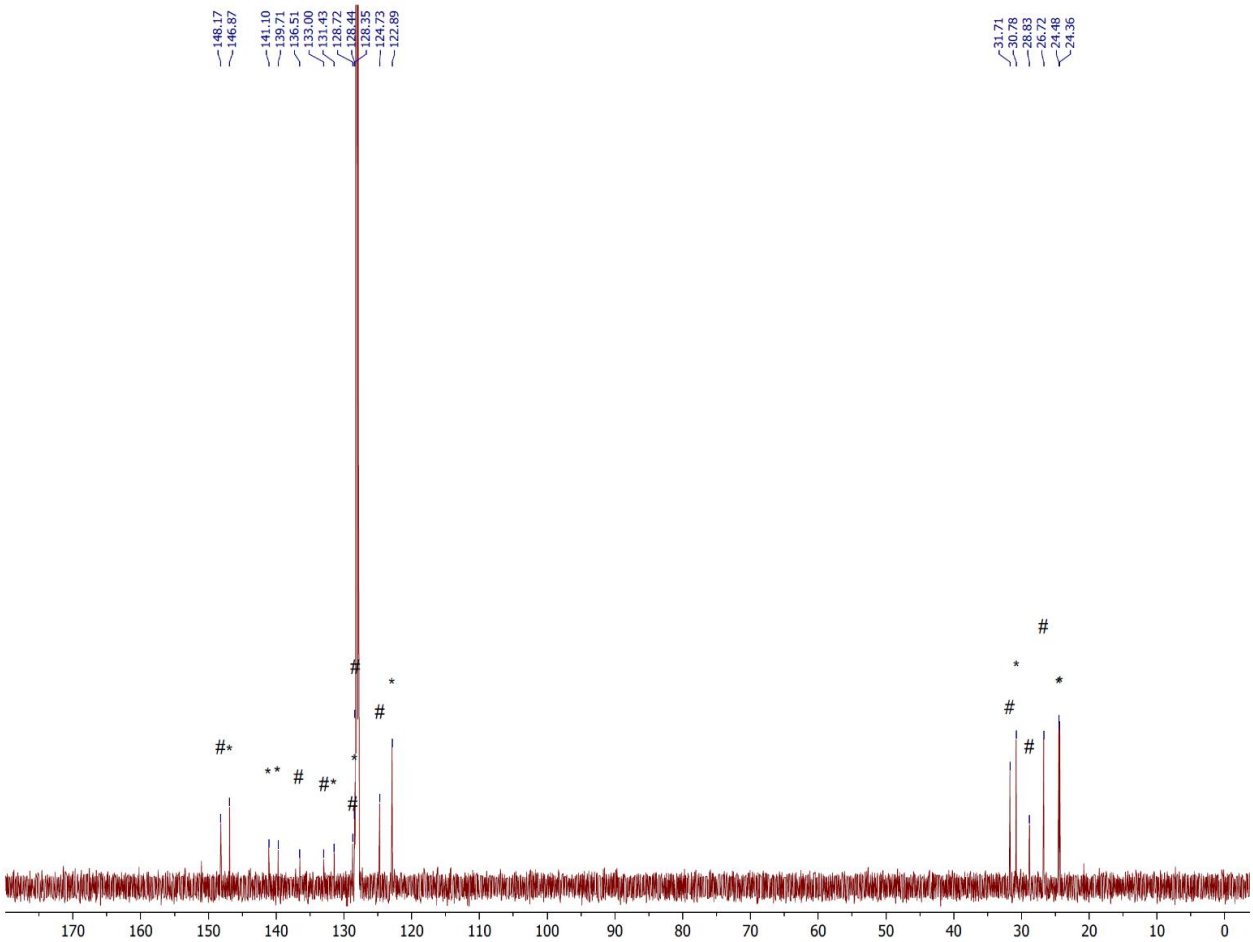


**Figure 2.S12.** $^{13}C\{^{1}H\}$ NMR of $(PbAr^{iPr4})_2$ (**7, #**) + $Ar^{iPr4}H$ (*) in $C_6D_6$ at 25°C.

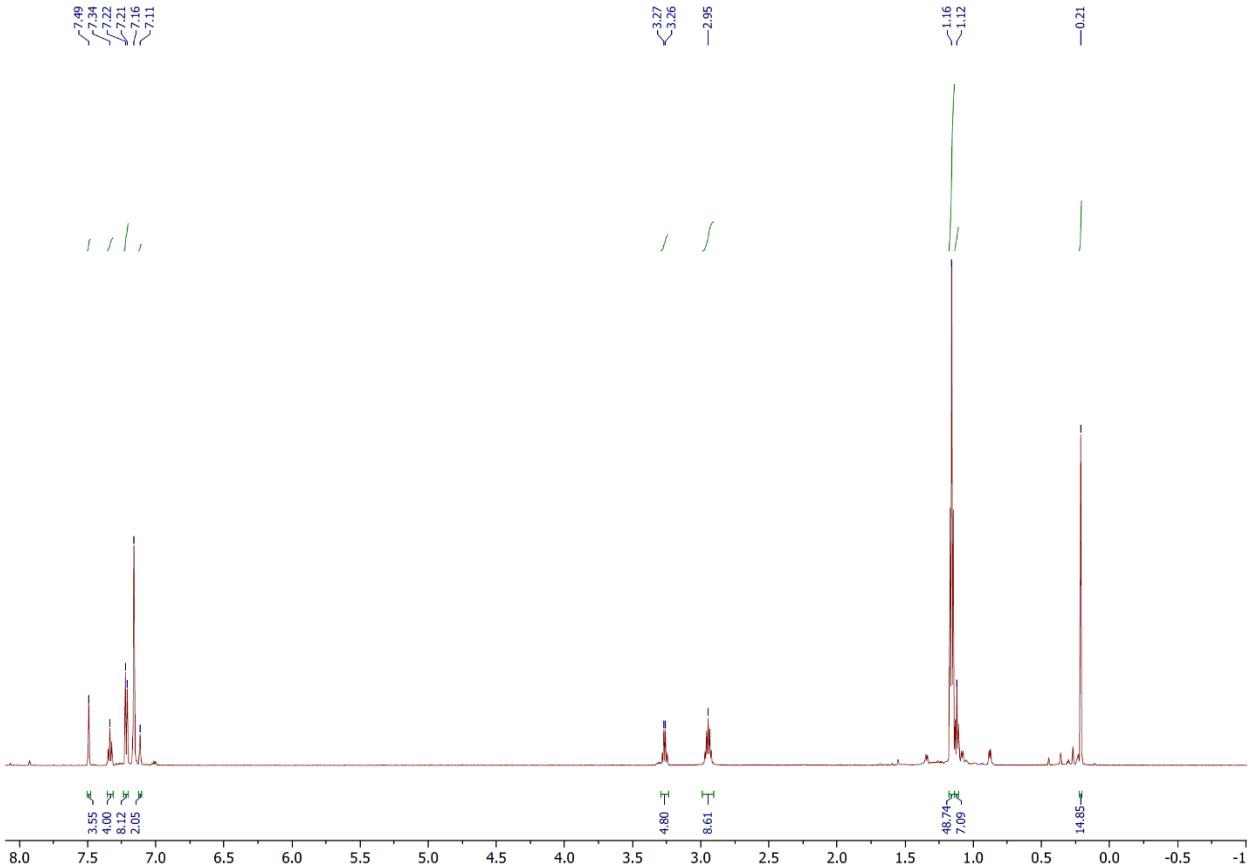


**Figure 2.S13.** $^{1}$H NMR spectrum of $\{Pb(4\text{-}SiMe_3\text{-}Ar^{iPr4})\}_2$ (**8**·$Et_2O$) in $C_6D_6$ at 25°C.

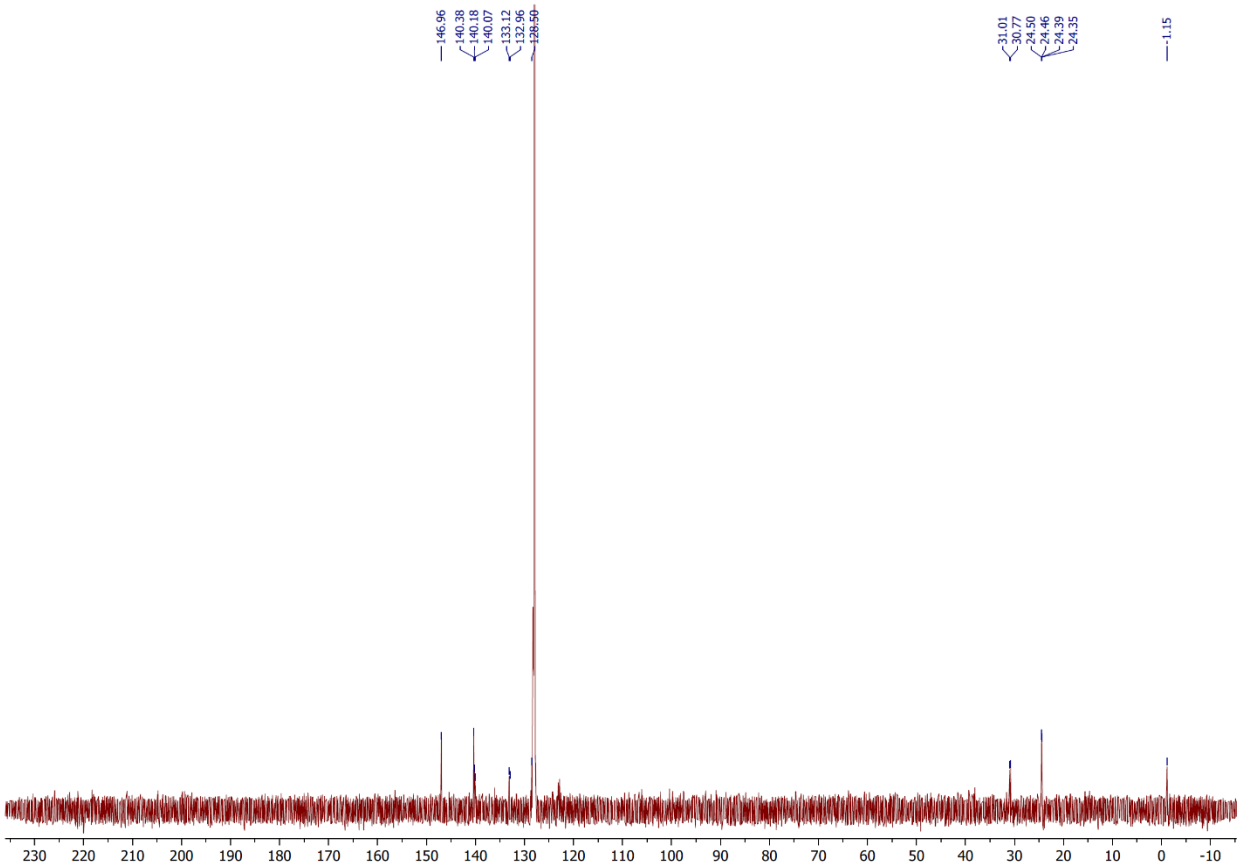


**Figure 2.S14.** $^{13}C\{^{1}H\}$ NMR spectrum of $\{Pb(4\text{-}SiMe_3\text{-}Ar^{iPr4})\}_2$ (**8**·$Et_2O$) in $C_6D_6$ at 25°C.

## UV-Visible Spectra

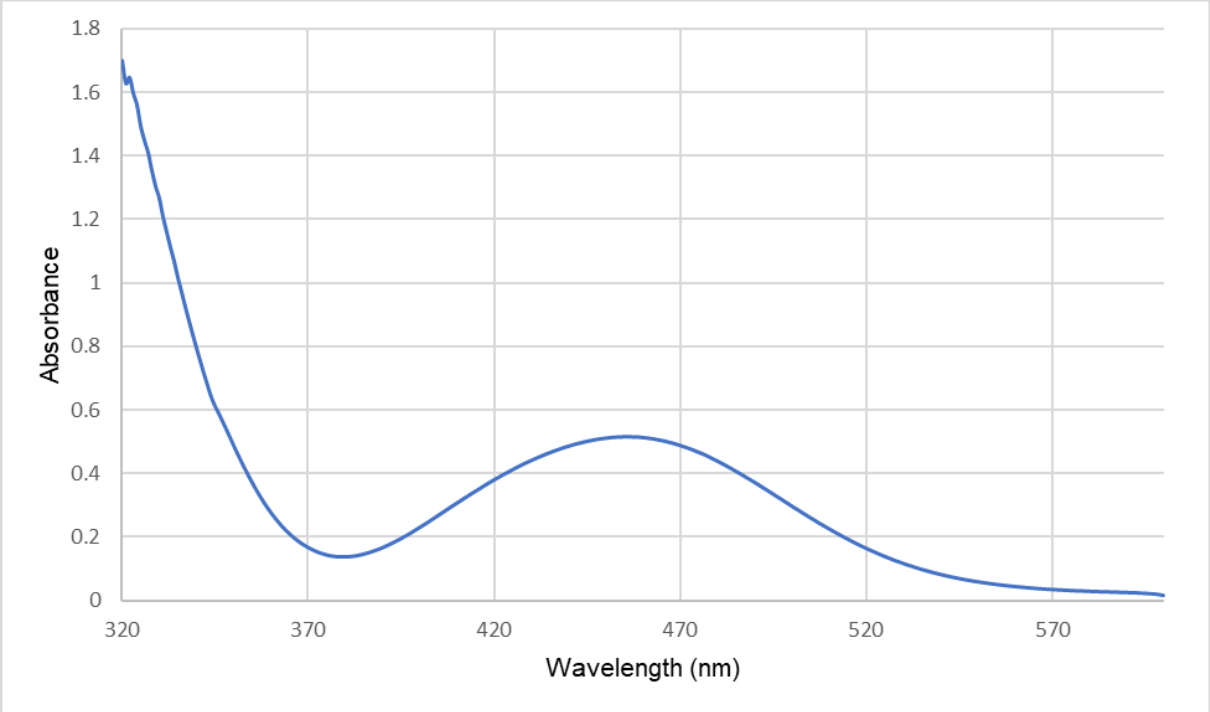


**Figure 2.S15.** UV-Visible spectrum of $\{Pb(\mu\text{-}Br)Ar^{iPr8}\}_2$ (**2**) in hexanes (685 μM).

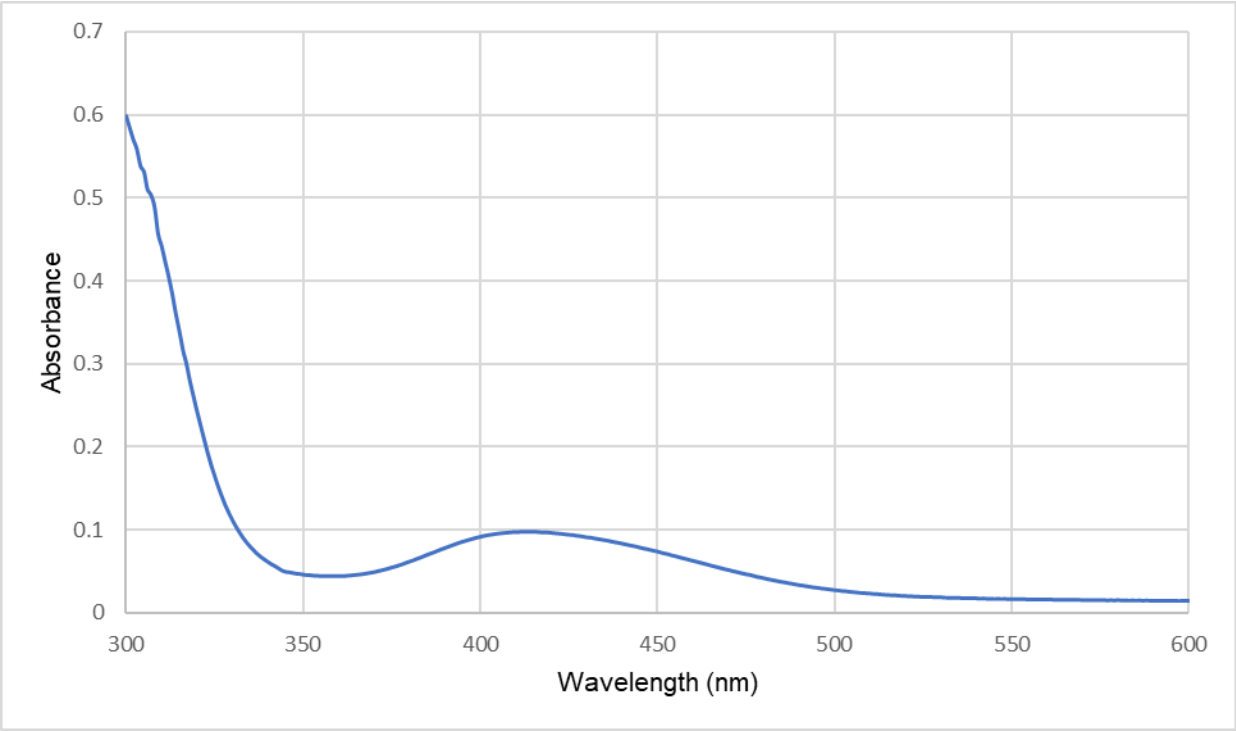


**Figure 2.S16.** UV-Visible spectrum of $\{Pb(\mu\text{-}Br)Ar^{tBu6}\}_2$ (**3**) in hexanes (101 mM).

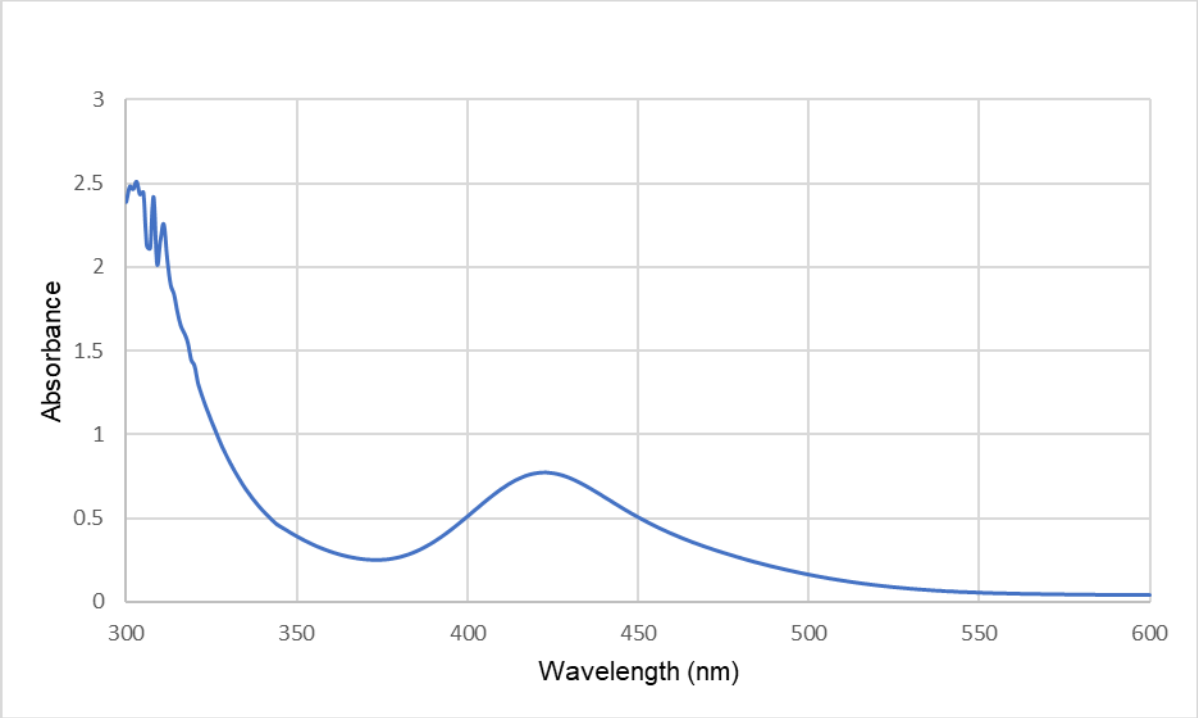


**Figure 2.S17.** UV-Visible spectrum of $\{Pb(\mu\text{-}Br)(4\text{-}SiMe_3\text{-}Ar^{iPr4})\}_2$ (**4**) in hexanes (921 μM).

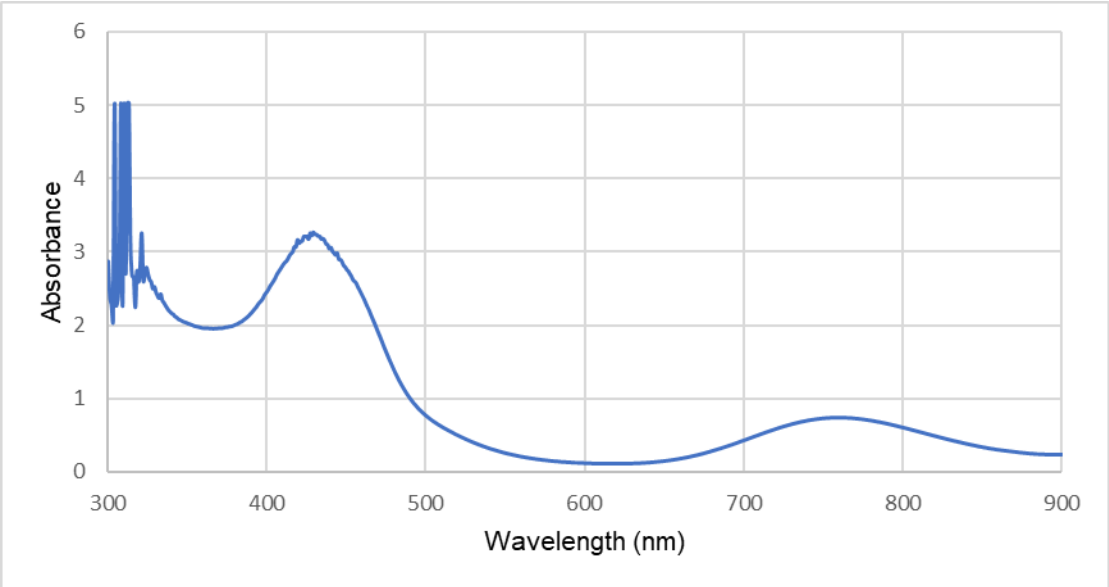


**Figure 2.S18.** UV-Visible spectrum of $(PbAr^{iPr8})_2$ (**5**) in hexanes (280 μM).

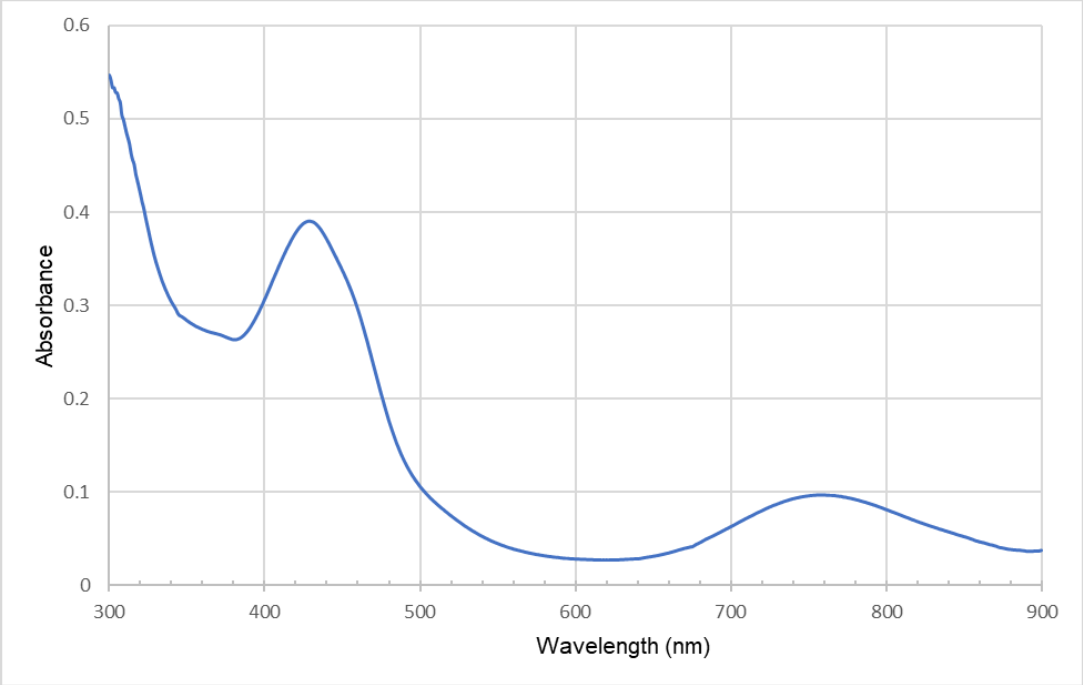


**Figure 2.S19.** UV-Visible spectrum of $(PbAr^{iPr8})_2$ (**5**) in hexanes (42.0 μM).

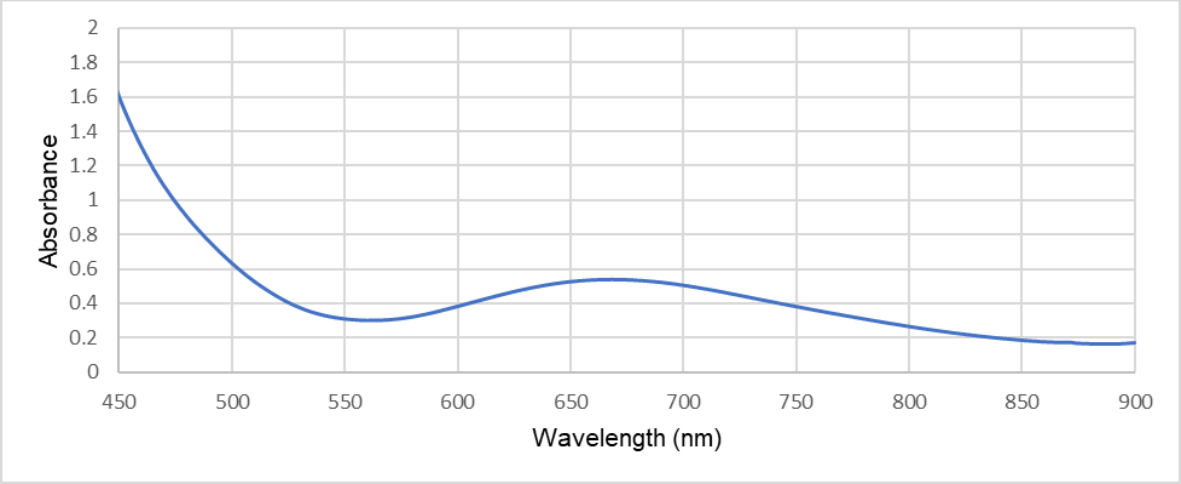


**Figure 2.S20**. UV-Visible spectrum of $(PbAr^{tBu6})_2$ (**6**) in hexanes (596 μM).

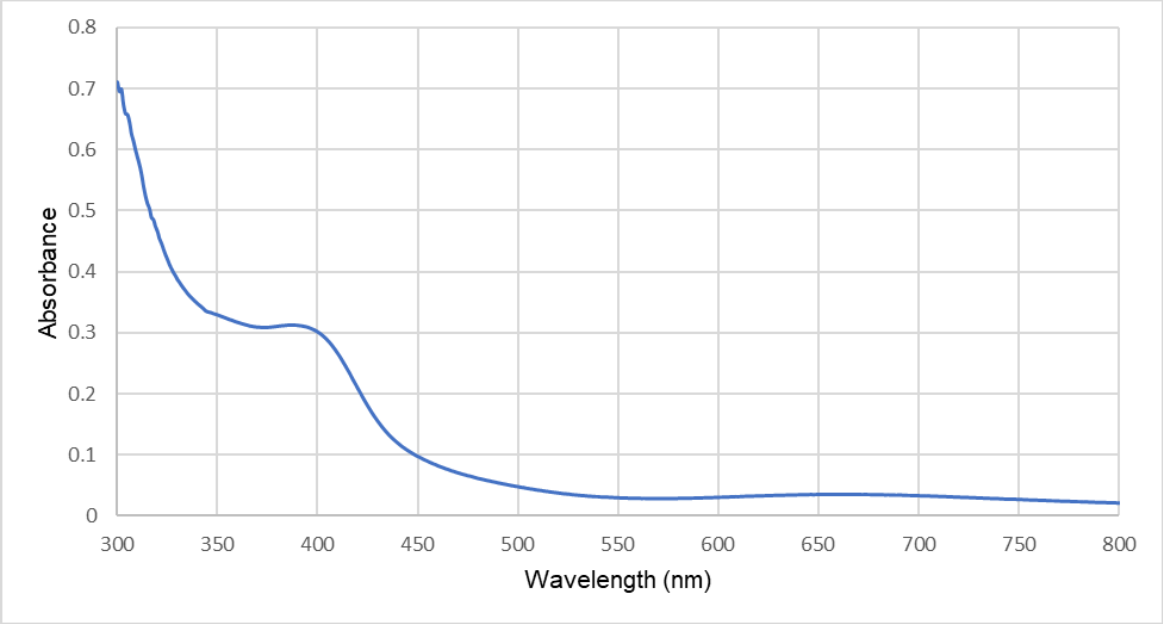


**Figure 2.S21**. UV-Visible spectrum of $(PbAr^{tBu6})_2$ (**6**) in hexanes (44.7 μM).

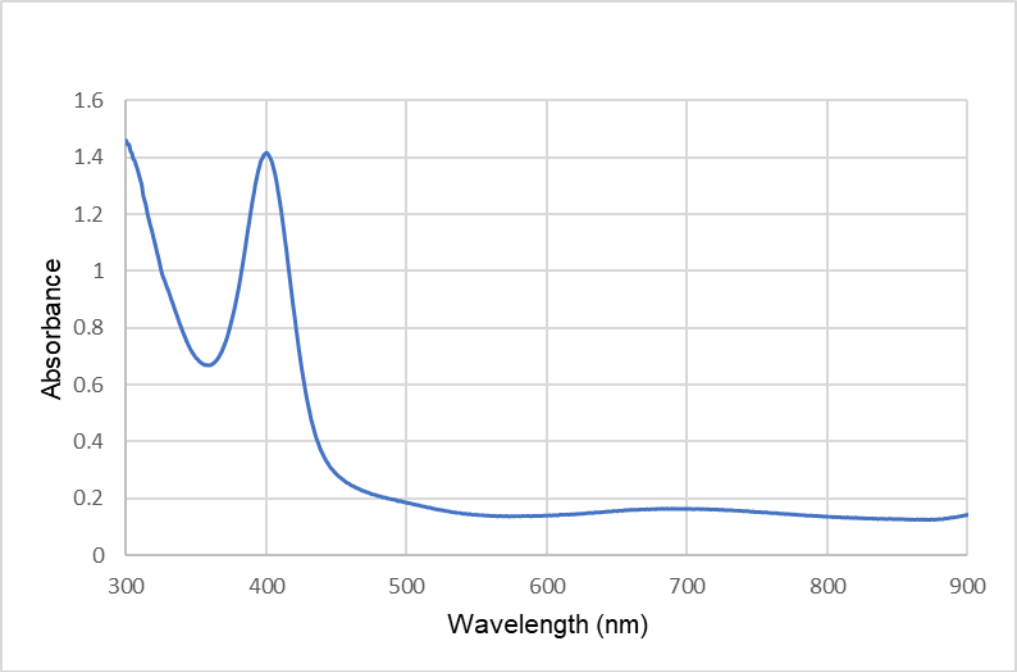


**Figure 2.S22.** UV-Visible spectrum of $(PbAr^{iPr4})_2$ (**7**) in hexanes (107μM).

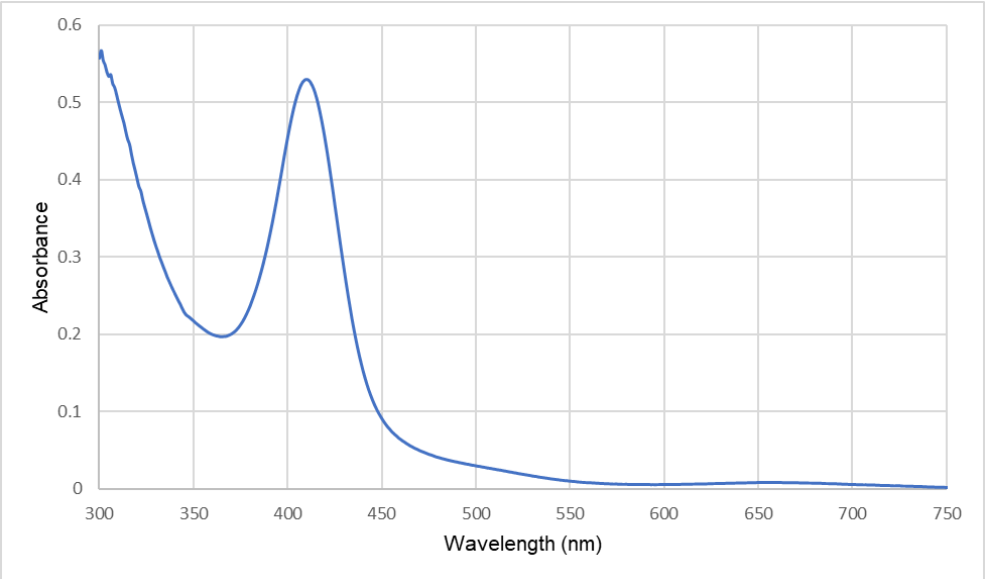


**Figure 2.S23.** UV-Visible spectrum of $\{Pb(4\text{-}SiMe_3\text{-}Ar^{iPr4})\}_2$ (**8**·$Et_2O$) in hexanes (30.3 μM).

## Crystal Structures

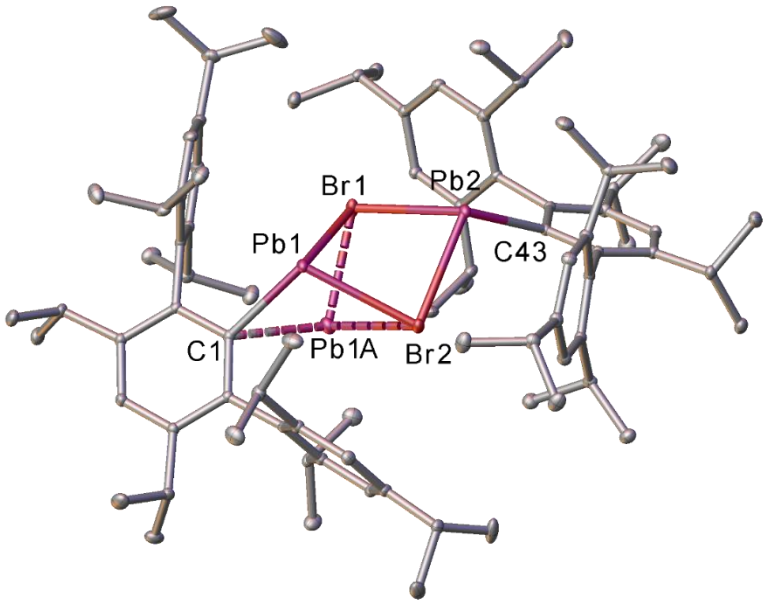


**Figure 2.S24.** Thermal ellipsoid plot of $\{Pb(Br)Ar^{iPr8}\}_2$ (**2**) (30%). H atoms not shown for clarity. Pb1 is disordered over two sites with a 1% occupancy at position Pb1A.

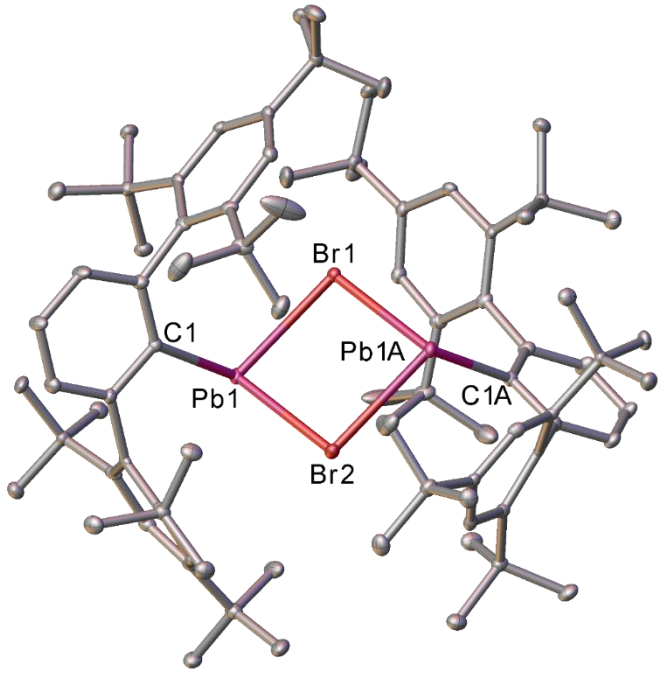


**Figure 2.S25.** Thermal ellipsoid plot of $\{Pb(\mu\text{-}Br)Ar^{tBu6}\}_2$ (**3**) (30%). H atoms not shown for clarity.

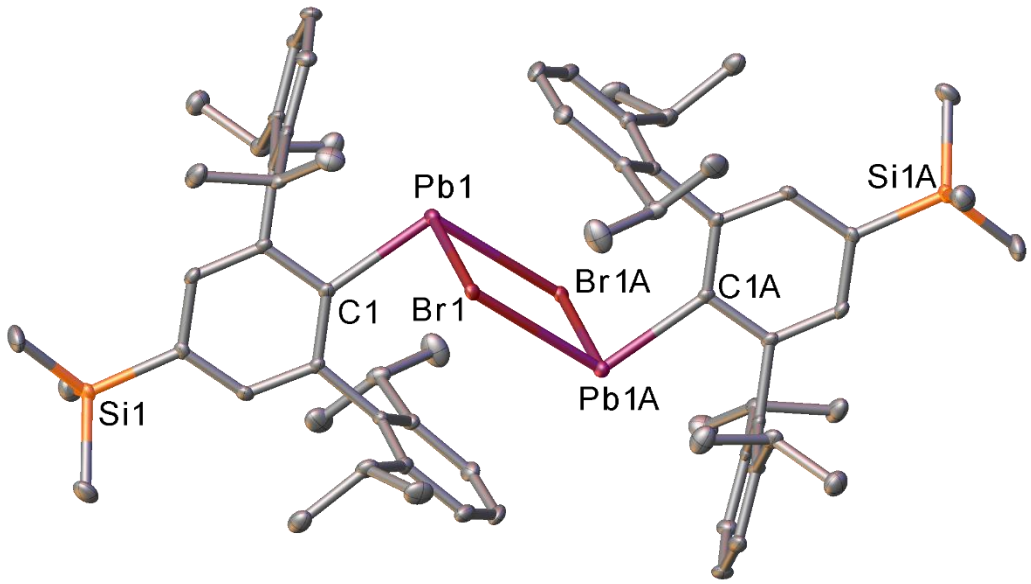


**Figure 2.S26.** Thermal ellipsoid plot of {Pb(μ-Br)(4-SiMe$_3$-Ar$^{iPr4}$)}$_2$ (**4**) (30%). H atoms not shown for clarity.

## Photos of Compounds

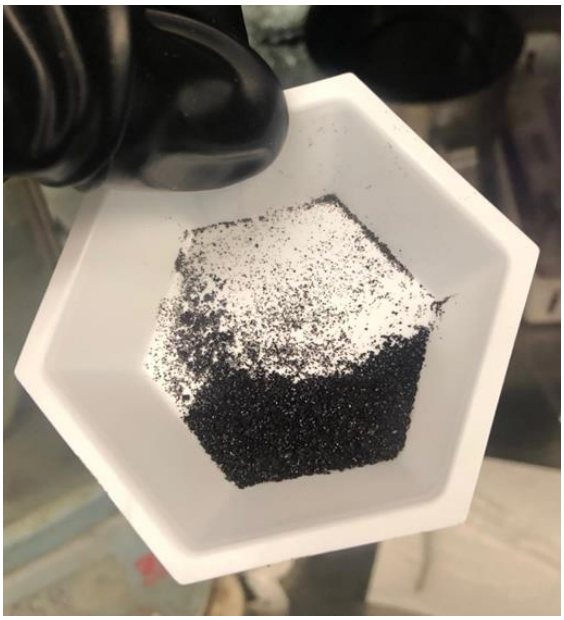

**Figure 2.S27.** Dark brown crystals of **1**.

**Figure 2.S28.** A red crystal of **5**.

**Figure 2.S29.** A green crystal of **6**.

**Figure 2.S30.** A crystal of **7** (left) and powdered **7** (right).

**Figure 2.S31.** A crystal of **8** under a microscope illustrating their dichroic character.

## Computational Details

### General remarks, geometry optimizations, energy calculations and vibrational frequency calculations

All visualizations of structures, MOs and NBOs were created with UCSF Chimera[S3] 1.10.2.

Quantum mechanical calculations were performed with the TURBOMOLE 7.0.2[S4,S5], ORCA 4.1[S6,S7] and xtb 6.1.0[S8] program packages unless otherwise stated.[S5,S9,S10] Geometries were pre-optimized with the GFN2-xTB[S11] extended tight binding method and finally optimized using the TPSS[S12] meta-GGA functional in combination with the triple-ζ def2-TZVP[S13] basis set. The numerical quadrature grid m4 grid was employed for the integration of the exchange-correlation contributions and default convergence criteria for energies and gradients were applied as implemented in TURBOMOLE. The default Stuttgart-Dresden effective core potential ecp-46[S14] was applied for all Pb atoms. All structures were pre-optimized applying the fast and robust GFN2-xTB[S11] Tight-Binding quantum mechanical method. Minimum structures were verified as minima on the potential energy hyper surface by the absence of imaginary frequencies ($i\omega > 35$ $cm^{-1}$) in the harmonic frequency calculation. Imaginary frequencies below this threshold were inverted and included in the thermostatistical correction calculation.

All geometry optimizations and single point energy calculations were performed applying the resolution-of-identity (RI) approximation for Coulomb integrals[S15] with matching default auxiliary basis sets.[S16] The D3[S17] and D4(EEQ)[S18,S19] dispersion correction schemes applying Becke-Johnson (BJ) damping[S20,S21] and including Axilrod-Teller-Muto (ATM)[S22,S23] type three-body dispersion to the total dispersion energy was applied (D3(BJ)-ATM generally applied for geometry optimizations). For a review on this topic see Ref. S24

Ro-vibrational corrections to obtain free energies were obtained from a modified rigid rotor harmonic oscillator statistical treatment[S25] ($T$ = 25.0 °C, 1 atm pressure) based on harmonic frequencies calculated at the geometry optimization level (TPSS-D3(BJ)-ATM/def2-TZVP). To avoid errors in the harmonic approximation, frequencies with wave numbers below 100 $cm^{-1}$ were treated partially as rigid rotors.[S25]

Final gas phase single point energies were calculated with the PBE0[S26] and B3LYP[S27] hybrid functionals with the large polarized quadruple-ζ Gaussian AO basis set def2-TZVPP[S13]and the m5 grid.

**Solvation corrections and Gibbs free energies**

Solvation effects were further considered by the COSMO-RS[S28,S29] model, used as implemented in COSMOtherm (Version C3.0, release 16.01)[S30] with the 2016 parameterization for toluene (parameter file: BP_TZVP_C30_1601.ctd; default $G_{solv}$ option). Calculated solvation corrections were further corrected for the volume work of 1 bar to 1 M ideal gas. The default BP86[S31,S32]/def-TZVP[S33] level of theory was used for single point calculations on the optimized geometries.

Final Gibbs free energies were obtained by summing the gas phase single point energy $E$, the dispersion correction $E_{Disp.}$, the ro-vibrational correction $G_{RRHO}$ and the solvation correction $\delta G_{solv}$ (Eq. 2.S1).

$G_{tot.} = E + E_{Disp.} + G_{RRHO} + \delta G_{solv., corr.}$ (Equation 2.S1)

**NBO analysis**

NBO analyses were carried out with the NBO6[S34] program package implementation in ORCA 4.1 at the geometry optimization level of theory.

**UV/vis spectra and molecular dynamics simulations**

UV/vis spectra were calculated applying simplified Tamm-Dancoff approximated[S35] time-dependent density functional theory (sTD-DFT) (ORCA 4.1). For the sTD-DFT calculations the BHLYP[S36] hybrid functional was applied with the triple-ζ def2-TZVP[S13] basis set. The RIJCOSX[S37] approximation (GridX6) was applied to accelerate the sTD-DFT calculations. All UV/vis spectra were calculated applying the conductor-like polarizable continuum solvation model[S38] (CPCM) for *n*-hexane.

To obtain averaged UV/vis spectra molecular dynamics (MD) simulations at GFN2-xTB(GBSA(toluene)) level were carried out starting from the corresponding DFT structures. The simulations were carried out for 1000 ps with preceding equilibration for 100 ps. A time step of 1 fs was used and the SHAKE[S39,S40] algorithm was applied, constraining all hydrogen containing bonds. From the resulting trajectory 200 snapshots were taken equidistantly and used as structural input for sTDA-xTB calculations. A standard threshold of 7 eV was applied for the sTDA part. The MD averaged absorption spectrum results from a mean over all individual spectra of the snapshots.

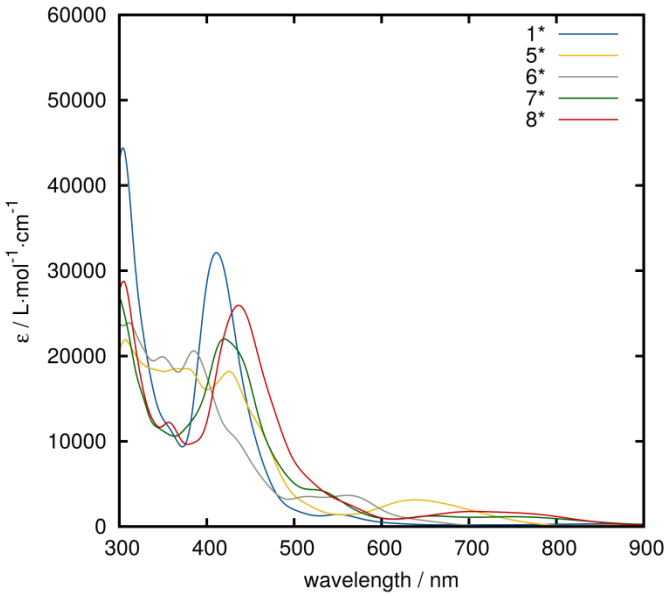


**Figure 2.S32.** Molecular dynamics averaged UV/vis spectra of all generated structures at sTD-BHLYP(CPCM(*n*-hexane) level.

## Tabulated data

**Table 2.S2.** Structure scan data for the model system Ph-Pb-Pb-Ph.

| **ϑ(C-Pb-Pb-C)** / ° | **φ(C-Pb-Pb)** / ° | **E(TPSS-D3(BJ)-ATM/def2-TZVP** / **kcal·mol$^{-1}$** | **d(Pb-Pb)** / **Å** | **ΣE(2)** / **kcal·mol$^{-1}$** | **NPA/NLMOBO** | **$E_{exc.}$(HOMO→LUMO+1)** / **eV** |
|---|---|---|---|---|---|---|
| 100 | 100 | -849.207 | 3.086 | 0.00 | 1.04 | 1.92 |
| 100 | 105 | -849.205 | 3.072 | 1.23 | 1.07 | 1.87 |
| 100 | 110 | -849.203 | 3.046 | 2.14 | 1.10 | 1.82 |
| 100 | 115 | -849.201 | 3.011 | 3.66 | 1.15 | 1.77 |
| 100 | 120 | -849.198 | 2.972 | 5.99 | 1.21 | 1.72 |
| 100 | 125 | -849.196 | 2.938 | 9.09 | 1.26 | 1.69 |
| 100 | 130 | -849.193 | 2.912 | 12.52 | 1.32 | 1.75 |
| 100 | 90 | -849.210 | 3.062 | 0.00 | 1.02 | 1.99 |
| 100 | 95 | -849.205 | 3.072 | 1.23 | 1.07 | 1.87 |
| 110 | 100 | -849.206 | 3.100 | 0.00 | 1.04 | 2.02 |
| 110 | 105 | -849.204 | 3.077 | 1.25 | 1.07 | 1.97 |
| 110 | 110 | -849.202 | 3.043 | 2.41 | 1.11 | 1.92 |
| 110 | 115 | -849.200 | 2.997 | 4.54 | 1.17 | 1.87 |

| | | | | | | |
|---|---|---|---|---|---|---|
| 110 | 120 | -849.198 | 2.949 | 7.92 | 1.24 | 1.83 |
| 110 | 125 | -849.196 | 2.910 | 12.28 | 1.30 | 1.79 |
| 110 | 130 | -849.193 | 2.883 | 16.73 | 1.36 | 1.75 |
| 110 | 90 | -849.210 | 3.070 | 0.00 | 1.03 | 2.10 |
| 110 | 95 | -849.204 | 3.077 | 1.25 | 1.07 | 1.97 |
| 120 | 100 | -849.205 | 3.114 | 0.00 | 1.03 | 2.09 |
| 120 | 105 | -849.204 | 3.090 | 1.14 | 1.06 | 2.06 |
| 120 | 110 | -849.201 | 3.044 | 2.59 | 1.11 | 2.01 |
| 120 | 115 | -849.199 | 2.984 | 5.60 | 1.18 | 1.97 |
| 120 | 120 | -849.197 | 2.923 | 10.73 | 1.27 | 1.95 |
| 120 | 125 | -849.195 | 2.881 | 16.79 | 1.35 | 1.92 |
| 120 | 130 | -849.193 | 2.856 | 22.17 | 1.41 | 1.88 |
| 120 | 90 | -849.209 | 3.081 | 0.00 | 1.03 | 2.21 |
| 120 | 95 | -849.204 | 3.090 | 1.14 | 1.06 | 2.06 |
| 130 | 100 | -849.205 | 3.126 | 0.00 | 1.02 | 2.18 |
| 130 | 105 | -849.203 | 3.107 | 0.00 | 1.05 | 2.13 |
| 130 | 110 | -849.200 | 3.052 | 2.59 | 1.10 | 2.09 |
| 130 | 115 | -849.198 | 2.968 | 7.16 | 1.20 | 2.07 |
| 130 | 120 | -849.196 | 2.893 | 15.22 | 1.32 | 2.07 |
| 130 | 125 | -849.195 | 2.852 | 23.01 | 1.40 | 2.06 |
| 130 | 130 | -849.193 | 2.831 | 28.90 | 1.46 | 2.02 |
| 130 | 90 | -849.208 | 3.097 | 0.00 | 1.02 | 2.30 |
| 130 | 95 | -849.203 | 3.107 | 0.00 | 1.05 | 2.13 |
| 140 | 100 | -849.204 | 3.141 | 0.00 | 1.02 | 2.25 |
| 140 | 105 | -849.202 | 3.128 | 0.00 | 1.03 | 2.19 |
| 140 | 110 | -849.199 | 3.074 | 2.23 | 1.09 | 2.15 |
| 140 | 115 | -849.196 | 2.944 | 9.89 | 1.24 | 2.15 |
| 140 | 120 | -849.195 | 2.859 | 22.44 | 1.38 | 2.22 |
| 140 | 125 | -849.195 | 2.825 | 31.26 | 1.46 | 2.21 |
| 140 | 130 | -849.193 | 2.808 | 36.72 | 1.50 | 2.16 |
| 140 | 90 | -849.207 | 3.116 | 0.00 | 1.02 | 2.36 |
| 140 | 95 | -849.202 | 3.128 | 0.00 | 1.03 | 2.19 |
| 150 | 100 | -849.204 | 3.158 | 0.00 | 1.01 | 2.31 |

| | | | | | | |
|---|---|---|---|---|---|---|
| 150 | 105 | -849.201 | 3.152 | 0.00 | 1.02 | 2.24 |
| 150 | 110 | -849.197 | 3.115 | 1.38 | 1.06 | 2.19 |
| 150 | 115 | -849.194 | 2.895 | 17.13 | 1.31 | 2.31 |
| 150 | 120 | -849.194 | 2.824 | 33.31 | 1.45 | 2.37 |
| 150 | 125 | -849.194 | 2.800 | 41.05 | 1.51 | 2.36 |
| 150 | 130 | -849.193 | 2.790 | 44.99 | 1.55 | 2.31 |
| 150 | 90 | -849.206 | 3.137 | 0.00 | 1.01 | 2.41 |
| 150 | 95 | -849.201 | 3.152 | 0.00 | 1.02 | 2.24 |
| 160 | 100 | -849.203 | 3.172 | 0.00 | 1.00 | 2.35 |
| 160 | 105 | -849.200 | 3.176 | 0.00 | 1.01 | 2.28 |
| 160 | 110 | -849.195 | 3.168 | 0.00 | 1.03 | 1.92 |
| 160 | 115 | -849.193 | 2.829 | 34.79 | 1.43 | 2.50 |
| 160 | 120 | -849.193 | 2.795 | 46.41 | 1.51 | 2.53 |
| 160 | 125 | -849.193 | 2.781 | 51.01 | 1.55 | 2.52 |
| 160 | 130 | -849.193 | 2.776 | 52.67 | 1.58 | 2.46 |
| 160 | 90 | -849.205 | 3.158 | 0.00 | 1.00 | 2.43 |
| 160 | 95 | -849.200 | 3.176 | 0.00 | 1.01 | 2.28 |
| 170 | 100 | -849.203 | 3.183 | 0.00 | 1.00 | 2.37 |
| 170 | 105 | -849.199 | 3.194 | 0.00 | 1.00 | 2.30 |
| 170 | 110 | -849.194 | 3.210 | 0.00 | 1.00 | 2.21 |
| 170 | 115 | -849.191 | 2.789 | 53.97 | 1.52 | 2.21 |
| 170 | 120 | -849.193 | 2.775 | 58.01 | 1.56 | 2.68 |
| 170 | 125 | -849.193 | 2.769 | 58.90 | 1.59 | 2.68 |
| 170 | 130 | -849.193 | 2.767 | 58.33 | 1.60 | 2.62 |
| 170 | 90 | -849.204 | 3.175 | 0.00 | 1.00 | 2.44 |
| 170 | 95 | -849.199 | 3.194 | 0.00 | 1.00 | 2.30 |
| 180 | 100 | -849.203 | 3.186 | 0.00 | 1.00 | 2.38 |
| 180 | 105 | -849.199 | 3.202 | 0.00 | 1.00 | 2.30 |
| 180 | 110 | -849.188 | 2.783 | 63.17 | 1.52 | 2.68 |
| 180 | 115 | -849.191 | 2.774 | 63.58 | 1.55 | 2.73 |
| 180 | 120 | -849.192 | 2.768 | 63.20 | 1.58 | 2.76 |
| 180 | 125 | -849.193 | 2.765 | 62.12 | 1.60 | 2.79 |
| 180 | 130 | -849.193 | 2.765 | 60.47 | 1.61 | 2.76 |

| | | | | | | |
|---|---|---|---|---|---|---|
| 180 | 90 | -849.203 | 3.185 | 0.00 | 1.00 | 2.43 |
| 180 | 95 | -849.199 | 3.202 | 0.00 | 1.00 | 2.30 |
| 90 | 90 | -849.211 | 3.057 | 0.00 | 1.03 | 1.88 |
| 90 | 100 | -849.207 | 3.081 | 0.00 | 1.05 | 1.82 |
| 90 | 105 | -849.206 | 3.071 | 1.12 | 1.07 | 1.78 |
| 90 | 110 | -849.203 | 3.051 | 1.83 | 1.10 | 1.74 |
| 90 | 115 | -849.201 | 3.025 | 2.94 | 1.13 | 1.74 |
| 90 | 120 | -849.198 | 2.994 | 4.56 | 1.18 | 1.75 |
| 90 | 125 | -849.195 | 2.966 | 6.69 | 1.23 | 1.78 |
| 90 | 130 | -849.192 | 2.942 | 9.23 | 1.27 | 1.83 |
| 90 | 95 | -849.206 | 3.071 | 1.12 | 1.07 | 1.78 |

**Table 2.S3.** Absolute contributions to $G_{tot}$ in kcal·mol$^{-1}$. All calculations were conducted applying the $C_1$ point group. "Frag" denotes the PbR fragment in the doublet ground state.

| | **TPSS-D3(BJ)-ATM/def2-TZVP / a.u.** | **PBE0/def2-TZVPP / a.u.** | **PBE0/def2-TZVPP / kcal mol$^{-1}$** | **$E_{D3,ATM}$ (PBE0) / kcal mol$^{-1}$** | **$E_{D4,ATM}$ (PBE0) / kcal mol$^{-}$** | **B3LYP/def2-TZVPP / a.u.** | **B3LYP/def2-TZVPP / kcal mol$^{-1}$** | **$E_{D3,ATM}$ (B3LYP) / kcal mol$^{-1}$** | **$E_{D4,ATM}$ (B3LYP) / kcal mol$^{-}$** | **$G_{RRHO}$ (25.0 °C) / kcal mol$^{-1}$** | **$\delta G_{solv.,corr.}$ (*n*-hexane, 25.0 °C) / kcal mol$^{-1}$** |
|---|---|---|---|---|---|---|---|---|---|---|---|
| **1** | -3190.236741 | -3186.098803 | -1999307.18 | -179.39 | -179.66 | -3187.563546 | -2000226.32 | -320.25 | -307.07 | 864.84 | -32.93 |
| **$1_{frag}$** | -1595.082561 | -1593.037289 | -999645.99 | -75.51 | -76.43 | -1593.779013 | -1000111.43 | -138.44 | -134.09 | 421.47 | -19.09 |
| **5** | -3662.300438 | -3657.429249 | -2295071.51 | -216.18 | -216.17 | -3659.128946 | -2296138.08 | -384.29 | -368.14 | 1063.90 | -37.32 |
| **$5_{frag}$** | -1831.116954 | -1828.707630 | -1147531.36 | -93.84 | -94.78 | -1829.567212 | -1148070.76 | -170.41 | -164.82 | 520.80 | -21.47 |
| **6** | -3662.182576 | -3657.284477 | -2294980.66 | -228.36 | -228.35 | -3658.963293 | -2296034.13 | -406.80 | -389.96 | 1069.93 | -34.73 |
| **$6_{frag}$** | -1831.053437 | -1828.633157 | -1147484.63 | -98.11 | -99.12 | -1829.482243 | -1148017.44 | -178.92 | -173.24 | 524.62 | -20.71 |
| **7** | -2718.169941 | -2714.749288 | -1703530.90 | -148.39 | -149.16 | -2715.971674 | -1704297.96 | -266.86 | -256.46 | 668.23 | -28.58 |

| | | | | | | | | | | | |
|---|---|---|---|---|---|---|---|---|---|---|---|
| **7frag** | -1359.049432 | -1357.359021 | -851755.65 | -62.57 | -63.64 | -1357.978125 | -852144.14 | -115.18 | -111.97 | 323.55 | -15.84 |
| **8** | -3535.759105 | -3531.672490 | -2216157.95 | -169.41 | -169.85 | -3533.187944 | -2217108.91 | -304.11 | -291.41 | 781.29 | -30.26 |
| **8frag** | -1767.843128 | -1765.820519 | -1108069.11 | -72.62 | -73.52 | -1766.586573 | -1108549.81 | -133.14 | -128.79 | 380.06 | -17.57 |
| **1*** | -3190.236233 | -3186.097238 | -1999306.20 | -177.07 | -177.47 | -3187.559052 | -2000223.50 | -318.10 | -305.03 | 864.95 | -32.89 |
| **5*** | -3662.289317 | -3657.418458 | -2295064.73 | -216.54 | -216.76 | -3659.115764 | -2296129.81 | -385.02 | -369.01 | 1066.59 | -37.16 |
| **6*** | -3662.160717 | -3657.269768 | -2294971.43 | -223.97 | -223.56 | -3658.951788 | -2296026.91 | -399.88 | -382.73 | 1069.44 | -35.63 |
| **7*** | -2718.165176 | -2714.739554 | -1703524.79 | -147.64 | -148.66 | -2715.957071 | -1704288.79 | -266.99 | -256.67 | 667.44 | -28.17 |
| **8*** | -3535.753441 | -3531.662529 | -2216151.70 | -168.09 | -168.79 | -3533.173468 | -2217099.83 | -303.50 | -290.92 | 781.89 | -29.67 |

$\Delta E_{Disp.} = E_{Disp., complex} - (E_{Disp., fragment\ 1} + E_{Disp., fragment\ 2})$ (Equation 2.S2)

**Table 2.S4.** $\Delta E_{Disp.}$ and absolute dispersion corrections for the full complex and its unrelaxed fragments in kcal·mol$^{-1}$.

| | | **PBE0** | | **B3LYP** | |
|---|---|---|---|---|---|
| | | **D3(BJ)-ATM** | **D4(EEQ)-ATM** | **D3(BJ)-ATM** | **D4(EEQ)-ATM** |
| **1** | $E_{Disp., complex}$ | -179.39 | -179.66 | -320.25 | -307.07 |
| | $E_{Disp., fragment\ 1}$ | -74.22 | -74.86 | -136.00 | -131.34 |
| | $E_{Disp., fragment\ 2}$ | -74.22 | -74.87 | -136.01 | -131.35 |
| | $\Delta E_{Disp.}$ | -30.94 | -29.93 | -48.24 | -44.39 |
| **5** | $E_{Disp., complex}$ | -216.18 | -216.17 | -384.29 | -368.14 |
| | $E_{Disp., fragment\ 1}$ | -93.77 | -94.43 | -170.25 | -164.17 |
| | $E_{Disp., fragment\ 2}$ | -93.61 | -94.29 | -169.94 | -163.91 |
| | $\Delta E_{Disp.}$ | -28.79 | -27.45 | -44.10 | -40.07 |
| **6** | $E_{Disp., complex}$ | -228.36 | -228.35 | -406.80 | -389.96 |
| | $E_{Disp., fragment\ 1}$ | -97.19 | -98.11 | -177.19 | -171.42 |
| | $E_{Disp., fragment\ 2}$ | -98.07 | -98.56 | -178.64 | -172.10 |
| | $\Delta E_{Disp.}$ | -33.10 | -31.69 | -50.97 | -46.44 |

| | | | | | |
|---|---|---|---|---|---|
| **7** | $E_{Disp., complex}$ | -148.39 | -149.16 | -266.86 | -256.46 |
| | $E_{Disp., fragment 1}$ | -61.73 | -62.49 | -113.44 | -109.86 |
| | $E_{Disp., fragment 2}$ | -61.73 | -62.50 | -113.44 | -109.86 |
| | $\Delta E_{Disp.}$ | -24.94 | -24.17 | -39.97 | -36.74 |
| **8** | $E_{Disp., complex}$ | -169.41 | -169.85 | -304.11 | -291.41 |
| | $E_{Disp., fragment 1}$ | -72.18 | -72.76 | -132.02 | -127.26 |
| | $E_{Disp., fragment 2}$ | -72.19 | -72.78 | -132.05 | -127.28 |
| | $\Delta E_{Disp.}$ | -25.04 | -24.31 | -40.04 | -36.87 |
| **1*** | $E_{Disp., complex}$ | -177.07 | -177.07 | -318.10 | -305.03 |
| | $E_{Disp., fragment 1}$ | -75.13 | -75.86 | -138.03 | -133.29 |
| | $E_{Disp., fragment 2}$ | -75.17 | -75.89 | -138.09 | -133.33 |
| | $\Delta E_{Disp.}$ | -26.76 | -25.32 | -41.99 | -38.41 |
| **5*** | $E_{Disp., complex}$ | -216.54 | -216.76 | -385.02 | -369.01 |
| | $E_{Disp., fragment 1}$ | -93.87 | -94.56 | -170.25 | -164.24 |
| | $E_{Disp., fragment 2}$ | -93.58 | -94.42 | -169.98 | -164.22 |
| | $\Delta E_{Disp.}$ | -29.09 | -27.78 | -44.79 | -40.54 |
| **6*** | $E_{Disp., complex}$ | -223.97 | -223.56 | -399.88 | -382.73 |
| | $E_{Disp., fragment 1}$ | -97.64 | -98.12 | -178.02 | -171.51 |
| | $E_{Disp., fragment 2}$ | -97.64 | -98.12 | -178.03 | -171.51 |
| | $\Delta E_{Disp.}$ | -28.69 | -27.32 | -43.83 | -39.72 |
| **7*** | $E_{Disp., complex}$ | -147.64 | -148.66 | -266.99 | -256.67 |
| | $E_{Disp., fragment 1}$ | -63.25 | -64.24 | -116.57 | -113.09 |
| | $E_{Disp., fragment 2}$ | -63.24 | -64.23 | -116.55 | -113.07 |
| | $\Delta E_{Disp.}$ | -21.15 | -20.19 | -33.87 | -30.52 |
| **8*** | $E_{Disp., complex}$ | -168.09 | -168.79 | -303.50 | -290.92 |
| | $E_{Disp., fragment 1}$ | -73.41 | -74.22 | -134.76 | -130.11 |
| | $E_{Disp., fragment 2}$ | -73.38 | -74.19 | -134.70 | -130.05 |
| | $\Delta E_{Disp.}$ | -21.29 | -20.38 | -34.05 | -30.76 |

## References


(S1) Stanciu, C.; Richards, A. F.; Fettinger, J. C.; Brynda, M.; Power, P. P. Synthesis and Characterization of New, Modified Terphenyl Ligands: Increasing the Rotational Barrier for Flanking Rings. *J. Organomet. Chem.* **2006**, *691*, 2540–2545.

(S2) Hino, S.; Olmstead, M. M.; Phillips, A. D.; Wright, R. J.; Power, P. P. Terphenyl Ligand Stabilized Lead(II) Derivatives: Steric Effects and Lead-Lead Bonding in Diplumbenes. *Inorg. Chem.* **2004**, *43*, 7346–7352.

(S3) Pettersen, E. F.; Goddard, T. D.; Huang, C. C.; Couch, G. S.; Greenblatt, D. M.; Meng, E. C.; Ferrin, T. E. UCSF Chimera - A Visualization System for Exploratory Research and Analysis. *J. Comput. Chem.* **2004**, *25*, 1605–1612.

(S4) Furche, F.; Ahlrichs, R.; Hättig, C.; Klopper, W.; Sierka, M.; Weigend, F. Turbomole. *WIREs Comput Mol Sci* **2014**, *4*, 91–100.

(S5) TURBOMOLE V7.0.2 2015, a Development of University of Karlsruhe and Forschungszentrum Karlsruhe GmbH, 1989-2007, TURBOMOLE GmbH, since 2007; Available from Http://Www.Turbomole.Com.

(S6) Neese, F. The ORCA Program System. *Wiley Interdiscip. Rev. Comput. Mol. Sci.* **2012**, *2*, 73–78.

(S7) Neese, F. ORCA: An Ab Initio, Density Functional and Semiempirical Program Package , V. 4.1.0; MPI Für Chemische Energiekonversion: Mülheim a. d. Ruhr, Germany, 2019.

(S8) Grimme, S. XTB, V. 6.1; Mulliken Center for Theoretical Chemistry, University of Bonn. **2019**.

(S9) Furche, F.; Ahlrichs, R.; Hättig, C.; Klopper, W.; Sierka, M.; Weigend, F. Turbomole. *WIREs Comput. Mol. Sci.* **2014**, *4*, 91–100.

(S10) TURBOMOLE V7.2 2017, a Development of University of Karlsruhe and Forschungszentrum Karlsruhe GmbH, 1989-2007, TURBOMOLE GmbH, since 2007; Available from Http://Www.Turbomole.Com.

(S11) Bannwarth, C.; Ehlert, S.; Grimme, S. GFN2-XTB—An Accurate and Broadly Parametrized Self-Consistent Tight-Binding Quantum Chemical Method with Multipole Electrostatics and Density-Dependent Dispersion Contributions. *J. Chem. Theory Comput.* **2019**, *15*, 1652–1671.

(S12) Tao, J.; Perdew, J. P.; Staroverov, V. N.; Scuseria, G. E. Climbing the Density Functional Ladder: Nonempirical Meta–Generalized Gradient Approximation Designed for Molecules and Solids. *Phys. Rev. Lett.* **2003**, *91*, 146401.

(S13) Weigend, F.; Ahlrichs, R. Balanced Basis Sets of Split Valence, Triple Zeta Valence and Quadruple Zeta Valence Quality for H to Rn: Design and Assessment of Accuracy. *Phys. Chem. Chem. Phys.* **2005**, *7*, 3297.

(S14) Metz, B.; Stoll, H.; Dolg, M. Small-Core Multiconfiguration-Dirac-Hartree-Fock-Adjusted Pseudopotentials for Post-d Main Group Elements: Application to PbH and PbO. *J. Chem. Phys.* **2000**, *113*, 2563–2569.

(S15) Eichkorn, K.; Treutler, O.; Öhm, H.; Häser, M.; Ahlrichs, R. Auxiliary Basis Sets to Approximate Coulomb Potentials. *Chem. Phys. Lett.* **1995**, *240*, 283–289.

(S16) Weigend, F. Accurate Coulomb-Fitting Basis Sets for H to Rn. *Phys. Chem. Chem. Phys.* **2006**, *8*, 1057.

(S17) Grimme, S.; Antony, J.; Ehrlich, S.; Krieg, H. A Consistent and Accurate Ab Initio Parametrization of Density Functional Dispersion Correction (DFT-D) for the 94 Elements H-Pu. *J. Chem. Phys.* **2010**, *132*, 154104.

(S18) Caldeweyher, E.; Ehlert, S.; Hansen, A.; Neugebauer, H.; Spicher, S.; Bannwarth, C.; Grimme, S. A Generally Applicable Atomic-Charge Dependent London Dispersion Correction. *J. Chem. Phys.* **2019**, *150*, 154122.

(S19) Caldeweyher, E.; Bannwarth, C.; Grimme, S. Extension of the D3 Dispersion Coefficient Model. *J. Chem. Phys.* **2017**, *147*, 034112.

(S20) Grimme, S.; Ehrlich, S.; Goerigk, L. Effect of the Damping Function in Dispersion Corrected Density Functional Theory. *J. Comput. Chem.* **2011**, *32*, 1456–1465.

(S21) Becke, A. D.; Johnson, E. R. A Density-Functional Model of the Dispersion Interaction. *J. Chem. Phys.* **2005**, *123*, 154101.

(S22) Axilrod, B. M.; Teller, E. Interaction of the van Der Waals Type between Three Atoms. *J. Chem. Phys.* **1943**, *11*, 299–300.

(S23) Muto, Y. Force between Nonpolar Molecules. *Proc. Phys. Math. Soc. Jpn.* **1943**, *17*, 629–631.

(S24) Grimme, S.; Hansen, A.; Brandenburg, J. G.; Bannwarth, C. Dispersion-Corrected Mean-Field Electronic Structure Methods. *Chem. Rev.* **2016**, *116*, 5105–5154.

(S25) Grimme, S. Supramolecular Binding Thermodynamics by Dispersion-Corrected Density Functional Theory. *Chem. - A Eur. J.* **2012**, *18*, 9955–9964.

(S26) Adamo, C.; Barone, V. Toward Reliable Density Functional Methods without Adjustable Parameters: The PBE0 Model. *J. Chem. Phys.* **1999**, *110*, 6158–6170.

(S27) Becke, A. D. Density-Functional Thermochemistry. III. The Role of Exact Exchange. *J. Chem. Phys.* **1993**, *98*, 5648–5652.

(S28) Klamt, A. Conductor-like Screening Model for Real Solvents: A New Approach to the Quantitative Calculation of Solvation Phenomena. *J. Phys. Chem.* **1995**, *99*, 2224–2235.

(S29) Eckert, F.; Klamt, A. Fast Solvent Screening via Quantum Chemistry: COSMO-RS Approach. *AIChE J.* **2002**, *48*, 369–385.

(S30) Klamt, A.; Eckert, F.; Pohler, L. COSMOtherm. COSMOlogic GmbH & Co. KG: Leverkusen, Germany 2013.

(S31) Becke, A. D. Density-Functional Exchange-Energy Approximation with Correct Asymptotic Behavior. *Phys. Rev. A* **1988**, *38*, 3098–3100.

(S32) Perdew, J. P. Density-Functional Approximation for the Correlation Energy of the Inhomogeneous Electron Gas. *Phys. Rev. B* **1986**, *33*, 8822–8824.

(S33) Schäfer, A.; Huber, C.; Ahlrichs, R.; Schafer, A.; Huber, C.; Ahlrichs, R. Fully Optimized Contracted Gaussian Basis Sets of Triple Zeta Valence Quality for Atoms Li to Kr Fully Optimized Contracted Gaussian Basis Sets of Triple Zeta Valence Quality for Atoms Li to Kr. *J. Chem. Phys.* **1994**, *100*, 5829–5835.

(S34) Glendening, E. D.; Badenhoop, J. K.; Reed, A. E.; Carpenter, J. E.; Bohmann, J. A.; Morales, C. M.; Landis, C. R.; Weinhold, F. NBO 6.0. Theoretical Chemistry Institute, University of Wisconsin: Madison 2013.

(S35) Grimme, S. A Simplified Tamm-Dancoff Density Functional Approach for the Electronic Excitation Spectra of Very Large Molecules. *J. Chem. Phys.* **2013**, *138*, 244104.

(S36) Becke, A. D. A New Mixing of Hartree-Fock and Local Density-Functional Theories. *J. Chem. Phys.* **1993**, *98*, 1372–1377.

(S37) Neese, F.; Wennmohs, F.; Hansen, A.; Becker, U. Efficient, Approximate and Parallel Hartree-Fock and Hybrid DFT Calculations. A “chain-of-Spheres” Algorithm for the Hartree-Fock Exchange. *Chem. Phys.* **2009**, *356*, 98–109.

(S38) Barone, V.; Cossi, M. Quantum Calculation of Molecular Energies and Energy Gradients in Solution by a Conductor Solvent Model. *J. Phys. Chem. A* **1998**, *102*, 1995–2001.

(S39) Ryckaert, J. P.; Ciccotti, G.; Berendsen, H. J. C. Numerical Integration of the Cartesian Equations of Motion of a System with Constraints: Molecular Dynamics of n-Alkanes. *J. Comput. Phys.* **1977**, *23*, 327–341.

(S40) Van Gunsteren, W. F.; Berendsen, H. J. C. Algorithms for Macromolecular Dynamics and Constraintdynamics. *Mol. Phys.* **1977**, *34*, 1311–1327.

## Chapter 3. Two Quasi-Stable Lead(II) Hydrides at Ambient Temperature

Joshua D. Queen, James C. Fettinger and Philip P. Power *

Department of Chemistry, University of California, Davis, One Shields Avenue, Davis, California 95616, United States

Reproduced from *Chem. Commun.* 2019, 55, 10285–10287 with permission from the Royal Society of Chemistry.

**Abstract.** Simple reaction of their terphenyl lead bromide precursors with DIBAL-H in diethyl ether solution at ca. -78°C leads to the isolation of the hydrides $\{Pb(\mu\text{-}H)Ar^{iPr4}\}_2$ ($Ar^{iPr4}$ = $C_6H_3$-2,6 ($C_6H_3$-2,6-$^iPr_2$)$_2$) (1) and $\{Pb(\mu\text{-}H)Ar^{Me6}\}_2$ ($Ar^{Me6}$ = $C_6H_3$-2,6($C_6H_2$-2,4,6-$Me_3$)$_2$) (2) in good yield (60-80%). The isolated solids are stable at up to ca. 5°C for several weeks but are thermally labile in solution. Hydride **1** decomposes to the diplumbyne $Ar^{iPr4}PbPbAr^{iPr4}$, while **2** decomposes to the plumbylene $Pb(Ar^{Me6})_2$. The decomposition of **1** was determined to be zero order with a rate constant of ca. $2.0\times10^{-5}$ M min$^{-1}$ at 298 K.

Since the initial report of a stable tin(II) hydride in 2000,[1] low valent hydride derivatives of the heavy group 14 elements have become well established for the elements Si-Sn[1–14] over the past two decades. They display a diverse range of structures and are of particular interest for their reactivity with small molecules[15–18] and potential uses in catalysis.[19,20] The existence of an unstable lead(II) hydride "$Pb(H)Ar^{iPr6}$" ($Ar^{iPr6}$ = $C_6H_3$-2,6-($C_6H_2$-2,4,6-$^iPr_3$)$_2$) was implicated in the synthesis of the terphenyl substituted diplumbyne $Ar^{iPr6}PbPbAr^{iPr6}$ which was obtained via treatment of $\{Pb(\mu\text{-}Br)Ar^{iPr6}\}_2$ with $LiAlH_4$.[21] However, it wasn't until recently that the existence of the lead(II) hydride was established by Wesemann and coworkers[22] who synthesized it by treatment of $Ar^{iPr6}Pb\{CH(Ph)(PPh_2)\}$

with catechol borane, and showed that it has the symmetrically bridged hydride structure $\{Pb(\mu\text{-}H)Ar^{iPr6}\}_2$ (**3**) and converts to the diplumbyne $Ar^{iPr6}PbPbAr^{iPr6}$ above -40°C in solution with $H_2$ elimination.

In related work on Sn(II) hydrides we have shown that they can be stabilized by a variety of terphenyl substituents.[1,23–25] Moreover, the structure of the hydride product was found to be dependent on the aryl substituent used.[24] and that bulkier substituents favored the unsymmetrical $ArSnSn(H)_2Ar$ (Ar = terphenyl group) over the symmetric $\{Sn(\mu\text{-}H)Ar\}_2$ structure. We applied this approach to the synthesis of lead(II) hydrides and their subsequent conversions to diplumbynes[26] and other low-valent lead species. We found that some of the intermediate lead hydrides that were formed precipitated out of diethyl ether as relatively stable solids and can be isolated in good yields (60-80%). We now report the isolation of the aryl lead(II) hydrides $\{Pb(\mu\text{-}H)Ar^{iPr4}\}_2$ ($Ar^{iPr4}$ = $C_6H_3$-2,6 ($C_6H_3$-2,6-$^iPr_2)_2$) (**1**) and $\{Pb(\mu\text{-}H)Ar^{Me6}\}_2$ ($Ar^{Me6}$ = $C_6H_3$-2,6($C_6H_2$-2,4,6-$Me_3)_2$) (**2**) and show that although **1** converts to the expected diplumbyne $Ar^{iPr4}PbPbAr^{iPr4}$ in solution,[26] **2** is transformed to the diarylplumbylene $Pb(Ar^{Me6})_2$.[27]

The lead hydrides were synthesized in a simple manner by treatment of $\{Pb(\mu\text{-}Br)Ar^{iPr4}\}_2$[28] or $\{Pb(\mu\text{-}Br)Ar^{Me6}\}_2$[29] with DIBAL-H (di-isobutyl aluminium hydride) in diethyl ether solution at -78°C (Scheme 3.1). This resulted in the precipitation of **1** and **2** as yellow-green solids. Decanting the supernatant liquid and washing the solid with ether and hexanes gave **1** in ca. 80% and **2** in ca. 60% yield. Extraction of a portion of the solids with either toluene or THF at ca. 0°C and storage of the resulting solutions at ca. -30°C gave yellow blocks of **1** or yellow-green blocks of **2** that were

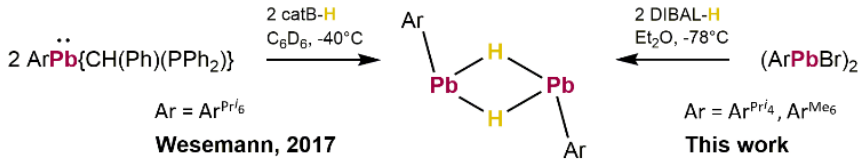


**Scheme 3.1** Current known synthetic routes to terphenyl substituted lead(II) hydrides.

suitable for X-ray diffraction studies (see photos in Supporting Information). Both **1** and **2** (Figure 3.1) display dimeric hydrogen-bridged structures with planar $Pb_2H_2$ cores (sum of the internal angles = 360°), which are similar to that seen for the structure of **3** reported by Wesemann and coworkers.[22] The dimeric structure of **2** contrasts with the analogous Sn hydride $\{Sn(H)Ar^{Me6}\}_4$,[25] which has a tetrameric structure containing four Sn–Sn bonds and a terminal hydrogen bound to each tin. The Pb–H distances are in the range 2.04(3) Å to 2.09(4) Å, similar to the distances reported in **3** (1.98(4)-2.03(5) Å). The ligands are bound to the lead atoms almost perpendicularly to the $Pb_2H_2$ core with Pb–$C_{ipso}$ angles of 89.61(11)° to 93.44(3)° (cf. 92.3(6) in the case of **3**) with respect to the $Pb_2H_2$ plane.

Wesemann and co-workers reported two observable $^1$H NMR signals in solution for the lead hydride **3** at 35.83 ppm and 31.43 ppm in $d_8$-toluene, which were attributed to the

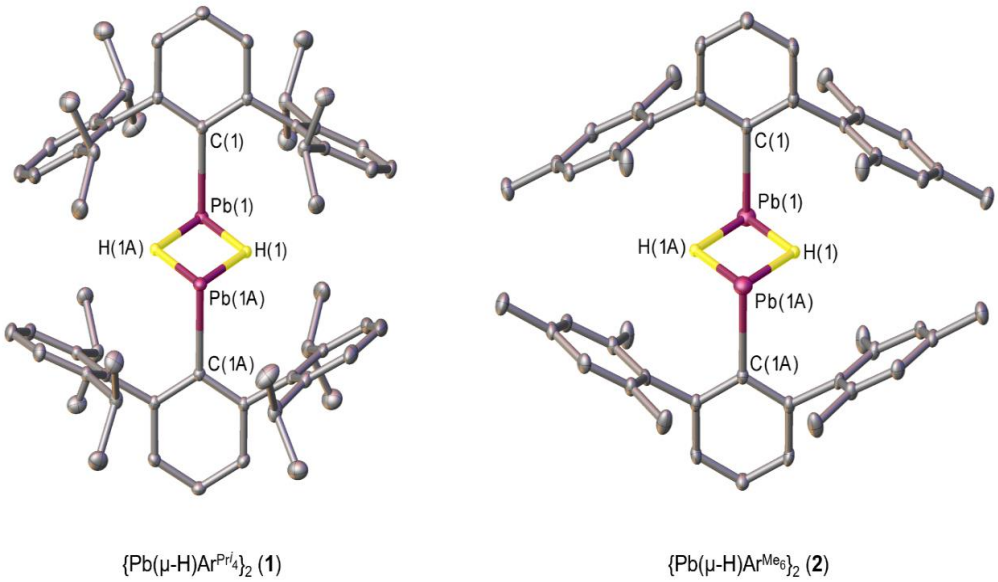


**Figure 3.1.** Thermal ellipsoid plots (50%) of **1** and **2**. Terphenyl hydrogen atoms and co-crystallized solvent molecules are not shown for clarity. Selected bond lengths [Å] and angles [°]: 1: Pb1–C1: 2.3066(12), Pb1–H1: 2.04(3), Pb1–H1A: 2.05(2), Pb1···Pb1A: 3.2662(3), Pb1–H1–Pb1A: 105.9(1), H1–Pb1–H1A: 74.1(1), (Pb1–C1)–(Pb2H2): 93.44(3). 2: Pb1–C1: 2.289(4), Pb1–H1: 2.08(4), Pb1–H1A: 2.09(4), Pb1···Pb1A: 3.2791(5), Pb1–H1–Pb1A: 104(3), H1–Pb1–H1A: 76(3), (Pb1–C1)–($Pb_2H_2$): 89.61(11).

presence of rotamers of **3** in solution.[22] The more downfield shifted signal is the prominent signal at 298 K while the more upfield signal is more prominent at 193 K, indicative of an equilibrium between the two rotamers in solution. The extreme downfield chemical shift of the hydride resonance has been determined by relativistic DFT methods to be due to the spin-orbit coupling effects of the heavy lead atoms.[30] Essentially, it was found that the relatively low HOMO-LUMO gap of low valent 6p elements allows for efficient magnetic coupling of the frontier orbitals; combined with the primarily 6p character of the metal contribution to the bonding orbitals, the result is a drastic deshielding of the bonded hydrogen atom.[31]

Our previous work on tin(II) hydrides showed that increasing the size of the terphenyl ligand affects the solution structure,[24] e.g. the symmetric hydrogen bridged structure of $\{Sn(\mu\text{-}H)Ar^{iPr6}\}_2$ in the solid state converts to the deep blue asymmetric structure $Ar^{iPr6}SnSn(H)_2Ar^{iPr6}$ in solution. The $^1$H NMR spectra of yellow solutions of **1** and **2** at 298 K display only one downfield singlet at 33.91 ppm ($^1J^{207}_{Pb\text{-}}{}^1_H$ = 696 Hz) in $C_6D_6$ for **1** and at 33.91 ppm in $C_6D_6$ or 33.65 ppm in $d_8$-THF ($^1J^{207}_{Pb\text{-}}{}^1_H$ = 708Hz) for **2** corresponding to the hydride signal. The signals are slightly upfield in comparison to that of the lead hydride $^1$H chemical shift for **3** at 35.83 ppm ($^1J^{207}_{Pb\text{-}}{}^1_H$ = 725 Hz) reported at 298 K and are in close agreement with the chemical shift calculated for the symmetric bridging hydride structure in solution.[30] The ATR-FTIR spectra of **1** and **2** both display a near identical feature in the range ca. 950 to 1050 cm$^{-1}$ which match Pb-H bands determined for **3** (900-1100 cm$^{-1}$).[22]

The hydrides **1** and **2** can be stored as solids under anaerobic and anhydrous conditions at 5°C in the absence of light but decompose slowly over several days if kept at ambient

temperature. When dissolved in hydrocarbon or ethereal solvents they both immediately begin to release $H_2$ and decompose. Monitoring the degradations by $^1$H NMR spectroscopy, we observed that **1** converts to the expected amber diplumbyne $Ar^{iPr4}PbPbAr^{iPr4}$ [26] and determined the rate to be zero order with a rate constant of ca. $2.0\times10^{-5}$ M min$^{-1}$ ($1.2\times10^{-3}$ M hr$^{-1}$). The hydride **2** instead converts to the purple plumbylene $Pb(Ar^{Me6})_2$[27] with concomitant deposition of Pb metal. This suggests the putative diplumbyne "$Ar^{Me6}PbPbAr^{Me6}$" that may form upon elimination of $H_2$ from **2** is not sufficiently stabilized by the smaller mesityl groups on the flanking rings of the terphenyl ligands compared to $Ar^{iPr6}PbPbAr^{iPr6}$ and $Ar^{iPr4}PbPbAr^{iPr4}$ and instead a rearrangement is preferred. We have previously found that $Ar^{Me6}$ is not sufficiently large to stabilize the digermyne $Ar^{Me6}GeGeAr^{Me6}$ and instead the cyclotregermenyl radical $(GeAr^{Me6})_3^{\cdot}$ is obtained.[32] Ziegler and co-workers have demonstrated computationally that isopropyl substituents on the terphenyl ligands play a crucial role in stabilizing group 14 dimetallynes through intramolecular London dispersion interactions which overcome the Pb–Pb bond dissociation energy (cf. -44 kcal·mol$^{-1}$).[33] Working with Stefan Grimme's group on a series of diplumbynes bearing terphenyl ligands of varying size, we have further confirmed that the Pb–Pb bond dissociation energy is compensated for by dispersion force attractions between ligands on opposing Pb atoms.[26]

Attempts to apply this protocol to the preparation of other terphenyl supported lead(II) hydrides has so far been unsuccessful and we have not observed any precipitation of other lead(II) hydride systems. We attribute this to the low solubility of **1** and **2** compared to other terphenyl lead systems we have investigated.[26] Examining the crystal structure of **2**, a network of close interligand H···H contacts can be observed between molecules with

distances of 2.368(25) Å, (see Supporting Information–Figure 3.S8) shorter than twice the van der Waals radius of hydrogen ($2r_H$ = 2.40 Å).[34] Such an interaction is not observed in the structure of **1** recrystallized from toluene, as several solvent molecules surround the structure which presumably contribute to the stability of the crystals. However, these crystals were found to be much more prone to thermal decomposition than crystals of **2** or powdered **1**. The results strongly suggest that as isolated solids, **1** and **2** may be stabilized by intermolecular London dispersion force energies (i.e. 'packing' forces) which stabilize the molecular structures.[35] When these are removed by dissolution of **1** or **2** in hydrocarbon or ethereal solvents, decomposition to the diplumbyne or plumbylene ensues.

Compounds **1** and **2** are very rare examples of hydride derivatives from the 6$^{th}$ period p-block elements that are isolable under ambient or near ambient conditions, the other notable example is $BiH(Ar^{Me6})_2$.[36]

In summary, the treatment of $\{Pb(\mu\text{-}Br)Ar^{iPr4}\}_2$ and $\{Pb(\mu\text{-}Br)Ar^{Me6}\}_2$ with DIBAL-H in diethyl ether at -78° gives the lead(II) hydrides **1** and **2** in ca. 60-80% yield as green-yellow powders. The products are thermally unstable in solution and degrade to diplumbyne $Ar^{iPr4}PbPbAr^{iPr4}$ in the case of **1** and plumbylene $Pb(Ar^{Me6})_2$ in the case of **2** . However, they can be stored in the solid state under a nitrogen or argon atmosphere and in low light conditions at ≤ 5°C for several weeks without noticeable decomposition.

We wish to acknowledge the US National Science Foundation (CHE-1565501) for support of this work

## References


(1) Eichler, B.E; Power, P.P. [2,6-$Trip_2H_3C_6Sn(\mu\text{-}H)]_2$ (Trip = $C_6H_2$-2,4,6-*i*-$Pr_3$): Synthesis and Structure of a Divalent Group 14 Element Hydride. *J. Am. Chem. Soc.* **2000**, *122*, 8785–8786.

(2) Pineda, L. W.; Jancik, V.; Starke, K.; Oswald, R. B.; Roesky, H. W. Stable Monomeric Germanium(II) and Tin(II) Compounds with Terminal Hydrides. *Angew. Chem. Int. Ed.* **2006**, *45*, 2602–2605.

(3) Takeuchi, K.; Ikoshi, M.; Ichinohe, M.; Sekiguchi, A. Addition of Amines and Hydroborane to the Disilyne RSi≡SiR (R = $Si^iPr[CH(SiMe_3)_2]_2$) Giving Amino- and Boryl-Substituted Disilenes. *J. Am. Chem. Soc.* **2010**, *132*, 930–931.

(4) Agou, T.; Sugiyama, Y.; Sasamori, T.; Sakai, H.; Furukawa, Y.; Takagi, N.; Guo, J.-D.; Nagase, S.; Hashizume, D.; and Tokitoh, N. Synthesis of Kinetically Stabilized 1,2-Dihydrodisilenes. *J. Am. Chem. Soc.* **2012**, *134*, 4120–4123.

(5) Peng, Y.; Ellis, B.D.; Wang, X.; Power, P. P. Diarylstannylene Activation of Hydrogen or Ammonia with Arene Elimination. *J. Am. Chem. Soc.* **2008**, *130*, 12268–12269.

(6) Richards, A.F.; Phillips, A.D.; Olmstead, M. M.; Power, P. P. Isomeric Forms of Divalent Heavier Group 14 Element Hydrides: Characterization of Ar‘(H)GeGe(H)Ar‘ and Ar‘$(H)_2$GeGeAr‘·$PMe_3$ (Ar‘ = $C_6H_3$-2,6-$Dipp_2$; Dipp = $C_6H_3$-2,6-$Pr^i_2$). *J. Am. Chem. Soc.* **2003**, *125*, 3204–3205.

(7) Spikes, G. H.; Fettinger, J. C.; Power, P. P. Facile Activation of Dihydrogen by an Unsaturated Heavier Main Group Compound. *J. Am. Chem. Soc.* **2005**, *127*, 12232–12233.

(8) Choong, S. L.; Woodul, W. D.; Schenk, C.; Stasch, A.; Richards, A. F.; Jones, C. Synthesis, Characterization, and Reactivity of an N-Heterocyclic Germanium(II) Hydride: Reversible Hydrogermylation of a Phosphaalkyne. *Organometallics* **2011**, *30*, 5543–5550.

(9) Inoue S.; Eisenhut C. A Dihydrodisilene Transition Metal Complex from an N-Heterocyclic Carbene-Stabilized Silylene Monohydride. *J. Am. Chem. Soc.* **2013**, *135*, 18315–18318.

(10) Hadlington, T. J.; Hermann, M.; Li, J.; Frenking, G.; Jones, C. Activation of $H_2$ by a Multiply Bonded Amido–Digermyne: Evidence for the Formation of a Hydrido–Germylene. *Angew. Chem. Int. Ed.* **2013**, *52*, 10199–10203.

(11) Mohapatra, C.; Kundu, S.; Paesch, A. N.; Herbst-Irmer, R.; Stalke, D.; Andrada, D. M.; Frenking, G.; Roesky, H. W. The Structure of the Carbene Stabilized $Si_2H_2$ May Be Equally Well Described with Coordinate Bonds as with Classical Double Bonds. *J. Am. Chem. Soc.* **2016**, *138*, 10429–10432.

(12) Arz, M. I.; Schnakenburg, G.; Meyer, A.; Schiemann, O.; Filippou, A. C. The $Si_2H$ radical supported by two N-heterocyclic carbenes. *Chem. Sci.* **2016**, *7*, 4973–4979.

(13) Lutters, D.; Severin, C.; Schmidtmann, M.; Müller, T. Activation of 7-Silanorbornadienes by N-Heterocyclic Carbenes: A Selective Way to N-Heterocyclic-Carbene-Stabilized Silylenes. *J. Am. Chem. Soc.* **2016**, *138*, 6061–6067.

(14) Do, D. C. H.; Keyser, A.; Protchenko, A. V.; Maitland, B.; Pernik, I.; Niu, H.; Kolychev, E. L.; Rit, A.; Vidovic, D.; Stasch, A.; Jones, C.; Aldridge, S. Highly Electron-Rich β-Diketiminato Systems: Synthesis and Coordination Chemistry of Amino-Functionalized "*N*-nacnac" Ligands. *Chem. Eur. J.* **2017**, *23*, 5830–5841.

(15) Mandal S. K.; Roesky, H. W. Group 14 Hydrides with Low Valent Elements for Activation of Small Molecules. *Acc. Chem. Res.* **2012**, *45*, 298–307.

(16) Wang, S.; McCrea-Hendrick, M. L.; Weinstein, C. M.; Caputo, C. A.; Hoppe, E.; Fettinger, J. C.; Olmstead, M. M.; Power, P. P. Dynamic Behavior and Isomerization Equilibria of Distannenes Synthesized by Tin Hydride/Olefin Insertions: Characterization of the Elusive Monohydrido Bridged Isomer. *J. Am. Chem. Soc.* **2017**, *139*, 6586–6595.

(17) Wang, S.; McCrea-Hendrick, M. L.; Weinstein, C. M.; Caputo, C. A.; Hoppe, E.; Fettinger, J. C.; Olmstead, M. M.; Power, P. P. Tin(II) Hydrides as Intermediates in Rearrangements of Tin(II) Alkyl Derivatives. *J. Am. Chem. Soc.* **2017**, *139*, 6596–6604.

(18) McCrea-Hendrick, M. L.; Wang, S.; Gullett, K. L.; Fettinger, J. C.; Power, P. P. The Reactions of Aryl Tin(II) Hydrides $\{Ar^{iPr6}Sn(\mu\text{-}H)\}_2$ ($Ar^{iPr6}$ = $C_6H_3$-2,6-($C_6H_2$-2,4,6-$^i$Pr$_3$)$_2$) and $\{Ar^{iPr4}Sn(\mu\text{-}H)\}_2$ ($Ar^{iPr4}$ = $C_6H_3$-2,6-($C_6H_3$-2,6-$^i$Pr$_2$)$_2$) with Aryl Alkynes: Substituent Dependent Structural Isomers. *Organometallics* **2017**, *36*, 3799–3805.

(19) Hadlington, T. J.; Driess, M.; Jones, C. Low-valent group 14 element hydride chemistry: towards catalysis. *Chem. Soc. Rev.* **2018**, *47*, 4176–4197.

(20) Villegas-Escobar, N.; Ortega, D. E.; Cortés-Arriagada, D.; Durán, R.; Yepes, D.; Gutiérrez-Oliva, S.; Toro-Labbé, A. Why Low Valent Lead(II) Hydride Complex Would be a Better Catalyst for $CO_2$ Activation than Its 14 Group Analogues? *J. Chem. Phys. C* **2017**, *121*, 12127–12135.

(21) Pu, L.; Twamley, B.; Power, P. P. Synthesis and Characterization of 2,6-Trip$_2$H$_3$C$_6$PbPbC$_6$H$_3$-2,6-Trip$_2$ (Trip = $C_6H_2$-2,4,6-*i*-Pr$_3$): A Stable Heavier Group 14 Element Analogue of an Alkyne. *J. Am. Chem. Soc.* **2000**, *122*, 3524–3525.

(22) Schneider, J.; Sindlinger, C. P.; Eichele, K.; Schubert, H.; Wesemann, L. Low-Valent Lead Hydride and Its Extreme Low-Field $^1$H NMR Chemical Shift. *J. Am. Chem. Soc.* **2017**, *139*, 6542–6545.

(23) Rivard, E.; Steiner, J.; Fettinger, J. C.; Giuliani, J. R.; Augustine, M. P.; Power, P. P. Convergent syntheses of [Sn$_7${$C_6H_3$-2,6-($C_6H_3$-2,6-$^i$Pr$_2$)$_2$}$_2$]: a cluster with a rare pentagonal bipyramidal motif. *Chem. Commun.* **2007**, *46*, 4919–4921.

(24) Rivard, E.; Fischer, R. C.; Wolf, R.; Peng, Y.; Merrill, A. W.; Schley, N. D.; Zhu, Z.; Pu, L.; Fettinger, J. C.; Teat, S. J.; Nowik, I.; Herber, R. H.; Takagi, N.; Nagase, S.; Power, P. P. Isomeric Forms of Heavier Main Group Hydrides: Experimental and Theoretical Studies of the [Sn(Ar)H]$_2$ (Ar = Terphenyl) System. *J. Am. Chem. Soc.* **2007**, *129*, 16197–16208.

(25) Vasko, P.; Wang, S.; Tuononen, H. M.; Power, P. P. Addition of Ethylene or Hydrogen to a Main-Group Metal Cluster under Mild Conditions. *Angew. Chem. Int. Ed.* **2015**, *54*, 3802–3805.

(26) Details of the synthesis and characterization of a series of new diplumbynes will be published in a separate paper.

(27) Simons, R. S.; Pu, L.; Olmstead, M. M.; Power, P. P. Synthesis and Characterization of the Monomeric Diaryls M{$C_6H_3$-2,6-$Mes_2$}$_2$ (M = Ge, Sn, or Pb; Mes = 2,4,6-$Me_3C_6H_2$−) and Dimeric Aryl−Metal Chlorides [M(Cl){$C_6H_3$-2,6-$Mes_2$}]$_2$ (M = Ge or Sn). *Organometallics* **1997**, *16*, 1920–1925.

(28) Hino, S.; Olmstead, M. M.; Phillips, A. D.; Wright, R. J.; Power, P. P. Terphenyl Ligand Stabilized Lead(II) Derivatives: Steric Effects and Lead−Lead Bonding in Diplumbenes. *Inorg. Chem.* **2004**, *43*, 7346–7352.

(29) Weiß, S.; Auer, M.; Eichele, K.; Schubert, H.; Wesemann, L. $\eta^3$-Allyl Coordination at Pb(II). *Organometallics* **2019**, *38*, 417–423.

(30) Vícha, J.; Marek, R.; Straka, M. High-Frequency $^1$H NMR Chemical Shifts of $Sn^{II}$ and $Pb^{II}$ Hydrides Induced by Relativistic Effects: Quest for $Pb^{II}$ Hydrides. *Inorg. Chem.* **2016**, *55*, 10302–10309.

(31) Vícha, J.; Marek, R.; Straka, M. High-Frequency $^{13}$C and $^{29}$Si NMR Chemical Shifts in Diamagnetic Low-Valence Compounds of $Tl^{I}$ and $Pb^{II}$: Decisive Role of Relativistic Effects. *Inorg. Chem.* **2016**, *55*, 1770–1781.

(32) Olmstead, M. M.; Pu, L.; Simons R. S.; Power, P. P. Reduction of Ge(Cl)$C_6H_3mes_2$-2,6 to give the cyclotrigermenyl radical (Ge$C_6H_3mes_2$-2,6)$_3$· and the trigermenyl anion salt K(Ge$C_6H_3mes_2$-2,6)$_3$. *Chem. Commun*. **1997**, 1595–1596.

(33) Seidu, I.; Seth, M.; Ziegler, T. Role Played by Isopropyl Substituents in Stabilizing the Putative Triple Bond in Ar′EEAr′ [E = Si, Ge, Sn; Ar′ = $C_6H_3$-2,6-($C_6H_3$-2,6-$Pr^i_2$)$_2$] and Ar*PbPbAr* [Ar* = $C_6H_3$-2,6-($C_6H_2$-2,4,6-$Pr^i_3$)$_2$]. *Inorg. Chem.* **2013**, *52*, 8378–8388.

(34) Bondi, A. van der Waals Volumes and Radii. *J. Phys. Chem.* **1964**, *68*, 441–451.

(35) Although the close contacts between the individual molecules in the structures are apparent from the structural data, calculations of the lattice anergies are no simple matter and few accurate calculations of such energies are known.

(36) Hardman, N. J.; Twamley, B.; Power, P. P. (2,6-$Mes_2H_3C_6$)$_2$BiH, a Stable, Molecular Hydride of a Main Group Element of the Sixth Period, and Its Conversion to the Dibismuthene (2,6-$Mes_2H_3C_6$)BiBi(2,6-$Mes_2C_6H_3$). *Angew. Chem. Int. Ed.* **2000**, *39*, 2771–2773.

**Author Contributions**

**J.D. Queen**: Synthesized and spectroscopically characterized the lead hydrides, collected X-Ray data, and prepared manuscript

**J. C. Fettinger**: Prepared X-ray crystallographic data for publication.

**P. P. Power:** Supervised synthetic work and manuscript preparation.

**Supporting Information**

**Experimental Details**

**General Procedures.** All manipulations were carried out using modified Schlenk techniques or in a Vacuum Atmospheres OMNI-Lab drybox under a $N_2$ or argon atmosphere. Manipulations of the lead compounds were carried out with careful exclusion of light due to the tendency for low valent lead compounds to decompose or disproportionate. Solvents were dried over columns of activated alumina using a Grubbs type purification system (Glass Contour)[S1], stored over Na ($Et_2O$) or K (hexanes, toluene) mirrors, and degassed via three freeze-pump-thaw cycles prior to use. $^1$H and $^{13}$C{$^1$H} spectra were recorded on Varian Inova 600 MHz or Bruker Avance III HD Nanobay 400 MHz spectrometers and were referenced to the residual solvent signals in $C_6D_6$ or $d_8$-THF.[S2] Infrared spectra were collected on a Bruker Tensor 27 ATR-FTIR spectrometer. Melting points were measured in glass capillary tubes sealed under argon using a Mel-Temp II apparatus and are uncorrected.

The starting materials $\{Pb(\mu\text{-}Br)Ar^{iPr4}\}_2$[S3] and $\{Pb(\mu\text{-}Br)Ar^{Me6}\}_2$[S4] were synthesized according to the literature procedures. DIBAL-H (1.0 M, hexanes) was purchased commercially and used without further purification.

**$\{Pb(\mu\text{-}H)Ar^{iPr4}\}_2$ (1)**. A solution of $\{Pb(\mu\text{-}Br)Ar^{iPr4}\}_2$ (0.950 g, 0.694 mmol) in diethyl ether (ca. 50 mL) was cooled to -78°C in an ethanol/dry ice bath and 1.0 M DIBAl-H in hexanes (1.42 mL, 1.42 mmol, 2.05 eq) was added dropwise via syringe. The mixture was stirred for 30 min, during which time it was warmed up to 0°C. The yellow precipitate was allowed to settle and the supernatant liquid was decanted. The solid was washed with cold, ca. 0°C ether (ca. 15 mL) and hexanes (ca. 20 mL). The product was dried under reduced pressure to give **1** as a green-yellow powder that was pure by $^1$H NMR spectroscopy. Yield: 0.690 g (82%). mp: 76-91°C (dec). 165-

169 (melts). $^1$H NMR (600 MHz, $C_6D_6$, 298 K): δ 32.63 (s, 2H, $^1J_{^{207}Pb-^1H}$ = 696 Hz, Pb*H*) 7.49 (d, 4H, $^3J$ = 7.5Hz, Ar*H*), 7.30 (t, 4H, $^3J$ = 7.7 Hz, Ar*H*), 7.05 (d, 8H, $^3J$ = 7.8 Hz, Ar*H*), 3.00 (sept, 8H, $^3J$ = 6.9 Hz, C*H*$(CH_3)_2$), 1.05 (d, 24H, $^3J$ = 6.7 Hz, CH(C$H_3$)$_2$) , 0.96 (d, 24H, 6.9 Hz, CH(C$H_3$)$_2$).

For crystal growth, toluene (ca. 20 mL) was added to 0.100 g of powdered **1** at ambient temperature (ca. 23°C) and stirred for 5 min. The pale-yellow solution was filtered away from undissolved **1** and stored at ca. -30°C for 2 weeks, after which time several pale-yellow crystals of **1**·4$C_7H_8$ suitable for X-ray diffraction studies were obtained.

**{Pb(μ-H)Ar$^{Me6}$}$_2$** (**2**). A solution of {Pb(μ-Br)Ar$^{Me6}$}$_2$ (0.825 g, 0.687 mmol) in diethyl ether (ca. 25 mL) was cooled to -78°C in an ethanol/dry ice bath and 1.0 M DIBAl-H in hexanes (1.41 mL, 1.41 mmol, 2.05 eq) was added dropwise via syringe. The mixture was stirred for 30 min, during which time it was warmed up to 0°C. The yellow precipitate was allowed to settle and the supernatant liquid was decanted. The solid was washed with cold, ca. 0°C ether (ca. 15 mL) and hexanes (ca. 20 mL). The product was dried under reduced pressure to give **2** as a green-yellow powder. Yield: 0.426 g (60%). mp: 76-91°C (dec). 165-169 (melts). $^1$H (400 MHz, $C_6D_6$, 298 K): δ 33.91 (s, 2H, Pb*H*). $^1$H (600 MHz, $d_8$-THF, 298 K): δ 33.65 (s, 2H, $^1J_{^{207}Pb-^1H}$ = 708 Hz, Pb*H*). The only other trace $^1$H and $^{13}$C{$^1$H} signals were assigned to Pb(Ar$^{Me6}$)$_2$.[S5]

For crystal growth, THF (ca. 25 mL) was added to 0.100 g of powdered **2** at ambient temperature (ca. 23°C) and stirred for 10 min. The brown solution was filtered away from undissolved **2** and stored at ca. -30°C for 3 days, after which time several yellow-green dichroic crystals of **2** suitable for X-ray diffraction studies were obtained.

**X-Ray Crystallography.** Crystals of **1** and **2** were removed from a Schlenk flask under a stream of nitrogen and immediately covered with hydrocarbon oil. A suitable crystal was selected,

attached to a glass fiber on a copper pin and placed in the cold $N_2$ stream on the diffractometer. Data were collected at 90 K on a Bruker APEX DUO diffractometer (**1**) or 100 K on a Bruker D8 VENTURE diffractometer (**2**) with Mo Kα radiation (λ = 0.71073 Å). Absorption corrections were applied using SADABS.[S6] The crystal structures were solved by intrinsic phasing methods using SHELXT[S7] and refined by full matrix least-squares procedures using SHELXL.[S8] All non-H atoms were refined anisotropically.

**Table 3.S1**. Selected X-ray Crystallographic data for **1** and **2**.

| **Compound** | **1·4 $C_7H_8$** | **2** |
|---|---|---|
| **Formula** | $C_{88}H_{108}Pb_2$ | $C_{48}H_{52}Pb_2$ |
| **Formula Weight (g mol$^{-1}$)** | 1580.12 | 1043.27 |
| **T (K)/λ (Å)** | 90(2)/0.71073 | 100(2)/0.71073 |
| **Crystal System** | Triclinic | Monoclinic |
| **Space Group** | P-1 | C2/m |
| **Z** | 1 | 2 |
| **Crystal color and habit** | Yellow block | Yellow block |
| **a (Å)** | 11.9074(15) | 10.0988(11) |
| **b (Å)** | 13.2780(17) | 22.633(2) |
| **c (Å)** | 13.7294(18) | 8.7512(9) |
| **α (°)** | 110.8199(14) | 90 |
| **β (°)** | 103.3533(16) | 99.263(2) |
| **γ (°)** | 102.2870(15) | 90 |
| **V (Å$^3$)** | 1867.4(4) | 1974.1(4) |
| **ρ (mg mm$^{-3}$)** | 1.405 | 1.755 |
| **Abs. coeff (mm$^{-1}$)** | 4.545 | 8.549 |
| **F(000)** | 800 | 1008 |
| **Crystal size (mm)** | 0.455 x 0.270 x 0.166 | 0.153 x 0.108 x 0.037 |
| **$\theta$ range (°)** | 2.047 to 30.553 | 2.967 to 27.488 |
| **Reflns collected** | 22485 | 7728 |
| **Ind. Reflns.** | 11379 | 2325 |
| **R(int)** | 0.0134 | 0.0164 |
| **Obs. reflns ($I$>2σ($I$))** | 10955 | 2221 |
| **Completeness to 2$\theta$ = 25.242°** | 99.9% | 99.8% |
| **Goodness-of-fit on $F^2$** | 1.058 | 1.158 |
| **Final R ($I$>2σ($I$))** | R1 = 0.0139 | R1 = 0.0211 |
| | wR2 = 0.0338 | wR2 = 0.0492 |
| **R (all data)** | R1 = 0.0149 | R1 = 0.0228 |
| | wR2 = 0.0341 | wR2 = 0.0499 |

## NMR Spectra

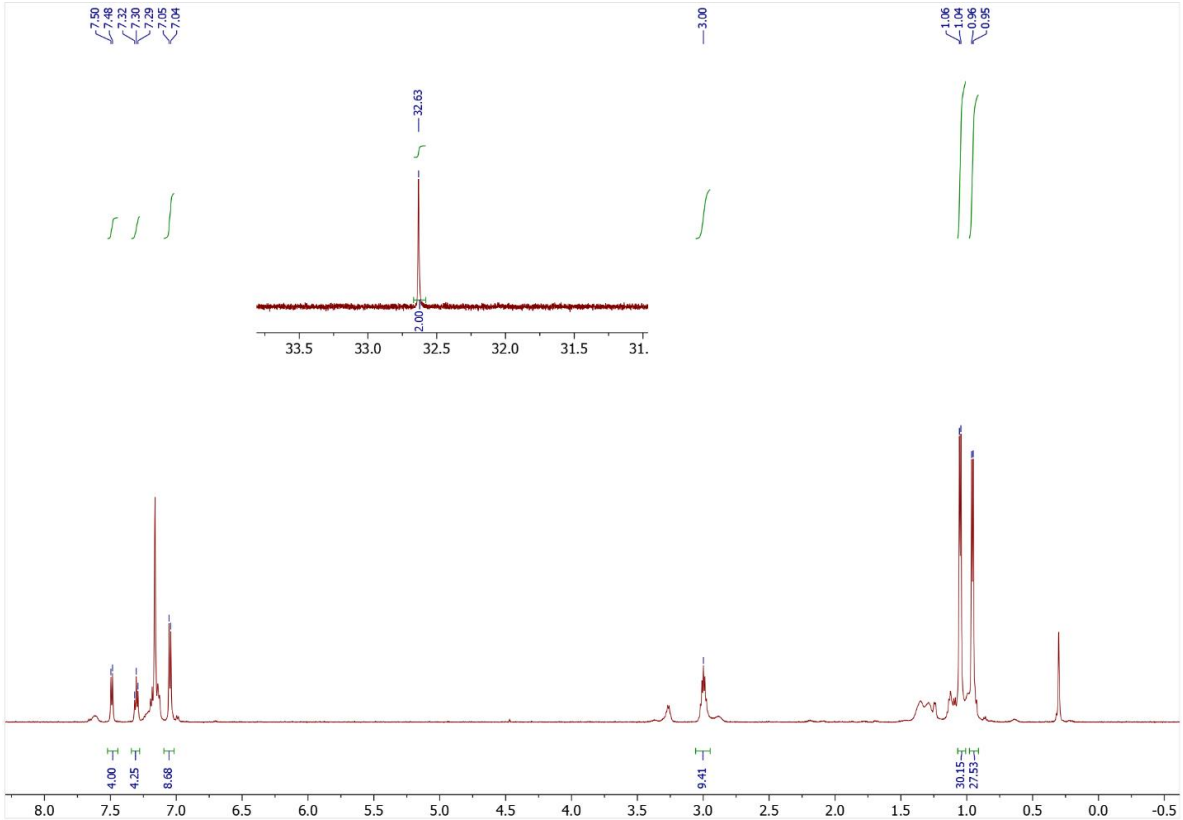


**Figure 3.S1.** $^{1}$H NMR spectrum of **1** in $C_6D_6$ at 298 K. The inset shows the Pb-H signal region.

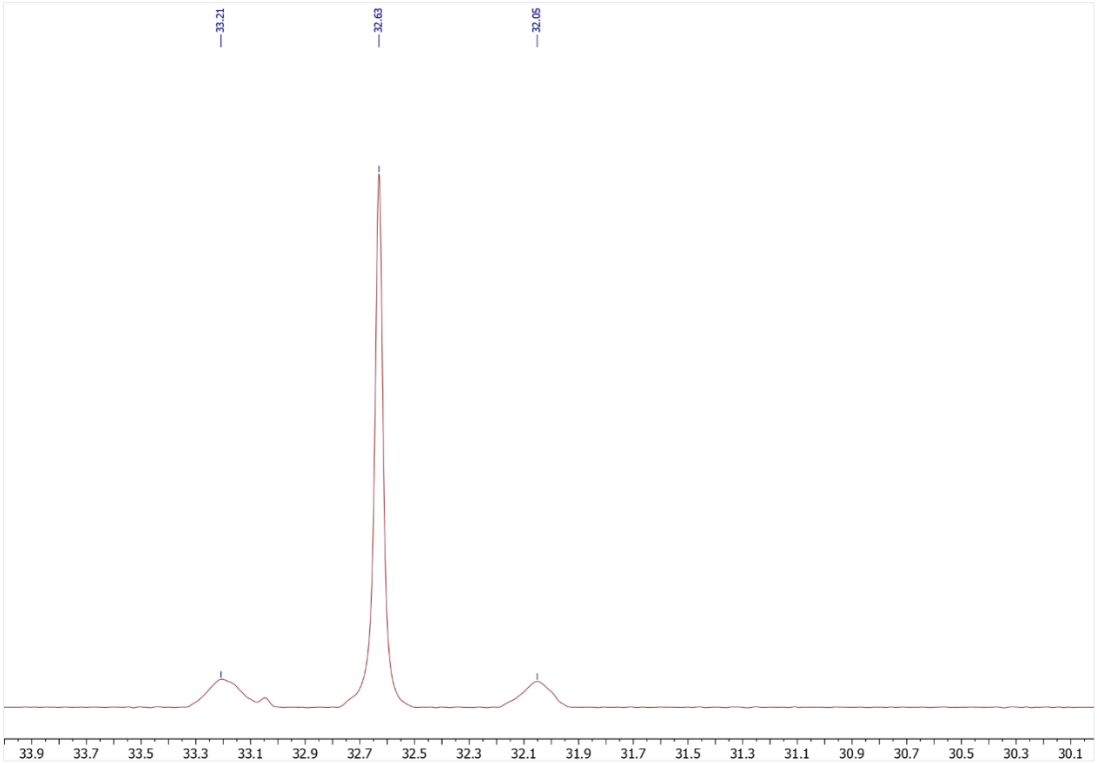


**Figure 3.S2.** $^{1}$H NMR spectrum of **1** in $C_6D_6$ at 298 K in the range 30-34 ppm.

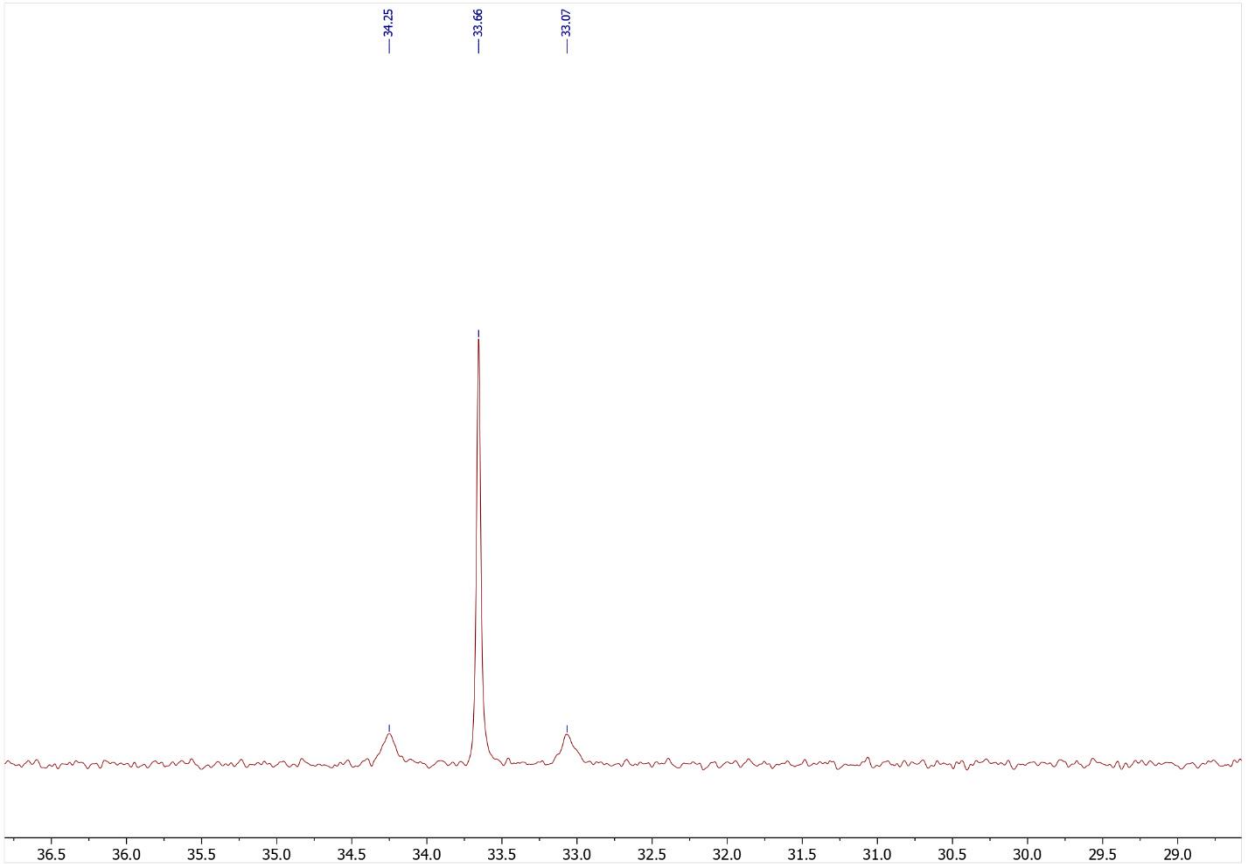


**Figure 3.S3.** $^{1}$H NMR spectrum of **2** in $d_8$-THF at 298K in the range 30-37 ppm.

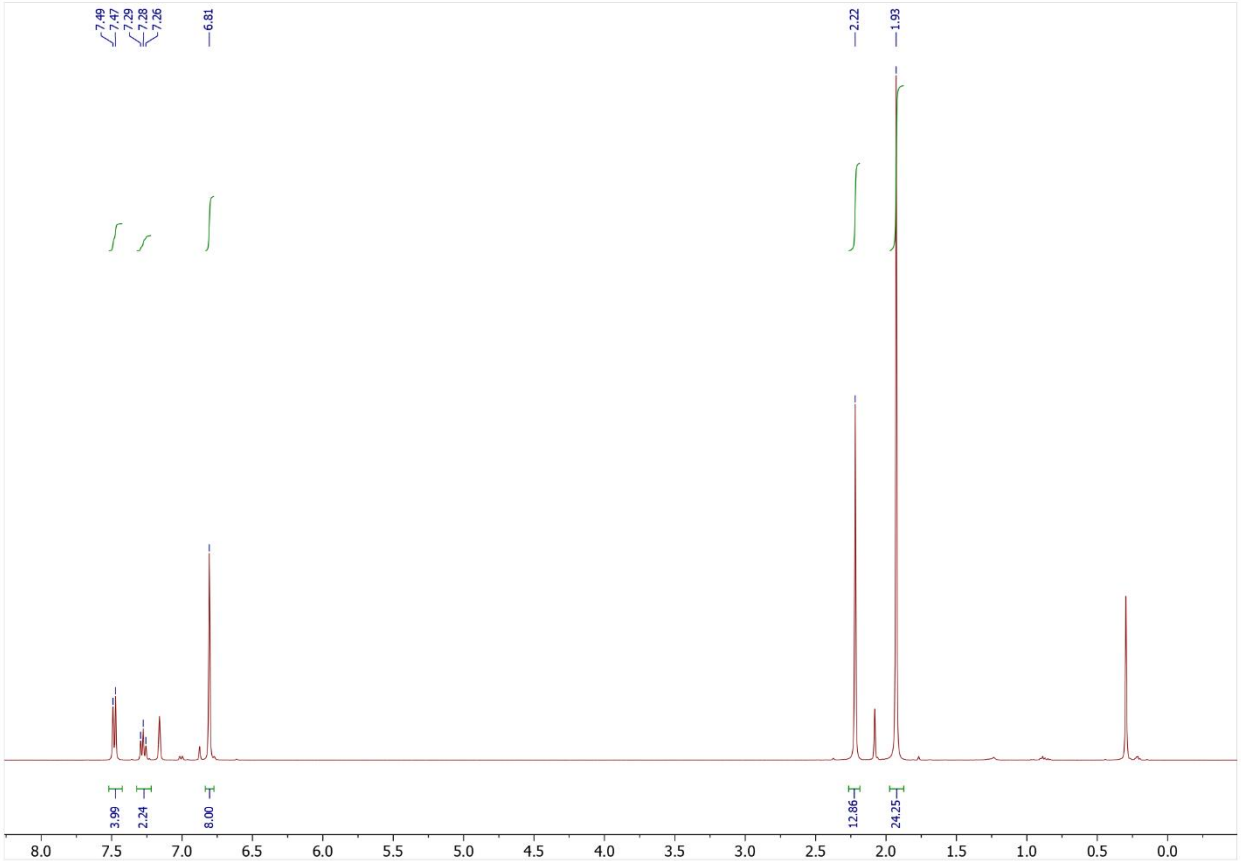


**Figure 3.S4.** $^{1}$H NMR spectrum in $C_6D_6$ of crystalline $Pb(Ar^{Me6})_2$ deposited from a hexane solution of **2** after 3 days at ambient temperature.

## Infrared Spectra

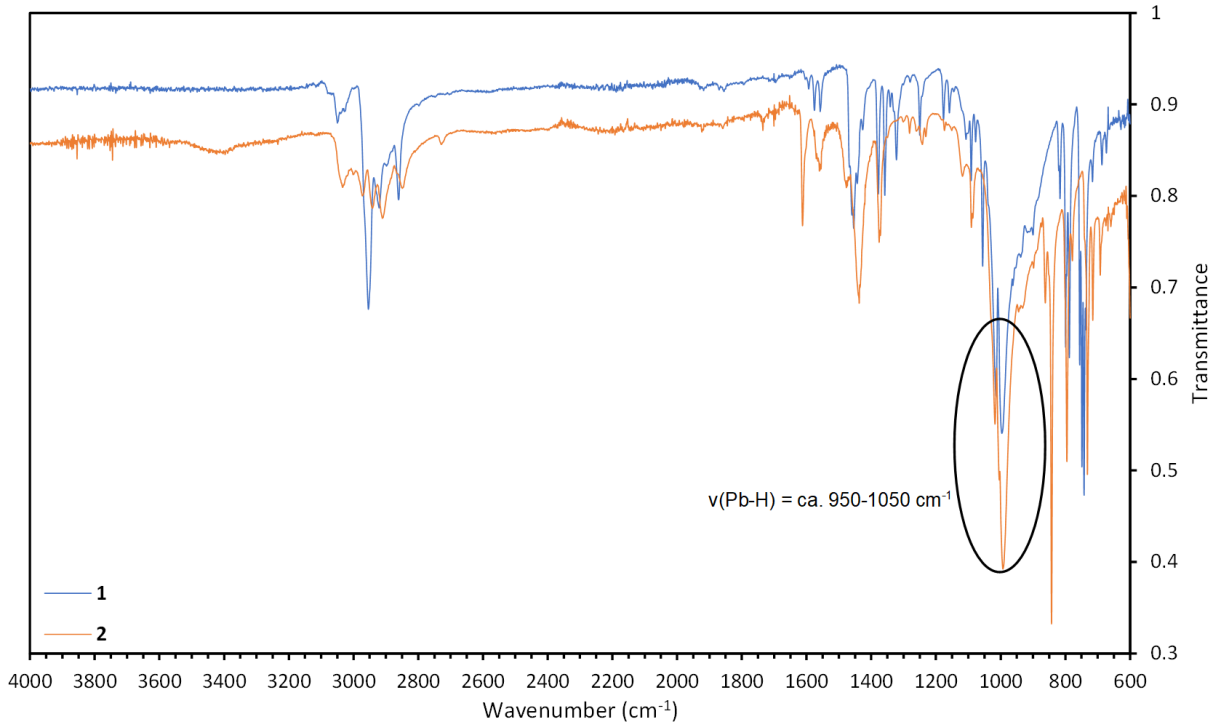


**Figure 3.S5** ATR-FTIR spectra of $\{Pb(\mu\text{-}H)Ar^{iPr4}\}_2$ (**1**, blue) and $\{Pb(\mu\text{-}H)Ar^{Me6}\}_2$ (**2**, orange).

## Kinetics Data

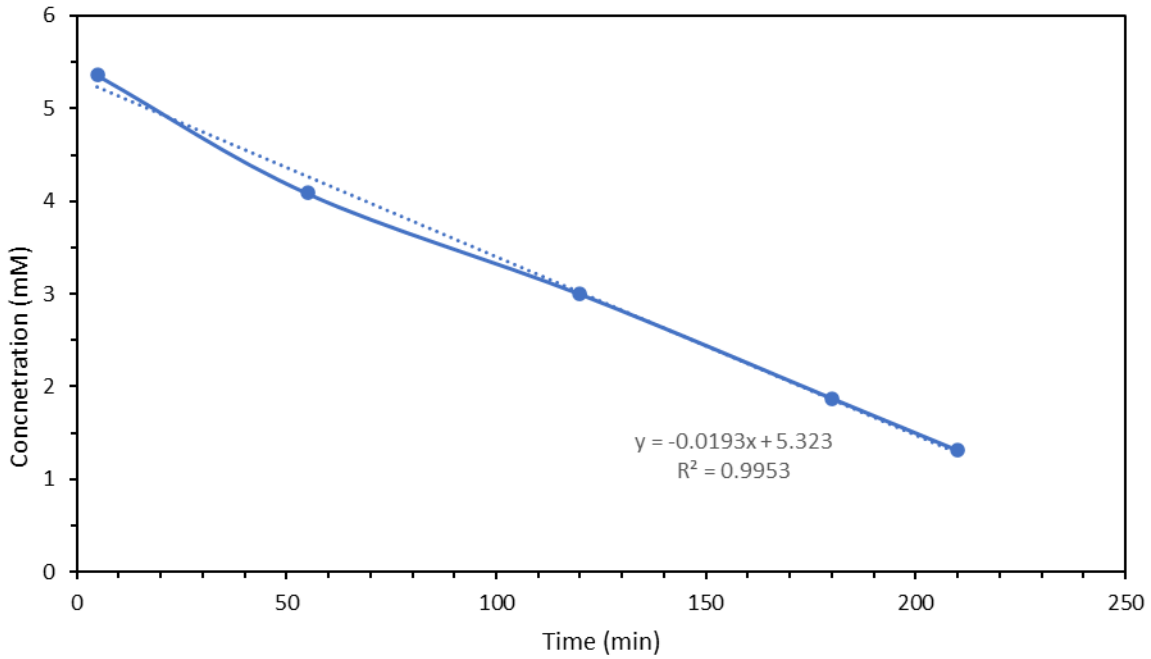


**Figure 3.S6.** Plot of time (min) vs concentration (mM) of a sample of $\{Pb(\mu\text{-}H)Ar^{iPr4}\}_2$ (**1**) in $C_6D_6$ at 25°C. Concentrations were referenced to an internal standard of ferrocene.

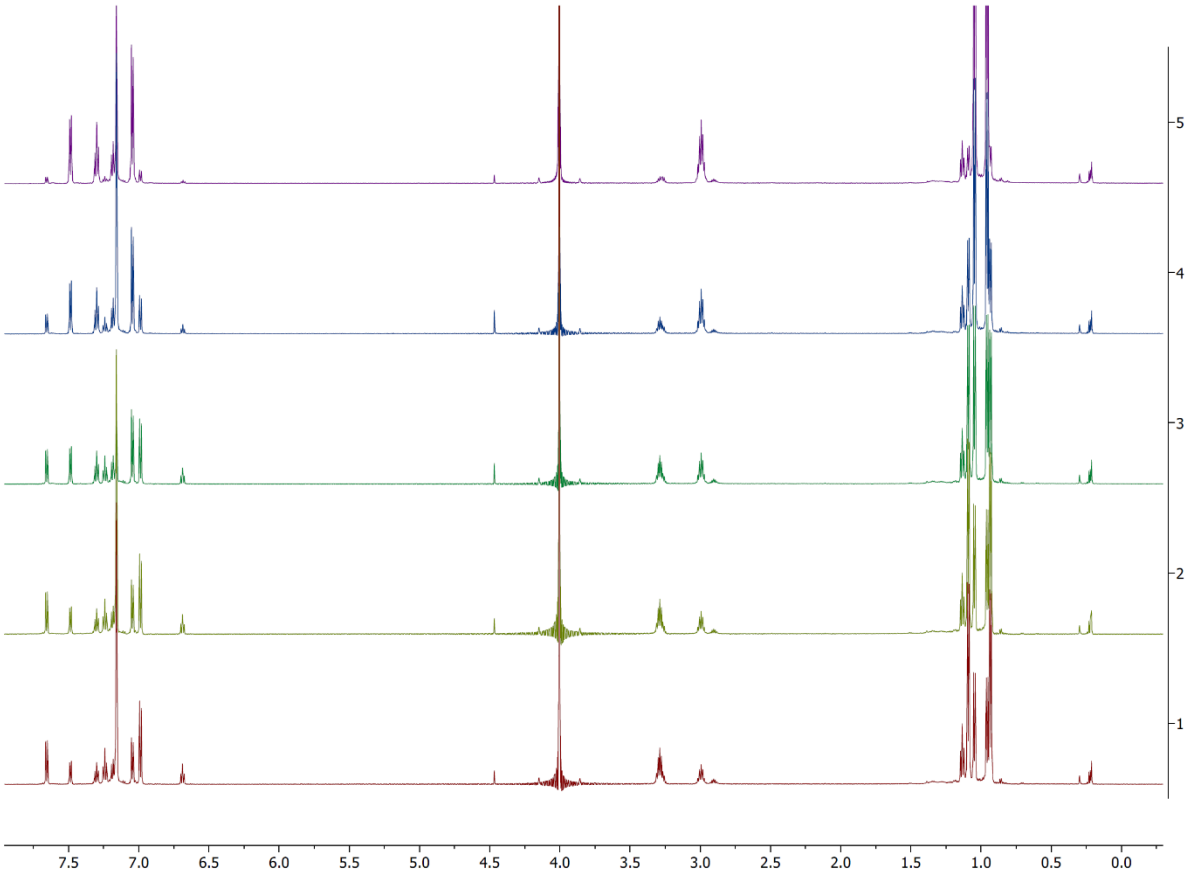


**Figure 3.S7.** $^{1}$H NMR spectra of the conversion of **1** into $Ar^{iPr4}PbPbAr^{iPr4}$. From top to bottom t = 5, 55, 120, 180, and 210 min**.**

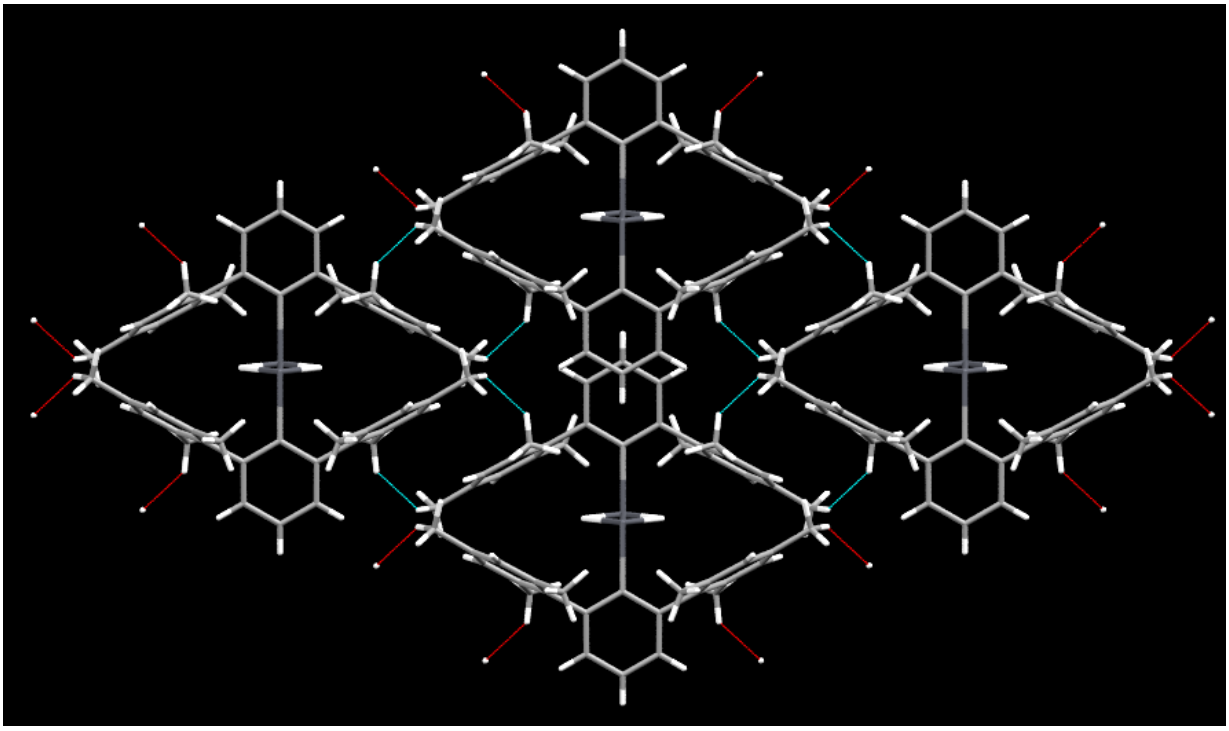

**Figure 3.S8.** Crystal packing of $\{Pb(\mu\text{-}H)Ar^{Me6}\}_2$ (**2**). Lines show short H···H contacts (2.368(25) Å) between adjacent molecules. Red lines are to molecules not depicted. Each flanking ring has two contacts to an adjacent molecule in the crystal–8 total per molecule of **2**.

## Photos of Compounds

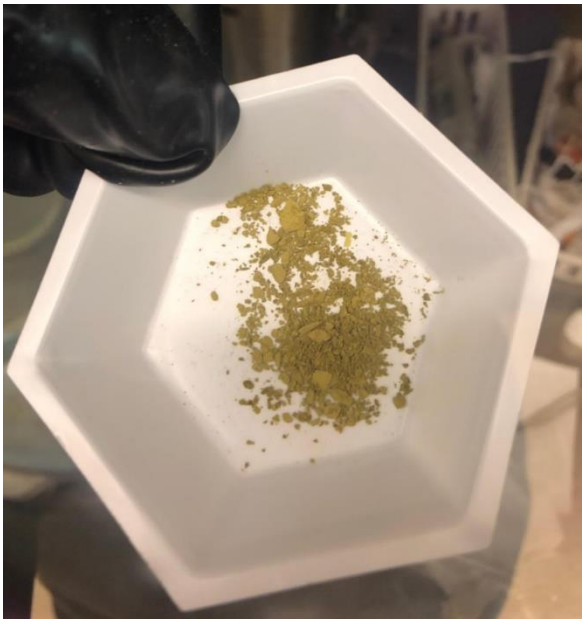

**Figure 3.S9.** Powdered $\{Pb(\mu\text{-}H)Ar^{iPr4}\}_2$ (**1**).

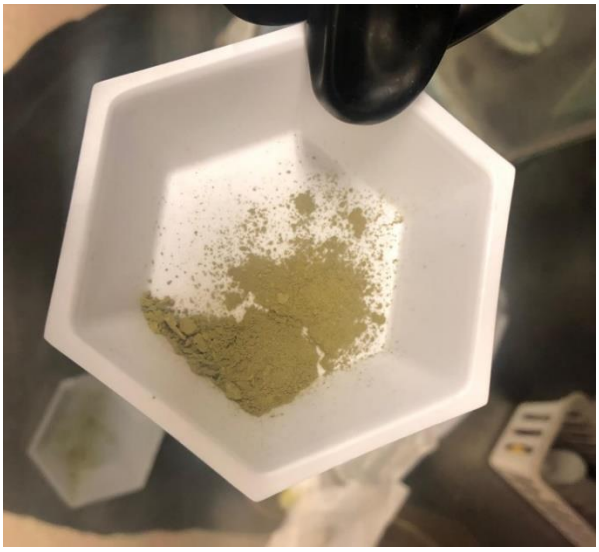

**Figure 3.S10.** Powdered $\{Pb(\mu\text{-}H)Ar^{Me6}\}_2$ (**2**).

## References


(S1) Pangborn, A. B.; Giardello, M. A.; Grubbs, R. H.; Rosen, R. K.; Timmers, F. J. Safe and Convenient Procedure for Solvent Purification. *Organometallics* **1996**, *15*, 1518–1520.

(S2) Fulmer, G. R.; Miller, A. J. M.; Sherden, N. H.; Gottlieb, H. E.; Nudelman, A.; Stoltz, B. M.; Bercaw, J. E.; Goldberg, K. I. NMR Chemical Shifts of Trace Impurities: Common Laboratory Solvents, Organics, and Gases in Deuterated Solvents Relevant to the Organometallic Chemist. *Organometallics* **2010**, *29*, 2176–2179.

(S3) Hino, S.; Olmstead, M. M.; Phillips, A. D.; Wright, R. J.; Power, P. P. Terphenyl Ligand Stabilized Lead(II) Derivatives: Steric Effects and Lead−Lead Bonding in Diplumbenes. *Inorg. Chem.* **2004**, *43*, 7346–7352.

(S4) Weiß, S.; Auer, M.; Eichele, K.; Schubert, H.; Wesemann, L. $\eta^3$-Allyl Coordination at Pb(II). Or*ganometallics* **2019**, *38*, 417–423.

(S5) Simons, R. S.; Pu, L.; Olmstead, M. M.; Power, P. P. Synthesis and Characterization of the Monomeric Diaryls M{$C_6H_3$-2,6-$Mes_2$}$_2$ (M = Ge, Sn, or Pb; Mes = 2,4,6-$Me_3C_6H_2$−) and Dimeric Aryl−Metal Chlorides [M(Cl){$C_6H_3$-2,6-$Mes_2$}]$_2$ (M = Ge or Sn). *Organometallics* **1997**, *16*¸1920–1925.

(S6) Krause, L.; Herbst-Irmer, R.; Sheldrick, G. M.; Stalke, D. Comparison of silver and molybdenum microfocus X-ray sources for single-crystal structure determination. *J. Appl. Crystallogr.* **2015**, *48*, 3–10.

(S7) Sheldrick, G. M. *SHELXT* – Integrated space-group and crystal-structure determination. *Acta Cryst. A.* **2015**, *71*, 3–8.

(S8) Sheldrick, G. M. Crystal structure refinement with *SHELXL*. Acta *Cryst. C.* **2015**, *71*, 3–8.

## Chapter 4. Metathetical Exchange between Metal−Metal Triple Bonds

Joshua D. Queen, Alice C. Phung, Christine A. Caputo†, James C. Fettinger, and Philip P. Power*

Department of Chemistry, University of California, One Shields Ave, Davis, CA, USA, 95616.

This work is in memory of Malcolm Chisholm and his contributions to the chemistry of transition-metal triple bonds.



**Abstract.** The reaction of the molybdenum-molybdenum triple-bonded dimer $(CO)_2CpMo{\equiv}MoCp(CO)_2$ (Cp = $\eta^5$-$C_5H_5$) with the triple-bonded dimetallynes $Ar^{iPr4}MMAr^{iPr4}$ or $Ar^{iPr6}MMAr^{iPr6}$ ($Ar^{iPr4}$ = $C_6H_3$-2,6-($C_6H_3$-2,6-$^iPr_2)_2$, $Ar^{iPr6}$ = $C_6H_3$-2,6-($C_6H_2$-2,4,6-$^iPr_3)_2$; M = Ge, Sn, or Pb) under mild conditions (≤80°C, 1 bar) afforded $Ar^{iPr4}M{\equiv}MoCp(CO)_2$ or $Ar^{iPr6}M{\equiv}MoCp(CO)_2$ in moderate to excellent yields. The reactions represent the first isolable products from a metathesis of two metal-metal triple bonds. Analogous exchange reactions with the single-bonded $(CO)_3CpMo–MoCp(CO)_3$ gave $Ar\ddot{M}–MoCp(CO)_3$ (Ar = $Ar^{iPr4}$ or $Ar^{iPr6}$ ; M = Sn or Pb). The products were characterized by NMR ($^1H$, $^{13}C$, $^{119}Sn$, or $^{207}Pb$), electronic, and IR spectroscopy and by X-ray crystallography.

Alkene and alkyne metathesis reactions are one of the cornerstones of organometallic chemistry and are of key importance in alkene and alkyne synthesis.[1] In 1974, Mortreux reported homogeneous alkyne metathesis catalyzed by $Mo(CO)_6$[2] and in 1981, Schrock and coworkers demonstrated the metathesis of acetylenes by tungsten(VI) alkylidyne complexes.[3] These stoichiometric metathesis reactions, for example the reaction of $^tBuC{\equiv}W(O^tBu)_3$ with PhC≡CPh

to give PhC≡W(O$^t$Bu)$_3$ and PhC≡C$^t$Bu, proceed in high yield under mild conditions. Also, it was found also that several tungsten(VI) alkylidyne complexes display catalytic metathesis reactions with acetylenes such as 3-hexyne.[3,4] Mechanistic investigations showed that tungstacyclobutadienes are intermediates in these reactions.[4] A similar chemistry was later observed for the analogous molybdenum species,[5–7] and triple bond metathesis of transition metal phosphides and nitrides have since been reported to proceed through similar intermediates.[8–10] Further work showed that the metal-metal triple-bonded dimers ($^t$BuO)$_3$M≡M(O$^t$Bu)$_3$ (M = Mo, W) exchange with alkynes under mild conditions to yield the metal alkylidynes RC≡M(O$^t$Bu)$_3$[5,11] and cleave N=N bonds to give imido complexes.[12] Alkyne metathesis and the related olefin metathesis has since found wide application in organic synthesis and polymerization.[13] The application of metathesis methods to organic synthesis led to the award of a Nobel Prize in 2005.[14]

The isolation of heavier group 14 element dimetallynes[15] of formula RMMR (M = Si, Ge, Sn, Pb; R = aryl, silyl, or amide ligand) and of stable complexes with triple bonds between heavier group 14 elements and transition metals by salt metathesis or ligand elimination[16–20] have suggested that triple bond metathesis reactions featuring the heavier group 14 elements might be feasible. However, the requirement for large substituents to stabilize these compounds suggested that steric effects might hamper or prevent such reactions. Nonetheless, we now show that the m-terphenyl supported

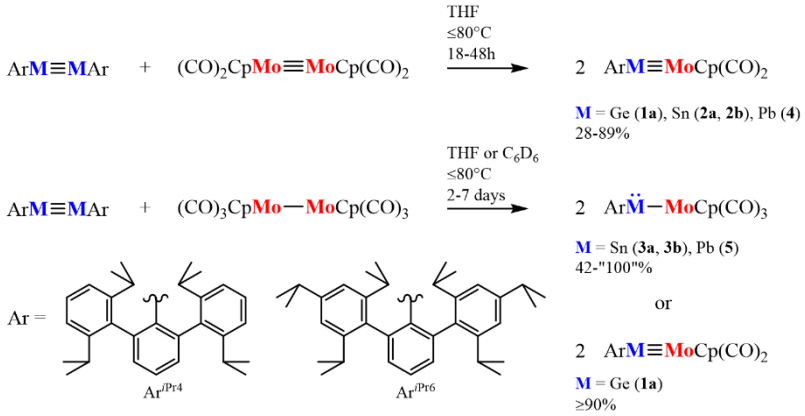


**Scheme 4.1**. Metathesis routes to compounds **1a-5.**

dimetallynes $Ar^{iPr4}MMAr^{iPr4}$ or $Ar^{iPr6}MMAr^{iPr6}$ ($Ar^{iPr4}$ = $C_6H_3$-2,6-($C_6H_3$-2,6-$^iPr_2)_2$, $Ar^{iPr6}$ = $C_6H_3$-2,6-($C_6H_2$-2,4,6-$^iPr_3)_2$; M = Ge, Sn, Pb) react readily with triple-bonded $(CO)_2CpMo{\equiv}MoCp(CO)_2$ (Cp = $\eta^5$-$C_5H_5$) or single-bonded $(CO)_3CpMo–MoCp(CO)_3$ to give triple-bonded $Ar^{iPr4}M{\equiv}MoCp(CO)_2$ (M = Ge, Sn) (**1a, 2a**) and $Ar^{iPr6}M{\equiv}MoCp(CO)_2$ (M = Sn, Pb) (**2b, 4**) or the single-bonded $Ar^{iPr4}\ddot{S}n–MoCp(CO)_3$ (**3a**) and $Ar^{iPr6}\ddot{M}–MoCp(CO)_3$ (M = Sn, Pb) (**3b, 5**) in moderate to excellent yields (Scheme 4.1).

Heating a solution of the digermyne $Ar^{iPr4}GeGeAr^{iPr4}$ and $(CO)_2CpMo{\equiv}MoCp(CO)_2$ in THF to 80°C for 18 h afforded the red-orange molybdogermylyne $Ar^{iPr4}Ge{\equiv}MoCp(CO)_2$ (**1a**) in ca. 89% yield as orange needles. Reaction of the digermyne with single-bonded $(CO)_3CpMo–MoCp(CO)_3$ in $C_6D_6$ at 80°C also gave **1a** with ≥ 90% conversion after 7 days. Previous attempts to prepare the single-bonded germylene complexes $Ar\ddot{G}e–MoCp(CO)_3$ (Ar = m-terphenyl ligand) from ArGeCl and $NaMoCp(CO)_3$ gave the triple-bonded germylyne complexes $Ar^{iPr6}Ge{\equiv}MoCp(CO)_2$ (**1b**)[21] and $Ar^{Me6}Ge{\equiv}MoCp(CO)_2$ (**1c**)[22] ($Ar^{Me6}$ = $C_6H_3$-2,6-($C_6H_2$-2,4,6-$Me_3)_2$) owing to facile CO elimination. It has since been found by Jones and coworkers that, by using a sterically demanding amide ligand, the molybdogermylenes {$C_6H_2$-2,6-$(CHPh_2)_2$-4-Me}(R)$N\ddot{G}e–MoCp(CO)_3$ (R = $SiMe_3$ or Ph) can be isolated.[23]

For distannynes, treatment with $(CO)_2CpMo{\equiv}MoCp(CO)_2$ in THF at ca. 25°C afforded a color change from dark green to red over 1-2 days to give the molybdostannylyne products $Ar^{iPr4}Sn{\equiv}MoCp(CO)_2$ (**2a**) or $Ar^{iPr6}Sn{\equiv}MoCp(CO)_2$ (**2b**) in 28% and 54% yields respectively. Similarly, the blue-purple single-bonded molybdostannylene $Ar^{iPr4}\ddot{S}n–MoCp(CO)_3$ (**3a**) was obtained in ca. 44% yield by stirring the distannyne with $(CO)_3CpMo–MoCp(CO)_3$ in THF for 2 days at ambient temperature. The metallostannylene $Ar^{iPr6}\ddot{S}n–MoCp(CO)_3$ (**3b**)[24] was prepared similarly in $C_6D_6$ in quantitative yield.

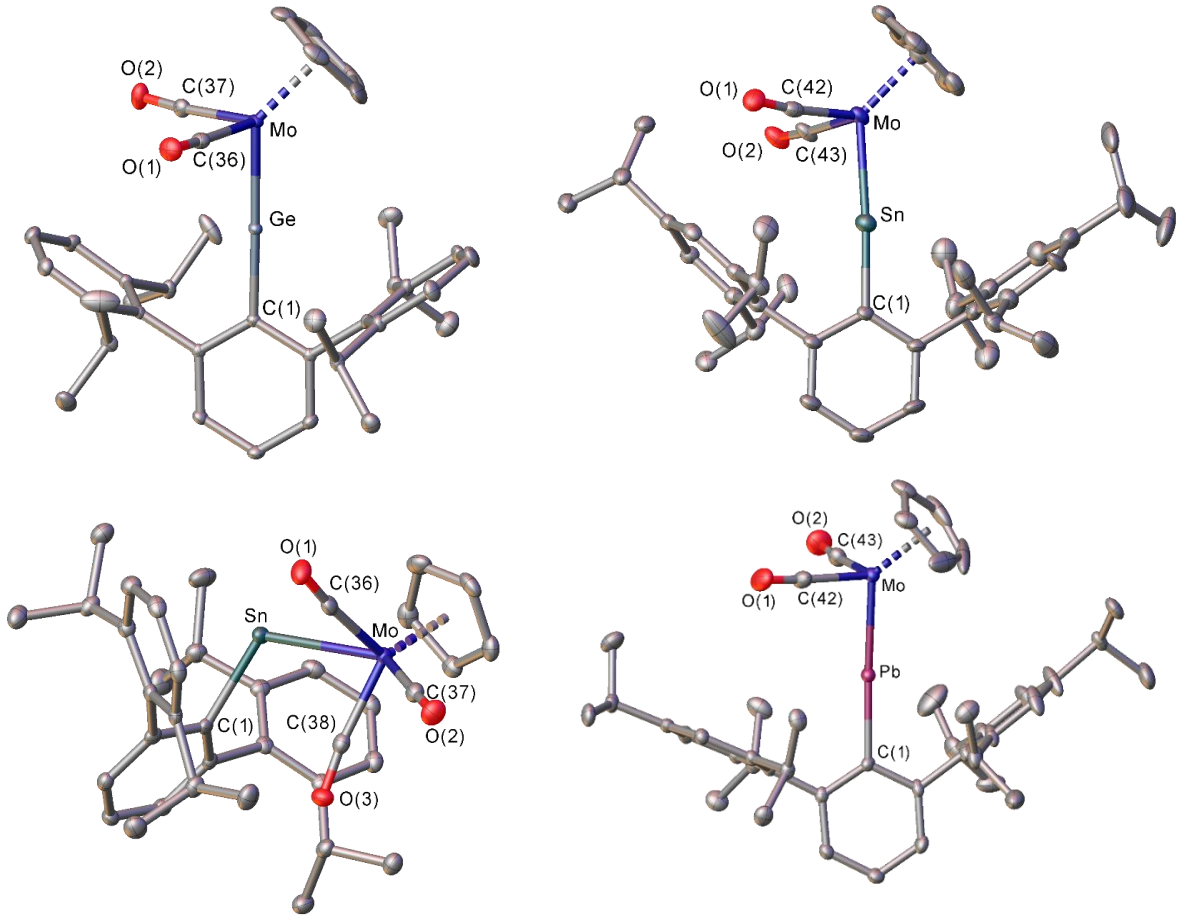


**Figure 4.1.** Thermal ellipsoid plots (50%) of $Ar^{iPr4}Ge{\equiv}MoCp(CO)_2$ (**1a**) (top left), $Ar^{iPr6}Sn{\equiv}MoCp(CO)_2$ (**2b**) (top right) $Ar^{iPr4}Sn–MoCp(CO)_3$ (**3a**) (bottom left), and $Ar^{iPr6}Pb{\equiv}MoCp(CO)_2$ (**4**) (bottom right). H atoms and disordered atoms in **2b** are not shown for clarity. Selected bond distances (Å) and angles (°): **1a**: Ge-Mo: 2.2831(2), Ge-C1: 1.9441(13), C1-Ge-Mo: 179.06(4). **2b:** Sn-Mo: 2.4691(7), Sn-C1: 2.036(4), C1-Sn-Mo: 173.1(3). **3a**: Sn-Mo: 2.9066(3), Sn-C1: 2.2030(18), C1-Sn-Mo: 113.88(5).**4:** Pb-Mo: 2.5143(2), Pb-C1: 2.201(2), C1-Pb-Mo: 175.03(7).

When the diplumbyne $Ar^{iPr6}PbPbAr^{iPr6}$ and $(CO)_2CpMo{\equiv}MoCp(CO)_2$ were stirred in THF at ca. 25°C for 18 h, a dark green solution of $Ar^{iPr6}Pb{\equiv}MoCp(CO)_2$ (**4**) was obtained from which **4** was isolated as dark blue-green crystals in 63% yield. Treatment of the diplumbyne with $(CO)_3CpMo–MoCp(CO)_3$ in $C_6D_6$ at ambient temperature for 2 days gave the molybdoplumbylene $Ar^{iPr6}\ddot{P}b–MoCp(CO)_3$(**5**) which had previously been obtained via a salt elimination route.[25]

The structures of **1a**, **2b**, **3a**, and **4** were determined by X-ray crystallography and are shown in Figure 4.1. The structures unequivocally establish the existence of metathesis products for both

triple and single-bonded species. For the triple-bonded species the M≡Mo bond lengths are consistent with the sum of the triple bond radii of the respective elements[26] and are ca. 0.45-0.50 Å shorter than those of the single-bonded congeners. With C–M≡Mo angles greater than ca. 170.0°, the triple-bonded structures are also consistent with those synthesized independently by salt elimination routes in conjunction with ligand (CO or $N_2$) elimination.[16–22]

Stannylyne **2b** is the second structurally characterized molybdostannylyne complex after $Tp'(CO)_2Mo{\equiv}SnAr^{Me6}$ (Tp′ = tris(3,5-dimethylpyrazolyl)borate) reported by Filippou.[20] The Sn-Mo distance is ca. 2.47 Å (cf. the sum of the triple bond radii $Sn(r_3)+Mo(r_3)$ = 2.45 Å[26] and the Sn≡Mo distance in $Tp'(CO)_2Mo{\equiv}SnAr^{Me6}$ = 2.5068(6) Å) and is much (ca. 0.45 Å) shorter than the Sn-Mo single bonds in **3a** (2.9065(6) Å) or in the known stannylenes **3b** (2.897(3) Å) and $Ar^{Me6}\ddot{S}n{-}MoCp(CO)_3$ (**3c**) (2.905(2) Å).[24] There is a wide $C_{ispo}$-Sn-Mo angle near 172.0° which may be contrasted with the much narrower angles in the molybdostannylenes (cf. 113.87(5)° in **3a**, 110.1(1)° in **3b**, or 110.7(1)° **3c**) in which repulsion from the non-bonding lone-pair on the Sn atom results in a strongly bent geometry. The Pb-Mo distance (2.5144(4) Å) in the plumbylyne **4** is similar to the sum of the triple bond radii (2.50 Å)[26] and slightly shorter than the bonds in *trans*-$Br(PMe_3)_4Mo{\equiv}PbAr^{iPr6}$ (2.5495(8) Å),[19] $Tp'(CO)_2Mo{\equiv}PbAr^{Me6}$ (2.5545(2) Å),[20] or $Tp'(CO)_2Mo{\equiv}PbAr^{iPr6}$ (2.5723(2) Å).[20]

The electronic spectra of the triple-bonded compounds display an intense absorption between 329-356 nm which tails into the visible region and may be due to transitions within the $MoCp(CO)_2$ moiety or possibly involving the M-Mo σ bond. They also display medium intensity absorptions at 423 nm for **1a**, 455 nm for **2a**, 457 nm for **2b**, and at 419 nm for **4** which are primarily responsible for the intense colors of these complexes (Figure 4.S39 of the SI). These likely correspond to the M-Mo π→π* transitions[21] and have weak lower-energy shoulders

probably due to Mo d→π* transitions.[21] The general red-shifting of the absorbances is consistent with a decrease in the M≡Mo bond energy as the group is descended from Ge to Pb.[27]

The infrared spectra of the triple-bonded complexes display two major bands in the CO stretching region with some shoulder features. The bands in **1a** appear at 1930 $cm^{-1}$ and 1872 $cm^{-1}$, while the two bands of **2a**, **2b**, and **4** are in the ranges 1899-1910 $cm^{-1}$ and 1847-1853 $cm^{-1}$. These data are consistent with decreasing transfer of electrons from Mo into the group 14 element p orbital as the group is descended from Ge to Pb, resulting in increased Mo(d)→CO(π*) donation. The bands are also of lower energy than those in triple-bonded **3a**-**3c** and **5** (1865-2020 $cm^{-1}$) as the group 14 element lone pair used in the triple bond increases electron density on the Mo and facilitates the Mo(d)→CO(π*) back-bonding.

The $^{119}Sn\{^1H\}$ NMR spectra of **2a** and **2b** each display a single resonance at 1021 ppm (**2a**) and 1040 ppm (**2b**). These values are further upfield than the signals of the single-bonded stannylene complexes **3a** and **3b** which appear at 2448 ppm (**3a**) and 2414 ppm (**3b**)[24] indicating increased shielding in the multiple-bonded species. The $^{207}Pb\{^1H\}$ NMR spectrum of **4** displays a singlet at 4686 ppm, which, like its tin counterpart, is further upfield than the plumbylene **5** which features a singlet at 9660 ppm.[25]

The formation of **1a**, **2a**, **2b**, and **4** represent the first report of products isolated from the metathesis of two metal-metal triple bonds. Previous investigations of the metathesis of $(CO)_2CpMo{\equiv}MoCp(CO)_2$ with $(CO)_2CpW{\equiv}WCp(CO)_2$ showed that after irradiation with UV light at 25°C or thermolysis at 120°C, Mo≡W containing ions could be observed in the mass spectra of the reaction products[28], but these were not isolated and their formation was deemed to result from single bond metathesis of $(CO)_3CpMo–MoCp(CO)_3$ with $(CO)_3CpW–WCp(CO)_3$ present in the reaction mixture followed by CO elimination.[29,30]

The ready formation of heavy group 14 element alkylidyne complexes via metathesis described here can be contrasted to the reaction of $(CO)_2CpMo{\equiv}MoCp(CO)_2$ with alkynes which give the isolable complexes $(CO)_2CpMoMoCp(CO)_2(\mu\text{-RCCR})$ in which the alkyne moiety is coordinated perpendicularly to the Mo-Mo bond.[31,32] Such structures are likely intermediates in the formation of group 6 metal alkylidyne complexes by isomerization to 1,3-metallocyclobutadienes.[33] Reactions of group 14 dimetallynes with unsaturated hydrocarbons are known to give formal [2+2] cycloaddition products which proceed through [1+2] cycloadditions.[34,35] However, the large steric demand of the ligands stabilizing the heavy alkyne analogues discussed here make it unlikely that the reactions proceed through π-bond complexes or tetrametallic-cyclobutadiene intermediates.

The reactivity may be attributed at least in part to the charge-shift nature of the triple bonds in group 14 dimetallynes.[36–39] We have recently reported studies of the reversible dissociation of the distannyne $Ar^{iPr4}SnSnAr^{iPr4}$ in solution[40] and showed that the terphenyl substituted distannynes exist in equilibrium with the corresponding Sn(I)Ar radicals ($K_{diss}$ = 1.78 × $10^{-6}$ for $Ar^{iPr4}SnSnAr^{iPr4}$ at 298 K). Therefore, we suspect the metathesis reactions are likely to proceed via interaction of Ge(I), Sn(I), or Pb(I) radical fragments with the Mo-Mo bonded species. The higher bond energy of the digermyne necessitates heating of the reaction mixture, while the tin and lead metathesis reactions proceed spontaneously at ambient temperature (ca. 25°C).

In each case the heavy alkylidyne species is thermodynamically favorable due to the formation of strong heterometallic triple bonds[27] (Table 4.S2). The higher bond strengths of the M≡Mo bonds in comparison to those of the homonuclear main group triple bond may be rationalized in terms of the CGMT (Carter, Goddard, Malrieu, and Trinquier) bonding model for their formation.[41–43] This model requires a doublet→quartet excitation in preparation of each main group MAr fragment for bonding. Only one such energy input is required for the heteronuclear main group-transition metal

triple bond whereas the homonuclear triple-bonded species requires double this amount. As a result, the linear isomer of dimetallynes H-M≡M-H (M = Si–Pb) is not an energetic minimum.[44-46] The calculated excitation energies (in kcal·mol$^{-1}$) for the group 14 species M–H are 47.1 (Ge), 45.9 (Sn), and 57.0 (Pb).[47] Hence there is a large energy difference between the homo- and heteronuclear triple bonds.

In conclusion, the germanium, tin, and lead analogues of alkynes undergo triple-bond metathesis with the Mo≡Mo bond in $(CO)_2CpMo{\equiv}MoCp(CO)_2$ to give the heavy alkylidyne products **1a**, **2a**, **2b**, and **4**. In addition, the molybdostannylenes **3a** and **3b** and molybdoplumbylene **5** are formed through metathesis with $(CO)_3CpMo–MoCp(CO)_3$. The relative facility of the metathetical exchange reactions described above lend further support to the view that many heavier main group multiple-bonded compounds feature charge-shift bonds which is consistent with their high reactivity.[37–39] Studies of metathesis reactions with other metal-metal triple-bonded molecules are in hand.

**Acknowledgements**

We thank the Office of Basic Energy Sciences, U.S. Department of Energy (DE-FG02-07ER4675) for support of this work.

**References**

(1) Elschenbroich, C. *Organometallics*, 3rd ed.; WILEY-VCH: Weinheim, 2006.

(2) Mortreux, A.; Blanchard, M. Metathesis of Alkynes by a Molybdenum Hexacarbonyl-Resorcinol Catalyst. *J. Chem. Soc., Chem. Commun.* **1974**, 786–787.

(3) Wengrovius, J. H.; Sancho, J.; Schrock, R. R. Metathesis of Acetylenes by Tungsten(VI)-Alkylidyne Complexes. *J. Am. Chem. Soc.* **1981**, *103*, 3932–3934.

(4) Churchill, M. R.; Ziller, J. W.; Freudenberger, J. H.; Schrock, R. R. Metathesis of Acetylenes by Triphenoxytungstenacyclobutadiene Complexes and the Crystal Structure of $W(C_3Et_3)[O\text{-}2,6\text{-}C_6H_3(i\text{-}Pr)_2]_3$. *Organometallics* **1984**, *3*, 1554–1562.

(5) Strutz, H.; Schrock, R. R. Multiple Metal-Carbon Bonds. 36. Metathesis of Molybdenum-Molybdenum Triple Bonds with Acetylenes to Give Alkylidyne Complexes. *Organometallics* **1984**, *3*, 1600–1601.

(6) McCullough, L. G.; Schrock, R. R. Multiple Metal-Carbon Bonds. 34. Metathesis of Acetylenes by Molybdenum(VI) Alkylidyne Complexes. *J. Am. Chem. Soc.* **1984**, *106*, 4067–4068.

(7) McCullough, L. G.; Schrock, R. R.; Dewan, J. C.; Murdzek, J. C. Multiple Metal-Carbon Bonds. 38. Preparation of Trialkoxymolybdenum(VI) Alkylidyne Complexes, Their Reactions with Acetylenes, and the x-Ray Structure of $Mo[C_3(CMe_3)_2][OCH(CF_3)_2](C_5H_5N)_2$. *J. Am. Chem. Soc.* **1985**, *107*, 5987–5998.

(8) Figueroa, J. S.; Cummins, C. C. Phosphaalkynes from Acid Chlorides via P for O(Cl) Metathesis: A Recyclable Niobium Phosphide ($P^{3-}$) Reagent That Effects C−P Triple-Bond Formation. *J. Am. Chem. Soc.* **2004**, *126*, 13916–13917.

(9) Gdula, R. L.; Johnson, M. J. A. Highly Active Molybdenum−Alkylidyne Catalysts for Alkyne Metathesis: Synthesis from the Nitrides by Metathesis with Alkynes. *J. Am. Chem. Soc.* **2006**, *128*, 9614–9615.

(10) Wiedner, E. S.; Gallagher, K. J.; Johnson, M. J. A.; Kampf, J. W. Synthesis of Molybdenum Nitrido Complexes for Triple-Bond Metathesis of Alkynes and Nitriles. *Inorg. Chem.* **2011**, *50*, 5936–5945.

(11) Schrock, R. R.; Listemann, M. L.; Sturgeoff, L. G. Metathesis of Tungsten-Tungsten Triple Bonds with Acetylenes and Nitriles to Give Alkylidyne and Nitrido Complexes. *J. Am. Chem. Soc.* **1982**, *104*, 4291–4293.

(12) Ikeda, H.; Nishi, K.; Tsurugi, H.; Mashima, K. Metathesis Cleavage of an N=N Bond in Benzo[*c*]Cinnolines and Azobenzenes by Triply-Bonded Ditungsten Complexes. *Chem. Commun.* **2018**, *54*, 3709–3711.

(13) Fürstner, A.; Davies, P. W. Alkyne Metathesis. *Chem. Commun.* **2005**, 2307–2320.

(14) The Nobel Prize in Chemistry 2005. NobelPrize.org. Nobel Media AB 2019. https://www.nobelprize.org/prizes/chemistry/2005/summary/ (accessed Nov 8, 2019).

(15) Power, P. P. Silicon, Germanium, Tin and Lead Analogues of Acetylenes. *Chem. Commun.* **2003**, 2091–2101.

(16) Hashimoto, H.; Tobita, H. Recent Advances in the Chemistry of Transition Metal–Silicon/Germanium Triple-Bonded Complexes. *Coord. Chem. Rev.* **2018**, *355*, 362–379.

(17) Filippou, A. C.; Hoffmann, D.; Schnakenburg, G. Triple Bonds of Niobium with Silicon, Germaniun and Tin: The Tetrylidyne Complexes $[(\kappa^3\text{-Tmps})(CO)_2Nb{\equiv}E{-}R]$ (E = Si, Ge, Sn; Tmps = $MeSi(CH_2PMe_2)_3$ ; R = Aryl). *Chem. Sci.* **2017**, *8*, 6290–6299.

(18) Filippou, A. C.; Portius, P.; Philippopoulos, A. I.; Rohde, H. Triple Bonding to Tin: Synthesis and Characterization of the Stannylyne Complex Trans-$[Cl(PMe_3)_4W{\equiv}Sn{-}C_6H_3\text{-}2,6\text{-}Mes_2]$. *Angew. Chem., Int. Ed.* **2003**, *42*, 445–447.

(19) Filippou, A. C.; Weidemann, N.; Schnakenburg, G.; Rohde, H.; Philippopoulos, A. I. Tungsten-Lead Triple Bonds: Syntheses, Structures, and Coordination Chemistry of the Plumbylidyne Complexestrans-[X($PMe_3$)$_4$W≡Pb(2,6-Trip$_2$C$_6$H$_3$)]. *Angew. Chem., Int. Ed.* **2004**, *43*, 6512–6516.

(20) Ghana, P. *Synthesis, Characterization, and Reactivity of Ylidyne and μ-Ylido Complexes Supported by Scorpionato Ligands*; Springer: Cham, 2019.

(21) Pu, L.; Twamley, B.; Haubrich, S. T.; Olmstead, M. M.; Mork, B. V.; Simons, R. S.; Power, P. P. Triple Bonding to Germanium: Characterization of the Transition Metal Germylynes ($\eta^5$-$C_5H_5$)(CO)$_2$M:Ge-$C_6H_3$-2,6-Mes$_2$ (M = Mo, W; Mes = −$C_6H_2$-2,4,6-Me$_3$. *J. Am. Chem. Soc.* **2000**, *122*, 650–656.

(22) Simons, R. S.; Power, P. P. ($\eta^5$-$C_5H_5$)(CO)$_2$MoGe$C_6H_3$-2,6-Mes$_2$: A Transition-Metal Germylyne Complex. *J. Am. Chem. Soc.* **1996**, *118*, 11966–11967.

(23) Hicks, J.; Hadlington, T. J.; Schenk, C.; Li, J.; Jones, C. Utilizing Steric Bulk to Stabilize Molybdenum Aminogermylyne and Aminogermylene Complexes. *Organometallics* **2013**, *32*, 323–329.

(24) Barrett E. Eichler; Andrew D. Phillips; Scott T. Haubrich; Benjamin V. Mork, A.; Power, P. P. Synthesis, Structures, and Spectroscopy of the Metallostannylenes ($\eta^5$-$C_5H_5$)(CO)$_3$M−S̈n−$C_6H_3$-2,6-Ar$_2$ (M = Cr, Mo, W; Ar = $C_6H_2$-2,4,6-Me$_3$, $C_6H_2$-2,4,6-Pr$^i_3$). *Organometallics* **2002**, *21*, 5622–5627.

(25) Pu, L.; Power, P. P.; Boltes, I.; Herbst-Irmer, R. Synthesis and Characterization of the Metalloplumbylenes ($\eta^5$-$C_5H_5$)(CO)$_3$M-P̈b-$C_6H_3$-2,6-Trip$_2$ (M = Cr, Mo, or W; Trip = −$C_6H_2$-2,4,6-i-Pr$_3$). *Organometallics* **2000**, *19*, 352–356.

(26) Pyykkö, P. Additive Covalent Radii for Single-, Double-, and Triple-Bonded Molecules and Tetrahedrally Bonded Crystals: A Summary. *J. Phys. Chem. A* **2015**, *119*, 2326–2337.

(27) Takagi, N.; Yamazaki, K.; Nagase, S. Theoretical Investigation of Triple Bonding between Transition Metal and Main Group Elements in ($\eta^5$-$C_5H_5$)(CO)$_2$M≡ER (M = Cr, Mo, W; E = Si, Ge, Sn, Pb; R = Terphenyl Groups). *Bull. Korean Chem. Soc.* **2003**, *24*, 832–836.

(28) Chisholm, M. H.; Extine, M. W.; Kelly, R. L.; Mills, W. C.; Murillo, C. A.; Rankel, L. A.; Reichert, W. W. In Search of Metal-Metal Metathesis in the Chemistry of Compounds Containing Metal-to-Metal Triple Bonds between Molybdenum and Tungsten Atoms. *Inorg. Chem.* **1978**, *17*, 1673–1675.

(29) Chisholm, M. H.; Macintosh, A. M. Linking Multiple Bonds between Metal Atoms: Clusters, Dimers of "Dimers", and Higher Ordered Assemblies. *Chem. Rev.* **2005**, *105*, 2949–2976.

(30) Cotton, F. A.; Murillo, C. A.; Walton, R. A. *Multiple Bonds Between Metal Atoms*, 3rd ed.; Springer: Boston, 2005.

(31) Klingler, R. J.; Butler, W.; Curtis, M. D. Synthesis, Reactivity, and Molecular Structure of Cyclopentadienylmolybdenum Dicarbonyl Dimer. Molybdenum–Molybdenum Triple Bond. *J. Am. Chem. Soc.* **1975**, *97*, 3535–3536.

(32) Bailey, W. I.; Chisholm, M. H.; Cotton, F. A.; Rankel, L. A. Reactions of Metal-to-Metal Multiple Bonds. 4.1 μ-Acetylene-Bis(Cyclopentadienyl)Tetracarbonyldimolybdenum Compounds. Preparations, Properties, Structural Characterizations, and Dynamical Solution Behavior. *J. Am. Chem. Soc.* **1978**, *100*, 5764–5773.

(33) Chisholm, M. H.; Heppert, J. A. Chemistry of 1,3-Ditungstacyclobutadienes. *Adv. Organomet. Chem.* **1986**, *26*, 97–124.

(34) Kinjo, R.; Ichinohe, M.; Sekiguchi, A.; Takagi, N.; Sumimoto, M.; Nagase, S. Reactivity of a Disilyne RSi≡SiR (R = $Si^iPr[CH(SiMe_3)_2]_2$) toward π-Bonds: Stereospecific Addition and a New Route to an Isolable 1,2-Disilabenzene. *J. Am. Chem. Soc.* **2007**, *129*, 7766–7767.

(35) Sasamori, T.; Sugahara, T.; Agou, T.; Sugamata, K.; Guo, J.-D.; Nagase, S.; Tokitoh, N. Reaction of a diaryldigermyne with ethylene. *Chem. Sci.* **2015**, *6*, 5526–5530.

(36) Shaik, S.; Danovich, D.; Wu, W.; Hiberty, P. C. Charge-Shift Bonding and Its Manifestations in Chemistry. *Nature Chem.* **2009**, *1*, 443–449.

(37) Shaik, S.; Danovich, D.; Braida, B.; Wu, W.; Hiberty, P. C. New Landscape of Electron-Pair Bonding: Covalent, Ionic, and Charge-Shift Bonds. *Struct. Bond.* **2016**, *170*, 169–212.

(38) Ploshnik, E.; Danovich, D.; Hiberty, P. C.; Shaik, S. The Nature of the Idealized Triple Bonds Between Principal Elements and the σ Origins of Trans-Bent Geometries—A Valence Bond Study. *J. Chem. Theory Comput.* **2011**, *7*, 955–968.

(39) Huo, S.; Li, X.; Zeng, Y.; Sun, Z.; Zheng, S.; Meng, L. Nature of E–E bonds in heavier ditetrel alkyne analogues ArEEAr (Ar = $C_6H_3$-2,6($C_6H_3$-2,6-$Pr^i_2$)$_2$; E = Si, Ge, Sn, and Pb). *New J. Chem.* **2013**, *37*, 3145–3151.

(40) Lai, T. Y.; Tao, L.; Britt, R. D.; Power, P. P. Reversible Sn–Sn Triple Bond Dissociation in a Distannyne: Support for Charge-Shift Bonding Character. *J. Am. Chem. Soc.* **2019**, *141*, 12527–12530.

(41) Carter, E. A.; Goddard, W. A. Relation between singlet-triplet gaps and bond energies *J. Phys. Chem.* **1986**, *90*, 998–1001.

(42) Trinquier, G.; Malrieu, J.-P. Nonclassical distortions at multiple bonds. *J. Am. Chem. Soc*. **1987**, *109*, 5303–5315.

(43) Trinquier, G.; Malrieu, J.-P. Trans-bending at double bonds. Occurrence and extent. *J. Am. Chem. Soc*. **1989**, *111*, 5916–5921.

(44) Colgegrove, B. T.; Schaefer, H. F. Disiylne ($Si_2H_2$) revisited. *J. Phys. Chem.* **1990**, *94*, 5593–5602.

(45) Grev, R. S.; Deleeuw, B. J.; Schaefer, H. F. Germanium–germanium multiple bonds: The singlet electronic ground state of $Ge_2H_2$. *Chem. Phys. Let.* **1990**, *165*, 257–264.

(46) Nagase, S.; Kobayashi, K.; Takagi, N. Triple bonds between heavier Group 14 elements. A theoretical approach. *J. Organomet. Chem.* **2000**, *611*, 264–271.

(47) Lein, M.; Krapp, A.; Frenking, G. Why Do the Heavy-Atom Analogues of Acetylene $E_2H_2$ (E = Si–Pb) Exhibit Unusual Structures? *J. Am. Chem. Soc.* **2005**, 127, 6290–6299.

**Author Contributions**

**J. D. Queen**: Synthesized and spectroscopically characterized compounds **1a**, **2a**, **2b**, and **4**, collected X-ray crystallographic data, and prepared manuscript.

**A. C. Phung**: Synthesized compound **3a** and helped prepare $(CO)_2CpMo{\equiv}MoCp(CO)_2$.

**C. A. Caputo**: Was the first to prepare **2a** and **3a** through the metathesis reaction with the distannyne.

**J. C. Fettinger**: Prepared X-ray crystallographic data for publication.

**P. P. Power**: Supervised synthetic work and manuscript preparation.

## Supporting Information

## Experimental Details

**General Procedures.** All manipulations were carried out using modified Schlenk techniques or in a Vacuum Atmospheres OMNI-Lab drybox under a $N_2$ or argon atmosphere. Manipulations of the lead compounds were carried out with careful exclusion of light when possible due to the tendency of low-valent lead compounds to decompose or disproportionate under illumination. Solvents were dried over columns of activated alumina using a Grubbs type purification system[S1] (Glass Contour), stored over Na (THF) or K (hexanes, pentane, toluene) mirrors, and degassed via three freeze-pump-thaw cycles prior to use. The $^{1}H$, $^{13}C\{^{1}H\}$, $^{119}Sn\{^{1}H\}$, and $^{207}Pb\{^{1}H\}$ NMR spectra were recorded on Varian Inova 600 MHz or Bruker Avance III HD Nanobay 400 MHz spectrometers. The $^{1}H$ and $^{13}C\{^{1}H\}$NMR spectra were referenced to the residual solvent signals in $C_6D_6$ (δ 7.16 ppm)[S2]. The $^{119}Sn\{^{1}H\}$ and $^{207}Pb\{^{1}H\}$ NMR spectra were referenced to external standards of $SnMe_4$ (δ 0.0 ppm) or $PbMe_4$ (δ 0.0 ppm) in $C_6D_6$. UV-Visible spectra were recorded in dilute hexane solutions in 3.5 mL quartz cuvettes using an Olis 17 Modernized Cary 14 UV-Vis/NIR spectrophotometer. Infrared spectra were collected on a Bruker Tensor 27 ATR-FTIR spectrometer. Melting points were measured in glass capillary tubes sealed under argon using a Mel-Temp II apparatus and are uncorrected.

$[Mo(\eta^5\text{-}C_5H_5)(CO)_3]_2$ was purchased commercially. $Ar^{iPr4}GeGeAr^{iPr4}$,[S3] $Ar^{iPr4}SnSnAr^{iPr4}$,[S4] $Ar^{iPr6}SnSnAr^{iPr6}$,[S5] $Ar^{iPr6}PbPbAr^{iPr6}\cdot C_6H_{14}$,[S6,S7] and $[Mo(\eta^5\text{-}C_5H_5)(CO)_2]_2$[S8] were prepared according to the literature procedures.

**$Ar^{iPr4}Ge{\equiv}Mo(\eta^5\text{-}C_5H_5)(CO)_2$ (1a).** $Ar^{iPr4}GeGeAr^{iPr4}$ (0.235 g, 0.250 mmol) and $[Mo(\eta^5\text{-}C_5H_5)(CO)_2]_2$ (0.108 g, 0.250 mmol) were placed in a heavy-walled Teflon screw-cap Schlenk flask and dissolved in ca. 40 mL of THF. The flask was sealed and the mixture was heated to 80 °C (oil bath temperature) for 18 h during which time there was a subtle color change from deep red to red-orange. The mixture was cooled to room temperature and the volatile components were removed under reduced pressure. The orange residue was extracted with hexanes (ca. 60 mL) and filtered through Celite. Storage of the filtrate at ca. -18 °C overnight afforded yellow-orange needles of $Ar^{iPr4}Ge{\equiv}Mo(\eta^5\text{-}C_5H_5)(CO)_2$. The mother liquor was decanted, concentrated to ca. 8 mL and stored at ca. 5°C for one week to afford X-ray quality crystals of $Ar^{iPr4}Ge{\equiv}Mo(\eta^5\text{-}C_5H_5)(CO)_2$ as red blocks. Yield: 0.304 g (89%) mp = 199-215 °C (decomposes with a color change to brown). $^1$H NMR (600 MHz, $C_6D_6$, 298K): δ 7.33 (t, $^3J_{H,H}$ = 7.7 Hz, 2H, Trip p-H), 7.24 (d, $^3J_{H,H}$ = 7.8 Hz, 4H, Trip m-H), 7.10 (t, $^3J_{H,H}$ = 7.6 Hz, 1H, p-H), 7.04 (d, $^3J_{H,H}$ = 7.6 Hz, 2H, m-H), 4.67 (s, 5H, $C_5H_5$), 2.92 (sept, $^3J_{H,H}$ = 7.0 Hz, 4H, -$CH(CH_3)_2$), 1.48 (d, $^3J_{H,H}$ = 6.9 Hz, 12H, -$CH(CH_3)_2$), 1.09 (d, $^3J_{H,H}$ = 6.9 Hz, 12H, -$CH(CH_3)_2$). $^{13}C\{^1H\}$ NMR (151 MHz, $C_6D_6$, 298 K): δ 231.3, 166.7, 148.1, 143.3, 135.8, 130.23, 130.19, 128.8, 123.9, 86.3, 31.4, 25.3, 23.9. ATR-FTIR: $\tilde{\nu}_{CO}$ ($cm^{-1}$) = 1961 (w), 1930 (s), 1918 (m), 1890 (w), 1872 (s), 1845 (m). UV-Vis (hexanes) $\lambda_{max}$ = nm ($\varepsilon$ = $L{\cdot}mol^{-1}{\cdot}cm^{-1}$): 325 (shoulder, 26000), 329 (27000), 423 (3400), 540 (shoulder, 290).

**Reaction of $Ar^{iPr4}GeGeAr^{iPr4}$ with $[Mo(\eta^5\text{-}C_5H_5)(CO)_3]_2$.** $Ar^{iPr4}GeGeAr^{iPr4}$ (9.5 mg, 0.010 mmol) and $[Mo(\eta^5\text{-}C_5H_5)(CO)_3]_2$ (6.0 mg, 0.012 mmol) were dissolved in ca. 0.8 mL $C_6D_6$ in an NMR tube. The mixture was heated to 80°C for 7 days, after which >90% conversion to $Ar^{iPr4}Ge{\equiv}Mo(\eta^5\text{-}C_5H_5)(CO)_2$ (**1a**) was determined by $^1$H NMR spectroscopy.

**$Ar^{iPr4}Sn{\equiv}Mo(\eta^5\text{-}C_5H_5)(CO)_2$ (2a).** A solution of $Ar^{iPr4}SnSnAr^{iPr4}$ (0.258 g, 0.250 mmol) and $[Mo(\eta^5\text{-}C_5H_5)(CO)_2]_2$ (0.108 g, 0.250 mmol) in THF (ca. 30 mL) was stirred at 25°C for 2 days, resulting in a color change from dark forest-green to dark red. The volatile components were removed under reduced pressure and the dark red-brown residue was extracted with ca. 40 mL hexanes. The dark red solution was filtered through Celite and concentrated to ca. 10 mL and stored at -30°C to give $Ar^{iPr4}Sn{\equiv}Mo(\eta^5\text{-}C_5H_5)(CO)_2$ as a red-purple solid. Several attempts to grow crystals of **2a** that were suitable for single crystal X-ray diffraction were unsuccessful due to extensive twinning. Yield: 0.102 g (28%). mp = 145-152°C (decomposes with a color change to black). $^1$H NMR (400 MHz, $C_6D_6$, 298 K) δ 7.34 (t, $^3J_{H,H}$ = 7.8 Hz, 2H, Dipp p-Ar*H*) 7.20-7.26 (m, 6H, m-Ar*H* and Dipp m-Ar*H*), 7.16 (triplet, overlapping with solvent residual peak, 1H, p-Ar*H*), 4.73 (s, 5H, $C_5H_5$), 2.92 (sept, $^3J_{H,H}$ = 7.1 Hz, 4H, -C*H*$(CH_3)_2$), 1.43 (d, $^3J_{H,H}$ = 6.9 Hz, 12H, -CH(C*H*$_3)_2$), 1.06 (d, $^3J_{H,H}$ = 6.8 Hz, 12H, -CH(C*H*$_3)_2$). $^{13}$C{$^1$H} NMR (101 MHz, $C_6D_6$, 298 K) δ 232.7, 187.4, 148.0, 143.4, 136.8, 130.4, 129.6, 129.5, 124.3, 84.8, 31.2, 25.4, 23.9. $^{119}$Sn{$^1$H} NMR (149 MHz, $C_6D_6$, 298 K) δ 1021. ATR-FTIR: $\tilde{\nu}_{CO}$ (cm$^{-1}$) = 1932 (w), 1899 (s), 1850 (s). UV-Vis (hexanes) $\lambda_{max}$ = nm ($\varepsilon$ = L·mol$^{-1}$·cm$^{-1}$): 356 (36100), 455 (3200), 570 (shoulder, 850).

**$Ar^{iPr6}Sn{\equiv}Mo(\eta^5\text{-}C_5H_5)(CO)_2$ (2b).** $Ar^{iPr6}SnSnAr^{iPr6}$ (0.300 g, 0.250 mmol) and $[Mo(\eta^5\text{-}C_5H_5)(CO)_2]_2$ (0.108 g, 0.250 mmol) were dissolved in THF (ca. 25 mL) and stirred for 1 day at 25°C during which time the solution changed from dark green to red. The volatile components were removed under reduced pressure and the red-brown was residue was extracted with pentane (ca. 40 mL). The solution was concentrated to ca. 3 mL and stored at ca. -30°C to give $Ar^{iPr6}Sn{\equiv}Mo(\eta^5\text{-}C_5H_5)(CO)_2$ as red plates. Yield: 0.221 g (54%). mp = 149-158°C (decomposes with color change to black). $^1$H NMR (600 MHz, $C_6D_6$, 298 K) δ 7.30 (s, 4H, Trip m-Ar*H*), 7.28

(d, 2H, $^3J_{H,H}$ = 7.8 Hz, m-Ar*H*), 7.21 (t, $^3J_{H,H}$ = 7.9 Hz, 1H, p-Ar*H*) 4.73 (s, 5H, $C_5H_5$), 2.99 (sept, $^3J_{H,H}$ = 6.9 Hz, 4H, o-C*H*$(CH_3)_2$), 2.92 (sept, 2H, $^3J_{H,H}$ = 6.9 Hz, p-C*H*$(CH_3)_2$), 1.50 (d, $^3J_{H,H}$ = 7.0 Hz, 12H, -CH(C*H*$_3)_2$), 1.36 (d, $^3J_{H,H}$ = 6.9 Hz 12H, -CH(C*H*$_3)_2$), 1.14 (d, $^3J_{H,H}$ = 6.8 Hz 12H, -CH(C*H*$_3)_2$). $^{13}C\{^1H\}$ NMR (101 MHz, $C_6D_6$, 298 K) δ 232.9, 187.7, 150.6, 148.1, 143.5, 134.5, 129.8, 129.5, 122.4, 84.7, 35.0, 31.3, 25.5, 24.2, 23.9. $^{119}Sn\{^1H\}$ NMR (149 MHz, $C_6D_6$, 298 K) δ 1040. ATR-FTIR: $\tilde{\nu}_{CO}$ ($cm^{-1}$) = 1958 (w) 1910 (s), 1853 (s). UV-Vis (hexanes) $\lambda_{max}$ = nm ($\varepsilon$ = $L\cdot mol^{-1}\cdot cm^{-1}$): 356 (33000), 457 (2700), 546 (shoulder, 570).

**$Ar^{iPr4}Sn–Mo(\eta^5\text{-}C_5H_5)(CO)_3$ (3a).** A dark forest-green solution of $Ar^{iPr4}SnSnAr^{iPr4}$ (0.516 g, 0.500 mmol) in THF (ca. 30 mL) was added to a red solution of $[Mo(\eta^5\text{-}C_5H_5)(CO)_3]_2$ (0.245 g, 0.500 mmol) in THF (ca. 10 mL) at 25°C. The mixture was stirred for two days after which the volatile components were removed under reduced pressure. The purple residue was dissolved in toluene (ca. 50 mL) and filtered through a Celite plug. The dark navy-blue filtrate was concentrated until incipient crystallization and stored at -30°C for two days to give X-ray quality purple crystals of $Ar^{iPr4}Sn–Mo(\eta^5\text{-}C_5H_5)(CO)_3$. Yield 0.335 g (44%). mp = 170-173°C. $^1H$ NMR (400 MHz, $C_6D_6$, 298 K): δ 1.00-1.16 (m, broad, 12H, -CH(C*H*$_3)_2$), 1.39 (d, $^3J_{H,H}$ = 6.8 Hz, 12H, -CH(C*H*$_3)_2$). 3.41-3.55 (m, br, 4H, -C*H*$(CH_3)_2$), 4,24 (s, 5H, $C_5H_5$), 6.95-7.44 (m, 9H, Ar*H*). $^{13}C\{^1H\}$ NMR (151 MHz, $C_6D_6$, 298 K): δ 184.7, 144.9, 135.9, 130.6, 129.5, 124.8, 123.6, 122.9, 92.5, 31.0, 30.8, 26.6, 26.5, 24.5, 24.4, 23.4, 23.1. $^{119}Sn\{^1H\}$ NMR (224 MHz, $C_6D_6$, 298 K): δ 2448. ATR-FTIR $\tilde{\nu}_{CO}$ ($cm^{-1}$) = 2016 (s), 1960 (s), 1870 (s). UV-Vis (hexanes) $\lambda_{max}$ = nm ($\varepsilon$ = $L\cdot mol^{-1}\cdot cm^{-1}$): 367 (5600) 580 (960).

**$Ar^{iPr6}Sn–Mo(\eta^5\text{-}C_5H_5)(CO)_3$ (3b).** $Ar^{iPr6}SnSnAr^{iPr6}$ (12.0 mg, 0.010 mmol) and $[Mo(\eta^5\text{-}C_5H_5)(CO)_3]_2$ (6.5 mg, 0.013 mmol) were combined in an NMR tube and dissolved in ca. 0.7 mL of $C_6D_6$. After 2 days, the dark green mixture had turned dark blue and the $^1H$ and $^{119}Sn\{^1H\}$

NMR spectra showed signals consistent with the formation of $Ar^{iPr6}Sn–Mo(\eta^5-C_5H_5)(CO)_3$ with no $Ar^{iPr6}SnSnAr^{iPr6}$ remaining.

**$Ar^{iPr6}Pb≡Mo(\eta^5-C_5H_5)(CO)_2$ (4).** $Ar^{iPr6}PbPbAr^{iPr6}·C_6H_{14}$ (0.100 g, 0.068 mmol) and $[Mo(\eta^5-C_5H_5)(CO)_2]_2$ (0.030 g, 0.069 mmol) were placed in a Schlenk tube and dissolved in ca. 10 mL THF. The mixture was stirred for 18 hours at ambient temperature and the volatile components were removed under reduced pressure. The dark green residue was extracted with ca. 10 mL hexanes and filtered through Celite. The green solution was concentrated to ca. 5 mL and stored at ca. 5 °C for 2 days to give dark blue-green crystals of $Ar^{iPr6}Pb≡Mo(\eta^5-C_5H_5)(CO)_2$. Yield: 0.078 g (63%). mp = 146-154°C (decomposes with a color change to black). $^1$H NMR (400 MHz, $C_6D_6$, 298 K): δ 7.94 (d, $^3J$ = 7.4 Hz, 2H, m-Ar*H*), 7.32 (t, $^3J$ = 7.4 Hz, 1H, p-Ar*H*), 7.29 (s, 4H, Trip Ar*H*), 4.72 (s, 5H, $C_5H_5$), 3.03 (sept, $^3J$ = 6.8 Hz, 4H, o-C*H*$(CH_3)_2$), 2.92 (sept, $^3J$ = 6.9 Hz, 2H, p-C*H*$(CH_3)_2$), 1.45 (d, $^3J$ = 6.9 Hz, 12H, -CH(C*H*$_3)_2$), 1.36 (d, $^3J$ = 6.9 Hz, 12H, -CH(C*H*$_3)_2$), 1.14 (d, $^3J$ = 6.8 Hz, 12H, -CH(C*H*$_3)_2$). $^{13}C\{^1H\}$ NMR (101 MHz, $C_6D_6$, 298K): δ 229.8, 150.4, 147.7, 143.0, 136.7, 135.2, 127.4, 122.3, 84.5, 35.0, 31.2, 25.4, 24.3, 23.9. $^{207}Pb\{^1H\}$ NMR (84 MHz, $C_6D_6$, 298 K): δ 4686. ATR-FTIR: $\tilde{\nu}_{CO}$ (cm$^{-1}$) = 1962(w), 1903(s), 1847(s), 1823(m). UV-Vis (hexanes): $\lambda_{max}$, ($\varepsilon$, L mol$^{-1}$ cm$^{-1}$) 357 nm (26000), 419 (3800), 480 (shoulder, 1900), 619 nm (550).

**$Ar^{iPr6}Pb–Mo(\eta^5-C_5H_5)(CO)_3$ (5).** $Ar^{iPr6}PbPbAr^{iPr6}·C_6H_{14}$ (16.0 mg, 0.011 mmol) and $[Mo(\eta^5-C_5H_5)(CO)_3]_2$ (8.0 mg, 0.016 mmol) were combined in an NMR tube and dissolved in ca. 0.7 mL of $C_6D_6$. After 2 days, the red mixture had turned blue-green and the $^1$H NMR and $^{207}Pb\{^1H\}$ showed signals consistent with formation of $Ar^{iPr6}Pb–Mo(\eta^5-C_5H_5)(CO)_3$ and no $Ar^{iPr6}PbPbAr^{iPr6}$ remaining.

## X-Ray Crystallography

Crystals of **1a**, **2b**, **3a**, and **4** were removed from a Schlenk flask under a stream of nitrogen and immediately covered with hydrocarbon oil. A suitable crystal was selected, attached to a MiTeGen microloop, and mounted on the goniometer of the diffractometer under a cold stream of $N_2$. Data were collected at 90 K on a Bruker APEXII diffractometer (**1a**, **3a**, **4**) or 100 K on a Bruker D8 VENTURE diffractometer (**2b**) with Mo Kα (λ = 0.71073 Å) or Cu (1.54178) radiation. Absorption corrections were applied using SADABS.[S9] The crystal structures were solved by intrinsic phasing methods using SHELXT[S10] and refined by full matrix least-squares procedures using SHELXL.[S11] All non-H atoms were refined anisotropically.

**Table 4.S1.** Summary of X-ray crystallographic data for **1a**, **2b**, **3a**, and **4**.

| **Compound** | **1a** | **2b** | **3a** | **4** |
|---|---|---|---|---|
| **Formula** | $C_{37}H_{42}MoO_2Ge$ | $C_{43}H_{54}MoO_2Sn$ | $C_{38}H_{42}MoO_3Sn$ | $C_{43}H_{54}MoO_2Pb$ |
| **Formula Weight (g mol$^{-1}$)** | 687.23 | 817.51 | 761.34 | 906.00 |
| **T (K) / λ (Å)** | 90(2) / 0.71037 | 100(2) / 1.54178 | 90(2) / 0.71073 | 90(2) / 0.71073 |
| **Crystal System** | Monoclinic | Triclinic | Monoclinic | Monoclinic |
| **Space Group** | $P2_1/n$ | P-1 | $P2_1/n$ | $P2_1/c$ |
| **Z** | 4 | 2 | 4 | 4 |
| **Crystal color and habit** | Red block | Red plate | Purple block | Blue-green rod |
| **a (Å)** | 11.3692(9) | 9.6023(4) | 8.5886(7) | 13.3557(4) |
| **b (Å)** | 16.3298(12) | 9.8505(4) | 17.4666(14) | 10.6317(3) |
| **c (Å)** | 18.4110(14) | 21.0495(8) | 22.6926(19) | 28.1313(8) |
| **α (°)** | 90 | 87.9879(15) | 90 | 90 |
| **β (°)** | 102.4620(10) | 82.7837(15) | 97.2770(10) | 94.2515(11) |
| **γ (°)** | 90 | 88.3199(14) | 90 | 90 |
| **V (Å$^3$)** | 3337.6(4) | 1973.41(14) | 3376.8(5) | 3983.5(2) |
| **ρ (mg mm$^{-3}$)** | 1.368 | 1.376 | 1.498 | 1.511 |
| **Abs. coeff (mm$^{-1}$)** | 1.306 | 7.876 | 1.146 | 4.568 |
| **F(000)** | 1416.0 | 840 | 1544 | 1808 |
| **Crystal size (mm)** | 0.239 × 0.190 × 0.160 | 0.377 × 0.163 × 0.067 | 0.256 × 0.146 × 0.064 | 0.179 × 0.086×0.037 |
| **2$\theta$ range (°)** | 4.436 to 61.116 | 4.236 to 72.626 | 4.306 to 55.02 | 1.452 to 30.605 |
| **Reflns collected** | 38995 | 13323 | 30122 | 40468 |
| **Ind. Reflns.** | 10223 | 7775 | 7760 | 12215 |
| **R(int)** | 0.0303 | 0.0336 | 0.0346 | 0.0393 |
| **Obs. reflns ($I$>2σ($I$))** | 8829 | 7301 | 6591 | 10171 |
| **Completeness** | 100% | 99.7% | 100% | 100% |
| **Goodness-of-fit on $F^2$** | 1.024 | 1.066 | 1.027 | 1.033 |
| **Final R ($I$>2σ($I$))** | R1 = 0.0243 | R1 = 0.0542 | R1 = 0.0221 | R1 = 0.0269 |
| | wR2 = 0.0576 | wR2 = 0.1236 | wR2 = 0.0443 | wR2 = 0.0512 |
| **R (all data)** | R1 = 0.0314 | R1 = 0.0568 | R1 = 0.0312 | R1 = 0.0378 |
| | wR2 = 0.0604 | wR2 = 0.1256 | wR2 = 0.0473 | wR2 = 0.0549 |

## Bond Energies

**Table 4.S2.** Calculated or experimental bond energies for triple bonds in the dimetallynes, the molybdenum dimers, and the group 14 M≡Mo triple bonds. [a]Ref S12. [b]Ref 34. [c]Ref S13. [d]Ref S14. [e]Ref 27.

| **Compound** | **Bond Energy (kcal mol$^{-1}$)** |
|---|---|
| $Ar^{iPr6}GeGeAr^{iPr6}$ | 33.8[a] |
| $Ar^{iPr6}SnSnAr^{iPr6}$<br>$Ar^{iPr4}SnSnAr^{iPr4}$ | 25.9[a]<br>17.2[b] |
| $Ar^{iPr6}PbPbAr^{iPr6}$ | 10.1[a] |
| $(CO)_2CpMoMoCp(CO)_2$ | 69[c] |
| $(CO)_3CpMoMoCp(CO)_3$ | 32.5[d] |
| $HGeMoCp(CO)_2$ | 76.3[e] |
| $HSnMoCp(CO)_2$ | 64.8[e] |
| $HPbMoCp(CO)_2$ | 58.8[e] |

## NMR Spectra

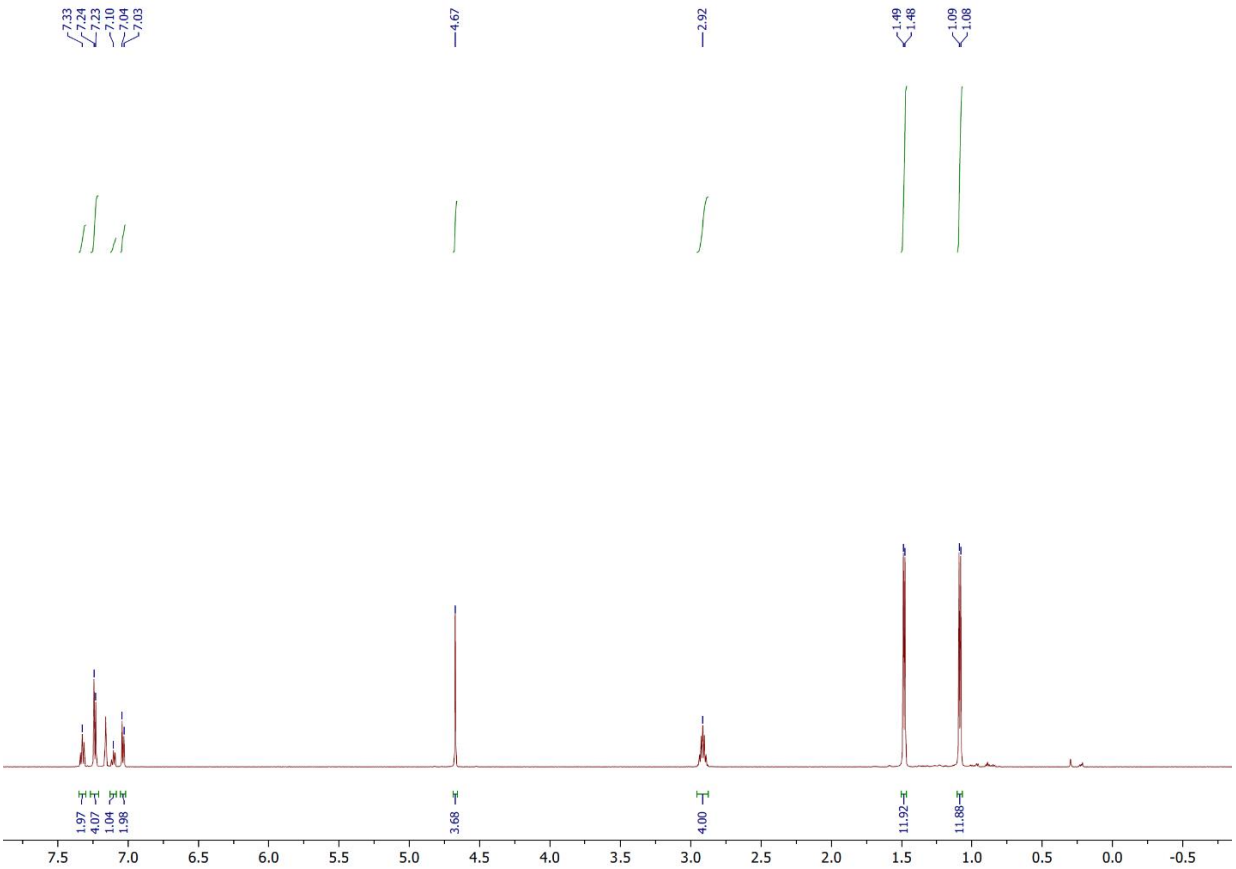


**Figure 4.S1.** $^{1}$H NMR spectrum of $Ar^{iPr4}Ge{\equiv}Mo(\eta^{5}\text{-}C_{5}H_{5})(CO)_{2}$ (**1a**) in $C_{6}D_{6}$ at 298 K.

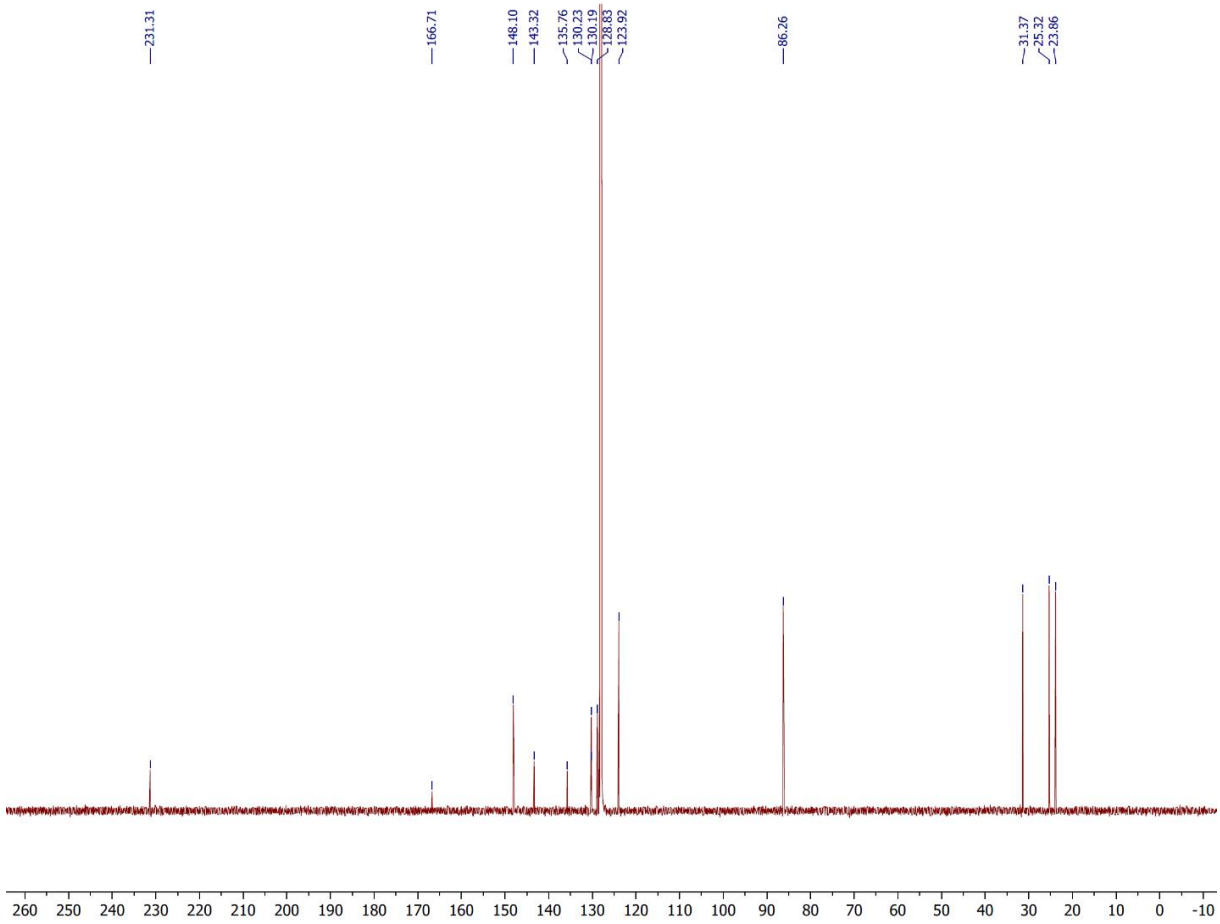


**Figure 4.S2.** $^{13}C\{^{1}H\}$ NMR spectrum of $Ar^{iPr4}Ge{\equiv}Mo(\eta^{5}\text{-}C_5H_5)(CO)_2$ (**1a**) in $C_6D_6$ at 298 K.

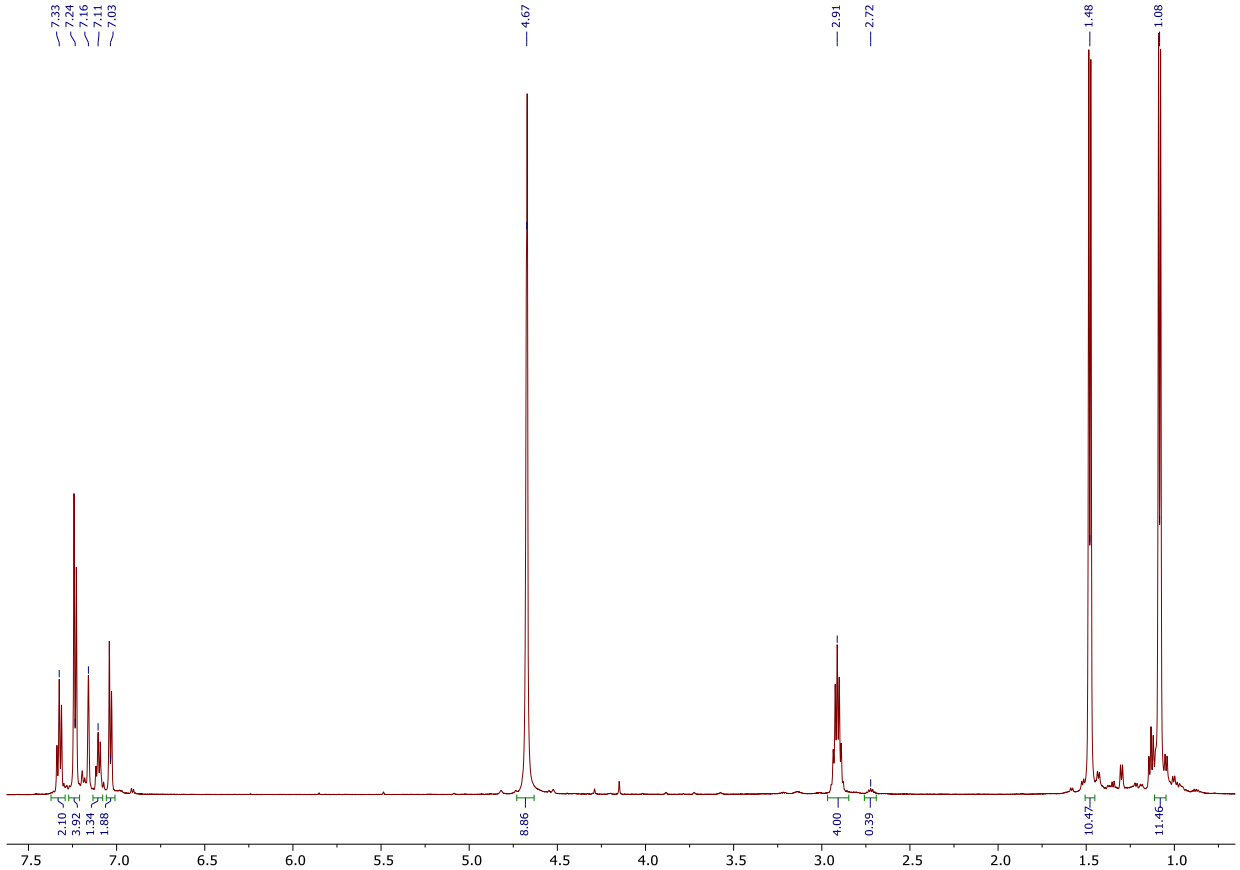


**Figure 4.S3.** $^1$H NMR spectrum of **1a** formed from the reaction of $Ar^{iPr4}GeGeAr^{iPr4}$ (#) and excess $[Mo(\eta^5\text{-}C_5H_5)(CO)_3]_2$ ($\delta$ = 4.67 ppm, overlapping with $C_5H_5$ resonance of **1a**) in $C_6D_6$ at 80°C for 1 week**.**



#

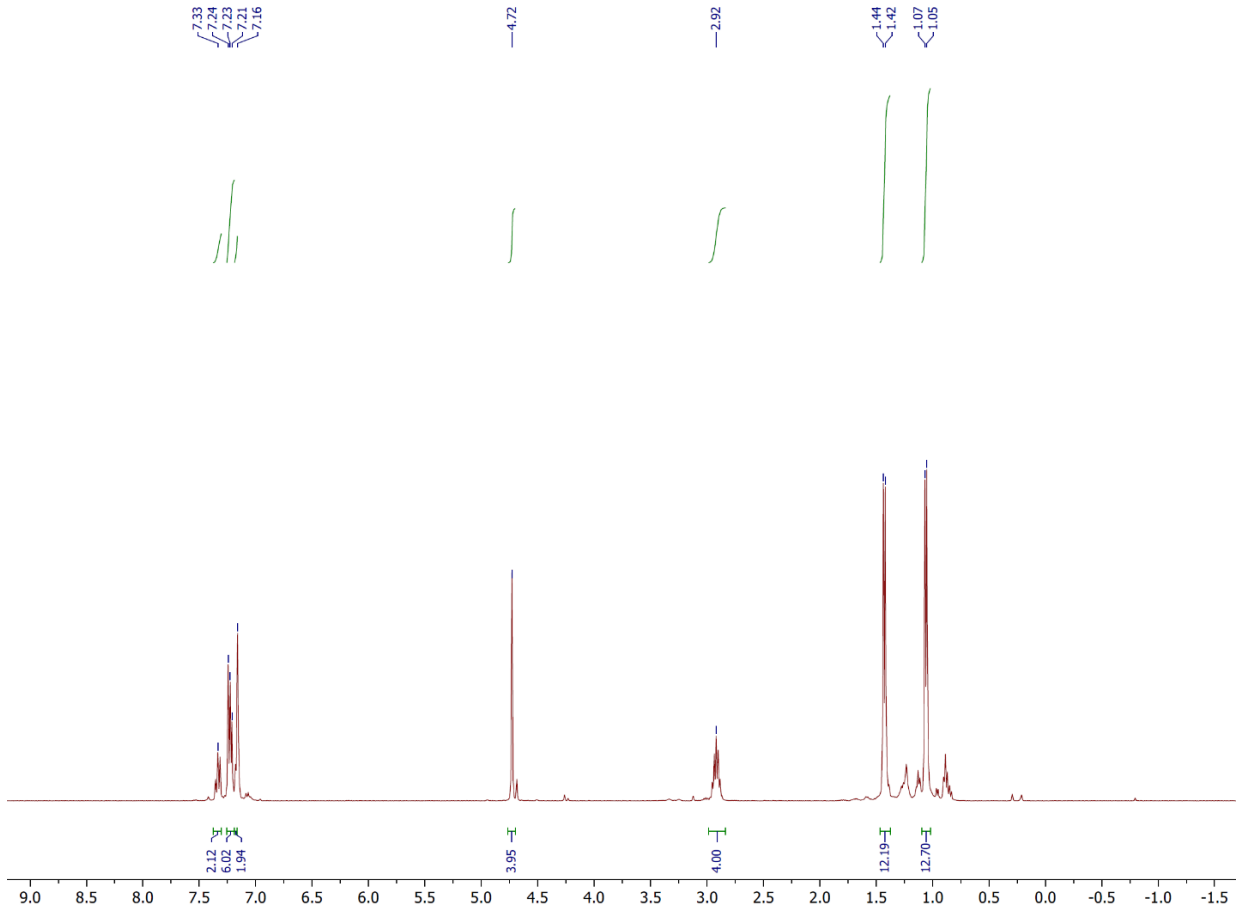


**Figure 4.S4.** $^{1}$H NMR spectrum of $Ar^{iPr4}Sn{\equiv}Mo(\eta^{5}\text{-}C_{5}H_{5})(CO)_{2}$ (**2a**) in $C_{6}D_{6}$ at 298 K.

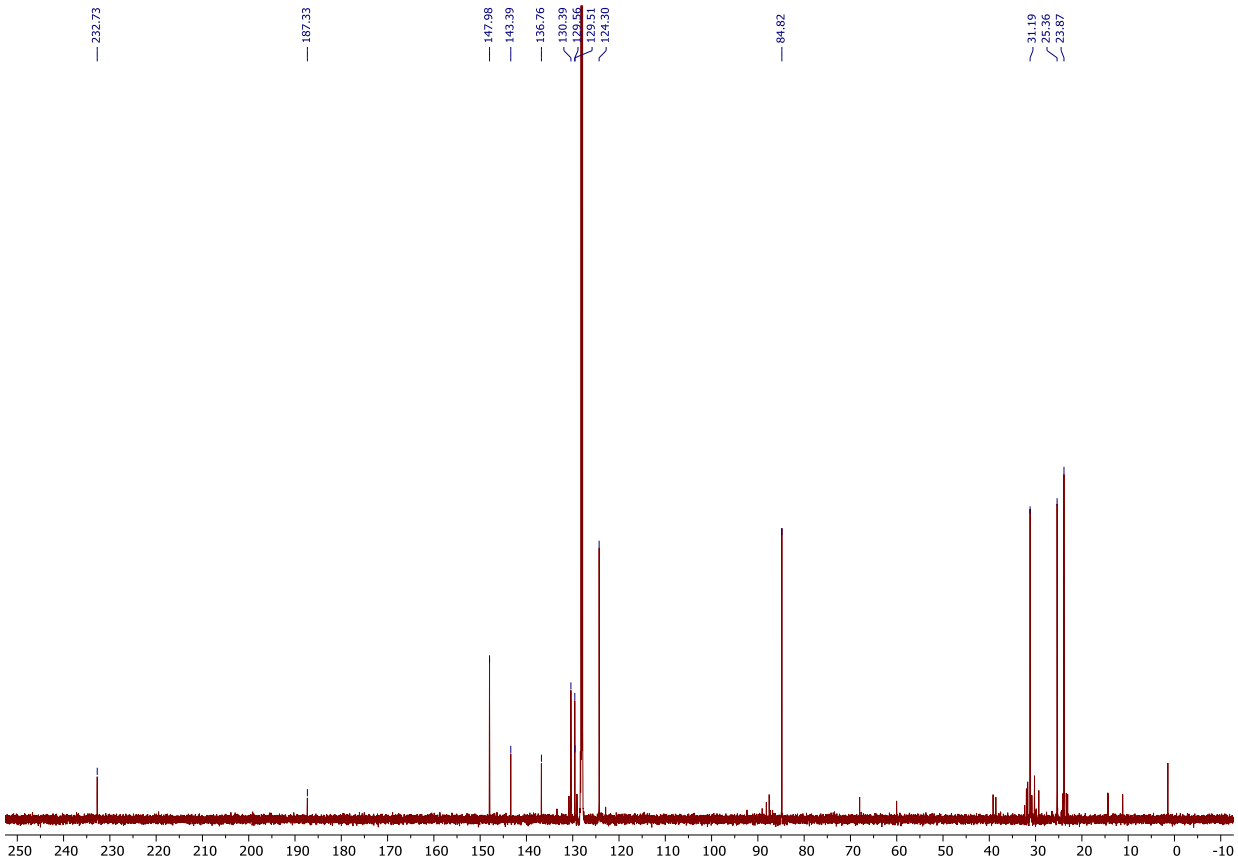


**Figure 4.S5.** $^{13}C\{^{1}H\}$ NMR spectrum of $Ar^{iPr4}Sn{\equiv}Mo(\eta^{5}\text{-}C_{5}H_{5})(CO)_{2}$ (**2a**) in $C_{6}D_{6}$ at 298 K**.**

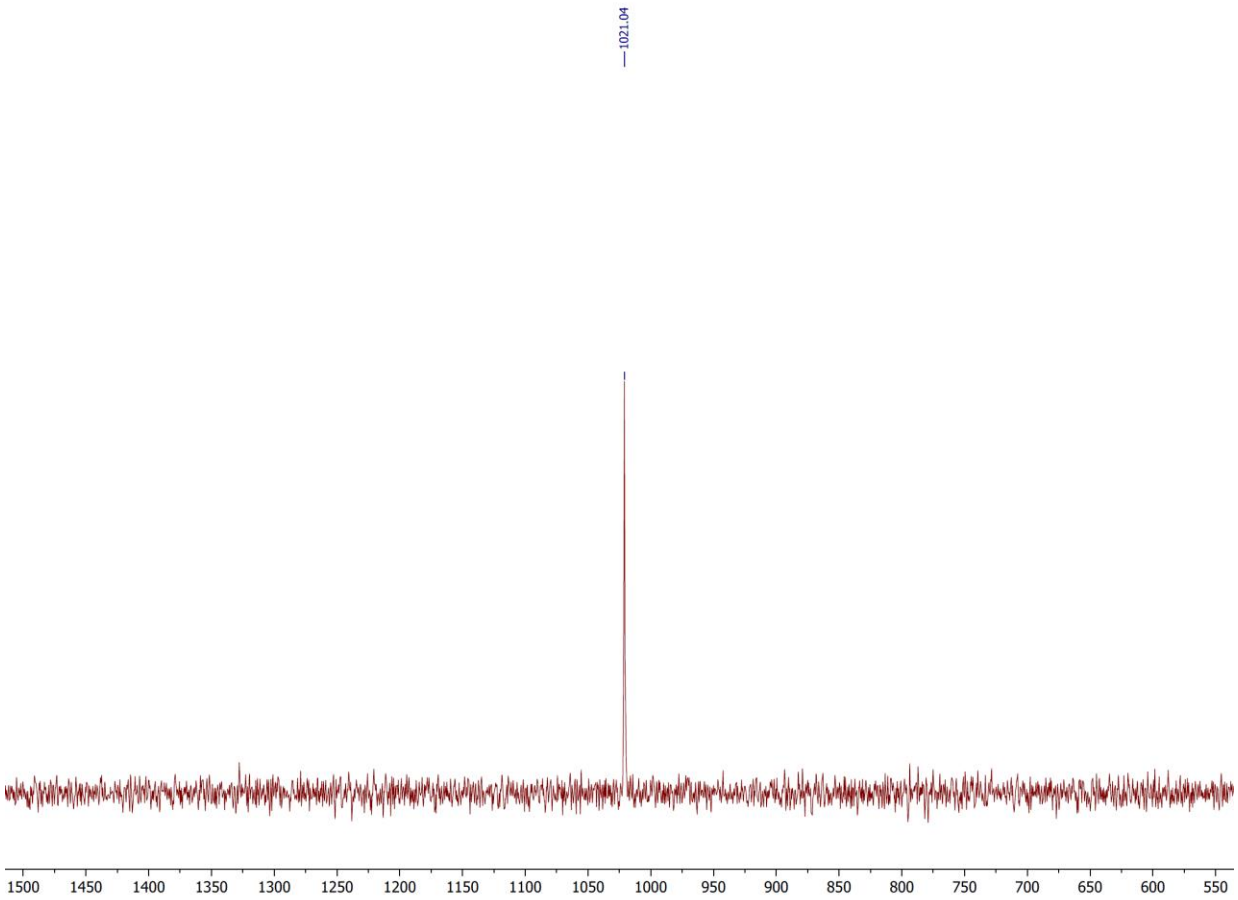


**Figure 4.S6.** $^{119}Sn\{^{1}H\}$ NMR spectrum of $Ar^{iPr4}Sn{\equiv}Mo(\eta^5\text{-}C_5H_5)(CO)_2$ (**2a**) in $C_6D_6$ at 298 K.

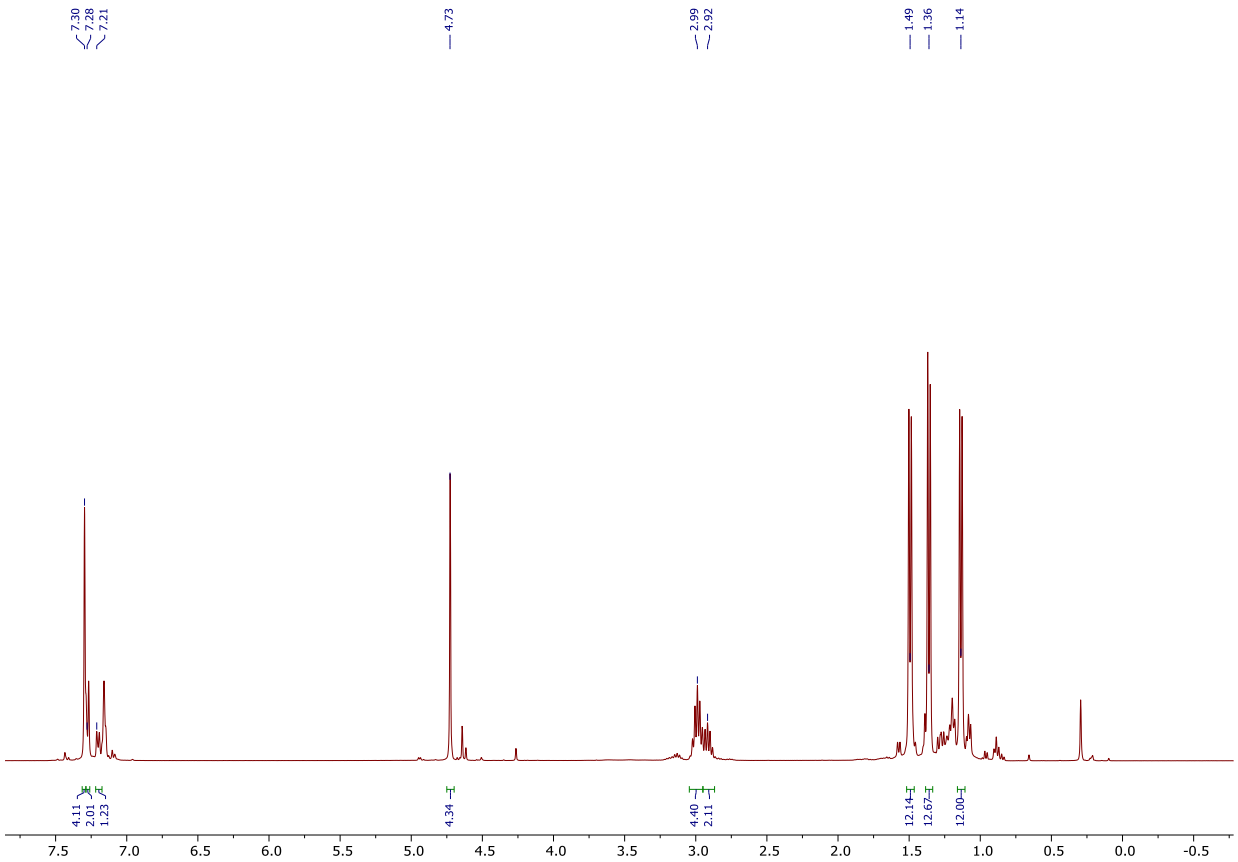


**Figure 4.S7.** $^1$H NMR spectrum of $Ar^{iPr6}Sn{\equiv}Mo(\eta^5\text{-}C_5H_5)(CO)_2$ (**2b**) in $C_6D_6$ at 298 K. Minor impurities of $[Mo(\eta^5\text{-}C_5H_5)(CO)_3]_2$ ($C_5H_5$ $\delta$ = 5.67 ppm), $[Mo(\eta^5\text{-}C_5H_5)(CO)_2]_2$, ($C_5H_5$ $\delta$ = 5.64 ppm), and **3b** ($C_5H_5$ $\delta$ = 4.26 ppm) are present in the sample.

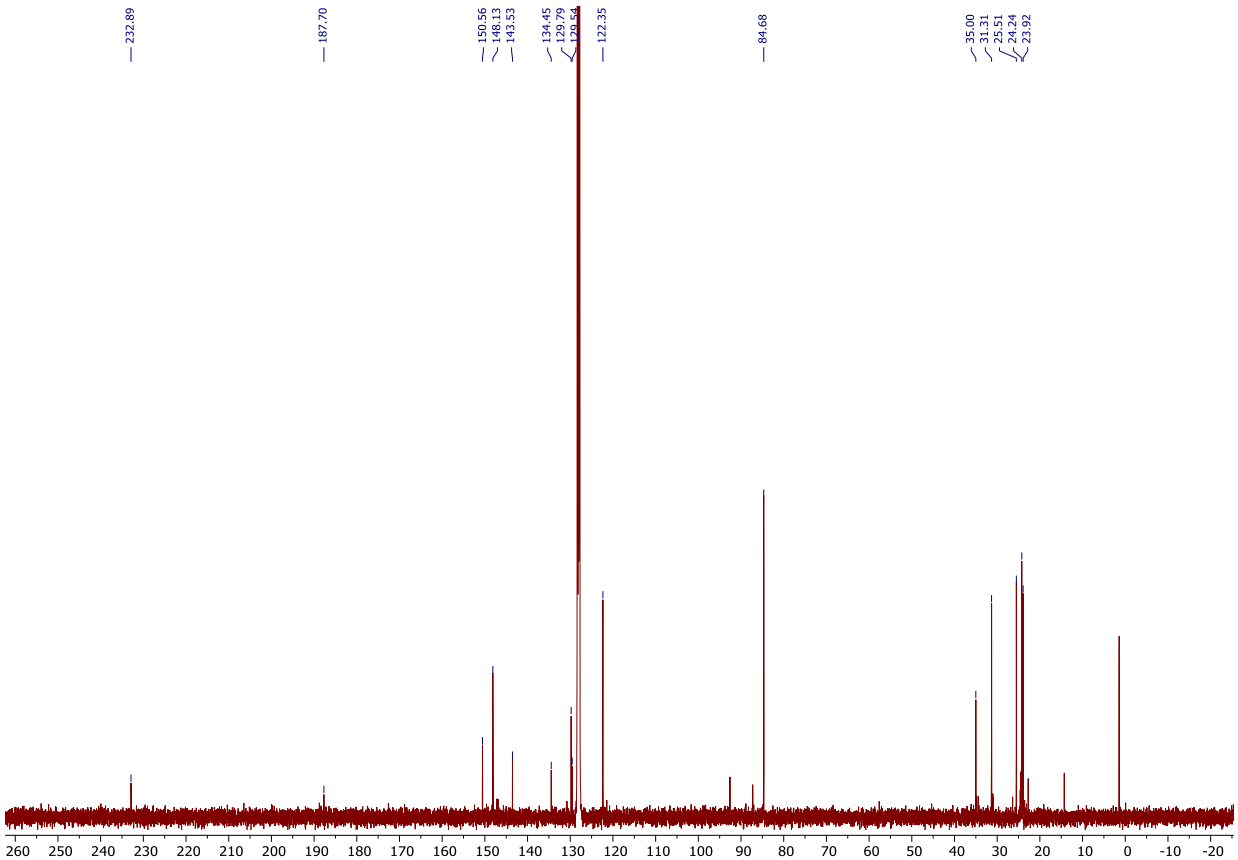


**Figure 4.S8.** $^{13}C\{^{1}H\}$ NMR spectrum of $Ar^{iPr6}Sn{\equiv}Mo(\eta^5\text{-}C_5H_5)(CO)_2$ (**2b**) in $C_6D_6$ at 298 K.

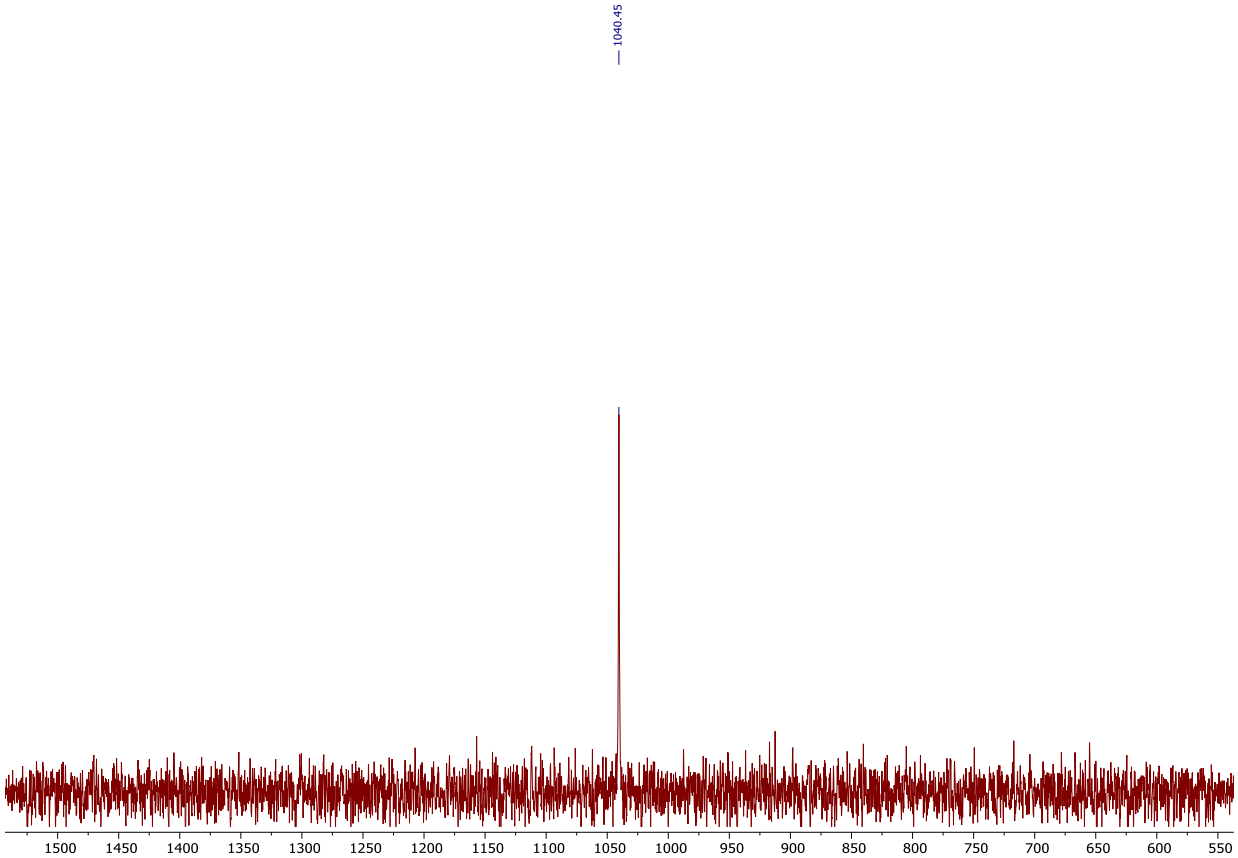


**Figure 4.S9.** $^{119}Sn\{^{1}H\}$ NMR spectrum of $Ar^{iPr6}Sn{\equiv}Mo(\eta^5\text{-}C_5H_5)(CO)_2$ (**2b**) in $C_6D_6$ at 298 K.

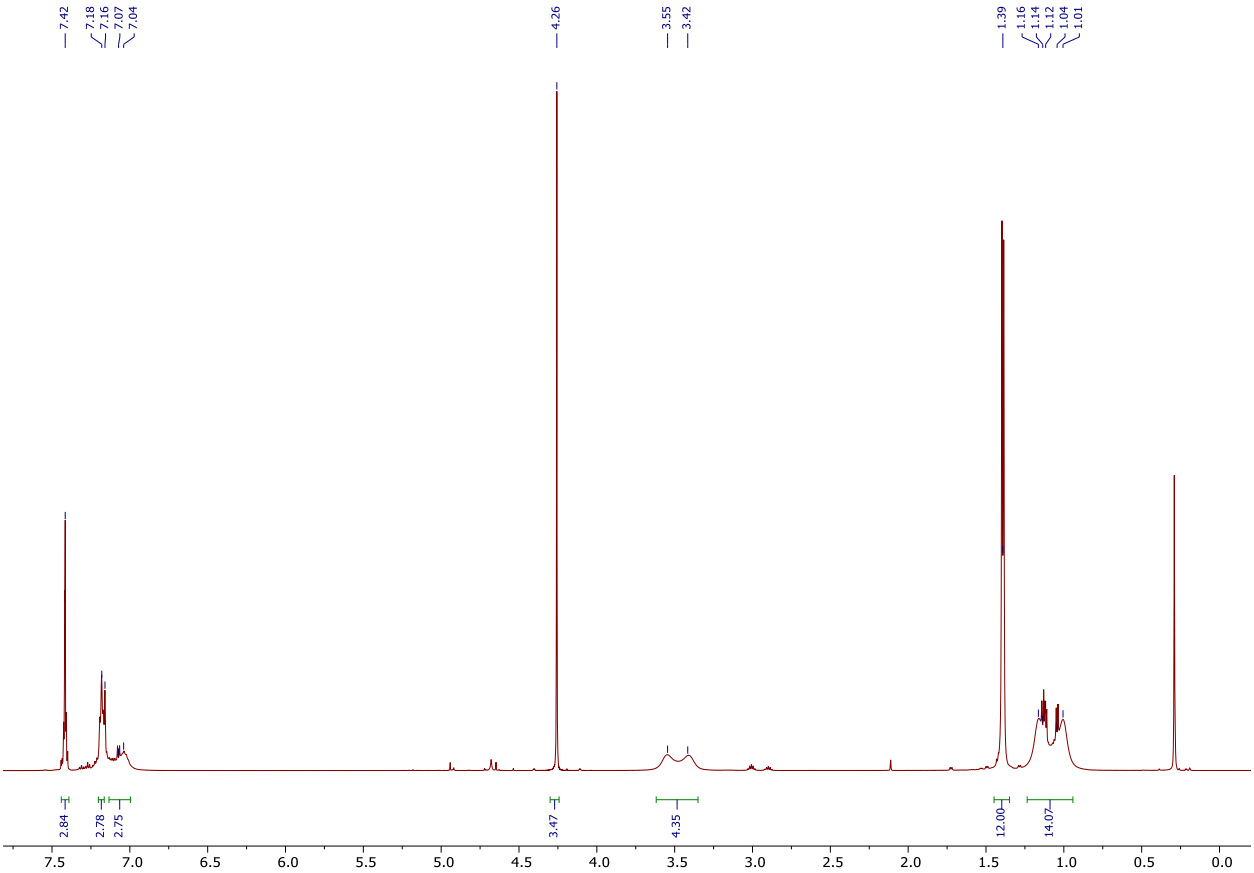


**Figure 4.S10**. $^{1}$H NMR spectrum of $Ar^{iPr4}Sn–Mo(\eta^{5}\text{-}C_5H_5)(CO)_3$ (**3a**) in $C_6D_6$ at 298 K.

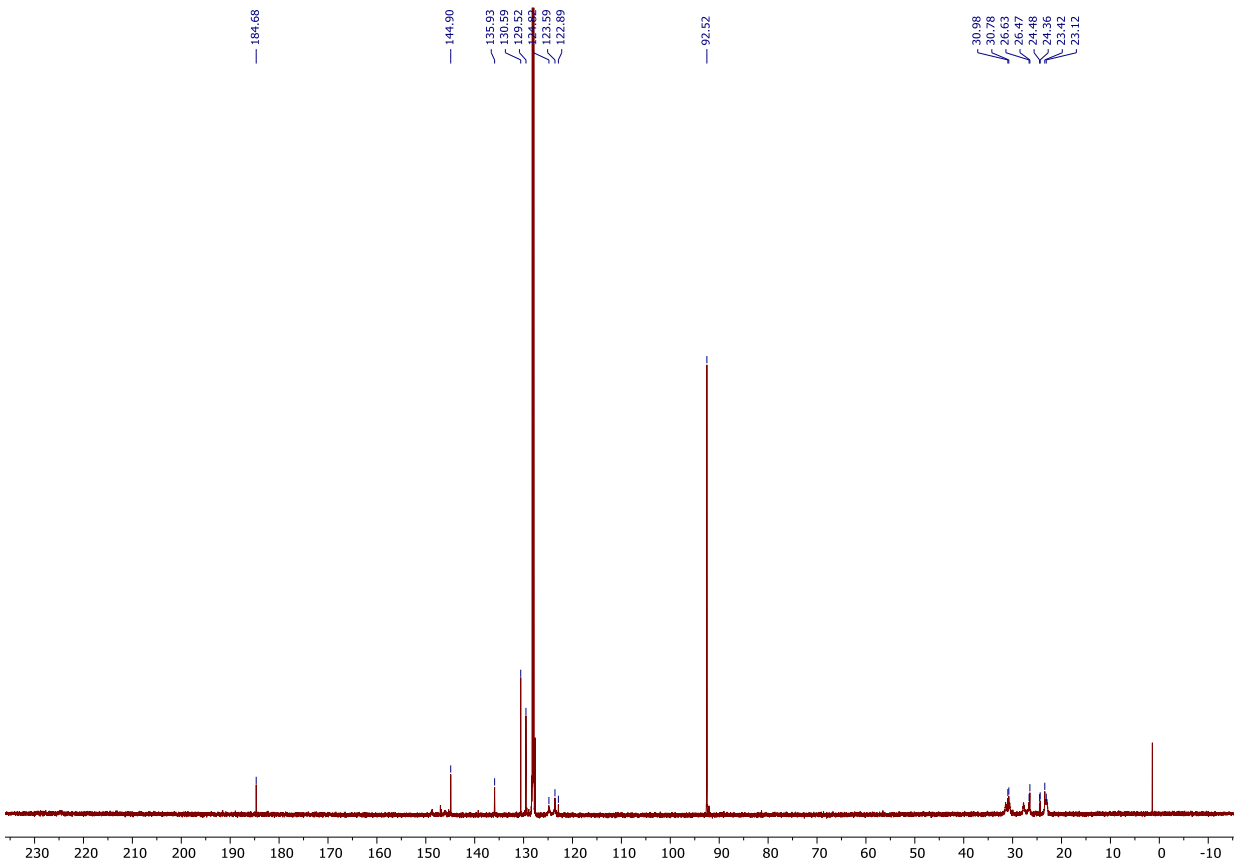


**Figure 4.S11.** $^{13}C\{^{1}H\}$ NMR spectrum of $Ar^{iPr4}Sn–Mo(\eta^5\text{-}C_5H_5)(CO)_3$ (**3a**) in $C_6D_6$ at 298 K.

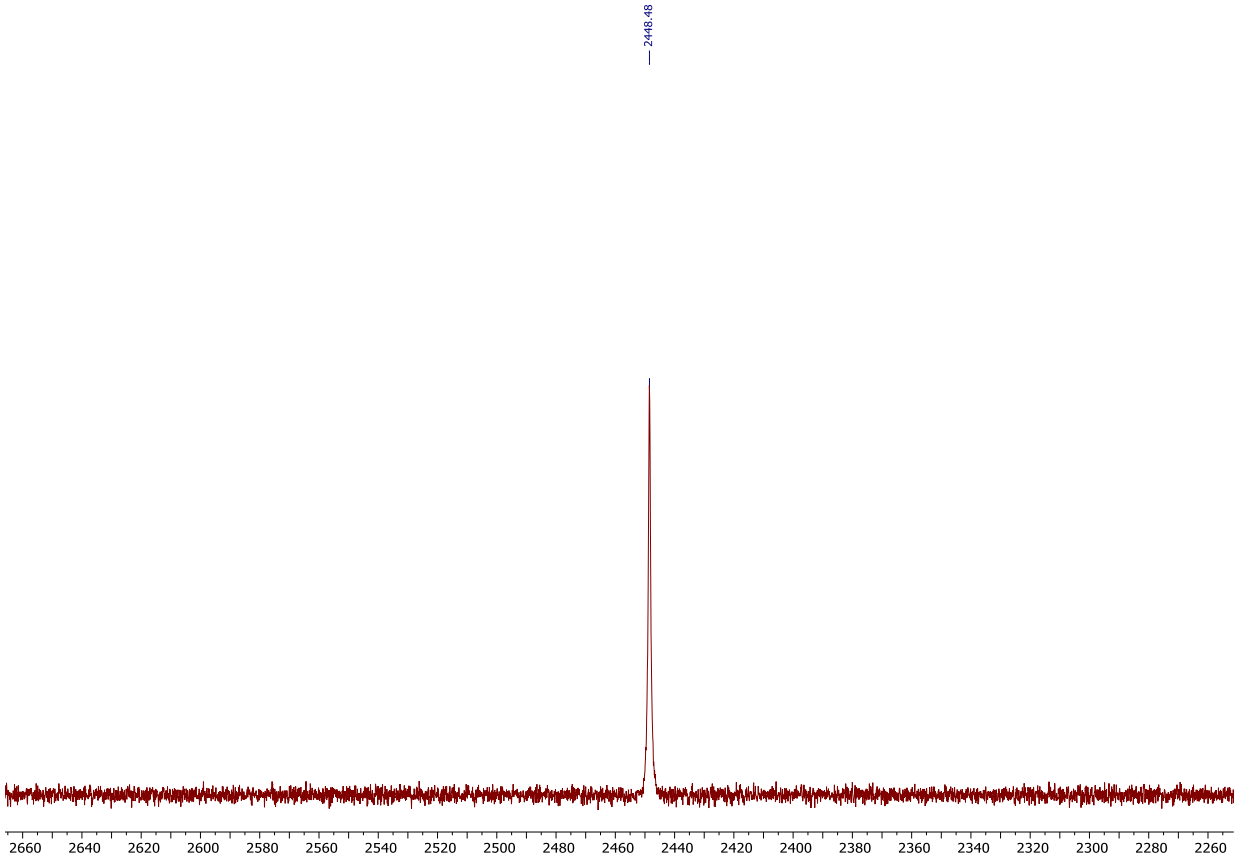


**Figure 4.S12.** $^{119}Sn\{^{1}H\}$ NMR spectrum of $Ar^{iPr4}Sn–Mo(\eta^{5}-C_{5}H_{5})(CO)_{3}$ (**3a**) in $C_{6}D_{6}$ at 298 K.

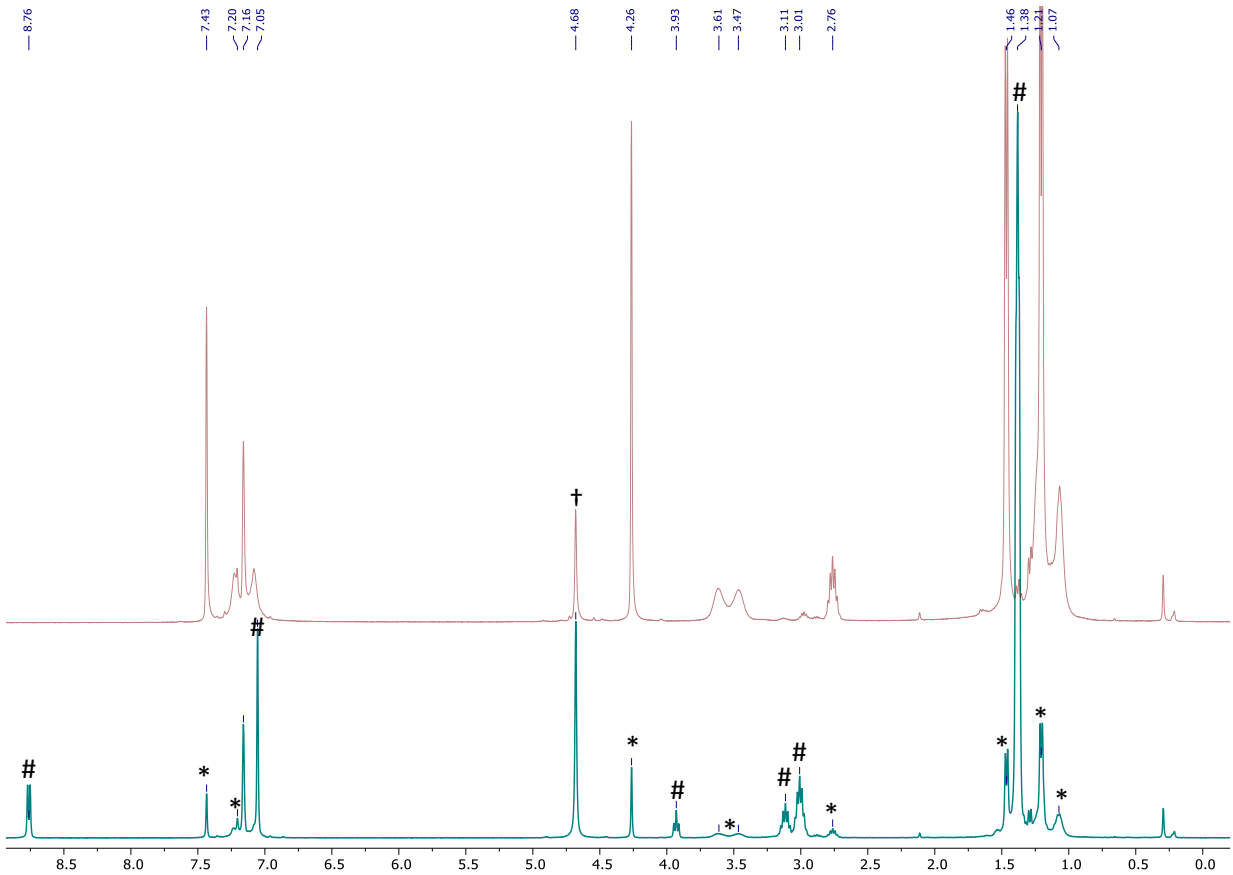


**Figure 4.S13.** $^1$H NMR spectra showing the formation of $Ar^{iPr6}Sn–Mo(\eta^5-C_5H_5)(CO)_3$ (**3b**) (*****) from the reaction of $Ar^{iPr6}SnSnAr^{iPr6}$ (#) with $[Mo(\eta^5-C_5H_5)(CO)_3]_2$ (†) in $C_6D_6$ at 298 K. Bottom: Reaction mixture just after preparation. Top: Reaction mixture after 2 days.

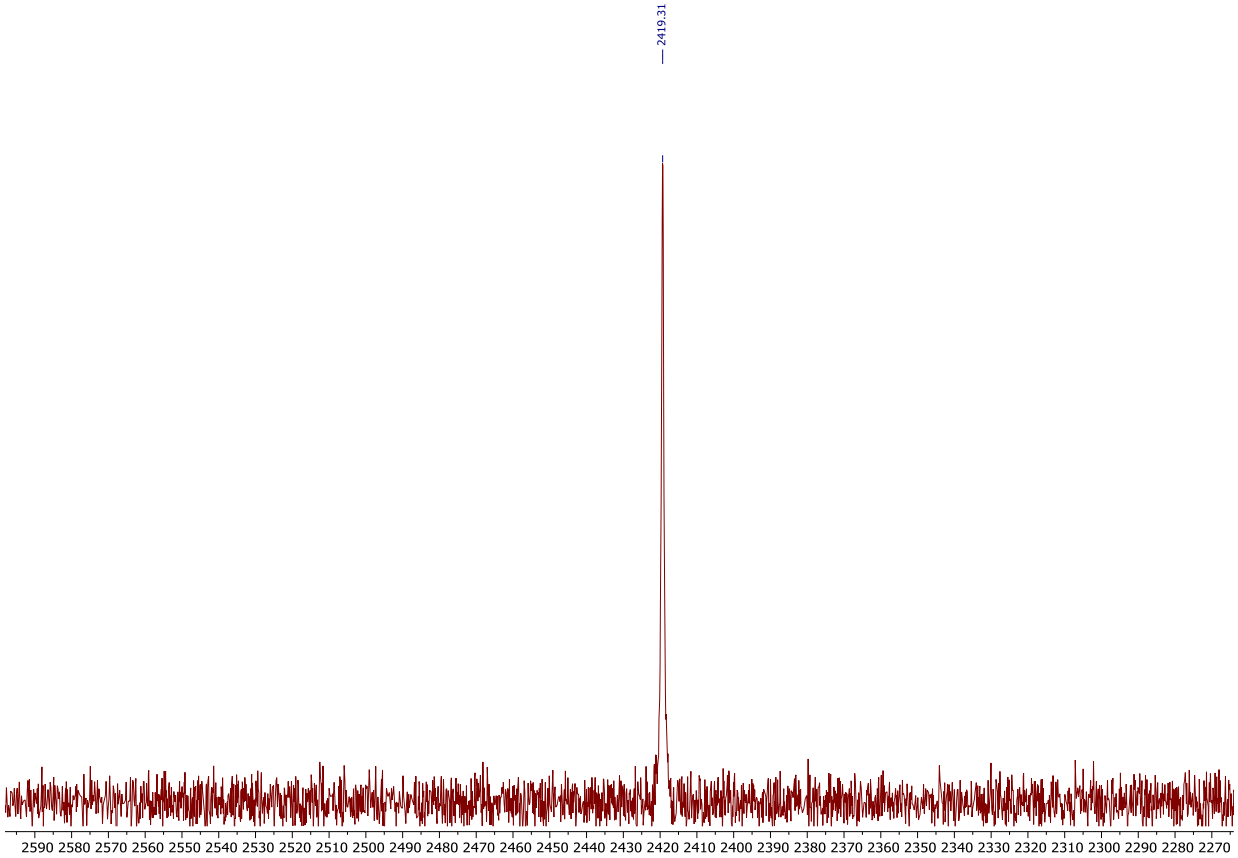


**Figure 4.S14.** $^{119}Sn\{^{1}H\}$ NMR spectrum of $Ar^{iPr6}Sn–Mo(\eta^5\text{-}C_5H_5)(CO)_3$ (**3b**) in $C_6D_6$ formed from the reaction of $Ar^{iPr6}SnSnAr^{iPr6}$ with $[Mo(\eta^5\text{-}C_5H_5)(CO)_3]_2$ in $C_6D_6$ at 298 K.

.

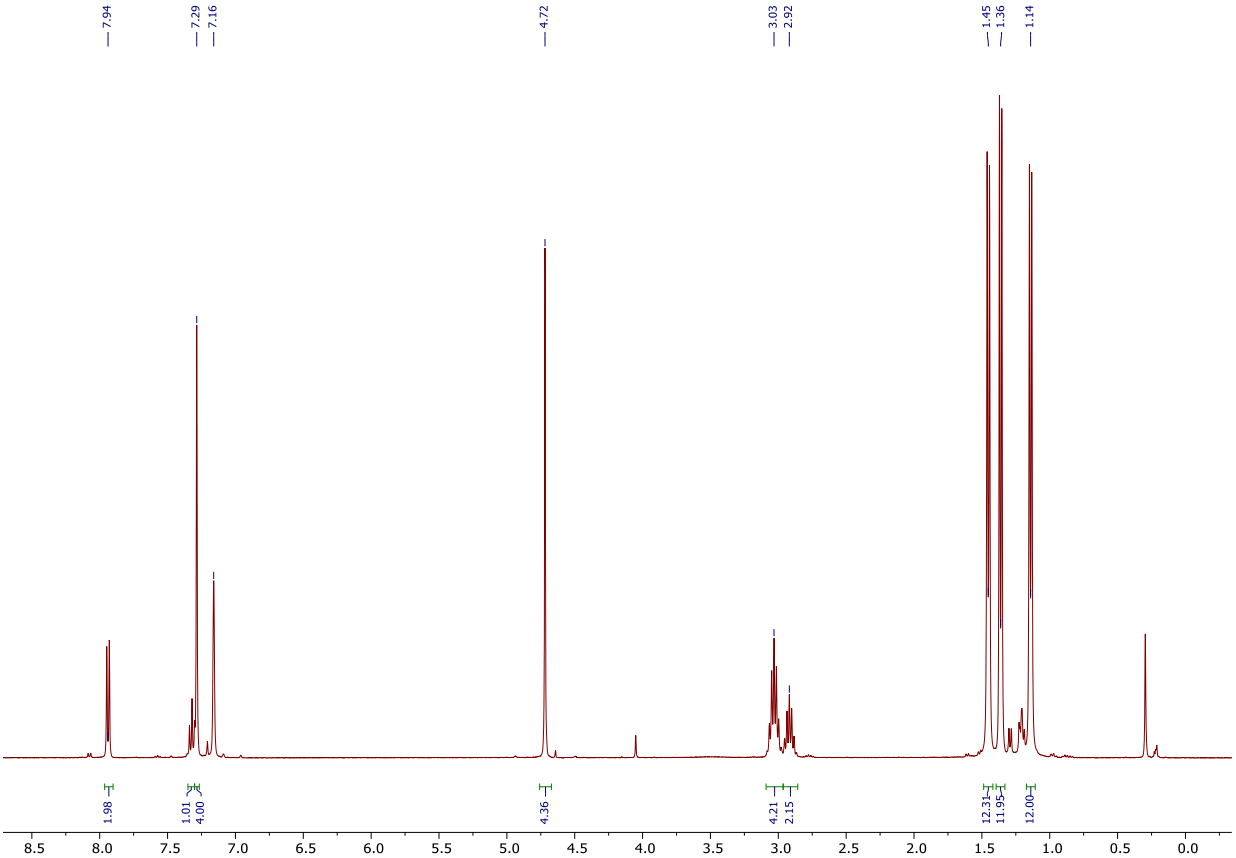


**Figure 4.S15**. $^1$H NMR spectrum of $Ar^{iPr6}PbMo(\eta^5\text{-}C_5H_5)(CO)_2$ (**4**) in $C_6D_6$ at 298 K.

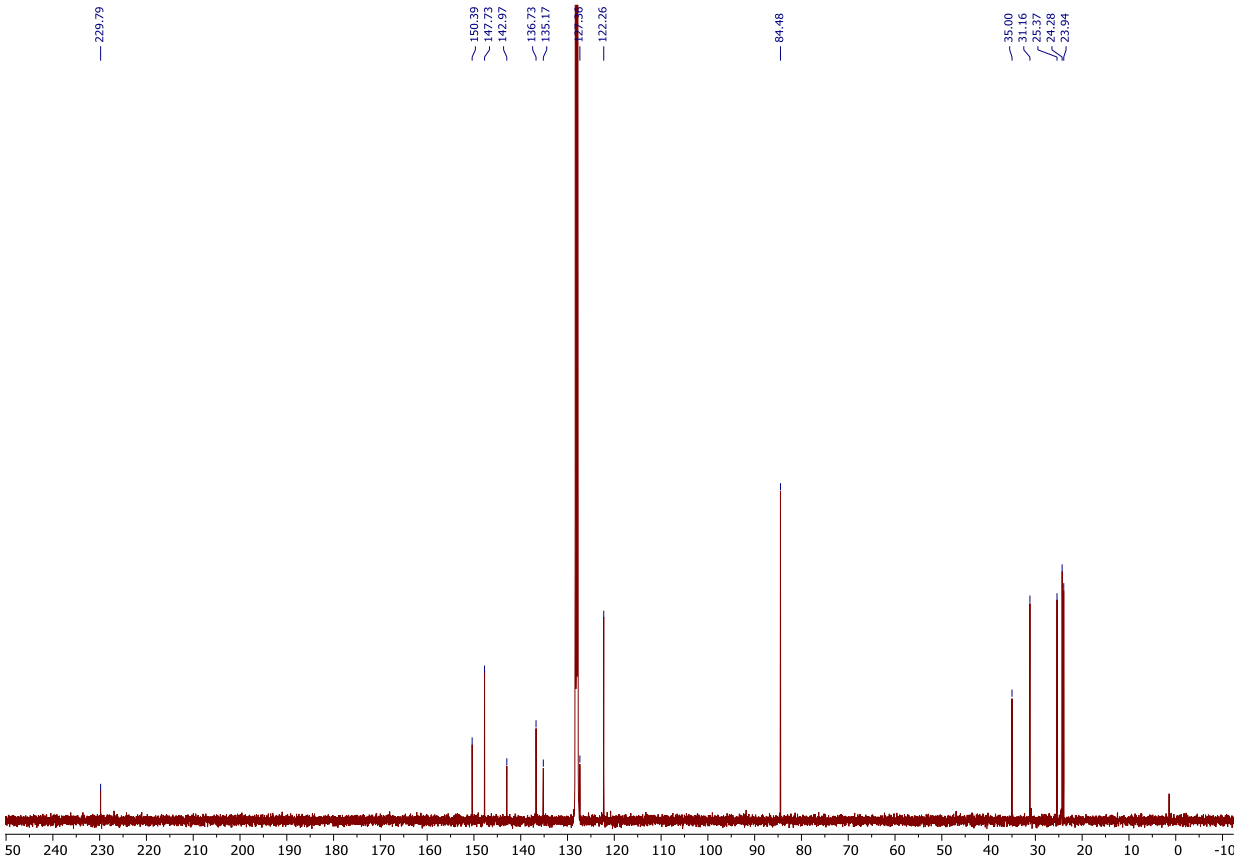


**Figure 4.S16.** $^{13}C\{^{1}H\}$ NMR spectrum of $Ar^{iPr6}PbMo(\eta^{5}\text{-}C_5H_5)(CO)_2$ (**4**) in $C_6D_6$ at 298 K.

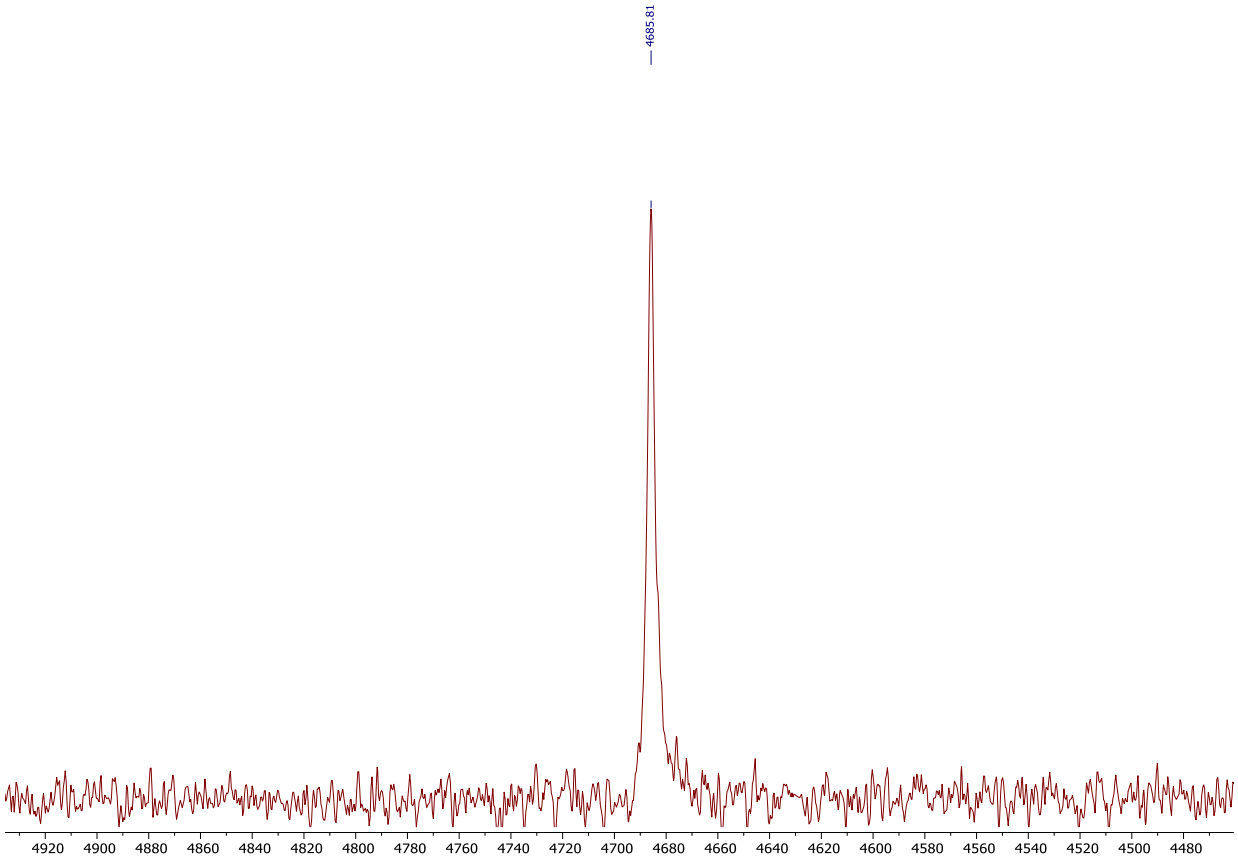


**Figure 4.S17.** $^{207}Pb\{^{1}H\}$ NMR spectrum of $Ar^{iPr6}Pb{\equiv}Mo(\eta^{5}\text{-}C_{5}H_{5})(CO)_{2}$ (**4**) in $C_{6}D_{6}$ at 298 K.

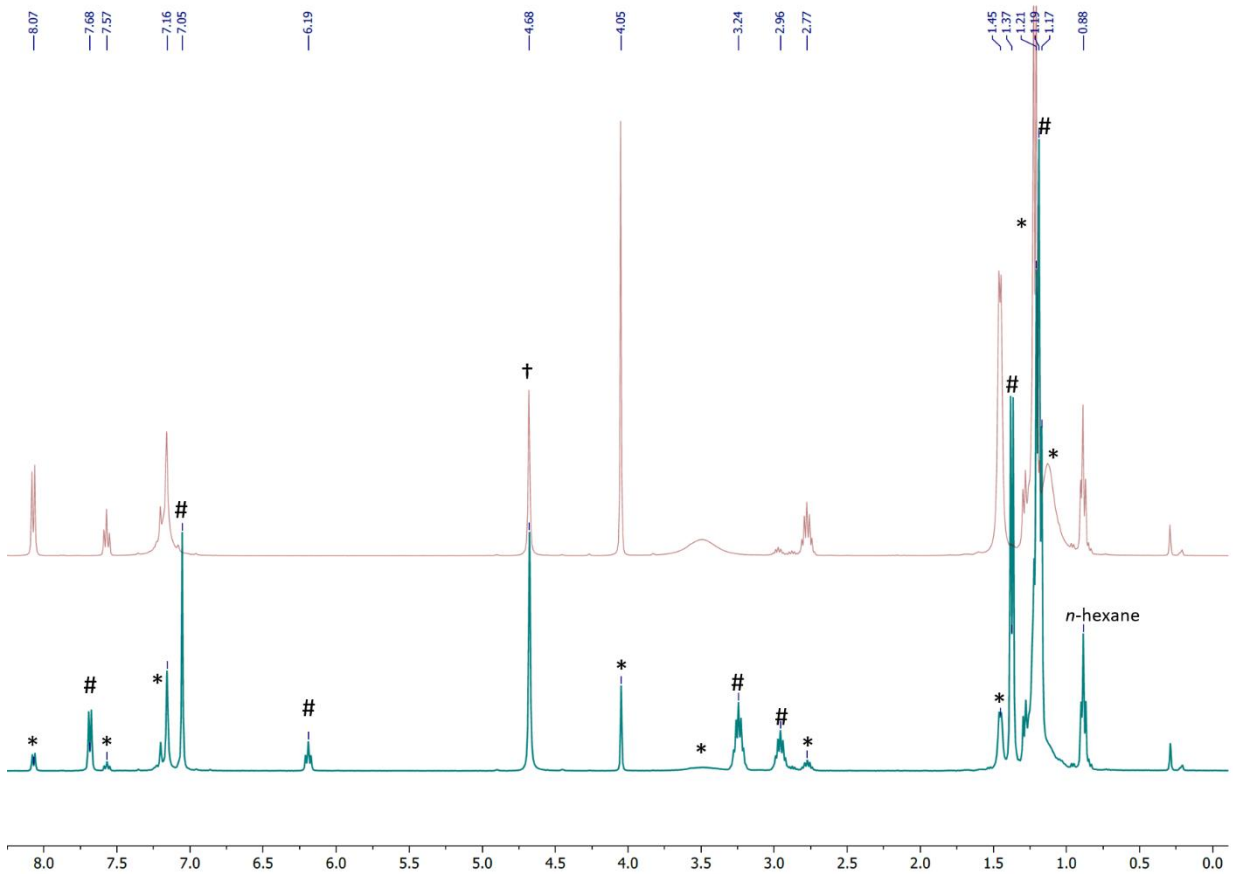


**Figure 4.S18.** $^1$H NMR spectra showing the formation of $Ar^{iPr6}Pb–Mo(\eta^5\text{-}C_5H_5)(CO)_3$ (**5**) (*) from the reaction of $Ar^{iPr6}PbPbAr^{iPr6}$ (#) with $[Mo(\eta^5\text{-}C_5H_5)(CO)_3]_2$ (†) in $C_6D_6$ at 298 K. Bottom: Reaction mixture just after preparation. Top: Reaction mixture after 2 days.

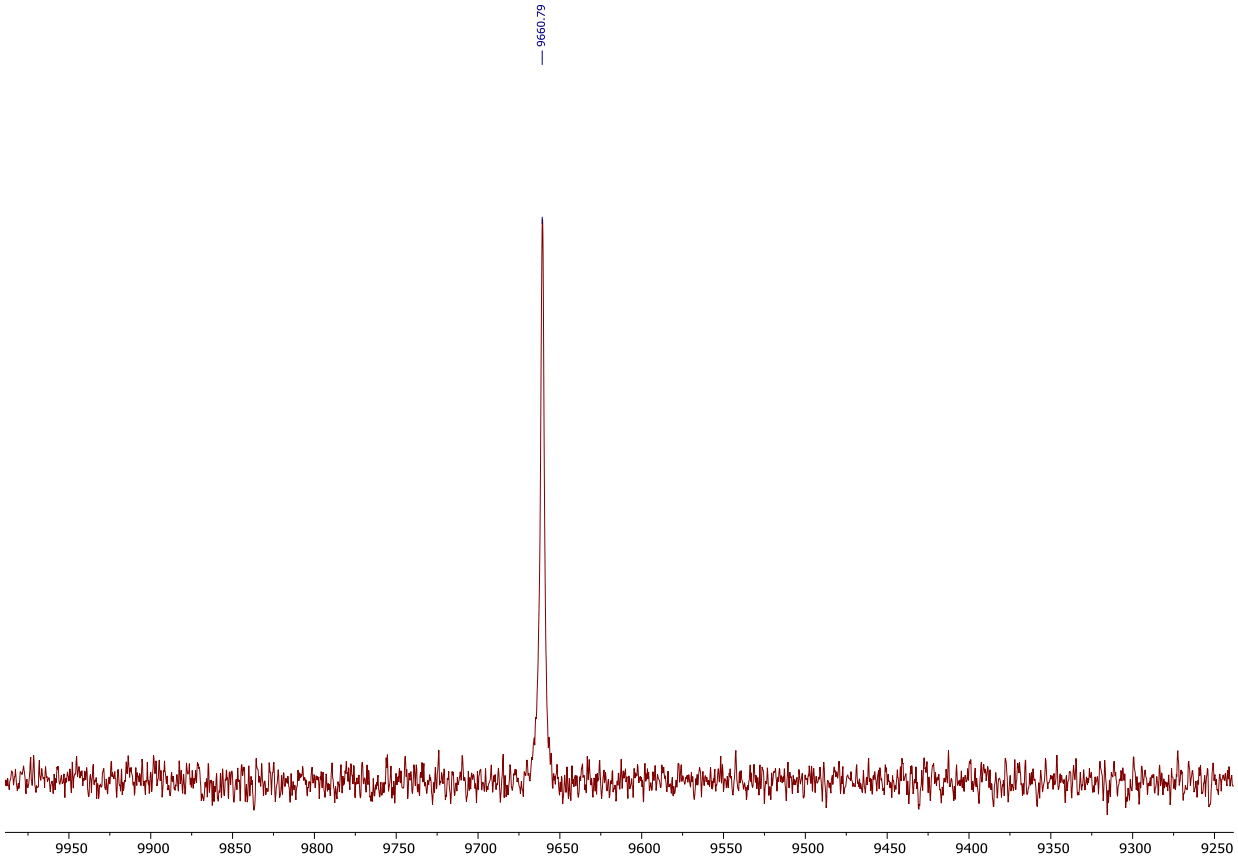


**Figure 4.S19.** $^{207}Pb\{^{1}H\}$ NMR spectrum of $Ar^{iPr6}Pb–Mo(\eta^5\text{-}C_5H_5)(CO)_3$ (**5**) formed from the reaction of $Ar^{iPr6}PbPbAr^{iPr6}$ with $[Mo(\eta^5\text{-}C_5H_5)(CO)_3]_2$ in $C_6D_6$ at 298 K.

## Infrared Spectra

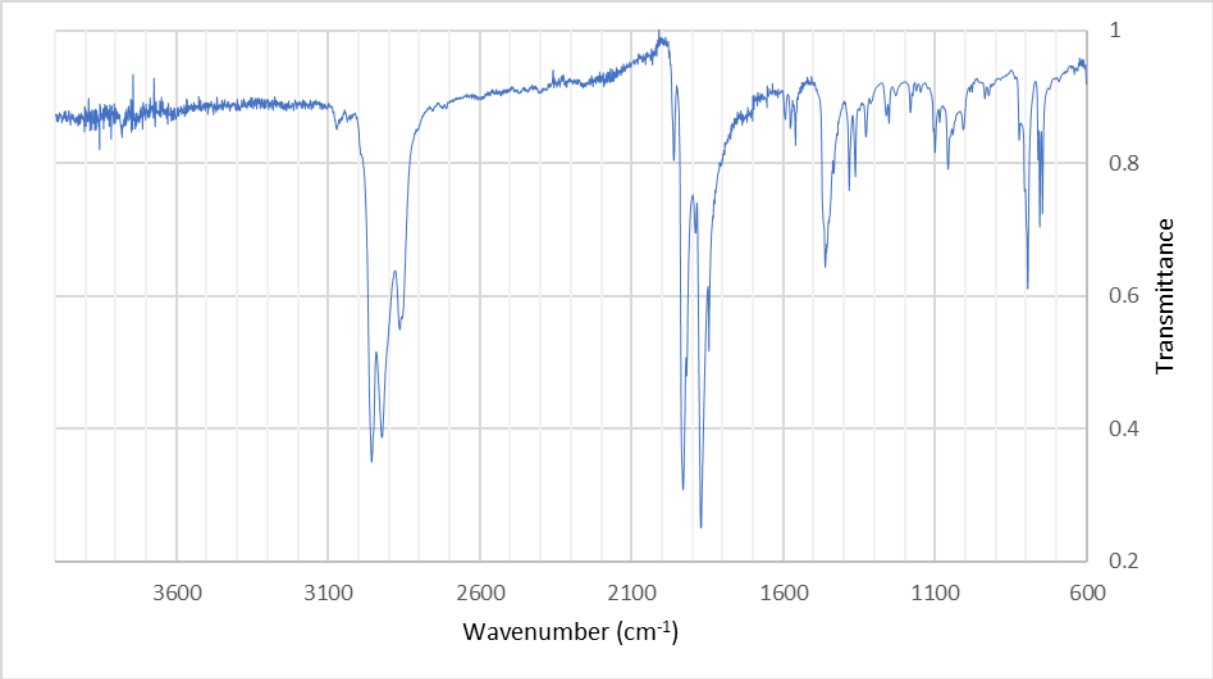


**Figure 4.S20.** ATR-FTIR spectrum of $Ar^{iPr4}Ge{\equiv}Mo(\eta^5\text{-}C_5H_5)(CO)_2$ (**1a**) at 298 K.

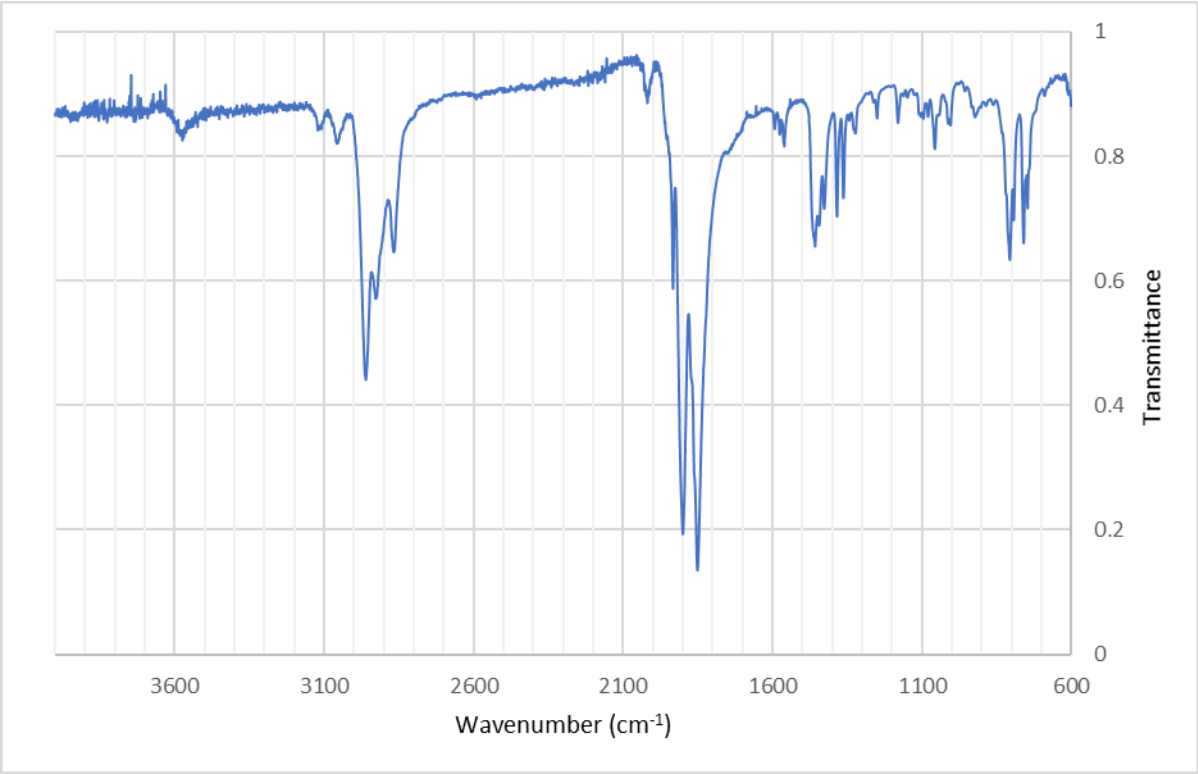


**Figure 4.S21.** ATR-FTIR spectrum of $Ar^{iPr4}Sn{\equiv}Mo(\eta^5\text{-}C_5H_5)(CO)_2$ (**2a**) at 298 K.

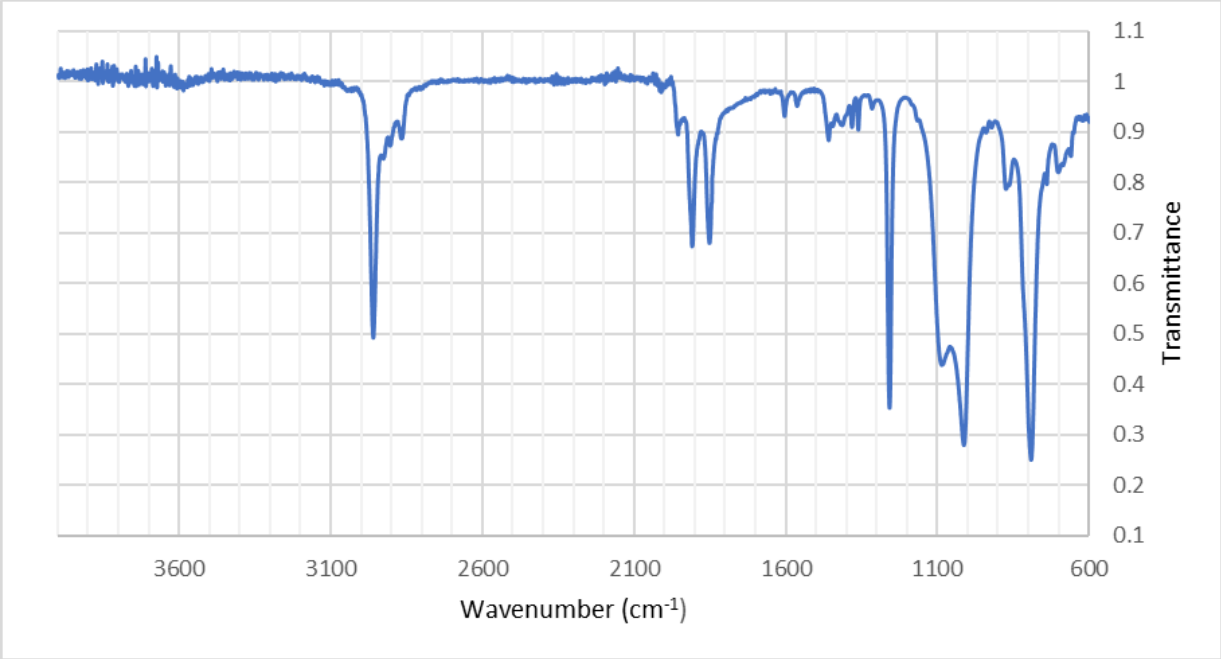


**Figure 4.S22.** ATR-FTIR spectrum of $Ar^{iPr6}Sn{\equiv}Mo(\eta^5\text{-}C_5H_5)(CO)_2$ (**2b**) at 298 K. A hydrocarbon impurity saturates the fingerprint region.

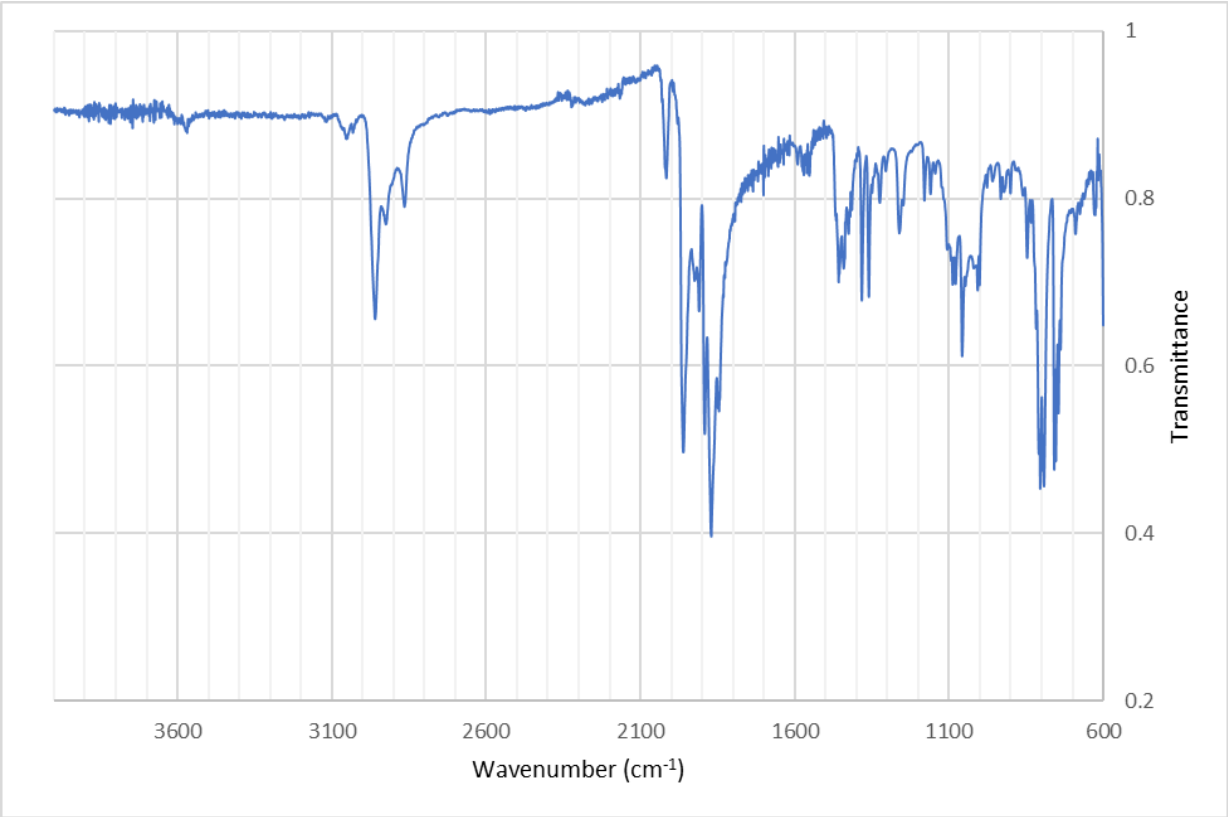


**Figure 4.S23.** ATR-FTIR spectrum of $Ar^{iPr4}Sn–Mo(\eta^5-C_5H_5)(CO)_3$ (**3a**) at 298 K.

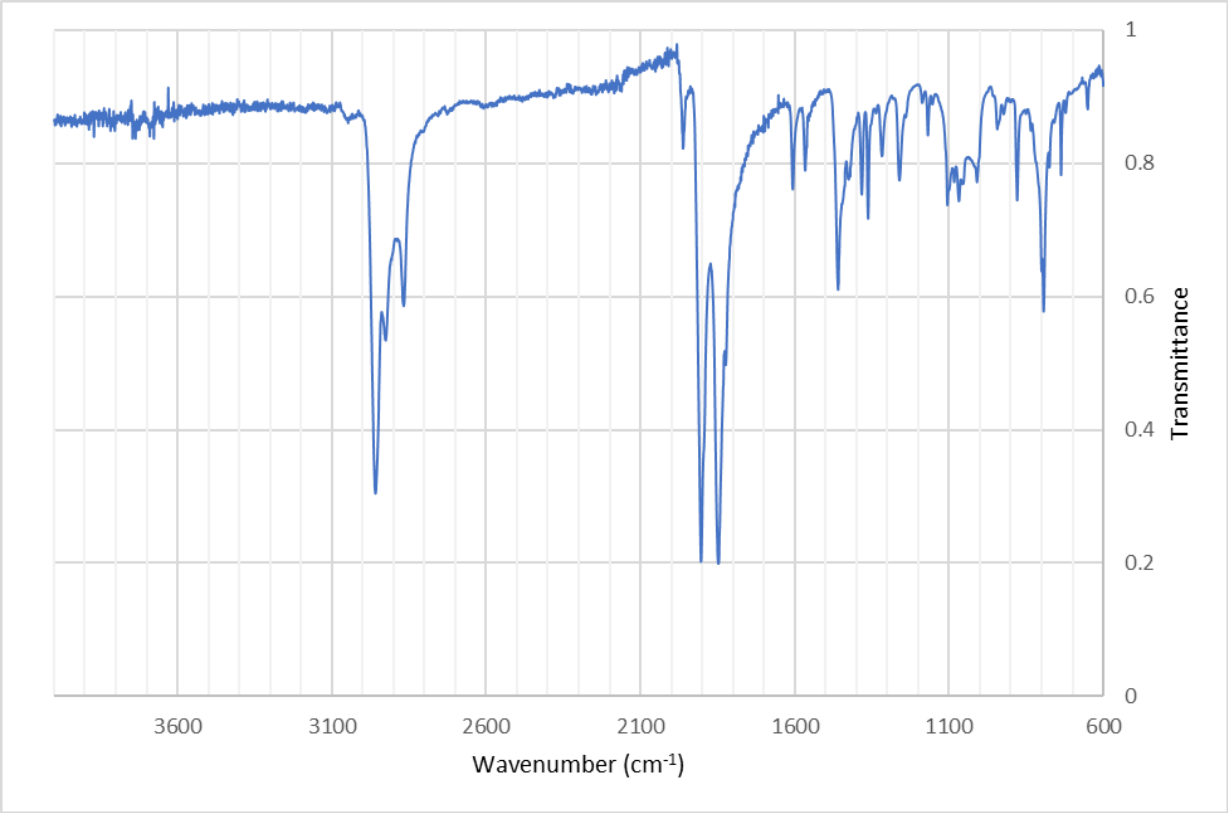


**Figure 4.S24.** ATR-FTIR spectrum of $Ar^{iPr6}Pb{\equiv}Mo(\eta^5\text{-}C_5H_5)(CO)_2$ (**4**) at 298 K.

## UV-Visible Spectra

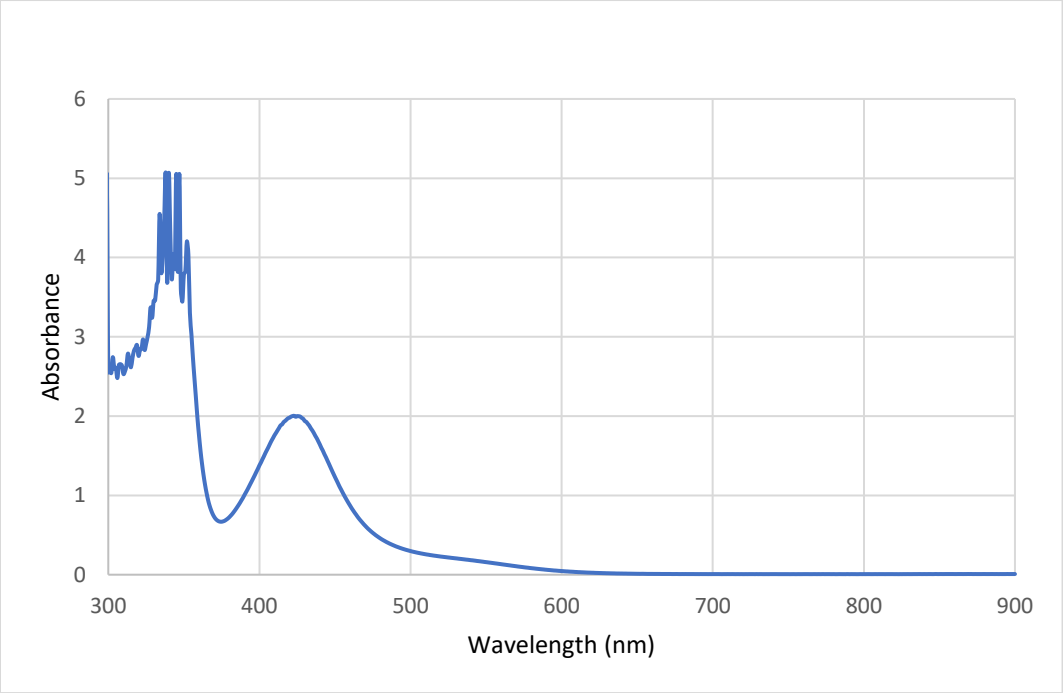


**Figure 4.S25.** UV-Visible spectrum of $Ar^{iPr4}Ge{\equiv}Mo(\eta^5\text{-}C_5H_5)(CO)_2$ (**1a**) 640 μM in hexanes at 298 K.

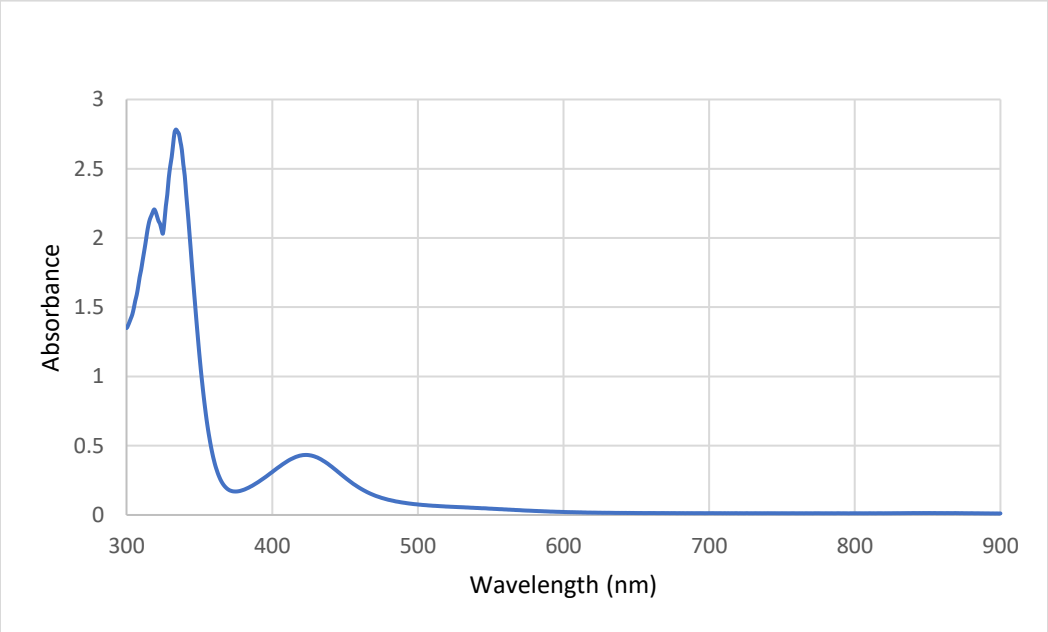


**Figure 4.S26.** UV-Visible spectrum of $Ar^{iPr4}Ge{\equiv}Mo(\eta^5\text{-}C_5H_5)(CO)_2$ (**1a**) 128 μM in hexanes at 298 K.

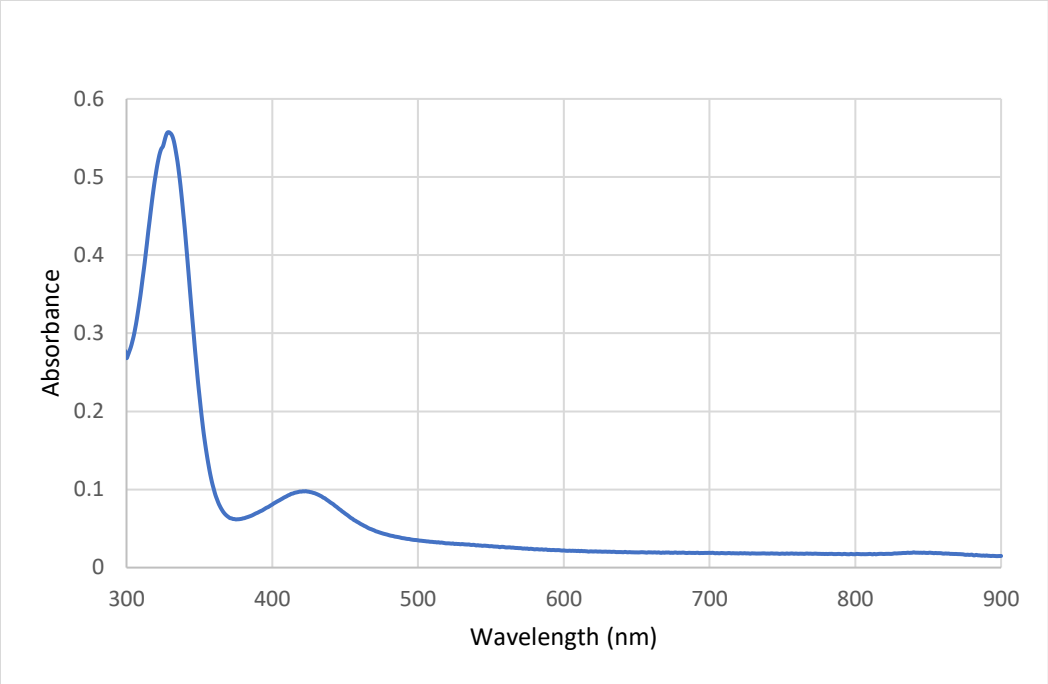


**Figure 4.S27.** UV-Visible spectrum of $Ar^{iPr4}Ge{\equiv}Mo(\eta^5\text{-}C_5H_5)(CO)_2$ (**1a**) 20 μM in hexanes at 298 K.

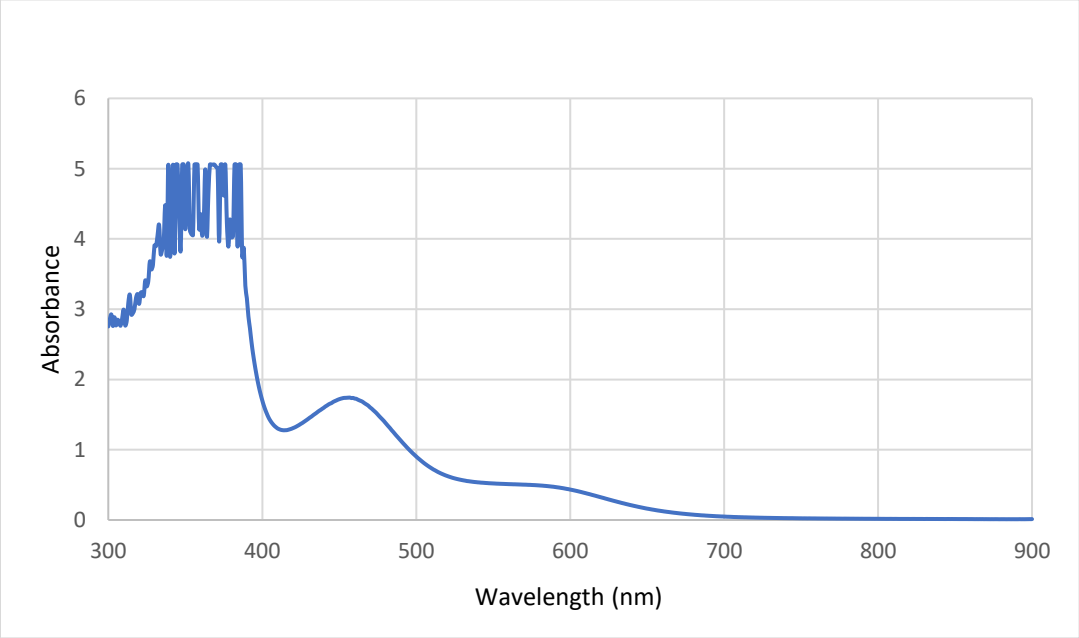


**Figure 4.S28.** UV-Visible spectrum of $Ar^{iPr4}Sn{\equiv}Mo(\eta^5\text{-}C_5H_5)(CO)_2$ (**2a**) 589 μM in hexanes at 298 K.

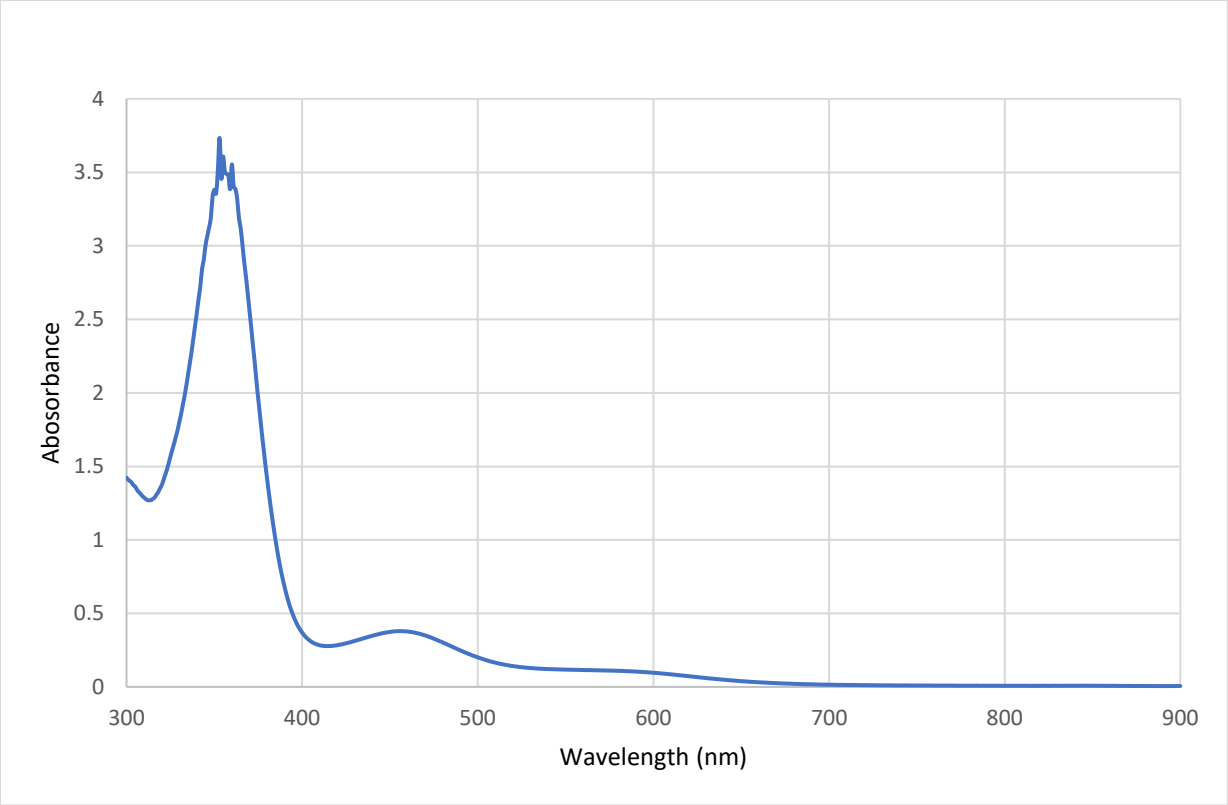


**Figure 4.S29.** UV-Visible spectrum of $Ar^{iPr4}Sn{\equiv}Mo(\eta^5\text{-}C_5H_5)(CO)_2$ (**2a**) 118 μM in hexanes at 298 K.

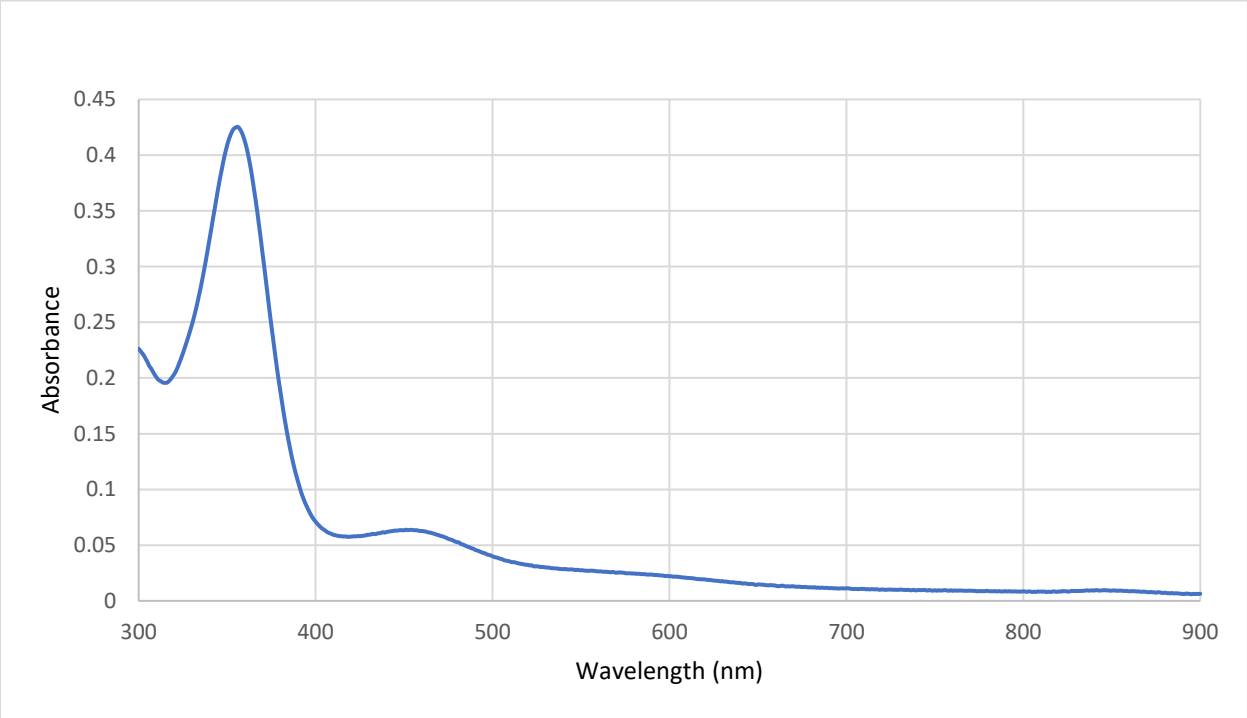


**Figure 4.S30.** UV-Visible spectrum of $Ar^{iPr4}Sn{\equiv}Mo(\eta^5\text{-}C_5H_5)(CO)_2$ (**2a**) 11.8 μM in hexanes at 298 K.

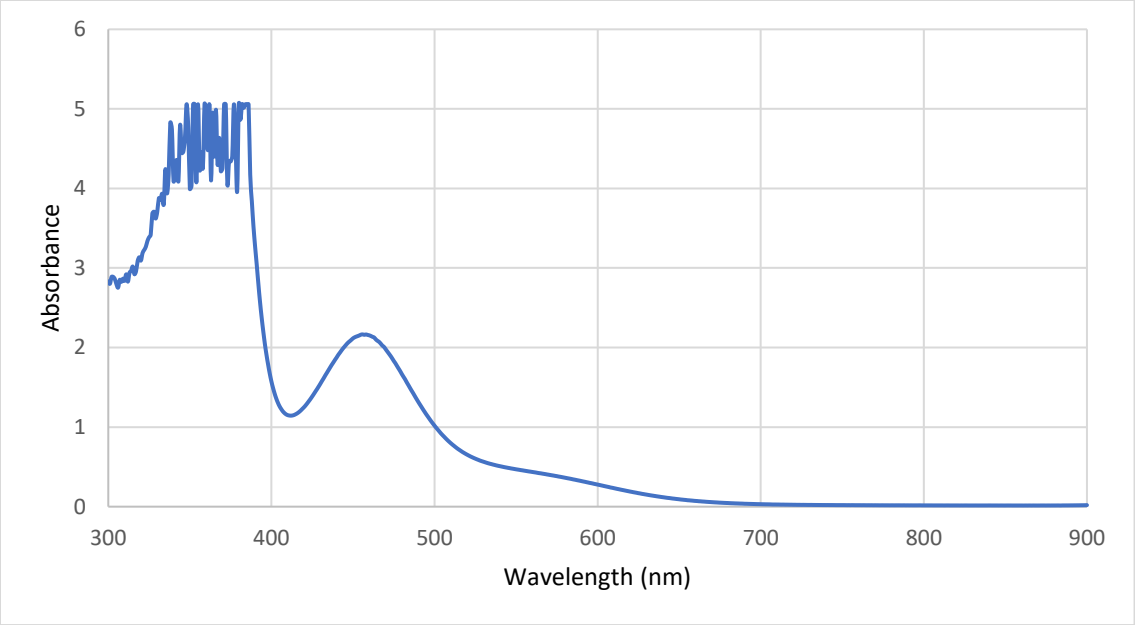


**Figure 4.S31.** UV-Visible spectrum of $Ar^{iPr6}Sn{\equiv}Mo(\eta^5\text{-}C_5H_5)(CO)_2$ (**2b**) 856 μM in hexanes at 298 K.

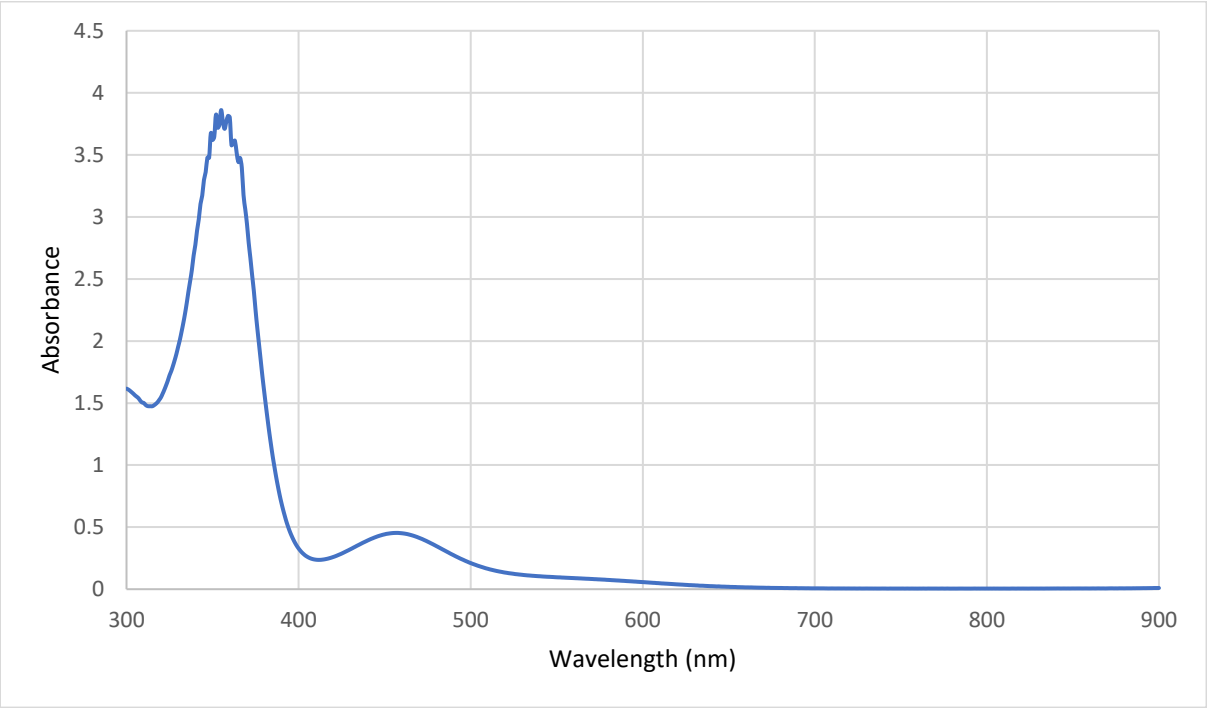


**Figure 4.S32.** UV-Visible spectrum of $Ar^{iPr6}Sn{\equiv}Mo(\eta^5\text{-}C_5H_5)(CO)_2$ (**2b**) 171 μM in hexanes at 298 K.

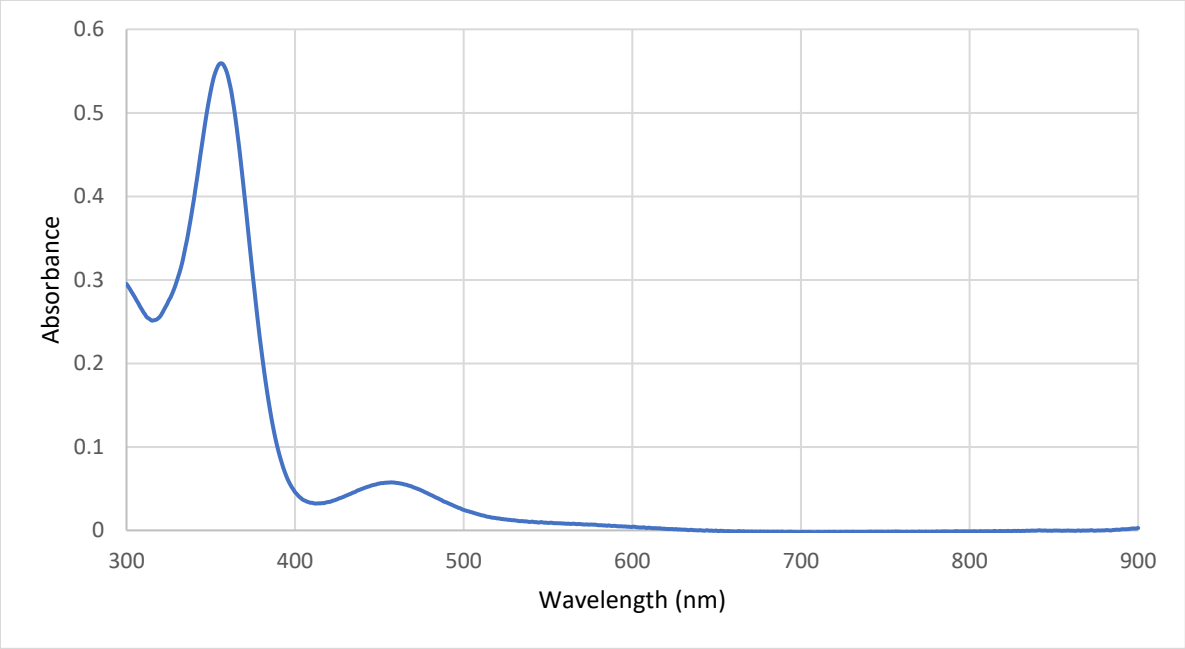


**Figure 4.S33.** UV-Visible spectrum of $Ar^{iPr6}Sn{\equiv}Mo(\eta^5\text{-}C_5H_5)(CO)_2$ (**2b**) 17.1 μM in hexanes at 298 K.

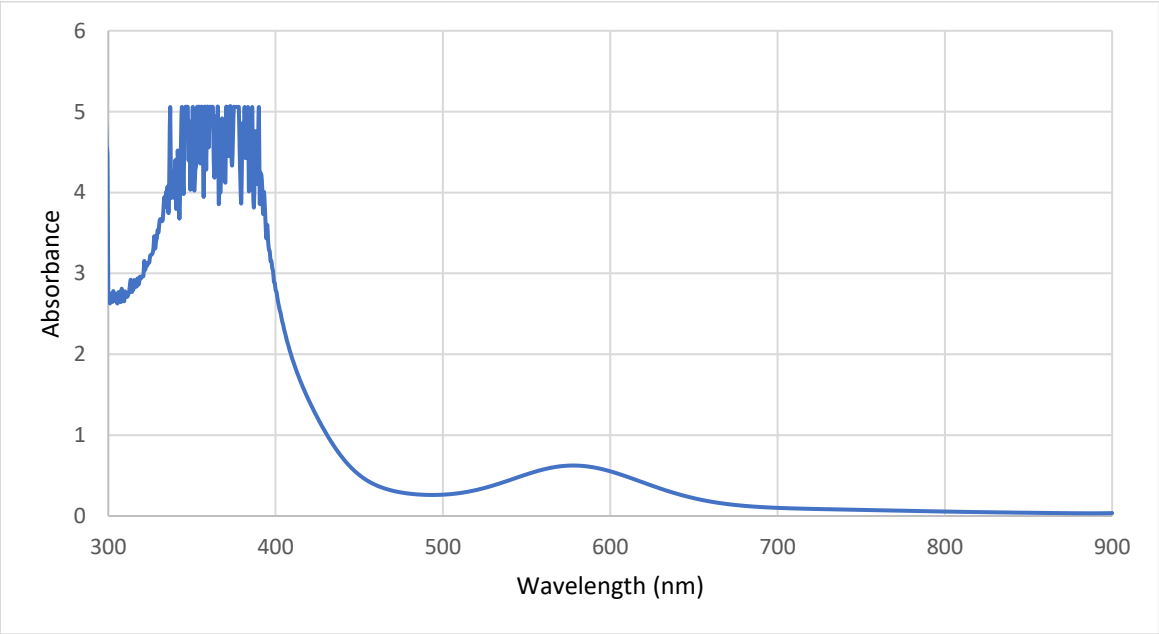


**Figure 4.S34.** UV-Visible spectrum of $Ar^{iPr4}Sn{-}Mo(\eta^5\text{-}C_5H_5)(CO)_3$ (**3a**) 650 μM in hexanes at 298 K.

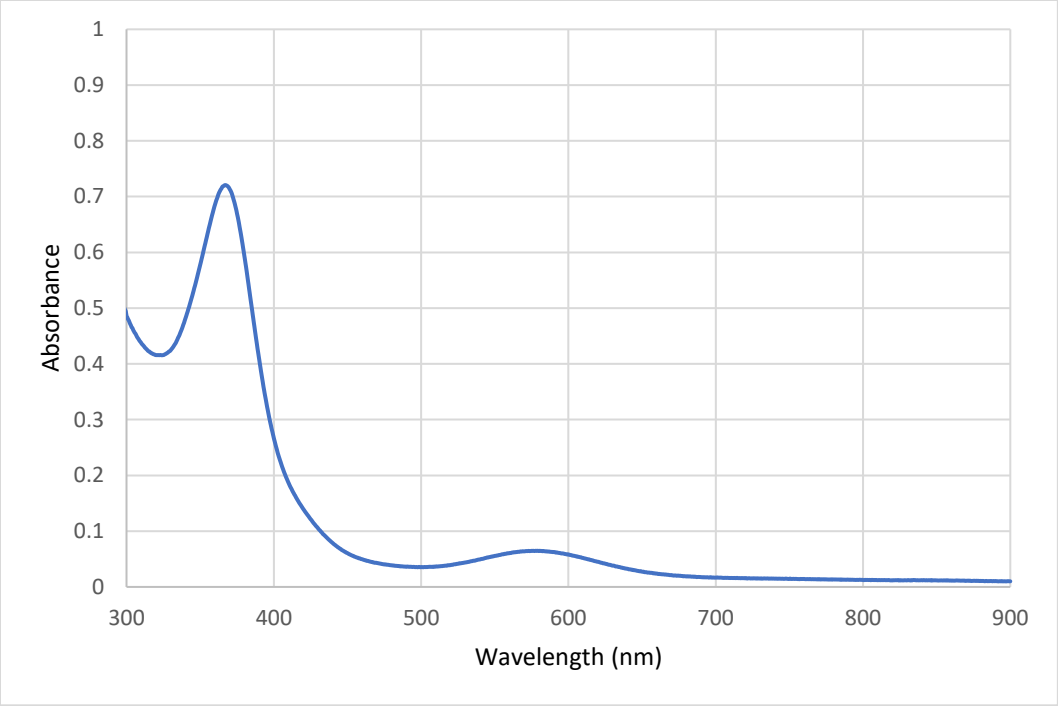


**Figure 4.S35.** UV-Visible spectrum of $Ar^{iPr4}Sn–Mo(\eta^5\text{-}C_5H_5)(CO)_3$ (**3a**) 65 μM in hexanes at 298 K.

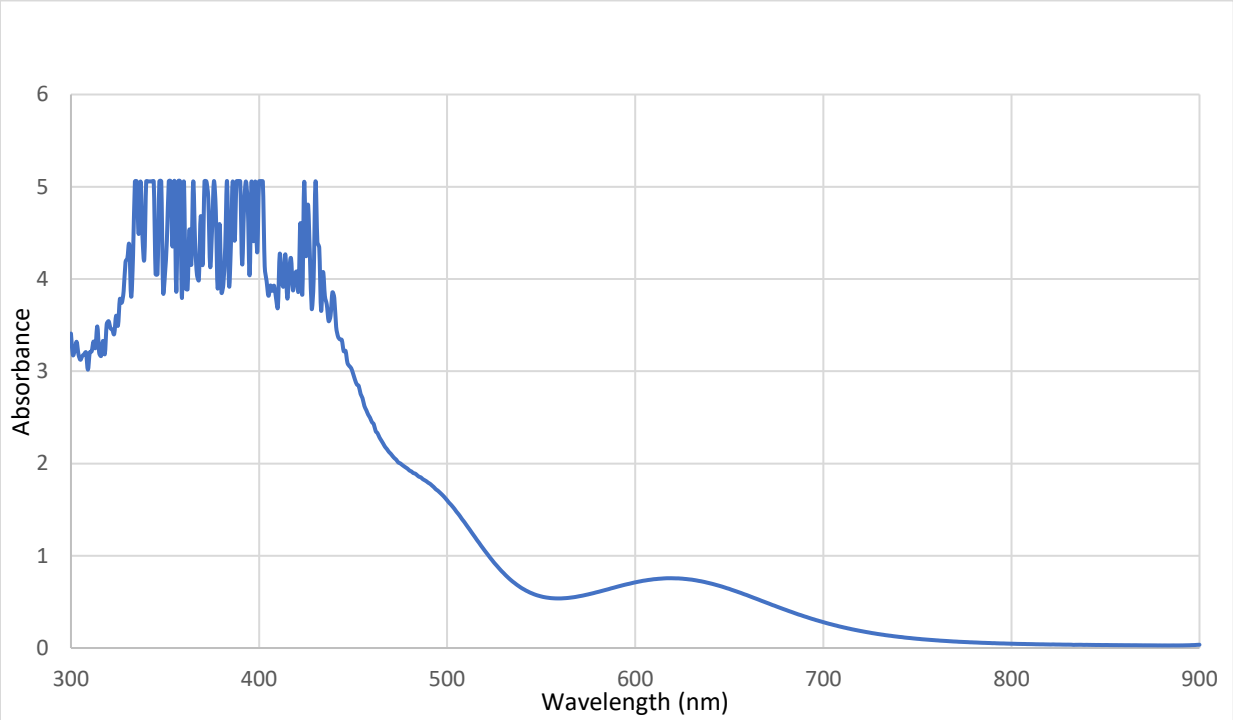


**Figure 4.S36.** UV-Visible spectrum of $Ar^{iPr6}Pb{\equiv}Mo(\eta^5\text{-}C_5H_5)(CO)_2$ (**4**) 1.37 mM in hexanes at 298 K.

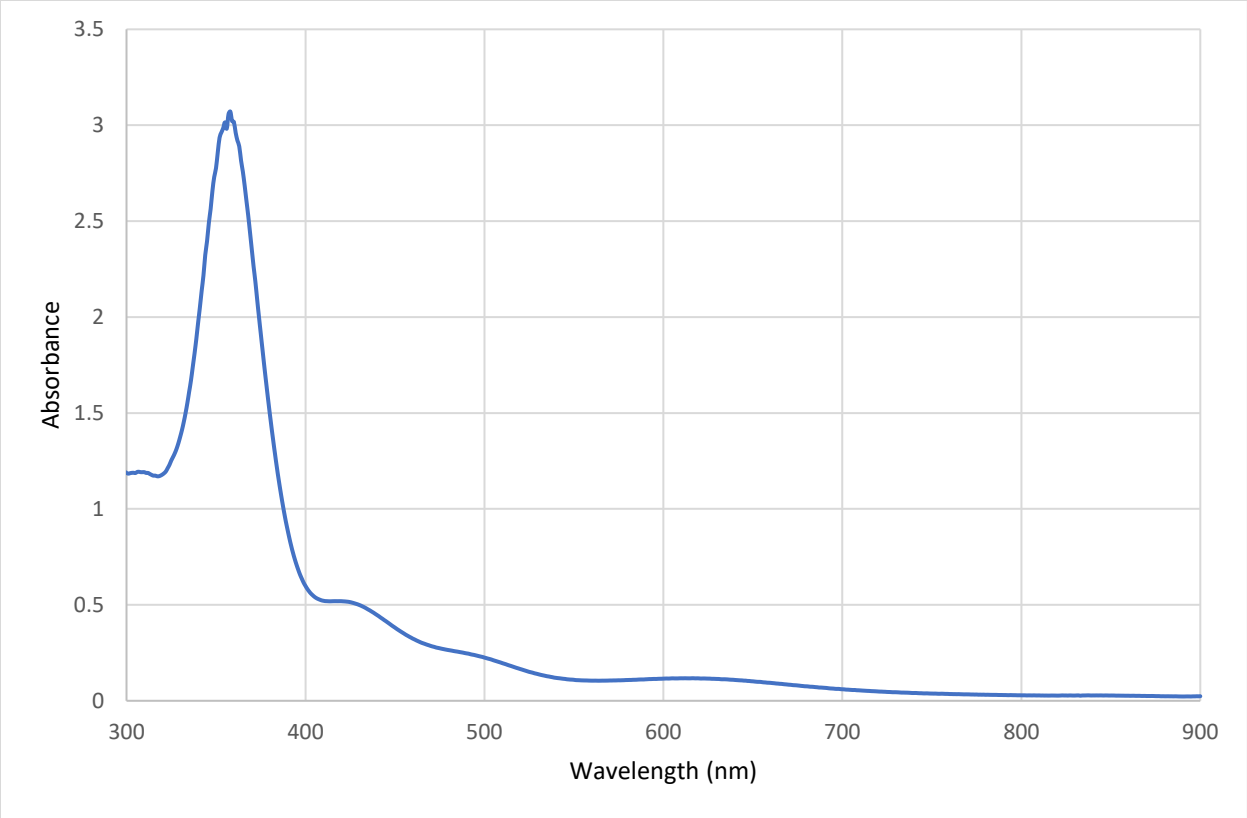


**Figure 4.S37.** UV-Visible spectrum of $Ar^{iPr6}Pb{\equiv}Mo(\eta^5\text{-}C_5H_5)(CO)_2$ (**4**) 137 μM in hexanes at 298 K.

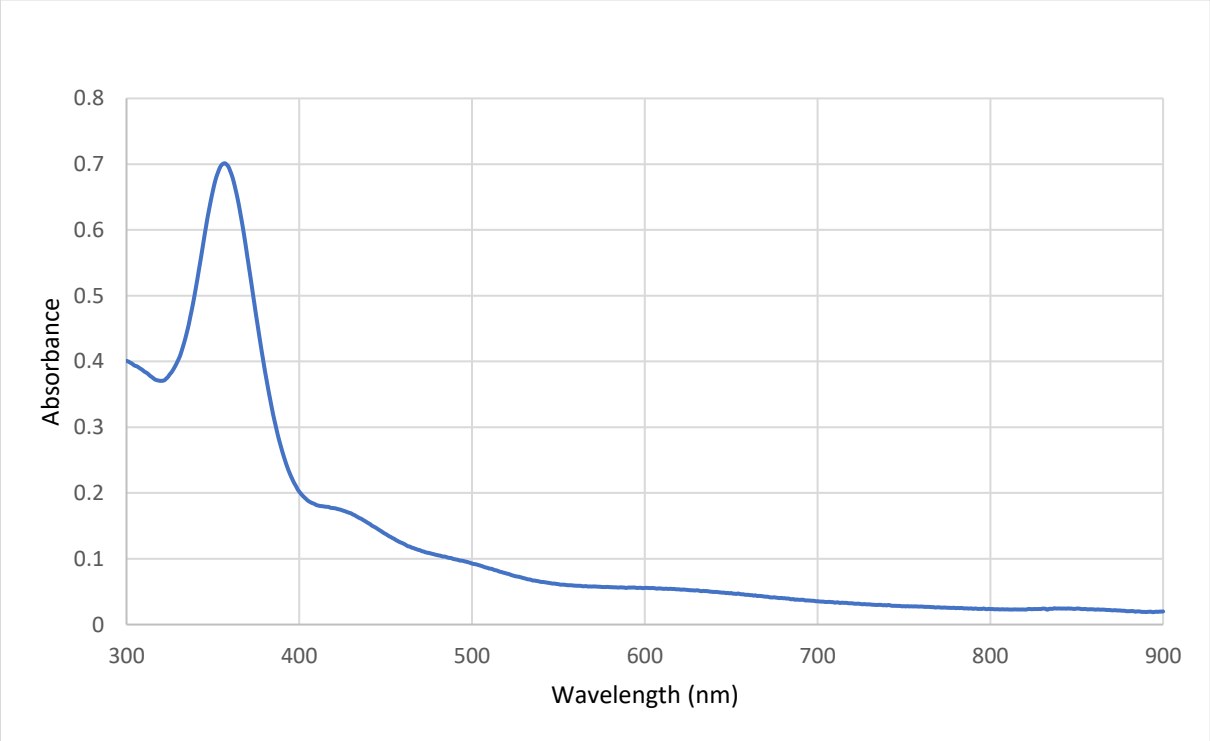


**Figure 4.S38.** UV-Visible spectrum of $Ar^{iPr6}Pb{\equiv}Mo(\eta^5\text{-}C_5H_5)(CO)_2$ (**4**) 27.4 μM in hexanes at 298 K.

## Photos of Compounds

**Figure 4.S39.** Photos of $C_6D_6$ solutions of compounds (left to right) **1a**, **2b**, **3a**, **4**, and **5**.

## References


(S1) Pangborn, A. B.; Giardello, M. A.; Grubbs, R. H.; Rosen, R. K.; Timmers, F. J. Safe and Convenient Procedure for Solvent Purification. *Organometallics*, **1996**, *15*, 1518-1520.

(S2) Fulmer, G. R.; Miller, A. J. M.; Sherden, N. H.; Gottlieb, H. E.; Nudelman, A.; Stoltz, B M.; Bercaw, J. E.; Goldberg, K. I. NMR Chemical Shifts of Trace Impurities: Common Laboratory Solvents, Organics, and Gases in Deuterated Solvents Relevant to the Organometallic Chemist. *Organometallics*, **2010**, *29*, 2176-2179.

(S3) Stender, M.; Phillips, A. D.; Wright, R. J.; Power, P. P. Synthesis and characterization of a digermanium analogue of an alkyne. *Angew. Chem., Int. Ed.* **2002** *41*, 1785-1787.

(S4) Phillips, A. D.; Wright, R. J.; Olmstead, M. M.; Power, P. P. Synthesis and characterization of 2,6-Dipp$_2$-H$_3$C$_6$SnSnC$_6$H$_3$-2,6-Dipp$_2$ (Dipp = C$_6$H$_3$-2,6-Pr$^i_2$): A tin analogue of an alkyne. *J. Am. Chem. Soc.* **2002**, *124*, 5930-5931.

(S5) Pu, L.; Phillips, A. D.; Richards, A. F.; Stender, M.; Simons, R. S.; Olmstead, M. M.; Power, P. P. Germanium and Tin Analogues of Alkynes and Their Reduction Products. *J. Am. Chem. Soc.* **2003**, *125*, 11626-11636.

(S6) Pu, L.; Twamley, B.; Power, P. P. Synthesis and characterization of 2,6-Trip$_2$H$_3$C$_6$PbPbC$_6$H$_3$-2,6-Trip$_2$ (Trip = C$_6$H$_2$-2,4,6-i-Pr$_3$): A stable heavier group 14 element analogue of an alkyne. *J. Am. Chem. Soc.* **2000**, *122*, 3524-3525.

(S7) Queen, J. D.; Bursch, M.; Seibert, J.; Maurer, L. R.; Ellis, B. D.; Fettinger, J. C.; Grimme, S.; Power, P. P. Isolation and Computational Studies of a Series of Terphenyl Substituted Diplumbynes with Ligand Dependent Lead–Lead Multiple-Bonding Character. *J. Am. Chem. Soc.* **2019**, *141*, 14370-14383.

(S8) Curtis, M. D.; Hay, M. S.; Choi, M. G.; Angelici, R. J. Cyclopentadienyl metal carbonyl dimers of molybdenum and tungsten. *Inorg. Synth.*, **1990**, *28* 150-154.

(S9) Sheldrick, G. M. *SADABS*; University of Göttingen, Germany, 1996.

(S10) Sheldrick, G. M. SHELXT - Integrated Space-Group and Crystal-Structure Determination.*Acta Cryst.* **2015**, *A71*, 3-8.

(S11) Sheldrick, G. M. Crystal Structure Refinement with SHELXL. *Acta Cryst.* **2015**, *C71*, 3-8.

(S12) Takagi, N.; S. Nagase, S. Substituent Effects on Germanium–Germanium and Tin–Tin Triple Bonds. *Organometallics*, **2001**, *20*, 5498-5500.

(S13) Nolan, S. P.; López de la Vega, R.; Hoff, C. D. Heats of Reaction of $[Mo(CO)_2Cp^*]_2$ ($Cp^*$ = $C_5H_5$, $C_5(CH_3)_5$, $C_9H_7$) with CO, HC≡CH, and $C_6H_5C$≡CH. Thermochemical Investigation of the Molybdenum-Molybdenum Triple Bond. *Inorg. Chem*. **1986**, *25*, 4446-4448.

(S14) Amer, S.; Kramer, G.; Poë, A. Thermal Homolytic Cleavage of Mo–Mo Bond in ($h^5$-$C_5H_5)_2Mo_2(CO)_6$. *J. Organomet. Chem.* **1981**, *209*, C28-C30.

## Chapter 5. The monomeric alanediyl :AlAr$^{iPr8}$ (Ar$^{iPr8}$ = C$_6$H-2,6-(C$_6$H$_2$-2,4,6-Pr$^i_3$)$_2$-3,5-Pr$^i_2$): an organoaluminum(I) compound with a one-coordinate aluminum atom.

Joshua D. Queen,[†] Annika Lehmann,[‡] James C. Fettinger,[†] Heikki M. Tuononen,*[,‡] and Philip P. Power*[,†]

[†]Department of Chemistry, University of California, Davis, One Shields Avenue, Davis CA, USA, 95616.

[‡]Department of Chemistry, NanoScience Centre, University of Jyväskylä, P.O. Box 35, FI-40014 Jyväskylä, Finland



**Abstract.** Reduction of the aluminum iodide AlI$_2$Ar$^{iPr8}$ (**1**; Ar$^{iPr8}$ = C$_6$H-2,6-(C$_6$H$_2$-2,4,6-Pr$^i_3$)$_2$-3,5-Pr$^i_2$) with 5% w/w Na/NaCl in hexanes gave a dark red solution from which the monomeric alanediyl :AlAr$^{iPr8}$ (**2**) was isolated in ca. 28% yield as yellow-orange crystals. Compounds **1** and **2** were characterized by X-ray crystallography, electronic and NMR spectroscopy, and theoretical calculations. The Al atom in **2** is one-coordinate and the compound displays two absorptions in its electronic spectrum at 354 nm and 455 nm. It reacts with H$_2$ under ambient conditions to give the aluminum hydride {AlH(μ-H)Ar$^{iPr8}$}$_2$, probably via a weakly bound dimer of **2** as an intermediate.

The chemistry of the group 13 elements is largely defined by the increasing stability of the +1 oxidation state as the group is descended from B to Tl.[1] For aluminum, low-oxidation-state compounds have generated much interest,[2–11] but they are more challenging to isolate in comparison to those of the other group 13 metals because of their higher reactivity and tendency to disproportionate.[2] The isolation of the landmark Al$^{II}$ compound R$_2$Al-AlR$_2$ (R = −CH(SiMe$_3$)$_2$),

the first Al–Al bonded molecular species, by Uhl[12] in 1988, and of the first organo $Al^{I}$ species $Al_4Cp^*_4$ ($Cp^*$ = $\eta^5$-$C_5Me_5$) by Schnöckel and co-workers[13] in 1991 as well as the icosahedral cluster $K_2[Al_{12}{}^{i}Bu_{12}]$[14] were major breakthroughs. Continued advancement has been made via the synthesis of further $Al_4R_4$ derivatives (R = alkyl, silyl, amide),[15–18] of dialuminenes RAl=AlR (R = large *m*-terphenyl, aryl, or silyl groups), which were trapped either as their cycloaddition products with aromatic species[19,20] or stabilized and isolated by complexation with NHC ligands,[21,22] and of the monomeric β-diketiminate complexes **:**Al($^{Dipp}$Nacnac) ($^{Dipp}$Nacnac = [R{C═N(2,6-$C_6H_3$-$^{i}Pr_2$)}$_2$], R = $CH_3$, $C(CH_3)_3$).[23,24]

Several anionic low-oxidation-state Al complexes have also been reported, such as the dialuminyne[25] $Na_2(AlAr^{iPr4})_2$ (oxidation state $Al^0$; $Ar^{iPr4}$ = $C_6H_3$-2,6-($C_6H_3$-2,6-$^{i}Pr_2$)$_2$) with a nonclassical Al–Al triple bond and the metalloaromatic cycloalane $Na_2(AlAr^{Me6})_3$ (oxidation state $Al^{0.33}$; $Ar^{Me6}$ = $C_6H_3$-2,6-($C_6H_2$-2,4,6-$Me_3$)$_2$), which are analogous to the corresponding Ga complexes $Na_2(GaAr^{iPr6})_2$ ($Ar^{iPr6}$ = $C_6H_3$-2,6-($C_6H_2$-2,4,6-$^{i}Pr_3$)$_2$) and $Na_2(GaAr^{Me6})_3$ of Robinson and co-workers.[26,27] Treatment of the dialanes $Trip_2AlAlTrip_2$ (Trip = $C_6H_2$-2,4,6-$^{i}Pr_3$) and $R_2AlAlR_2$ (R = $CH(SiMe_3)_2$) with alkali metals in donor solvents gave the radical anion complexes $[Li(TMEDA)_2][Trip_2AlAlTrip_2]$,[28] $[Li(TMEDA)_2][R_2AlAlR_2]$[29] (TMEDA = *N,N,N′,N′*-tetramethylethane-1,2-diamine), and $[K(DME)_3][R_2AlAlR_2]$[30] (DME = 1,2-dimethoxyethane) with Al−Al bond orders of 1.5. The chelating NON/$NON^{Dipp}$ scaffolds (NON = 4,5-bis(2,6-diisopropylanilido)-2,7-di-*tert*-butyl-9,9-dimethylxanthene; $NON^{Dipp}$ = $O(SiMe_2NDipp)_2$; Dipp = $C_6H_3$-2,6-$^{i}Pr_2$)[31,32] also stabilize the $Al^{I}$ compounds $[KAl(NON)]_2$ or $[KAl(NON^{Dipp})]_2$, and the structurally related $[KAl\{N(Dipp)_2SiMe_2CH_2\}_2]_2$ has also been reported.[33] In addition alkyl or alkyl-amino ligands stabilize the cyclic $Al^{(I)}$ salts $[K(toluene)_2]$

[$AlC(SiMe_3)_2CH_2CH_2C(SiMe_3)_2$][34] and [K(12-crown-4][$AlN(Ad)CHCHC(SiMe_3)_2$].[35] These "aluminyl" complexes have nucleophilic Al centers that display a diverse reaction chemistry.[36]

Despite these advances, monomeric compounds of $Al^I$ remain especially rare, with the only well-characterized examples being the aforementioned **:**Al($^{Dipp}$Nacnac) and the more recently reported **:**$Al^{3t}Cp$ ($^{3t}Cp$ = $C_5H_2$-1,2,4-$^tBu_3$),[37] although $Al_4Cp^*_4$ had been shown earlier to dissociate into **:**AlCp* monomers at elevated temperature.[38] Wiberg and co-workers have also shown that the dialane $R_2AlAlR_2$ (R = $Si^tBu_3$) dissociates into $R_2Al^\bullet$ radicals upon heating to 50 °C.[39,40] These compounds have a rich chemistry[5,6] that involves oxidative additions,[41] reversible olefin coordination,[42] C–F and C–H bond activation,[42,43] and C–C bond coupling.[44,45]

However, no compound containing a singly coordinated Al atom has been isolated. A common theme among the low-oxidation-state aluminum compounds has been the use of chelating or π-bonding ligands to stabilize the reactive Al center. Although AlH and the monohalides AlX (X = F, Cl, Br, I) have been studied, they are only observed in the gas phase at high temperature and low pressure,[46] or as metastable solutions when condensed in toluene/ether at cryogenic temperatures.[47,48] Driess and co-workers characterized an AlBr moiety using a push–pull strategy by coordination of one $Fe(CO)_4$ and two NHC ligands to the Al atom.[49] Recently Braunschweig and co-workers characterized monomeric AlH trapped by two cyclic (alkyl)(amino)carbene (CAAC) ligands,[50] although a non-negligible resonance structure (36%) involving an Al(III) diradical centered on the two CAAC ligands contributes to its stability.

Our group has shown that the use of sterically demanding terphenyl ligands allowed the structural characterization of one-coordinate univalent compounds of Ga,[51] In,[52] and Tl[53] and transition-metal M(I) (M = Mn, Fe, Co) fragments, which form coordination complexes with arenes.[54,55] These results suggested that a similar stabilization of a one-coordinate compound of Al

was feasible. However, numerous attempts to isolate such a compound via a reduction of aryl aluminum dihalides were unsuccessful owing to the extreme reactivity of the reduced aluminum species. We turned to the use of the extremely sterically crowding terphenyl ligand $Ar^{iPr8}$ ($Ar^{iPr8}$ = $C_6H$-2,6-($C_6H_2$-2,4,6-$^iPr_3)_2$-3,5-$^iPr_2$) in combination with the reducing agent Na/NaCl, which, upon reduction of the precursor $AlI_2Ar^{iPr8}$, afforded the monomeric alanediyl **:**$AlAr^{iPr8}$ containing a one-coordinate aluminum atom.

The precursor aluminum iodide **1** (Figure 5.1) was prepared by treatment of the corresponding trihydridoaluminate salt [$LiAlH_3Ar^{iPr8}$][56] with an excess of methyl iodide in diethyl ether at 0 °C (Scheme 5.1). Crystallization from hexanes gave **1** as colorless blocks in 91% yield. Compound **1** is an uncommon example of a three-coordinate monomeric aluminum(III) halide.[57,58] The coordination environment of the Al atom is slightly pyramidalized (sum of the interligand angles at Al = 356.5(4)°), and the sterically demanding ligand prevents dimerization or the coordination of $Et_2O$ solvent that is normally seen for similar compounds.[59] One of the flanking phenyl rings is bent toward the Al atom (Al–C(1)–C(6) = 110.89(39)° vs Al–C(1)–C(2) = 128.45(40)°), and two of the Al···$C_{(ring)}$ distances (Al–C(22) = 2.745(5) Å, Al–C(23) = 2.766(6) Å) are the closest Al···C approaches, indicating a weak attraction between the electron-rich π-system and the Lewis acidic Al atom.

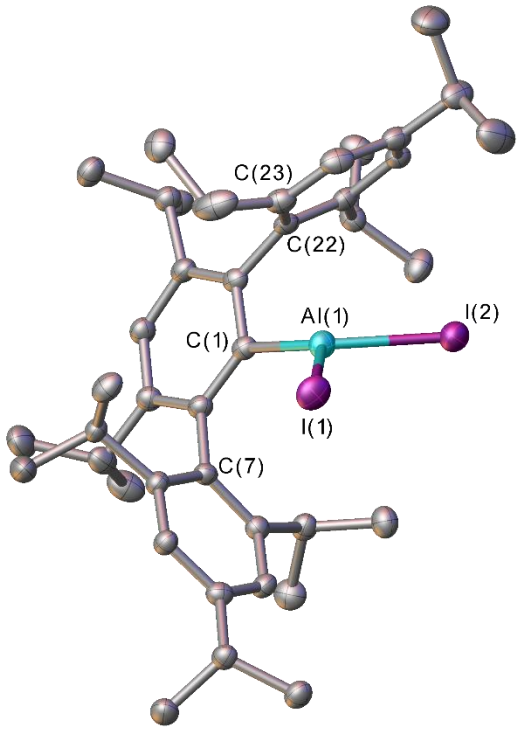


**Figure 5.1.** Thermal ellipsoid plot (50%) of $AlI_2Ar^{iPr8}$ (**1**). Hydrogen atoms are not shown. Selected distances (Å) and angles (°): Al(1)-I(1): 2.5125(18) Al(1)-I(2): 2.4840(18), Al(1)-C(1): 1.9653(57), Al(1)···C(7): 3.347(5) Al(1)···C(22): 2.745(5), Al(1)···C(23): 2.766(6), I(1)-Al(1)-I(2): 103.88(6), C(1)-Al(1)-I(1): 124.85(17), C(1)-Al(1)-I(2): 127.80(17), Al(1)-C(1)-C(2): 128.48(40), Al(1)-C(1)-C(6): 110.89(39).

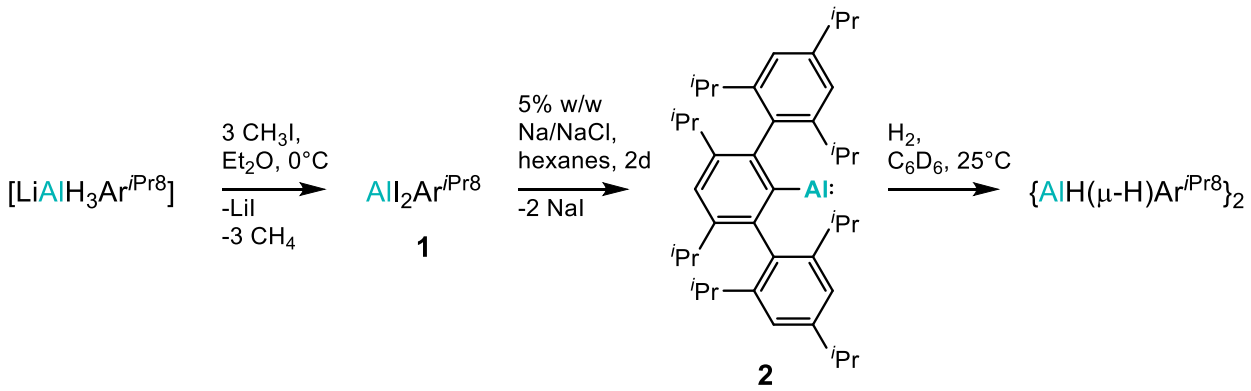


**Scheme 5.1** Synthesis of compounds **1** and **2** and the reaction of **2** with $H_2$.

These are, however, much longer than, for example, the Al–C distances in $Al_4Cp^*_4$ (Al–C = 2.29(1)–2.38(1) Å)[13] and are expected to be very weakly bonding at most.

The unusual monomeric structure of **1** suggested that the $Ar^{iPr8}$ ligand could be effective for the stabilization of other low-coordinate Al complexes. Attempts at a reductive dehalogenation of **1** with $KC_8$ or Na mirrors gave pale yellow-green solutions from which only $Ar^{iPr8}H$ could be isolated. A recent report by Jones and co-workers showed that alkali metals supported on their halide salts are effective reagents for the preparation of Mg(I) and Al(I) β-diketiminate complexes,[60] and we chose 5% weight Na on NaCl as a reducing agent for **1**. A hexanes solution of **1** stirred over an excess of freshly prepared Na/NaCl yielded a dark red solution after 2 d. Filtration and removal of the solvent, followed by recrystallization from benzene at ca. 8 °C, gave the compound **:**$AlAr^{iPr8}$ (**2**) as yellow crystals in ca. 28% yield, which were thermally stable up to their melting point of 228–231 °C. Upon isolation and drying under reduced pressure these crystals of **2** darkened to an orange color.

The crystal structure of **2** (Figure 5.2) revealed two crystallographically independent molecules in which the Al atoms are bound only to the *ipso* carbon of the central ring of the $Ar^{iPr8}$ ligand. The Al–C distances of 1.988(4) and 2.003(4) Å (calculated value 2.023 Å at the PBE1PBE-

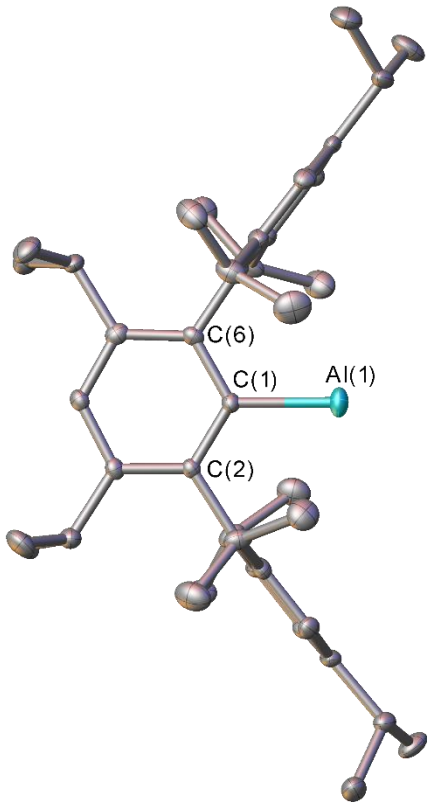


**Figure 5.2.** Thermal ellipsoid plot (50%) of one of the crystallographically independent molecules of :AlAr$^{iPr8}$ (**2**). Hydrogen atoms and solvent benzene molecules are not shown (cf. Figure 5.S7). Selected bond lengths (Å) and angles (°) {values in braces correspond to the other crystallographically independent molecule of 2}: Al(1)-C(1): 1.9883(36) {2.0028(37)}, Al(1)-C(1)-C(2): 121.29(28) {121.22(29)}, Al(1)-C(1)-C(6): 119.41(30) {119.46(31)} C(2)-C(1)-C(6): 119.27(29) {119.31(31)}.

G3BJ/def2-TZVP level) are only slightly longer than the Al–C single bond in **1**. It crystallizes from benzene in the space group *Pc* and is packed in a head-to-tail fashion (Figure 5.S7 in Supporting Information) preventing any Al–Al bonding in the crystal structure. The long Al···H and Al···C separations for atoms in the nearby methyl groups (>2.9 Å), flanking rings (>3.0 Å), or benzene molecules of crystallization (>4.8 Å) indicate no strong secondary bonding interactions in the crystal structure. An analysis of generalized compliance constants calculated for the optimized structure of **2** supports this conclusion. However, the Quantum Theory of Atoms in Molecules shows a bond path and a bond critical point between the C–H atoms and the aluminum center with very low electron density value of 0.006 e bohr$^{-3}$. An examination of the Natural Bond Orbitals further revealed that the C–H···Al donor–acceptor interactions, calculated at the second-order perturbation level, have a stabilization energy of only 7–8 kJ mol$^{-1}$, that is, considerably less than that typically found for C–H···metal agostic interactions.[61] Thus, **2** is an example of a compound containing a singly coordinated aluminum atom. The Al atom lies almost symmetrically between the two flanking rings, and nearly in the extended plane of the central ring of the terphenyl ligand. This is similar to its Ga congener but not to the related In and Tl compounds **:**MAr$^{iPr6}$ (M = In, Tl),[52,53] where the metal atoms lie 0.23 and 0.28 Å from the extended plane.

The frontier molecular orbitals of **2** are the n-type highest occupied molecular orbital (HOMO) occupied by the Al nonbonding lone pair, while the lowest unoccupied molecular orbital (LUMO) ($\pi_{out\text{-}of\text{-}plane}$) and LUMO+1 ($\pi_{in\text{-}plane}$) orbitals are mainly composed of the Al 3p orbitals (Figure 5.3). The electronic spectrum of **2** shows two absorptions at 455 and 354 nm (calculated values 467 and 351 nm), which are responsible for its yellow-orange color. These are calculated to correspond to the lone pair n → $\pi_{out\text{-}of\text{-}plane}$ and n → $\pi_{in\text{-}plane}$ transitions, respectively, both of which are symmetry-allowed. The absorptions are slightly lower in energy than those of the gallium congener **:**GaAr$^{iPr8}$ (437 and 351 nm).[51]

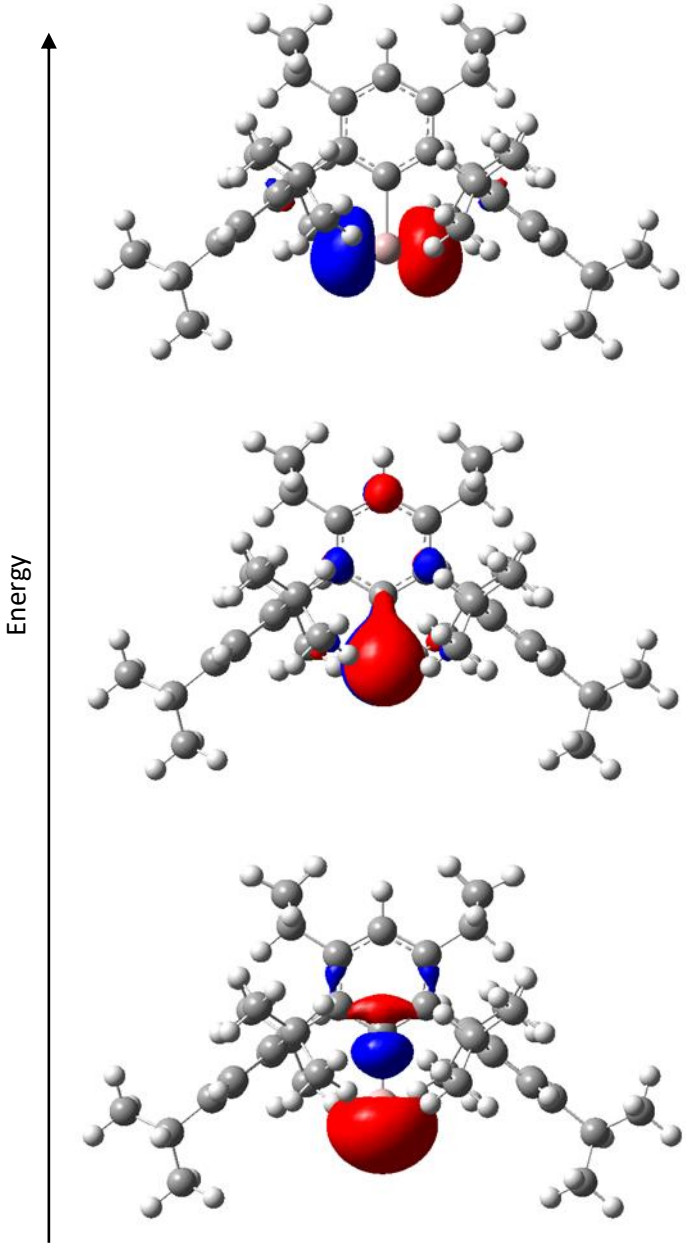


**Figure 5.3.** LUMO+1 (top), LUMO (middle), and HOMO (bottom) of AlAr$^{iPr8}$ (**2**) (±0.05 isovalue).

Compound **2** was found to react rapidly with $H_2$ in $C_6D_6$, giving the known compound {AlH(μ-H)Ar$^{iPr8}$}$_2$,[56] identified by its $^1$H NMR spectrum, in high yield. The facile formation of {AlH(μ-H)Ar$^{iPr8}$}$_2$ is surprising, considering that its gallium congener **:**GaAr$^{iPr8}$ shows no such reactivity.[62] In contrast, the related digallene Ar$^{iPr4}$GaGaAr$^{iPr4}$ readily reacts with $H_2$ to afford {GaH(μ-H)Ar$^{iPr4}$}$_2$, suggesting that the metal–

metal bonded dimer $Ar^{iPr8}AlAlAr^{iPr8}$ is the reactive species in solution. Similar reactivity was seen for the dialuminene-benzene cycloaddition products reported by Tokitoh and co-workers.[63] Upon retro-cycloaddition, free dialuminene is liberated in solution and was further found to react with $H_2$ to give the corresponding aluminum dihydride product. Inoue and co-workers also demonstrated that $H_2$ adds to the classical double bond in the dialuminene Trip(NHC)AlAl(NHC)Trip to give the dialane Trip(NHC)HAl-AlH(NHC)Trip.[22] Analysis of the frontier orbitals of **2** indicates that its direct reactivity with $H_2$ is likely to involve a very high-energy transition state, and all attempts to follow this reaction path computationally were met with steep increases in energy with no identifiable transition state. Consequently, a weak association of 2 equivalents of **2** to form the corresponding dialuminene could be crucial for the observed reactivity by lowering the activation energy. Calculations probing the energetics of this process indicated that dimerization of **2** is energetically slightly favored ($\Delta G = -20$ kJ mol$^{-1}$) in the gas phase. Thus, a judicious choice of solvent may allow the characterization of the dialuminene $Ar^{iPr8}AlAlAr^{iPr8}$.

In conclusion, we have isolated the monomeric alanediyl **:**$AlAr^{iPr8}$ (**2**) containing a one-coordinate aluminum atom by reduction of the precursor arylaluminum diiodide $AlI_2Ar^{iPr8}$ (**1**) with excess 5% w/w Na/NaCl in hexanes. Two absorbances at 455 and 354 nm in the electronic spectrum of **2** correspond to the Al lone pair n $\rightarrow$ $\pi_{\text{out-of-plane}}$ and n $\rightarrow$ $\pi_{\text{in-plane}}$ transitions. Compound **2** appears to have good thermal stability and reacts with $H_2$ to give the aluminum hydride complex $\{AlH(\mu\text{-}H)Ar^{iPr8}\}_2$ in contrast with its heavier congener **:**$GaAr^{iPr8}$. Further reactivity studies of **2** with small molecules and the preparation of other low-coordinate aluminum complexes are in hand along with computational investigations of the mechanisms involved.

**Acknowledgements**

We thank the Office of Basic Energy Sciences, U.S. Department of Energy (DE-FG02-07ER4675), for support of this work and the U.S. National Science Foundation for the purchase of a dual source X-ray diffractometer (Grant No. CHE-0840444). This project received funding from the European Research Council under the European Union's Horizon 2020 research and innovation programme (Grant No. 772510 to H.M.T.). This paper is dedicated to the memory of Alan H. Cowley, who made many important contributions to main-group element chemistry.

**References**

(1) Cotton, F. A.; Wilkinson, G. *Advanced Inorganic Chemistry*, 4th ed.; Wiley: New York, 1980, pp 327.

(2) Aldridge, S.; Downs, A. J. *The Group 13 Metals Aluminium, Gallium, Indium and Thallium: Chemical Patterns and Peculiarities*; Wiley: Chichester, 2011.

(3) Downs, A. J. Recent Advances in the Chemistry of the Group 13 Metals: Hydride Derivatives and Compounds Involving Multiply Bonded Group 13 Metal Atoms. *Coord. Chem. Rev.* **1999**, *189*, 59–100.

(4) Bag, P.; Weetman, C.; Inoue, S. Experimental Realisation of Elusive Multiple-Bonded Aluminium Compounds: A New Horizon in Aluminium Chemistry. *Angew. Chem., Int. Ed.* **2018**, *57*, 14394–14413.

(5) Roesky, H. W.; Kumar, S. S. Chemistry of Aluminium(I). *Chem. Commun.* **2005**, 4027–4038.

(6) Zhong, M.; Sinhababu, S.; Roesky, H. W. The Unique β-Diketiminate Ligand in Aluminum(I) and Gallium(I) Chemistry. *Dalton Trans.* **2020**, *49*, 1351–1364.

(7) Wang, Y.; Robinson, G. H. Unique Homonuclear Multiple Bonding in Main Group Compounds. *Chem. Commun.* **2009**, 5201–5213.

(8) Wang, Y.; Robinson, G. H. Organometallics of the Group 13 M−M Bond (M = Al, Ga, In) and the Concept of Metalloaromaticity. *Organometallics* **2007**, *26*, 2–11.

(9) Robinson, G. H. Multiple Bonds Involving Aluminum and Gallium Atoms. *Adv. Organomet. Chem.* **2001**, *47*, 283–294.

(10) Power, P. P. Multiple Bonding Between Heavier Group 13 Elements. *Struct. Bond.* **2002**, *103*, 57–84.

(13) Hobson, K.; Carmalt, C. J.; Bakewell, C. Recent Advances in Low Oxidation State

Aluminium Chemistry. *Chem. Sci*. **2020**, *11*, 6942–6956.

(12) Uhl, W. Tetrakis[Bis(Trimethylsilyl)Methyl]Dialan(4), Eine Verbindung Mit Aluminium—Aluminium-Bindung. *Z. Naturforsch. B* **1988**, *43*, 1113–1118.

(13) Dohmeier, C.; Robl, C.; Tacke, M.; Schnöckel, H. The Tetrameric Aluminum(I) Compound [{Al($\eta^5$-$C_5Me_5$)}$_4$]. *Angew. Chem., Int. Ed.* **1991**, *30*, 564–565.

(14) Klinkhammer, K-W.; Uhl, W.; Wagner, J.; Hiller, W. $K_2[Al_{12}iBu_{12}]$, a Compound with $Al_{12}$ Icosahedra. Angew. Chem. Int. Ed. **1991**, 30, 179–180.

(15) Purath, A.; Dohmeier, C.; Ecker, A.; Schnöckel, H.; Amelunxen, K.; Passler, T.; Wiberg, N. Synthesis and Crystal Structure of the Tetraaluminatetrahedrane $Al_4[Si(t\text{-}Bu)_3]_4$, the Second $Al_4R_4$ Compound. *Organometallics* **1998**, *17*, 1894–1896.

(16) Purath, A.; Schnöckel, H. Tetrakis[Tris(Trimethylsilyl)Silylaluminium(I)] $Al_4[Si(SiMe_3)_3]_4$—Eine SiliziumreicheVerbindung Mit Zentralem Tetraedrischem $Al_4$-Kern. *J. Organomet. Chem.* **1999**, *579*, 373–375.

(17) Schiefer, M.; Reddy, N. D.; Roesky, H. W.; Vidovic, D. Synthesis and Structural Characterization of an Exclusively N-Based Tetrameric Aluminum(I) Compound. *Organometallics* **2003**, *22*, 3637–3638.

(18) Schnitter, C.; Roesky, H. W.; Röpken, C.; Herbst-Irmer, R.; Schmidt, H.-G.; Noltemeyer, M. The Behavior of [$RAlX_2$·THF] Compounds under Reductive Conditions: Tetrakis[Tris(Trimethylsilyl)Methylaluminum(I)]—A Neutral Aluminum(I) Compound with σ-Bound Alkyl Groups and a Tetrahedral Structure. *Angew. Chem., Int. Ed.* **1998**, *37*, 1952–1955.

(19) Wright, R. J.; Phillips, A. D.; Power, P. P. The [2 + 4] Diels−Alder Cycloadditon Product of a Probable Dialuminene, Ar‘AlAlAr‘ (Ar‘ = $C_6H_3$- 2,6-$Dipp_2$; Dipp = $C_6H_3$-2,6-$Pr^i_2$), with Toluene. *J. Am. Chem. Soc.* **2003**, *125*, 10784–10785.

(20) Agou, T.; Nagata, K.; Tokitoh, N. Synthesis of a Dialumene-Benzene Adduct and Its Reactivity as a Synthetic Equivalent of a Dialumene. *Angew. Chem., Int. Ed.* **2013**, *52*, 10818–10821.

(21) Bag, P.; Porzelt, A.; Altmann, P. J.; Inoue, S. A Stable Neutral Compound with an Aluminum–Aluminum Double Bond. *J. Am. Chem. Soc.* **2017**, *139*, 14384–14387.

(22) Weetman, C.; Porzelt, A.; Bag, P.; Hanusch, F.; Inoue, S. Dialumenes – Aryl vs. Silyl Stabilization for Small Molecule Activation and Catalysis. *Chem. Sci.* **2020**, *11*, 4817–4827.

(23) Cui, C.; Roesky, H. W.; Schmidt, H.-G.; Noltemeyer, M.; Hao, H.; Cimpoesu, F. Synthesis and Structure of a Monomeric Aluminum(I) Compound [{HC(CMeNAr)$_2$}Al] (Ar=2,6–$i$Pr$_2$C$_6$H$_3$): A Stable Aluminum Analogue of a Carbene. *Angew. Chem., Int. Ed.* **2000**, *39*, 4274–4276.

(24) Li, X.; Cheng, X.; Song, H.; Cui, C. Synthesis of HC[(CBut)(NAr)]$_2$Al (Ar = 2,6-$Pr^i_2C_6H_3$) and Its Reaction with Isocyanides, a Bulky Azide, and $H_2O$. *Organometallics* **2007**, *26*, 1039–1043.

(25) Wright, R. J.; Brynda, M.; Power, P. P. Synthesis and Structure of the "Dialuminyne" $Na_2[Ar'AlAlAr']$ and $Na_2[(Ar''Al)_3]$: Al—Al Bonding in $Al_2Na_2$ and $Al_3Na_2$ Clusters. *Angew. Chem., Int. Ed.* **2006**, *45*, 5953–5956.

(26) Su, J.; Li, X.-W.; Crittendon, R. C.; Robinson, G. H. How Short Is a -Ga:Ga- Triple Bond? Synthesis and Molecular Structure of $Na_2[Mes^*_2C_6H_3\text{-}Ga{:}Ga\text{-}C_6H_3Mes^*_2]$ (Mes* = 2,4,6-i-$Pr_3C_6H_2$): The First Gallyne. *J. Am. Chem. Soc.* **1997**, *119*, 5471–5472.

(27) Li, X.-W.; Pennington, W. T.; Robinson, G. H. Metallic System with Aromatic Character. Synthesis and Molecular Structure of $Na_2[[(2,4,6\text{-}Me_3C_6H_2)_2C_6H_3]Ga]_3$ The First Cyclogallane. *J. Am. Chem. Soc.* **1995**, *117*, 7578–7579.

(28) Wehmschulte, R. J.; Ruhlandt-Senge, K.; Olmstead, M. M.; Hope, H.; Sturgeon, B. E.; Power, P. P. Reduction of a Tetraaryldialane to Generate Al–Al π-Bonding. *Inorg. Chem.* **1993**, *32*, 2983–2984.

(29) Uhl, W. Organoelement Compounds with AlAl, GaGa, and InIn Bonds. *Angew. Chem. Int. Ed.* **1993**, *32*, 1386-1397.

(30) Pluta, C.; Pörschke, K-R.; Krüger, C.; Hildenbrand, K. An Al–Al One-Electron π Bond. *Angew. Chem. Int. Ed.* **1993**, *32*, 388–390.

(31) Hicks, J.; Vasko, P.; Goicoechea, J. M.; Aldridge, S. Synthesis, Structure and Reaction Chemistry of a Nucleophilic Aluminyl Anion. *Nature* **2018**, *557*, 92–95.

(32) Schwamm, R. J.; Anker, M. D.; Lein, M.; Coles, M. P. Reduction vs. Addition: The Reaction of an Aluminyl Anion with 1,3,5,7-Cyclooctatetraene. *Angew. Chem., Int. Ed.* **2019**, *58*, 1489–1493.

(33) Schwamm, R. J.; Coles, M. P.; Hill, M. S.; Mahon, M. F.; McMullin, C. L.; Rajabi, N. A.; Wilson, A. S. S. A Stable Calcium Alumanyl. *Angew. Chem. Int. Ed.* **2020**, *59*, 3928–3932.

(34) Kurumada, S.; Takamori, S.; Yamashita, M. An Alkyl-Substituted Aluminium Anion with Strong Basicity and Nucleophilicity. *Nature Chem.* **2020**, *12*, 36–39.

(35) Koshino, K.; Kinjo, R. Construction of σ-Aromatic $AlB_2$ Ring via Borane Coupling with a Dicoordinate Cyclic (Alkyl)(Amino)Aluminyl Anion. *J. Am. Chem. Soc.* **2020**, *142*, 9057–9062.

(36) Hicks, J.; Vasko, P.; Goicoechea, J. M.; Aldridge, S. The Aluminyl Anion: A New Generation of Aluminium Nucleophile. *Angew. Chem., Int. Ed.* **2020**, *59*, 2–14.

(37) Hofmann, A.; Tröster, T.; Kupfer, T.; Braunschweig, H. Monomeric $Cp^{3t}Al(I)$: Synthesis, Reactivity, and the Concept of Valence Isomerism. *Chem. Sci.* **2019**, *10*, 3421–3428.

(38) Sitzmann, H.; Lappert, M. F.; Dohmeier, C.; Üffing, C.; Schnöckel, H. Cyclopentadienylderivate von Aluminium(I). *J. Organomet. Chem.* **1998**, *561*, 203–208.

(39) Wiberg, N.; Amelunxen, K.; Blank, T.; Nöth, H.; Knizek, J. Tetrasupersilyldialuminum $[(t\text{-}Bu)_3Si]_2Al{-}Al[Si(t\text{-}Bu)_3]_2$: The Dialane(4) with the Longest Al−Al Bond to Date. *Organometallics* **1998**, *17*, 5431–5433.

(40) Wiberg, N.; Blank, T.; Kaim, W.; Schwederski, B.; Linti, G. Tri(Supersilyl)Dialanyl ($t$Bu$_3$Si)$_3$Al$_2$• and Tetra(Supersilyl)Cyclotrialanyl ($t$Bu$_3$Si)$_4$Al$_3$• − New Stable Radicals of a Group 13 Element from Thermolysis of ($t$Bu$_3$Si)$_4$Al$_2$. *Eur. J. Inorg. Chem.* **2000**, *2000*, 1475–1481.

(41) Chu, T.; Korobkov, I.; Nikonov, G. I. Oxidative Addition of σ Bonds to an Al(I) Center. *J. Am. Chem. Soc.* **2014**, *136*, 9195–9202.

(42) Bakewell, C.; White, A. J. P.; Crimmin, M. R. Reversible Alkene Binding and Allylic C–H Activation with an Aluminium(I) Complex. *Chem. Sci.* **2019**, *10*, 2452–2458.

(43) Bakewell, C.; White, A. J. P.; Crimmin, M. R. Reactions of Fluoroalkenes with an Aluminium(I) Complex. *Angew. Chem., Int. Ed.* **2018**, *57*, 6638–6642.

(44) Urwin, S. J.; Nichol, G. S.; Cowley, M. J. Aluminium-Mediated Carbon–Carbon Coupling of an Isonitrile. *Chem. Commun.* **2018**, *54*, 378–380.

(45) Kong, R. Y.; Crimmin, M. R. Reversible Insertion of CO into an Aluminium–Carbon Bond. *Chem. Commun.* **2019**, *55*, 6181–6184.

(46) Nagendran, S.; Roesky, H. W. The Chemistry of Aluminum(I), Silicon(II), and Germanium(II). *Organometallics* **2008**, *27*, 457–492.

(47) Tacke, M.; Schnöckel, H. Metastable Aluminum Chloride, AlCl, as a Solid and in Solution. *Inorg. Chem.* **1989**, *28*, 2895–2896.

(48) Dohmeier, C.; Loos, D.; Schnöckel, H. Aluminum(I) and Gallium(I) Compounds: Syntheses, Structures, and Reactions. *Angew. Chem., Int. Ed*. **1996**, *35*, 129–149.

(49) Tan, G.; Szilvási, T.; Inoue, S.; Blom, B.; Driess, M. An Elusive Hydridoaluminum(I) Complex for Facile C–H and C–O Bond Activation of Ethers and Access to Its Isolable Hydridogallium(I) Analogue: Syntheses, Structures, and Theoretical Studies. *J. Am. Chem. Soc.* **2014**, *136*, 9732–9742.

(50) Mellerup, S. K.; Cui, Y.; Fantuzzi, F.; Schmid, P.; Goettel, J. T.; Bélanger-Chabot, G.; Arrowsmith, M.; Krummenacher, I.; Ye, Q.; Engel, V.; Engels, B.; Braunschweig, H. Lewis-Base Stabilization of the Parent Al(I) Hydride under Ambient Conditions. *J. Am. Chem. Soc.* **2019**, *141*, 16954–16960.

(51) Zhu, Z.; Fischer, R. C.; Ellis, B. D.; Rivard, E.; Merrill, W. A.; Olmstead, M. M.; Power, P. P.; Guo, J. D.; Nagase, S.; Pu, L. Synthesis, Characterization and Real Molecule DFT Calculations for Neutral Organogallium(I) Aryl Dimers and Monomers: Weakness of Gallium—Gallium Bonds in Digallenes and Digallynes. *Chem. Eur. J.* **2009**, *15*, 5263–5272.

(52) Haubrich, S. T.; Power, P. P. Monomeric InC$_6$H$_3$-2,6-Trip$_2$ (Trip = -C$_6$H$_2$-2,4,6-i-Pr$_3$) and Its Manganese Complex ($\eta^5$-C$_5$H$_5$)(CO)$_2$MnInC$_6$H$_3$-2,6-Trip$_2$: One-Coordinate Indium in the Solid State. *J. Am. Chem. Soc.* **1998**, *120*, 2202–2203.

(53) Niemeyer, M.; Power, P. P. Synthesis and Solid-State Structure of 2,6-Trip$_2$C$_6$H$_3$Tl (Trip=2,4,6-$i$Pr$_3$C$_6$H$_2$): A Monomeric Arylthallium(I) Compound with a Singly Coordinated Thallium Atom. *Angew. Chem., Int. Ed.* **1998**, *37*, 1277–1279.

(54) Ni, C.; Ellis, B. D.; Fettinger, J. C.; Long, G. J.; Power, P. P. Univalent Transition Metal Complexes of Arenes Stabilized by a Bulky Terphenyl Ligand: Differences in the Stability of Cr(I), Mn(I) or Fe(I) Complexes. *Chem. Commun.* **2008**, 1014–1016.

(55) Lei, H.; Ellis, B. D.; Ni, C.; Grandjean, F.; Long, G. J.; Power, P. P. An Arene-Stabilized Cobalt(I) Aryl: Reactions with CO and NO. *Inorg. Chem.* **2008**, *47*, 10205–10207.

(56) Melton, C. E.; Dube, J. W.; Ragogna, P. J.; Fettinger, J. C.; Power, P. P. Synthesis and Characterization of Primary Aluminum Parent Amides and Phosphides. *Organometallics* **2014**, *33*, 329–337.

(57) Wehmschulte, R. J.; P. Power, P. New Routes to Synthetically Useful, Sterically Encumbered Arylaluminum Halides and Hydride Halides. *Inorg. Chem.* **1996**, *35*, 3262–3267.

(58) A. Petrie, M.; P. Power, P.; V. Rasika Dias, H.; Ruhlandt-Senge, K.; M. Waggoner, K.; J. Wehmschulte, R. Synthesis and Characterization of Bulky Aryl Derivatives of the Heavier Main Group 3 Elements. *Organometallics* **2002**, *12*, 1086–1093.

(59) Wehmschulte, R. J.; Grigsby, W. J.; Schiemenz, B.; Bartlett, R. A.; Power, P. P. Synthesis and Characterization of Sterically Encumbered Derivatives of Aluminum Hydrides and Halides: Assessment of Steric Properties of Bulky Terphenyl Ligands. *Inorg. Chem.* **1996**, *35*, 6694–6702.

(60) Hicks, J.; Juckel, M.; Paparo, A.; Dange, D.; Jones, C. Multigram Syntheses of Magnesium(I) Compounds Using Alkali Metal Halide Supported Alkali Metals as Dispersible Reducing Agents. *Organometallics* **2018**, *37*, 4810–4813.

(61) Lein, M. Characterization of Agostic Interactions in Theory and Computation. *Coord. Chem. Rev.* **2009**, *253*, 625–634.

(62) Caputo, C. A.; Koivistoinen, J.; Moilanen, J.; Boynton, J. N.; Tuononen, H. M.; Power, P. P. Counterintuitive Mechanisms of the Addition of Hydrogen and Simple Olefins to Heavy Group 13 Alkene Analogues. *J. Am. Chem. Soc.* **2013**, *135*, 1952–1960.

(63) Nagata, K.; Murosaki, T.; Agou, T.; Sasamori, T.; Matsuo, T.; Tokitoh, N. Activation of Dihydrogen by Masked Doubly Bonded Aluminum Species. *Angew. Chem. Int. Ed.* **2016**, *55*, 12877–12880.

**Author Contributions**

**J. D. Queen:** Synthesized and spectroscopically characterized reported compounds, collected X-ray crystallography data, and prepared the manuscript.

**A. Lehmann and H. M. Tuononen**: Perfomed DFT calculations on reported compounds includting optimizing geometries, simulating electronic spectra and prepared the related figures and portions of the manuscript.

**J. C. Fettinger**: Prepared the X-ray crystallographic data for publication.

**P. P. Power**: Supervised synthetic work and manuscript preparation.

## Supporting Information

### Experimental Details

**General Procedures.** All manipulations were carried out using modified Schlenk techniques or in a Vacuum Atmospheres OMNI-Lab drybox under argon atmosphere. Solvents were dried over columns of activated alumina using a Grubbs type purification system[S96] (Glass Contour), stored over an Na mirror ($Et_2O$), K mirror (hexanes), or 3 Å molecular sieves (benzene), and degassed via three freeze-pump-thaw cycles prior to use. The $^1H$ and $^{13}C\{^1H\}$ NMR spectra were recorded on Varian Inova 600 MHz spectrometer and were referenced to the residual solvent signals in $C_6D_6$ ($^1H$: δ 7.16 ppm, $^{13}C\{^1H\}$: δ 128.06 ppm).[S97] UV-Visible spectra were recorded in dilute hexane solutions in 3.5 mL quartz cuvettes using an Olis 17 Modernized Cary 14 UV-Vis/NIR spectrophotometer. Melting points were measured in glass capillary tubes sealed under argon using a Mel-Temp II apparatus using a partial immersion thermometer.

[$LiAlH_3Ar^{iPr8}$][S98] and 5% w/w Na/NaCl[S99] were prepared according to the literature methods. $CH_3I$ was purchased commercially, dried over $CaH_2$, and degassed via the freeze-pump-thaw method before use. $H_2$ gas was dried by passage through a column containing $P_2O_5$ and Drierite™.

### Synthesis of Compounds

$AlI_2Ar^{iPr8}$ (**1**). A solution of [$LiAlH_3Ar^{iPr8}$] (3.15 g, 5.23 mmol) in $Et_2O$ was cooled to 0°C in an ice/water bath. Neat $CH_3I$ (1.65 ml, 26.5 mmol) was added dropwise via syringe with rapid stirring. The mixture was kept in the bath and allowed to warm slowly (over ca. 8 h) to ambient temperature under a flow of inert gas to allow venting of the $CH_4$ byproduct. The volatile components were removed under reduced pressure and the white residue was extracted twice

with ca. 40 mL of hot (ca. 60°C) hexanes. The combined colorless filtrates were concentrated to ca. 40 mL and stored at -18°C overnight to give colorless blocks of **1** (1.92 g). The mother liquor was concentrated to ca. 15 mL and stored at -18°C to yield a further 2.10 g.

Yield: 4.02 g, 4.75 mmol (91%).

mp = 217-220°C (dec).

$^{1}$H NMR (600 MHz, $C_6D_6$, 298 K): δ 7.62 (s, 1H, p-Ar*H*), 7.32 (s, 4H, Trip m-Ar*H*), 3.07 (sept, $^{3}J$ = 6.8 Hz, 4H, -CH(C*H*$_3$)$_2$), 2.82 (sept, $^{3}J$ = 6.8 Hz, 4H, -C*H*(CH$_3$)$_2$), 1.50 (d, $^{3}J$ = 6.8 Hz, 12H, -CH(C*H*$_3$)$_2$), 1.29 (d, $^{3}J$ = 6.9 Hz, 12H, -CH(C*H*$_3$)$_2$), 1.25 (d, $^{3}J$ = 6.7 Hz, 12H, -CH(C*H*$_3$)$_2$), 1.14 (d, $^{3}J$ = 6.7 Hz, 12H, -CH(C*H*$_3$)$_2$).

$^{13}$C{$^{1}$H} NMR (151 MHz, $C_6D_6$, 298 K): δ 150.7, 147.1, 147.0, 143.5, 138.6, 125.8, 124.5, 34.9, 30.6, 30.1, 26.4, 25.4, 25.3, 24.5.

$^{27}$Al NMR (156 MHz, $C_6D_6$, 298 K): Not observed.

**:**AlAr$^{iPr8}$ (**2**): Crystalline **1** (0.850 g 1.00 mmol) was added to a flask containing 2.30 g of freshly prepared 95:5% w/w Na/NaCl powder (prepared from 0.115g/5.00 mmol Na (5.0 eq) and 2.19 g NaCl). Hexanes (ca. 100 mL) was added and the mixture was vigorously stirred for 3 days. The resulting dark red solution was filtered and the volatile components were removed under reduced pressure to afford a red oil that slowly solidified upon standing. Recrystallization from benzene (ca. 5 ml) at ca. 8°C for 2 days afforded bright yellow crystals of **2**. Upon isolation and drying under vacuum, crystals of **2** darken to an orange color.

Yield: 0.166 g, 0.280 mmol (28%)

Mp = 228-231°C (dec).

$^{1}$H (600 MHz, $C_6D_6$, 298 K): 7.46 (s, 1H, Ar*H*), 7.28 (s, 4H, Ar*H*), 2.98 (sept, $^{3}J$ = 6.8Hz, 4H, o-C*H*($CH_3$)$_2$), 2.85 (sept, $^{3}J$ = 7.0 Hz, 2H, -C*H*($CH_3$)$_2$), 2.76 (sept, $^{3}J$ = 6.7 Hz, 2H, -C*H*($CH_3$)$_2$), 1.42 (d, $^{3}J$ = 6.7 Hz, 12H, -CH(C*H*$_3$)$_2$), 1.25-1.23 (mult, 24H, -CH(C*H*$_3$)$_2$), 1.18 (d, $^{3}J$ = 6.8 Hz, 12H, -CH(C*H*$_3$)$_2$).

$^{13}$C{$^{1}$H} (151 MHz, $C_6D_6$, 298 K): 162.0, 148.9, 148.7, 145.4, 139.5, 134.4, 123.7, 121.8, 34.7, 30.4, 28.9, 26.1, 25.0, 24.9, 25.3

$^{27}$Al NMR (156 MHz, $C_6D_6$, 298 K): Not observed.

UV-Vis (hexanes): 354 nm (2800), 455 nm (730).

**Reaction of :AlAr$^{iPr8}$ with $H_2$**

Yellow crystals of **2** (10.0 mg 16.9 μmol) were dissolved in ca. 0.7 mL $C_6D_6$ in a J. Young NMR tube. The tube was evacuated, placed under an atmosphere of dry $H_2$ and agitated, resulting in an immediate change of the solution from orange to colorless. $^{1}$H NMR spectroscopy revealed complete conversion of **2** to the known hydride {AlH(μ-H)Ar$^{iPr8}$}$_2$.[S3]

## NMR Spectra

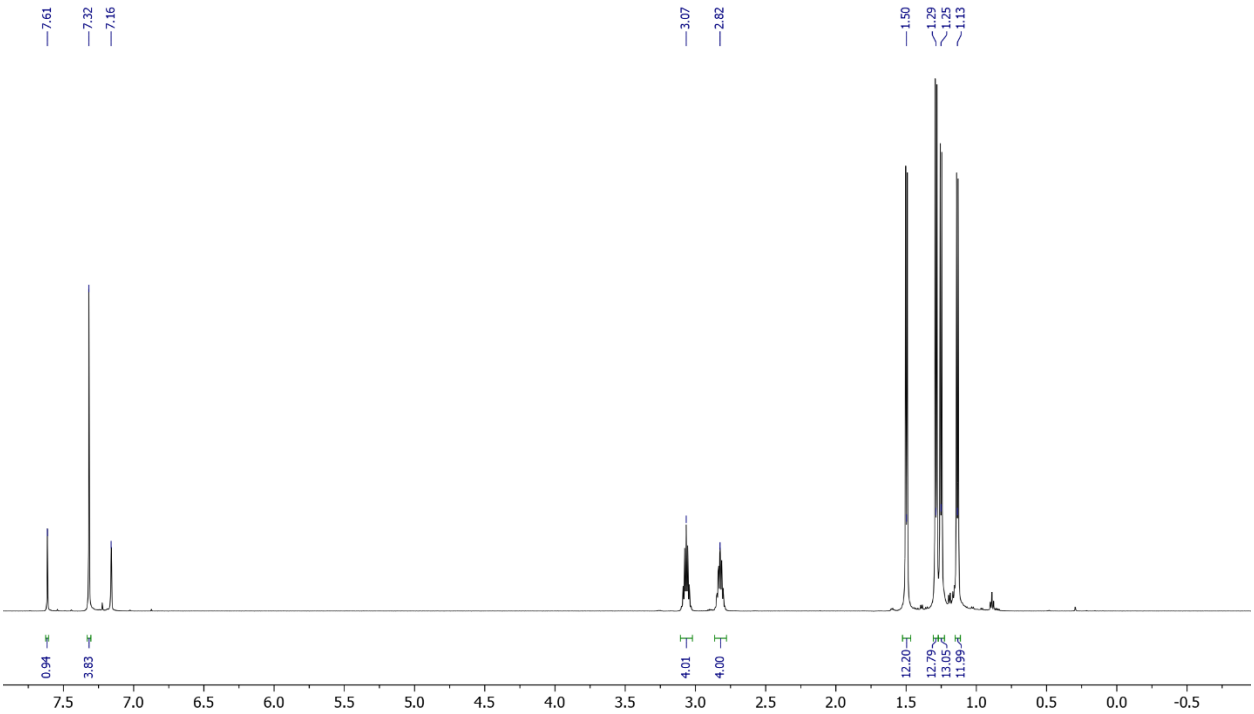


**Figure 5.S1.** $^{1}$H NMR spectrum of $AlI_2Ar^{iPr8}$ (**1**) in $C_6D_6$ at 298 K.

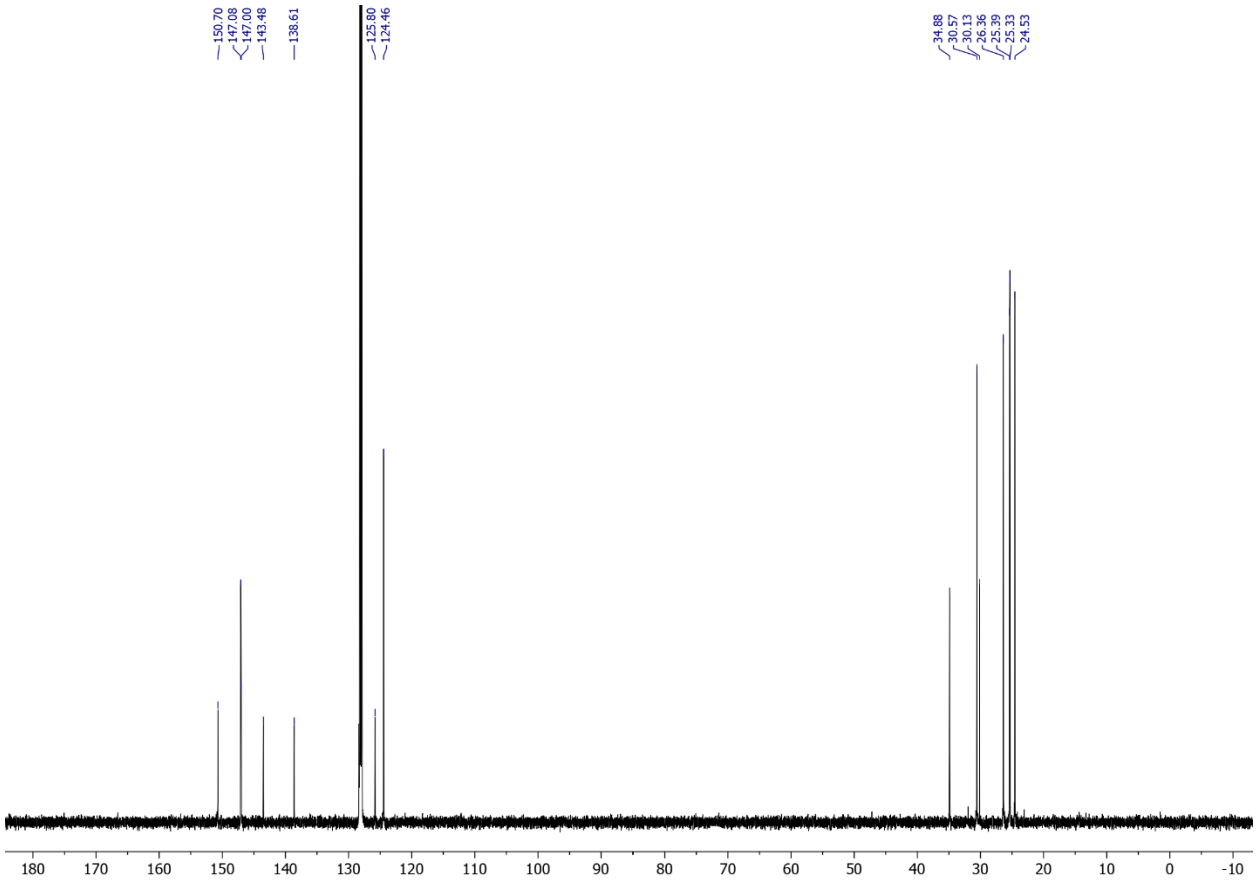


**Figure 5.S2.** $^{13}C\{^{1}H\}$ NMR spectrum of $AlI_2Ar^{iPr8}$ (**1**) in $C_6D_6$ at 298 K.

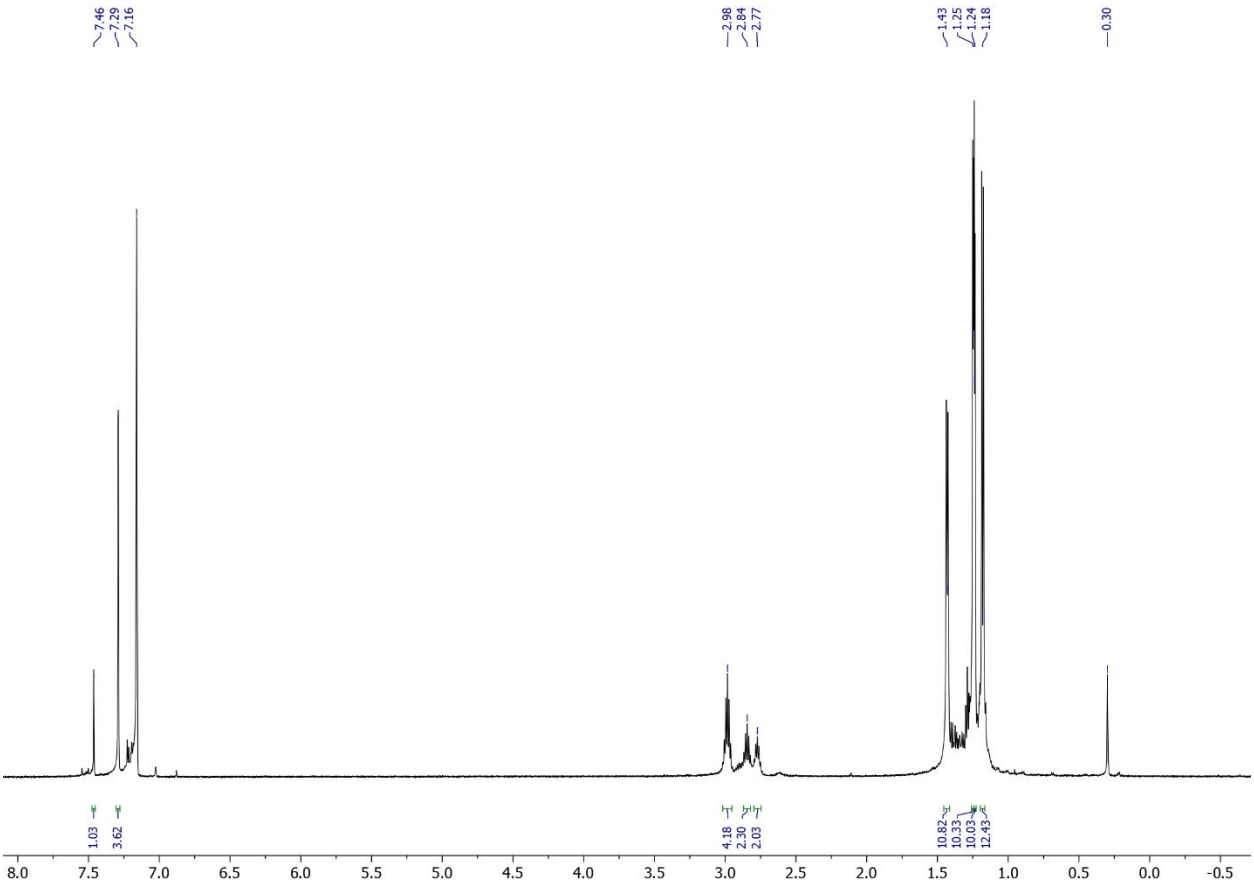


**Figure 5.S3.** $^{1}$H NMR spectrum of **:**AlAr$^{iPr8}$ (**2**) in $C_6D_6$ at 298 K.

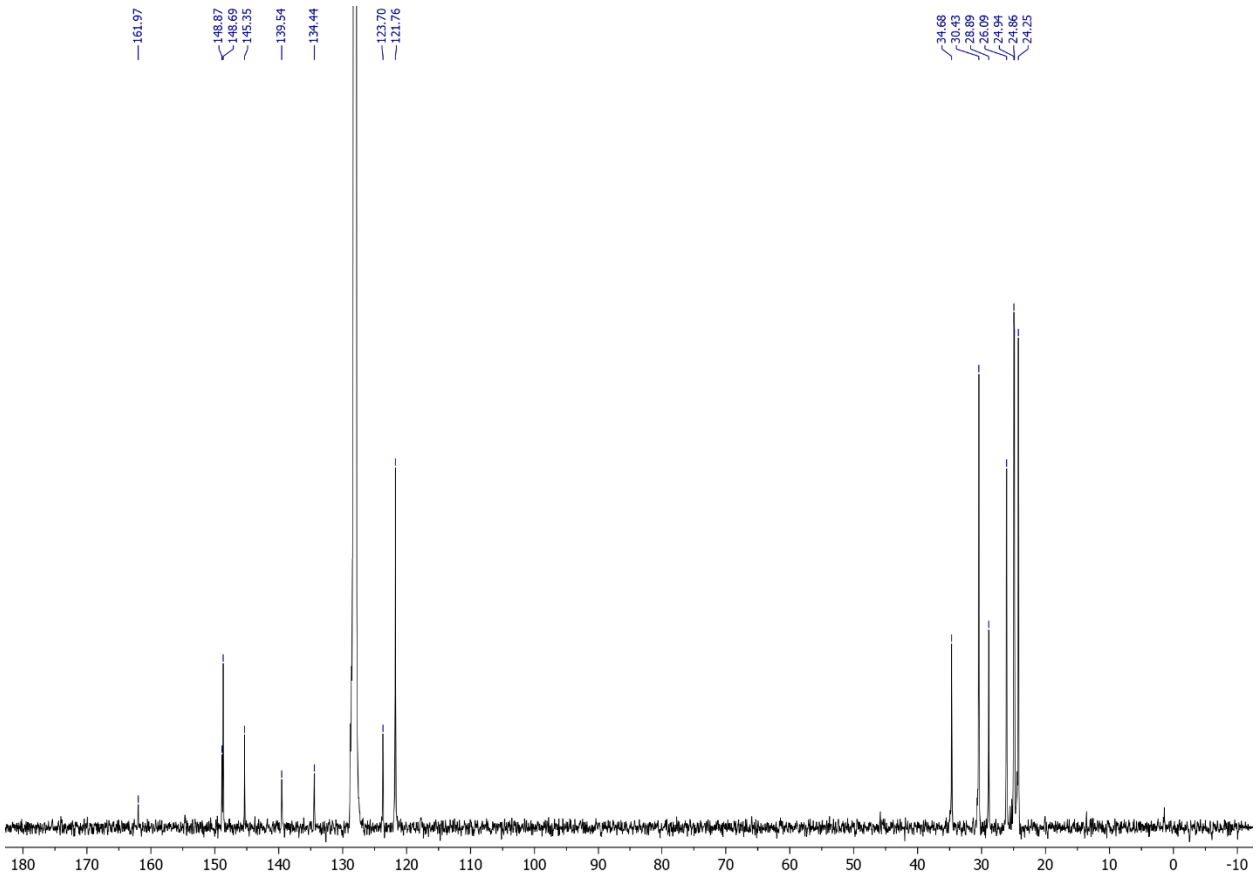


**Figure 5.S4.** $^{13}C\{^{1}H\}$ NMR spectrum of **:**AlAr$^{iPr8}$ **(2)** in $C_6D_6$ at 298 K.

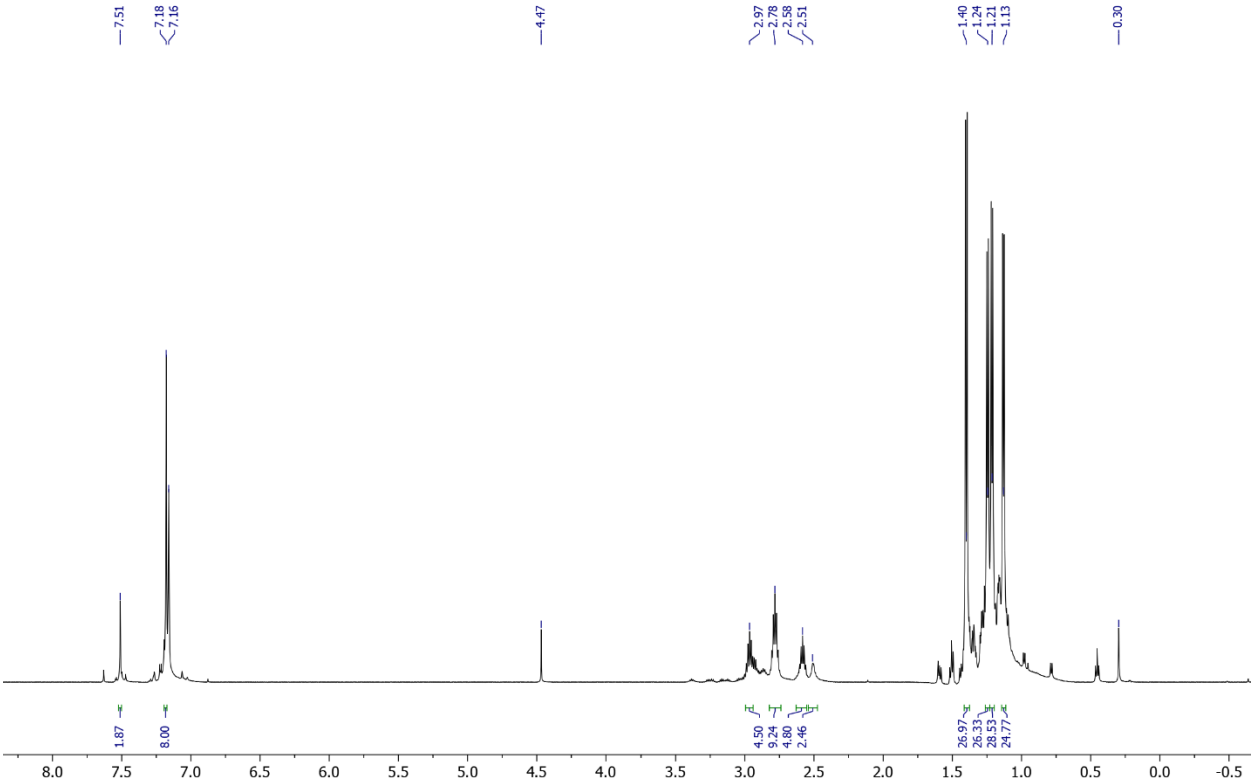


**Figure 5.S5.** $^{1}$H NMR spectrum of $\{Al(\mu\text{-}H)_2Ar^{iPr8}\}_2$ formed from the reaction of $:AlAr^{iPr8}$ (**2**) with $H_2$ in $C_6D_6$ at 298 K.

## UV-Visible Spectrum

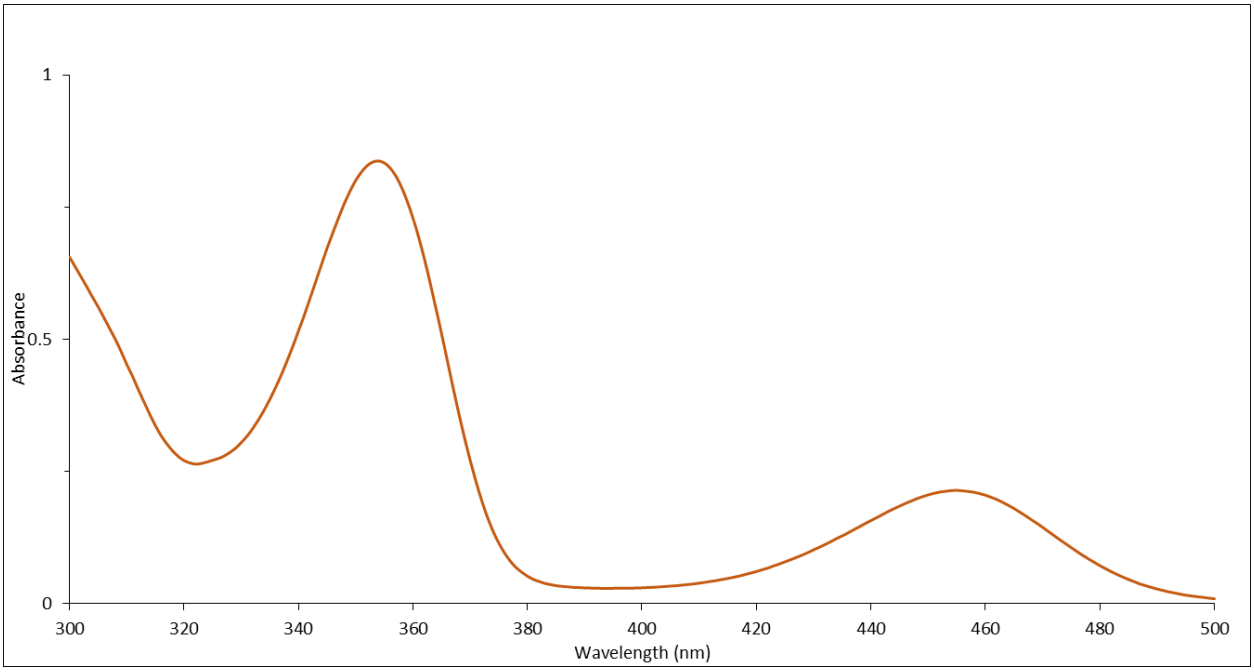


**Figure 5.S6.** UV-Visible spectrum of **:**AlAr$^{iPr8}$ (**2**), 295 μM in hexanes.

**X-Ray Crystallography**

**Compound 1:** Crystals of **1** were removed from a Schlenk flask under a stream of nitrogen and immediately covered with hydrocarbon oil. A suitable crystal was selected, attached to a MiTeGen microloop, and mounted on the goniometer of the diffractometer under a cold stream of $N_2$. Data were collected at 90 K on a Bruker Duo[S5]APEXII CCD system at –183°C (90K) using Cu Kα (λ = 1.54178) radiation. Data were integrated with SAINT[S5] and an absorption correction (multi-scan) was applied using SADABS.[S6] The structure was solved using SHELXTL[S7] program package by intrinsic phasing methods using SHELXT[S8] and was refined by full matrix least-squares procedures using SHELXL.[S9] All non-H atoms were refined anisotropically. Solvent accessible voids in the crystal structure (V = 108 $Å^3$) were treated with the SQUEEZE algorithm.[S10]

**Compound 2:** A yellow block with approximate dimensions 0.379 x 0.220 x 0.164$mm^3$ was placed and optically centered on a Bruker Duo[S5] APEXII CCD system at –183°C (90K). Indexing of the unit cell used a random set of reflections collected from three series of 0.5° wide ω-scans, 10 seconds per frame, and 30 frames per series that were well distributed in reciprocal space. Four ω-scan data frame series were collected [$MoK_\alpha$] with 0.3° wide scans, 20 seconds per frame and 606 frames collected per series at varying φ angles (φ=0°, 90°, 180°, 270°). The crystal to detector distance was 5.15cm, thus providing a complete sphere of data to $2\theta_{max}$=54.99°.

All crystallographic calculations were performed on an Intel Xeon E5-1620v2 at 3.70GHz with eight core processor and 16GB of extended memory. Cellnow[S11] determined the twin relationship between the two components, a rotation of 179.9° about the real axis 0 0 1 produced the transformation matrix -1 0 -0.5 0 1 0 0 0 1, generated the orientation matrices for the components and output a useable multiple matrices input file for the integration program SAINT[S5]. Saint was run three times using the output optimized merged matrix file from the

previous run. Data collected were now corrected for absorption using TWINABS[S12,S13] and Blessing's method and merged generating both single component HKLF4 and multi-component HKLF5 files. The SHELXTL[S7] program package was now implemented to determine, based upon systematic absences and intensity statistics, the non-centrosymmetric monoclinic space group Pc (no. 7). The structure was determined by direct methods with a majority of the non-hydrogen atoms being located for the two unique molecules of interest directly using the program XT[S8]. Refinement of the structure was achieved using the program XL[S9]. The two molecules refined well along with the six benzene solvent molecules being refined as perfect hexagons (AFIX66) The HKLF5, the 2 component twin data file contained 23587 unique data was chosen for the final refinement cycles. All non-hydrogen atoms were refined anisotropically. Hydrogen atoms were idealized. The final structure was refined to convergence with R(F)=7.47%, wR($F^2$)=11.29%, GOF=1.003 for all 23587 unique reflections [R(F)=4.79, wR($F^2$)=9.98% for those 17285 data with Fo > 4σ(Fo)]. The final difference-Fourier map was featureless indicating that the structure is both correct and complete

**Table 5.S1.** Selected X-ray crystallographic data for compounds **1** and **2**

| **Compound** | **1+[solvent]** | **2·($C_6H_6$)$_3$** |
|---|---|---|
| **Formula** | $C_{42}H_{61}AlI_2$ | $C_{60}H_{79}Al$ |
| **Formula Weight (g mol$^{-1}$)** | 846.68 | 827.21 |
| **T (K) / λ (Å)** | 90(2) | 90(2) |
| **Crystal System** | Trigonal | Monoclinic |
| **Space Group** | R-3 | Pc |
| **Z** | 18 | 4 |
| **Crystal color and habit** | Colorless plate | Yellow block |
| **a (Å)** | 28.5955(5) | 14.0683(8) |
| **b (Å)** | 28.5955(5) | 21.4815(13) |
| **c (Å)** | 25.8675(5) | 17.9802(11) |
| **α (°)** | 90 | 90 |
| **β (°)** | 90 | 108.6180(10) |
| **γ (°)** | 120 | 90 |
| **V (Å$^3$)** | 18318.1(8) | 5149.4(5) |
| **ρ (mg mm$^{-3}$)** | 1.382 | 1.067 |
| **Abs. coeff (mm$^{-1}$)** | 12.522 | 0.075 |
| **F(000)** | 7776 | 1808 |
| **Crystal size (mm)** | 0.149 × 0.109 × 0.042 | 0.379 × 0.220 × 0.164 |
| **2*θ* range (°)** | 4.94 to 144.272 | 1.798 to 27.513 |
| **Reflns collected** | 28384 | 23587 |
| **Ind. Reflns.** | 7912 | 23587 |
| **Obs. reflns ($I$>2σ($I$))** | 7672 | 17285 |
| **Completeness** | 100 | 99.9 |
| **Goodness-of-fit on $F^2$** | 1.201 | 1.003 |
| **Final R ($I$>2σ($I$))** | 0.0570 | 0.0479 |
| **wR2** | 0.1532 | 0.0998 |
| **R (all data)** | 0.0581 | 0.0747 |
| **wR2** | 0.1539 | 0.1129 |

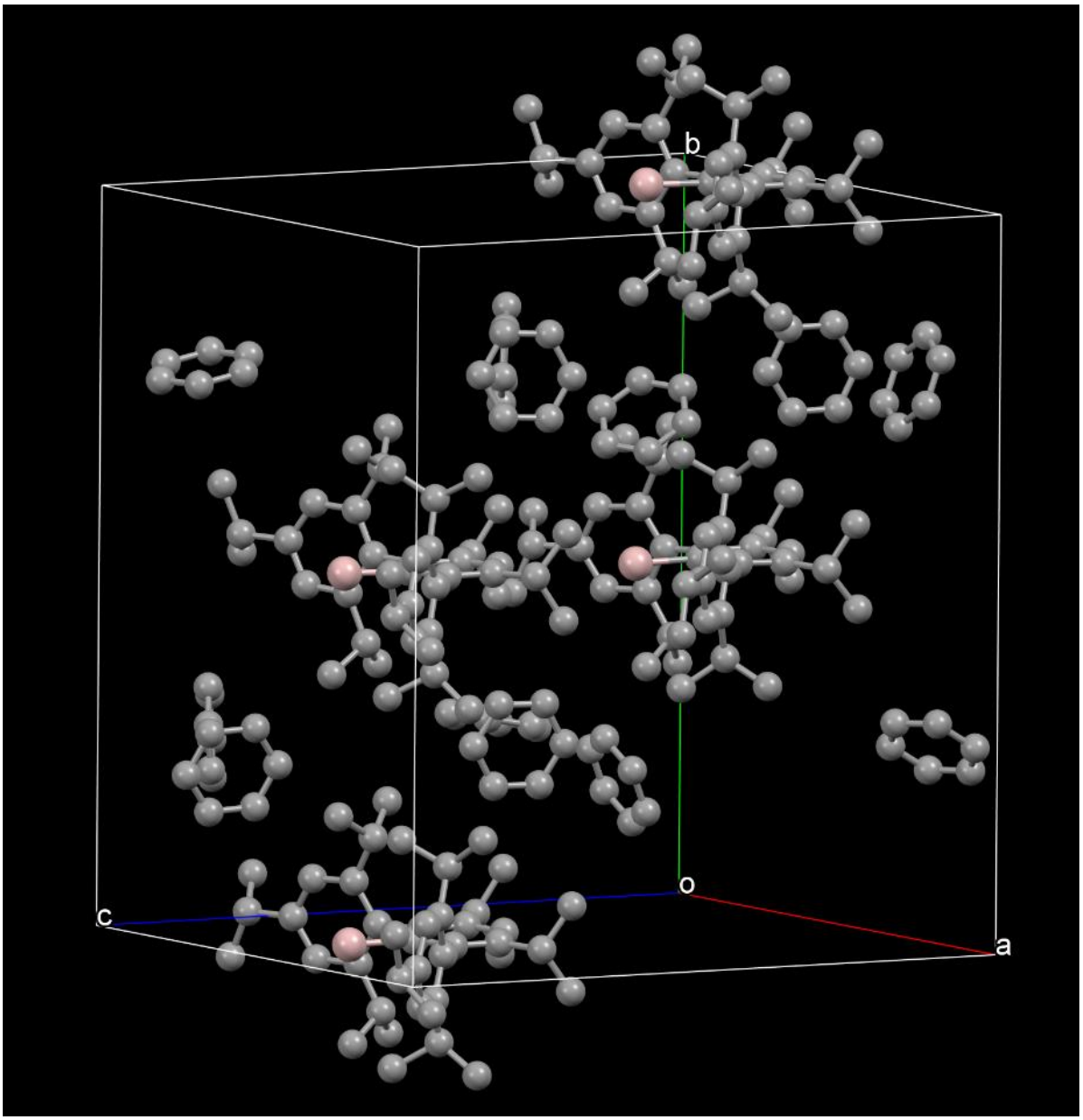


**Figure 5.S7.** Unit cell packing of **2**·$(C_6H_6)_3$

## Computational Details

Geometries of :AlAr$^{iPr8}$ (**2**) and Ar$^{iPr8}$AlAlAr$^{iPr8}$ were optimized in the gas phase with dispersion corrected density functional theory, namely the PBE1PBE functional,[S14-S17] def2-TZVP basis sets[S18] and Grimme's D3 correction with Becke-Johnson damping,[S19,S20] using the Gaussian 16-C.01 program suite.[S21] The structures were confirmed to be minima on the potential energy hypersurface via calculation of the associated vibrational frequencies (all positive). Compliance constants,[S22,S23] Quantum Theory of Atoms in Molecules bond paths and bond critical points,[S24] and second-order perturbative estimates of donor-acceptor interactions in Natural Bond Orbital basis,[S25] as descriptors of non-covalent C···Al and H···Al interaction strengths, were calculated for **2** using programs Compliance 3.0.2, AIMAll 19.10.12, and NBO 7.0.5.[S26-S28] Vertical excitation energies and associated oscillator strengths were calculated for **2** with the time-dependent density functional theory as implemented in the Gaussian 16-C.01 program package.[S29] The same functional-basis set combination was used as with prior geometry optimizations.

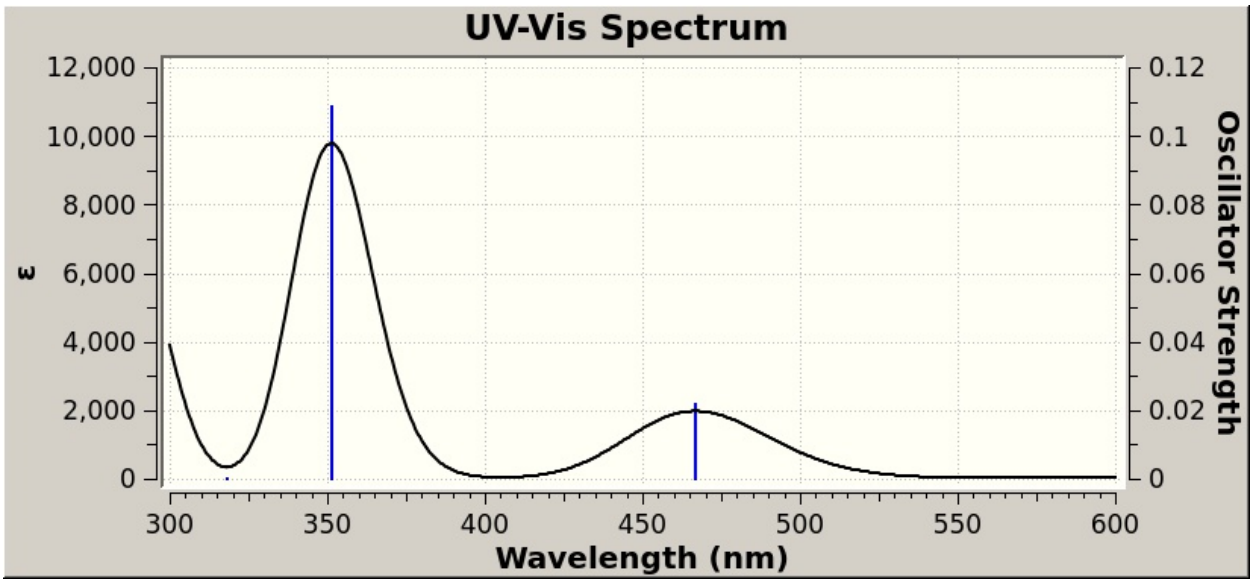


**Figure 5.S8.** Calculated UV-Visible spectrum of **:**AlAr$^{iPr8}$ (**2**).

**Table 5.S2.** xyz-Coordinates of $AlAr^{iPr8}$ (**2**)

104
$AlAr^{iPr8}$ (**2**)

| | | | |
|---|---|---|---|
| C | -3.056044 | -0.433751 | -1.076284 |
| C | -2.458510 | 0.040500 | 0.104559 |
| C | -2.990897 | -0.339011 | 1.346559 |
| C | -4.086922 | -1.194198 | 1.382500 |
| C | -4.680026 | -1.682319 | 0.229326 |
| C | -4.150894 | -1.283704 | -0.990042 |
| C | -1.210590 | 0.864271 | 0.043563 |
| C | 0.000034 | 0.159286 | 0.000035 |
| C | 1.210593 | 0.864392 | -0.043542 |
| C | 1.223455 | 2.261730 | -0.037175 |
| C | -0.000091 | 2.921255 | -0.000040 |
| C | -1.223573 | 2.261605 | 0.037118 |
| C | 2.458557 | 0.040677 | -0.104527 |
| C | 2.990963 | -0.338818 | -1.346535 |
| C | 4.086958 | -1.194038 | -1.382479 |
| C | 4.680027 | -1.682219 | -0.229307 |
| C | 4.150893 | -1.283617 | 0.990060 |
| C | 3.056067 | -0.433628 | 1.076311 |
| C | 2.391563 | 0.143912 | -2.648428 |
| C | 3.426216 | 0.840258 | -3.526938 |
| C | 2.544897 | -0.036279 | 2.443375 |
| C | 3.603418 | 0.735846 | 3.226023 |
| C | 5.855457 | -2.624953 | -0.301903 |
| C | 7.091949 | -2.038199 | 0.371429 |
| Al | 0.000509 | -1.864141 | -0.000063 |
| C | -2.505037 | 3.060519 | 0.070203 |
| C | -2.597677 | 3.919054 | 1.328413 |
| C | 2.504840 | 3.060768 | -0.070257 |
| C | 2.655419 | 3.924914 | 1.178490 |
| C | -2.391432 | 0.143644 | 2.648446 |
| C | -3.426044 | 0.839779 | 3.527163 |
| C | -5.855608 | -2.624870 | 0.301868 |
| C | -7.092172 | -2.037432 | -0.370749 |
| C | -2.544801 | -0.036454 | -2.443336 |
| C | -3.603297 | 0.735527 | -3.226158 |
| C | -1.728744 | -1.003742 | 3.402588 |
| C | -2.071503 | -1.249830 | -3.236094 |
| C | -5.508081 | -3.989771 | -0.285028 |
| C | 2.597335 | 3.919486 | -1.328352 |
| C | -2.655645 | 3.924795 | -1.178447 |
| C | 2.071780 | -1.249618 | 3.236300 |
| C | 5.507356 | -3.990053 | 0.284204 |
| C | 1.729071 | -1.003436 | -3.402793 |
| H | -0.000150 | 4.007361 | -0.000062 |
| H | 4.601627 | -1.649108 | 1.907178 |
| H | 4.491983 | -1.496874 | -2.343394 |
| H | 1.686242 | 0.623475 | 2.295425 |
| H | 1.326777 | -1.826219 | 2.680825 |
| H | 1.625578 | -0.943467 | 4.185654 |
| H | 2.902384 | -1.925067 | 3.457375 |
| H | 4.466039 | 0.102850 | 3.450435 |
| H | 3.196249 | 1.091828 | 4.176091 |
| H | 3.964615 | 1.598371 | 2.663158 |
| H | 6.086636 | -2.765009 | -1.363868 |
| H | 5.278872 | -3.910196 | 1.350393 |
| H | 6.344739 | -4.683904 | 0.173614 |
| H | 4.634499 | -4.420894 | -0.210414 |
| H | 7.357230 | -1.071861 | -0.062534 |
| H | 7.946885 | -2.710511 | 0.262726 |
| H | 6.921816 | -1.887977 | 1.440887 |
| H | 1.614281 | 0.871470 | -2.401996 |
| H | 2.463372 | -1.761135 | -3.688742 |
| H | 1.241255 | -0.642648 | -4.311981 |
| H | 0.973154 | -1.499090 | -2.788181 |
| H | 3.928690 | 1.646072 | -2.988519 |
| H | 2.949752 | 1.265833 | -4.413978 |
| H | 4.193661 | 0.141308 | -3.869057 |
| H | -4.601669 | -1.649145 | -1.907162 |
| H | -4.491942 | -1.497051 | 2.343412 |
| H | -1.686212 | 0.623383 | -2.295364 |
| H | -1.326485 | -1.826294 | -2.680494 |
| H | -1.625260 | -0.943751 | -4.185454 |
| H | -2.902025 | -1.925393 | -3.457139 |
| H | -4.465864 | 0.102467 | -3.450594 |
| H | -3.196061 | 1.091438 | -4.176224 |
| H | -3.964588 | 1.598091 | -2.663411 |
| H | -6.086459 | -2.765391 | 1.363842 |
| H | -5.280020 | -3.909495 | -1.351275 |
| H | -6.345590 | -4.683467 | -0.174423 |
| H | -4.635131 | -4.421059 | 0.209038 |
| H | -7.357105 | -1.071299 | 0.063884 |
| H | -7.947237 | -2.709612 | -0.262228 |
| H | -6.922276 | -1.886572 | -1.440157 |
| H | -1.614252 | 0.871314 | 2.402021 |
| H | -2.462951 | -1.761538 | 3.688521 |
| H | -1.240847 | -0.643031 | 4.311763 |
| H | -0.972862 | -1.499244 | 2.787814 |
| H | -3.928608 | 1.645660 | 2.988927 |
| H | -2.949518 | 1.265230 | 4.414229 |
| H | -4.193426 | 0.140741 | 3.869243 |
| H | 3.332512 | 2.345028 | -0.088217 |
| H | 2.486787 | 3.317416 | -2.231659 |
| H | 3.560819 | 4.433862 | -1.375692 |
| H | 1.813229 | 4.681483 | -1.340000 |
| H | 1.877137 | 4.691805 | 1.219858 |
| H | 3.622997 | 4.433722 | 1.182563 |
| H | 2.578678 | 3.327489 | 2.088528 |
| H | -3.332639 | 2.344697 | 0.088037 |
| H | -1.877453 | 4.691783 | -1.219700 |
| H | -3.623281 | 4.433492 | -1.182505 |
| H | -2.578800 | 3.327477 | -2.088548 |
| H | -2.487188 | 3.316849 | 2.231639 |
| H | -3.561183 | 4.433390 | 1.375747 |
| H | -1.813592 | 4.681070 | 1.340244 |

**Table 5.S3.** xyz-Coordinates of $Ar^{iPr8}AlAlAr^{iPr8}$

208

$Ar^{iPr8}AlAlAr^{iPr8}$

| | | | |
|---|---|---|---|
| C | 2.222400 | 3.232300 | -1.087000 |
| C | 2.553500 | 2.017300 | -1.708700 |
| C | 1.995000 | 1.709000 | -2.958000 |
| C | 1.137900 | 2.620900 | -3.565300 |
| C | 0.813000 | 3.831400 | -2.974700 |
| C | 1.355200 | 4.106700 | -1.727100 |
| C | 3.500900 | 1.075400 | -1.040100 |
| C | 3.008800 | 0.141900 | -0.112500 |
| C | 3.906900 | -0.749600 | 0.503300 |
| C | 5.278200 | -0.696400 | 0.243600 |
| C | 5.723500 | 0.247800 | -0.669800 |
| C | 4.871600 | 1.124000 | -1.330900 |
| C | 3.324900 | -1.797000 | 1.398100 |
| C | 2.863600 | -2.995800 | 0.826200 |
| C | 2.273500 | -3.948700 | 1.647300 |
| C | 2.132300 | -3.759300 | 3.014300 |
| C | 2.601500 | -2.573200 | 3.561400 |
| C | 3.199100 | -1.590400 | 2.782900 |
| C | 2.989700 | -3.242800 | -0.662000 |
| C | 1.707100 | -2.865200 | -1.393100 |
| C | 3.724100 | -0.335300 | 3.445500 |
| C | 2.611600 | 0.463700 | 4.116100 |
| C | 1.537400 | -4.843900 | 3.878700 |
| C | 0.383000 | -4.342300 | 4.736800 |
| Al | 1.146700 | -0.008600 | 0.643700 |
| Al | -1.193400 | 0.238200 | -0.639400 |
| C | -3.029700 | -0.081400 | 0.110400 |
| C | -3.788000 | -1.029100 | -0.599700 |
| C | -5.152300 | -1.195100 | -0.350600 |
| C | -5.728900 | -0.406000 | 0.634700 |
| C | -5.013700 | 0.523900 | 1.379300 |
| C | -3.650100 | 0.689700 | 1.107200 |
| C | 5.462300 | 2.119400 | -2.304400 |
| C | 6.216000 | 3.219800 | -1.561600 |
| C | 6.261700 | -1.637100 | 0.900500 |
| C | 7.389500 | -0.883700 | 1.598300 |
| C | -3.054400 | -1.870300 | -1.595900 |
| C | -2.890600 | -1.441300 | -2.927100 |
| C | -2.128700 | -2.211300 | -3.794400 |
| C | -1.541200 | -3.408400 | -3.404800 |
| C | -1.731600 | -3.825100 | -2.096300 |
| C | -2.473800 | -3.080600 | -1.184200 |
| C | -6.001500 | -2.193800 | -1.102000 |
| C | -6.500500 | -3.305300 | -0.182600 |
| C | -5.743300 | 1.333300 | 2.426900 |
| C | -6.463300 | 0.444100 | 3.436900 |
| C | -2.819300 | 1.676600 | 1.863400 |
| C | -2.623300 | 2.973800 | 1.357300 |
| C | -1.823900 | 3.863000 | 2.063800 |
| C | -1.219900 | 3.524000 | 3.266700 |
| C | -1.425900 | 2.242700 | 3.750700 |
| C | -2.215400 | 1.315700 | 3.078500 |
| C | -3.588000 | -0.205800 | -3.454800 |
| C | -2.623900 | 0.806200 | -4.060600 |
| C | -0.761300 | -4.213600 | -4.420700 |
| C | 0.026100 | -5.372200 | -3.830400 |
| C | -2.640600 | -3.587700 | 0.231800 |
| C | -1.378200 | -3.365300 | 1.056500 |
| C | -3.294000 | 3.446400 | 0.085000 |
| C | -4.120100 | 4.708700 | 0.322100 |
| C | -0.428800 | 4.565400 | 4.023000 |
| C | -1.377600 | 5.523300 | 4.743300 |
| C | -2.441600 | -0.035100 | 3.721500 |
| C | -3.180800 | 0.119000 | 5.050000 |
| C | 2.325300 | 0.427600 | -3.693000 |
| C | 1.076800 | -0.385100 | -4.017700 |
| C | -0.032600 | 4.876900 | -3.662400 |
| C | -1.044900 | 4.308400 | -4.643900 |
| C | 2.785000 | 3.606400 | 0.266800 |
| C | 1.743500 | 3.412600 | 1.359700 |
| C | -7.176400 | -1.517000 | -1.802200 |
| C | -6.733300 | 2.297800 | 1.778400 |
| C | -4.655200 | -0.596600 | -4.475300 |
| C | -1.690500 | -4.721900 | -5.522900 |
| C | -3.055900 | -5.054500 | 0.278800 |
| C | -2.285400 | 3.689700 | -1.030000 |
| C | 0.582200 | 3.985100 | 4.999500 |
| C | -1.142400 | -0.801200 | 3.939800 |
| C | 6.376300 | 1.456200 | -3.330300 |
| C | 6.823400 | -2.639900 | -0.103700 |
| C | 3.104500 | 0.716700 | -4.974300 |
| C | 0.868100 | 5.900700 | -4.353200 |
| C | 3.314800 | 5.036900 | 0.310900 |
| C | 4.827700 | -0.663100 | 4.447500 |
| C | 2.615000 | -5.496100 | 4.741700 |
| C | 3.389000 | -4.674600 | -0.998600 |
| H | -6.788900 | -0.523400 | 0.837000 |
| H | -1.991200 | -1.869400 | -4.815700 |
| H | -1.291600 | -4.758400 | -1.767500 |
| H | -4.088200 | 0.273400 | -2.608800 |
| H | -1.847500 | 1.096900 | -3.346600 |
| H | -3.164700 | 1.704100 | -4.369800 |
| H | -2.123500 | 0.401100 | -4.944400 |
| H | -4.196400 | -1.027400 | -5.369300 |
| H | -5.231600 | 0.279500 | -4.784500 |
| H | -5.346700 | -1.336500 | -4.069500 |
| H | -0.045200 | -3.522300 | -4.883900 |
| H | 0.702600 | -5.047800 | -3.038000 |
| H | 0.624000 | -5.852400 | -4.608100 |
| H | -0.641100 | -6.133900 | -3.416800 |

| | | | |
|---|---|---|---|
| H | -2.426100 | -5.416000 | -5.106900 |
| H | -1.124000 | -5.249000 | -6.295000 |
| H | -2.236500 | -3.905700 | -5.998900 |
| H | -3.436800 | -2.999700 | 0.694000 |
| H | -0.538400 | -3.938800 | 0.657300 |
| H | -1.534500 | -3.681100 | 2.091000 |
| H | -1.084500 | -2.312700 | 1.072400 |
| H | -3.933300 | -5.244200 | -0.342800 |
| H | -3.293200 | -5.346100 | 1.305100 |
| H | -2.254200 | -5.711700 | -0.067800 |
| H | -1.675500 | 4.865400 | 1.671500 |
| H | -0.966500 | 1.947200 | 4.686700 |
| H | -3.973100 | 2.654700 | -0.241900 |
| H | -4.805500 | 4.589200 | 1.162700 |
| H | -4.705500 | 4.954400 | -0.567800 |
| H | -3.478100 | 5.566200 | 0.539500 |
| H | -1.565800 | 4.461500 | -0.745000 |
| H | -2.788300 | 4.014400 | -1.944700 |
| H | -1.705700 | 2.790600 | -1.269500 |
| H | 0.123500 | 5.147800 | 3.275700 |
| H | -2.079200 | 5.985800 | 4.046300 |
| H | -0.820900 | 6.317300 | 5.248500 |
| H | -1.961300 | 4.985000 | 5.495100 |
| H | 0.087000 | 3.492100 | 5.840500 |
| H | 1.206400 | 4.780200 | 5.413700 |
| H | 1.233700 | 3.252600 | 4.519200 |
| H | -3.069100 | -0.622300 | 3.046400 |
| H | -2.549100 | 0.621600 | 5.787400 |
| H | -3.449200 | -0.860000 | 5.456400 |
| H | -4.092600 | 0.707400 | 4.941700 |
| H | -0.581600 | -0.920200 | 3.010700 |
| H | -1.352500 | -1.791100 | 4.351600 |
| H | -0.494500 | -0.280900 | 4.650500 |
| H | -5.367200 | -2.650900 | -1.867600 |
| H | -5.673700 | -3.813500 | 0.315600 |
| H | -7.068100 | -4.049600 | -0.747600 |
| H | -7.157400 | -2.901600 | 0.592700 |
| H | -7.882900 | -1.105800 | -1.076300 |
| H | -7.721000 | -2.234500 | -2.421700 |
| H | -6.843300 | -0.696700 | -2.440200 |
| H | -4.996500 | 1.925900 | 2.962900 |
| H | -7.291500 | -0.093700 | 2.967900 |
| H | -6.881500 | 1.045300 | 4.248600 |
| H | -5.791300 | -0.297300 | 3.871200 |
| H | -6.244600 | 2.937900 | 1.043100 |
| H | -7.203800 | 2.936100 | 2.531200 |
| H | -7.526100 | 1.748300 | 1.262900 |
| H | 6.786100 | 0.299900 | -0.884700 |
| H | 0.719600 | 2.372300 | -4.533900 |
| H | 1.101400 | 5.047800 | -1.248100 |
| H | 2.958900 | -0.174900 | -3.036800 |
| H | 0.473300 | -0.569100 | -3.127200 |
| H | 1.352100 | -1.347700 | -4.457600 |
| H | 0.444200 | 0.138100 | -4.739500 |
| H | 2.482400 | 1.263000 | -5.688600 |
| H | 3.419700 | -0.215000 | -5.452400 |
| H | 3.992300 | 1.319600 | -4.781800 |
| H | -0.587700 | 5.401800 | -2.876200 |
| H | -0.553700 | 3.860700 | -5.512000 |
| H | -1.696900 | 5.102100 | -5.016400 |
| H | -1.667000 | 3.542900 | -4.178700 |
| H | 1.568500 | 6.351800 | -3.647300 |
| H | 0.274900 | 6.698800 | -4.808100 |
| H | 1.453500 | 5.419700 | -5.141800 |
| H | 3.619800 | 2.931700 | 0.473900 |
| H | 0.862200 | 4.029900 | 1.174500 |
| H | 2.149300 | 3.672600 | 2.340400 |
| H | 1.387500 | 2.376200 | 1.421800 |
| H | 4.003000 | 5.238000 | -0.512100 |
| H | 3.842300 | 5.215800 | 1.251400 |
| H | 2.503800 | 5.767000 | 0.249900 |
| H | 2.505900 | -2.407300 | 4.629600 |
| H | 1.917800 | -4.878300 | 1.215100 |
| H | 4.157000 | 0.290500 | 2.660500 |
| H | 1.813900 | 0.709700 | 3.408800 |
| H | 3.006200 | 1.395400 | 4.529900 |
| H | 2.157800 | -0.101000 | 4.935100 |
| H | 4.437300 | -1.249800 | 5.283300 |
| H | 5.257700 | 0.254300 | 4.858000 |
| H | 5.630600 | -1.239200 | 3.984200 |
| H | 1.142200 | -5.609100 | 3.201000 |
| H | 0.716100 | -3.580200 | 5.445900 |
| H | -0.051400 | -5.163000 | 5.313200 |
| H | -0.401400 | -3.900900 | 4.120900 |
| H | 3.429400 | -5.886400 | 4.127800 |
| H | 2.198500 | -6.320200 | 5.326700 |
| H | 3.042300 | -4.770700 | 5.439500 |
| H | 3.778500 | -2.582500 | -1.031500 |
| H | 0.858400 | -3.452800 | -1.040500 |
| H | 1.809200 | -3.026100 | -2.469000 |
| H | 1.461300 | -1.807800 | -1.257200 |
| H | 4.280500 | -4.982900 | -0.448100 |
| H | 3.599500 | -4.762500 | -2.067300 |
| H | 2.591200 | -5.385200 | -0.767700 |
| H | 4.631500 | 2.586900 | -2.839400 |
| H | 5.574700 | 3.721400 | -0.836300 |
| H | 6.595800 | 3.970300 | -2.260000 |
| H | 7.068900 | 2.803100 | -1.018200 |
| H | 7.290300 | 1.078200 | -2.864800 |
| H | 6.676200 | 2.176600 | -4.095900 |
| H | 5.884700 | 0.616600 | -3.824500 |
| H | 5.713700 | -2.201700 | 1.660400 |
| H | 8.018700 | -0.353300 | 0.878800 |
| H | 8.031900 | -1.577300 | 2.147200 |

| | | | |
|---|---|---|---|
| H | 6.999400 | -0.147600 | 2.303900 |
| H | 6.027100 | -3.218300 | -0.575500 |
| H | 7.506600 | -3.338400 | 0.386700 |
| H | 7.376900 | -2.127800 | -0.895800 |

## Photos of Compounds

**Figure 5.S9**. Crystals (left) and solution in $C_6D_6$ (right) of :AlAr$^{iPr8}$ (**2**).

## References


(S1) Pangborn, A. B.; Giardello, M. A.; Grubbs, R. H.; Rosen, R. K.; Timmers, F. J. Safe and Convenient Procedure for Solvent Purification. *Organometallics* **1996**, *15*, 1518–1520.

(S2) Fulmer, G. R.; Miller, A. J. M.; Sherden, N. H.; Gottlieb, H. E.; Nudelman, A.; Stoltz, B. M.; Bercaw, J. E.; Goldberg, K. I. NMR Chemical Shifts of Trace Impurities: Common Laboratory Solvents, Organics, and Gases in Deuterated Solvents Relevant to the Organometallic Chemist. *Organometallics* **2010**, *29*, 2176–2179.

(S3) Melton, C. E.; Dube, J. W.; Ragogna, P. J.; Fettinger, J. C.; Power, P. P. Synthesis and Characterization of Primary Aluminum Parent Amides and Phosphides. *Organometallics* **2014**, *33*, 329–337.

(S4) Hicks, J.; Juckel, M.; Paparo, A.; Dange, D.; Jones, C. Multigram Syntheses of Magnesium(I) Compounds Using Alkali Metal Halide Supported Alkali Metals as Dispersible Reducing Agents. *Organometallics* **2018**, *37*, 4810–4813.

(S5) Bruker (2013) APEXII (Version 2014.9-1) and (2016) SAINT (Version 8.37a). Bruker AXS Inc., Madison, Wisconsin, USA.

(S6) Sheldrick, G. M., (1996) SADABS. University of Göttingen, Germany.

(S7) Sheldrick, G.M., (2002). SHELXTL. Version 6.1. Siemens Analytical X-ray Instruments Inc., Madison, Wisconsin, USA.

(S8) Sheldrick, G. M., (2014). SHELXT. Universität Göttingen: Göttingen, Germany.

(S9) Sheldrick, G. M., (2015). SHELXL Universität Göttingen: Göttingen, Germany.

(S10) Spek, A. L. PLATON SQUEEZE: A Tool for the Calculation of the Disordered Solvent Contribution to the Calculated Structure Factors. *Acta Cryst.* **2015**, *C71*, 9-18.

(S11) Sheldrick, G.M., CELLNOW, Twin matrix determination program, Universität Göttingen: Göttingen, Germany, Version 2008/3.

(S12) Blessing, R. H. An Empirical Correction for Absorption Anisotropy. *Acta Cryst*. **1995**, *A51*, 33-38.

(S13) Sheldrick, G.M., TWINABS Version 2012/1‘An Empirical Correction for Absorption Anisotropy applied to Twinned crystals’. Universität Göttingen: Göttingen, Germany.

(S14) Perdew, J. P.; Burke, K.; Ernzerhof, M. Generalized Gradient Approximation Made Simple. *Phys. Rev. Lett.* **1996**, *77*, 3865–3868.

(S15) Perdew, J. P.; Burke, K.; Ernzerhof, M. Generalized Gradient Approximation Made Simple. *Phys. Rev. Lett.* **1996**, *78*, 1396–1396.

(S16) Adamo, C.; Barone, V. Toward Reliable Density Functional Methods without Adjustable Parameters: The PBE0 Model. *J. Chem. Phys.* **1999**, *110*, 6158–6170.

(S17) Ernzerhof, M.; Scuseria, G. E. Assessment of the Perdew-Burke-Ernzerhof Exchange-Correlation Functional. *J. Chem. Phys.* **1999**, *110*, 5029–5036.

(S18) Weigend, F.; Ahlrichs, R. Balanced Basis Sets of Split Valence, Triple Zeta Valence and Quadruple Zeta Valence Quality for H to Rn: Design and Assessment of Accuracy. *Phys. Chem. Chem. Phys.* **2005**, *7*, 3297–3305.

(S19) Grimme, S.; Antony, J.; Ehrlich, S.; Krieg, H. A Consistent and Accurate Ab Initio Parametrization of Density Functional Dispersion Correction (DFT-D) for the 94 Elements H-Pu. *J. Chem. Phys.* **2010**, *132*, 154104.

(S20) Grimme, S.; Ehrlich, S.; Goerigk, L. Effect of the Damping Function in Dispersion Corrected Density Functional Theory. *J. Comput. Chem.* **2011**, *32*, 1456–1465.

(S21) Gaussian 16, Revision C.01, Frisch, M. J.; Trucks, G. W.; Schlegel, H. B.; Scuseria, G. E.; Robb, M. A.; Cheeseman, J. R.; Scalmani, G.; Barone, V.; Petersson, G. A.; Nakatsuji, H.; Li, X.; Caricato, M.; Marenich, A. V.; Bloino, J.; Janesko, B. G.; Gomperts, R.; Mennucci, B.; Hratchian, H. P.; Ortiz, J. V.; Izmaylov, A. F.; Sonnenberg, J. L.; Williams-Young, D.; Ding, F.; Lipparini, F.; Egidi, F.; Goings, J.; Peng, B.; Petrone, A.; Henderson, T.; Ranasinghe, D.; Zakrzewski, V. G.; Gao, J.; Rega, N.; Zheng, G.; Liang, W.; Hada, M.; Ehara, M.; Toyota, K.; Fukuda, R.; Hasegawa, J.; Ishida, M.; Nakajima, T.; Honda, Y.; Kitao, O.; Nakai, H.; Vreven, T.; Throssell, K.; Montgomery, J. A., Jr.; Peralta, J. E.; Ogliaro, F.; Bearpark, M. J.; Heyd, J. J.; Brothers, E. N.; Kudin, K. N.; Staroverov, V. N.; Keith, T. A.; Kobayashi, R.; Normand, J.; Raghavachari, K.; Rendell, A. P.; Burant, J. C.; Iyengar, S. S.; Tomasi, J.; Cossi, M.; Millam, J. M.; Klene, M.; Adamo, C.; Cammi, R.; Ochterski, J. W.; Martin, R. L.; Morokuma, K.; Farkas, O.; Foresman, J. B.; Fox, D. J. Gaussian, Inc., Wallingford CT, 2016.

(S22) Brandhorst, K.; Grunenberg, J. Efficient Computation of Compliance Matrices in Redundant Internal Coordinates from Cartesian Hessians for Nonstationary Points. *J. Chem. Phys.* **2010**, *132*, 184101–184107.

(S23) Brandhorst, K.; Grunenberg, J. How strong is it? The Interpretation of Force and Compliance Constants as Bond Strength Descriptors. *Chem. Soc. Rev.* **2008**, *37*, 1558–1567.

(S24) Bader, R. F. W. Atoms in Molecules: A Quantum Theory, Oxford University Press, Oxford, 1990.

(S25) Foster, J. P.; Weinhold, F. Natural Hybrid Orbitals. *J. Am. Chem. Soc.* **1980**, *102*, 7211–7218.

(S26) Compliance, Version 3.0.2. Grunenberg, J.

(S27) AIMAll, Version 19.10.12, Keith, T. A. TK Gristmill Software, Overland Park KS 2019.

(S28) NBO 7.0. Glendening, E. D.; Badenhoop, J. K.; Reed, A. E.; Carpenter, J. E.; Bohmann, J. A.; Morales, C. M.; Karafiloglou, P.; Landis, C. R.; Weinhold, F. Theoretical Chemistry Institute, University of Wisconsin, Madison WI 2018.

(S29) Stratmann, R. E.; Scuseria, G. E.; Frisch, M. J. An efficient implementation of time-dependent density-functional theory for the calculation of excitation energies of large molecules *J. Chem. Phys.* **1998**, *109*, 8218–8224.

**Chapter 6. A Monomeric Aluminum Imide (Iminoalane) with Al-N Triple-Bonding: Bonding Analysis and Dispersion Energy Stabilization.**

Joshua D. Queen,[†] Sini Irvankoski,[‡] James C. Fettinger,[†] Heikki M. Tuononen,*[,‡] and Philip P. Power*[,†]

[†]Department of Chemistry, University of California, Davis, One Shields Avenue, Davis CA, USA, 95616.

[‡]Department of Chemistry, NanoScience Centre, University of Jyväskylä, P.O. Box 35, FI-40014 Jyväskylä, Finland



**Abstract.** Reaction of :AlAr$^{iPr8}$ (Ar$^{iPr8}$ = $C_6H$-2,6-($C_6H_2$-2,4,6-$^iPr_3)_2$-3,5-$^iPr_2$) with Ar$^{Me6}N_3$ (Ar$^{Me6}$ = $C_6H_3$-2,6-($C_6H_2$-2,4,6-$Me_3)_2$) in hexanes at ambient temperature gave the aluminum imide Ar$^{iPr8}$AlNAr$^{Me6}$ (**1**). Its crystal structure displayed short Al-N distances of 1.625(4) and 1.628(3) Å with linear (C-Al-N-C = 180°) or almost linear (C-Al-N = 172.4(2)°; Al-N-C = 172.5(3)°) geometries. DFT calculations confirm linear geometry with an Al-N distance of 1.635 Å. According to energy decomposition analysis, the Al-N bond has three orbital components totaling –1350 kJ mol$^{-1}$ and instantaneous interaction energy of –551 kJ mol$^{-1}$ with respect to :AlAr$^{iPr8}$ and Ar$^{Me6}$N̈:. Dispersion accounts for –89 kJ mol$^{-1}$, which is similar in strength to one Al-N π-interaction. The electronic spectrum has an intense transition at 290 nm which tails into the visible region. In the IR spectrum the Al-N stretching band is calculated to appear at ca. 1100 cm$^{-1}$. In contrast, reaction of AlAr$^{iPr8}$ with 1-Ad$N_3$ or $Me_3SiN_3$ gave transient imides that immediately

reacted with a second equivalent of the azide to give $Ar^{iPr8}Al[(NAd)_2N_2]$ (**2**) or $Ar^{iPr8}Al(N_3)\{N(SiMe_3)_2\}$ (**3**).

The chemistry of compounds with group 13 element-nitrogen bonding has been extensively studied.[1-9] Current interest is driven by their applications as precursors for group III-V materials,[10] $H_2$ storage media,[11-13] and an interest in M–N (M = Al–Tl) multiple bonding. Early work on the group 13 amine complexes showed they could be condensed at elevated temperature with release of RR′ (R,R′ = organic group or hydrogen); a common route to amide, imide, and nitride compounds[14] (Scheme 6.1).

$$\underset{\text{amine complex}}{R_3MNR'_3} \xrightarrow{-RR'} \underset{\text{amide}}{R_2MNR'_2} \xrightarrow{-RR'} \underset{\text{imide}}{RMNR'} \xrightarrow{-RR'} \underset{\text{nitride}}{MN}$$

**Scheme 6.1.** Stepwise condensation of group 13 amine complexes to nitrides.

The group 13 metal imides (also called N-iminometallanes) of formula $[RMNR']_n$ (R = alkyl, aryl, hydrogen, halide; R′ = alkyl, aryl, silyl, hydrogen; M = Al–In; n = 4–8) were first studied in detail by Cesari and coworkers in the 1960s and ’70s and several examples featuring cage structures with alternating metal and nitrogen vertices were structurally characterized.[15-19] Roesky and coworkers characterized the quasi-isomeric tetrameric amido-Al(I) compound $[AlN(Dipp)(SiMe_3)]_4$ (Dipp = 2,6-$^i$Pr$_2$-$C_6H_3$) with a tetrahedral $Al_4$ core and terminal amide groups.[20] The lower imido aggregates (n = 1–3) remain scarce but are especially interesting since M-N multiple bonding becomes possible. Thus the unique trimer $[Al(Me)N(Dipp)]_3$,[21] which is an Al analogue of borazine (i.e. an “alumazine”), features relatively short (ca. 1.78 Å) Al-N bonds. The planar $Al_3N_3$ ring has 6-π electrons but has little aromatic character as shown by its reaction chemistry.[22,23] Several dimeric, $[RAlNR']_2$ compounds with $Al_2N_2$ cores and short Al-N distances in the range 1.796-1.842 Å, which is slightly longer than that seen in the alumazine derivative, have also been reported.[24-29]

Monomeric RAlNR′ compounds remain unknown, which is probably a result of high association energies (cf. dimerization of HAlNH is exothermic by ca. 580 kJ $mol^{-1}$).[30] Their synthesis via hydrocarbon or dihydrogen elimination usually proceeds at elevated temperatures that often results in C-H activation of the ligands.[31] However an alternative synthesis by the reaction of organoazides with M(I) species at low temperatures avoids C-H activation. For example, Roesky and coworkers reported that the reaction of :AlCp* (Cp* = $\eta^5$-$C_5Me_5$), formed by dissociation of $(AlCp^*)_4$ at elevated temperature, with $R_3SiN_3$ (R = $^i$Pr, Ph, $^t$Bu), gave the imido dimers $\{Cp^*Al(\mu\text{-}NSiR_3)\}_2$.[26] Using the larger, chelated Al(I) β-diketiminate :Al$^{Dipp}$NacNac ($^{Dipp}$NacNac = $HC\{(CMe)(NDipp)\}_2$) gave the transient imides $^{Dipp}$NacNacAl=NR which reacted with a second equivalent of the azide to give cyclic $AlN_4$ products $^{Dipp}$NacNacAl$[(NR)_2N_2]$.[32,33] Attempts to stabilize the imide using more sterically demanding m-terphenyl azides failed to give an isolable aluminum imide, although this route did yield a corresponding Ga imide.[34] The Al imide underwent C-H activation of a methyl group on a flanking ring of the $^{Dipp}$NacNac ligand or C-C activation of the aryl ring of the nitrogen terphenyl ligand.[35]

Nonetheless, monomeric aluminum imides were obtained by coordinative blocking of the Al atoms. Cui and coworkers showed that addition of an NHC (N-heterocyclic carbene) to $:Al[HC\{(C^tBu)(NDipp)\}_2]$ resulted in insertion of the Al atom into the N-C bond of the β-diketiminate ligand.[36] This gave the four-coordinate terminal Al imide **I** (Figure 6.1) with a short (1.705(2) Å) Al-N bond. Recently the groups of Coles and Aldridge

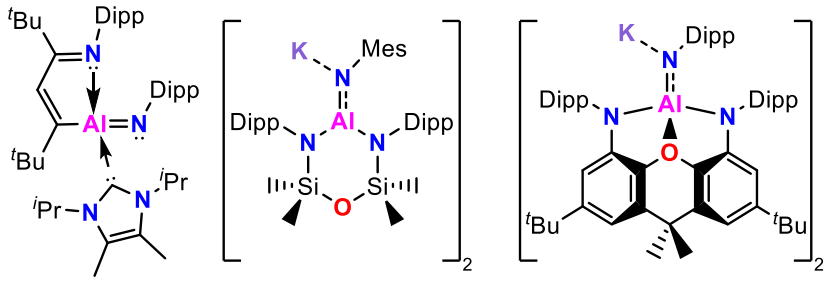


I II III

**Figure 6.1.** Structurally characterized terminal aluminum imides. Mes = 2,4,6-$Me_3C_6H_2$; Dipp = 2,6-$^iPr_2C_6H_3$.

separately reported that the reaction of anionic Al(I) aluminyls with organoazides gave terminal aluminum imides **II** and **III** (Figure 6.1) with Al-N distances of 1.7251(11) and 1.723(2) Å, supported by multidentate NON ligands that exist as dimers with bridging $K^+$ cations.[37,38] It was shown that the Al=N bonds reacted readily with small molecules such as CO and $CO_2$.[36-38]

No compounds of formula RAlNR′ in which Al and N are two-coordinate have been isolated and characterized. The reaction of laser-ablated Al atoms with $NH_3$ gas gave the planar trans-bent parent compound HAlNH as a minor product, identified by IR spectroscopy in a solid argon matrix.[39] *Ab initio* computations by Davy and Jaffrey found HAlNH to be "quasi-linear" with only a 0.2 kcal $mol^{-1}$ barrier between the linear and bent geometries and a short Al-N bond distance of 1.63 Å, which may be interpreted on the basis of Al-N triple bonding. Computations for HAlNH and MeAlNMe showed linear geometries with short (ca. 1.63-1.65Å) Al-N distances[11,30,40,41] and NBO analysis of MeAlNMe by Gilbert indicated that it had an Al-N triple bond composed of one σ- and 2 π-bonds.[42]

Previously, our group described the synthesis of gallium and indium imides with two-coordination at both the group 13 metal and N atoms by reaction of an m-terphenyl azide with the dimetallenes $Ar^{iPr4}MMAr^{iPr4}$ (M = Ga, In; $Ar^{iPr4}$ = $C_6H_3$-2,6-($C_6H_3$-2,6-$^iPr_2)_2$), which exist in equilibrium with :$MAr^{iPr4}$ monomers in solution.[43] This suggested that a similar Al species could be isolable, but the lack of an analogous Al(I) precursor (i.e. ArAlAlAr or :AlAr) precluded its synthesis. Recently we reported the monomeric alanediyl :$AlAr^{iPr8}$ ($Ar^{iPr8}$ = $C_6H$-2,6-($C_6H_2$-2,4,6-$^iPr_3)_2$-3,5-$^iPr_2$) with a one-coordinate Al atom.[44] We show here that its reaction with $Ar^{Me6}N_3$ ($Ar^{Me6}$ = $C_6H_3$-2,6-($C_6H_2$-2,4,6-$Me_3)_2$ gives the aluminum imide $Ar^{iPr8}AlNAr^{Me6}$ having two-coordinate Al and N atoms with a notably short Al-N bond length of 1.625(4) or 1.628(3) Å consistent with Al-N triple bonding. Additionally, the reaction of :$AlAr^{iPr8}$ with the less sterically

demanding azides 1-Ad$N_3$ (1-Ad = adamantyl) or $Me_3SiN_3$ give transient imides which react immediately with a second equivalent of azide to give products featuring ring closure or silyl migration.

Compound **1** was prepared by reaction of :AlAr$^{iPr8}$ with Ar$^{Me6}N_3$ (Scheme 6.2, a) in hexanes at ambient temperature, giving immediate vigorous evolution of $N_2$ and formation of a red solution. After ca. 5 min, the solids had dissolved and gas evolution had ceased. Storage at ca. -30°C for 3 days gave orange plates of **1** in ca. 91% yield. The crystal structure of **1** (Figure 6.2) contains two crystallographically independent molecules. One of these lies along the 2-fold proper rotation axis of the I2/a space group and contains a strictly linear C-Al-N-C core. The second molecule maintains a planar C-Al-N-C array but deviates slightly from linearity at the Al (C-Al-N = 172.5(3)°) and N (Al-N-C = 171.4(2)°) atoms. The Al-N bond lengths of 1.625(4) and 1.628(3) Å are the shortest reported to date and agree with those calculated for HAlNH and MeAlNMe.[11,30,40,41] The linear structure of **1** is in marked contrast to the heavier congeners Ar$^{iPr4}$M=NAr′ (M = Ga, In; Ar′ = $C_6H_3$-2,6-($C_6H_2$-2,6-$Me_2$-4-$^t$Bu)$_2$) which are strongly bent at the M and N atoms (Ga-N = 1.701(2) Å; C-Ga-N = 148.2(2)°; Ga-N-C = 141.7(3)°; In-N = 1.928(2) Å; C-In-N = 142.2(1)°; In-N-C = 134.9(2)°).[43]

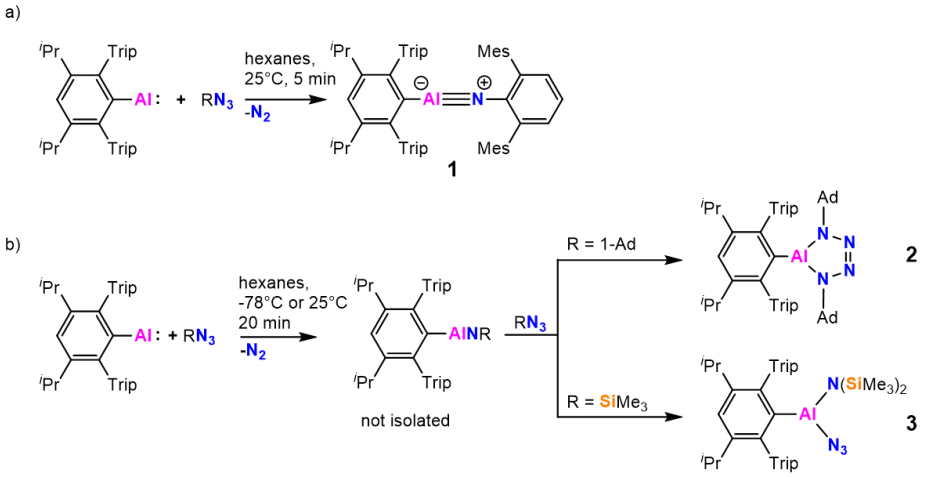


**Scheme 6.2.** a) Synthesis of compound **1**. b) synthesis of compounds **2** and **3**. Trip = 2,4,6-$^i$Pr$_3$C$_6$H$_2$; Mes = 2,4,6-Me$_3$C$_6$H$_2$; 1-Ad = 1-adamantyl).

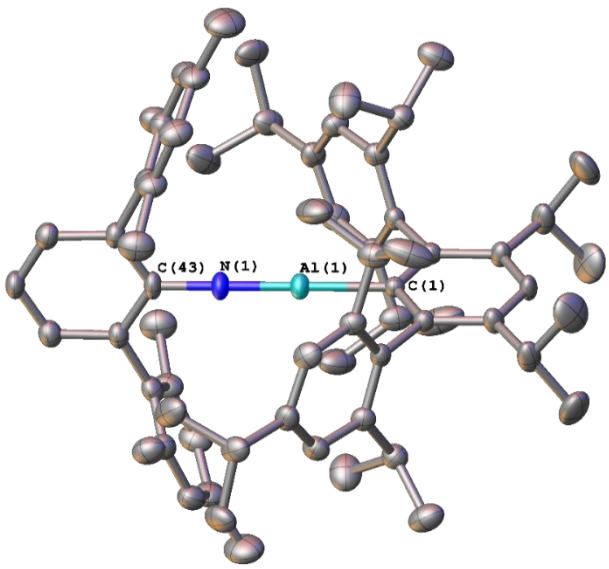


**Figure 6.2**. Thermal ellipsoid plot (50%) of one of the crystallographically independent molecules of $Ar^{iPr8}AlNAr^{Me6}$ (**1**). H atoms and n-hexane solvent not shown. Selected bond lengths (Å) and angles (°) {values in braces correspond to the other crystallographically independent molecule of **1**}: Al(1)-N(1): 1.625(4) {1.628(3)}, Al(1)-C(1): 1.935(4) {1.931(3)}, N(1)-C(43): 1.378(5) {1.366(4)}, C(1)-Al(1)-N(1): 180 {172.4 (2)}, Al(1)-N(1)-C(43): 180 {172.5(3)}, C(1)-Al(1)-N(1)-C(43): 0 {167.0(2)}.

The UV-Vis electronic spectrum of 1 has a single absorbance at 290 nm which tails into the visible region, producing an orange color. Time-dependent DFT calculations on **1** suggest that the low-intensity absorption tail is mostly due to the HOMO→LUMO+1 transition at 387 nm, whereas the main feature is due to two high-intensity transitions at 287 and 316 nm. The Al-N stretching band of **1** was calculated to be ca. 1100 $cm^{-1}$, however no distinct spectral features are apparent for assignment of the band.

Imide **1** slowly decomposes in solution over ca. 12 hours at ambient temperature as indicated by fading of the orange color to colorless. $^{1}H$ NMR spectroscopy (Figure 6.S3, supporting information) is consistent with decomposition via C-H activation of one of the methyl groups on the flanking rings that is analogous to that in $^{Dipp}NacNacAl{=}NAr^{iPr4}$.[35] A singlet at δ 3.50 ppm is assigned to the resulting amine proton, while the Al-$CH_2$ group gives a multiplet at δ 0.05-0.13 ppm. Solid **1** is thermally stable at ambient temperature for at least several days, but rapidly decomposes to a white solid above 83°C.

Dispersion corrected DFT calculations for **1** at the PBE1PBE- GD3BJ/def2-TZVP level yield an optimized structure with a linear C-Al-N-C core and an Al-N bond length of 1.635 Å in excellent agreement with the crystal structure. The Kohn-Sham orbitals (Figure 6.S15,

supporting information) and those of the model system Ph-NAl-Ph (Figure 6.3) show three major components to the Al-N bond, one of σ-type and two nondegenerate of π-type. NBO analysis yielded three two-center Al-N bonding orbitals with occupations close to 2 electrons and ca. 90% localization on the N atom.[45] Consequently, the calculated Wiberg bond index for the Al-N bond is only 0.89. More detailed bonding analyses using the ETS-NOCV method and the fragments :AlAr$^{iPr8}$ and Ar$^{Me6}$N̈: at the geometries they adopt in **1** also revealed three primary contributions to the Al-N bond. The major component (–1120 kJ mol$^{-1}$, ca. 83 % of the total orbital interaction –1350 kJ mol$^{-1}$) involves charge flow from Al to N, whereas the two minor components (–100 and –102 kJ mol$^{-1}$, each ca. 8 % of the total orbital interaction) describe backdonation from N to Al. Taken as a whole, the Al-N bond in 1 has the format characteristics of a triple bond with donation from Al to N greatly exceeding backdonation from N to Al. The calculated instantaneous interaction energy between :AlAr$^{iPr8}$ and Ar$^{Me6}$N is –551 kJ mol$^{-1}$ (cf. Gibbs interaction energy of –429 kJ mol$^{-1}$ taking into account fragment relaxation) with significant stabilization, –89 kJ mol$^{-1}$, from dispersion interactions. The possibility of charge-shift character in the Al-N bond has not yet been supported by computational data.[46-48]

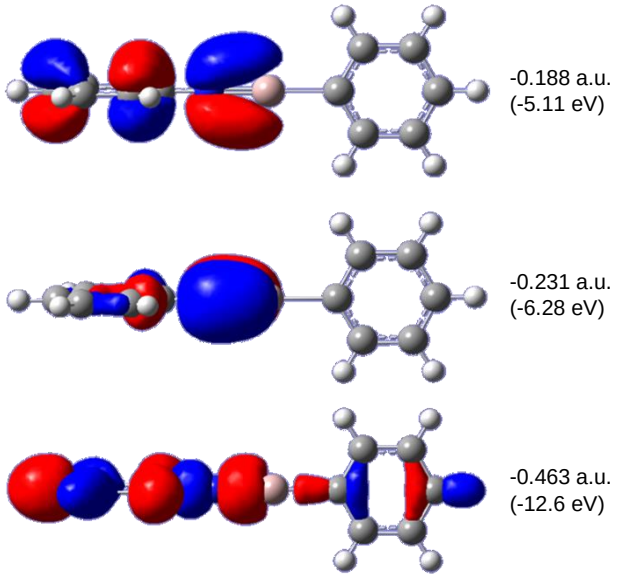


**Figure 6.3.** Occupied PBE1PBE-GD3BJ/def2-TZVP orbitals of Ph-NAl-Ph localized on the AlN bond (NPh moiety on the left, AlPh moiety on the right; isosurface value ± 0.05 a.u.).

Addition of AdN$_3$ or Me$_3$SiN$_3$ to **:**AlAr$^{iPr8}$ gives the tran-sient imides Ar$^{iPr8}$AlNR (R = 1-Ad, SiMe$_3$), which immediately reacts with a second equivalent of the azide (Scheme 6.2, b).

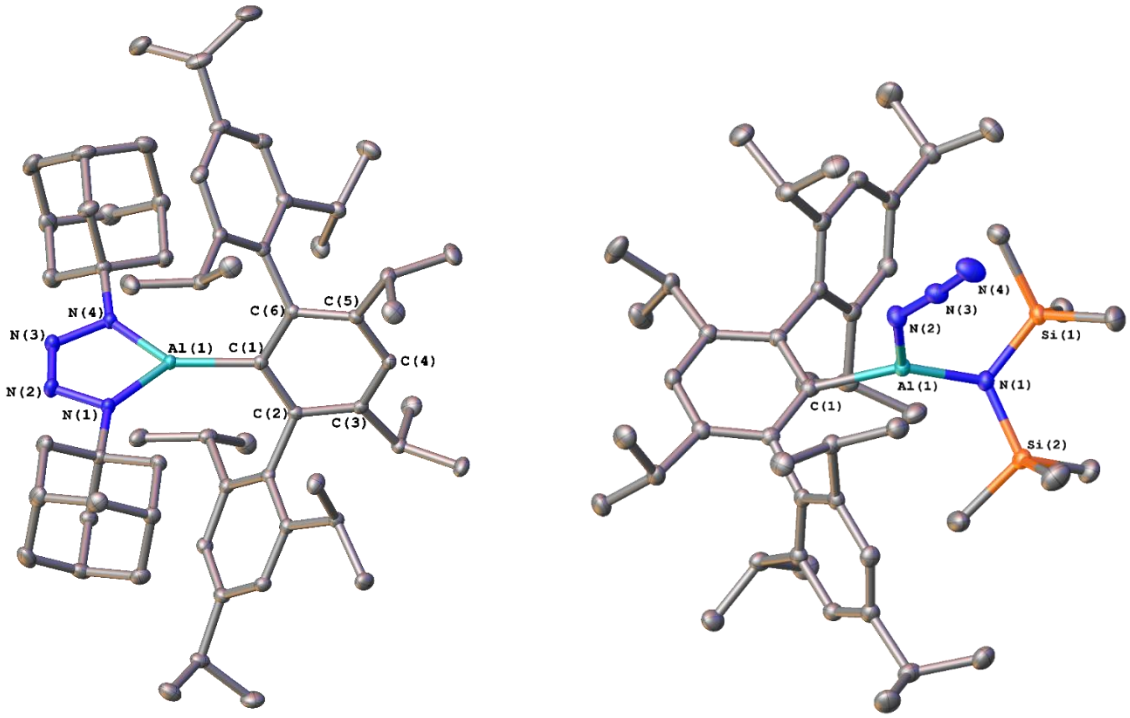


**2** **3**

**Figure 6.4**. Thermal ellipsoid plots (50%) of $Ar^{iPr8}Al(NAd)_2N_2$ (**2**, left) and $Ar^{iPr8}Al(N_3)N(SiMe_3)_2$ (**3**, right). Hydrogen atoms and toluene are not shown. Selected bond lengths (Å) and angles (°): **2**: Al(1)-C(1): 1.9710(12), Al(1)-N(1): 1.8126(9), Al(1)-N(4): 1.8220(11), N(1)-N(2): 1.3899(15), N(2)-N(3): 1.2643(16), N(3)-N(4): 1.3853(12), C(1)-Al(1)-N(1): 135.49(4), C(1)-Al(1)-N(4): 138.11(4), N(1)-Al(1)-N(4): 86.39(4). **3**: Al(1)-C(1): 1.9775(14), Al(1)-N(1): 1.8088(12), N(1)-Si(1): 1.7518(12), N(1)-Si(2): 1.7546(12), Al(1)-N(2): 1.8210(13), N(2)-N(3): 1.2132(18), N(3)-N(4): 1.1407(19), C(1)-Al(1)-N(1): 143.91(6), C(1)-Al(1)-N(2): 102.62(6), N(1)-Al(1)-N(2): 113.44(6), N(2)-N(3)-N(4): 175.71(16).

Roesky, Aldridge, and coworkers have shown that organic azides with small substituents such as -$SiMe_3$, -$SiPh_3$, and 1-Ad react in a 2:1 ratio with :Al[DippNacac] or an aluminyl anion to give planar $AlN_4$ heterocycles.[32,33,38] Reaction with the first equivalent of azide results in $N_2$ loss and a highly reactive species with a terminal Al=NR moiety, which undergoes ring closure with a second equivalent of the azide. The reaction of :$AlAr^{iPr8}$ with 2 equivalents of 1-$AdN_3$ gave **2** (Figure 6.4, left) as colorless crystals. The Al-N bonds are 1.8126(9) and 1.8220(11) Å which are in the typical range for these $AlN_4$ compounds.[32,33,38] However steric congestion between the terphenyl flanking rings and the adamantyl groups result in a deformation of the central ring of the terphenyl ligand, illustrated by torsion angles of C(1)-C(2)-C(3)-C(4) = 20.43(14)° and C(1)-C(6)-C(5)-C(4) = 20.06(14)°. The $^1H$ and $^{13}C\{^1H\}$ NMR spectra of 2 also display broad signals

indicating restricted movement of the 1-adamantyl and terphenyl flanking groups**.** The reaction of **:**AlAr$^{iPr8}$ with 2 equivalents of $Me_3SiN_3$ gives the amido- azido-alane **3** (Figure 6.4, right) as colorless crystals in which silyl migration from the second equivalent of azide to the nitrogen atom of the transient imide has occurred. Such migrations have been observed in a number of reactions of $Me_3SiN_3$ with low valent main group compounds.[49-54]

Computationally, the reaction of AlAr$^{iPr8}$ with $Me_3SiN_3$ yielded Ar$^{iPr8}$AlN($N_2$)$SiMe_3$ which readily releases $N_2$ with a free energy barrier of 46 kJ mol$^{-1}$ to afford Ar$^{iPr8}$AlN$SiMe_3$ at –306 kJ mol$^{-1}$ (Figure 6.S17, supporting information). Addition of a second equivalent of $Me_3SiN_3$ gave two products, *cis*- and *trans*-Ar$^{iPr8}$Al[N($SiMe_3$)$N_2$]N$SiMe_3$, depending on the relative orientation of Ar$^{iPr8}$AlN$SiMe_3$ and $Me_3SiN_3$. The *cis*-isomer has the two $SiMe_3$ groups on the same side of the dative Al-N bond and readily forms **3** via silyl migration, whereas the *trans*-isomer can form the $SiMe_3$ analogue of **2** via ring closure. Of the two possible products, **3** is kinetically preferred and thermodynamically favoured by 113 kJ mol$^{-1}$. The potential energy surface is expected to be largely similar for the :AlAr$^{iPr8}$ Ad$N_3$ pair with the exception that substituent migration is energetically unfeasible and **2** is formed rapidly via ring closure.

In summary, the alanediyl **:**AlAr$^{iPr8}$ reacts with the *m*-terphenyl azide Ar$^{Me6}N_3$ to yield the monomer Ar$^{iPr8}$AlNAr$^{Me6}$ (**1**) in which the Al and N atoms have linear, or almost linear coordination and short Al-N distances of 1.625(4) or 1.628(3) Å, consistent with Al-N triple bonding. Calculations show that the Al-N bond is composed of strong σ-donation from the **:**AlAr$^{iPr8}$ moiety to the :N̈Ar$^{Me6}$ nitrene and weak π-donation from the latter to **:**AlAr$^{iPr8}$. The calculations also indicate a key contribution from dispersion energies that, together with steric effects from the terphenyl substituents, provide sufficient stabilization for the room-temperature characterization of **1**.

**Acknowledgements**

We thank the US National Science Foundation (CHE-156551) for supporting this work and for the purchase of a dual source X-ray diffractometer (CHE-0840444). This project received funding from the European Research Council under the European Union's Horizon 2020 research and innovation programme (grant agreement #772510 to H.M.T.).

**References**

(1) Downs, A. Aldridge, S. The Group 13 Metals Aluminium, Gallium, Indium and Thallium: Chemical Patterns and Peculiarities. Wiley: Chichester, 2011 pp 122-131, 257–264.

(2) Timoshkin, A. Y. Group 13 Imido Metallanes and their Heavier Analogs $[RMYR']_n$ (M = Al, Ga, In; Y = P, N, As, Sb) *Coord. Chem. Rev.* **2005**, *249*, 2094–2131.

(3) Gardiner, M. G.; Raston, C. L. Advances in the chemistry of Lewis base adducts of alane and gallane *Coord. Chem. Rev.* **1997**, *166*, 1–34.

(4) Carmalt, C. J. Amido compounds of gallium and indium *Coord. Chem. Rev.* **2001**, *223*, 217–264.

(5) Brothers, P. J.; Power, P. P. Multiple Bonding Involving the Heavier Main Group 3 Elements Al, Ga, In, and Tl. *Adv. Organomet. Chem.* **1996**, *39*, 1–69.

(6) Schauer, S. J.; Robinson, G. H. Aminoalane Dimers and Trimers. An Examination of Structural and Steric Trends. *J. Coord. Chem.* **1993**, *30*, 197–214.

(7) Uhl, W. Aluminum and Gallium Hydrazides. *Struct. Bond.* **2003**, *105*, 41–66.

(8) Veith, M. Cage Compounds with Main-Group Metals. *Chem. Rev.* **1990**, *90*, 3–16.

(9) Lappert, M. F.; Power, P. P.; Sanger, A. R.; Srivastava, R. C. *Metal and Metalloid Amides*; Ellis Horwood-Wiley: Chichester, 1979, Chapter 4.

(10) Jegier, J. A.; Gladfelter, W. L. The Use of Aluminum and Gallium Hydrides in Materials Science. *Coord. Chem. Rev.* **2000**, *206–207*, 631–650.

(11) Grant, D. J.; Dixon, D. A. Thermodynamic Properties of Molecular Borane Phosphines, Alane Amines, and Phosphine Alanes and the $[BH_4^-][PH_4^+]$, $[AlH_4^-][NH_4^+]$, and $[AlH_4^-][PH_4^+]$ Salts for Chemical Hydrogen Storage Systems from ab Initio Electronic Structure Theory. *J. Phys. Chem. A.* **2005**, *109*, 10138–10147.

(12) Marder, T. B. Will We Soon Be Fueling our Automobiles with Ammonia–Borane? *Angew. Chem. Int. Ed*. **2007**, *46*, 8116–8118.

(13) Langmi, H. W.; McGrady, G. S. Non-hydride systems of the main group elements as hydrogen storage materials *Coord. Chem. Rev.* **2007**, *251*, 925–935.

(14) Laubengayer, A. W.; Smith, J. D.; Ehrlich, G. G. Aluminum-Nitrogen Polymers by Condensation Reactions. *J. Am. Chem. Soc.* **1961**, *83*, 542–546.

(15) Cesari, M.; Perego, G,; Del Piero, G.; Cucinella, S.; Cernia, E. The chemistry and the stereochemistry of poly(*N*-alkyliminoalanes): II. The crystal and molecular structure of the hexamer, $(HAlN\text{-}i\text{-}Pr)_6$. *J. Organomet. Chem.* **1974**, *78*, 203–213.

(16) Del Piero, G.; Cesari, M. C.; Perego, G.; Cucinella, S.; Cernia, E. The chemistry and the stereochemistry of poly (N-alkyliminoalanes) : XI. The crystal and molecular structure of the hexamer $(HAlN\text{-}n\text{-}Pr)_6$ and the octamer $(HAlN\text{-}n\text{-}Pr)_8$ *J. Organomet. Chem.* **1977**¸*129*, 289–298.

(17) Del Piero, G.; Cesari, M.; Dozzi, G.; Mazzei, A.; *J. Organomet. Chem.* **1977**, *129*, 281–288.

(18) Belgardt, T.; Waezsada, S. D.; Roesky, H. W.; Gornitzka, H.; Häming, L.; Stalke, D. Synthesis and Characterization of (Pentafluorophenyl)amino-based Amino- and Iminometallanes. Crystal Structures of $(MeAlNC_6F_5)_4$ and $NHC_6F_5Ga(MesGa)_3(\mu_3\text{-}NC_6F_5)_4$ (Mes = 2,4,6-$Me_3C_6H_2$). *Inorg. Chem.* **1994**, *33*, 6247–6251

(19) Reddy, N. D.; Roesky, H. W.; Noltemeyer, N.; Schmidt, H.-G. Reactions of $AlH_3{\cdot}NMe_3$ with Nitriles: Structural Characterization and Substitution Reactions of Hexameric Aluminum Imides *Inorg. Chem.* **2002**, *41*, 2374–2378.

(20) Schiefer, M.; Reddy, N.D.; Roesky, H. W.; Vidovic, D. Synthesis and Structural Characterization of an Exclusively N-Based Tetrameric Aluminum(I) Compound. *Organometallics*, **2003**¸*22*, 3637–3638.

(21) Waggoner, K. M.; Hope, H.; Power, P. P. Synthesis and Structure of $[MeAlN(2,6\text{-}i\text{Pr}_2C_6H_3)]_3$: An Aluminum-Nitrogen Analogue of Borazine. *Angew. Chem. Int. Ed.* **1988**, *27*, 1699–1700.

(22) Pinkas, J.; Löbl, J.; Roesky, H. W. Chemical Reactivity of Alumazene. *Phosph. Sulfur Silicon Relat. Elements*, **2004**, *179*, 759–763.

(23) Löbl, J.; Necas, M.; Pinkas, J. Alumazene adducts with triphenylphosphine oxide *Main Group Chem.* **2006**, *5*, 79–88.

(24) Wehmschulte, R. J.; Power, P. P. Reactions of $(H_2AlMes^*)_2$ (Mes* = 2,4,6-$(t\text{-}Bu)_3C_6H_2$) with $H_2EAr$ (E = N, P, or As; Ar = aryl): Characterization of the Ring Compounds $(Mes^*AlNPh)_2$ and $(Mes^*AlEPh)_3$ (E = P or As). *J. Am. Chem. Soc.* **1996**, *118*, 791–797.

(25) Wehmschulte, R. J.; Power, P. P. Reaction of the Primary Alane $(2,4,6\text{-}t\text{-}Bu_3H_2C_6AlH_2)_2$ with Nitriles, Isonitriles, and Primary Amines. *Inorg. Chem.* **1998**, *37*, 6906–6911.

(26) Schulz, S.; Voigt, A.; Roesky, H. W.; Häming, L.; Herbst-Irmer, R. Synthesis of Dimeric Iminoalanes by Oxidative Addition of Azides to $(Cp^*Al)_4$: Structural Characterization of $(Cp^*AlNSi^tBu_3)_2$ ($Cp^* = C_5Me_5$). *Organometallics* **1996**, *15*, 5252–5253.

(27) Schulz, S; Häming, L.; Herbst-Irmer, R.; Roesky, H. W.; Sheldrick, G. M. Synthesis and Structure of the First Dimeric Iminoalane Containing an $Al_2N_2$ Heterocycle *Angew. Chem. Int. Ed.* **1994**, *33*, 969–970.

(28) Fischer, J. D.; Shapiro, P. J.; Yap, G. P. A.; Rheingold, A. L. $[CpAlN(2,6\text{-}i\text{-}Pr_2C_6H_3)]_2$: A Dimeric Iminoalane Obtained by Alkane Elimination. *Inorg. Chem.* **1996**, *35*, 271–272.

(29) Schulz, S.; Thomas, F.; Priesmann, W. F.; Nieger, M. Synthesis and X-Ray Structurse of Base-Stabilized Iminoalanes. *Organometallics* **2006**, *25*, 1392–1398.

(30) Hamilton, T. P.; Shaikh, A. D. Theoretical Study of the Dimerization of Multiply-Bonded Aluminum-Nitrogen Compounds. *Inorg. Chem.* **1997**, *36*, 754–755.

(31) Waggoner, K. M.; Power, P. P. Reactions of trimethylaluminum or trimethylgallium with bulky primary amines: structural characterization of the thermolysis products. *J. Am. Chem. Soc.* **1991**, *113*, 3385–3393.

(32) Cui, C.; Roesky, H. W.; Schmidt, H.-G.; Noltemeyer, M. $[HC\{(CMe)(NAr)\}_2Al[(NSiMe_3)_2N_2]$ (Ar=2,6-$i$Pr$_2$C$_6$H$_3$): The First Five-Membered $AlN_4$ Ring System. *Angew. Chem. Int. Ed*. **2000**, *39*, 4531–4533.

(33) Zhu, H. Yang, Z.; Magull, J.; Roesky, H. W.; Schmidt, H.-G.; Noltemeyer, M. Synthesis and Structural Characterization of a $LAl(N_3)N[\mu\text{-}Si(N_3)(t\text{Bu})]_2NAl(N_3)L$ and a Monomeric Aluminum Hydride Amide LAlH(NHAr) (L = $HC[(CMe)(NAr)]_2$, Ar = 2,6-$^i$Pr$_2$C$_6$H$_3$). *Organometallics* **2005**, *24*, 6420–6425.

(34) Hardman, N. J.; Cui, C.; Roesky, H. W.; Fink, W. H.; Power, P. P. Stable, Monomeric Imides of Aluminum and Gallium: Synthesis and Characterization of $[\{HC(CMeDippN)_2\}MN\text{-}2,6\text{-}Trip_2C_6H_3]$ (M=Al or Ga; Dipp=2,6-$i$Pr$_2$C$_6$H$_3$; Trip=2,4,6-$i$Pr$_3$C$_6$H$_2$). *Angew. Chem. Int. Ed.* **2001**, *40*, 2172–2174.

(35) Zhu, H.; Chai, J.; Chandrasekhar, V.; Roesky, H. W.; Magull, J.; Vidovic, D.; Schmidt, H.-G.; Noltemeyer, M.; Power, P. P.; Merrill, W. A. Two Types of Intramolecular Addition of an Al−N Multiple-Bonded Monomer LAlNAr‘ Arising from the Reaction of LAl with $N_3$Ar‘ (L = $HC[(CMe)(NAr)]_2$, Ar‘ = 2,6-Ar$_2$C$_6$H$_3$, Ar = 2,6-$i$Pr$_2$C$_6$H$_3$). *J. Am. Chem. Soc.* **2004**, *126*, 9472–9473.

(36) Li, J.; Li, X.; Huang, W.; Hu, H. Zhang, J.; Cui, C. Synthesis, Structure, and Reactivity of a Monomeric Iminoalane. *Chem. Eur. J.* **2012**, *18*, 15263–15266.

(37) Anker, M. D.; Schwamm, R. J.; Coles, M. P. Synthesis and Reactivity of a Terminal Aluminum-Imide Bond. *Chem Commun.* **2020**, *56*, 2288–2291.

(38) Heilmann, A.; Hicks, J.; Vasko, P.; Goicoechea, J. M.; Aldridge, S. Carbon Monoxide Activation by a Molecular Aluminium Imide: C−O Bond Cleavage and C−C Bond Formation. *Angew. Chem. Int. Ed.* **2020**, *59*, 4897–4901.

(39) Lanzisera, D. V.; Andrews, L. Reactions of Laser-Ablated Aluminum Atoms with Ammonia. Infrared Spectra of $HAlNH_2$, $AlNH_2$, and HAlNH in Solid Argon. *J. Phys. Chem. A* **1997**, *101*, 5082–5089.

(40) Timoshkin, A. Y.; Schaefer, H. F. Theoretical Studies of $[MYR_2]_n$ Isomers (M = B, Al, Ga; Y = N, P, As; R = H, $CH_3$): Structures and Energetics of Monomeric and Dimeric Compounds ($n$ = 1, 2). *J. Phys. Chem. A.* **2008**, *112*, 13180–13196.

(41) Zhang, S-L.; Yang, M-C.; Su, M.-D. A computational study to determine whether substituents make $E_{13}$=nitrogen ($E_{13}$ = B, Al, Ga, In, and Tl) triple bonds synthetically accessible. *RSC. Adv.* **2019**, *9*, 12195–12208.

(42) Gilbert, T. M. Ab Initio Computational Studies of Heterocycloalkynes: Structures, Natural Bond Orders, Ring Strain Energies, and Isomerizations of Cyclic Iminoboranes and Iminoalanes. *Organometallics* **2000**, *19*, 1160–1165.

(43) Wright, R. J.; Phillips, A. D.; Allen, T. L.; Fink, W. H.; Power, P. P. Synthesis and Characterization of the Monomeric Imides Ar‘MNAr“ (M = Ga or In; Ar‘ or Ar“ = Terphenyl Ligands) with Two-Coordinate Gallium and Indium. *J. Am. Chem. Soc.* **2003**, *125*, 1694–1695.

(44) Queen, J. D.; Lehmann, A.; Fettinger, J. C.; Tuononen, H. M.; Power, P. P. The Monomeric Alanediyl :$AlAr^{iPr8}$ ($Ar^{iPr8}$ = $C_6H$-2,6-($C_6H_2$-2,4,6-$Pr^i_3)_2$-3,5-$Pr^i_2$): An Organoaluminum(I) Compound with a One-Coordinate Aluminum Atom. *J. Am. Chem. Soc.* **2020**, *142*, 20554–20559.

(45) This is consistent with the Al-N bond having similar polarity t the Li-I bond ($\Delta\chi_p$(Al-N) = 1.43; $\Delta\chi_p$(Li-I) = 1.68). Source of $\chi_p$ values: Huheey, J. E. Inorganic Chemistry, 2nd Ed. pp 162. New York, 1978.

(46) Ploshnik, E.; Danovich, D.; Hiberty, P. C.; Shaik, S. The Nature of the Idealized Triple Bonds Between Principal Elements and the σ Origins of Trans-Bent Geometries—A Valence Bond Study. *J. Chem. Theory Comput.* **2011**, *7*, 955–968.

(47) Huo, S.; Li, X.; Zeng, Y.; Sun, Z.; Zheng, S.; Meng, L. Nature of E–E bonds in heavier ditetrel alkyne analogues ArEEAr (Ar = $C_6H_3$-2,6($C_6H_3$-2,6-$Pr^i_2)_2$; E = Si, Ge, Sn, and Pb). *New J. Chem.* **2013**, *37*, 3145–3151.

(48) Power, P. P. An Update on Multiple Bonding between Heavier Main Group Elements: The Importance of Pauli Repulsion, Charge-Shift Character, and London Dispersion Force Effects. *Organometallics* **2020**, *39*, 4127–4138.

(49) Jutzi, P.; Neumann, B.; Reumann, G. Stammler, H.-G. Novel $Ga_2N_2$ Ring Systems by Reaction of Pentamethylcyclopentadienylgallium with Organic Azides. *Organometallics* **1999**, *18*, 2037–2039.

(50) Schulz, A.; Thomas, M.; Villinger, A. Tetrazastannoles *versus* distannadiazanes – a question of the tin(II) source. *Dalton. Trans.* **2019**, *48*, 125–132.

(51) Pfeiffer, J.; Maringgele, W.; Noltemeyer, M.; Meller, A. Reaktionen von Germylenen mit Aziden: Iminogermane, Azidogermane, Tetrazagermole und Hexaazadigermadispirododecane. *Chem. Ber.* **1989**, *122*, 245–252.

(52) Hitchcock, P. B.; Lappert, M. F.; Protchenko, A. V.; Uiterweerd, P. G. H. Synthesis and structures of halides and pseudohalides of bis[2,6-bis(dimethylamino)phenyl]tin(IV). *Dalton Trans.* **2009**, 353–361.

(53) Hardman, N. J.; Power, P. P. Unique structural isomerism involving tetrazole and amide/azide derivatives of gallium. *Chem. Commun.* **2001**, 1184–1185.

(54) Krahfuss, M. J.; Radius, U. *N*-Heterocyclic Silylene Main Group Element Chemistry: Adduct Formation, Insertion into E-X Bonds and Cyclization of Organoazides. *Eur. J. Inorg. Chem.* **2021**, 548–561.

## Author Contributions

**J. D. Queen:** Synthesized and spectroscopically characterized reported compounds, collected X-ray crystallographic data, and prepared the manuscript.

**S. Irvankoski and H. M. Tuononen:** Performed DFT calculations including geometry optimizations, calculated molecular orbitals, and determination of transition state geometries. Prepared the relevant figures and text in the manuscript.

**J. C. Fettinger**: Prepared X-ray crystallography data for publication.

**P. P. Power**: Supervised synthetic work and manuscript preparation.

## Supporting Information

## Experimental Details

## General Procedures

All manipulations were carried out using modified Schlenk techniques or in a Vacuum Atmospheres OMNI-Lab drybox under an argon atmosphere. Solvents were dried over columns of activated alumina using a Grubbs type purification system[S1] (Glass Contour), stored over an Na mirrors (hexanes, toluene), or 3 Å molecular sieves (benzene), and degassed via the freeze-pump-thaw method prior to use. The $^{1}H$ and $^{13}C\{^{1}H\}$ NMR spectra were recorded on Varian Inova 600 MHz spectrometer and were referenced to the residual solvent signals in $C_6D_6$ ($^{1}H$: δ 7.16 ppm, $^{13}C\{^{1}H\}$: δ 128.06 ppm).[S2] UV-Visible spectra were recorded in dilute hexane solutions in 3.5 mL quartz cuvettes using an Olis 17 Modernized Cary 14 UV-Vis/NIR spectrophotometer. Infrared spectra were recorded in nujol on a Perkin Elmer 1430 spectrophotometer. Melting points were measured in glass capillary tubes sealed under argon using a Mel-Temp II apparatus using a partial immersion thermometer.

$AlAr^{iPr8}$ and $Ar^{Me6}N_3$ were synthesized according to the literature procedures.[S3,S4] $Me_3SiN_3$ and 1-$AdN_3$ were purchased commercially and used without further purification.

## Synthesis of 1-3.

**$Ar^{iPr8}AlNAr^{Me6}$ (1).** A mixture of solid $AlAr^{iPr8}$ (0.150 g, 0.253 mmol) and $Ar^{Me6}N_3$ (0.090 g, 0.253 mmol) was dissolved in ca. 4 mL hexanes resulting in immediate gas evolution and the formation of a red solution. After ca. 5 min, the solution was concentrated to ca. 2 mL under reduced pressure and stored at ca. –30 °C for 2 days to give red-orange crystals of **1**·$C_6H_{14}$.

Yield: 0.210 g, 0.228 mmol (91%).

mp. 83°C dec to white solid without melting.

$^1$H NMR (600 MHz, $C_6D_6$, 298 K): δ 7.44 (s, 1H, Ar$^{iPr8}$ *p*-Ar*H*), 7.17 (s, 4H, Ar*H*), 6.89 (d, overlapping with signal at 6.88, 2H, Ar$^{Me6}$ *m*-Ar*H*), 6.88 (s, 4H, Ar*H*), 6.76 (t, $^3J$ = 7.1 Hz, 1H, Ar$^{Me6}$ *p*-Ar*H*), 2.82 (sept, $^3J$ = 6.8 Hz, 2H, C*H*($CH_3$)$_2$), 2.53 (sept, $^3J$ = 6.8 Hz, 6H, C*H*($CH_3$)$_2$ ), 2.37 (s, 6H, Ar$^{Me6}$ *p*-C*H*$_3$), 2.10 (s, 12 H, Ar$^{Me6}$ *p*-C*H*$_3$), 1.23 (d, $^3J$ = 6.9 Hz, 12H, -CH(C*H*$_3$)$_2$), 1.12 (d, $^3J$ = 6.7Hz, 12H, -CH(C*H*$_3$)$_2$), 1.04 (d, $^3J$ = 6.7 Hz, 12H, -CH(C*H*$_3$)$_2$), 0.93 (d, $^3J$ = 6.8 Hz, 12H, -CH(C*H*$_3$)$_2$).

$^{13}$C{$^1$H} NMR (151 MHz, $C_6D_6$, 298 K): δ 150.33, 148.63, 148.07, 147.42, 145.43, 142.10, 137.76, 136.51, 136.15, 133.30, 128.94, 128.57, 126.34, 123.06, 115.97, 31.98, 30.80, 30.72, 27.50, 24.81, 24.63, 24.12, 21.31, 21.26, 14.37.

UV-Vis (hexanes): $\lambda_{max}$ = 292 nm ($\varepsilon$ = 5500 L mol$^{-1}$ cm$^{-1}$).

**Decomposition of 1**: ca. 15 mg of the imide **1** was placed in a J-Young NMR tube and dissolved in ca. 0.6 mL $C_6D_6$ to give an orange solution. After ca. 24 hours the now colorless solution showed new signals in the $^1$H and $^{13}$C{$^1$H} NMR spectra that were assigned as the product [$C_6$H-2-{$C_6H_2$-2-CH($CH_3$)($CH_2$)-4,6-$^i$Pr$_2$}-6-($C_6H_2$,-2,4-6-$^i$Pr$_3$)-3,5-$^i$Pr$_2$]Al-N(H)Ar$^{Me6}$.

$^1$H NMR (600 MHz, $C_6D_6$, 298 K): δ 7.46 (s, 1H, Ar*H*), 7.27 (s, 1H, Ar*H*), 7.24 (s, 1H, Ar*H*), 7.19 (s, 2H, Ar*H*), 6.98-6.77 (mult, br, 4H, Ar*H*), 6.71 (mult, 3H, Ar*H*), 3.50 (s, 1H, N*H*), 3.00 (br, 1H, -C*H*$CH_2$Al), 2.93 (sept, *J* = 6.9 Hz, 1H, -C*H*($CH_3$)$_2$), 2.85 (sept, *J* = 6.9 Hz, 1H, -C*H*($CH_3$)$_2$), 2.76 (mult, 4H, -C*H*($CH_3$)$_2$), 2.64 (sept, *J* = 6.8 Hz, 1H -C*H*($CH_3$)$_2$), 2.59 (sept, *J* = 6.7 H,z 1H, -C*H*($CH_3$)$_2$), 2.27 (s, 12H, Mes o-$CH_3$), 1.75 (s, 6H, Mes p-$CH_3$), 1.50 (d, *J* = 6.7 Hz, 3H, -CH(C*H*$_3$)$CH_2$Al) 1.33 (dd, *J* = 6.9 Hz, *J* = 12 Hz, 6H -CH(C*H*$_3$)$_2$), 1.27-1.22 (mult,

18H, -CH(C*H*$_3$)$_2$), 1.19 (mult, 6H, CH(C*H*$_3$)$_2$), 1.07 (d, *J* = 6.7 Hz, 3H, -CH(C*H*$_3$)$_2$,), 1.03 (d, *J* = 6.8 Hz, 3H, -CH(C*H*$_3$)$_2$), 0.94 (d, *J* = 6.8 Hz, 3H, -CH(C*H*$_3$)$_2$), 0.79 (d, *J* = 6.7 Hz, 3H, -CH(C*H*$_3$)$_2$) 0.55 (d, *J* = 6.8 Hz, 3H, -CH(C*H*$_3$)$_2$), 0.14-0.04 (mult, 2H, -C*H*$_2$Al).

$^{13}$C{$^1$H} NMR (151 MHz, $C_6D_6$, 298 K): δ 149.78, 149.33, 149.11, 148.11, 147.47, 146.42, 146.00, 144.80, 144.33, 144.12, 141.80, 139.65, 134.42, 128.93, 122.56, 122.53, 122.02, 121.31, 119.30, 119.22, 34.98, 34.78, 34.63, 34.32, 31.98, 30.38, 30.26, 30.13, 30.09, 30.06, 29.44, 26.71, 26.35, 25.73, 25.65, 25.36,25.26, 24.95, 24.87, 24.79, 24.69, 23.95, 23.48, 23.07, 2.27, 21.82, 21.25, 20.90, 20.34, 14.38, 11.69.

**Ar$^{iPr8}$Al[(NAd)$_2$N$_2$] (2)**. Solid :AlAr$^{iPr8}$ (0.200 g, 0.337 mmol) and 1-AdN$_3$ (0.120 g, 0.677 mmol) were combined in a flask and dissolved in ca. 10 mL hexanes at ambient temperature giving a pale yellow solution. After ca. 20 min the volatile components were removed under reduced pressure and the yellow residue was dissolved in ca. 0.5 mL toluene. Storage at ca. 8 °C for 3 days gave colorless blocks of **3**·2C$_7$H$_8$.

Yield: 0.273 g, 0.297 mmol (88%).

mp. 231-236 °C (dec).

$^1$H NMR (600 MHz, $C_6D_6$, 298 K): δ 7.59-7.19 (mult, 5H, Ar*H*), 3.50 (sept, *J* = 6.6 Hz, 1H -C*H*(CH$_3$)$_2$), 3.29-2.49 (mult, 7H, -C*H*(CH$_3$)$_2$), 2.05 (s, 1H), 2.02 (s, 2H), 1.75 (s, 3H), 1.65 (br, 7H), 1.60 (br, 5H), 1.48 (mult, 3H), 1.40-1.29, (mult, br, 24H), 1.27 (d, *J* = 7.0 Hz, 6H), 1.22 (d, *J* = 6.5 Hz, 6H), 1.17 (d, *J* = 6.5 Hz, 6H), 1.11 (d, *J* = 6.6 Hz, 6H), 1.06 (d, *J* = 6.7 Hz, 6H), 0.91 (mult, 3H).

$^{13}$C{$^1$H} NMR (151 MHz, $C_6D_6$, 298 K): δ 148.69, 148.46, 146.09, 143.62, 140.25, 123.95, 122.85, 121.86, 121.03, 55.28, 44.07, 43.80, 43.25, 42.41, 42.00, 41.60, 37.34, 37.05, 36.77, 36.41,

36.11, 35.93, 34.94, 34.46, 33.73, 31.37, 30.86, 30.77, 30.39, 30.26, 30.23, 30.04, 26.49, 25.91, 25.58, 25.46, 24.78, 24.46, 24.16, 24.08, 23.93, 23.62, 23.33.

**$Ar^{iPr8}Al\{N(SiMe_3)_2\}N_3$ (3).** A solution of $AlAr^{iPr8}$ (0.200 g, 0.337 mmol) in ca. 10 mL of hexanes was cooled to ca. −78°C (ethanol/dry ice bath) and neat $Me_3SiN_3$ (0.090 mL, 0.68 mmol) was added via syringe, resulting in the immediate formation of a colorless solution. The mixture was stirred for ca. 20 min then removed from the cold bath and the volatile components were removed under reduced pressure, affording a white residue. After drying under reduced pressure for 1 hour at ambient temperature, the white powder was dissolved in benzene and stored at ca. 8°C. After 3 days, colorless blocks of **2**·$C_6H_6$ formed.

Yield: 0.225 g, 0.283 mmol (84%).

mp. Softens at 89°C then melts rapidly at 133-135°C.

$^1$H NMR (600 MHz, $C_6D_6$, 298 K): δ 7.56 (s, 1H, *p*-Ar*H*), 7.24 (s, 4H, Trip *m*-Ar*H*), 3.08 (sept, $^3J$ = 6.7 Hz, 4H, -C*H*$(CH_3)_2$), 2.83 (sept, $^3J$ = 2.9Hz, 2H, -C*H*$(CH_3)_2$), 2.51 (sept, $^3J$ = 6.7 Hz, 2H, -C*H*$(CH_3)_2$), 1.48 (d, $^3J$ = 6.7 Hz, 12H, -CH(C*H*$_3)_2$), 1.27 (d, $^3J$ = 6.9 Hz, 12H, -CH(C*H*$_3)_2$), 1.19 (d, $^3J$ = 6.7Hz, 12H, -CH(C*H*$_3)_2$), 1.12 (d, $^3J$ = 6.7 Hz, 12H, -CH(C*H*$_3)_2$), -0.04 (s, 18H, -Si(C*H*$_3)_3$).

$^{13}C\{^1H\}$ NMR (151 MHz, $C_6D_6$, 298 K): δ 149.56, 149.36, 147.53, 142.54, 137.36, 128.59, 124.97, 123.17, 34.70, 30.61, 29.81, 26.11, 25.86, 25.56, 24.12, 5.03.

IR (CsI, nujol): $\tilde{\nu}_{N_3}$ = 2120 cm$^{-1}$

**X-Ray Crystallography**

Crystals of **1**-**3** were removed from a Schlenk flask under a stream of argon and immediately covered with hydrocarbon oil. A suitable crystal was selected, attached to a MiTeGen microloop, and mounted on the goniometer of the diffractometer under a cold stream of $N_2$. Data were collected at 90 K on a Bruker Duo[S5]APEXII CCD system at –183°C (90K) using Cu Kα (λ = 1.54178) radiation. Data were integrated with SAINT[S5] and an absorption correction (multi-scan) was applied using SADABS[S6] (**2**,**3**) or TWINABS (**1**).[S7] The structures were solved using SHELXTL[S8] program package by intrinsic phasing methods using SHELXT[S9] and were refined by full matrix least-squares procedures using SHELXL.[S10] All non-H atoms were refined anisotropically.

**Table 6.S1**. Crystal data and structure refinement for $[C_{66}H_{86}AlN]_{1.5}[C_6H_{14}]$ (**1**).

| | | |
|---|---|---|
| Empirical formula | $C_{105}H_{143}Al_{1.50}N_{1.50}$ | |
| Formula weight | 1466.67 | |
| Temperature | 90(2) K | |
| Wavelength | 1.54178 Å | |
| Crystal system | Monoclinic | |
| Space group | I2/a | |
| Unit cell dimensions | a = 18.7125(4) Å | α = 90°. |
| | b = 18.0528(4) Å | β = 91.0212(13)°. |
| | c = 55.2534(12) Å | γ = 90°. |
| Volume | 18662.4(7) $Å^3$ | |
| Z | 8 | |
| Density (calculated) | 1.044 g $cm^{-3}$ | |
| Absorption coefficient | 0.563 $mm^{-1}$ | |
| F(000) | 6424 | |
| Crystal size | 0.453 x 0.438 x 0.186 $mm^3$ | |
| Crystal color and habit | Orange plate | |
| Diffractometer | Bruker APEX-II CCD | |
| Theta range for data collection | 3.428 to 68.588° | |
| Index ranges | –22<=h<=22, 0<=k<=21, 0<=l<=66 | |
| Reflections collected | 16602 | |
| Independent reflections | 16602 [Rint = 0.0459, Rsigma = 0.0615] | |
| Observed reflections (I > 2sigma(I)) | 15677 | |
| Completeness to theta = 67.679° | 98.8 % | |
| Absorption correction | Semi-empirical from equivalents | |
| Max. and min. transmission | 0.8637 and 0.6754 | |
| Solution method | SHELXT (Sheldrick, 2014) | |
| Refinement method | SHELXL-2017/1 (Sheldrick, 2017) Full-matrix least-squares on $F^2$ | |
| Data / restraints / parameters | 16602 / 97 / 1102 | |
| Goodness-of-fit on $F^2$ | 1.057 | |
| Final R indices [I>2sigma(I)] | R1 = 0.0762, wR2 = 0.2098 | |
| R indices (all data) | R1 = 0.0791, wR2 = 0.2121 | |
| Largest diff. peak and hole | 0.366 / −0.347 e $Å^{-3}$ | |

**Table 6.S2.** Crystal data and structure refinement for $[C_{62}H_{91}AlN_4][C_7H_8]_2$ (**2**).

| | | |
|---|---|---|
| Empirical formula | $C_{76}H_{107}AlN_4$ | |
| Formula weight | 1103.63 | |
| Temperature | 90(2) K | |
| Wavelength | 1.54178 Å | |
| Crystal system | Triclinic | |
| Space group | P-1 | |
| Unit cell dimensions | a = 11.2344(8) Å | α = 72.801(6)° |
| | b = 17.5443(18) Å | β = 77.326(5)° |
| | c = 17.8281(18) Å | γ = 76.613(9)° |
| Volume | 3222.2(5) $Å^3$ | |
| Z | 2 | |
| Density (calculated) | 1.137 g $cm^{-3}$ | |
| M | 0.609 $mm^{-1}$ | |
| F(000) | 1208.0 | |
| Crystal size | 0.489 × 0.36 × 0.329 $mm^3$ | |
| Crystal habit and color | Colorless block | |
| Diffractometer | Bruker APEX-II CCD | |
| 2Θ range for data collection/° | 5.258 to 144.492 | |
| Index ranges | $-13 \leq h \leq 13$, $-21 \leq k \leq 21$, $-21 \leq l \leq 21$ | |
| Reflections collected | 22226 | |
| Independent reflections | 12207 [Rint = 0.0155, Rsigma = 0.0224] | |
| Observed reflections (I> 2sigma(I)) | 12207 | |
| Completeness to theta = 67.679 | 96.7% | |
| Absorption correction | Semi-empirical from equivalents | |
| Max. and min. transmission | 0.4162 and 0.3273 | |
| Solution method | SHELXT (Sheldrick, 2014) | |
| Refinement method | SHELXL-2017/1 (Sheldrick, 2017) Full-matrix least-squares on $F^2$ | |
| Data / restraints / parameters | 12207 / 0 / 748 | |
| Goodness-of-fit on F2 | 1.015 | |
| Final R indexes [I>=2σ (I)] | R1 = 0.0357, wR2 = 0.0898 | |
| Final R indexes [all data] | R1 = 0.0374, wR2 = 0.0912 | |
| Largest diff. peak/hole | 0.31 / −0.22 e $Å^{-3}$ | |

**Table 6.S3.** Crystal data and structure refinement for $[C_{48}H_{79}AlN_4Si_2][C_6H_6]$ (**3**).

| | | |
|---|---|---|
| Empirical formula | $C_{54}H_{85}AlN_4Si_2$ | |
| Formula weight | 873.41 | |
| Temperature | 90(2) K | |
| Wavelength | 1.54178 $Å^3$ | |
| Crystal system | Monoclinic | |
| Space group | P21/c | |
| Unit cell dimensions | a = 13.4017(2) | α = 90 |
| | b = 18.6679(2) | β = 96.50 |
| | c = 21.3897(3) | γ = 90 |
| Volume | 5316.93(12) $Å^3$ | |
| Z | 4 | |
| Density (calculated) | 1.091 g $cm^{-3}$ | |
| Absorption coefficient | 1.035 $mm^{-1}$ | |
| F(000) | 1912.0 | |
| Crystal size | 0.384 × 0.316 × 0.312 $mm^3$ | |
| Crystal color and habit | Colorless block | |
| Diffractometer | Bruker APEX-II CCD | |
| 2Θ range for data collection | 6.302 to 139.018° | |
| Index ranges | $-16 \leq h \leq 16$, $-22 \leq k \leq 22$, $-25 \leq l \leq 25$ | |
| Reflections collected | 26033 | |
| Independent reflections | 9694 [Rint = 0.0181, Rsigma = 0.0192] | |
| Observed reflections (I> 2sigma(I)) | 9483 | |
| Completeness to theta = 67.679 | 99.0% | |
| Absorption correction | Semi-empirical from equivalents | |
| Max. and min. transmission | 0.6210 and 0.5333 | |
| Solution method | SHELXT (Sheldrick, 2014) | |
| Refinement method | SHELXL-2017/1 (Sheldrick, 2017) Full-matrix least-squares on $F^2$ | |
| Data / restraints / parameters | 9694 / 0 / 572 | |
| Goodness-of-fit on $F^2$ | 1.036 | |
| Final R indexes [I>=2σ (I)] | R1 = 0.0402, wR2 = 0.1025 | |
| Final R indexes [all data] | R1 = 0.0408, wR2 = 0.1032 | |
| Largest diff. peak/hole | 0.80 / −0.49 e $Å^{-3}$ | |

**NMR Spectra**

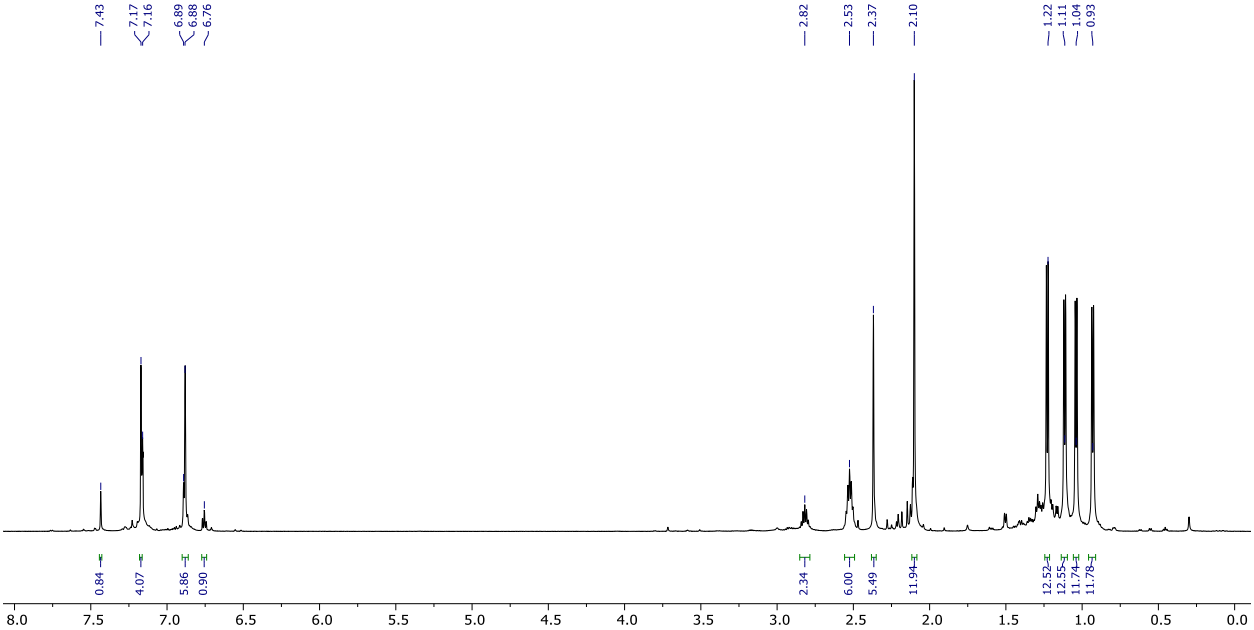


**Figure 6.S1.** $^{1}$H NMR spectrum (600 MHz, $C_6D_6$, 298 K) of $Ar^{iPr8}AlN^{Me6}$ (**1**).

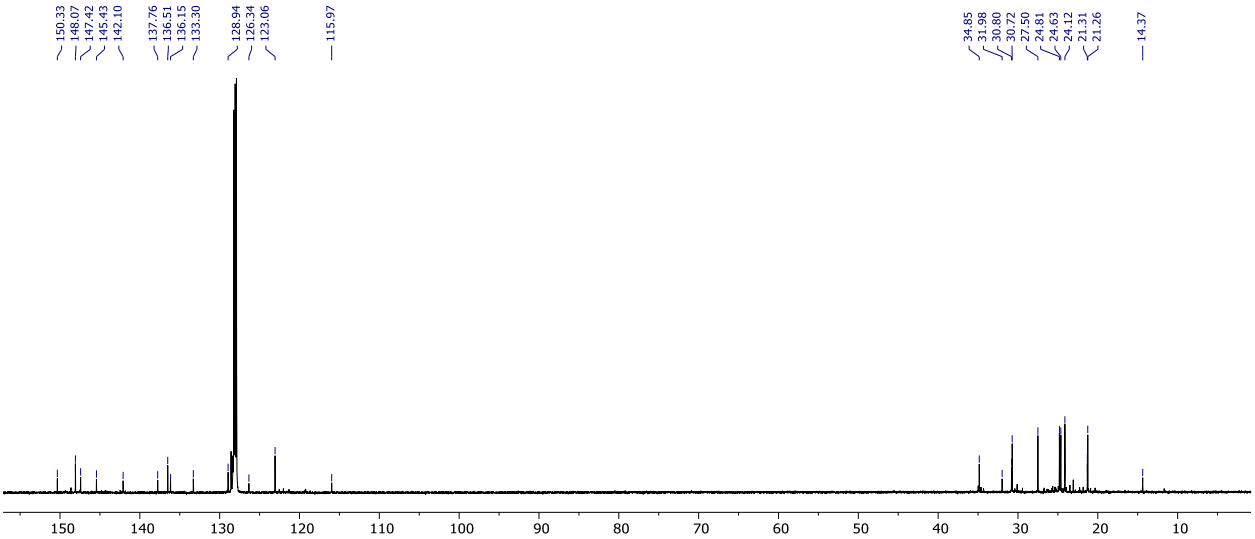


**Figure 6.S2.** $^{13}C\{^{1}H\}$ NMR spectrum (151 MHz, $C_6D_6$, 298 K) of $Ar^{iPr8}AlN^{Me6}$ (**1**).

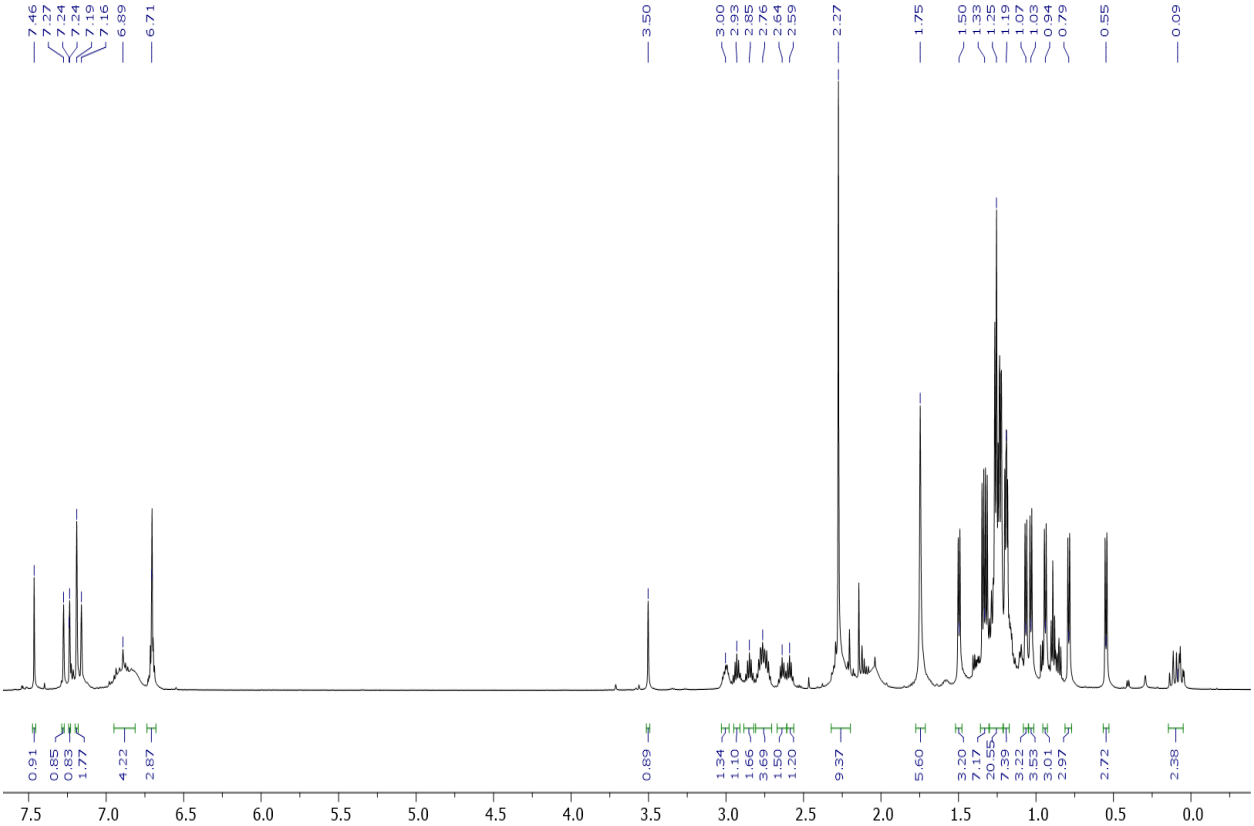


**Figure 6.S3.** $^{1}$H NMR spectrum (600 MHz, $C_6D_6$, 298 K) of the decomposition product of **1** after ca. 24 hours at ambient temperature.

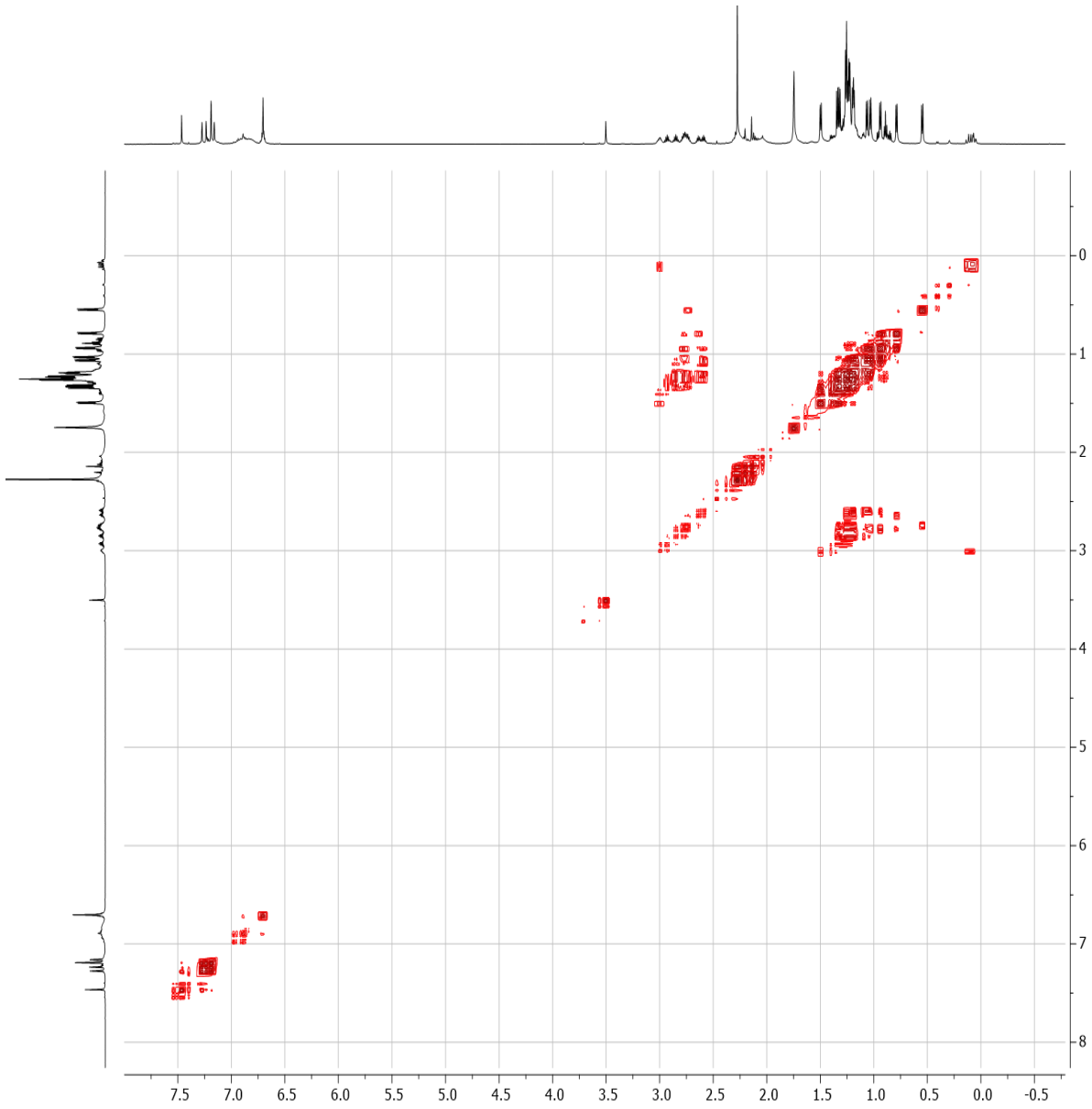


**Figure 6.S4.** $^{1}$H-$^{1}$H COSY NMR spectrum of the decomposition product of **1** after ca. 24 hours at ambient temperature.

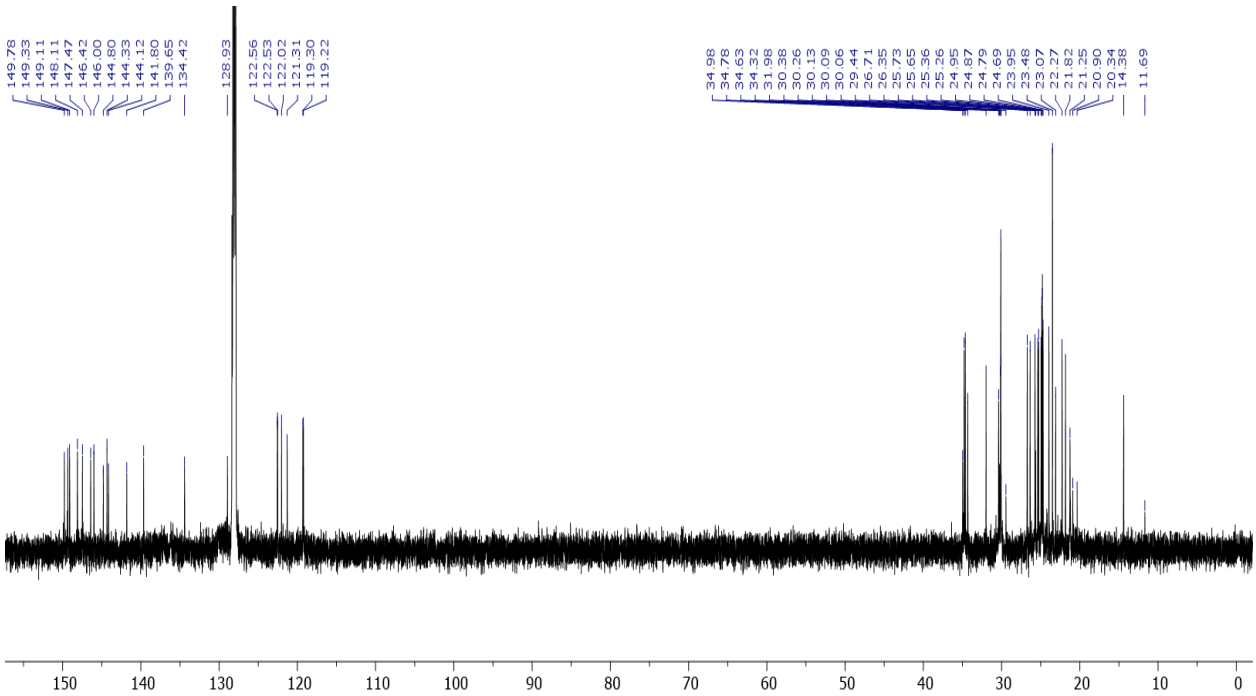


**Figure 6.S5.** $^{13}C\{^{1}H\}$ NMR spectrum (151 MHz, $C_6D_6$, 298 K) of the decomposition product of **1** after ca. 24 hours at ambient temperature.

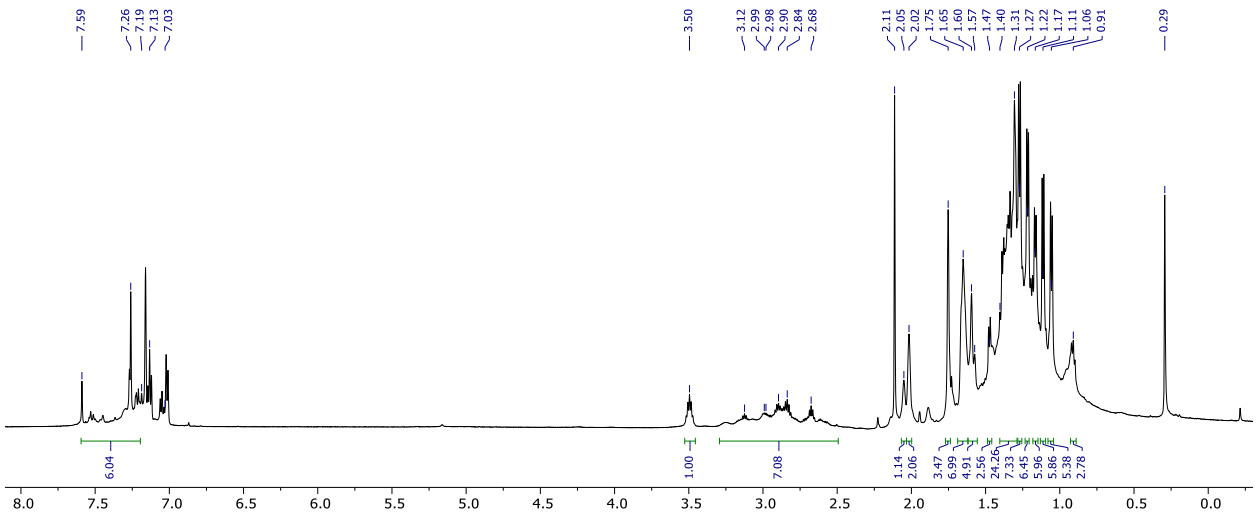


**Figure 6.S6.** $^1$H NMR spectrum (600 MHz, $C_6D_6$, 298 K) of $Ar^{iPr8}Al[(NAd)_2N_2]$ (**2**). Signals at 7.13, 7.03, and 2.11 correspond to toluene solvent of crystallization. A silicone grease impurity appears at 0.29 ppm.

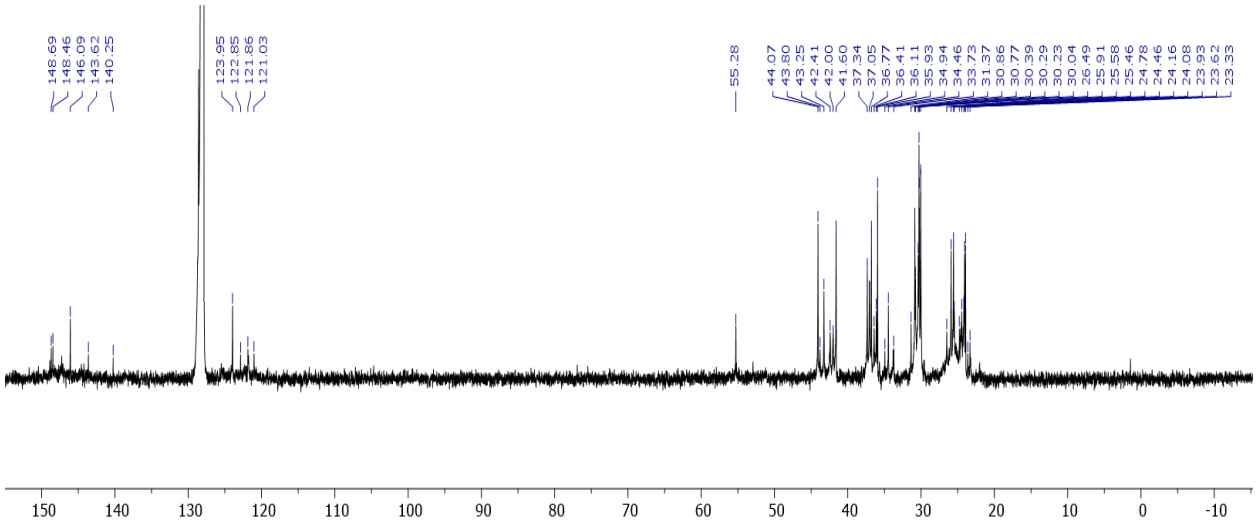


**Figure 6.S7.** $^{13}C\{^{1}H\}$ NMR spectrum (151 MHz, $C_6D_6$, 298 K) of $Ar^{iPr8}Al[(NAd)_2N_2]$ (**2**).

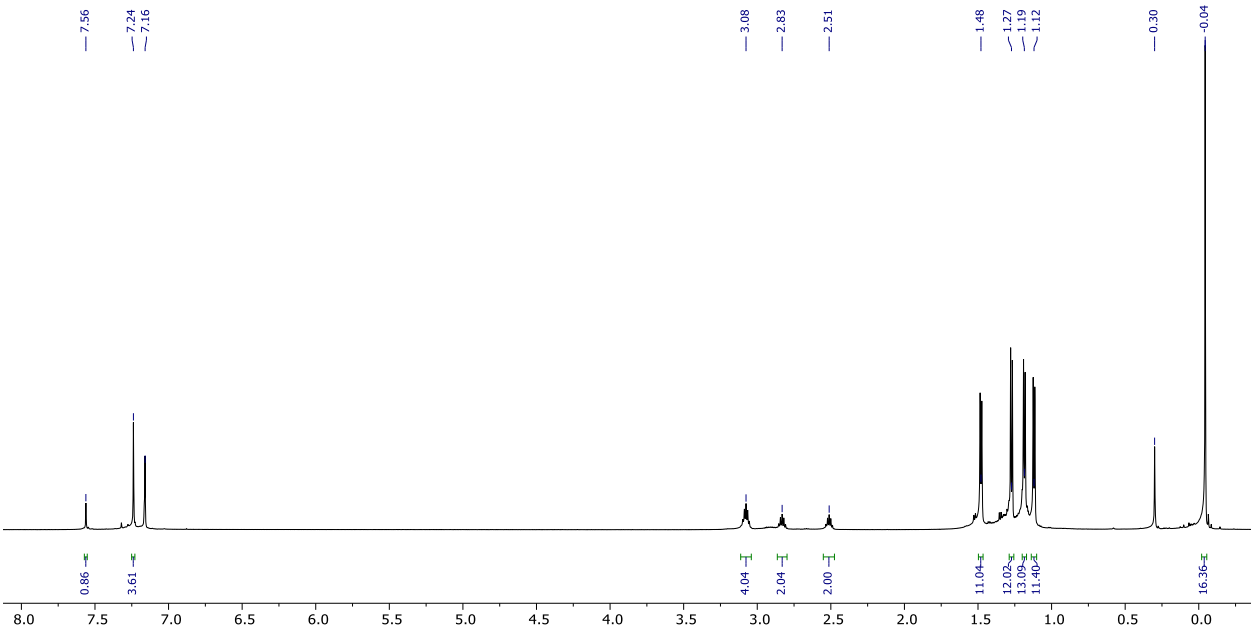


**Figure 6.S8.** $^{1}$H NMR spectrum (600 MHz, $C_6D_6$, 298 K) of $Ar^{iPr8}Al(N_3)N(SiMe_3)_2$ (**3**). A silicone grease impurity gives a signal at 0.30.

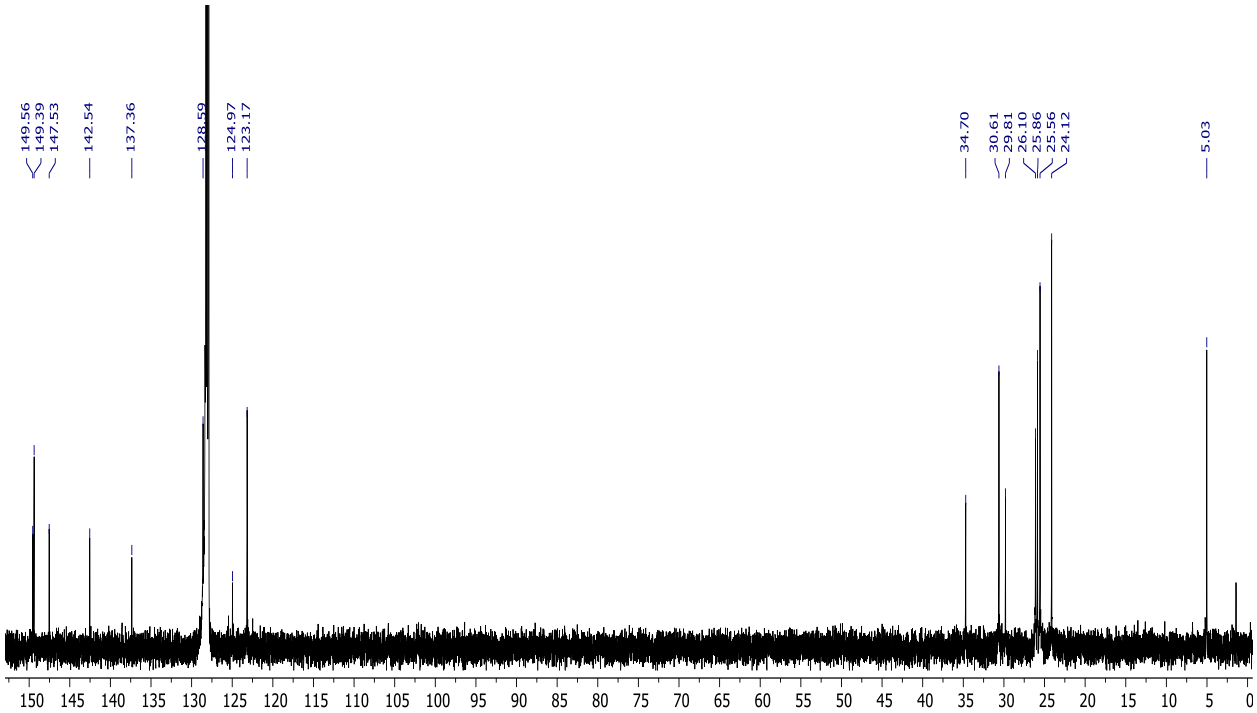


**Figure 6.S9.** $^{13}C\{^{1}H\}$ NMR spectrum (151 MHz, $C_6D_6$, 298K) of $Ar^{iPr8}Al(N_3)N(SiMe_3)_2$ (**3**).

**Electronic Spectrum and Photo of 1**

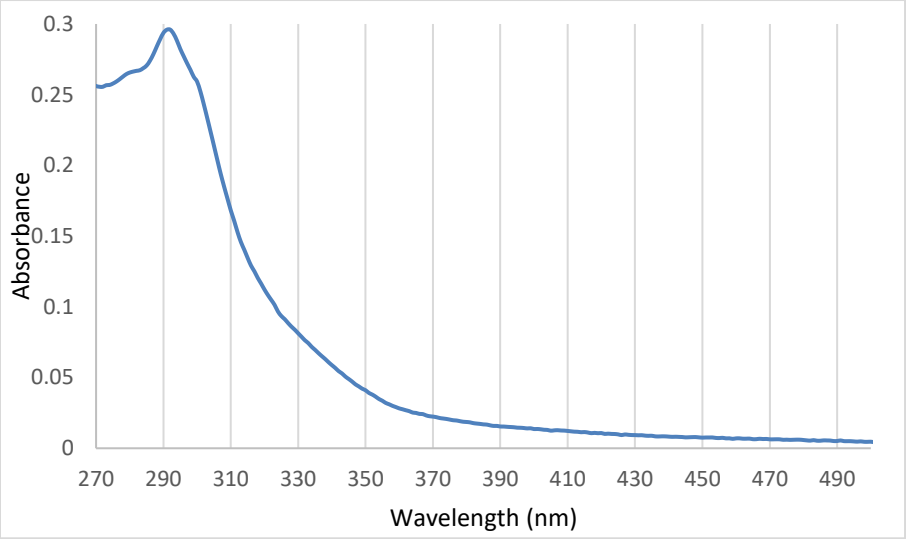


**Figure 6.S10**. UV-Visible spectrum (54 μM, hexanes) of $Ar^{iPr8}AlN^{Me6}$ (**1**). $\lambda_{max}$ = 292 nm.

**Figure 6.S11**. Photo of solid $Ar^{iPr8}AlNAr^{Me6}$ (**1**).

## Infrared Spectra

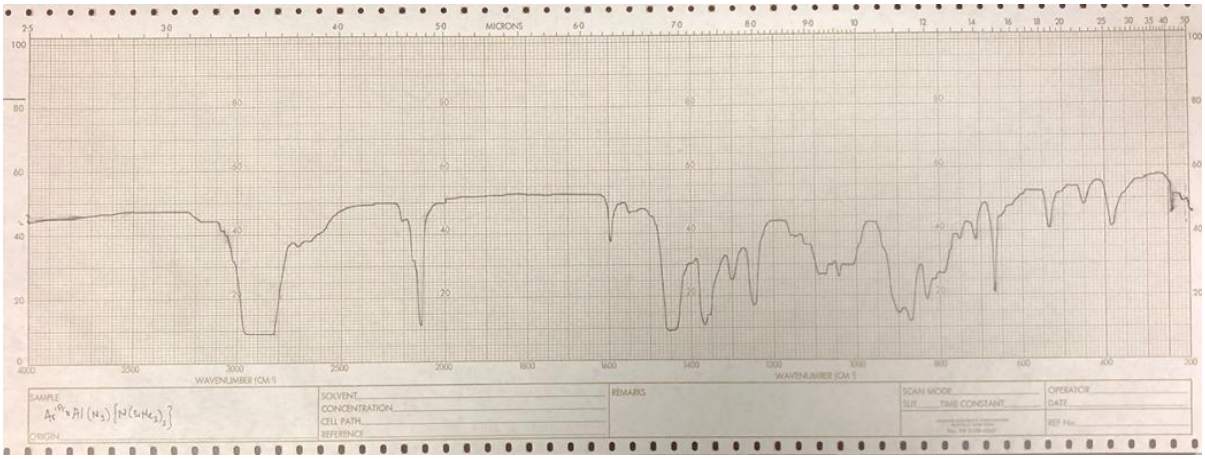


**Figure 6.S12.** Infrared spectrum (nujol, CsI) of **1.**

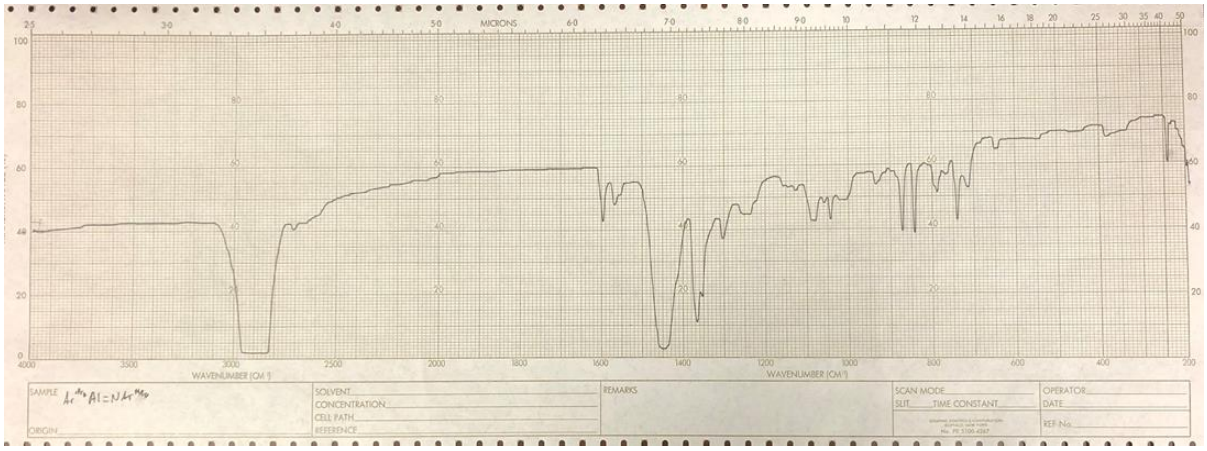


**Figure 6.S13**. Infrared spectrum (nujol, CsI) of **3**.

## Computational Details

The geometry of **1** was optimized in the gas phase with density functional theory using the PBE1PBE functional,[S11-S14] def2-TZVP basis sets,[S15] and Grimme's D3 dispersion correction with Becke-Johnson damping[S16,S17] and employing the Gaussian 16-C.01 program suite.[S18] The structure was confirmed to be a minimum on the potential energy hypersurface *via* calculation of the associated vibrational frequencies (all positive). Vertical excitation energies and associated oscillator strengths were calculated for **1** with the time-dependent density functional theory (TD-DFT), as implemented in the Gaussian program package,[S19] using the same functional-basis set combination as with prior geometry optimization (Figure S14). The bonding in **1** was analyzed by examining its Kohn-Sham orbitals (Figure S15), using Natural Atomic Orbital and Natural Bond Orbital analysis,[S20] and via energy decomposition analysis (Table S4 and Figure S16) within the extended transition state-natural orbitals for chemical valence (ETS-NOCV) framework,[S21] as available in the ADF 2019.3 program package.[S22,S23] These calculations employed the PBE1PBE functional,[S11-S14] TZ2P STO-basis sets[S24], Grimme's D3 dispersion correction with Becke-Johnson damping,[S16,S17] and treatment of scalar relativistic effects using the zero-order regular-approximated (ZORA) Hamiltonian.[S25] Finally, the formation of $Ar^{iPr8}Al(N_3)N(SiMe_3)_2$ (**3**) and $Ar^{iPr8}Al[(NSiMe_3)_2N_2]$ (the $SiMe_3$ analogue of **2**) from $Ar^{iPr8}Al$ and 2 equivalents of $Me_3SiN_3$ was examined computationally (Figure S17) by calculating the associated transformations and their free energies (kJ $mol^{-1}$).

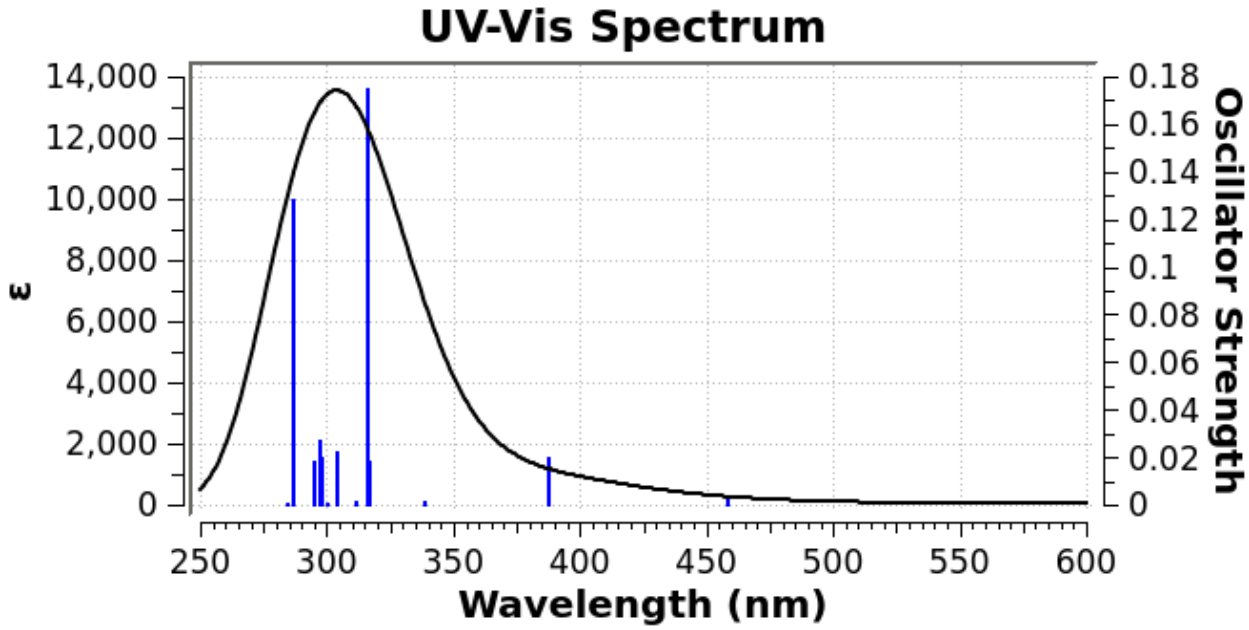


**Figure 6.S14.** Calculated UV-Visible spectrum of $Ar^{iPr8}AlNAr^{Me6}$ (**1**).

**Table 6.S4.** Summary of Results from Energy Decomposition Analysis for **1** [kJ mol$^{-1}$]

| | |
|---|---|
| Pauli repulsion | 1886 |
| Electrostatic interaction | -998 |
| Orbital interaction | -1350 |
| Dispersion | -89 |
| Total interaction energy | -551 |

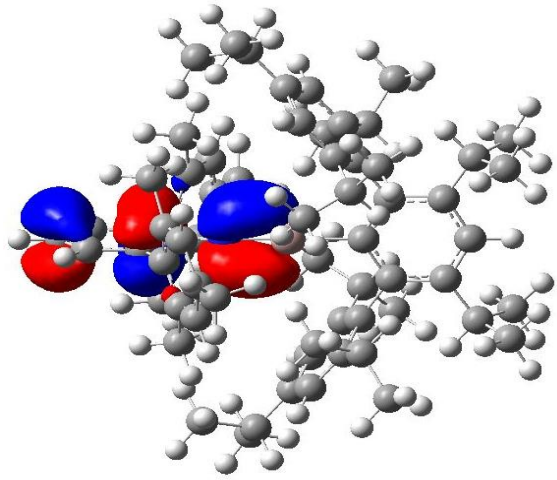

−0.180 a.u.
(−4.90 eV)

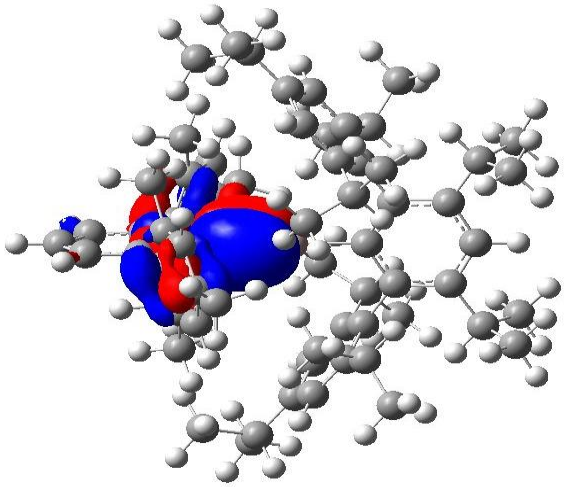

−0.216 a.u.
(−5.88 eV)

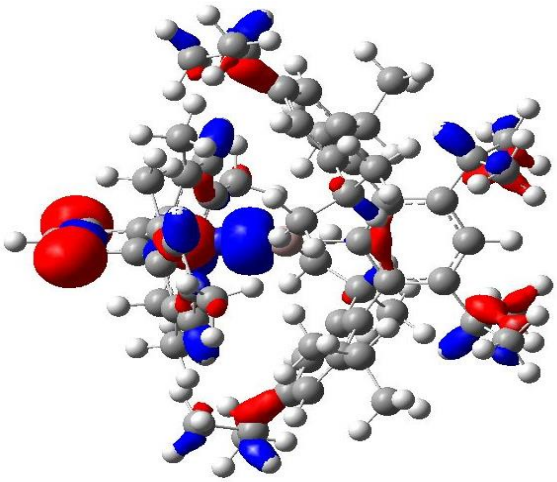

−0.481 a.u.
(−13.1 eV)

**Figure 6.S15.** Occupied PBE1PBE-GD3BJ/def2-TZVP orbitals of **1** primarily localized on the NAl bond (N moiety on the left, Al moiety on the right; isosurface value ± 0.03 a.u.).

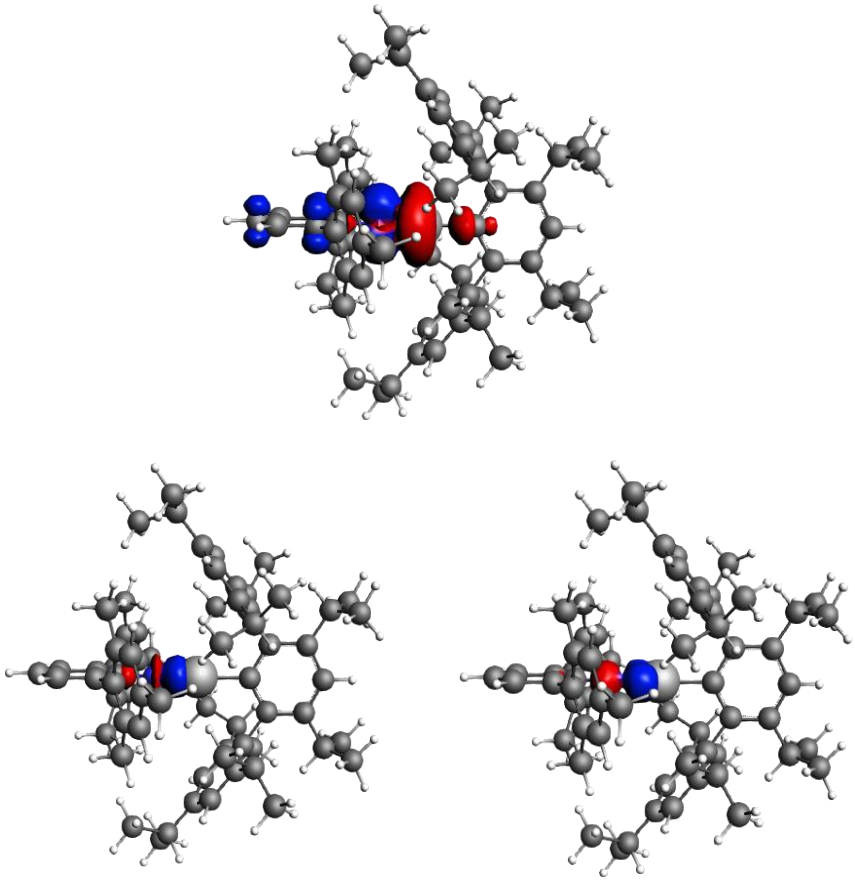

**Figure 6.S16.** Three most important ETS-NOCV deformation density contributions to AlN bonding in **1** (N moiety on the left, Al moiety on the right; isovalue = 0.001 a.u.). Donation from Al to N (top, 83 %) and back-donation from N to Al (bottom left and right, 8 % each). Red contour corresponds to depletion of electron density, whereas blue contour indicates accumulation of electron density.

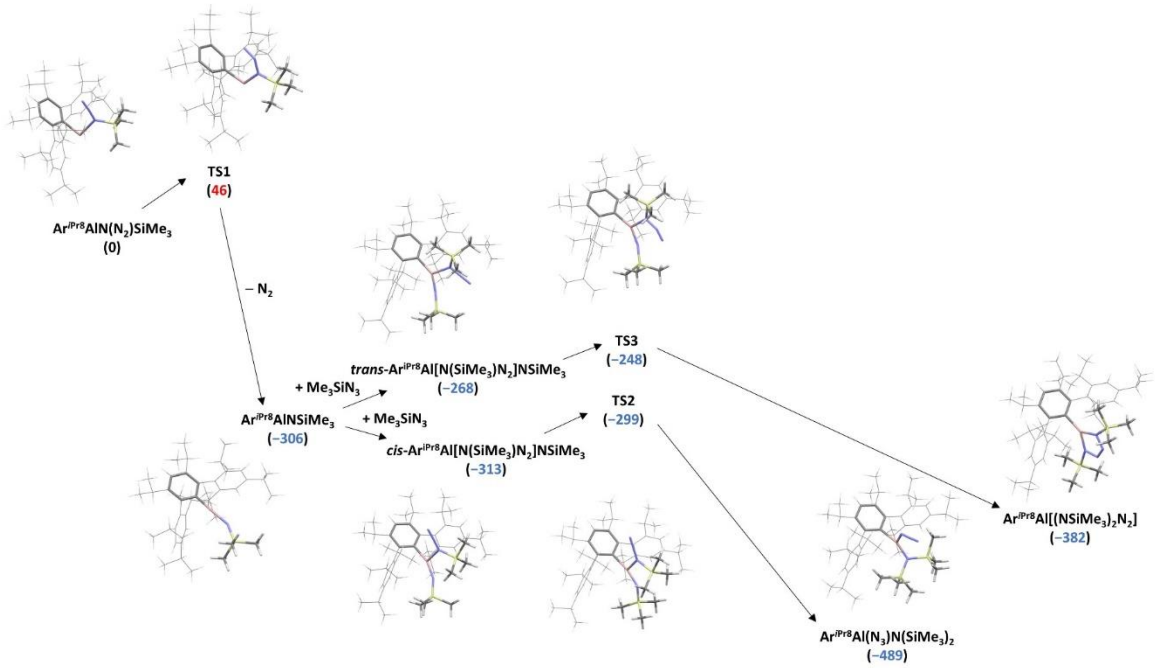


**Figure 6.S17.** Calculated pathways for the formation of $Ar^{iPr8}Al(N_3)N(SiMe_3)_2$ (**3**) and $Ar^{iPr8}Al[(NSiMe_3)_2N_2]$ from $Ar^{iPr8}Al$ and 2 equivalents of $Me_3SiN_3$. Standard Gibbs free energies are reported in kJ $mol^{-1}$.

## Optimized Coordinates

**Table 6.S5.** XYZ coordinates for $Ar^{iPr8}AlNAr^{Me6}$

154
1 - AriPr8AlNArMe6

| | | | |
|---|---|---|---|
| Al | 0.000000000000 | 0.000000000000 | 0.081800610963 |
| C | 0.000000000000 | 0.000000000000 | 3.063153812097 |
| N | 0.000000000000 | 0.000000000000 | 1.717171910523 |
| C | 1.114112895537 | 0.470008501502 | 3.804227448870 |
| C | 1.094754673585 | 0.463135791856 | 5.192633965908 |
| H | 1.970212464405 | 0.829671503220 | 5.719974644437 |
| C | 0.000000000000 | 0.000000000000 | 5.902703885829 |
| H | 0.000000000000 | 0.000000000000 | 6.986107599782 |
| C | 2.345795844748 | 0.977553321597 | 3.150422255374 |
| C | 3.338321005592 | 0.086664528907 | 2.733517838017 |
| C | 4.546696313130 | 0.586605373563 | 2.259278090315 |
| H | 5.317812796324 | -0.111247926923 | 1.945358420496 |
| C | 4.798102995475 | 1.949475005299 | 2.190359653251 |
| C | 3.794389498392 | 2.819046605063 | 2.597635087781 |
| H | 3.964419273951 | 3.891099798726 | 2.541109187800 |
| C | 2.569861295980 | 2.356010170284 | 3.060254864672 |
| C | 3.102110504830 | -1.389278329962 | 2.808549079045 |
| H | 2.263713742702 | -1.678481682378 | 2.167906505281 |
| H | 2.842290383331 | -1.698424516391 | 3.823948778456 |
| H | 3.987624580438 | -1.944168543451 | 2.493835676636 |
| C | 6.096572418017 | 2.472459528479 | 1.655720828567 |
| H | 6.465989456819 | 3.309747095399 | 2.252360152968 |
| H | 5.981502875193 | 2.834560223823 | 0.628545260828 |
| H | 6.863975779566 | 1.696472839456 | 1.647135506287 |
| C | 1.486391828721 | 3.320900147767 | 3.433330053971 |
| H | 1.230038137002 | 3.256743867499 | 4.493504816237 |
| H | 0.573505567625 | 3.094122333703 | 2.875924416414 |
| H | 1.784089113165 | 4.347740419874 | 3.212416109486 |
| C | 0.000000000000 | 0.000000000000 | -1.857771210275 |
| C | -0.357601196316 | 1.170039601984 | -2.542342752502 |
| C | -0.358787219589 | 1.171884487738 | -3.939097163557 |
| C | 0.000000000000 | 0.000000000000 | -4.594692014774 |
| H | 0.000000000000 | 0.000000000000 | -5.680379808194 |
| C | -0.727100351541 | 2.397403743894 | -4.741070702124 |
| H | -0.971148610253 | 3.189886013491 | -4.027389863843 |
| C | -1.955947765116 | 2.147419903823 | -5.610708187614 |
| H | -1.749577345427 | 1.390958788871 | -6.372660436561 |
| H | -2.254198607338 | 3.063637885942 | -6.126454744301 |
| H | -2.802806017045 | 1.799192509874 | -5.017389389031 |
| C | 0.444922815449 | 2.873881067860 | -5.594455406982 |
| H | 1.336539572609 | 3.044830562756 | -4.989258927192 |
| H | 0.194038467199 | 3.806386622159 | -6.106175857644 |
| H | 0.698898024236 | 2.134305311504 | -6.358685616648 |
| C | -0.706110120682 | 2.359043334892 | -1.711252972562 |
| C | -2.040742568350 | 2.599092740610 | -1.337446967589 |
| C | -2.313793376317 | 3.640461426796 | -0.463676944726 |
| H | -3.343052319056 | 3.825557384926 | -0.171166613060 |
| C | -1.315954057808 | 4.460205907910 | 0.053001646654 |
| C | -0.012017634068 | 4.222992337979 | -0.350798044977 |
| H | 0.784738067238 | 4.856122206563 | 0.019594903831 |

| | | | |
|---|---|---|---|
| C | 0.312517549059 | 3.195506492028 | -1.232274808703 |
| C | -3.175635856537 | 1.754014737065 | -1.870473918075 |
| H | -2.753369427527 | 1.057957827764 | -2.599990123366 |
| C | -3.818343335235 | 0.931270635106 | -0.761717252258 |
| H | -4.284708830265 | 1.579215990514 | -0.016358818706 |
| H | -3.089753851424 | 0.312920414103 | -0.233948173826 |
| H | -4.589974001345 | 0.268782315211 | -1.161831651800 |
| C | -4.220559276226 | 2.604620638009 | -2.586105824190 |
| H | -4.981498482815 | 1.967994239966 | -3.044920432339 |
| H | -3.770402009744 | 3.218950186533 | -3.368292071565 |
| H | -4.729286775332 | 3.275156214841 | -1.889043765325 |
| C | -1.689768873233 | 5.561035325945 | 1.020314070103 |
| H | -2.555800015611 | 6.074581989679 | 0.583528984796 |
| C | -2.132968759793 | 4.975495068195 | 2.360237566387 |
| H | -2.953652841987 | 4.267548402314 | 2.238400929530 |
| H | -2.464128499594 | 5.768852494920 | 3.035086892911 |
| H | -1.307509908644 | 4.444652489461 | 2.840146209889 |
| C | -0.596570813736 | 6.596116682136 | 1.229619477804 |
| H | -0.966296042863 | 7.408702410449 | 1.858501300451 |
| H | -0.256974836211 | 7.026907430771 | 0.284899268595 |
| H | 0.269025673518 | 6.161565510305 | 1.737395370338 |
| C | 1.748066573689 | 3.033181183843 | -1.678114730908 |
| H | 1.788164595103 | 2.186088992487 | -2.367576951083 |
| C | 2.669988968204 | 2.733712659231 | -0.505481030450 |
| H | 3.683953058131 | 2.518304110707 | -0.850321919687 |
| H | 2.329056435132 | 1.882477844722 | 0.089371335507 |
| H | 2.725095197756 | 3.582858512309 | 0.177629181994 |
| C | 2.228458578885 | 4.271509398142 | -2.430886867987 |
| H | 1.566524789145 | 4.518320183514 | -3.263063712842 |
| H | 3.234733370013 | 4.111753905315 | -2.826921856706 |
| H | 2.266490003771 | 5.140606743419 | -1.769166009239 |
| C | -1.114112895537 | -0.470008501502 | 3.804227448870 |
| C | -1.094754673585 | -0.463135791856 | 5.192633965908 |
| H | -1.970212464405 | -0.829671503220 | 5.719974644437 |
| C | -2.345795844748 | -0.977553321597 | 3.150422255374 |
| C | -3.338321005592 | -0.086664528907 | 2.733517838017 |
| C | -4.546696313130 | -0.586605373563 | 2.259278090315 |
| H | -5.317812796324 | 0.111247926923 | 1.945358420496 |
| C | -4.798102995475 | -1.949475005299 | 2.190359653251 |
| C | -3.794389498392 | -2.819046605063 | 2.597635087781 |
| H | -3.964419273951 | -3.891099798726 | 2.541109187800 |
| C | -2.569861295980 | -2.356010170284 | 3.060254864672 |
| C | -3.102110504830 | 1.389278329962 | 2.808549079045 |
| H | -2.263713742702 | 1.678481682378 | 2.167906505281 |
| H | -2.842290383331 | 1.698424516391 | 3.823948778456 |
| H | -3.987624580438 | 1.944168543451 | 2.493835676636 |
| C | -6.096572418017 | -2.472459528479 | 1.655720828567 |
| H | -6.465989456819 | -3.309747095399 | 2.252360152968 |
| H | -5.981502875193 | -2.834560223823 | 0.628545260828 |
| H | -6.863975779566 | -1.696472839456 | 1.647135506287 |
| C | -1.486391828721 | -3.320900147767 | 3.433330053971 |
| H | -1.230038137002 | -3.256743867499 | 4.493504816237 |
| H | -0.573505567625 | -3.094122333703 | 2.875924416414 |
| H | -1.784089113165 | -4.347740419874 | 3.212416109486 |
| C | 0.357601196316 | -1.170039601984 | -2.542342752502 |
| C | 0.358787219589 | -1.171884487738 | -3.939097163557 |

| | | | |
|---|---|---|---|
| C | 0.727100351541 | -2.397403743894 | -4.741070702124 |
| H | 0.971148610253 | -3.189886013491 | -4.027389863843 |
| C | 1.955947765116 | -2.147419903823 | -5.610708187614 |
| H | 1.749577345427 | -1.390958788871 | -6.372660436561 |
| H | 2.254198607338 | -3.063637885942 | -6.126454744301 |
| H | 2.802806017045 | -1.799192509874 | -5.017389389031 |
| C | -0.444922815449 | -2.873881067860 | -5.594455406982 |
| H | -1.336539572609 | -3.044830562756 | -4.989258927192 |
| H | -0.194038467199 | -3.806386622159 | -6.106175857644 |
| H | -0.698898024236 | -2.134305311504 | -6.358685616648 |
| C | 0.706110120682 | -2.359043334892 | -1.711252972562 |
| C | 2.040742568350 | -2.599092740610 | -1.337446967589 |
| C | 2.313793376317 | -3.640461426796 | -0.463676944726 |
| H | 3.343052319056 | -3.825557384926 | -0.171166613060 |
| C | 1.315954057808 | -4.460205907910 | 0.053001646654 |
| C | 0.012017634068 | -4.222992337979 | -0.350798044977 |
| H | -0.784738067238 | -4.856122206563 | 0.019594903831 |
| C | -0.312517549059 | -3.195506492028 | -1.232274808703 |
| C | 3.175635856537 | -1.754014737065 | -1.870473918075 |
| H | 2.753369427527 | -1.057957827764 | -2.599990123366 |
| C | 3.818343335235 | -0.931270635106 | -0.761717252258 |
| H | 4.284708830265 | -1.579215990514 | -0.016358818706 |
| H | 3.089753851424 | -0.312920414103 | -0.233948173826 |
| H | 4.589974001345 | -0.268782315211 | -1.161831651800 |
| C | 4.220559276226 | -2.604620638009 | -2.586105824190 |
| H | 4.981498482815 | -1.967994239966 | -3.044920432339 |
| H | 3.770402009744 | -3.218950186533 | -3.368292071565 |
| H | 4.729286775332 | -3.275156214841 | -1.889043765325 |
| C | 1.689768873233 | -5.561035325945 | 1.020314070103 |
| H | 2.555800015611 | -6.074581989679 | 0.583528984796 |
| C | 2.132968759793 | -4.975495068195 | 2.360237566387 |
| H | 2.953652841987 | -4.267548402314 | 2.238400929530 |
| H | 2.464128499594 | -5.768852494920 | 3.035086892911 |
| H | 1.307509908644 | -4.444652489461 | 2.840146209889 |
| C | 0.596570813736 | -6.596116682136 | 1.229619477804 |
| H | 0.966296042863 | -7.408702410449 | 1.858501300451 |
| H | 0.256974836211 | -7.026907430771 | 0.284899268595 |
| H | -0.269025673518 | -6.161565510305 | 1.737395370338 |
| C | -1.748066573689 | -3.033181183843 | -1.678114730908 |
| H | -1.788164595103 | -2.186088992487 | -2.367576951083 |
| C | -2.669988968204 | -2.733712659231 | -0.505481030450 |
| H | -3.683953058131 | -2.518304110707 | -0.850321919687 |
| H | -2.329056435132 | -1.882477844722 | 0.089371335507 |
| H | -2.725095197756 | -3.582858512309 | 0.177629181994 |
| C | -2.228458578885 | -4.271509398142 | -2.430886867987 |
| H | -1.566524789145 | -4.518320183514 | -3.263063712842 |
| H | -3.234733370013 | -4.111753905315 | -2.826921856706 |
| H | -2.266490003771 | -5.140606743419 | -1.769166009239 |

**Table 6.S6.** XYZ Coordinates for $Ar^{iPr8}AlN(N_2)SiMe_3$

120

$Ar^{iPr8}AlN(N_2)SiMe_3$

| | | | |
|---|---|---|---|
| C | 3.352058620033 | -0.288738780025 | -0.573026741444 |
| C | 2.337045983488 | -0.722292582388 | 0.300777947472 |
| C | 2.503328991089 | -0.481394877667 | 1.691463978542 |

| | | | |
|---|---|---|---|
| C | 3.626930717688 | 0.200720169892 | 2.138028824271 |
| C | 4.616978871270 | 0.653669185527 | 1.278771245413 |
| C | 4.460799950950 | 0.384913306744 | -0.065434153866 |
| C | 1.057534435430 | -1.357802811957 | -0.176945845163 |
| C | -0.122122016141 | -0.610765317824 | 0.009883311103 |
| C | -1.371293536757 | -1.166071551832 | -0.311842831304 |
| C | -1.449433982062 | -2.450034063655 | -0.864728151623 |
| C | -0.265398815364 | -3.147309121016 | -1.054045476715 |
| C | 0.987234565118 | -2.652695163619 | -0.712232004620 |
| C | -2.592107433357 | -0.369803724787 | 0.063920884715 |
| C | -3.018533266579 | -0.378153890654 | 1.409593377743 |
| C | -4.065766374051 | 0.442136438331 | 1.806411863486 |
| C | -4.728766916555 | 1.275942290411 | 0.919730460269 |
| C | -4.334190500950 | 1.239136777871 | -0.405551901524 |
| C | -3.294128967289 | 0.430515590243 | -0.854369871760 |
| C | -2.420932705151 | -1.306286187975 | 2.445356377501 |
| C | -1.938576791126 | -0.559480948818 | 3.683277795232 |
| C | -3.003294423248 | 0.426543255604 | -2.337650999171 |
| C | -2.721219601032 | 1.827845645235 | -2.875247289816 |
| C | -5.838038301767 | 2.189292503936 | 1.377306535158 |
| C | -5.314879524130 | 3.246939617319 | 2.344916525758 |
| Al | -0.040432379723 | 1.258771025594 | 0.823923592448 |
| N | 0.415167931405 | 2.055627050681 | -1.295371474273 |
| Si | 0.893194434571 | 3.783393945786 | -1.436503397967 |
| C | 2.432755908264 | 3.964713217657 | -0.414555528460 |
| C | 2.187424084553 | -3.546297415522 | -0.940854227936 |
| C | 2.143513496935 | -4.820106341484 | -0.098852334627 |
| C | -2.752043416169 | -3.111367762911 | -1.248567683043 |
| C | -2.989011950991 | -4.396969566367 | -0.460401963641 |
| C | 1.523838641160 | -1.006612971511 | 2.727834686102 |
| C | 1.618820142444 | -0.310736930943 | 4.076716473249 |
| C | 5.810461510070 | 1.420488382101 | 1.790211495264 |
| C | 5.389479939678 | 2.762612745999 | 2.382348543360 |
| C | 3.328379448411 | -0.500606124650 | -2.072352565164 |
| C | 3.438316406784 | 0.820102531291 | -2.834577192377 |
| C | 1.669690638474 | -2.514853089702 | 2.898525615604 |
| C | 4.472568662440 | -1.406820335760 | -2.527450182743 |
| C | 6.618790699522 | 0.607827586705 | 2.796303888012 |
| C | -2.798581324872 | -3.404408314305 | -2.746489102087 |
| C | 2.313209789876 | -3.928700624548 | -2.415011976668 |
| C | -4.168833388481 | -0.185287308580 | -3.113794158701 |
| C | -6.997571669544 | 1.410973475155 | 1.990401375960 |
| C | -3.435479930710 | -2.376577392361 | 2.843448414316 |
| C | 1.169889503956 | 4.119662266592 | -3.248423266413 |
| C | -0.523063188054 | 4.768260338843 | -0.751144965458 |
| H | -0.322190967972 | -4.146585030757 | -1.474091712960 |
| H | -4.860637529611 | 1.864523400467 | -1.120161607214 |
| H | -4.372244681982 | 0.426966512469 | 2.846969083508 |
| H | -2.118708664497 | -0.192623406540 | -2.502457368010 |
| H | -4.425245321143 | -1.177954227211 | -2.744118371506 |
| H | -3.923223095445 | -0.268974758853 | -4.175990040156 |
| H | -5.059844023396 | 0.441851180881 | -3.024545481870 |
| H | -3.629209778266 | 2.436092919347 | -2.876920424461 |
| H | -2.356808754300 | 1.777921327123 | -3.904221527230 |
| H | -1.984607570633 | 2.351671095551 | -2.265460087457 |
| H | -6.214428190378 | 2.705399805328 | 0.486683850518 |

| | | | |
|---|---|---|---|
| H | -7.386849074335 | 0.667033156807 | 1.292161842596 |
| H | -7.813080277208 | 2.084857601246 | 2.265555524168 |
| H | -6.682245525321 | 0.885480915174 | 2.895680707783 |
| H | -4.932610936518 | 2.783441973787 | 3.258285540633 |
| H | -6.110359553110 | 3.941016682569 | 2.628862622364 |
| H | -4.498928068392 | 3.819515729601 | 1.899109495692 |
| H | -1.563048717927 | -1.807912794656 | 1.991980531202 |
| H | -4.282994183249 | -1.929147575308 | 3.369930295858 |
| H | -2.978015262303 | -3.113453808978 | 3.509177909213 |
| H | -3.830411132466 | -2.898444480059 | 1.970987277871 |
| H | -1.243340172954 | 0.243087227749 | 3.425051855232 |
| H | -1.437575617015 | -1.246431771390 | 4.369757950065 |
| H | -2.773951584049 | -0.108080189312 | 4.224601159813 |
| H | 5.230390920324 | 0.720823169363 | -0.753757216198 |
| H | 3.734791042574 | 0.389506062394 | 3.197855783612 |
| H | 2.377140822447 | -0.968912137673 | -2.333168017884 |
| H | 5.435373298435 | -0.923326328871 | -2.343470664623 |
| H | 4.400697672846 | -1.604973263661 | -3.600110668600 |
| H | 4.479649291566 | -2.362804100226 | -2.006472732735 |
| H | 2.770226054757 | 1.578551904524 | -2.431686179210 |
| H | 3.203614808180 | 0.675096112366 | -3.891546938776 |
| H | 4.452790911380 | 1.222050134857 | -2.772704287376 |
| H | 6.454737718671 | 1.621419640168 | 0.926488721103 |
| H | 6.028283845071 | 0.391182846475 | 3.690348168776 |
| H | 7.508532531615 | 1.158620320709 | 3.112199601520 |
| H | 6.937919348381 | -0.344988585419 | 2.368816018244 |
| H | 4.839899950964 | 3.360869052173 | 1.652567914669 |
| H | 6.262477319097 | 3.333668242111 | 2.709270272562 |
| H | 4.739374305298 | 2.618409353796 | 3.249420849431 |
| H | 0.513115313284 | -0.837107397239 | 2.346733755840 |
| H | 1.444252317313 | -3.030618092830 | 1.967204229652 |
| H | 0.978900455611 | -2.880589183924 | 3.663082053853 |
| H | 2.687123065465 | -2.775750418254 | 3.203286265648 |
| H | 2.555761365654 | -0.541917038337 | 4.590837751872 |
| H | 0.808239750380 | -0.652591415382 | 4.721775664352 |
| H | 1.534275497816 | 0.773967817444 | 3.976198881348 |
| H | -3.558413424404 | -2.412938774599 | -1.005026964591 |
| H | -2.591132449442 | -2.512236590524 | -3.338563861780 |
| H | -3.779656676664 | -3.789926766650 | -3.037304120771 |
| H | -2.053622940926 | -4.158325391782 | -3.014456796201 |
| H | -2.246947963780 | -5.156243367146 | -0.721269445811 |
| H | -3.976862769189 | -4.809424829929 | -0.682475104752 |
| H | -2.921110473586 | -4.227805595893 | 0.614657384515 |
| H | 3.076030984346 | -2.985011729441 | -0.642626449204 |
| H | 1.491354489493 | -4.584840124284 | -2.712614634289 |
| H | 3.246322498741 | -4.468228234715 | -2.597100080094 |
| H | 2.289113898318 | -3.055984234256 | -3.068162042310 |
| H | 2.145960167562 | -4.607609297109 | 0.969861552265 |
| H | 3.012938984140 | -5.446061265737 | -0.317437794615 |
| H | 1.248187128113 | -5.406106681059 | -0.322021419014 |
| H | -0.266164767993 | 5.830977386887 | -0.720190284431 |
| H | -1.422833887627 | 4.650575265143 | -1.359195679852 |
| H | -0.749740186035 | 4.437525431682 | 0.265502943289 |
| H | 2.774591548021 | 5.003613320329 | -0.413403829307 |
| H | 2.226265942290 | 3.667733438595 | 0.617112884169 |
| H | 3.239551166250 | 3.332276953283 | -0.791045481255 |

| | | | |
|---|---|---|---|
| H | 1.431875438823 | 5.171432847467 | -3.392405520208 |
| H | 1.981692774349 | 3.515328323763 | -3.659356721241 |
| H | 0.266138726959 | 3.921286849816 | -3.830598221466 |
| N | 0.345284937825 | 1.293165337841 | -2.248564041103 |
| N | 0.251783390836 | 0.529190977945 | -3.064909187666 |

**Table 6.S7.** XYZ Coordinates for Transition state 1.

120

TS1

| | | | |
|---|---|---|---|
| C | -2.639039213519 | -0.613141294191 | 1.577611330540 |
| C | -2.371275029877 | -0.763898729929 | 0.198135070471 |
| C | -3.307532012862 | -0.254547622255 | -0.723760400178 |
| C | -4.419345734154 | 0.437550770416 | -0.253919622353 |
| C | -4.660936476663 | 0.642556435034 | 1.092911883513 |
| C | -3.762946888093 | 0.090892341678 | 1.991664932071 |
| C | -1.067389101977 | -1.383728491867 | -0.222571293170 |
| C | 0.097653434750 | -0.619530230822 | -0.018144236993 |
| C | 1.373016775313 | -1.136805294128 | -0.302576854119 |
| C | 1.480855678217 | -2.405683969913 | -0.891277156683 |
| C | 0.314649700447 | -3.135438096203 | -1.076537497921 |
| C | -0.952275839233 | -2.680991696975 | -0.731483913214 |
| C | 2.579846197709 | -0.349848177512 | 0.122715502770 |
| C | 2.895994065852 | -0.273678892693 | 1.503607835234 |
| C | 4.027414961334 | 0.423611421032 | 1.901728696188 |
| C | 4.867722177760 | 1.061789668822 | 0.999609038828 |
| C | 4.536336605444 | 0.995171361347 | -0.338316142308 |
| C | 3.414976469768 | 0.308406502961 | -0.796576851962 |
| C | 2.045258425528 | -0.948871412468 | 2.564928163822 |
| C | 2.248192969121 | -2.460625302524 | 2.587395136395 |
| C | 3.144322967811 | 0.352679072737 | -2.283738502874 |
| C | 4.292924691028 | -0.238683527754 | -3.098188550928 |
| C | 6.085784226416 | 1.818941170864 | 1.465660567706 |
| C | 7.075580228418 | 0.905882698629 | 2.182249644685 |
| Al | -0.096058781910 | 1.279923537344 | 0.485894455775 |
| N | -0.335950772394 | 2.219646270588 | -1.111752587793 |
| N | -0.300765706925 | 1.576430878589 | -2.426232295265 |
| N | -0.080387660036 | 0.562796938775 | -2.873931407455 |
| C | -2.123933754759 | -3.623475475702 | -0.866090488364 |
| C | -2.260026289958 | -4.175158624599 | -2.281974666630 |
| C | 2.792628980488 | -3.016056046398 | -1.334426104166 |
| C | 2.763746089956 | -3.307598501412 | -2.833756592890 |
| C | -3.196142544064 | -0.439979555394 | -2.221276237253 |
| C | -4.273008372286 | -1.402100930079 | -2.724960360394 |
| C | -5.859708332429 | 1.430223471260 | 1.558369455374 |
| C | -6.781235958539 | 0.591660059757 | 2.438149675095 |
| C | -1.803841614975 | -1.286283602529 | 2.646139865439 |
| C | -2.595128257554 | -2.427729993623 | 3.283804696649 |
| C | -3.331470527308 | 0.878615024215 | -2.981495336263 |
| C | -1.330011323006 | -0.314674672282 | 3.719024049457 |
| C | -5.434991794617 | 2.710399705804 | 2.271989060635 |
| Si | -0.806336602435 | 3.935499782478 | -1.181731134492 |
| C | 0.526635388557 | 4.971202733430 | -0.384091294166 |
| C | -0.977167557633 | 4.405235462426 | -2.982658425788 |
| C | -2.438996503576 | 4.160855528531 | -0.300654096250 |
| C | 3.149161265391 | -4.286438837339 | -0.567147726474 |
| C | -2.009480267699 | -4.770517571861 | 0.135933897763 |

| | | | |
|---|---|---|---|
| C | 2.894711378353 | 1.790418088355 | -2.739221846669 |
| C | 5.699914701772 | 3.005353617231 | 2.344171937350 |
| C | 2.246884193155 | -0.379532250533 | 3.961603685903 |
| H | 0.401231475384 | -4.133637915646 | -1.493739158718 |
| H | -5.126141529078 | 0.840793898893 | -0.972138892229 |
| H | -3.946369642174 | 0.198575924193 | 3.055274072770 |
| H | -2.213323303557 | -0.866153733512 | -2.437213362845 |
| H | -4.250003654922 | -2.359402459833 | -2.206434871748 |
| H | -4.148804063873 | -1.590270944527 | -3.794741500467 |
| H | -5.265589870294 | -0.968836460416 | -2.575522204834 |
| H | -4.367372921758 | 1.226982912356 | -2.978962201280 |
| H | -3.031368751357 | 0.749425815808 | -4.023814274126 |
| H | -2.718791430754 | 1.665206222605 | -2.544904399783 |
| H | -6.421081754742 | 1.716199487918 | 0.661697005026 |
| H | -7.101039363129 | -0.316522362685 | 1.922978946352 |
| H | -7.671720785047 | 1.160885945261 | 2.716763108883 |
| H | -6.277731487677 | 0.292034204844 | 3.361118520106 |
| H | -4.867341676891 | 2.480813688007 | 3.177866082159 |
| H | -6.308700829072 | 3.298338068537 | 2.565000274191 |
| H | -4.803014246961 | 3.328403061853 | 1.631156207456 |
| H | -0.926179670618 | -1.720618076580 | 2.163243379894 |
| H | -3.452423067478 | -2.042442725691 | 3.842223450685 |
| H | -1.966038301723 | -2.990318321193 | 3.978782370907 |
| H | -2.977480855403 | -3.117576544158 | 2.529961827698 |
| H | -0.735951680783 | 0.499616245095 | 3.293264269666 |
| H | -0.718716092804 | -0.832927069665 | 4.460407933714 |
| H | -2.172256750764 | 0.137552535356 | 4.247952245491 |
| H | 5.170840029809 | 1.503573301054 | -1.057508990698 |
| H | 4.264094029556 | 0.477840581498 | 2.956318288264 |
| H | 2.240820034603 | -0.229271829739 | -2.479415448256 |
| H | 5.193233078715 | 0.373524055724 | -3.001910206192 |
| H | 4.028827054453 | -0.270688156493 | -4.158374330342 |
| H | 4.545519111110 | -1.250475065506 | -2.781945839005 |
| H | 2.144903168578 | 2.283362340739 | -2.120441064057 |
| H | 2.556199692966 | 1.810926362086 | -3.777983898094 |
| H | 3.813620675501 | 2.379022385749 | -2.675680828717 |
| H | 6.579442706974 | 2.211392300596 | 0.569413208443 |
| H | 6.637913374830 | 0.493669738435 | 3.095346530446 |
| H | 7.975728231681 | 1.457710750791 | 2.465104942039 |
| H | 7.371167377495 | 0.068286540941 | 1.547015096234 |
| H | 5.010543815658 | 3.673605008609 | 1.823914472262 |
| H | 6.585081920199 | 3.578838205335 | 2.631418347068 |
| H | 5.208478094551 | 2.668580880138 | 3.260869464546 |
| H | 1.001668917789 | -0.775405189357 | 2.292653221996 |
| H | 1.938984463432 | -2.914318583132 | 1.647441295436 |
| H | 1.654597777998 | -2.910191008367 | 3.388242512109 |
| H | 3.298850778529 | -2.708008599053 | 2.764305754183 |
| H | 3.237481841313 | -0.615862987224 | 4.359346591901 |
| H | 1.518553700282 | -0.818911602805 | 4.644985887930 |
| H | 2.118701185064 | 0.705148165150 | 3.982427819678 |
| H | -3.027408967875 | -3.057900825198 | -0.622315897627 |
| H | -2.279503395474 | -3.377709792535 | -3.025829445330 |
| H | -3.178544069890 | -4.759518563508 | -2.381424189882 |
| H | -1.424624326044 | -4.836225904770 | -2.526059717413 |
| H | -1.136086032691 | -5.390295167518 | -0.084486522443 |
| H | -2.894474748954 | -5.411129182834 | 0.094602522036 |

| | | | |
|---|---|---|---|
| H | -1.900516185077 | -4.400180676549 | 1.156171985698 |
| H | 3.578585396296 | -2.283181251152 | -1.138511527564 |
| H | 2.050506418651 | -4.104422970248 | -3.060259305756 |
| H | 3.746533783791 | -3.635649850313 | -3.182398127108 |
| H | 2.470391059264 | -2.428933500267 | -3.409790310106 |
| H | 3.278776301902 | -4.094218403116 | 0.497826500610 |
| H | 4.083053706702 | -4.707191790604 | -0.949053553949 |
| H | 2.372316310081 | -5.047438665322 | -0.680497053979 |
| H | -2.799157851524 | 5.189250553625 | -0.400513304692 |
| H | -3.195431595223 | 3.489506328152 | -0.715426524386 |
| H | -2.340494302353 | 3.934275162516 | 0.763420370558 |
| H | 0.290777716469 | 6.035860572996 | -0.476080945394 |
| H | 0.630474327744 | 4.734403732706 | 0.676616547520 |
| H | 1.491784761408 | 4.794130631501 | -0.865662260758 |
| H | -1.241623887739 | 5.463759960560 | -3.061645956354 |
| H | -0.041044768069 | 4.251331887764 | -3.524851839991 |
| H | -1.756093949443 | 3.826329165065 | -3.483930675679 |

**Table 6.S7.** XYZ coordinates for $Ar^{iPr8}AlNSiMe_3$

118

AriPr8AlNSiMe3

| | | | |
|---|---|---|---|
| C | 2.903292172200 | -0.619282452395 | -1.070720817962 |
| C | 2.212084121135 | -0.962986886325 | 0.107037934711 |
| C | 2.704447342782 | -0.532900255316 | 1.350871854064 |
| C | 3.873164533032 | 0.221683909034 | 1.388290334891 |
| C | 4.565077739997 | 0.571573702294 | 0.241330405661 |
| C | 4.060112784906 | 0.140092759328 | -0.978724024162 |
| C | 0.899088219743 | -1.670710074017 | 0.017253942365 |
| C | -0.241377900268 | -0.859864291150 | 0.025951468094 |
| C | -1.529937441574 | -1.391581702987 | -0.083306274769 |
| C | -1.685462755898 | -2.773144239782 | -0.215869161508 |
| C | -0.538888860741 | -3.562334424019 | -0.208975107005 |
| C | 0.751337937935 | -3.055059243021 | -0.090919382421 |
| C | -2.653251317571 | -0.410733169997 | -0.030368708552 |
| C | -2.985648084215 | 0.349336246228 | -1.166502793602 |
| C | -3.929831074579 | 1.360473692886 | -1.047087355096 |
| C | -4.549953263285 | 1.652554405701 | 0.158499286535 |
| C | -4.223278795320 | 0.878527111138 | 1.260988873941 |
| C | -3.290377503028 | -0.148757693602 | 1.193134753577 |
| C | -2.364163535884 | 0.087826647056 | -2.521469529796 |
| C | -3.393352870182 | -0.511646399872 | -3.476658677188 |
| C | -2.945705481904 | -0.918651055148 | 2.448221660476 |
| C | -4.182797401199 | -1.495373322217 | 3.127753800045 |
| C | -5.518735631852 | 2.801797474380 | 0.278766461091 |
| C | -6.718805505839 | 2.635966787655 | -0.647418778476 |
| Al | 0.050204514268 | 1.043352579131 | 0.148858139860 |
| C | 1.935747778708 | -3.991665811818 | -0.080840374118 |
| C | 1.897591946627 | -4.914261378697 | 1.134215051894 |
| C | -3.042850889972 | -3.416546507717 | -0.372185403806 |
| C | -3.341779658712 | -4.393395977384 | 0.761198901972 |
| C | 2.015456097103 | -0.874151413784 | 2.653746902983 |
| C | 2.879131912875 | -1.806248808491 | 3.499435589279 |
| C | 5.830609540828 | 1.388888459339 | 0.319610891047 |
| C | 7.036312653794 | 0.576816982902 | -0.145056145672 |
| C | 2.390655310361 | -1.018316940492 | -2.436372598762 |
| C | 3.447352155211 | -1.753504748188 | -3.253845880513 |

| | | | |
|---|---|---|---|
| C | 2.025329988838 | -4.803481873585 | -1.369588485359 |
| C | -3.168591830701 | -4.111738818453 | -1.725112011768 |
| C | 1.649593409494 | 0.380716541404 | 3.441652506601 |
| C | 5.714948057350 | 2.694798812669 | -0.459208531317 |
| C | 1.870579026522 | 0.201028212571 | -3.191683933157 |
| C | -2.149197441103 | -0.046876264450 | 3.414042166051 |
| C | -4.812653044168 | 4.132980916315 | 0.034053238690 |
| C | -1.746561449912 | 1.348006725665 | -3.121551288171 |
| H | -0.658451938730 | -4.637430035383 | -0.303394635703 |
| H | 4.254402317349 | 0.557244047100 | 2.347467653913 |
| H | 4.579276587720 | 0.413219976352 | -1.891270072223 |
| H | 1.089989538065 | -1.403993750564 | 2.412865958417 |
| H | 3.152126661481 | -2.707271971171 | 2.946972163515 |
| H | 2.347073028542 | -2.106381141375 | 4.405840138469 |
| H | 3.804938493839 | -1.311124266204 | 3.803535841288 |
| H | 2.543273925468 | 0.915427567495 | 3.772388202465 |
| H | 1.068100474120 | 0.120845630359 | 4.329221504075 |
| H | 1.066097992119 | 1.087993775174 | 2.844101293955 |
| H | 5.981120967522 | 1.641035998012 | 1.375150123359 |
| H | 7.139006570922 | -0.345836801411 | 0.430266519045 |
| H | 7.956674676545 | 1.155695867315 | -0.034324695093 |
| H | 6.938980091807 | 0.303802374748 | -1.199396869243 |
| H | 5.573103617167 | 2.507085738494 | -1.526822302345 |
| H | 6.626070303994 | 3.287634451336 | -0.346302646039 |
| H | 4.871088442739 | 3.292368314405 | -0.111988581695 |
| H | 1.549006885316 | -1.699617562294 | -2.288622419489 |
| H | 4.286534669710 | -1.099378963121 | -3.502571822986 |
| H | 3.020452511243 | -2.110610716381 | -4.194499364232 |
| H | 3.845709743863 | -2.612794782746 | -2.710640029200 |
| H | 1.096683613557 | 0.725662071650 | -2.626409749328 |
| H | 1.445514579957 | -0.091119914480 | -4.155425751510 |
| H | 2.672657856460 | 0.919914748323 | -3.377244815017 |
| H | -4.699199589769 | 1.100495438730 | 2.211090117581 |
| H | -4.174143350587 | 1.951030471799 | -1.923381586147 |
| H | -2.304550515397 | -1.754481319356 | 2.158083159103 |
| H | -4.834207986255 | -0.706168227829 | 3.510691326181 |
| H | -3.894079807654 | -2.121943630776 | 3.975601267765 |
| H | -4.769466281504 | -2.104174268252 | 2.436719469201 |
| H | -1.239439399290 | 0.335094694911 | 2.946280307681 |
| H | -1.859218300983 | -0.615141100450 | 4.301853808259 |
| H | -2.736147782563 | 0.815899790175 | 3.738990441052 |
| H | -5.888180056603 | 2.801297908236 | 1.310412929662 |
| H | -6.410166618559 | 2.644861983784 | -1.696156368369 |
| H | -7.429857990114 | 3.453697099742 | -0.505667299101 |
| H | -7.237589203109 | 1.693374152624 | -0.459862213569 |
| H | -3.955654392414 | 4.255782985515 | 0.699066774093 |
| H | -5.498876900890 | 4.968827586411 | 0.192536524909 |
| H | -4.441946249136 | 4.194090382846 | -0.992541844746 |
| H | -1.566596714645 | -0.647926955815 | -2.387072887581 |
| H | -3.843230623604 | -1.415783498201 | -3.062416831165 |
| H | -2.930441883588 | -0.764567114327 | -4.434133965556 |
| H | -4.200525561879 | 0.199526261632 | -3.671302337162 |
| H | -2.515213431547 | 2.081612576451 | -3.377210640774 |
| H | -1.203043828525 | 1.107727139393 | -4.038256561223 |
| H | -1.056646482884 | 1.839770044556 | -2.429129472814 |
| H | 2.835143388277 | -3.372711089730 | -0.007454441666 |

| | | | |
|---|---|---|---|
| H | 1.832334108507 | -4.346458340185 | 2.063996437844 |
| H | 2.795222327056 | -5.536383436064 | 1.174367354136 |
| H | 1.032040687489 | -5.581073241503 | 1.091682302648 |
| H | 1.167949858480 | -5.473994839356 | -1.472676997168 |
| H | 2.928341421882 | -5.419025542048 | -1.373205435801 |
| H | 2.050016816384 | -4.157713255758 | -2.248872735555 |
| H | -3.785612556696 | -2.614014781603 | -0.333231920341 |
| H | -2.647867245970 | -5.238165460817 | 0.745359579021 |
| H | -4.353436421713 | -4.795158252936 | 0.663885715473 |
| H | -3.259578785827 | -3.913287466810 | 1.737554222265 |
| H | -2.950205398040 | -3.427780574991 | -2.547014308113 |
| H | -4.179050828647 | -4.504109151995 | -1.864285798184 |
| H | -2.472519948149 | -4.951755858638 | -1.799216204444 |
| N | 0.205991718121 | 2.686502507027 | 0.210174211930 |
| Si | 1.177163505188 | 4.062982812499 | 0.178755320836 |
| C | 0.132915337328 | 5.620041921389 | 0.333341154093 |
| C | 2.424656813944 | 4.063766508585 | 1.593994812172 |
| C | 2.143262495573 | 4.174104324215 | -1.437480494664 |
| H | 3.085691706700 | 4.935584847912 | 1.565233653262 |
| H | 1.907349802451 | 4.064492618086 | 2.557819136539 |
| H | 3.042282951278 | 3.161844570101 | 1.551352873801 |
| H | 2.792363120425 | 5.054350133919 | -1.477217793371 |
| H | 2.766877612336 | 3.284664732473 | -1.566063489557 |
| H | 1.455267806181 | 4.222814484557 | -2.286555169650 |
| H | 0.743149202322 | 6.527862623768 | 0.308877966258 |
| H | -0.591912553378 | 5.675136492401 | -0.483753412959 |
| H | -0.427019345860 | 5.612136951839 | 1.272701516161 |

**Table 6.S8.** XYZ coordinates for cis-Ar$^{iPr8}$Al($N_3$)N($SiMe_3$)$_2$

134

cis-AriPr8Al(N3)N(SiMe3)2

| | | | |
|---|---|---|---|
| C | 3.566194807210 | 1.166850287204 | 0.443812342873 |
| C | 2.421566869763 | 1.112048192466 | -0.376823066568 |
| C | 2.435507190524 | 0.226853950725 | -1.490169567818 |
| C | 3.480454802384 | -0.678129204577 | -1.631823749144 |
| C | 4.570294153729 | -0.693760412439 | -0.772251330088 |
| C | 4.604929756691 | 0.264570107743 | 0.223276308451 |
| C | 1.157301785905 | 1.849171342318 | -0.046565001277 |
| C | 0.013166476060 | 1.052045927272 | 0.194376164685 |
| C | -1.226627571784 | 1.644157460420 | 0.484314142953 |
| C | -1.290663289520 | 3.023902338391 | 0.731612077778 |
| C | -0.163147221499 | 3.780561844130 | 0.462537462237 |
| C | 1.030671202572 | 3.244205311052 | -0.007443377556 |
| C | -2.497352717396 | 0.861213036752 | 0.331756829930 |
| C | -3.099522500153 | 0.851588442666 | -0.943564090436 |
| C | -4.296596929287 | 0.175668352281 | -1.125605026841 |
| C | -4.934334045498 | -0.494752391642 | -0.091338955307 |
| C | -4.327053873677 | -0.478401283919 | 1.151237836762 |
| C | -3.126545472998 | 0.185239544400 | 1.382571039929 |
| C | -2.482121068434 | 1.542761306443 | -2.140865616573 |
| C | -2.077739994338 | 0.523559060125 | -3.201354168145 |
| C | -2.540669016106 | 0.132240263218 | 2.772100663022 |
| C | -2.163451597333 | -1.303204133498 | 3.125735408077 |
| C | -6.249509484654 | -1.203237476401 | -0.301703778682 |
| C | -6.147286679226 | -2.301076065179 | -1.354702582594 |
| Al | 0.067647265286 | -0.887298315422 | -0.072644456121 |

| | | | |
|---|---|---|---|
| N | -0.591867276725 | -2.138695383635 | -0.957869284368 |
| Si | -1.840330358511 | -3.213800945815 | -0.704518615058 |
| C | -3.306729832448 | -2.958370340666 | -1.866428457722 |
| C | 2.061473485265 | 4.201419524447 | -0.561012391925 |
| C | 1.524244777372 | 4.854243732840 | -1.836509067088 |
| C | -2.533427232815 | 3.697549208079 | 1.264433029134 |
| C | -2.948097576536 | 4.927123303439 | 0.464222694249 |
| C | 1.487690326156 | 0.409049272266 | -2.666771164124 |
| C | 1.239751470927 | -0.841835780519 | -3.497138341214 |
| C | 5.708097479654 | -1.667212800932 | -0.955450071488 |
| C | 5.257654357871 | -3.106438560465 | -0.730314785195 |
| C | 3.797550247513 | 2.221293003248 | 1.509532868538 |
| C | 4.170011141803 | 1.668708074136 | 2.881707434088 |
| C | 2.070503709837 | 1.510366883835 | -3.556018502185 |
| C | 4.922036648328 | 3.160193709277 | 1.063592806870 |
| C | 6.365797492546 | -1.509620197594 | -2.323167295337 |
| C | -2.321580387496 | 4.073939301950 | 2.730445880839 |
| C | 2.469931719687 | 5.294326314916 | 0.422353927449 |
| C | -3.486613470909 | 0.706859659911 | 3.821867531128 |
| C | -7.356715459409 | -0.212213881310 | -0.649360295145 |
| C | -3.415779029152 | 2.591873281763 | -2.736467040034 |
| C | -1.307397828689 | -5.010187380247 | -0.962318933652 |
| C | -2.518544169678 | -3.097794955345 | 1.058291607167 |
| H | -0.233288107693 | 4.858306910767 | 0.563270016181 |
| H | -4.808548547175 | -1.003771070751 | 1.970346154677 |
| H | -4.744849550112 | 0.171093978940 | -2.113715462487 |
| H | -1.633988710637 | 0.745112977302 | 2.764300662634 |
| H | -3.800903468947 | 1.719120048828 | 3.564134273355 |
| H | -3.002133252211 | 0.738030709613 | 4.801930112472 |
| H | -4.386158110717 | 0.094044046851 | 3.917314088864 |
| H | -3.048995442369 | -1.942559543858 | 3.139873928664 |
| H | -1.698000175540 | -1.360127041670 | 4.114005880405 |
| H | -1.484395177540 | -1.732618018510 | 2.383450695789 |
| H | -6.510341060140 | -1.676900811616 | 0.651658179916 |
| H | -7.454201797060 | 0.558607201953 | 0.118334150301 |
| H | -8.317496111882 | -0.724325958954 | -0.747683933021 |
| H | -7.146487396427 | 0.287597766288 | -1.598786484199 |
| H | -5.905673894863 | -1.885350371109 | -2.336228486339 |
| H | -7.097885435498 | -2.833240976910 | -1.444848027829 |
| H | -5.368869583805 | -3.022534572355 | -1.102995355878 |
| H | -1.578536469939 | 2.056819192858 | -1.805874373737 |
| H | -4.309163005218 | 2.127872640521 | -3.162087359373 |
| H | -2.913002920922 | 3.136885375828 | -3.539745629513 |
| H | -3.745486846395 | 3.312368665459 | -1.986535431604 |
| H | -1.484042396647 | -0.284062890466 | -2.768898751459 |
| H | -1.505678586004 | 1.007936091123 | -3.998106938417 |
| H | -2.959376830541 | 0.066487499572 | -3.658136684868 |
| H | 5.484739729532 | 0.315917187587 | 0.858063342881 |
| H | 3.458947493435 | -1.363137072475 | -2.470205068460 |
| H | 2.875644495215 | 2.794827200378 | 1.620491953802 |
| H | 5.870701213652 | 2.618508579978 | 1.029063642472 |
| H | 5.037370855679 | 3.986118038710 | 1.769749151220 |
| H | 4.748775209093 | 3.579485494916 | 0.073219780092 |
| H | 3.417137723012 | 0.992408960138 | 3.276136278983 |
| H | 4.285211234108 | 2.492323321744 | 3.590890353116 |
| H | 5.122227953205 | 1.133225384316 | 2.852044612499 |

| | | | |
|---|---|---|---|
| H | 6.458841367164 | -1.426303084298 | -0.193887399216 |
| H | 5.669155931054 | -1.765351843627 | -3.125617480719 |
| H | 7.231038996511 | -2.171163546365 | -2.412359153211 |
| H | 6.699697749651 | -0.482671671942 | -2.485139434813 |
| H | 4.852614642722 | -3.242171596655 | 0.274484275334 |
| H | 6.095541493676 | -3.797224693873 | -0.853245316565 |
| H | 4.480759780767 | -3.392314482007 | -1.443756340999 |
| H | 0.525378889110 | 0.765526583421 | -2.293928939099 |
| H | 2.287149946071 | 2.414873435268 | -2.988345359665 |
| H | 1.373302488187 | 1.761439665671 | -4.359655562525 |
| H | 3.005600973107 | 1.170558226460 | -4.010041788591 |
| H | 2.145458138544 | -1.168567538048 | -4.015229463369 |
| H | 0.498021866456 | -0.619829487034 | -4.266815831794 |
| H | 0.847281294878 | -1.655365840772 | -2.882471080026 |
| H | -3.347768381177 | 2.970054054195 | 1.210989365695 |
| H | -2.023394189870 | 3.210124028896 | 3.326896092998 |
| H | -3.236163512578 | 4.490031441330 | 3.161775544625 |
| H | -1.533581286955 | 4.827057470457 | 2.821239613064 |
| H | -2.221455884654 | 5.737190258763 | 0.568384825136 |
| H | -3.908669081402 | 5.305317512616 | 0.822477288338 |
| H | -3.045154885294 | 4.701947377617 | -0.598270991025 |
| H | 2.943453954911 | 3.615932499915 | -0.830868807948 |
| H | 1.636769259062 | 5.974687954050 | 0.614538537137 |
| H | 3.286924858703 | 5.891726650103 | 0.010412110782 |
| H | 2.795607015635 | 4.891450813267 | 1.381304479761 |
| H | 1.178827857248 | 4.112797794170 | -2.557173573860 |
| H | 2.296613046314 | 5.464588305933 | -2.312188138762 |
| H | 0.677263679951 | 5.504804027638 | -1.603881718215 |
| H | -3.363412811904 | -3.772863544686 | 1.229044665534 |
| H | -1.738248314847 | -3.348277938798 | 1.784404525973 |
| H | -2.846743207736 | -2.074808558170 | 1.263745534052 |
| H | -4.105000331561 | -3.682038703675 | -1.673638699733 |
| H | -3.720501210779 | -1.955112664043 | -1.746203234208 |
| H | -2.996667340367 | -3.068333669382 | -2.909812692170 |
| H | -2.152421292460 | -5.698141449616 | -0.857742608708 |
| H | -0.889167735487 | -5.144605413850 | -1.964745668795 |
| H | -0.541335306289 | -5.311203247709 | -0.242181019922 |
| N | 1.393633548540 | -1.822954077292 | 1.182942933072 |
| N | 2.257656237458 | -0.999860070109 | 1.526679404151 |
| N | 3.021106623861 | -0.251367682262 | 1.833378867962 |
| Si | 1.852427536511 | -3.552847233121 | 1.531962588086 |
| C | 0.470535090723 | -4.547737853891 | 0.805074487210 |
| C | 3.483108813484 | -3.847390374350 | 0.686224687219 |
| C | 2.080896507957 | -3.679731077738 | 3.371873166228 |
| H | -0.508681087786 | -4.118136605537 | 1.020569817961 |
| H | 0.581504261600 | -4.601720667300 | -0.276871739921 |
| H | 0.498244757442 | -5.568710320788 | 1.193954438815 |
| H | 3.802815424260 | -4.880403546463 | 0.852583488828 |
| H | 3.422492091859 | -3.679984706167 | -0.389731911020 |
| H | 4.263090795911 | -3.197169754715 | 1.091007475083 |
| H | 2.221690991087 | -4.722841818550 | 3.668031049687 |
| H | 2.972984194677 | -3.127511971959 | 3.679996753227 |
| H | 1.223325023756 | -3.278582782067 | 3.911071219105 |

**Table 6.S9.** XYZ coordinates for Transition State 2.

134

TS2

| | | | |
|---|---|---|---|
| C | 2.592461663787 | 0.286297250312 | -1.615003885460 |
| C | 2.480922661951 | 0.907540480489 | -0.350597027479 |
| C | 3.545458592778 | 0.753704315183 | 0.564225901105 |
| C | 4.643320837585 | -0.023488946015 | 0.213679031402 |
| C | 4.754135319158 | -0.653221223949 | -1.014213785093 |
| C | 3.714878197203 | -0.479227473903 | -1.910936199277 |
| C | 1.247517183201 | 1.700670274670 | -0.021062642098 |
| C | 0.020731065539 | 1.022680551050 | 0.136639159801 |
| C | -1.175528442284 | 1.728444360405 | 0.353581516137 |
| C | -1.134690580380 | 3.113055722523 | 0.555807270026 |
| C | 0.082182129868 | 3.754551363401 | 0.389892313743 |
| C | 1.259269289630 | 3.100939722886 | 0.046492505996 |
| C | -2.480413542631 | 1.002133166470 | 0.221246790974 |
| C | -3.031657172312 | 0.220246656244 | 1.247608049139 |
| C | -4.221102801940 | -0.467265665579 | 1.019004752580 |
| C | -4.890253702668 | -0.409217389489 | -0.189165786747 |
| C | -4.343110043045 | 0.383464922397 | -1.188551346299 |
| C | -3.164270926418 | 1.090042422460 | -1.010654201404 |
| C | -2.418785945853 | 0.136750084475 | 2.627023542679 |
| C | -2.299684076265 | -1.304854038783 | 3.114771786779 |
| C | -2.633977070180 | 1.899330405322 | -2.174772520403 |
| C | -2.041290999919 | 0.977277938206 | -3.233874794077 |
| C | -6.176864917893 | -1.166462694804 | -0.403414473323 |
| C | -6.096087567627 | -2.102432434761 | -1.604545618676 |
| Al | -0.062982577040 | -0.922398014587 | 0.226718441491 |
| N | -0.424821793019 | -2.509398232380 | -0.222527585458 |
| Si | 1.331206513911 | -3.249676963960 | 1.786484196602 |
| C | 2.473640748512 | -3.318959704431 | 3.286162691922 |
| C | 2.459860793666 | 3.943695705479 | -0.313711909394 |
| C | 2.235491225401 | 4.618022582804 | -1.666511910834 |
| C | -2.351786684064 | 3.922785148057 | 0.937816223384 |
| C | -2.622891969728 | 5.068775704586 | -0.032273905757 |
| C | 3.588529904291 | 1.409003890116 | 1.928805375661 |
| C | 3.842112483924 | 0.391278210672 | 3.040154255325 |
| C | 5.983652246650 | -1.450729287889 | -1.370816512420 |
| C | 5.646305556541 | -2.855957662874 | -1.855769545933 |
| C | 1.589859283743 | 0.482358821121 | -2.733697931662 |
| C | 1.065815899666 | -0.844611700029 | -3.272828848501 |
| C | 4.690130686576 | 2.467359638853 | 2.002135477314 |
| C | 2.209326119783 | 1.297675687273 | -3.867745939860 |
| C | 6.824160447463 | -0.704411129745 | -2.403907244201 |
| N | 0.854730475471 | -1.451348021268 | 1.894820051025 |
| N | 0.848039242662 | -0.847129379673 | 2.960735777867 |
| N | 0.812485981163 | -0.274224121481 | 3.920782530486 |
| C | -0.027386383215 | -4.452111732939 | 2.182307904618 |
| C | 2.400885061538 | -3.516114919406 | 0.295156637941 |
| C | -2.197704007727 | 4.467647014289 | 2.356832010976 |
| C | 2.779110032614 | 4.997399593395 | 0.742617735589 |
| C | -3.696469514036 | 2.803605088036 | -2.791014487938 |
| C | -7.358258161181 | -0.208628216099 | -0.532461865172 |
| C | -3.228230788184 | 0.963633272486 | 3.623805429625 |
| Si | -1.487596625117 | -3.488567754483 | -1.086727613791 |

| | | | |
|---|---|---|---|
| C | -0.611045901812 | -5.047495875227 | -1.697526121153 |
| C | -2.958033866474 | -4.037516659230 | -0.031609948910 |
| C | -2.260150577590 | -2.685526589526 | -2.607773408402 |
| H | 0.108760627551 | 4.834092001003 | 0.492978369821 |
| H | -4.641867680962 | -1.073005626258 | 1.814479029915 |
| H | -4.847452710018 | 0.446301400225 | -2.146630097679 |
| H | -1.419483722908 | 0.580724505251 | 2.573851944296 |
| H | -3.339046374577 | 1.995683572254 | 3.290191578225 |
| H | -2.746500584142 | 0.966930867914 | 4.605106782068 |
| H | -4.230600877083 | 0.542829289786 | 3.739204420962 |
| H | -3.283706869899 | -1.732528863052 | 3.317853293430 |
| H | -1.735292360106 | -1.347852186272 | 4.049394184137 |
| H | -1.819833007197 | -1.944075903233 | 2.369657683461 |
| H | -6.336520968885 | -1.781259428116 | 0.489444087760 |
| H | -7.438088067717 | 0.441884145306 | 0.341228858726 |
| H | -8.295352297619 | -0.761529805927 | -0.637166185752 |
| H | -7.245457030938 | 0.428956950909 | -1.413672249244 |
| H | -5.956700070431 | -1.542885071166 | -2.533204166208 |
| H | -7.019452857494 | -2.679049779808 | -1.701727456297 |
| H | -5.262595007711 | -2.799195689323 | -1.507713128044 |
| H | -1.827713482103 | 2.534900391293 | -1.803289558830 |
| H | -4.462097641337 | 2.224027182115 | -3.312545557655 |
| H | -3.241809097043 | 3.472955884692 | -3.525928880459 |
| H | -4.198182077291 | 3.412236681838 | -2.036647634915 |
| H | -1.303184849539 | 0.304532790621 | -2.799679486425 |
| H | -1.560603279669 | 1.555651559946 | -4.027981302474 |
| H | -2.817328736045 | 0.355396543178 | -3.687334273197 |
| H | 5.452107410062 | -0.140667969474 | 0.928053385187 |
| H | 3.779984187582 | -0.940242633525 | -2.890073251699 |
| H | 2.622421602906 | 1.890163108020 | 2.105365227225 |
| H | 5.670934901165 | 1.992762424979 | 1.915182956780 |
| H | 4.658211432312 | 2.987000817625 | 2.963453466897 |
| H | 4.613697470010 | 3.210192383073 | 1.211399196532 |
| H | 3.247353533989 | -0.509091170844 | 2.913677199124 |
| H | 3.620319579153 | 0.821074068556 | 4.019134994816 |
| H | 4.889839851285 | 0.080990177511 | 3.047801502245 |
| H | 6.579582166424 | -1.545024734149 | -0.455918450102 |
| H | 6.269407933832 | -0.585898990121 | -3.338774822833 |
| H | 7.743548066615 | -1.252276358480 | -2.626144979470 |
| H | 7.094568340962 | 0.292345377336 | -2.048940604060 |
| H | 5.058147637884 | -3.402377184794 | -1.116611058861 |
| H | 6.560304065338 | -3.420755310050 | -2.055297127199 |
| H | 5.068446187859 | -2.827287470296 | -2.783008580814 |
| H | 0.746909361623 | 1.050856104272 | -2.337770449560 |
| H | 2.646259750193 | 2.229161920302 | -3.505248374263 |
| H | 1.452676251011 | 1.540080108232 | -4.618453904738 |
| H | 3.003291313194 | 0.733918803585 | -4.364685856395 |
| H | 1.873348449305 | -1.440966162660 | -3.704780699393 |
| H | 0.330757562291 | -0.671829272734 | -4.061850404077 |
| H | 0.596400415992 | -1.448520481986 | -2.491565246244 |
| H | -3.213487801487 | 3.249330053979 | 0.919173557985 |
| H | -1.978511132926 | 3.673172522871 | 3.071833324969 |
| H | -3.109786270148 | 4.978053421408 | 2.677043463575 |
| H | -1.376533489424 | 5.188208305778 | 2.404723298761 |
| H | -1.832460562312 | 5.822330197488 | 0.016837763744 |
| H | -3.563529537636 | 5.565625515547 | 0.218246976037 |

| | | | |
|---|---|---|---|
| H | -2.686323212999 | 4.720010800087 | -1.063042123722 |
| H | 3.317358649712 | 3.274953066523 | -0.416072376633 |
| H | 2.015046629410 | 5.778357174239 | 0.763982664054 |
| H | 3.731356597703 | 5.485584788826 | 0.520140669661 |
| H | 2.842184512245 | 4.566233188207 | 1.742497178775 |
| H | 1.995226332824 | 3.888681283951 | -2.440401423515 |
| H | 3.126595735500 | 5.169789399099 | -1.977276385827 |
| H | 1.403047809290 | 5.324801440091 | -1.609250683814 |
| H | -3.652474764562 | -4.661193466864 | -0.603395909482 |
| H | -2.655914350568 | -4.602765787435 | 0.852832364752 |
| H | -3.501217105920 | -3.153195932891 | 0.313989286554 |
| H | -2.961048800056 | -3.368473250255 | -3.098262739832 |
| H | -2.813612253392 | -1.787825569026 | -2.320976957188 |
| H | -1.505801870541 | -2.396359138250 | -3.343617696562 |
| H | -1.293152619329 | -5.708632166304 | -2.240120208123 |
| H | 0.205697496831 | -4.782853101026 | -2.376579608192 |
| H | -0.179155809455 | -5.622297754612 | -0.872954414389 |
| H | 1.818715664533 | -3.902288967107 | -0.538048365439 |
| H | 2.859400526865 | -2.574800159513 | -0.019821875715 |
| H | 3.206948500886 | -4.212259578440 | 0.549557337572 |
| H | 2.846946449655 | -4.342905312344 | 3.382467581154 |
| H | 3.344147431801 | -2.666159518430 | 3.185487765577 |
| H | 1.972446859401 | -3.077287157740 | 4.228199942765 |
| H | 0.395138004478 | -5.271133027201 | 2.773330826128 |
| H | -0.802867973914 | -3.977251296116 | 2.787941977423 |
| H | -0.498081105671 | -4.848300304549 | 1.288166084603 |

**Table 6.S10.** XYZ Coordinates for $Ar^{iPr8}Al(N_3)N(SiMe_3)_2$.

134

AriPr8Al(N3)N(SiMe3)2

| | | | |
|---|---|---|---|
| C | -3.243451776269 | 0.198277298812 | 1.109092789841 |
| C | -2.641278053992 | 0.924201145108 | 0.064407645597 |
| C | -3.281774412775 | 0.971576143550 | -1.192086282483 |
| C | -4.445040404980 | 0.237975433700 | -1.389511952961 |
| C | -5.002346386889 | -0.550099805382 | -0.395713351779 |
| C | -4.391247454491 | -0.543497592143 | 0.847297802562 |
| C | -1.350114142531 | 1.669984377577 | 0.216814661445 |
| C | -0.116081470782 | 0.994957111422 | 0.095277311819 |
| C | 1.076617889690 | 1.737138257455 | -0.036461150624 |
| C | 1.039986227444 | 3.139430366647 | -0.037514445733 |
| C | -0.175265171935 | 3.758179833545 | 0.200193575182 |
| C | -1.367783029587 | 3.066855182396 | 0.338383410155 |
| Al | 0.130606104633 | -0.909310326536 | 0.546335425121 |
| N | 0.190334555091 | -0.964627830954 | 2.365360172919 |
| N | 0.223703349627 | -1.874298616874 | 3.147852112080 |
| N | 0.256616030038 | -2.687089222395 | 3.933289800395 |
| C | 2.379123779078 | 1.018754733735 | -0.216051109781 |
| C | 2.675642547609 | 0.397838282442 | -1.446518946603 |
| C | 3.902801769250 | -0.237876225539 | -1.611851723625 |
| C | 4.868439443697 | -0.255817303142 | -0.621982864752 |
| C | 4.572985014770 | 0.381751999706 | 0.575463887084 |
| C | 3.361178714603 | 1.019926646892 | 0.800805526905 |
| C | 2.245188933755 | 4.007660362870 | -0.319826140061 |
| C | 2.458636098832 | 5.079025829253 | 0.745809415871 |
| C | -2.622140411416 | 3.860938651875 | 0.631985942171 |
| C | -2.498232668285 | 4.550208238713 | 1.990971845797 |

| | | | |
|---|---|---|---|
| C | 1.770795199049 | 0.503153349474 | -2.655675610824 |
| C | 1.358669625299 | -0.857934204642 | -3.203491560970 |
| C | 6.200217609906 | -0.926162779821 | -0.852394592743 |
| C | 6.363768821728 | -2.165646236492 | 0.021329013910 |
| C | 3.166910512531 | 1.716359630978 | 2.132092811089 |
| C | 3.029650805626 | 0.719766670895 | 3.279382711730 |
| C | -2.734162095823 | 1.780789608443 | -2.351555408495 |
| C | -1.921398425038 | 0.914168212121 | -3.305878784228 |
| C | -6.239686366644 | -1.372166176964 | -0.656871887084 |
| C | -5.960240086988 | -2.862632304397 | -0.489802986319 |
| C | -2.781666009884 | 0.308207399284 | 2.545829121338 |
| C | -2.818609629602 | -1.015080194933 | 3.301768699847 |
| N | 0.277413421078 | -2.544793227430 | -0.195200256591 |
| Si | -1.081604549000 | -3.401378332904 | -0.887492234999 |
| C | -2.191416403219 | -4.068823364965 | 0.466936300409 |
| Si | 1.695706388870 | -3.495752237093 | 0.212837357767 |
| C | 1.247080584314 | -5.082803932925 | 1.107346170756 |
| C | 2.834057697236 | -2.564945978324 | 1.367511419551 |
| C | 2.708052106207 | -3.882603391116 | -1.316153077877 |
| C | -2.089376963630 | -2.258436193101 | -1.953435522417 |
| C | -0.559574167032 | -4.806133004578 | -2.018007534197 |
| C | 2.443645216378 | 1.322543731576 | -3.755816948140 |
| C | 7.360273291465 | 0.043271298798 | -0.650654325020 |
| C | 4.310316867149 | 2.685717040715 | 2.426707323723 |
| C | -3.824541412283 | 2.522510604891 | -3.117885862512 |
| C | -7.404566894424 | -0.931745279460 | 0.224175369852 |
| C | -3.659377430557 | 1.323410779624 | 3.279184189663 |
| C | 2.109348871559 | 4.664686851133 | -1.692430957432 |
| C | -2.932825925740 | 4.902971024717 | -0.439043784829 |
| H | -0.200753082970 | 4.841235029075 | 0.254898363097 |
| H | 4.128183720596 | -0.702995599034 | -2.566553252718 |
| H | 5.313927635306 | 0.384148043796 | 1.367378957621 |
| H | 0.870165338025 | 1.035553592173 | -2.347433275058 |
| H | 2.804566310523 | 2.281629230209 | -3.382637036123 |
| H | 1.740798337125 | 1.511824066446 | -4.571392862511 |
| H | 3.301205044463 | 0.787936828926 | -4.172598307631 |
| H | 2.225541471531 | -1.413192317706 | -3.571571524257 |
| H | 0.669236715693 | -0.734744806445 | -4.042526664851 |
| H | 0.875703479950 | -1.469819445787 | -2.441174407714 |
| H | 6.214153935229 | -1.251720687122 | -1.898591276440 |
| H | 7.252570495555 | 0.926279643392 | -1.284004733275 |
| H | 8.310249363873 | -0.439722137274 | -0.892482717255 |
| H | 7.416454593029 | 0.381508069069 | 0.387236112969 |
| H | 6.319235610132 | -1.905122583299 | 1.082220914941 |
| H | 7.327922854226 | -2.644635621389 | -0.167179183162 |
| H | 5.575401428846 | -2.893322542780 | -0.177994075873 |
| H | 2.237254863076 | 2.287261432300 | 2.077077819706 |
| H | 5.236738956867 | 2.147874140644 | 2.642654642557 |
| H | 4.074998855043 | 3.290427750352 | 3.306066262634 |
| H | 4.504545505860 | 3.359309867112 | 1.591115933802 |
| H | 2.160507387393 | 0.078675706792 | 3.141700356255 |
| H | 2.916532633854 | 1.250676155764 | 4.228224397364 |
| H | 3.917460710477 | 0.085702006594 | 3.353065664376 |
| H | -4.925316443419 | 0.260467831522 | -2.361939870277 |
| H | -4.835583971541 | -1.112521213722 | 1.656127624077 |
| H | -2.051337055216 | 2.525223758212 | -1.939769486649 |

| | | | |
|---|---|---|---|
| H | -4.441796044421 | 1.839208872465 | -3.706188952095 |
| H | -3.373372167198 | 3.230027360446 | -3.818285502088 |
| H | -4.486404876593 | 3.076796475564 | -2.449647674535 |
| H | -1.114661622235 | 0.405503079060 | -2.780558241376 |
| H | -1.483653120753 | 1.526679097950 | -4.099142433273 |
| H | -2.550732894923 | 0.150870211186 | -3.770556797830 |
| H | -6.524171850856 | -1.197968087929 | -1.700690921943 |
| H | -7.180749851342 | -1.097881851647 | 1.281256331397 |
| H | -8.307420829705 | -1.498624683747 | -0.016961894895 |
| H | -7.620087454945 | 0.130569342979 | 0.091826334320 |
| H | -5.147422136075 | -3.187460899917 | -1.142130345840 |
| H | -6.849406137054 | -3.452148764130 | -0.727459608007 |
| H | -5.670276269858 | -3.093936428882 | 0.538480788676 |
| H | -1.753564058080 | 0.676559498184 | 2.548495964812 |
| H | -3.682064351629 | 2.285148743034 | 2.769427379285 |
| H | -3.294625021968 | 1.482272557901 | 4.297558221438 |
| H | -4.688013835096 | 0.957186373896 | 3.341136016748 |
| H | -3.844997498321 | -1.321220256280 | 3.519775326676 |
| H | -2.303893460998 | -0.917210914632 | 4.259616408434 |
| H | -2.343959572324 | -1.823878194959 | 2.746839599637 |
| H | 3.127313236675 | 3.363282830548 | -0.341751413080 |
| H | 1.935395722403 | 3.925616571777 | -2.474866109648 |
| H | 3.011647304653 | 5.228204777163 | -1.944186075629 |
| H | 1.264695201049 | 5.359168941852 | -1.702529652066 |
| H | 1.665670340487 | 5.830427043114 | 0.715179675872 |
| H | 3.404421142355 | 5.600151484389 | 0.577409725728 |
| H | 2.477857196025 | 4.655871861230 | 1.750529751870 |
| H | -3.459100313835 | 3.158791557722 | 0.672998828442 |
| H | -2.151543041702 | 5.666360120721 | -0.481997354881 |
| H | -3.873928426645 | 5.410360670653 | -0.212021378744 |
| H | -3.019124921114 | 4.459142862041 | -1.429995883362 |
| H | -2.218546485537 | 3.848260028880 | 2.777504982940 |
| H | -3.442505182007 | 5.024704837361 | 2.270817042265 |
| H | -1.731836353488 | 5.329261849014 | 1.958326907804 |
| H | 3.049298534404 | -1.545149982582 | 1.044034869965 |
| H | 3.791268312007 | -3.094142511317 | 1.373616376689 |
| H | 2.479060672684 | -2.540799328116 | 2.397307957384 |
| H | 2.137889863356 | -4.390414579089 | -2.094024872158 |
| H | 3.552962853090 | -4.523135861603 | -1.045338582590 |
| H | 3.109127682661 | -2.957479649557 | -1.736072611512 |
| H | 0.755308455352 | -4.853826928364 | 2.056406754657 |
| H | 2.166585298583 | -5.629665178908 | 1.338006366938 |
| H | 0.598775706986 | -5.752941610251 | 0.541619688851 |
| H | -2.428639574605 | -1.371272428438 | -1.417821185674 |
| H | -2.983123270952 | -2.778356659612 | -2.309709019897 |
| H | -1.521827627703 | -1.933472426541 | -2.826486992872 |
| H | -0.024605682684 | -4.420825845939 | -2.889575427904 |
| H | -1.470045326069 | -5.292771181514 | -2.381804691138 |
| H | 0.057879254990 | -5.573281624863 | -1.550837899729 |
| H | -1.639726553839 | -4.668518061269 | 1.193451298396 |
| H | -2.988000955974 | -4.689597705757 | 0.046651263571 |
| H | -2.670613904285 | -3.244849875152 | 1.003243428583 |

**Table 6.S11.** XYZ Coordinates for trans-Ar$^{iPr8}$Al[N(SiMe$_3$)N$_2$]NSiMe$_3$

134

trans-AriPr8Al[N(SiMe3)N2]NSiMe3

| | | | |
|---|---|---|---|
| C | 3.616365323912 | -0.952573595255 | -0.139387845431 |
| C | 2.437105031577 | -0.846527773903 | 0.625169216613 |
| C | 2.368668877172 | 0.171868324816 | 1.615901947452 |
| C | 3.369528625590 | 1.133941834990 | 1.678616813738 |
| C | 4.492913228156 | 1.090237924848 | 0.864407262841 |
| C | 4.607823709318 | 0.016397784255 | 0.001587040322 |
| C | 1.218488581639 | -1.675942665872 | 0.346087578062 |
| C | 0.054262087670 | -0.968158634043 | -0.036385189567 |
| C | -1.147358323265 | -1.647748898832 | -0.293172826055 |
| C | -1.145410820059 | -3.049082057248 | -0.364103372793 |
| C | -0.000616894696 | -3.713880984764 | 0.040479165981 |
| C | 1.149932038248 | -3.069038100775 | 0.481171516703 |
| C | -2.453889993106 | -0.910093881414 | -0.288457702317 |
| C | -3.108947928156 | -0.766817204744 | 0.952315454299 |
| C | -4.338785124483 | -0.128243282900 | 1.002634491105 |
| C | -4.959137873010 | 0.376668500946 | -0.131538611750 |
| C | -4.300130169274 | 0.231146127342 | -1.338759578847 |
| C | -3.065188687484 | -0.401375547351 | -1.439412365191 |
| C | -2.514890173029 | -1.272597999709 | 2.249928099023 |
| C | -2.196740009365 | -0.110409579761 | 3.185317316228 |
| C | -2.424211835978 | -0.497811965857 | -2.801955951026 |
| C | -2.090611797453 | 0.897086884906 | -3.322408721151 |
| C | -6.309401808993 | 1.045780080957 | -0.061618319644 |
| C | -6.295675801173 | 2.271253021529 | 0.845328859125 |
| Al | 0.019379303811 | 0.989775523069 | -0.017917845386 |
| N | -0.726525138461 | 2.311762070978 | 0.675274612567 |
| Si | -1.770355319439 | 3.587597649791 | 0.922918013100 |
| C | -2.942910027746 | 3.334215305772 | 2.381170997811 |
| C | 2.194273195158 | -3.900965497126 | 1.189850522487 |
| C | 1.630819151256 | -4.411214277669 | 2.518012926844 |
| C | -2.336622062825 | -3.840174813107 | -0.851277558470 |
| C | -2.734637358497 | -4.976351911580 | 0.084009203873 |
| C | 1.380513753413 | 0.096984143347 | 2.770820373921 |
| C | 1.047816095842 | 1.430207882561 | 3.424687432053 |
| C | 5.581933202751 | 2.129451334516 | 0.962865142694 |
| C | 5.083739804273 | 3.506871778645 | 0.539224925766 |
| C | 3.934515546864 | -2.121630017690 | -1.052275431541 |
| C | 4.341612236222 | -1.730353759313 | -2.469366934993 |
| C | 1.969403692008 | -0.855666522160 | 3.814305317392 |
| C | 5.076181664020 | -2.944819964614 | -0.449190125393 |
| C | 6.187451564486 | 2.175830434713 | 2.362581793083 |
| C | -2.048533119754 | -4.388707340409 | -2.248412807330 |
| C | 2.687284469024 | -5.089692076852 | 0.369980099800 |
| C | -3.301356232072 | -1.242614042451 | -3.803449590903 |
| C | -7.389400775549 | 0.057462132563 | 0.369414681567 |
| C | -3.429664012572 | -2.279265914852 | 2.940394754540 |
| C | -0.858567827121 | 5.203196470309 | 1.291585009000 |
| C | -2.853952147728 | 3.911364347472 | -0.594294513260 |
| H | -0.022960030046 | -4.797825493836 | 0.075962066064 |
| H | -4.767575154243 | 0.626499660923 | -2.235446000022 |

| | | | |
|---|---|---|---|
| H | -4.827896405800 | -0.019247982126 | 1.965032621040 |
| H | -1.494694159085 | -1.063097942389 | -2.682813519284 |
| H | -3.585240515210 | -2.227412013343 | -3.429945220487 |
| H | -2.775356736275 | -1.375282503322 | -4.753055541640 |
| H | -4.220052110224 | -0.688124746592 | -4.009198971861 |
| H | -2.999787507191 | 1.488799284070 | -3.450541929750 |
| H | -1.586830007252 | 0.849834717950 | -4.292183527709 |
| H | -1.461082204729 | 1.447123568310 | -2.616905572998 |
| H | -6.548880054715 | 1.382998194604 | -1.076572015346 |
| H | -7.423474312015 | -0.807722546606 | -0.296426216402 |
| H | -8.373262710358 | 0.533944738953 | 0.366274372179 |
| H | -7.199178578661 | -0.308431646241 | 1.382032279471 |
| H | -6.078946619008 | 1.994194982449 | 1.880148406871 |
| H | -7.269903322366 | 2.766965422749 | 0.831890535272 |
| H | -5.537100240492 | 2.989747384854 | 0.531884136439 |
| H | -1.578059663089 | -1.783376012761 | 2.016642885635 |
| H | -4.358115158614 | -1.806172805733 | 3.270340187597 |
| H | -2.939498055463 | -2.695164369917 | 3.824645331333 |
| H | -3.698402238729 | -3.102939764700 | 2.277303180123 |
| H | -1.618402621356 | 0.662209632708 | 2.674959101966 |
| H | -1.639510650176 | -0.463917381924 | 4.057800732361 |
| H | -3.114406681286 | 0.360327520020 | 3.547388103885 |
| H | 5.514768155224 | -0.074830911257 | -0.588869140097 |
| H | 3.285273055088 | 1.917593438217 | 2.421102775259 |
| H | 3.041884315300 | -2.745734158649 | -1.122546327408 |
| H | 5.999997506459 | -2.360725825115 | -0.449655184474 |
| H | 5.254244772730 | -3.847166473408 | -1.039150466826 |
| H | 4.878589786503 | -3.243092932693 | 0.579732804914 |
| H | 3.579301405442 | -1.144068553536 | -2.974285828970 |
| H | 4.519496240230 | -2.630855643839 | -3.062684042967 |
| H | 5.269352063463 | -1.152929367191 | -2.473821852623 |
| H | 6.372975116012 | 1.828583963939 | 0.266294590545 |
| H | 5.448142642733 | 2.499048560492 | 3.099750117852 |
| H | 7.020852869989 | 2.881818431513 | 2.397876819804 |
| H | 6.555419941708 | 1.193738131744 | 2.666663539050 |
| H | 4.716011459117 | 3.496234301983 | -0.488845684498 |
| H | 5.887152911931 | 4.244913890411 | 0.603187034556 |
| H | 4.266736021112 | 3.845104076027 | 1.181366744269 |
| H | 0.449753442962 | -0.346919452976 | 2.411763477450 |
| H | 2.245903451466 | -1.813902358255 | 3.375277769110 |
| H | 1.249815109727 | -1.034636328391 | 4.617480287714 |
| H | 2.870217306056 | -0.419310677747 | 4.254906603288 |
| H | 1.917097245480 | 1.860357327352 | 3.929375058687 |
| H | 0.283999285090 | 1.273845325384 | 4.188900739093 |
| H | 0.648976882638 | 2.140983830799 | 2.697136711808 |
| H | -3.181085124262 | -3.149429919760 | -0.921081497231 |
| H | -1.760623808618 | -3.594514811257 | -2.939196312960 |
| H | -2.926669498065 | -4.896892370857 | -2.655999417475 |
| H | -1.227725973485 | -5.110832844915 | -2.213283438260 |
| H | -1.972221952311 | -5.759417871770 | 0.110865459562 |
| H | -3.663262506137 | -5.439943590846 | -0.257679958702 |
| H | -2.885139504438 | -4.623493875824 | 1.104678740897 |
| H | 3.039865503818 | -3.246792246881 | 1.414584891286 |
| H | 1.891001678079 | -5.825896860138 | 0.236207735327 |
| H | 3.509681936661 | -5.592722437290 | 0.884457149185 |
| H | 3.036429278386 | -4.796826633876 | -0.620147709732 |

| | | | |
|---|---|---|---|
| H | 1.225917041050 | -3.601078497510 | 3.124788660619 |
| H | 2.406472807844 | -4.921017764691 | 3.095687628816 |
| H | 0.821155136825 | -5.123625480172 | 2.339846010764 |
| H | -3.570275607431 | 4.723665696139 | -0.433774162730 |
| H | -2.233604507958 | 4.177966277397 | -1.456241265301 |
| H | -3.410556837206 | 3.006191361856 | -0.853568945078 |
| H | -3.610681784944 | 4.190996611738 | 2.515507075462 |
| H | -3.557224617818 | 2.444470484095 | 2.228721143115 |
| H | -2.380683888967 | 3.196126875178 | 3.309547636505 |
| H | -1.556965734272 | 6.015405018263 | 1.517130080699 |
| H | -0.198290264894 | 5.080679828015 | 2.155799355850 |
| H | -0.240731196454 | 5.519840580347 | 0.446609519646 |
| N | 1.358130167120 | 1.818488144876 | -1.333730495439 |
| N | 1.607396848761 | 2.977442616230 | -0.963564367326 |
| N | 1.828402751211 | 4.011056808969 | -0.617504805295 |
| Si | 1.884835927709 | 1.468295229159 | -3.043919879206 |
| C | 1.275994183726 | -0.250074147695 | -3.366833195517 |
| C | 1.064253229191 | 2.744445667225 | -4.120737614171 |
| C | 3.726346512228 | 1.713479109033 | -3.092084572513 |
| H | 1.451284031771 | -0.918396654181 | -2.522653673675 |
| H | 0.205062522872 | -0.233384001399 | -3.563599953709 |
| H | 1.770271990298 | -0.663650370578 | -4.249403162568 |
| H | 1.336692951993 | 2.573775710918 | -5.166492359735 |
| H | -0.022850153657 | 2.708018926043 | -4.042899903301 |
| H | 1.393148634063 | 3.753911511853 | -3.860309848356 |
| H | 4.130003484793 | 1.385793016113 | -4.054012184229 |
| H | 3.968553678685 | 2.773693952475 | -2.978157495865 |
| H | 4.225705165844 | 1.158232499243 | -2.298818951906 |

**Table 6.S12**. XYZ Coordinates for Transition State 3.

134

TS3

| | | | |
|---|---|---|---|
| C | 2.272769883373 | -0.255551859368 | -1.672580290834 |
| C | 2.420792734281 | 0.801311712770 | -0.730352886192 |
| C | 3.621461870288 | 0.874284141176 | 0.002038734683 |
| C | 4.531983973662 | -0.177469103521 | -0.084921398562 |
| C | 4.307143615150 | -1.303972651369 | -0.855089097402 |
| C | 3.186492565816 | -1.301749115277 | -1.673960747993 |
| C | 1.234558835918 | 1.674612259621 | -0.447708571047 |
| C | 0.072895173469 | 0.988200248979 | -0.018950929299 |
| C | -1.114222660627 | 1.684709268722 | 0.251784551895 |
| C | -1.094921978514 | 3.087069831693 | 0.286764330308 |
| C | 0.048362011745 | 3.731125533864 | -0.155709413379 |
| C | 1.181634804829 | 3.064899421312 | -0.608996669105 |
| C | -2.417514304288 | 0.944956372205 | 0.303055376106 |
| C | -2.974960070464 | 0.433096341419 | 1.479882666817 |
| C | -4.181370377853 | -0.258131198909 | 1.423924190373 |
| C | -4.870509365315 | -0.446901307333 | 0.239885885740 |
| C | -4.317323729116 | 0.086600504703 | -0.916270638004 |
| C | -3.115094217441 | 0.777873996455 | -0.911575251426 |
| C | -2.328805576698 | 0.630977642039 | 2.828688355127 |
| C | -1.978243561381 | -0.707012133655 | 3.468456293070 |
| C | -2.604022470650 | 1.333653026528 | -2.224147770833 |
| C | -2.260516177315 | 0.212935492056 | -3.198144109110 |
| C | -6.187819108314 | -1.181975003890 | 0.218811754157 |
| C | -6.135059694625 | -2.424350269643 | -0.663451991999 |

| | | | |
|---|---|---|---|
| Al | 0.122571071552 | -0.973297408602 | 0.050527883701 |
| N | -0.520168070110 | -2.380193015397 | -0.628281124048 |
| Si | -1.574920918050 | -3.622176895727 | -1.030127148611 |
| C | -0.673860426584 | -5.130695944276 | -1.719982351215 |
| C | 2.219825613603 | 3.866833441294 | -1.359901323400 |
| C | 1.626760704223 | 4.371979526097 | -2.677024089677 |
| C | -2.269042317004 | 3.903500629693 | 0.773074486159 |
| C | -2.676958560407 | 5.009878885775 | -0.193749385415 |
| C | 4.035213139288 | 2.084693488380 | 0.814789254135 |
| C | 4.499603067299 | 1.781767938922 | 2.234905846864 |
| C | 5.258111478694 | -2.473327113248 | -0.833164514548 |
| C | 4.573677713337 | -3.714186870961 | -0.266141083934 |
| C | 1.304483163443 | -0.136321757861 | -2.839714957026 |
| C | 0.938174647212 | -1.452534802664 | -3.507150509685 |
| C | 5.172773484860 | 2.811363827211 | 0.091747046304 |
| C | 1.943895690662 | 0.800593325620 | -3.867763429258 |
| C | 5.848811685138 | -2.756064571050 | -2.210660929178 |
| N | 1.219298893573 | -1.714244950993 | 1.607669680821 |
| N | 1.228578007171 | -2.964605386296 | 1.430548351870 |
| N | 0.941434320960 | -3.914396151405 | 0.904569290627 |
| Si | 1.911517902870 | -1.194396866900 | 3.192607691444 |
| C | 1.175583447816 | -2.286782015520 | 4.511778896915 |
| C | 3.744392049706 | -1.510999710139 | 3.151023003728 |
| C | 1.395110656543 | 0.578310952982 | 3.377548998779 |
| C | -1.947602167109 | 4.498827436743 | 2.143407158466 |
| C | 2.766015154449 | 5.053853718036 | -0.572055114677 |
| C | -3.605628024464 | 2.296813446694 | -2.854773980493 |
| C | -7.326897245036 | -0.258408763011 | -0.203321112671 |
| C | -3.220021998105 | 1.444940808926 | 3.763227543694 |
| C | -2.580724024148 | -4.181099000075 | 0.468431918728 |
| C | -2.822933196988 | -3.153859748813 | -2.364576958067 |
| H | 0.036320264197 | 4.814341582377 | -0.213339503197 |
| H | -4.605996112335 | -0.656773506761 | 2.340242580089 |
| H | -4.839542620547 | -0.040424073493 | -1.858914158488 |
| H | -1.405912935902 | 1.195186743126 | 2.665065455841 |
| H | -3.516958990569 | 2.391182530709 | 3.309186191803 |
| H | -2.700147648382 | 1.662965562736 | 4.700367408640 |
| H | -4.131547322242 | 0.894670992901 | 4.009149752155 |
| H | -2.877714192181 | -1.300388840941 | 3.647584720739 |
| H | -1.483142017746 | -0.560870706321 | 4.432271469061 |
| H | -1.327528058799 | -1.301378222844 | 2.822769684849 |
| H | -6.384594585028 | -1.508863154754 | 1.246224748492 |
| H | -7.387154133039 | 0.618549810746 | 0.444980703844 |
| H | -8.284876344016 | -0.783338136064 | -0.163133459462 |
| H | -7.182984801784 | 0.093875586496 | -1.228300741284 |
| H | -5.954319240652 | -2.158861939472 | -1.708135879708 |
| H | -7.083469801100 | -2.966007170618 | -0.617256512488 |
| H | -5.335941796692 | -3.099167859070 | -0.353228595096 |
| H | -1.688540774837 | 1.892848302183 | -2.019976596627 |
| H | -4.511008557592 | 1.772046831188 | -3.170286512907 |
| H | -3.173895254549 | 2.770152978023 | -3.740624393133 |
| H | -3.906953951163 | 3.080316139147 | -2.157906329994 |
| H | -1.616994904702 | -0.534013557961 | -2.732642286348 |
| H | -1.758587489381 | 0.614389043823 | -4.083222052414 |
| H | -3.162749724944 | -0.304815468496 | -3.532713936751 |
| H | 5.451440084464 | -0.120721769328 | 0.490136571310 |

| | | | |
|---|---|---|---|
| H | 3.026544730937 | -2.125055040285 | -2.358310238214 |
| H | 3.172511770973 | 2.749259433854 | 0.883295989661 |
| H | 6.069854022391 | 2.186751938232 | 0.085674236203 |
| H | 5.420617507011 | 3.745073320417 | 0.602474381756 |
| H | 4.929523926364 | 3.042528419530 | -0.944987352644 |
| H | 3.740527581452 | 1.268596819616 | 2.817928998858 |
| H | 4.742834012538 | 2.715841399195 | 2.747695039830 |
| H | 5.402767681429 | 1.166933853433 | 2.240236350246 |
| H | 6.082517848608 | -2.204894522267 | -0.162524486678 |
| H | 5.072126273945 | -3.059462241372 | -2.917106696734 |
| H | 6.580089731038 | -3.566242717778 | -2.156033685717 |
| H | 6.344827367653 | -1.872273192962 | -2.617319938509 |
| H | 4.205169236017 | -3.532621687114 | 0.745573937038 |
| H | 5.267673687690 | -4.557584492867 | -0.229440007551 |
| H | 3.719627573563 | -4.007006016230 | -0.882201452858 |
| H | 0.386940946610 | 0.339486562272 | -2.488739731310 |
| H | 2.234177915558 | 1.751634343077 | -3.422280831023 |
| H | 1.248804307948 | 0.997791031712 | -4.688150376647 |
| H | 2.843063487090 | 0.340370077991 | -4.286781189636 |
| H | 1.796393382079 | -1.892135731764 | -4.023114748391 |
| H | 0.171238270554 | -1.273365141744 | -4.263406620977 |
| H | 0.542444033326 | -2.163773866254 | -2.779249263999 |
| H | -3.116817093753 | 3.221733037665 | 0.883950503486 |
| H | -1.650514973824 | 3.727926968687 | 2.856178258580 |
| H | -2.813077115978 | 5.028325909892 | 2.550920707328 |
| H | -1.122744177283 | 5.212762881238 | 2.064600686116 |
| H | -1.912789043579 | 5.789299144080 | -0.254191216692 |
| H | -3.600213517647 | 5.487048501736 | 0.143911332576 |
| H | -2.839684913513 | 4.625198034363 | -1.200913981394 |
| H | 3.043568719368 | 3.191544531365 | -1.601460443165 |
| H | 1.987236178358 | 5.802720228770 | -0.408288484866 |
| H | 3.571899175869 | 5.540118052308 | -1.127144353967 |
| H | 3.155371397703 | 4.763308530279 | 0.403825411332 |
| H | 1.187151609835 | 3.562460898151 | -3.260273597983 |
| H | 2.395209109276 | 4.857203061970 | -3.284661337088 |
| H | 0.838344657557 | 5.104214242615 | -2.484624889967 |
| H | -3.315235623061 | -4.952618553634 | 0.216568092774 |
| H | -1.924977370397 | -4.583617489356 | 1.246321515231 |
| H | -3.113729075759 | -3.324287977619 | 0.892466586156 |
| H | -3.506713166536 | -3.985972593268 | -2.560528925702 |
| H | -3.416361048552 | -2.290299485429 | -2.060503977442 |
| H | -2.320020672168 | -2.905024613201 | -3.303111418684 |
| H | -1.379570742454 | -5.906234969093 | -2.033677797614 |
| H | -0.081400154722 | -4.847141462130 | -2.595569978178 |
| H | 0.006172098546 | -5.567714693708 | -0.985530174505 |
| H | 1.531217889762 | 1.151766537098 | 2.459010615614 |
| H | 0.340207771027 | 0.626966170871 | 3.647130124865 |
| H | 1.963963432055 | 1.059951487709 | 4.176461906974 |
| H | 1.547372171139 | -1.976445244507 | 5.492884476767 |
| H | 0.086688768224 | -2.243837326591 | 4.533484623034 |
| H | 1.474175293002 | -3.328274223116 | 4.366135944348 |
| H | 4.229654559720 | -1.092612845410 | 4.037053838485 |
| H | 3.927906301237 | -2.589132169615 | 3.151656470241 |
| H | 4.211595918314 | -1.084734976903 | 2.264934633314 |

**Table 6.S13.** XYZ Coordinates for $Ar^{iPr8}Al[N(SiMe_3)N]_2$

134

AriPr8Al[N(SiMe3)N]2

| | | | |
|---|---|---|---|
| C | -3.860500166337 | -0.848750304319 | 1.504625608209 |
| C | -2.676651810024 | -0.117905382616 | 1.542646273356 |
| C | -2.440557963157 | 0.854476421310 | 0.556316281786 |
| C | -3.442328265049 | 1.126996878313 | -0.405954919003 |
| C | -4.608737383050 | 0.375056706680 | -0.386900627961 |
| C | -4.833568477058 | -0.628512288580 | 0.546282487713 |
| C | -3.300135749440 | 2.267536378063 | -1.403995822155 |
| C | -4.619558712533 | 2.711856027379 | -2.018657916627 |
| C | -1.762690077984 | -0.285807713888 | 2.739885985230 |
| C | -2.283479528805 | 0.583790928205 | 3.885312073631 |
| C | -1.141919571512 | 1.577364987664 | 0.426985867614 |
| C | -1.069544435720 | 2.970083142669 | 0.586659796472 |
| C | -0.000995304273 | 3.631877966011 | 0.002456823062 |
| C | 1.067817510805 | 2.971629809701 | -0.582976385799 |
| C | 1.140932783463 | 1.578729087525 | -0.425385887452 |
| C | -0.000175402342 | 0.869501529810 | 0.000491595634 |
| C | 2.439580505309 | 0.856255627307 | -0.556560374186 |
| C | 2.674842688805 | -0.114783450631 | -1.544462483861 |
| C | 3.858432342742 | -0.846172286603 | -1.508033410697 |
| C | 4.832146256234 | -0.627443927332 | -0.550007560967 |
| C | 4.608236301218 | 0.375083841474 | 0.384544795570 |
| C | 3.442056389263 | 1.127335339816 | 0.405365851668 |
| C | -2.064578302642 | 3.748177732631 | 1.420924833875 |
| C | -1.420912373408 | 4.047108733220 | 2.777806951790 |
| C | 6.118863074587 | -1.417465242290 | -0.592566801064 |
| C | 7.086458810897 | -0.789118475728 | -1.595045178020 |
| C | 2.062172314258 | 3.751479817656 | -1.416363157802 |
| C | 1.418531497400 | 4.050802927902 | -2.773167756747 |
| Al | 0.001570894293 | -1.106205090584 | 0.000417237256 |
| N | -0.862841620987 | -2.427054741751 | -0.912296527653 |
| Si | -2.069100527003 | -2.853006797714 | -2.129665051177 |
| C | 1.760780449616 | -0.279883795584 | -2.742046951998 |
| C | 2.283116249692 | 0.590490749181 | -3.886192250290 |
| C | 3.301012829407 | 2.267139236714 | 1.404434892055 |
| C | 4.620840452996 | 2.709316348244 | 2.019784632718 |
| C | -6.120493333831 | -1.418259527101 | 0.586960704683 |
| C | -7.089661342248 | -0.789381843024 | 1.587565852500 |
| N | 0.864807964360 | -2.426315582583 | 0.915378298102 |
| Si | 2.072766474764 | -2.851946378172 | 2.131201431946 |
| N | 0.429946545521 | -3.656656742094 | 0.451934615440 |
| N | -0.429235215853 | -3.657010344335 | -0.446832280581 |
| C | 2.272042305998 | 2.047980135481 | 2.513218998166 |
| C | 1.618914426426 | -1.717355523381 | -3.225286149582 |
| C | 2.539651345622 | 5.063179804208 | -0.799887884219 |
| C | -2.543756438142 | 5.059868879182 | 0.805741960098 |
| C | -1.622642940195 | -1.724131251604 | 3.221128922881 |
| C | 6.785513782109 | -1.580467969620 | 0.765473758213 |
| C | -2.271653517573 | 2.047666767096 | -2.513044836290 |
| C | -6.784763332001 | -1.581679036925 | -0.772203709699 |
| H | 5.369499410470 | 0.574700265854 | 1.126055606558 |

| | | | |
|---|---|---|---|
| H | -0.001308852210 | 4.716151924292 | 0.003361779927 |
| H | 2.935650713923 | 3.112572974719 | 0.824998782261 |
| H | 4.033630649199 | -1.604914940027 | -2.263192802499 |
| H | 0.767668560877 | 0.095796624126 | -2.472366535630 |
| H | -5.369411593122 | 0.575812115208 | -1.128714670938 |
| H | 2.933329269053 | 3.109357239418 | -1.580721389517 |
| H | -4.036318392185 | -1.608550793456 | 2.258568735346 |
| H | -2.934967769052 | 3.104944536459 | 1.584935082068 |
| H | -0.769086631808 | 0.088886006102 | 2.470572425067 |
| H | 5.861525821861 | -2.417609765212 | -0.960996822297 |
| H | -2.933412128871 | 3.112064843176 | -0.824143294970 |
| H | 1.720755178799 | 5.781253191278 | -0.709610074558 |
| H | 3.296568931391 | 5.519810495943 | -1.441826070198 |
| H | 2.979336378099 | 4.932251666650 | 0.190180306878 |
| H | 2.547573614426 | -2.080143455070 | -3.671932232984 |
| H | 0.851059113813 | -1.769226412728 | -3.999999381296 |
| H | 1.334991076610 | -2.402097047085 | -2.425847232087 |
| H | 1.325568373236 | 1.669238767285 | 2.127891754240 |
| H | 2.071853476927 | 2.998724352670 | 3.013957618886 |
| H | 2.643940404667 | 1.348322025867 | 3.261552351407 |
| H | 4.461311037584 | 3.617222683740 | 2.606391463307 |
| H | 5.375490009988 | 2.925651599237 | 1.260239953488 |
| H | 5.027135237920 | 1.956201023234 | 2.700651055128 |
| H | 2.425319401763 | 1.624251751903 | -3.573769811449 |
| H | 1.590912472436 | 0.575326892702 | -4.732261748398 |
| H | 3.249542875909 | 0.212161362235 | -4.230445733159 |
| H | -2.551559181493 | -2.086075165919 | 3.667930742733 |
| H | -0.854376799275 | -1.778083600050 | 3.995271471261 |
| H | -1.340213375231 | -2.408301419415 | 2.420685409337 |
| H | 7.173640128845 | -0.628819664157 | 1.138490100835 |
| H | 7.632670919639 | -2.265537112519 | 0.688122747000 |
| H | 6.091933345560 | -1.979538633609 | 1.507930076938 |
| H | -1.725573094727 | 5.778717720820 | 0.715144315739 |
| H | -3.300445060881 | 5.515407628276 | 1.448727727834 |
| H | -2.984348618840 | 4.929218044671 | -0.183947835618 |
| H | -2.423990800343 | 1.618219441481 | 3.574360777193 |
| H | -1.591243600052 | 0.566282609188 | 4.731309076833 |
| H | -3.250506181225 | 0.206559045889 | 4.229085171783 |
| H | 1.015790161588 | 3.150677466183 | -3.238013974152 |
| H | 2.142309321172 | 4.502206715436 | -3.457008654467 |
| H | 0.588814377960 | 4.751849288088 | -2.646533374082 |
| H | -5.863944307151 | -2.418324450110 | 0.956153382957 |
| H | -2.644000189146 | 1.347921705025 | -3.261090246698 |
| H | -1.325301007653 | 1.668577526046 | -2.127713807090 |
| H | -2.071117583049 | 2.998184278343 | -3.014085502019 |
| H | 6.636624034029 | -0.713934515110 | -2.587135801614 |
| H | 8.001414592020 | -1.381807558535 | -1.676406858978 |
| H | 7.362254555638 | 0.219962048431 | -1.275997143843 |
| H | -5.026768889908 | 1.960046179236 | -2.700415074927 |
| H | -4.459174290590 | 3.620333604903 | -2.604151692547 |
| H | -5.373865737041 | 2.927992063918 | -1.258714411548 |
| H | -1.016891073984 | 3.147094271517 | 3.241763709167 |
| H | -2.145069953475 | 4.496997349102 | 3.462241272839 |
| H | -0.592118457831 | 4.749319749227 | 2.651575364756 |
| H | -7.172083308018 | -0.630150654105 | -1.146350450693 |
| H | -7.632158951462 | -2.266595102892 | -0.696102303907 |

| | | | |
|---|---|---|---|
| H | -6.089862460320 | -1.981150188985 | -1.513212360062 |
| H | -6.641465537724 | -0.713962953488 | 2.580381285909 |
| H | -8.004883018448 | -1.381845313053 | 1.667581637097 |
| H | -7.364690883998 | 0.219659214110 | 1.267728835192 |
| C | 2.592978300346 | -1.310493121695 | 3.032197994382 |
| C | 1.358181924521 | -4.069433909775 | 3.356170416954 |
| C | 3.527574504064 | -3.641241343396 | 1.267805604482 |
| C | -2.588245234403 | -1.311348985665 | -3.030908178186 |
| C | -1.352661337604 | -4.070592264561 | -3.353473112260 |
| C | -3.525053048056 | -3.642568640147 | -1.268463125197 |
| H | -3.288844879029 | -1.568842348993 | -3.830379475023 |
| H | -3.086013065814 | -0.614624317634 | -2.357789305269 |
| H | -1.733487777385 | -0.805492051490 | -3.485939845533 |
| H | -2.120935592773 | -4.368802120652 | -4.073243926448 |
| H | -0.516021098770 | -3.646771309462 | -3.912079264383 |
| H | -0.998663262962 | -4.964127267883 | -2.836967059996 |
| H | -4.314571117250 | -3.909862256106 | -1.976286607142 |
| H | -3.199657566932 | -4.551733944625 | -0.757784796275 |
| H | -3.941462556788 | -2.963733023669 | -0.522371229937 |
| H | 2.127508925805 | -4.367565985530 | 4.074842942623 |
| H | 0.522428330567 | -3.645402878294 | 3.915962313175 |
| H | 1.003255953421 | -4.962985359573 | 2.840355892557 |
| H | 4.318031861103 | -3.909044588800 | 1.974379306273 |
| H | 3.201350549951 | -4.550085290068 | 0.757068529671 |
| H | 3.943031486354 | -2.962083108167 | 0.521470745968 |
| H | 3.294653399909 | -1.568369216873 | 3.830611677232 |
| H | 3.089758108534 | -0.613283680540 | 2.358869688665 |
| H | 1.738715989684 | -0.805115396631 | 3.488698637771 |

## References


(S1) Pangborn, A. B.; Giardello, M. A.; Grubbs, R. H.; Rosen, R. K.; Timmers, F. J. Safe and Convenient Procedure for Solvent Purification. *Organometallics* **1996**, *15*, 1518–1520.

(S2) Fulmer, G. R.; Miller, A. J. M.; Sherden, N. H.; Gottlieb, H. E.; Nudelman, A.; Stoltz, B. M.; Bercaw, J. E.; Goldberg, K. I. NMR Chemical Shifts of Trace Impurities: Common Laboratory Solvents, Organics, and Gases in Deuterated Solvents Relevant to the Organometallic Chemist. *Organometallics* **2010**, *29*, 2176–2179.

(S3) Queen, J. D.; Lehmann, A.; Fettinger, J. C.; Tuononen, H. M.; Power, P. P. The Monomeric Alanediyl :AlAr$^{iPr8}$ (Ar$^{iPr8}$ = $C_6H$-2,6-($C_6H_2$-2,4,6-Pr$^i_3$)2-3,5-Pr$^i_2$): An Organoaluminum(I) Compound with a One-Coordinate Aluminum Atom. *J. Am. Chem. Soc.* **2020**, *142*, 20554–20559.

(S4) Gavenonis, J.; Schüwer, N.; Tilley, T. D. 2,6-Dimesitylaniline ($H_2NC_6H_3$-2,6-$Mes_2$) and 2,6-Bis(2,4,6-triisopropylphenyl)aniline ($H_2NC_6H_3$-2,6-$Trip_2$). *Inorg. Synth.* **2018**, *37*, 98–102.

(S5) Bruker (2013) APEXII (Version 2014.9-1) and (2016) SAINT (Version 8.37a). Bruker AXS Inc., Madison, Wisconsin, USA

(S6) Sheldrick, G. M., (1996) SADABS. University of Göttingen, Germany.

(S7) Sheldrick, G. M. (2012) TWINABS; University of Göttingen, Germany.

(S8) Sheldrick, G.M., (2002). SHELXTL. Version 6.1. Siemens Analytical X-ray Instruments Inc., Madison, Wisconsin, USA.

(S9) Sheldrick, G. M., (2014). SHELXT. University of Göttingen, Germany.

(S10) Sheldrick, G. M., (2015). SHELXL University of Göttingen, Germany

(S11) Perdew, J. P.; Burke, K.; Ernzerhof, M. Generalized Gradient Approximation Made Simple. *Phys. Rev. Lett.* **1996**, *77*, 3865–3868.

(S12) Perdew, J. P.; Burke, K.; Ernzerhof, M. Generalized Gradient Approximation Made Simple. *Phys. Rev. Lett.* **1996**, *78*, 1396–1396.

(S13) Adamo, C.; Barone, V. Toward Reliable Density Functional Methods without Adjustable Parameters: The PBE0 Model. *J. Chem. Phys.* **1999**, *110*, 6158–6170.

(S14) Ernzerhof, M.; Scuseria, G. E. Assessment of the Perdew-Burke-Ernzerhof Exchange-Correlation Functional. *J. Chem. Phys.* **1999**, *110*, 5029–5036.

(S15) Weigend, F.; Ahlrichs, R. Balanced Basis Sets of Split Valence, Triple Zeta Valence and Quadruple Zeta Valence Quality for H to Rn: Design and Assessment of Accuracy. *Phys. Chem. Chem. Phys.* **2005**, *7*, 3297–3305.

(S16) Grimme, S.; Antony, J.; Ehrlich, S.; Krieg, H. A Consistent and Accurate Ab Initio Parametrization of Density Functional Dispersion Correction (DFT-D) for the 94 Elements H-Pu. *J. Chem. Phys.* **2010**, *132*, 154104.

(S17) Grimme, S.; Ehrlich, S.; Goerigk, L. Effect of the Damping Function in Dispersion

Corrected Density Functional Theory. *J. Comput. Chem.* **2011**, *32*, 1456–1465.

(S18) Gaussian 16, Revision C.01, Frisch, M. J.; Trucks, G. W.; Schlegel, H. B.; Scuseria, G. E.; Robb, M. A.; Cheeseman, J. R.; Scalmani, G.; Barone, V.; Petersson, G. A.; Nakatsuji, H.; Li, X.; Caricato, M.; Marenich, A. V.; Bloino, J.; Janesko, B. G.; Gomperts, R.; Mennucci, B.; Hratchian, H. P.; Ortiz, J. V.; Izmaylov, A. F.; Sonnenberg, J. L.; Williams-Young, D.; Ding, F.; Lipparini, F.; Egidi, F.; Goings, J.; Peng, B.; Petrone, A.; Henderson, T.; Ranasinghe, D.; Zakrzewski, V. G.; Gao, J.; Rega, N.; Zheng, G.; Liang, W.; Hada, M.; Ehara, M.; Toyota, K.; Fukuda, R.; Hasegawa, J.; Ishida, M.; Nakajima, T.; Honda, Y.; Kitao, O.; Nakai, H.; Vreven, T.; Throssell, K.; Montgomery, J. A., Jr.; Peralta, J. E.; Ogliaro, F.; Bearpark, M. J.; Heyd, J. J.; Brothers, E. N.; Kudin, K. N.; Staroverov, V. N.; Keith, T. A.; Kobayashi, R.; Normand, J.; Raghavachari, K.; Rendell, A. P.; Burant, J. C.; Iyengar, S. S.; Tomasi, J.; Cossi, M.; Millam, J. M.; Klene, M.; Adamo, C.; Cammi, R.; Ochterski, J. W.; Martin, R. L.; Morokuma, K.; Farkas, O.; Foresman, J. B.; Fox, D. J. Gaussian, Inc., Wallingford CT, 2016.

(S19) Stratmann, R. E.; Scuseria, G. E.; Frisch, M. J. An efficient implementation of time-dependent density-functional theory for the calculation of excitation energies of large molecules *J. Chem. Phys.* **1998**, *109*, 8218–8224

(S20) NBO 7.0. Glendening, E. D.; Badenhoop, J. K.; Reed, A. E.; Carpenter, J. E.; Bohmann, J. A.; Morales, C. M.; Karafiloglou, P.; Landis, C. R.; Weinhold, F. Theoretical Chemistry Institute, University of Wisconsin, Madison, WI 2018.

(S21) Mitoraj, M. P.; Michalak, A.; Ziegler, T. A Combined Charge and Energy Decomposition Scheme for Bond Analysis. *J. Chem. Theory Comput.* **2009**, *5*, 962–975.

(S22) te Velde, G.; Bickelhaupt, F. M.; Baerends, E. J.; Fonseca Guerra, C.; van Gisbergen, S. J. A.; Snijders, J. G.; Ziegler, T. Chemistry with ADF. *J. Comput. Chem.* **2001**, *22*, 931–967.

(S23) ADF 2019.3, SCM, Theoretical Chemistry; Vrije Universiteit; Amsterdam; The Netherlands, http://www.scm.com.

(S24) van Lenthe, E.; Baerends, E. J. Optimized Slater-Type Basis Sets for the Elements 1-118. J. Comp. Chem. **2003**, *24*, 1142–1156.

(S25) van Lenthe, E.; Baerends, E. J,; Snijders, J. G. Relativistic Total Energy Using Regular Approximations. *J. Chem. Phys.* **1994**, *101*, 9783–9792.

## Chapter 7. Comproportionation of a Dialuminyne with Alane or Dialane Dihalides as a Clean Route to Dialuminenes

Joshua D. Queen and Philip P. Power*

**Abstract.** Dialuminenes RAlAlR (R = m-terphenyl or bulky aryl) react with the aromatic solvents (e.g. benzene or toluene) in which they dissolve. We synthesized -$SiMe_3$ substituted derivatives of known terphenyl ligands to increase their solubility in alkanes which have lower reactivity than arenes. The new dialuminene was synthesized via the comproportionation reaction of $Na_2(AlAr^{iPr4}\text{-}4\text{-}SiMe_3)_2$ (**3**) ($Ar^{iPr4}$-4-$SiMe_3$ = 2,6-(2,6-$^iPr_2C_6H_3)_2$-4-$SiMe_3C_6H_2$) with either the diiodide $Al(Et_2O)I_2Ar^{iPr4}$-4-$SiMe_3$ (**1**) or the 1,2-diiododialane 4-$SiMe_3Ar^{iPr4}$(I)Al-Al(I)$Ar^{iPr4}$-4-$SiMe_3$ (**2**). This cleanly generates the dialuminene 4-$SiMe_3Ar^{iPr4}$AlAl$Ar^{iPr4}$-4-$SiMe_3$ which was trapped as its cycloaddition product (**4**) with benzene. Even in non-aromatic essentially inert solvents, red **4** decomposes to colorless solutions. This indicates that the instability of the free dialuminene is an inherent property rather than arising from of the method of synthesis or the presence of impurities.

The recognition in the 1970s and 80s that the heavier p-block elements can form multiple bonds to each other[1–3] led to the synthesis of series of alkene and alkyne analogues derived from the heavier members of the group 13, 14, and 15 elements.[4] The compounds with multiple bonds between aluminium atoms are of special interest due to their very high reactivity[5–9] and their calculated diradical

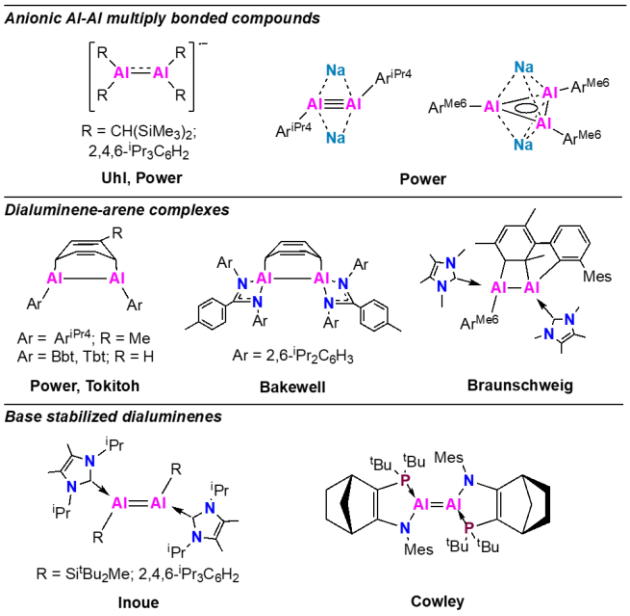


**Scheme 7.1.** Representative Al-Al multiple bonded species. $Ar^{iPr4}$ = 2,6-(2,6-$^iPr_2C_6H_3)_2C_6H_3$, $Ar^{Me6}$ = 2,6-$Mes_2C_6H_3$, Bbt = 2,6-{$CH(SiMe_3)_2$}$_2C_6H_3$, Tbt = 2,6-

character.[10] However this apparent diradical character makes them difficult to isolate as neutral species. Thus, structurally characterized Al-Al multiply bonded molecules (Scheme 7.1) tend to be anionic[11–13] and derived from the occupation of a bonding π-type LUMO in a neutral species. Alternatively, complexation of the aluminium atoms by Lewis bases confers stability to the multiple bonded compounds.[14–16] Another important compound class related to the multiple bonded species are the cycloaddition derivatives of Al=Al bonded moieties and solvent arenes.[17–21] This is a reversible process in some cases.[18–20]

The first isolated Al-Al π-bonded compounds resulted from one electron reduction of the tetraorganodialanes $R_2Al\text{-}AlR_2$ (R = $CH(SiMe_3)_2$, $C_6H_3$-2,4,6-$^iPr_3$).[12,22] Their EPR spectra showed the unpaired electron to be located predominantly in the π-type SOMO between the two Al atoms thereby generating multiple bond character and shortened Al-Al bonds.[11,12]

While the sterically demanding terphenyl ligand $Ar^{iPr4}$ ($Ar^{iPr4}$ = 2,6-(2,6-$^iPr_2C_6H_3)_2C_6H_3$) allowed the isolation of the neutral dimetallenes $Ar^{iPr4}EEAr^{iPr4}$ (E = Ga–Tl)[23–25] which dissociated to :$EAr^{iPr4}$ monomers in solution, the Al congener $Ar^{iPr4}AlAlAr^{iPr4}$ could not be isolated from hexanes or ether, due to its poor solubility.[17] Rather it could only be trapped and characterized as its cycloaddition products with toluene or $Me_3SiCCSiMe_3$ following the reduction of the halide derivative $AlI_2Ar^{iPr4}$ in $Et_2O$.[17,26] However, the dianionic dialuminyne $Na_2(AlAr^{iPr4})_2$ and the trimeric $Na_2(AlAr^{Me6})_3$ ($Ar^{Me6}$ = 2,6-(2,4,6-$Me_3C_6H_2)_2C_6H_3$) were isolable by reduction of $AlI_2Ar^{iPr4}$ and $AlI_2Ar^{Me6}$ with excess Na metal.[13] These are analogues of the corresponding Ga species $Na_2(GaAr^{iPr6})_2$[27] ($Ar^{iPr6}$ = 2,6-(2,4,6-$^iPr_3C_6H_2)_2C_6H_3$) and $Na_2(GaAr^{Me6})_3$[28] isolated earlier by Robinson and coworkers. By increasing the steric demand of the terphenyl ligand on the group 13 elements, the crystalline metallanediyls :$EAr^{iPr6}$ (E = In, Tl)[29,30], :$GaAr^{iPr8}$ ($Ar^{iPr8}$= 2,6-(2,4,6-$^iPr_3C_6H_2)_2$-3,5-$^iPr_2C_6H$) and :Ga(2,6-(2,6-$^iPr_2C_6H_3)_2$-3,5-$^iPr_2C_6H$)[31] were isolated. Following these

results, we recently reported the synthesis of a stable one-coordinate aluminium species :$AlAr^{iPr8}$.[32] A favorable dimerization energy of :$AlAr^{iPr8}$ to yield $Ar^{iPr8}AlAlAr^{iPr8}$ ($\Delta G$ = -20 kJ $mol^{-1}$) was calculated although this dimer was not isolated and only the monomer :$AlAr^{iPr8}$ was obtained from solution. Nonetheless, calculations suggested $Ar^{iPr8}AlAlAr^{iPr8}$ as the reactive species with $H_2$ (cf. monomeric :$GaAr^{iPr8}$ does not react with $H_2$ although the dimer $Ar^{iPr4}GaGaAr^{iPr4}$ is highly reactive).[33]

Tokitoh and coworkers isolated dialuminene-benzene cycloaddition products by reduction of the 1,2-dibromodialanes Bbt(Br)Al-Al(Br)Bbt (Bbt = 2,6-$\{CH(SiMe_3)_2\}_2C_6H_3$) and Tbt(Br)Al-Al(Br)Tbt (Tbt = 2,6-$\{CH(SiMe_3)_2\}_2$-4-$^tBuC_6H_2$) with $KC_8$ in benzene.[18,34] They further showed that these complexes act as synthetic equivalents to dialuminenes by the reversible dissociation of the benzene to yield ArAlAlAr in solution. The complexed benzene could also be irreversibly exchanged with naphthalene, anthracene, or $Me_3SiCCSiMe_3$ while the reaction with $H_2$ to give $\{AlH(\mu\text{-}H)Ar\}_2$ (Ar = Bbt, Tbt) was also observed under ambient conditions.[19]

As mentioned above, stable compounds containing Al=Al double bonds were only recently isolated through coordination of Lewis bases to the reactive Al centers and are so far limited to a few examples. Thus Inoue and coworkers reported the carbene complexed dialuminenes (NHC)RAl=AlR(NHC) (R = $Si^tBu_2Me$, 2,4,6-$^iPr_3C_6H_2$; NHC = 1,3-diisopropyl-4,5-dimethyl-imidazolin-2-ylidene)[14,15] and Cowley and coworkers reported the synthesis of an amidophosphine supported dialuminene which reversibly dissociates to monomers in solution.[16] However the coordination of Lewis bases to the aluminium atoms does not guarantee stability of the Al=Al bonded species. The amidinate supported dialuminene $(Am^{Dipp})Al{=}Al(Am^{Dipp})$ ($Am^{Dipp}$ = $C\{N(2,6\text{-}^iPr_2C_6H_3)\}_2(4\text{-}MeC_6H_4)$) generated by hydrogen abstraction from $AlH_2Am^{Dipp}$ by $Al(BDI^{Dipp})$ ($BDI^{Dipp}$ = $C\{C(Me)N(2,6\text{-}^iPr_2C_6H_3)\}_2$) at 80°C went on to react with the benzene

solvent to give the respective cycloaddition product.[21] Reduction of the carbene supported terphenyl aluminium diiodide $Al(NHC')I_2Ar^{Me6}$ (NHC′ = 1,3,4,5-tetramethylimidazol-2-ylidene) apparently gave $Ar^{Me6}(NHC')AlAl(NHC')Ar^{Me6}$ which added across a C=C bond of a flanking aryl ring, and the monomer $Al(NHC')Ar^{Me6}$ which ring opened the benzene or toluene solvent to give dihydropentalene type structures.[20]

Despite these advances, compounds of the type RAlAlR free of complexing ligands remain unisolated. Recent reports on the synthesis of the one-coordinate Al species[32,35,36] have illustrated the importance of reducing agent selection to access low oxidation state Al compounds—the products are only obtained when Na metal dispersed on NaCl powder is used. As the chemistry of dialuminenes remains underdeveloped, we revisited their synthesis with the objective of developing isolable ArAlAlAr species that are soluble in solvents with which they do not react. The direct stoichiometric reduction of the aluminium iodide precursors with alkali metals did not yield the targeted dialuminene, instead decomposition occured with elimination of the terphenyl arene. This led us to investigate alternative methods of their preparation free of alkali metal reductants. We found that the comproportionation reaction between a dialuminyne salt and aluminium iodides proceeded rapidly in benzene to cleanly afford a dialuminene-benzene complex. However, the comproportionation reaction in nonreactive ether or alkane solvents led to decomposition of the mixture, indicating an inherent instability of the dialuminene. Despite this, the reaction offers a new synthetic route to reactive Al-Al multiple bonded species.

Using the $-SiMe_3$ modified ligand $Ar^{iPr4}$-4-$SiMe_3$ ($Ar^{iPr4}$-4-$SiMe_3$ = 2,6-(2,6-$^iPr_2C_6H_3)_2$-4-$SiMe_3C_6H_2$), we anticipated that the extra aliphatic groups would increase the solubility of ArAlAlAr sufficiently to permit its handling in non-aromatic solvents with which it does not react (e.g. hexane, ether). The Hammett constant $\sigma_{para}$ = -0.07 for $-SiMe_3$[37] also suggested it would have

minimal electronic effects on the Al=Al moiety in comparison to the $Ar^{iPr4}$ derivative ($\sigma_{para}$ for H = 0). Addition of $LiAr^{iPr4}$-4-$SiMe_3$ to $AlH_3NMe_3$ in $Et_2O$ afforded the aluminate salt $Li(Et_2O)AlH_3Ar^{iPr4}$-4-$SiMe_3$ as a white solid. Subsequent treatment with $CH_3I$ (5 eq) gave the iodide $Al(Et_2O)I_2Ar^{iPr4}$-4-$SiMe_3$ (**1**). The Al-I distances in **1** (Figure 7.1, left) are 2.5288(7) Å and 2.5578(7) Å, an Al-C bond length of 1.9936(19) Å and Al-O bond being 1.8703(15) Å. Treating **1** with $KC_8$ (Scheme 7.2) gave the yellow 1,2-diiododialane 4-$SiMe_3Ar^{iPr4}$(I)Al-Al(I)$Ar^{iPr4}$-4-$SiMe_3$ (**2**) Figure 7.1, middle). The Al-Al distance of 2.604(2) Å in **2** is nearly identical to that of $Ar^{iPr4}$(I)Al-Al(I)$Ar^{iPr4}$ (2.609(2)Å). The I atoms are disordered over two sites with Al-I distances of 2.5083(11) and 2.5354(13) Å but in each case the coordination around the Al atom is trigonal planar. The UV-Visible spectrum of **2** showed a single absorbance at 386 nm.

The reduction of **1** with excess Na in the form of either Na mirror or 5% w/w Na/NaCl in $Et_2O$ gave a dark green-brown solution. Removal of the volatile components and extraction of the residue with hexanes and then

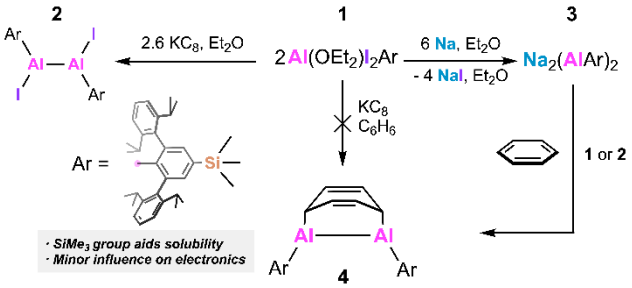


**Scheme 7.2.** Synthetic routes to compounds **2**, **3** and **4**.

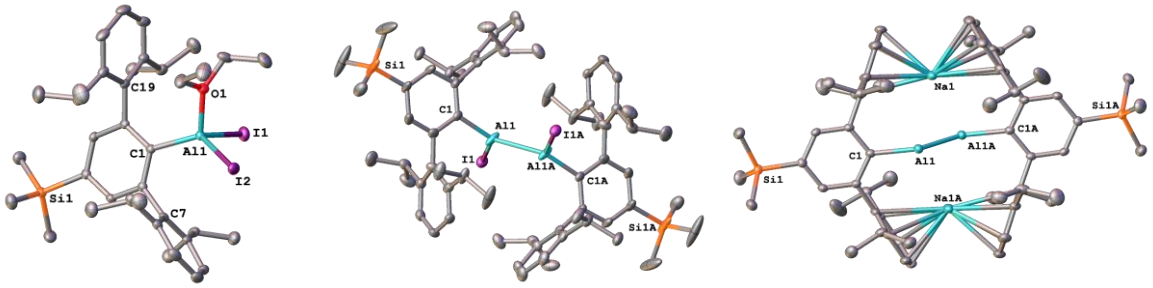

**Figure 7.1.** Thermal ellipsoid plots (30%) of **1** (left), **2** (middle), and **3** (right). Disordered atoms, solvent molecules, and hydrogen atoms are not shown. Selected bond distances (Å) and angles (°): [**1**]: Al(1)-I(1): 2.5287(7), Al(1)-I(2): 2.5578(8), Al(1)-C(1): 1.993(2), Al(1)-O(1): 1.8704(16), C(1)-Al(1)-I(1): 124.12(6), C(1)-Al(1)-I(2): 108.44(6), I(1)-Al(1)-I(2): 106.87(2), I(1)-Al(1)-O(1): 104.87(5) I(2)-Al(1)-O(1): 96.68(5). [**2**]: Al(1)-Al(1A): 2.604(3), Al(1)-I(1): 2.5087(17), Al(1)-C(1): 1.955(4), C(1)-Al(1)-Al(1A): 130.09(12), C(1)-Al(1)-I(1): 113.73(11), I(1)-Al(1)-Al(1A): 115.95(10), C(1)-Al(1)-Al(1A)-C(1A): 180. [**3**]: Al(1)-Al(1A): 2.4255(9), Al(1)-C(1): 2.0410(15), Al(1)-Na(1): 3.1403(8), Al(1)-Na(1A): 3.1138(9), Na-C(avg):2.968, C(1)-Al(1)-Al(1A)-C(1A): 180.

toluene gave two fractions: the hexanes extract, despite having a dark red color, contained 4-$SiMe_3$-$Ar^{iPr4}$H as the only identifiable product (isolated 62% based on **1**), indicating a significant amount of decomposition under reducing conditions. From the dark green toluene extract the anionic dialuminyne complex $Na_2$(4-$SiMe_3$-$Ar^{iPr4}$AlAl$Ar^{iPr4}$-4-$SiMe_3$) **3** was isolated as dark green-black crystals in ca. 30% yield. The structure of **3** (Figure 7.1, right) shows two crystallographically independent molecules with Al-Al distances of ca. 2.43 Å which is near to that of 2.428(1) Å in $Na_2$($Ar^{iPr4}$AlAl$Ar^{iPr4}$).[13] The Na-Al distances are in the range 3.1016(8) to 3.1403(8) Å, and the average Na-C distance is 2.968 Å. The UV-Visible spectrum of **3** displays absorbances at 344 nm, 470 nm, and at 612 nm with a shoulder at 660 nm (cf. 354, 456, and 600 nm in $Na_2$($Ar^{iPr4}$AlAl$Ar^{iPr4}$). Overall, the new compounds showed little deviation from their $Ar^{iPr4}$ substituted counterparts while having the desired increased solubility properties. However, attempts to reduce **1** or **2** with alkali metals to the dialuminene 4-$SiMe_3$-$Ar^{iPr4}$AlAl$Ar^{iPr4}$-4-$SiMe_3$ under a variety of conditions were unsuccessful.

As a result of the difficulty in direct reduction to the dialuminene (see above), we tested the comproportionation reaction of the dialuminyne **3** with the aluminium iodides **1** or **2**. Treating **3** with excess **1** in $C_6D_6$ showed formation of **2** with a trace amount of a new product that was later determined to be the dialuminene-benzene cycloaddition product **4**. Mixtures of **1** or **2** with a slight excess of **3** in $C_6D_6$ gave dark brown solutions that indicated consumption of the iodide materials along with formation of **4** in the $^1$H NMR spectra. On a preparative scale an equimolar mixture of **1** and **3** was dissolved in benzene, resulting in rapid formation of a red solution. Filtration and concentration of the solution to ca. 1 mL followed by storage at ca. 8°C afforded X-ray quality red

crystals of the dialuminene-benzene cycloaddition complex **4** (Figure 7.2) that were suitable for X-ray crystallography. $^1$H NMR monitoring of the reaction indicated the formation of no other Ar$^{iPr4}$-4-SiMe$_3$ substituted species except **4**.

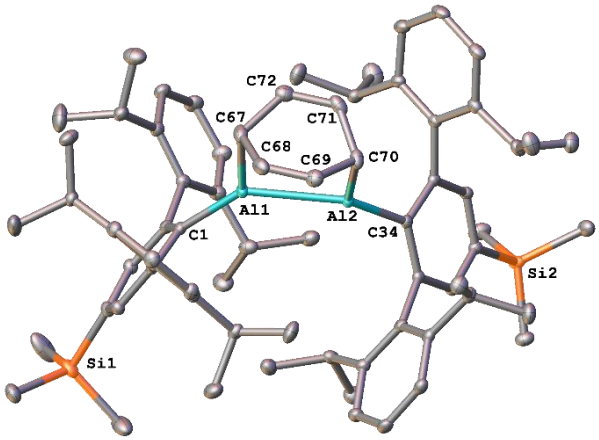


**Figure 7.2.** Thermal ellipsoid plot (30%) of **4.** Selected bond lengths (Å) and angles (°): Al(1)-Al(2): 2.5585(6), Al(1)-C(1): 1.9681(14), Al(2)-C(34): 1.9743(13), Al(1)-C(67): 2.0000(15), Al(2)-C(70): 1.9976(14), C(67)-C(68): 1.500(3), C(68)-C(69): 1.337(2), C(69)-C(70): 1.502(2), C(70)-C(71): 1.498(2), C(71)-C(72): 1.338(2), C(72)-C(67): 1.500(2), C(1)-Al(1)-Al(2): 136.83(4), C(1)-Al(1)-C(67): 128.87(6), C(67)-Al(1)-Al(2): 93.87(4), C(34)-Al(2)-Al(1): 136.76(4), C(34)-Al(2)-C(70): 127.02(6), C(70)-Al(2)-Al(1): 94.79(4).

The Al-Al bond length in **4** is 2.5585(6) Å with Al-C$_{ipso}$ distances of 1.9681(14) and 1.9743(13) Å while the Al-C distances to the bridging cyclohexadiene moiety are 2.0000(15) and 1.9976(14) Å. The Al atoms are almost planar coordinated (Σ°Al = 358.57(9)°, 359.57(9)°) and the C$_{ipso}$-Al-Al-C$_{ipso}$ torsion angle is 34.18(9)°. UV-Visible spectroscopy in hexanes showed an absorbance at 323 nm with a weaker shoulder spanning the range ca. 430 to 530 nm. A broad absorbance in the same region was found for the BbtAlAlBbt benzene complex mentioned above.[18]

The isolation of **4** is consistent with the growing number of cycloaddition products that have been isolated from the reaction of arenes and Al=Al bonded species.[17,18,20,21] Its formation serves as an indicator that the dialuminene ArAlAlAr is cleanly obtained from the reaction between **3** and **1** or **2**. The direct reduction of **1** in benzene with ≥2 eq alkali metal reducing agents did not afford the dialuminene but instead gave red solutions for which $^1$H NMR spectroscopy showed the generation of the free arene 4-SiMe$_3$-Ar$^{iPr4}$H as the major product and no signals assignable to **4**.

Complex **4** was observed to be soluble in benzene and cyclohexane as well as being sparingly soluble in hexanes or ether. While **4** showed no signs of decomposition in benzene after several

days, solutions of **4** in hexane or cyclohexane gradually lost their color overnight. This is probably due to reversible disassociation of **4** and a shift of the equilibrium toward benzene and the free dialuminene, which subsequently decomposes. Attempting the comproportionation reaction between **1** and **3** in $Et_2O$ or hexanes afforded a dark purple solution that also rapidly faded to colorless. We conclude that the instability of the dialuminene 4-$SiMe_3$-$Ar^{iPr4}$AlAl$Ar^{iPr4}$-4-$SiMe_3$ is an inherent property of the compound rather than an artifact of the synthetic route employed.

In summary, we have shown that the dialuminene 4-$SiMe_3$-$Ar^{iPr4}$AlAl$Ar^{iPr4}$-4-$SiMe_3$ is cleanly generated stoichiometrically in solution via the reaction of **1** or **2** with **3**. Its decomposition in hexanes or ether indicates that it is inherently unstable, probably as a result of its singlet diradical character.[10,38] However, it can be trapped as **4** by its reaction with benzene. Further investigations into the use of **3** as a reducing agent to generate Al-Al multiply bonded species are underway.

**References**


(1) Goldberg, D. E.; Harris, D. H.; Lappert, M. F.; Thomas, K. M. A New Synthesis of Divalent Group 4B Alkyls $M[CH(SiMe_3)_2]_2$(M = Ge or Sn), and the Crystal and Molecular and Molecular Strcuture of the Tin Compound. *J. Chem. Soc. Chem. Commun.* **1976**, 261–262.

(2) West, R.; Fink, M. J.; Michl, J. Tetramesityldisilene, a Stable Compound Containing a Silicon-Silicon Double Bond. *Science* **1981**, *214*, 1343–1344.

(3) Yoshifuji, M.; Shima, I.; Inamoto, N.; Hirotsu, K.; Higuchi, T. Synthesis and Structure of Bis(2,4,6-Tri-Tert-Butylphenyl)Diphosphene: Isolation of a True Phosphobenzene. *J. Am. Chem. Soc.* **1981**, *103*, 4587–4589.

(4) Fischer R. C.; Power, P. P. π-Bonding and the Lone Pair Effect in Multiple Bonds Involving Heavier Main Group Elements: Developments in the New Millennium. *Chem. Rev.* **2010**, *110*, 3877–3923.

(5) Downs, A. J. Recent advances in the chemistry of the Group 13 metals: hydride derivatives and compounds involving multiply bonded Group 13 metal atoms. *Coord. Chem. Rev.* **1999**, *189*, 59–100.

(6) Robinson, G. J. Multiple bonds involving aluminum and gallium atoms. *Adv. Organomet. Chem.* **2001**, *47*, 283–294.

(7) Wang, Y.; Robinson, G. H. Organometallics of the Group 13 M−M Bond (M = Al, Ga, In) and the Concept of Metalloaromaticity. *Organometallics*, **2007**, *26*, 2–11.

(8) Wang, Y.; G. H. Robinson, G. H. Unique homonuclear multiple bonding in main group compounds. *Chem. Commun.* **2009**, 5201–5213.

(9) Bag, P.; Weetman C.; Inoue, S. Experimental Realisation of Elusive Multiple-Bonded Aluminium Compounds: A New Horizon in Aluminium Chemistry. *Angew. Chem. Int. Ed.* **2018**, *57*, 14394–14413.

(10) Moilanen, J.; Power P. P.; Tuononen, H. M. Nature of Bonding in Group 13 Dimetallenes: a Delicate Balance between Singlet Diradical Character and Closed Shell Interactions. *Inorg. Chem.* **2010**, *49*, 10992–11000.

(11) Uhl, W.; Vester, A.; Kaim W.; Poppe, J. Dialan-Radikalanionen $[R_2Al\text{-}AlR_2]^{\cdot-}$ *J. Organomet. Chem.*, **1993**, *454*, 9–13.

(12) Wehmschulte, R. J.; Ruhlandt-Senge, K.; Olmstead, M. M.; Hope, H.; Sturgeon B. E.; Power, P.P. *Inorg. Chem.* **1993**, *32*, 2983–2984.

(13) Wright, R. J.; Brynda M.; Power, P. P. Synthesis and Structure of the "Dialuminyne" $Na_2[Ar'AlAlAr']$ and $Na_2[(Ar''Al)_3]$: Al—Al Bonding in $Al_2Na_2$ and $Al_3Na_2$ Clusters. *Angew. Chem., Int. Ed.* **2006**, *45*, 5953–5956.

(14) Bag, P.; Porzelt, A.; Altmann P. J.; Inoue, S. A Stable Neutral Compound with an Aluminum–Aluminum Double Bond. *J. Am. Chem. Soc.* **2017**, *139*, 14384–14387.

(15) Weetman, C.; Porzelt, A.; Bag, P.; Hanusch F.; Inoue, S. Dialumenes – Aryl vs. Silyl Stabilization for Small Molecule Activation and Catalysis *Chem. Sci.*, **2020**, *11*, 4817–4827.

(16) Falconer, R. L.; Byrne, K. M.; Nichol, G. S.; Krämer T.; Cowley, M. J. Reversible Dissociation of a Dialumene. *Angew. Chem. Int. Ed.* **2021**, *60*, 24702–24708.

(17) Wright, R. J.; Phillips A. D.; Power, P. P. The [2 + 4] Diels−Alder Cycloadditon Product of a Probable Dialuminene, Ar'AlAlAr' (Ar' = $C_6H_3$- 2,6-$Dipp_2$; Dipp = $C_6H_3$-2,6-$Pr^i_2$), with Toluene. *J. Am. Chem. Soc.* **2003**, *125*, 10784–10785.

(18) Agou, T.; Nagata K.; Tokitoh, N. Synthesis of a Dialumene-Benzene Adduct and Its Reactivity as a Synthetic Equivalent of a Dialumene. *Angew. Chem. Int. Ed.* **2013**, *52*, 10818–10821.

(19) Nagata, K.; Murosaki, T.; Agou, T.; Sasamori, T.; Matsuo T.; Tokitoh, N. Activation of Dihydrogen by Masked Doubly Bonded Aluminum Species. *Angew. Chem. Int. Ed.* **2016**, *55*, 12877–12880.

(20) Dhara, D.; Jayaraman, A.; Härterich, M.; Dewhurst R. D.; Braunschweig, H. Generation of a transient base-stabilised arylalumylene for the facile deconstruction of aromatic molecules. *Chem. Sci.* **2022**, *13*, 5631–5638.

(21) Bakewell, C.; Hobson K.; Carmalt, C. J. Exploring Equilibria between Aluminium(I) and Aluminium(III): The Formation of Dihydroalanes, Masked Dialumenes and Aluminium(I) Species*Angew. Chem. Int. Ed.* **2022**, *61*, e202205901.

(22) Uhl, W. *Z.* Tetrakis[bis(trimethylsilyl)methyl]dialan(4), eine Verbindung mit Aluminium—Aluminium-Bindung. *Naturforsch. B*, **1988**, *43*, 1113–1118.

(23) Hardman, N. J.; Wright, R. J.; Phillips A. D.; Power, P. P. Synthesis and Characterization of the Neutral "Digallene" Ar′GaGaAr′ and Its Reduction to $Na_2$Ar′GaGaAr′ (Ar′=2,6-$Dipp_2C_6H_3$, Dipp=2,6-$^iPr_2C_6H_3$). *Angew. Chem. Int. Ed.* **2002**, *41*, 2842–2844.

(24) Wright, R. J.; Phillips, A. D.; Hardman N. J.; Power, P. P. The "Diindene" ArInInAr (Ar = $C_6H_3$-2,6-$Dipp_2$, Dipp = $C_6H_3$-2,6-$Pr^i_2$). Dimeric versus Monomeric In(I) Aryls: para-Substituent Effects in Terphenyl Ligands. *J. Am. Chem. Soc.* **2002**, *124*, 8538–8539.

(25) Wright, R. J.; Phillips, A. D.; Hino S.; Power, P. P. Synthesis and Reactivity of Dimeric Ar'TlTlAr' and Trimeric $(Ar''Tl)_3$ (Ar', Ar'' = Bulky Terphenyl Group) Thallium(I) Derivatives: Tl(I)−Tl(I) Bonding in Species Ligated by Monodentate Ligands. *J. Am. Chem. Soc.* **2005**, *127*, 4794–4799.

(26) Cui, C.; Li, X.; Wang, C.; Zhang, J.; Cheng J.; Zhu, X. Isolation of a 1,2-Dialuminacyclobutene *Angew. Chem. Int. Ed.* **2006**, *45*, 2245–2247.

(27) Su, J.; Li, X.-W.; Crittendon R. C.; Robinson, G. H. How Short is a -Ga:Ga- Triple Bond? Synthesis and Molecular Structure of $Na_2[Mes^*_2C_6H_3$-Ga:Ga-$C_6H_3Mes^*_2]$ (Mes* = 2,4,6-i-$Pr_3C_6H_2$): The First Gallyne. *J. Am. Chem. Soc.* **1997**, *119*, 5471–5472.

(28) Li, X.-W.; Pennington W. T.; Robinson, G. H. Metallic System with Aromatic Character. Synthesis and Molecular Structure of $Na_2[[(2,4,6\text{-}Me_3C_6H_2)_2C_6H_3]Ga]_3$ The First Cyclogallane. *J. Am. Chem. Soc.* **1995**, *117*, 7578–7579.

(29) Haubrich S. T.; Power, P. P. Monomeric $InC_6H_3$-2,6-$Trip_2$ (Trip = -$C_6H_2$-2,4,6-i-$Pr_3$) and Its Manganese Complex $(\eta^5\text{-}C_5H_5)(CO)_2MnInC_6H_3$-2,6-$Trip_2$: One-Coordinate Indium in the Solid State. *J. Am. Chem. Soc.* **1998**, *120*, 2202–2203.

(30) Niemeyer M.; Power, P. P. Synthesis and Solid-State Structure of 2,6-$Trip_2C_6H_3Tl$ (Trip=2,4,6-$^iPr_3C_6H_2$): A Monomeric Arylthallium(I) Compound with a Singly Coordinated Thallium Atom. *Angew. Chem. Int. Ed.* **1998**, *37*, 1277–1279.

(31) Zhu, Z.; Fischer, R. C.; Ellis, B. D.; Rivard, E.; Merrill, W. A.; Olmstead, M. M.; Power, P. P.; Guo, J. D.; Nagase S.; Pu, L. Synthesis, Characterization and Real Molecule DFT Calculations for Neutral Organogallium(I) Aryl Dimers and Monomers: Weakness of Gallium—Gallium Bonds in Digallenes and Digallynes. *Chem. Eur. J.* **2009**, *15*, 5263–5272.

(32) Queen, J. D.; Lehmann, A.; Fettinger, J.C.; Tuononen, H. M.; Power, P. P. The Monomeric Alanediyl :$AlAr^{iPr8}$ ($Ar^{iPr8}$ = C$_6$H-2,6-$(C_6H_2$-2,4,6-$Pr^i_3)_2$-3,5-$Pr^i_2$): An Organoaluminum(I) Compound with a One-Coordinate Aluminum Atom *J. Am. Chem. Soc.* **2020**, *142*, 20554–20559.

(33) Caputo, C. A.; Koivistoinen, J.; Moilanen, J.; Boynton, J. N.; Tuononen H. M.; Power, P. P. Counterintuitive Mechanisms of the Addition of Hydrogen and Simple Olefins to Heavy Group 13 Alkene Analogues. *J. Am. Chem. Soc.* **2013**, *135*, 1952–1960.

(34) Nagata, K.; Agou, T.; Sasamori T.; Tokitoh, N. Formation of a Diaminoalkyne Derivative by Dialumane-mediated Homocoupling of t-Butyl Isocyanide. *Chem. Lett.* **2015**, *44*, 1610–1612.

(35) Zhang X.; Liu, L. L. A Free Aluminylene with Diverse σ-Donating and Doubly σ/π-Accepting Ligand Features for Transition Metals. *Angew. Chem. Int. Ed.* **2021**, *60*, 27062–27069.

(36) Hinz A.; Müller, M. P. Attempted reduction of a carbazolyl-diiodoalane. *Chem. Commun.* **2021,** *57*, 12532–12535.

(37) Hansch, C.; Leo A.; Taft, R. W. A survey of Hammett substituent constants and resonance and field parameters. *Chem. Rev.* **1991**, *91*, 165–195.

(38) Jung, Y.; Brynda, M.; Power, P. P.; Head-Gordon, M. Ab Initio Quantum Chemistry Calculations on the Electronic Structure of Heavier Alkyne Congeners: Diradical Character and Reactivity. *J. Am. Chem. Soc.* **2006**, *128*, 7185-7192.

## Author Contributions

**J. D. Queen**: Synthesized and spectroscopically characterized reported compounds, collected and prepared X-ray crystallography data for publication, and prepared the manuscript.

**P. P. Power**: Supervised synthetic work and manuscript preparation.

**Supporting Information**

**Experimental Details**

**General Procedures.** All manipulations were carried out using modified Schlenk techniques or in a Vacuum Atmospheres OMNI-Lab drybox under a $N_2$ or argon atmosphere. Solvents were dried over columns of activated alumina using a Grubbs type purification system[S1], stored over Na ($Et_2O$, hexanes), K (toluene) or 3 Å molecular sieves (benzene). $^1$H and $^{13}$C{$^1$H} spectra were recorded on Varian Inova 600 MHz or Bruker Avance III HD Nanobay 400 MHz spectrometers and were referenced to the residual solvent signals in $C_6D_6$.[S2] UV-Visible spectra were recorded in 3.5 mL quartz cuvettes using an Olis 17 Modernized Cary 14 UV-Vis/NIR spectrophotometer. Melting points were measured in glass capillary tubes sealed under argon using a Mel-Temp II apparatus using a partial immersion thermometer.

LiAr$^{iPr4}$-4-SiMe$_3$[S3] and AlH$_3$·NMe$_3$[S4] were prepared according to the literature procedures.

**[LiAlH$_3$Ar$^{iPr4}$-4-SiMe$_3$].** A solution of LiAr$^{iPr4}$-4-SiMe$_3$ (7.15 g, 15.0 mmol) in $Et_2O$ (ca. 50 mL) was added dropwise onto a solution of AlH$_3$·NMe$_3$ (1.34 g, 15.0 mmol) in $Et_2O$ (ca. 10 mL) cooled to 0°C in an ice/water bath. The mixture was warmed to room temperature and stirred for 18 h. The volatile components removed under reduced pressure and the residue dried at 40°C for 2 h. The solid was dissolved in ca. 90 mL of hot (ca. 60°C) hexanes and filtered. Removal of the solvent afforded [LiAlH$_3$Ar$^{iPr4}$-4-SiMe$_3$] as a white solid. Yield: 6.18 g (81%).

$^1$H NMR (600 MHz, $C_6D_6$, 298 K): δ 7.38 (s, 2H m-Ar***H***), 7.27 (t, $^3J$ = 7.6 Hz, 2H, Dipp p-Ar***H***), 7.18 (d, $^3J$ = 7.7 Hz, 4H, Dipp m-Ar***H***), 3.04 (sept, $^3J$ = 7.2 Hz, 4H, -C***H***(CH$_3$)$_2$), 2.25 (br, 3H, Al***H***), 1.29 (d, $^3J$ = 7.0 Hz, 12H, -CH(C***H***$_3$)$_2$), 1.12 (d, $^3J$ = 6.8 Hz, 12H, -CH(C***H***$_3$)$_2$), 0.29 (s, 9H, -Si(C***H***$_3$)$_3$).

$^{13}C\{^1H\}$ NMR (151 MHz, $C_6D_6$, 298 K): δ 146.57, 146.29, 143.22, 139.77, 133.50, 129.01, 123.37, 31.43, 25.04, 23.59, -1.37.

**Al(Et$_2$O)I$_2$Ar$^{iPr4}$-4-SiMe$_3$ (1).** A solution of [LiAlH$_3$Ar$^{iPr4}$-4-SiMe$_3$] (3.67 g, 7.25 mmol) in Et$_2$O (ca. 40 mL) was cooled to 0°C in an ice/water bath and CH$_3$I (2.3 mL, 36 mmol, 5 eq) was added via syringe. The mixture was allowed to slowly come to room temperature overnight with stirring (ca. 12 h). The volatile components were removed under reduced pressure and the white residue extracted with hexanes (ca. 60 mL). The colorless solution was filtered, concentrated to ca. 15 mL, and stored at ca. -18°C overnight to give colorless blocks of **1**. Yield: 3.87 g (65%).
m.p. = 185-188°C.

$^1H$ NMR (600 MHz, $C_6D_6$, 298 K): δ 7.40 (s, 2H, m-Ar***H***), 7.31 (t, $^3J$ = 7.7 Hz, 2H, Dipp p-Ar***H***), 7.21 (d, $^3J$ = 7.7 Hz, 4H, Dipp m-Ar***H***), 3.57 (q, $^3J$ = 7.1 Hz, 4H, O(C***H***$_2$CH$_3$)$_2$), 3.15 (sept, $^3J$ = 6.8 Hz, 4H, -C***H***(CH$_3$)$_2$), 1.43 (d, $^3J$ = 6.8 Hz 12H, -CH(C***H***$_3$)$_2$), 1.06 (d, $^3J$ = 6.7 Hz, 12H -CH(C***H***$_3$)$_2$), 0.73 (t, $^3J$ = 7.1 Hz, 6H, O(CH$_2$C***H***$_3$)$_2$), 0.21 (s, 9H, -Si(C***H***$_3$)$_3$).

$^{13}C\{^1H\}$ NMR (151 MHz, $C_6D_6$, 298 K): δ 147.68, 147.51, 143.03, 138.59, 136.15, 128.8, 123.47, 71.65, 31.09, 26.35, 23.51, 13.95, -1.45.

**{Al(I)Ar$^{iPr4}$-4-SiMe$_3$}$_2$. (2)** Ether (ca. 30 mL) was added to a mixture of solid **1** (1.65 g, 2.00 mmol) and KC$_8$ (0.350 g 2.60 mmol) at ambient temperature. The mixture was stirred for ca. 18 h during which time the color changed to yellow. The volatile components were removed under reduced pressure and the yellow residue dissolved in toluene (ca. 30 mL). The solution was filtered, concentrated to ca. 8 mL, and stored at ca. -18°C for 2 days to give pale yellow blocks of **2**. Yield: 0.536 g (43%).
m.p. = 198-201°C (dec).

$^{1}$H NMR (600 MHz, $C_6D_6$, 298 K): δ 7.37 (s, overlapping with triplet, 4H, m-Ar***H***), 7.37 (t, overlapping with singlet, $^{3}J$ = 7.8 Hz, 4H, Dipp, p-Ar***H***), 7.18 (d, $^{3}J$ = 7.8 Hz, 8H, Dipp m-Ar***H***), 3.03 (sept, $^{3}J$ = 6.7 Hz. 8H, -C***H***$(CH_3)_2$), 1.16 (d, 24H, $^{3}J$ = 6.8 Hz, -CH(C***H***$_3)_2$), 1.04 (d, $^{3}J$ = 6.7 Hz, 24H, -CH(C***H***$_3)_2$), 0.19 (s, 18H, -Si(C***H***$_3)_3$)

$^{13}$C{$^{1}$H} NMR (101 MHz, $C_6D_6$, 298 K): δ 147.83, 146.01, 140.29, 139.70, 134.83, 129.99, 124.16, 30.57, 26.44, 25.18, -1.49.

UV-Visible (hexanes): $\lambda_{max}$ 386 nm (ε =2300 L mol$^{-1}$ cm$^{-1}$).

**$Na_2$(AlAr$^{iPr4}$-4-SiMe$_3$)$_2$ (3).** *Method A*: A 100-mL Schlenk flask containing Na (0.201 g, 10.0 mmol, 5 eq) metal was heated under vacuum to mirror the interior wall of the flask with Na. The flask was then charged with a magnetic stirbar and **1** (1.65 g, 2.00 mmol). $Et_2O$ (ca. 70 mL) was added and the mixture was vigorously stirred for 3 days, during which time the mixture turned dark green-brown to black. The volatile components were removed under reduced pressure and the residue washed with hexanes (ca. 50 mL) to remove a dark red colored fraction containing mostly 4-SiMe$_3$-Ar$^{iPr4}$H (62% with respect to **1**). The residue was then extracted with toluene (ca. 40 mL) and the inky dark green solution filtered. Concentration to ca. 15 mL and storage at ca. -30°C overnight gave dark green/black blocks of **3**. Yield: 0.354 g (34%).

*Method B:* $Et_2O$ (ca. 70 mL) was added to mixture of **1** (1.65 g, 2.00 mmol) and 5% w/w Na/NaCl (4.60 g, 5 eq) and stirred for 3 days. The volatile components were removed under reduced pressure and the residue washed with hexanes (ca. 50 mL) then extracted with toluene (ca. 40 mL). The dark green toluene filtrate was concentrated to ca. 20 mL and stored at ca. -30°C overnight to give dark green blocks of **3**. Yield: 0.302 g (29%)

m.p. = 204-208°C (dec).

$^1$H NMR (600 MHz, $C_6D_6$, 298 K0): δ 7.20 (s, 4H, m-Ar***H***), 7.16 (t, overlapping with solvent signal, 4H, Dipp, p-Ar***H***), 6.97 (d, $^3J$ = 7.6 Hz, 8H, Dipp m-Ar***H***), 2.95 (sept, $^3J$ = 6.9 Hz, 8H, -C***H***$(CH_3)_2$), 1.46 (d, $^3J$ = 6.9 Hz, 24H, -CH(C***H***$_3)_2$) 1.03 (d, $^3J$ = 6.8 Hz 24H, -CH(C***H***$_3)_2$), 0.28 (s, 18H, -Si(C***H***$_3)_3$)

$^{13}$C{$^1$H} NMR (101 MHz, $C_6D_6$, 298 K): δ 165.10, 149.70, 148.38, 133.62, 130.98, 126.08, 122.06, 31.03, 25.27, 24.59, -0.95.

UV-Visible (toluene): $\lambda_{max}$ 344 nm (ε = 9400 L mol$^{-1}$ cm$^{-1}$), 470 nm (shoulder, ε = 4800 L mol$^{-1}$ cm$^{-1}$), 612 nm (ε = 4400 L mol$^{-1}$ cm$^{-1}$), 660 nm (shoulder, ε = 4100 L mol$^{-1}$ cm$^{-1}$).

**[(AlAr$^{iPr4}$-4-SiMe$_3$)$_2$(C$_6$H$_6$)] (4).** A mixture of solid [Na$_2$(AlAr$^{iPr4}$-4-SiMe$_3$)$_2$] (73.4 mg, 70.6μmol) and Al(Et$_2$O)I$_2$Ar$^{iPr4}$-4-SiMe$_3$ (58.2 mg, 70.6μmol) was dissolved in ca. 5 mL benzene. The mixture was stirred for ca. 15 min during which time the color changed from dark green to red with formation of a white precipitate. The mixture was filtered via cannula and concentrated under reduced pressure to ca. 1 mL. Storage of the solution at ca. 8°C yielded red blocks of **4**. Yield: 0.045 g (42%)

$^1$H NMR (600 MHz, $C_6D_6$, 298 K): δ 7.27 (t, $^3J$ = 7.7 Hz, 4H, Dipp p-Ar***H***), 7.14 (d, $^3J$ = 7.7 Hz, 8H, Dipp m-Ar***H***), 7.11 (s, 4H, m-Ar***H***), 3.04-2.91 (mult, br, 8H, -C***H***$(CH_3)_2$), 1.24-0.85 (mult, br, 48H, -CH(C***H***$_3)_2$), 0.13 (s, 18H, -Si(C***H***$_3)_3$). Complexed $C_6H_6$ signals not observed.

$^{13}$C{$^1$H} NMR (101 MHz, $C_6D_6$, 298 K): δ 146.15, 142.30, 138.90, 133.79, 129.19, 123.80, 30.91 (br), 25.54 (br), 23.25, -1.39.

UV-Visible (hexanes): $\lambda_{max}$ 323 nm (ε = 2200 L mol$^{-1}$ cm$^{-1}$), 460 (shoulder, ε = 230 L mol$^{-1}$ cm).

**4-SiMe$_3$-Ar$^{iPr4}$H NMR data:**

$^1$H NMR (400 MHz, $C_6D_6$, 298K): δ 7.49 (d, $^4J$ = 1.7 Hz, m-Ar***H***, 2H), 7.33 (t, $^3J$ = 7.6 Hz, 2H, Dipp p-Ar***H***), 7.21 (d, $^3J$ = 7.6 Hz, 4H, Dipp, m-Ar***H***), 7.11 (t, $^4J$ = 1.7 Hz, 1H, i-Ar***H***), 2.94 (sept, $^3J$ = 6.9 Hz, 4H, -C***H***$(CH_3)_2$), 1.16 (mult, 24 H, -CH(C***H***$_3)_2$), 0.21 (s, 9H, -Si(C***H***$_3)_3$).

$^{13}$C{$^1$H} NMR (101 MHz, $C_6D_6$, 298K) δ 146.97, 140.39, 140.18, 140.07, 133.05, 131.85, 122.97, 30.89, 24.44, 24.41, -1.10.

**NMR Scale Comproportionation Reactions:**

**1 + 3 to 2:** Solid **1** (5.0 mg, 6.1 μmol) was added to a solution of **3** (3.0 mg, 3.0 μmol) in ca. 0.5 mL $C_6D_6$ resulting in a color change from dark green to yellow.

**1 + 3 to 4** A mixture of solid **1** (2.1 mg, 2.5 μmol) and **3** (2.6 mg, 2.6 μmol) were dissolved in ca. 0.5 mL $C_6D_6$. The resulting spectrum showed **4**, excess **3**, and $Et_2O$.

**2 + 3 to 4** A mixture of solid **2** (3.1 mg, 2.5 μmol) and **3** (2.6 mg, 2.6 μmol) were dissolved in ca. 0.5 mL $C_6D_6$. The resulting spectrum showed **4** and excess **3**.

## NMR Spectra

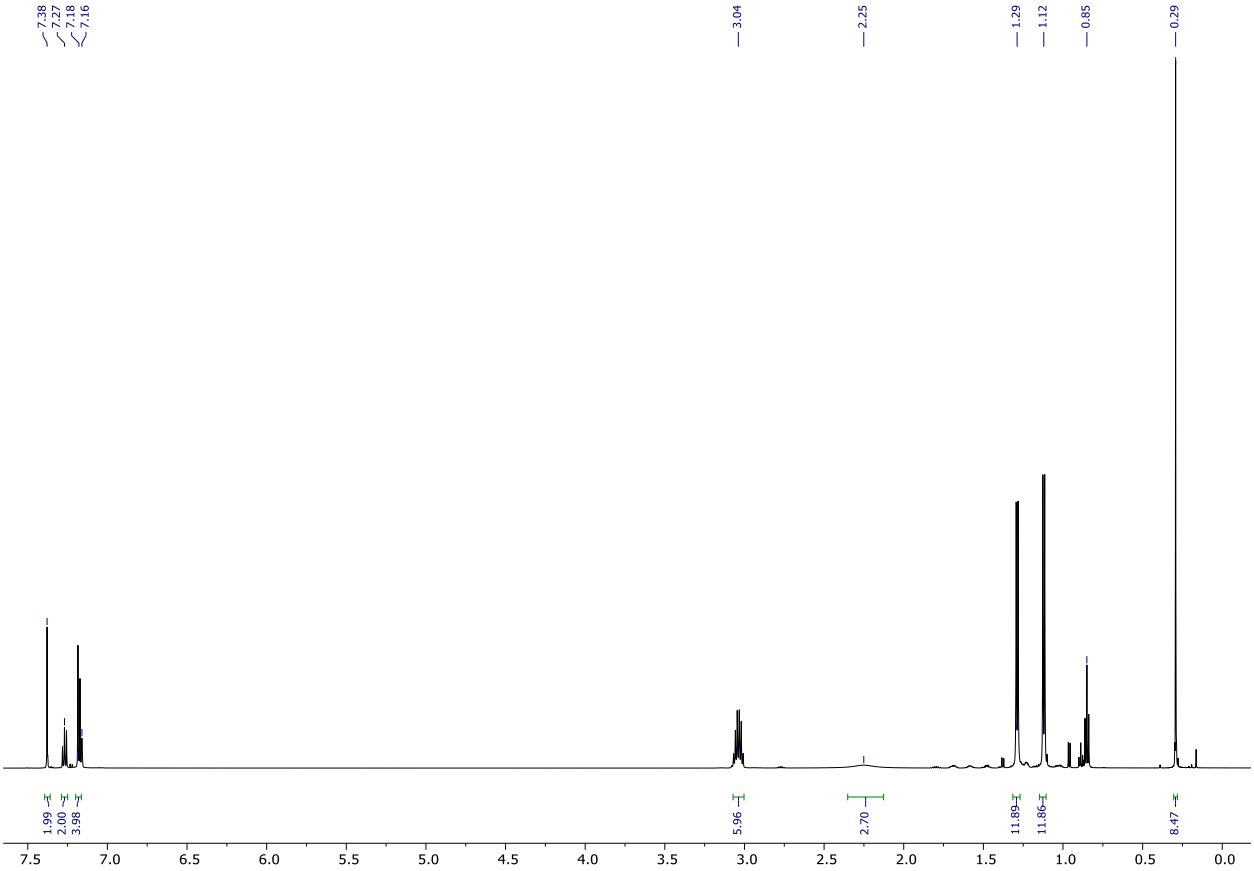


**Figure 7.S1.** $^{1}$H NMR (600 MHz, $C_6D_6$, 298 K) spectrum of [$LiAlH_3Ar^{iPr4}$-4-$SiMe_3$].

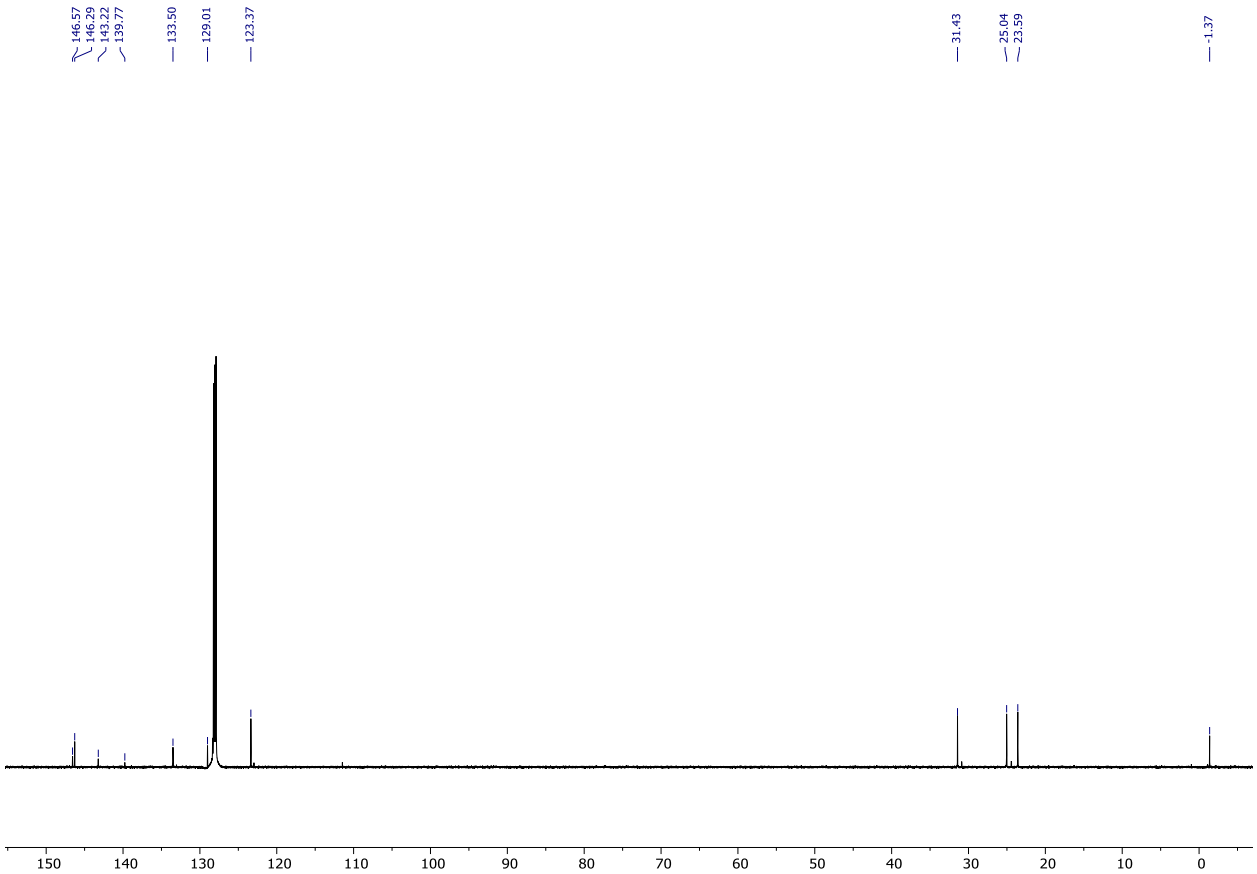


**Figure 7.S2.** $^{13}C\{^{1}H\}$ NMR (600 MHz, $C_6D_6$, 298 K) spectrum of [$LiAlH_3Ar^{iPr4}$-4-$SiMe_3$].

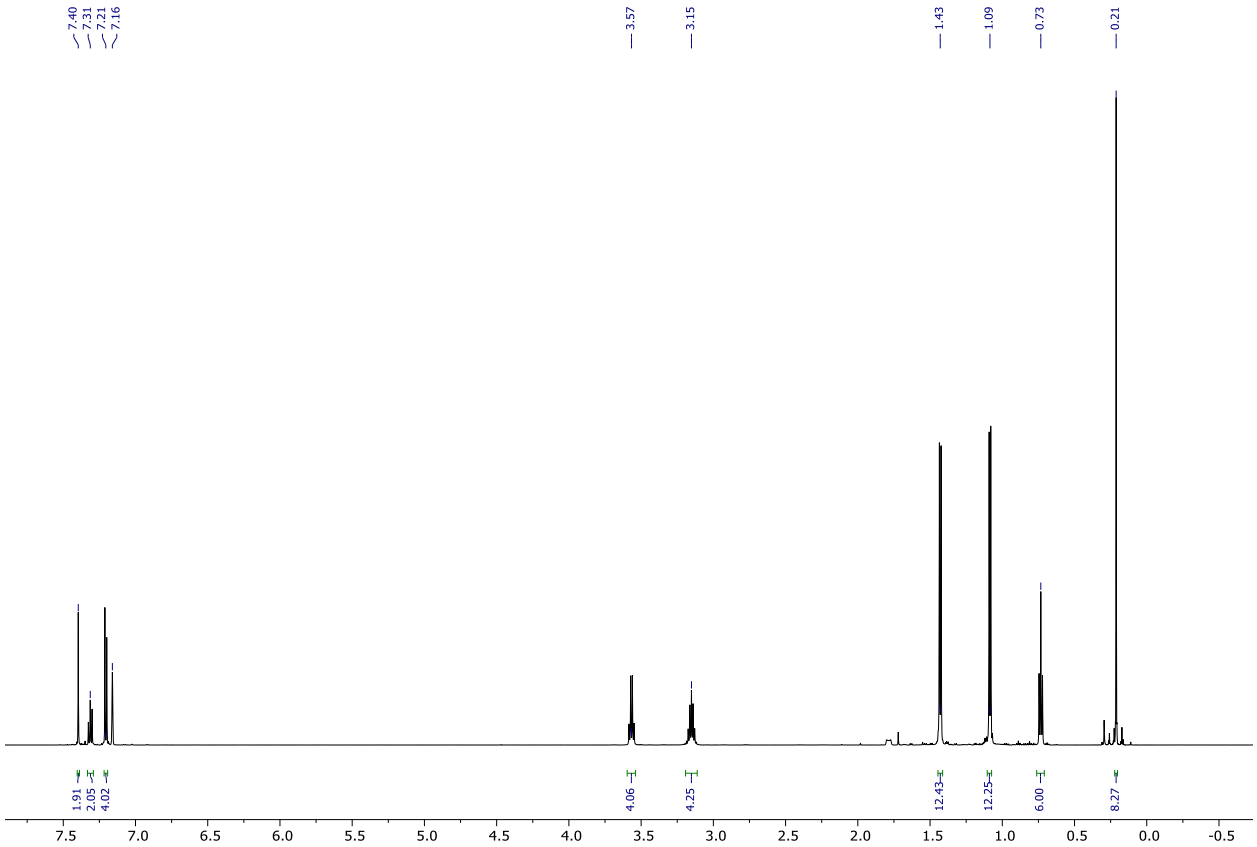


**Figure 7.S3.** $^{1}$H NMR (600 MHz, $C_6D_6$, 298 K) spectrum of $Al(Et_2O)I_2(4\text{-}SiMe_3\text{-}Ar^{iPr4})$ (**1**).

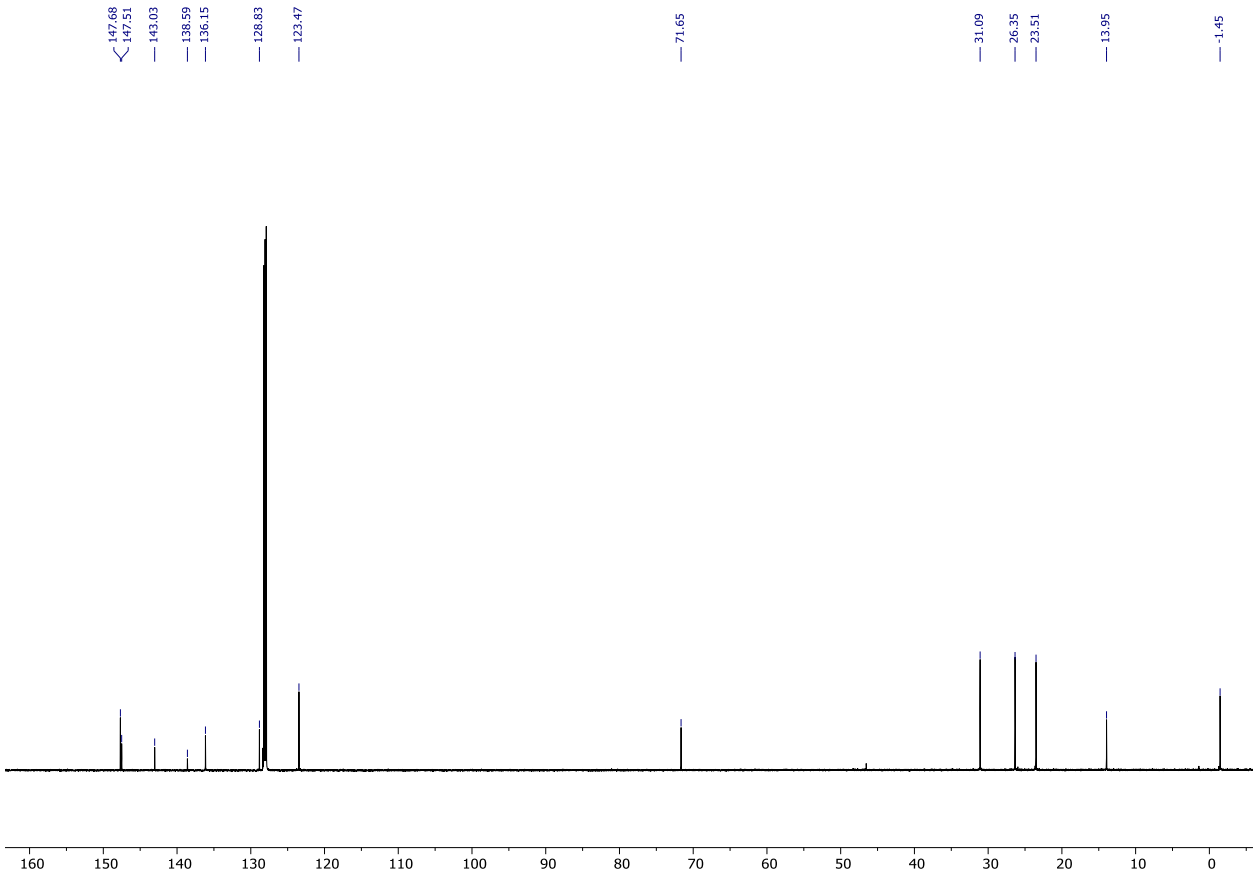


**Figure 7.S4.** $^{13}C\{^{1}H\}$ NMR (151 MHz, $C_6D_6$, 298 K) spectrum $Al(Et_2O)I_2(4\text{-}SiMe_3\text{-}Ar^{iPr4})$ (**1**).

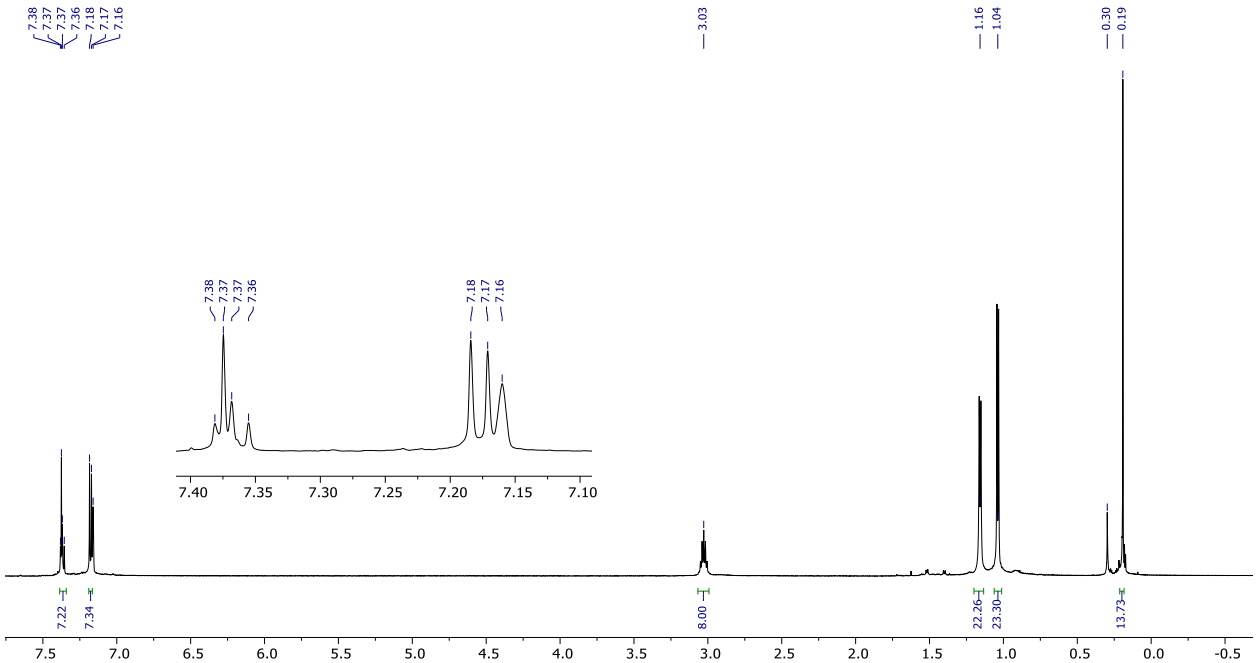


**Figure 7.S5.** $^{1}$H NMR (600 MHz, $C_6D_6$, 298 K) spectrum of $\{Al(I)Ar^{iPr4}\text{-}4\text{-}SiMe_3\}_2$ (**2**).

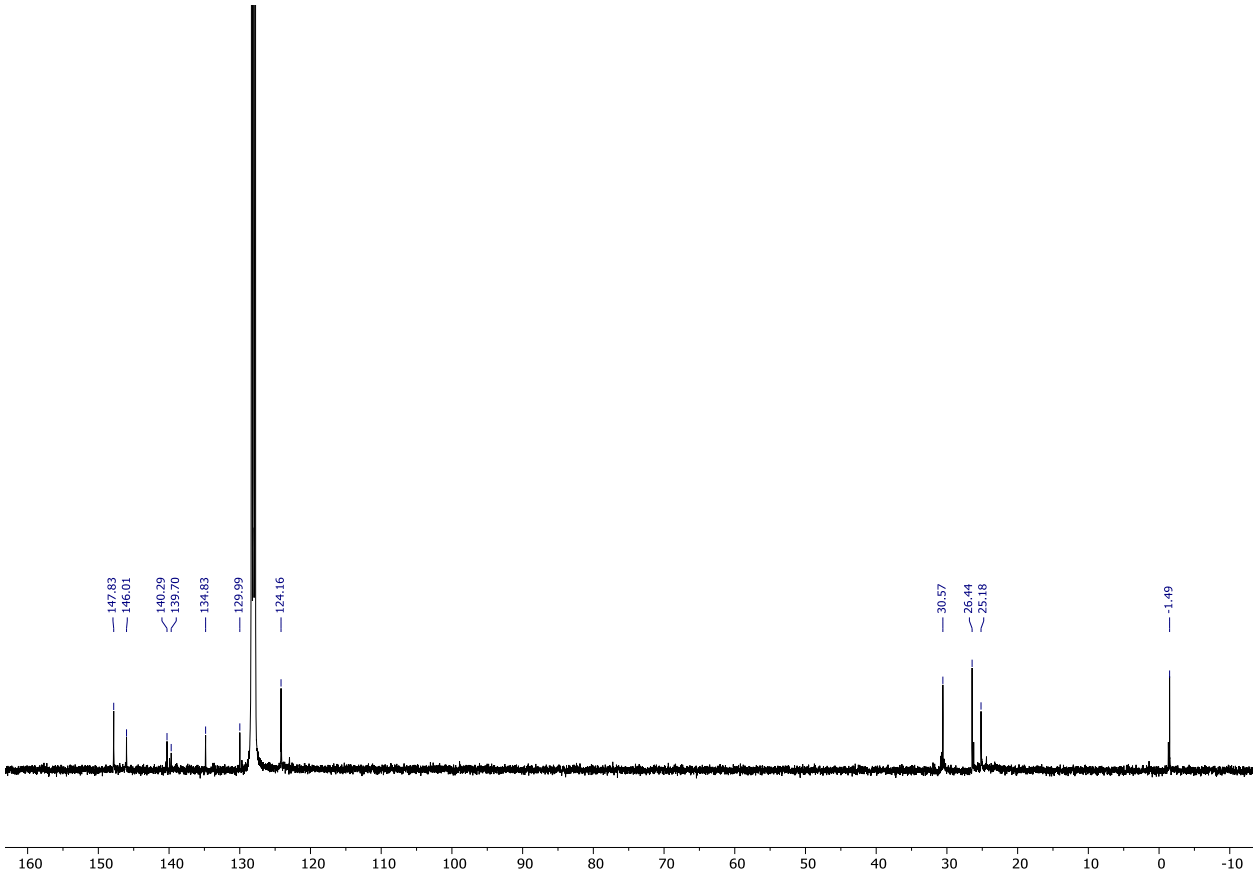


**Figure 7.S6. .**$^{13}C\{^{1}H\}$ NMR (101 MHz, $C_6D_6$, 298 K) spectrum of $\{Al(I)Ar^{iPr4}\text{-}4\text{-}SiMe_3\}_2$ (**2**).

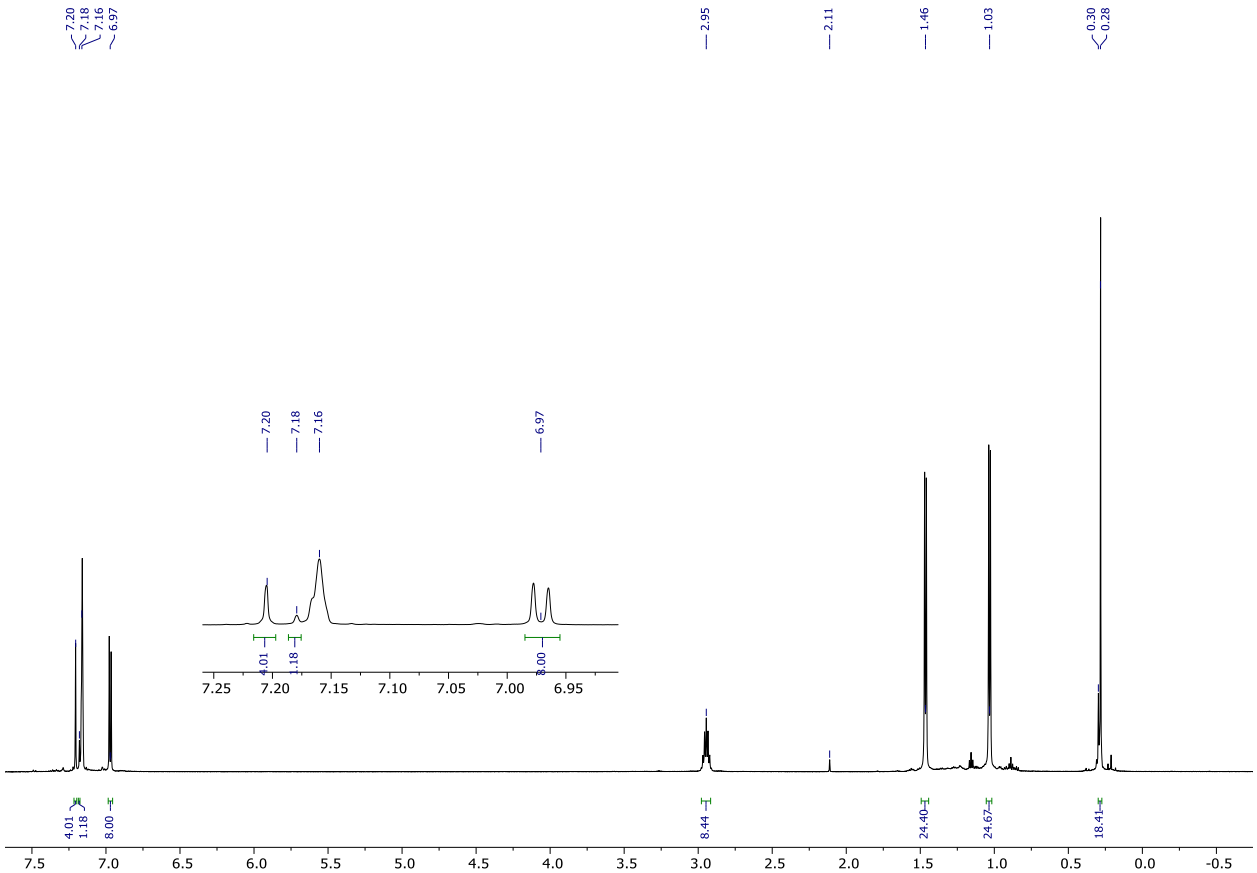


**Figure 7.S7**. $^{1}$H NMR (600 MHz, $C_6D_6$, 298 K) spectrum of $Na_2(AlAr^{iPr4}\text{-}4\text{-}SiMe_3)_2$ (**3**) The signal at 7.18 ppm corresponds to 25% of the 1:2:1 triplet overlapping with the benzene solvent signal.

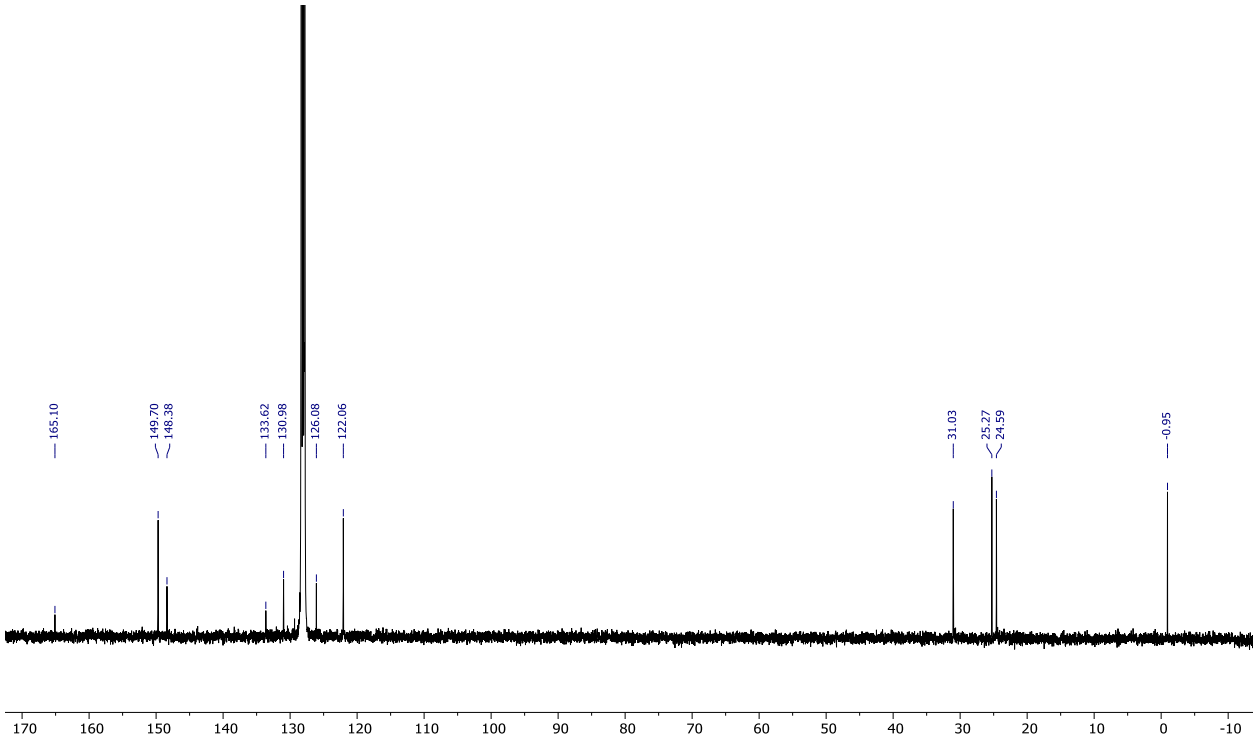


**Figure 7.S8.** $^{13}C\{^{1}H\}$ NMR (101 MHz, $C_6D_6$, 298 K) spectrum of $Na_2(AlAr^{iPr4}\text{-}4\text{-}SiMe_3)_2$ (**3**).

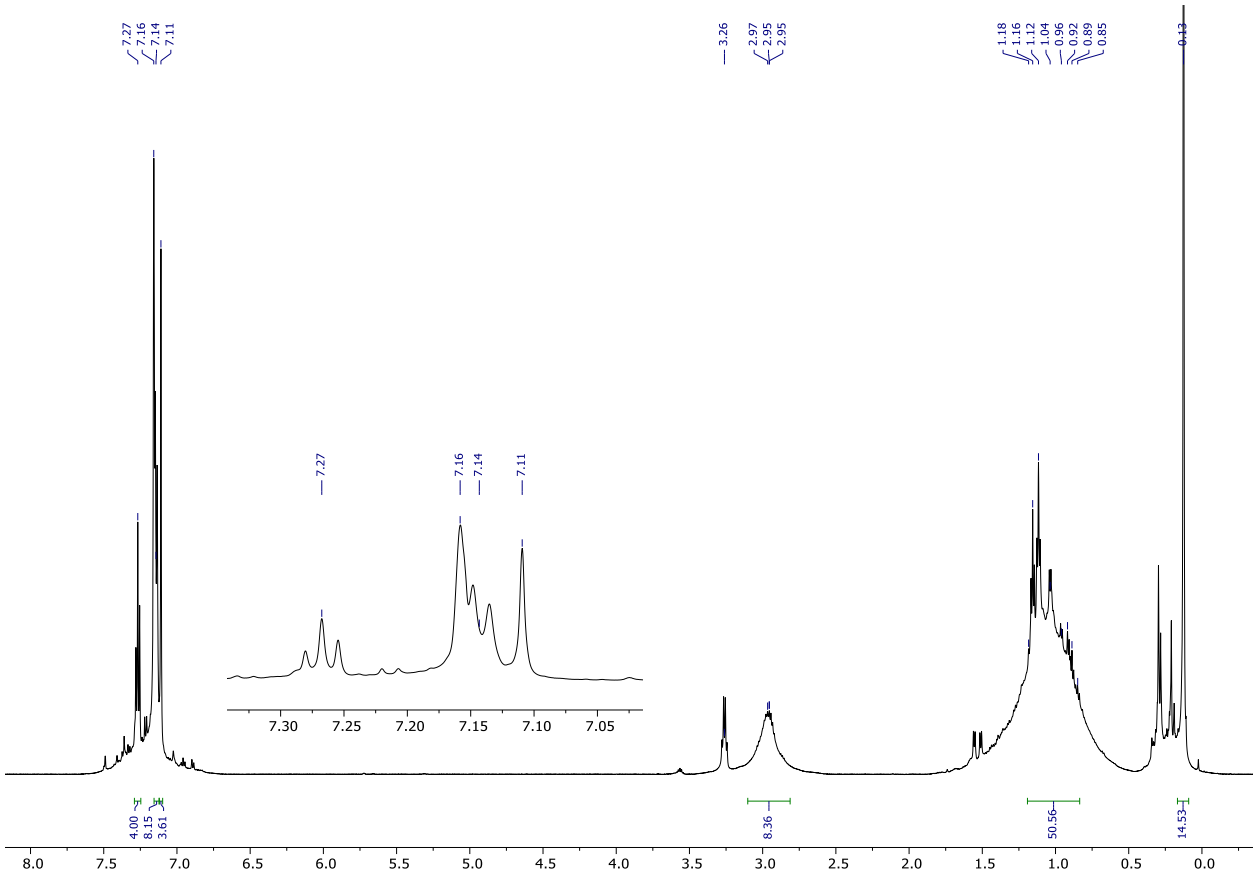


**Figure 7.S9.** $^{1}$H NMR (600 MHz, $C_6D_6$, 298 K) spectrum of the dialuminene-benzene cycloaddition product **4**.

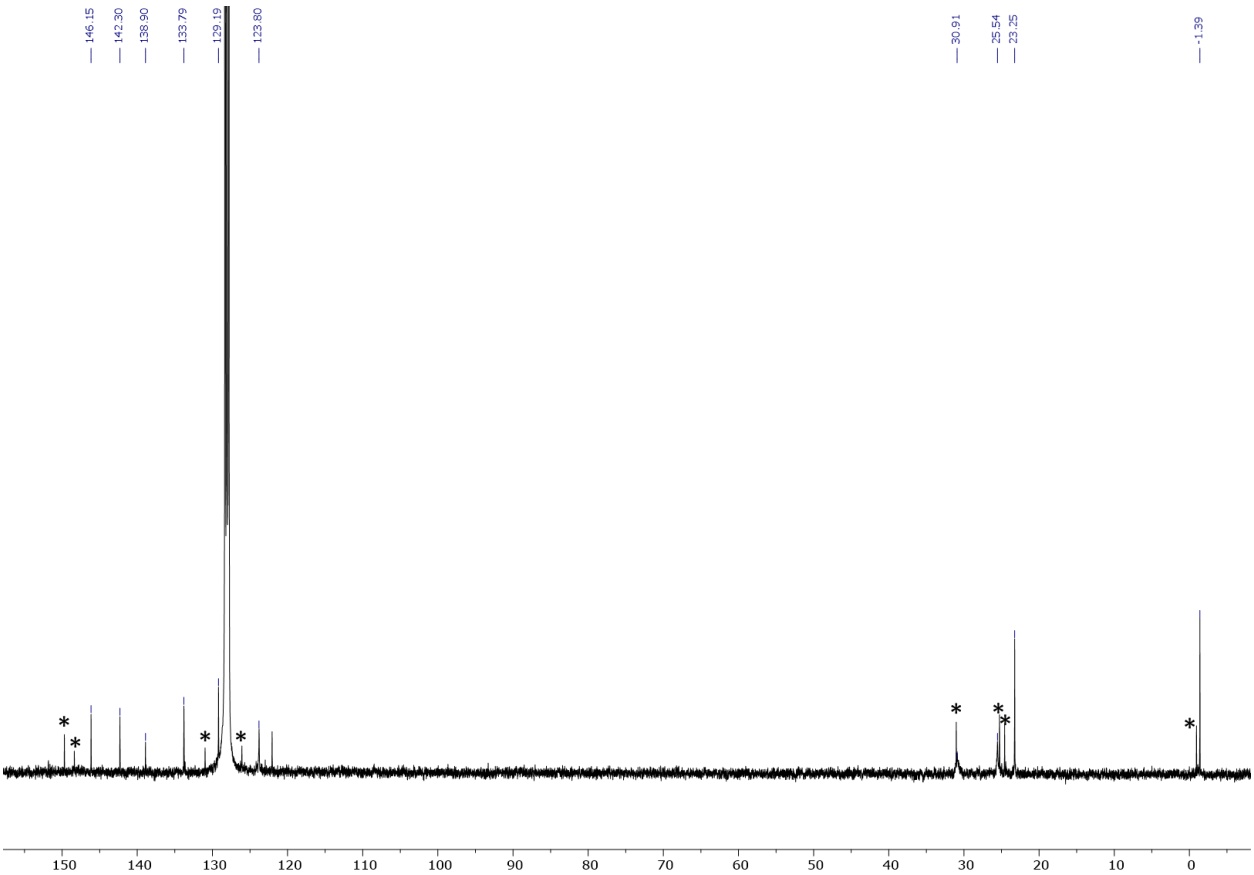


**Figure 7.S10.** $^{13}C\{^{1}H\}$ NMR (101 MHz, $C_6D_6$, 298 K) of 4 generated by the reaction between **2** and **3**. Signals marked with * correspond to excess **3**

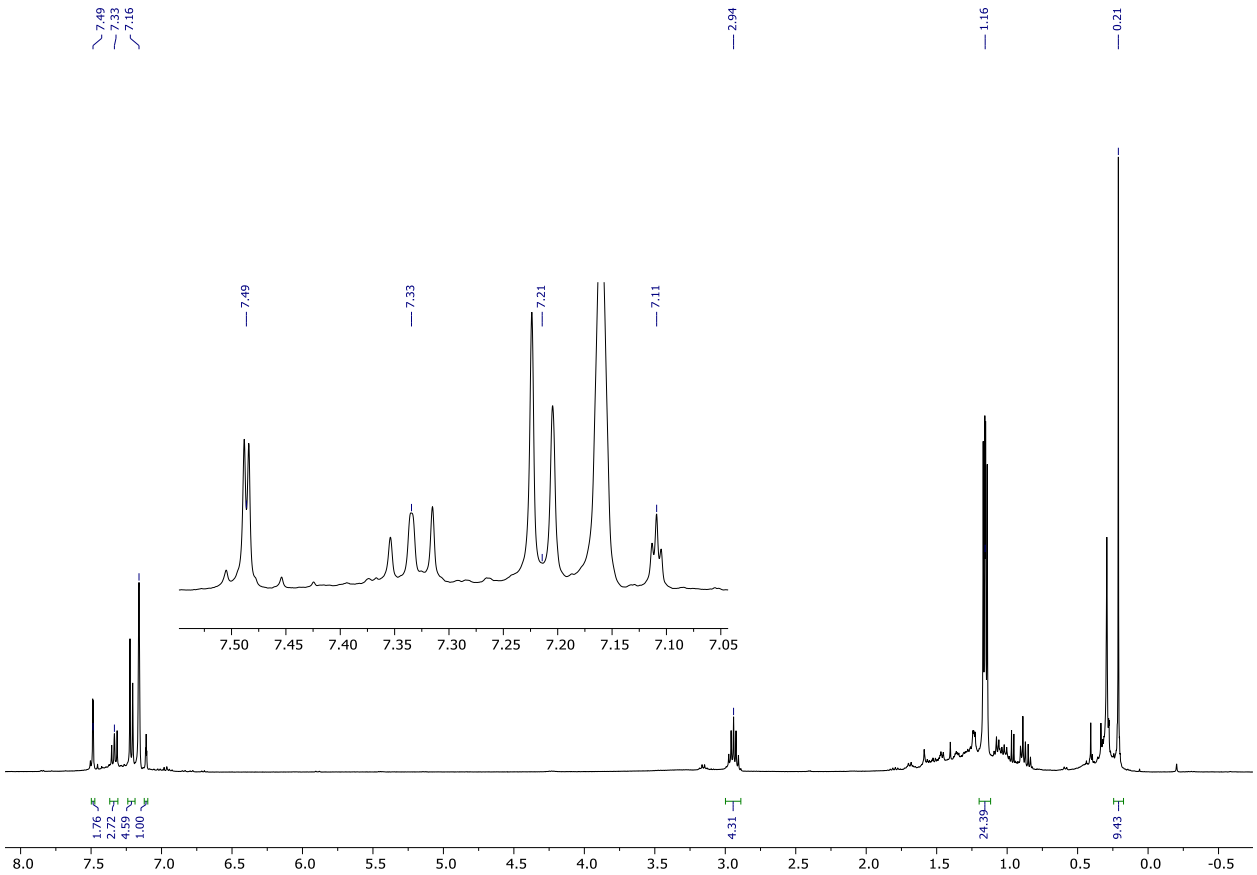


**Figure 7.S11.** $^{1}$H NMR (400 MHz, $C_6D_6$, 298 K) spectrum of 4-$SiMe_3Ar^{iPr4}H$

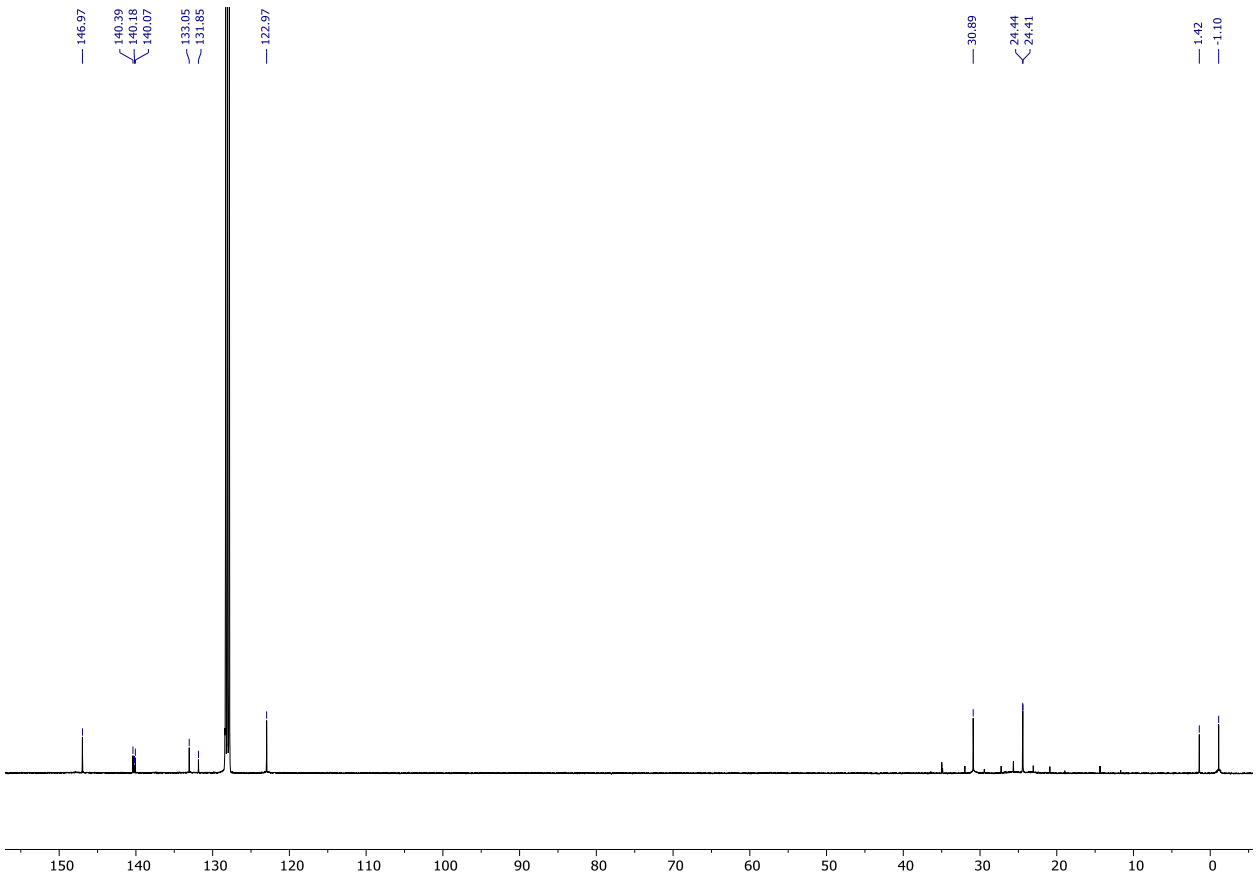


**Figure 7.S12.** $^{13}C\{^{1}H\}$ NMR (101 MHz, $C_6D_6$, 298 K) spectrum of 4-$SiMe_3Ar^{iPr4}H$

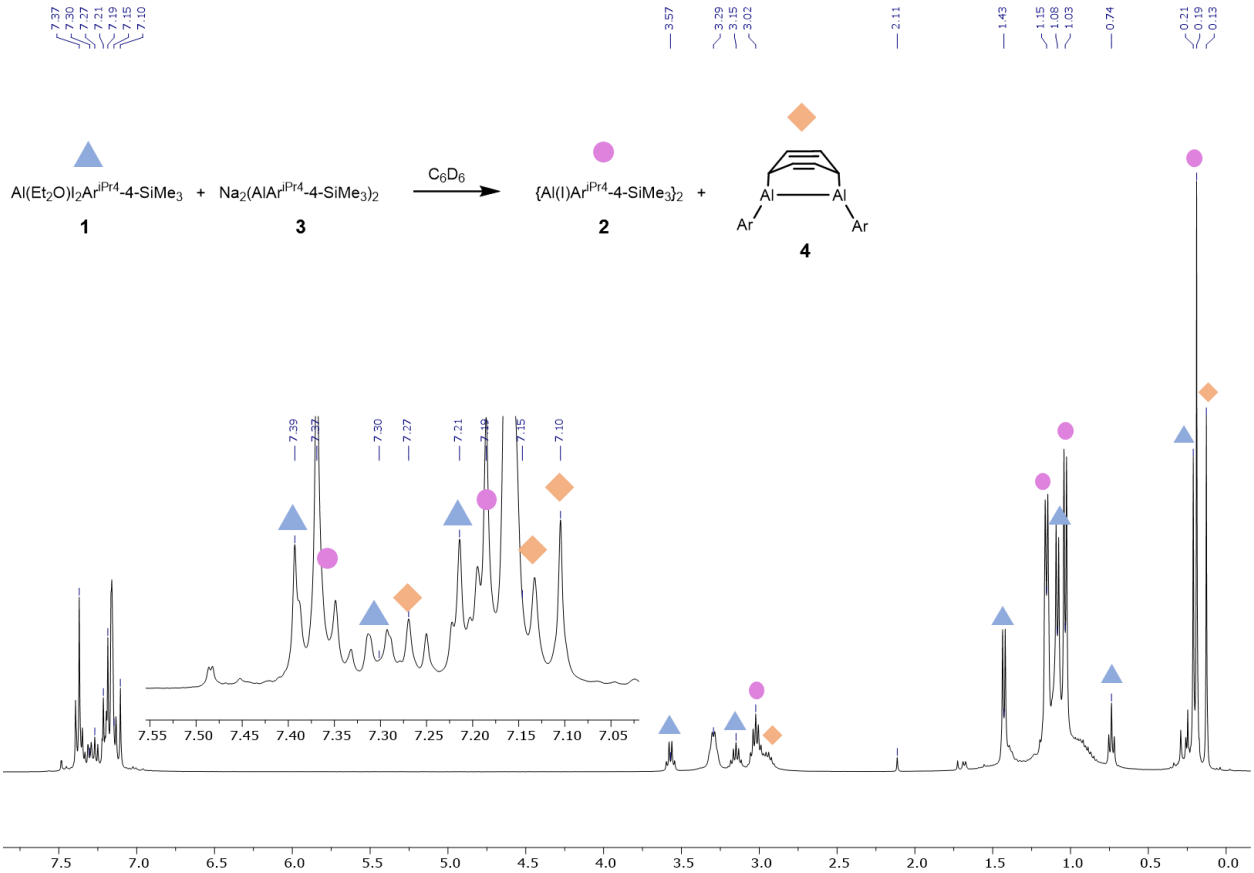


**Figure 7.S13.** $^1$H NMR spectrum of the comproportionation reaction between excess **1** (blue ▲) and **3** in $C_6D_6$ to give **2** (magenta ●) and **4** (orange ♦).

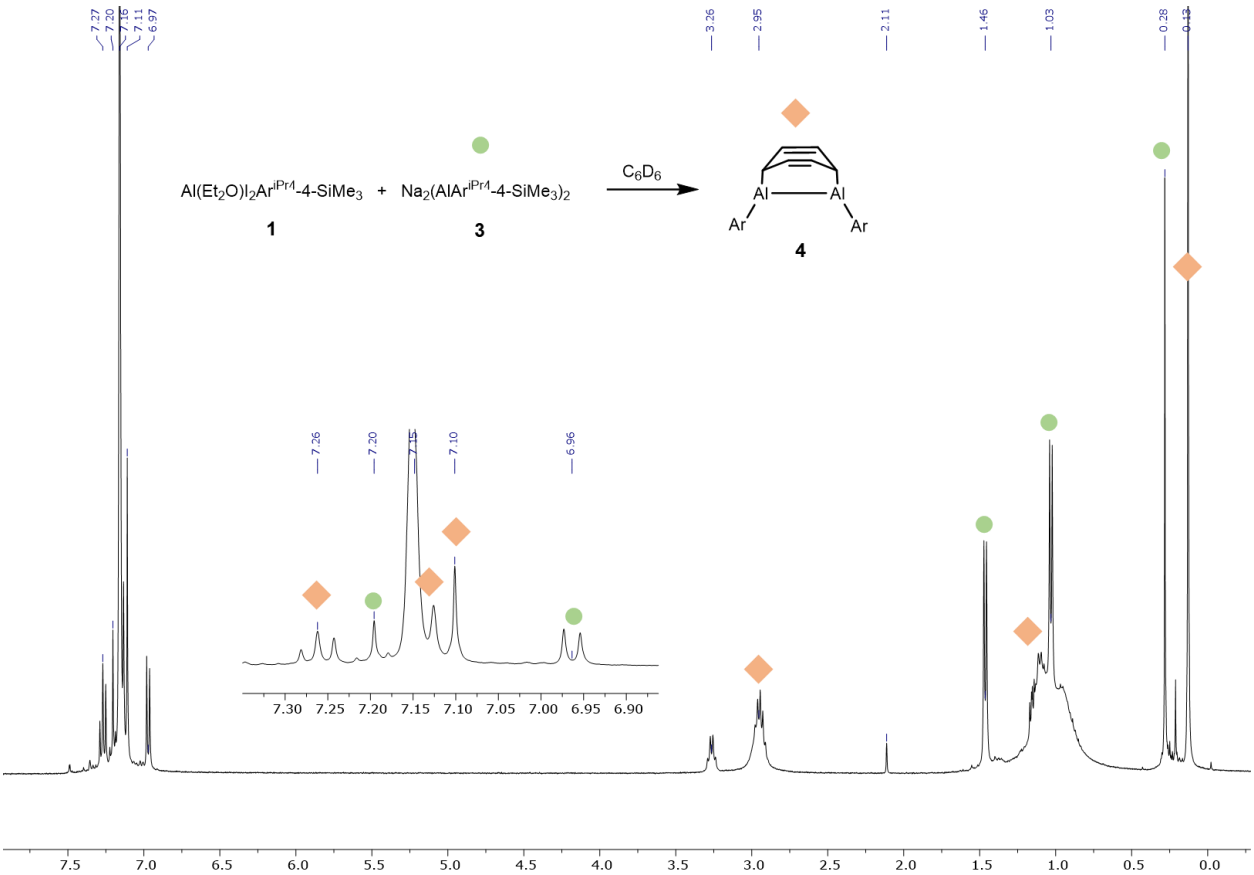


**Figure 7.S14.** $^1$H NMR spectrum of the comproportionation reaction **1** and excess **3** (green ●) in $C_6D_6$ to give **4** (orange ♦).

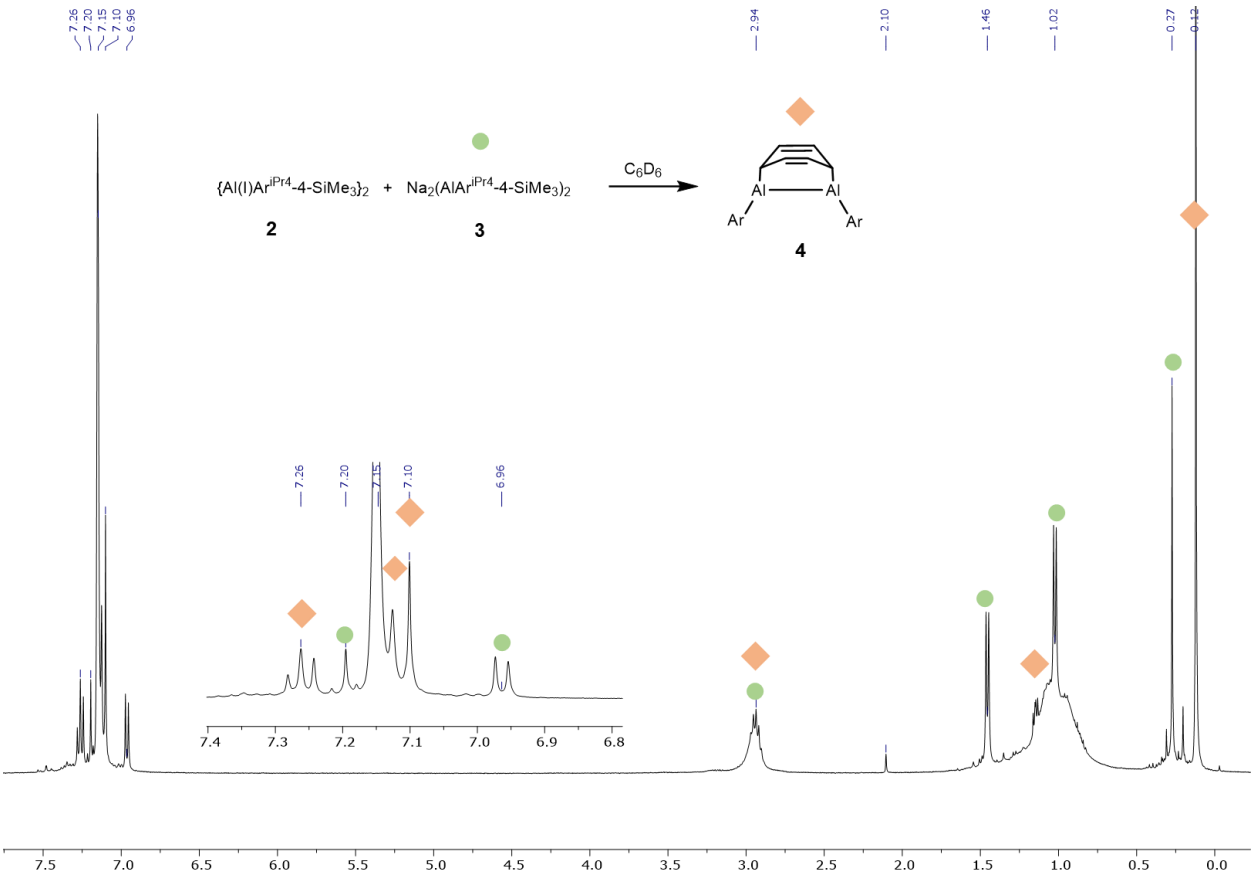


**Figure 7.S15.** $^1$H NMR spectrum of the comproportionation reaction **2** and excess **3** (green ●) in $C_6D_6$ to give 4 (orange ♦).

## UV-Visible Spectra

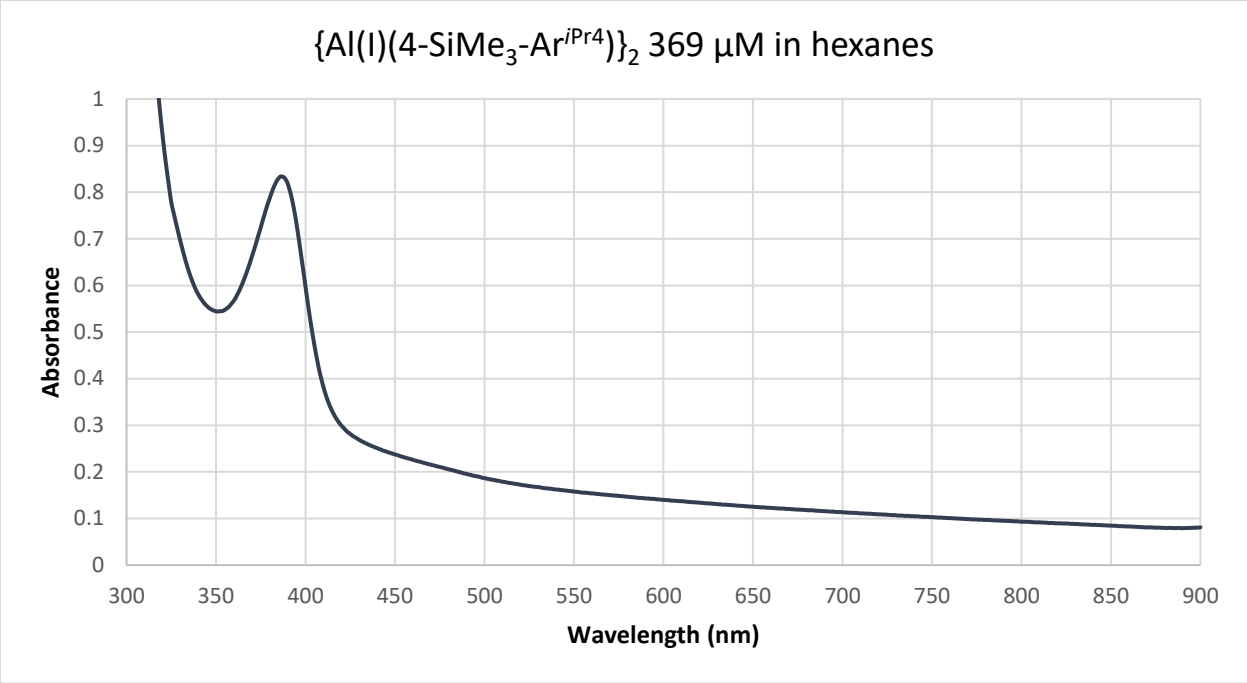


**Figure 7.S16.** UV-Visible spectrum of **2** in hexanes**.**

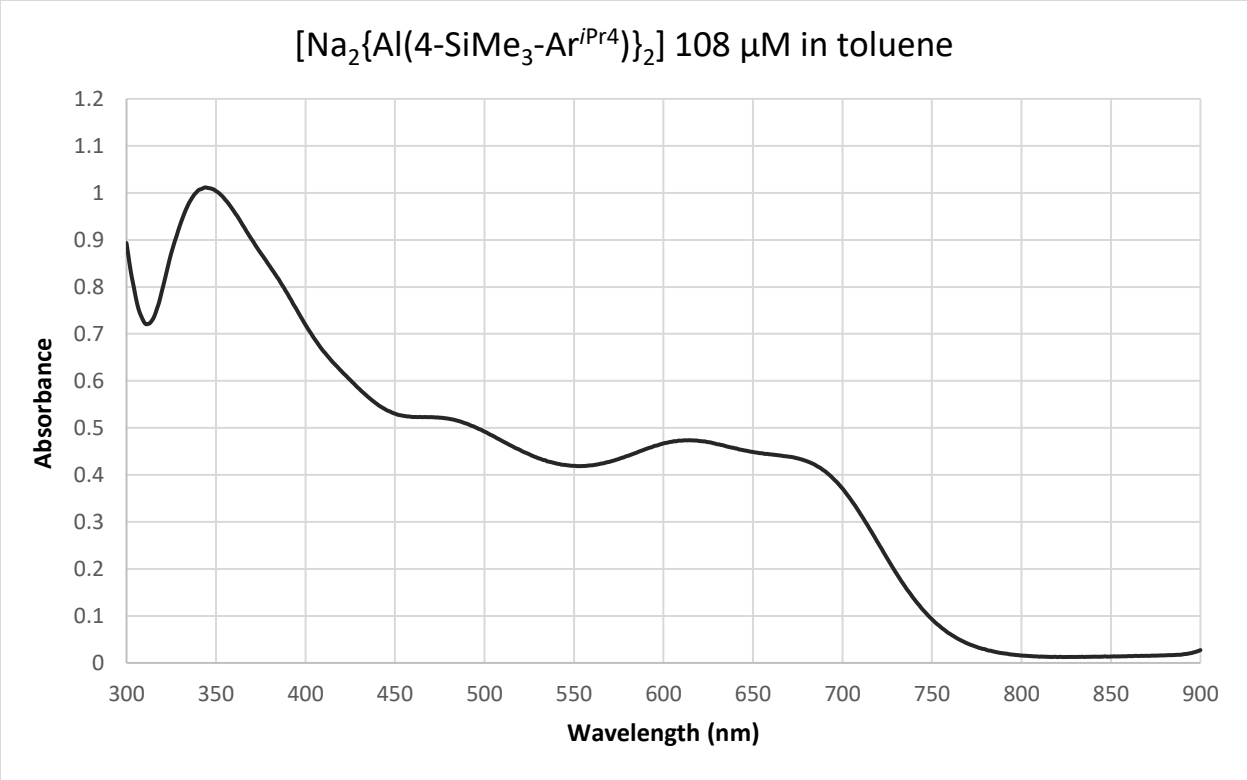


**Figure 7.S17.** UV-Visible spectrum of **3** in toluene.

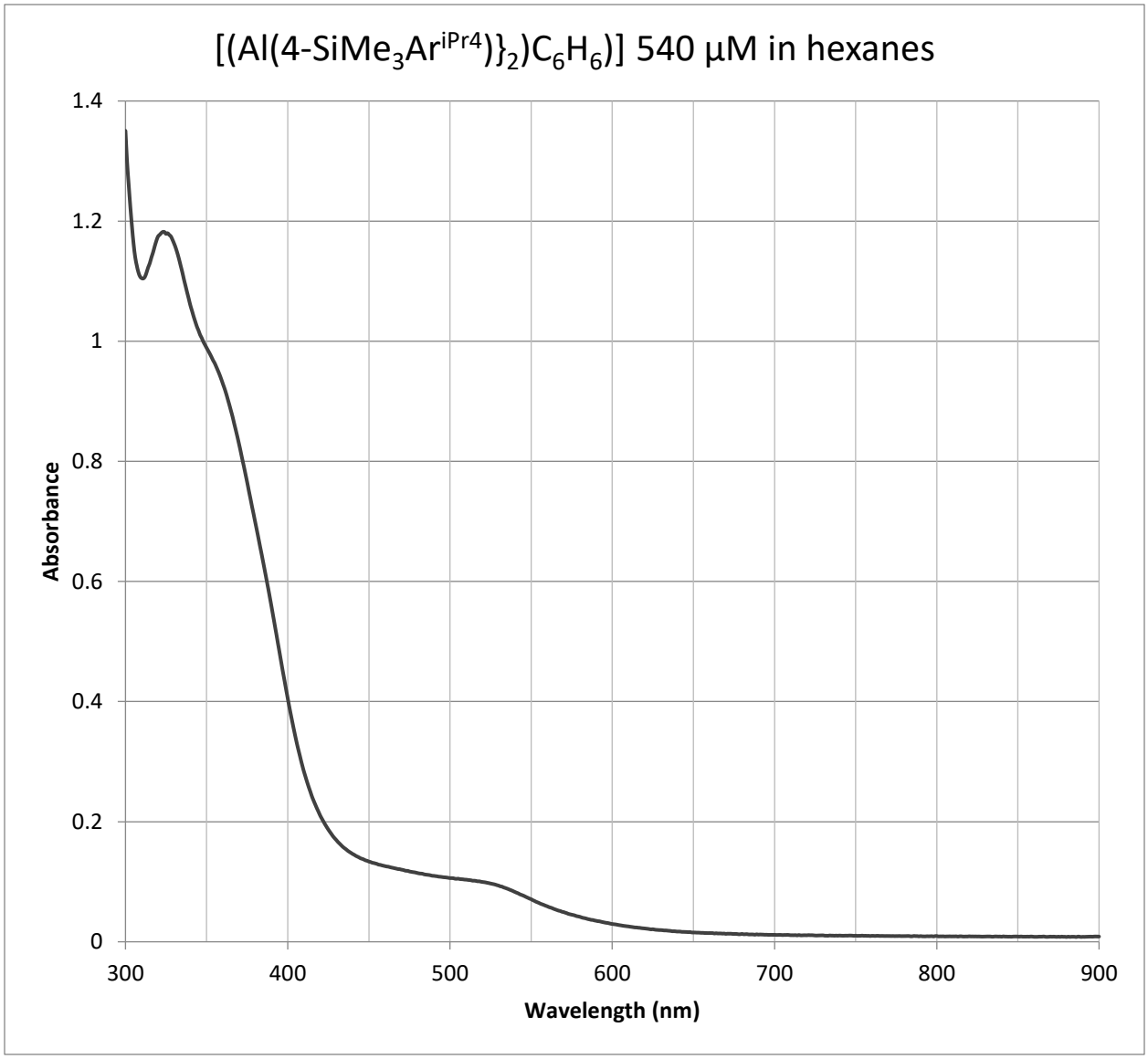


**Figure 7.S18.** UV-Visible spectrum of **4** in hexanes.

**X-Ray Crystallography**

Crystals of **1**-**4** were removed from a Schlenk flask under a stream of argon and immediately covered with hydrocarbon oil. A suitable crystal was selected, attached to a MiTeGen microloop, and mounted on the goniometer of the diffractometer under a cold stream of $N_2$. Data were collected at 90 K on a Bruker Duo APEXII CCD diffractometer (**1**, **2**, **3**) or 100 K on a Bruker D8 VENTURE diffractometer (**4**) with Mo Kα radiation (λ = 0.71073 Å) (**1**, **3**, **4**) or Cu Kα radiation λ = 1.54178 (**2**). Data were integrated with SAINT[S5] and an absorption correction (multi-scan) was applied using SADABS[S6]. The structures were solved using SHELXTL program package[S7] by intrinsic phasing methods using SHELXT[S8] and were refined by full matrix least-squares procedures using SHELXL.[S9] All non-H atoms were refined anisotropically.

**Table 7.S1**. X-ray crystallographic data for **1**.

| | |
|---|---|
| Empirical formula | $C_{37}H_{55}OAlSiI_2$ |
| Formula weight | 824.68 |
| Temperature/K | 90.15 |
| Crystal system | monoclinic |
| Space group | $P2_1/c$ |
| a/Å | 10.998(2) |
| b/Å | 13.500(3) |
| c/Å | 26.336(5) |
| α/° | 90 |
| β/° | 97.410(3) |
| γ/° | 90 |
| Volume/Å$^3$ | 3877.6(13) |
| Z | 4 |
| $\rho_{calc}$g/cm$^3$ | 1.413 |
| μ/mm$^{-1}$ | 1.701 |
| F(000) | 1672.0 |
| Crystal size/mm$^3$ | 0.163 × 0.111 × 0.076 |
| Radiation | MoKα (λ = 0.71073) |
| 2Θ range for data collection/° | 3.118 to 54.932 |
| Index ranges | $-14 \leq h \leq 14$, $-17 \leq k \leq 17$, $-34 \leq l \leq 34$ |
| Reflections collected | 34107 |
| Independent reflections | 8898 [$R_{int}$ = 0.0287, $R_{sigma}$ = 0.0221] |
| Data/restraints/parameters | 8898/0/392 |
| Goodness-of-fit on $F^2$ | 1.058 |
| Final R indexes [I>=2σ (I)] | $R_1$ = 0.0238, $wR_2$ = 0.0566 |
| Final R indexes [all data] | $R_1$ = 0.0289, $wR_2$ = 0.0596 |

**Table 7.S2**. X-ray crystallographic data for **2**.

| | |
|---|---|
| Empirical formula | $C_{40}H_{53}AlISi$ |
| Formula weight | 715.79 |
| Temperature/K | 90.15 |
| Crystal system | monoclinic |
| Space group | $P2_1/n$ |
| a/Å | 17.4939(8) |
| b/Å | 12.7921(7) |
| c/Å | 18.3769(9) |
| α/° | 90 |
| β/° | 109.048(2) |
| γ/° | 90 |
| Volume/Å$^3$ | 3887.3(3) |
| Z | 4 |
| $\rho_{calc}$g/cm$^3$ | 1.223 |
| μ/mm$^{-1}$ | 7.154 |
| F(000) | 1492.0 |
| Crystal size/mm$^3$ | 0.209 × 0.155 × 0.121 |
| Radiation | CuKα (λ = 1.54178) |
| 2Θ range for data collection/° | 6.058 to 144.582 |
| Index ranges | $-17 \leq h \leq 21$, $-15 \leq k \leq 15$, $-22 \leq l \leq 20$ |
| Reflections collected | 15859 |
| Independent reflections | 7423 [$R_{int}$ = 0.0265, $R_{sigma}$ = 0.0341] |
| Data/restraints/parameters | 7423/20/464 |
| Goodness-of-fit on $F^2$ | 1.012 |
| Final R indexes [I>=2σ (I)] | $R_1$ = 0.0554, $wR_2$ = 0.1441 |
| Final R indexes [all data] | $R_1$ = 0.0583, $wR_2$ = 0.1464 |

**Table 7.S3.** X-ray crystallographic data for **3**.

| | |
|---|---|
| Empirical formula | $C_{43.5}H_{57}AlNaSi$ |
| Formula weight | 657.95 |
| Temperature/K | 90.15 |
| Crystal system | triclinic |
| Space group | P-1 |
| a/Å | 11.4744(10) |
| b/Å | 17.7494(15) |
| c/Å | 21.1607(18) |
| α/° | 98.4810(10) |
| β/° | 90.4220(10) |
| γ/° | 106.9270(10) |
| Volume/Å$^3$ | 4072.1(6) |
| Z | 4 |
| $\rho_{calc}$g/cm$^3$ | 1.073 |
| μ/mm$^{-1}$ | 0.117 |
| F(000) | 1424.0 |
| Crystal size/mm$^3$ | 0.629 × 0.326 × 0.282 |
| Radiation | MoKα (λ = 0.71073) |
| 2Θ range for data collection/° | 3.342 to 54.982 |
| Index ranges | $-14 \leq h \leq 14$, $-23 \leq k \leq 23$, $-27 \leq l \leq 27$ |
| Reflections collected | 37051 |
| Independent reflections | 18661 [$R_{int}$ = 0.0203, $R_{sigma}$ = 0.0303] |
| Data/restraints/parameters | 18661/34/982 |
| Goodness-of-fit on $F^2$ | 1.020 |
| Final R indexes [I>=2σ (I)] | $R_1$ = 0.0496, $wR_2$ = 0.1363 |
| Final R indexes [all data] | $R_1$ = 0.0632, $wR_2$ = 0.1480 |

**Table 7.S4**. X-ray crystallographic data for **4**.

| | |
|---|---|
| Empirical formula | $C_{81}H_{105}Al_2Si_2$ |
| Formula weight | 1188.78 |
| Temperature/K | 100.0 |
| Crystal system | monoclinic |
| Space group | $P2_1/n$ |
| a/Å | 11.3894(11) |
| b/Å | 19.669(2) |
| c/Å | 32.660(6) |

| | |
|---|---|
| α/° | 90 |
| β/° | 91.426(6) |
| γ/° | 90 |
| Volume/Å$^3$ | 7314.1(16) |
| Z | 4 |
| $\rho_{calc}$g/cm$^3$ | 1.080 |
| μ/mm$^{-1}$ | 0.113 |
| F(000) | 2580.0 |
| Crystal size/mm$^3$ | 0.244 × 0.196 × 0.18 |
| Radiation | MoKα (λ = 0.71073) |
| 2Θ range for data collection/° | 2.418 to 52.844 |
| Index ranges | $-12 \leq h \leq 14$, $-24 \leq k \leq 24$, $-40 \leq l \leq 39$ |
| Reflections collected | 43076 |
| Independent reflections | 14960 [$R_{int}$ = 0.0330, $R_{sigma}$ = 0.0307] |
| Data/restraints/parameters | 14960/0/789 |
| Goodness-of-fit on $F^2$ | 1.044 |
| Final R indexes [I>=2σ (I)] | $R_1$ = 0.0443, $wR_2$ = 0.1137 |
| Final R indexes [all data] | $R_1$ = 0.0471, $wR_2$ = 0.1157 |

## Photos of Compounds

**Figure 7.S19.** An ice-cold solution of **1** and **3** in $Et_2O$ turns dark purple before rapidly fading to colorless.

**Figure 7.S20.** A pale yellow crystal of **2** mounted on a goniometer.

**Figure 7.S21.** A dark green crystal of **3** mounted on a goniometer.

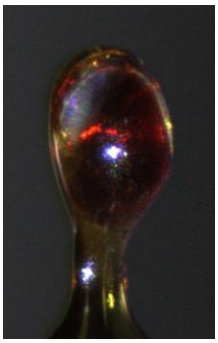

**Figure 7.S22.** A red crystal of **4** mounted on a goniometer.

## References


(S1) Pangborn, A. B.; Giardello, M. A.; Grubbs, R. H.; Rosen, R. K.; Timmers, F. J. Safe and Convenient Procedure for Solvent Purification. *Organometallics* **1996**, *15*, 1518–1520.

(S2) Fulmer, G. R.; Miller, A. J. M.; Sherden, N. H.; Gottlieb, H. E.; Nudelman, A.; Stoltz, B. M.; Bercaw, J. E.; Goldberg, K. I. NMR Chemical Shifts of Trace Impurities: Common Laboratory Solvents, Organics, and Gases in Deuterated Solvents Relevant to the Organometallic Chemist. *Organometallics* **2010**, *29*, 2176–2179.

(S3) Rivard, E.; Fischer, R. C.; Wolf, R.; Peng, Y.; Merrill, W. A.; Schley, N. D.; Zhu, Z.; Pu, L.; Fettinger, J. C.; Teat, S. J.; Nowik, I.; Herber, R. H.; Takagi, N.; Nagase S.; Power, P. P. Isomeric Forms of Heavier Main Group Hydrides: Experimental and Theoretical Studies of the $[Sn(Ar)H]_2$ (Ar = Terphenyl) System. *J. Am. Chem. Soc.* **2007**, *129*, 16197–16208.

(S4) Ruff. J. K.; Hawthorne, M. F. The Amine Complexes of Aluminum Hydride. I. *J. Am. Chem. Soc.* 1960, **82**, 2141-2144.

(S5) Bruker (2016) SAINT (Version 8.37a). Bruker AXS Inc., Madison, Wisconsin, USA

(S6) Sheldrick, G. M. (2015) SADABS. University of Göttingen, Germany.

(S7) Sheldrick, G. M. (2002). SHELXTL. Version 6.1. Siemens Analytical X-ray Instruments Inc., Madison, Wisconsin, USA.

(S8) Sheldrick, G. M. (2014). SHELXT. University of Göttingen, Germany.

(S9) Sheldrick, G. M. (2015). SHELXL University of Göttingen, Germany.